Reproduced by NTIS

N8019183

BA

BIN: M109 11-13-97
INVOICE: 511582
SHIPTO: 1*85776
PAYMENT: NONE

JPL PUBLICATION 80-14

Attitude Control Study for a Large Flexible Spacecraft Using a Solar Electric Propulsion System (SEPS)

Final Report

A. F. Tolivar
R. W. Key

March 1, 1980

National Aeronautics and
Space Administration

Jet Propulsion Laboratory
California Institute of Technology
Pasadena, California

JPL PUBLICATION 80-14

Attitude Control Study for a Large Flexible Spacecraft Using a Solar Electric Propulsion System (SEPS)

Final Report

A. F. Tolivar
R. W. Key

March 1, 1980

National Aeronautics and
Space Administration

Jet Propulsion Laboratory
California Institute of Technology
Pasadena, California

The research described in this publication was carried out by the Jet Propulsion Laboratory, California Institute of Technology, under NASA Contract No. NAS7-100

FOREWORD

The authors wish to express their appreciation to R. Bamford, J.A. Garba, K.K. Gupta, E.H. Kopf, G.E. Fleischer, P.H. Mak, and S.L. Miller for valuable contributions and assistance received during the course of this study.

The research performed for this report was carried out under NASA Contract NAS7-100, Task Order RD-65, Amendment Number 356, Change 1, paragraph 2(b) dated May 24, 1979. The Task Leader for Marshall Space Flight Center was Mr. Donald D. Tomlin and the Technical Manager at the Jet Propulsion Laboratory was Mr. Kenneth M. Russ.

ABSTRACT

This report describes work done to analyze and evaluate the attitude control performance of the Solar Electric Propulsion System (SEPS). A thrust vector control system for powered flight control is examined along with a gas jet reaction control system, and a reaction wheel system, both of which have been proposed for non-powered flight control. Comprehensive computer simulations of each control system were made and evaluated using a 30-mode spacecraft model.

Results obtained indicate that thrust vector control and reaction wheel systems offer acceptable smooth proportional control. The gas jet control system is shown to be risky for a flexible structure such as SEPS, and is therefore, not recommended as a primary control method.

CONTENTS

Figures

Figures (continued)

Tables

SECTION 1

INTRODUCTION AND SUMMARY

This report presents the results of a comprehensive study undertaken to establish the attitude control performance provided by the Solar Electric Propulsion System (SEPS) for the planned International Comet Mission.

1.1 BACKGROUND

The "Halley Flyby/Tempel 2 Rendezvous (HFB/T2R) International Comet Mission" presents a rare opportunity to fly by the comet Halley enroute to rendezvous with a second comet (Tempel 2). This mission[1] is possible by using a Solar Electric Propulsion System (SEPS) with a modest performance level based on current technology. An ecliptic plane projection of the overall heliocentric trajectory is illustrated in Figure 1-1.

The scientific objectives of the mission are the determination of the chemical composition and physical structure of cometary nuclei and comae, investigation of the dynamic processes occurring at the surface of nuclei and within the comae, and investigation of the interaction of comets with the solar wind, including study of the formation of and structure of cometary tails.

The mission plan calls for a single flight system to be launched by the space shuttle/inertial upper stage in the summer of 1985. The flight system (Figure 1-2) is composed of three basic elements:

i) THE SPACECRAFT, which includes all rendezvous science electronics, booms, and platforms, will provide deployment, pointing, power, commanding, and data collection for the science payload. It will also provide sequencing control for the probe and the SEPS.

ii) THE PROBE, which will be released at Halley, will contain its own set of science instruments.

iii) THE SEPS, which is a standard space transportation venicle capable of carrying planetary or Earth orbital payloads

[1] International Comet Mission: Halley/Tempel 2 Mission Baseline, NASA/ESA Document JPL 626-2, November 1979 (JPL Internal Document).

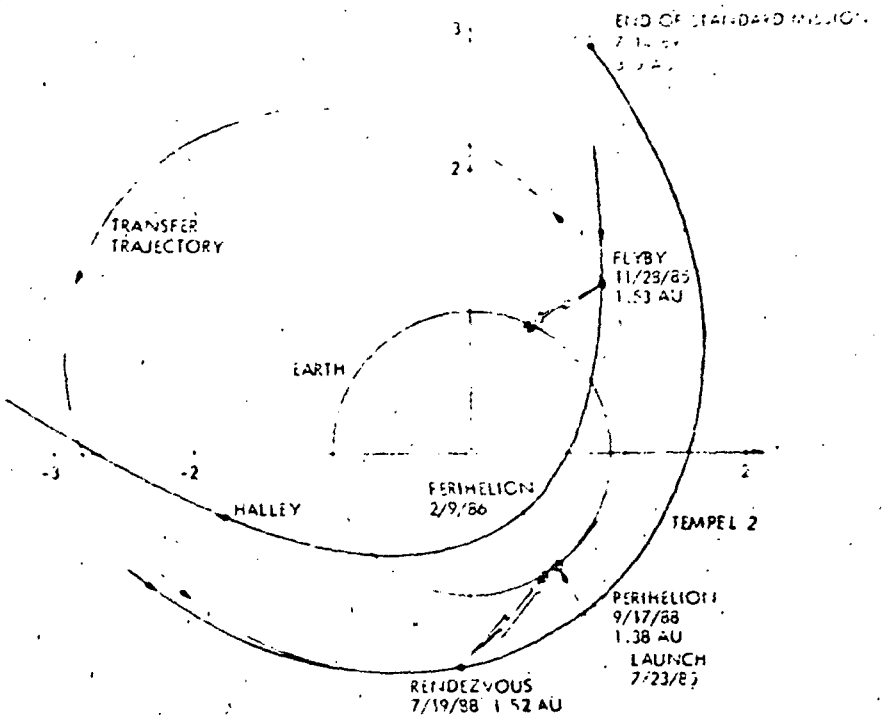

Figure 1-1. HFB/T2R Typical Transfer Trajectory

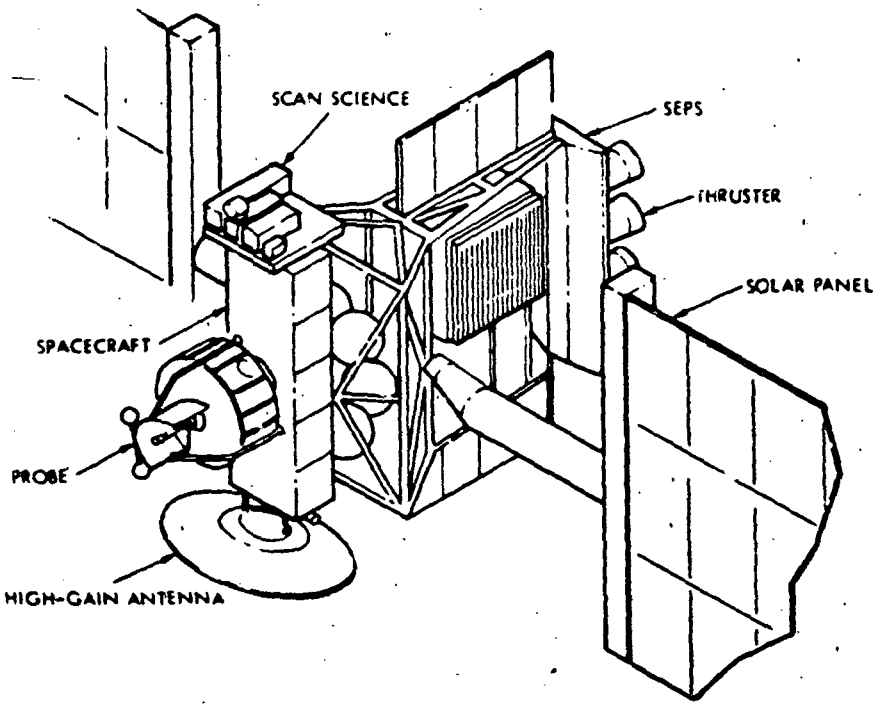

Figure 1-2. HFB/T2R Flight System Configuration

on missions for which ion propulsion is appropriate. It includes the mercury ion drive thrusters, mercury storage tanks, and two large (each 32 m long) solar panels which provide the energy for the electric propulsion. Besides power and propulsion, the SEPS provides flight system attitude control and maneuvering and contains associated celestial sensors and gyros.

The fast flyby (57 km/s) encounter with Halley occurs only four months after launch, when Halley is approaching perihelion about 1.5 AU solar range. The Halley probe is released from the spacecraft to acquire data on a ballistic path through the atmosphere of Halley, while the rendezvous spacecraft is deflected by the SEPS for safe flyby to the sunward side of Halley. The spacecraft makes remote observations of Halley during flyby as well as serving as a relay link for the data acquired by the probe and transmitted in real time to the spacecraft.

The SEPS provides thrust virtually continuously throughout the heliocentric transfer portion of the mission, with thruster-off periods restricted to brief intervals required for Halley probe deployment, Halley encounter data acquisition, and a few special engineering and science instrument calibration sequences during cruise. The number of thrusters operating and the thruster throttle level are programmed for optimum utilization of the available solar array power as the solar distance changes.

Rendezvous with Tempel 2 requires a total flight time of nearly three years, and is scheduled to occur about two months before comet perihelion. The standard mission is scheduled to extend for a year after initial rendezvous with Tempel 2 to permit extensive exploration of the cometary environment and nucleus until Tempel 2 is 3.0 AU from the Sun.

Attitude control and maneuvering throughout the mission is provided by the SEPS, both during powered flight to and around Tempel 2, as well as during unpowered orbital operations about Tempel 2.

Attitude control during powered flight is achieved by gimballing of the ion drive thrusters under what will be called "thrust vector control." This control method is used virtually continuously during

the first 3 years of the mission while in the heliocentric transfer portion of the mission. After Tempel 2 rendezvous the ion engines must be turned off and will only be used infrequently (a few hours a week) to permit the desired circumnavigation of the nucleus.

With the thrusters off most of the time following rendezvous, a second means of attitude control must be provided. Two candidates that have been proposed are 1) gas jet reaction control, and 2) momentum wheel control.

1.2 STUDY OBJECTIVES AND SCOPE

The SEPS/ICM Flight System represents a new kind of space vehicle. What makes it different from past spacecraft, from the point of view of attitude control, is its shear size and flexibility. The 2 large solar panels (required to provide the large amounts of energy needed to operate the ion thrusters) give the vehicle a wing span of ~75 m (246 ft) and result in very large vehicle inertias (200,000 kg-m^2). Available control torques to handle these large inertias are low. Constraints on system weight force the solar panels to be thin, lightweight structures, and, hence, quite flexible.

The objectives of this study have been to understand the nature of the control problems associated with this large flexible vehicle and to evaluate the attitude control performance provided by the baseline SEPS for the International Comet Mission for the 3 control methods under consideration:

1. Thrust vector control
2. Gas jet reaction control
3. Reaction wheel control.

The baseline attitude control performance requirements for SEPS/ICM are given in ref. [1]. Those requirements are to provide a pointing of the vehicle within $\pm$ 1° of a celestial reference direction with a maximum inertial rate not to exceed 1°/s.

The approach used has been one of time domain analysis (through digital computer simulation) of a comprehensive flexible dynamics model of the vehicle, augmented with the corresponding control laws and control hardware models. Each of the 3 control methods has been studied by simulation of the following four specific maneuvers:

[1] Ibid

1. Complete vehicle turn about the sun-line.
2. Reorientation turn of the SEPS bus while simultaneously rotating the solar panels so as to keep them pointed to the sun, as the bus turns.
3. Acquisition of small initial position errors and rates.
4. Attitude control in the disturbance environment created by Science Scan Platform slewing.

Section 2 presents the model of SEPS/ICM along with a description of the specific maneuvers considered, and several other study assumptions. The systems description, and performance evaluation for thrust vector, gas jet, and reaction wheel control are included in sections 3, 4, and 5, respectively.

1.3 CONCLUSIONS AND RECOMMENDATIONS

The main contribution of this study is that it establishes the Attitude Control Performance characteristics of SEPS for the 3 proposed control methods: TVC, Gas Jets, and Moment Wheel Control. The performance characteristics obtained are given as maneuver performance plots in sections 3, 4, and 5.

In addition to the performance characteristics, considerable insight and experience has been gained during this study, pertaining to the control of flexible spacecraft in general, and of the proposed flexible SEPS/ICM, in particular. Advanced simulation programs have been created which simulate SEPS flexible dynamics and constitute a sophisticated analysis and decision making tool immediately available for further use, should it become desirable.

A principal conclusion of this study is that both of the proposed TVC and Reaction Wheel attitude control (A/C) systems constitute acceptable control options for SEPS/ICM in that they both

1. Are based on currently existing technology. Require no advanced enabling technology.
2. Meet baseline performance requirements.

3. Do so in a very smooth and satisfactory manner, without exciting vehicle flexible dynamics significantly and without exhibiting control/structure interaction.
4. (because of 3) both control methods are not judged to be very sensitive to SEPS structural uncertainties, a very important advantage.

For the 2 Gas Jet Reaction Control Systems considered, it is concluded that

1. One of the systems appears to meet performance requirements, the other does not.
2. Performance for both is characterized by high vibration levels of the structure with substantial excitation of the vehicle flexible appendages. These high vibration levels are due to the impulsive nature of the loads produced by the nearly-square gas jet pulses. Such loads have a very high frequency content and, thus, tend to excite all resonant frequencies in the structure. The higher vibration levels are very dangerous and, in fact, in 2 out of the 6 simulations, have been shown to lead to severe control/structure interaction resulting in exceedingly high limit cycle rates, and unacceptable propellant consumption.
3. Gas jet RCS systems, as a class, tend to be highly interactive with the structures and their performance highly sensitive to model uncertainties. Performance will be reliably known only after launch, when it may be too late.
4. Because of the above, RCS systems are judged very risky for SEPS, and therefore, are not recommended as a primary control method.

To further elaborate on the above, it must be understood that the attitude control problem of guaranteeing stability and performance of the SEPS with the proposed large, flexible solar arrays is a sizeable engineering challenge.

It has been our experience at JPL that flexibility (even slight) can cause serious problems. To name a few, Explorer I, Mariner Venus-Mercury, and Voyager, all exhibited flexible appendage effects which caused serious in-flight attitude control anomalies (unstable behavior, excessive gas consumption, etc.) and ultimately, resulted in costly and extensive "fixes" and/or mission limitations. All this happened in spite of considerable ground testing and efforts to accommodate model uncertainties. These S/C were only slightly flexible. The SEPS on the other hand, is quite flexible. The solar arrays are complex non-linear structures and their large size, mass, and flexibility will have a predominant effect on the total vehicle dynamics. The arrays are, in fact so complex and non-linear that even the best available structural dynamics modeling techniques yield models with uncertainty levels too high for reliable attitude control work. Thus, we have a paradox where the array characteristics are more difficult to model than for previous spacecraft, but their potentially disastrous effects on attitude control make accurate modeling more critical.

Structural analysts provided the solar array dynamics model used in this report. It is the best available model that can be developed using current state-of-the-art modeling techniques. More accurate dynamics models of the solar arrays are unlikely to become available in the near future because the development of such accurate models would require costly in-orbit dynamic testing[2] of the solar arrays.

In view of the above, it is clear that the designer of the A/C system must aim for a control method which is tolerant of model uncertainties. It is precisely in this area that gas jet systems show their bad side-effects. They are highly interactive with flexible structures, and hence not forgiving of model uncertainties. The risk associated with an RCS system in a highly flexible vehicle is simply too great.

[2] Tolivar, A.F., and Garba, J.A., "Attitude Control Considerations for Enhanced Instrumentation on SEPS Solar Array Flight Experiment," Engineering Memorandum EM 347-30, 31 May 1979, Jet Propulsion Laboratory Internal Document.

TABLE 1-1. RCS & RWH Advantages and Disadvantages

R C S	R W H
• ADVANTAGES	• ADVANTAGES

• Provides high control authority	• Provides sufficient control authority to handle transients during
	  • SA axis turns @ 0.1 to 0.2°/s
	  • Scan platform slewing (no expendable mass required)
	• Very low control/structure interaction, very low instability risk
	• Very smooth proportional control

• DISADVANTAGES	• DISADVANTAGES

• Life & reliability, leak problem in long missions
• Potential instability problem
• Potential high mass expenditures during scan slewing
• Will require high contingency mass, all heavily impacted by uncertainties such as
  • Structural vibrations/control interactions
  • CM/CP uncertainties (1° misalignment in SA, deployment can increase amount of gas used to offset SP by 100%)
• Will not know real performance and consumption until after launch. Real performance may be off from predictions 100% or more
• Very likely to require extensive in-flight fixes and reprogramming (impact on mission operations difficulties)
	• Requires backup control method for
	  • Momentum dumping when wheels saturate
	  • Control of large disturbances such as initial rate reduction after IUS separation

1.4 PROPOSAL FOR AN ALTERNATE CONTROL METHOD

The purpose of this study has been to evaluate the 3 proposed A/C methods, and not to generate new candidates. In the process of this evaluation, however, we have gained a considerable amount of new information which suggests that all of the objectionable drawbacks associated with a single gas jet or reaction wheel system, may be eliminated if we judiciously incorporate both of them into the design. Table 1-1 presents a summary of advantages and disadvantages for individual RCS and reaction wheel systems.

After examining Table 1-1 in detail, it becomes clear that neither a Gas Jet RCS, nor a Reaction Wheel (RWH) system by itself will meet all non-powered flight A/C requirements in a satisfactory manner, nor will provide a reliable, low risk, control method.

The following combination of both may provide an acceptable solution by taking the best from each method:

1. Use Reaction Wheels for normal cruise momentum management and maneuvering. (This provides smooth and reliable control and considerable mass savings for turns and slewing.)
2. Use a much smaller RCS system to provide high control reserve needed to handle initial rate reduction and emergency situations, as well as to unload RWH when saturated. (This provides the reserve when needed.)

The following additional option may improve SEPS A/C problems substantially at very minor cost:

3. Provide a center of mass/center of solar pressure trim by including a capability of realigning solar array axes (2 to 3°). This will
   - eliminate gas needed to offset solar pressure torques
   - maintain wheels at lower speed improving their life and reliability

- eliminate almost entirely the need for wheel momentum dumping
- allow possibility of correction for SA deployment misalignments
- enhance multimission applicability

A possible mechanization[3] for achieving this vehicle turn capability is shown in Figures 1-3 and 1-4.

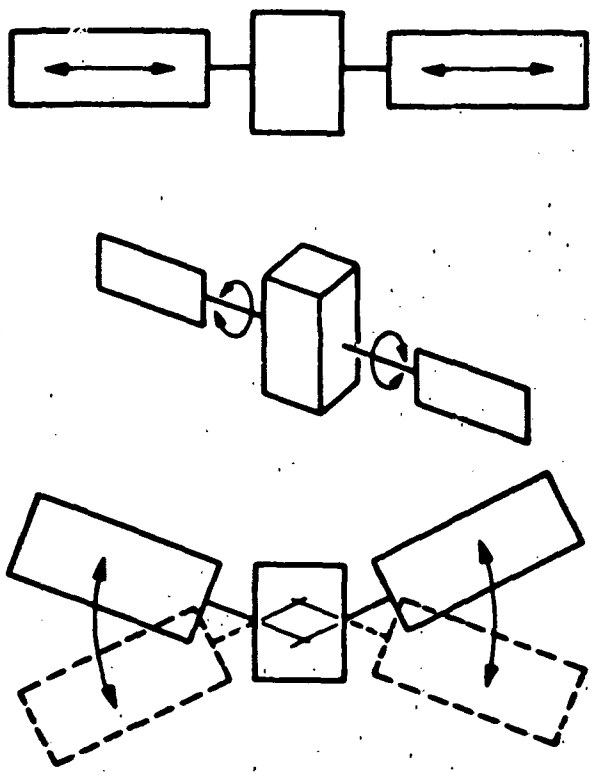

Figure 1-3. CM/CP Trim Concept

[3] Cork, M.J., et al., "Planetary Mission Requirements, Technologies and Design Considerations for a Solar Electric Propulsion Stage," AIAA Paper 79-0908, presented at the AIAA Conference on Advanced Technologies for Future Space Systems, Hampton, Virginia, May 8-11, 1979.

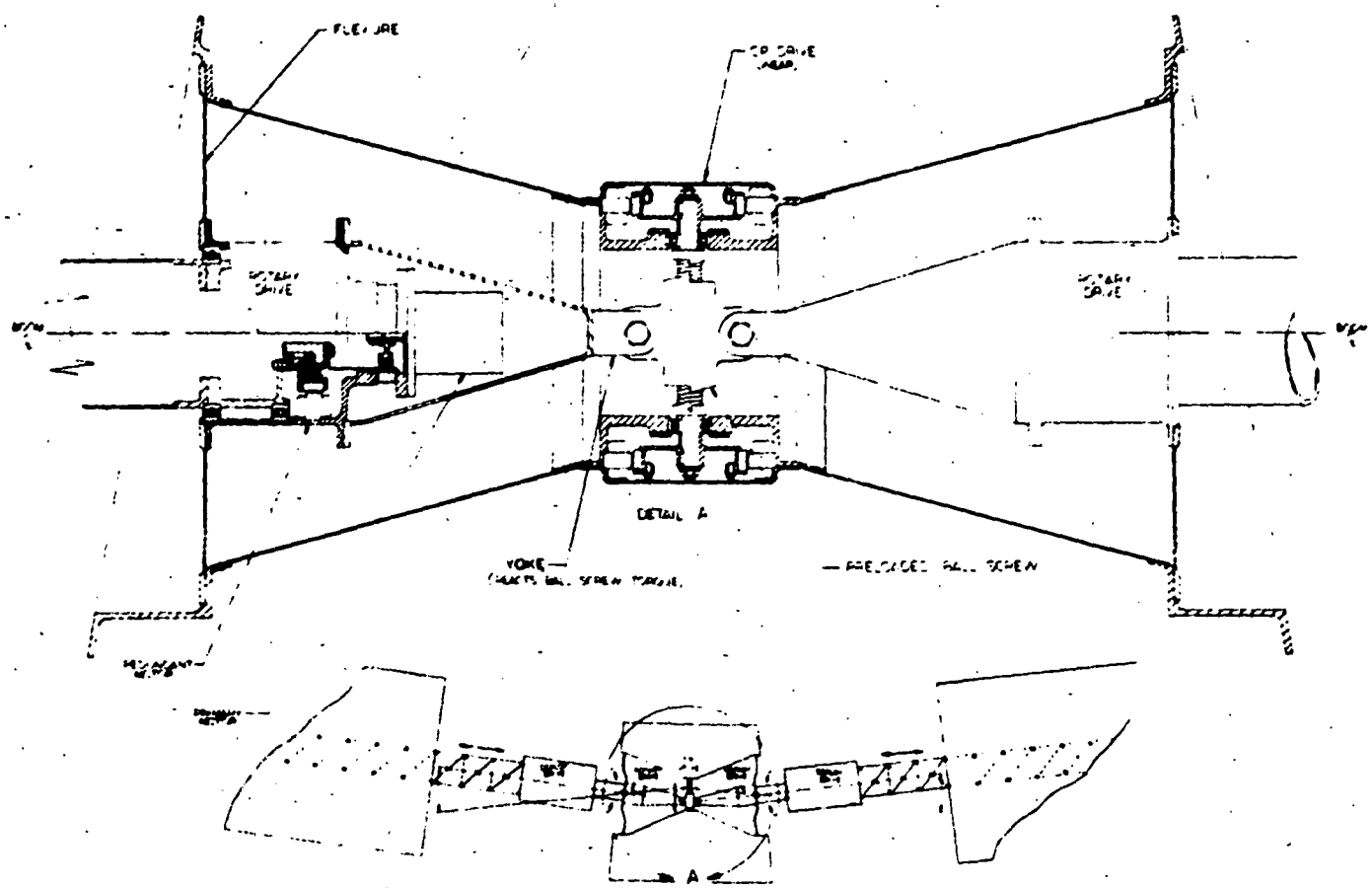

Figure 1-4. Solar Array wing CM/CP trim possible mechanization

SECTION 2

SEPS/ICM DYNAMIC MODELING

In order to evaluate the proposed attitude control schemes, the SEPS/ICM vehicle must be modeled into a form suitable for digital computer simulation. This section presents the assumptions made in this modeling and the abstraction process which takes the vehicle into a dynamic model consisting of a series of hinge-connected rigid bodies with flexible appendages.

The model to be developed here will correspond to vehicle characteristics near the time of rendezvous with comet Tempel 2, since that is the time when gas jets or reaction wheels will provide the primary attitude control. At that time most of the mercury propellant has been spent and the vehicle is significantly lighter than the initially launched mass.

This section is organized as follows:

2.1 SEPS/ICM DESCRIPTION AND ASSUMPTIONS

The SEPS/ICM Vehicle will be assumed to consist of the following components:

1) The SEPS Stage, consisting of 2 articulated flexible Lockheed/MSFC solar array wings plus a rigid SEPS bus (comprising the remainder of SEPS, including the interface adapter, propulsion module, etc.).

2) The ICM spacecraft, consisting of a rigid ICM bus plus an articulated (2 degree-of-freedom) rigid science scan platform (SP), as shown in Figure 2-1.

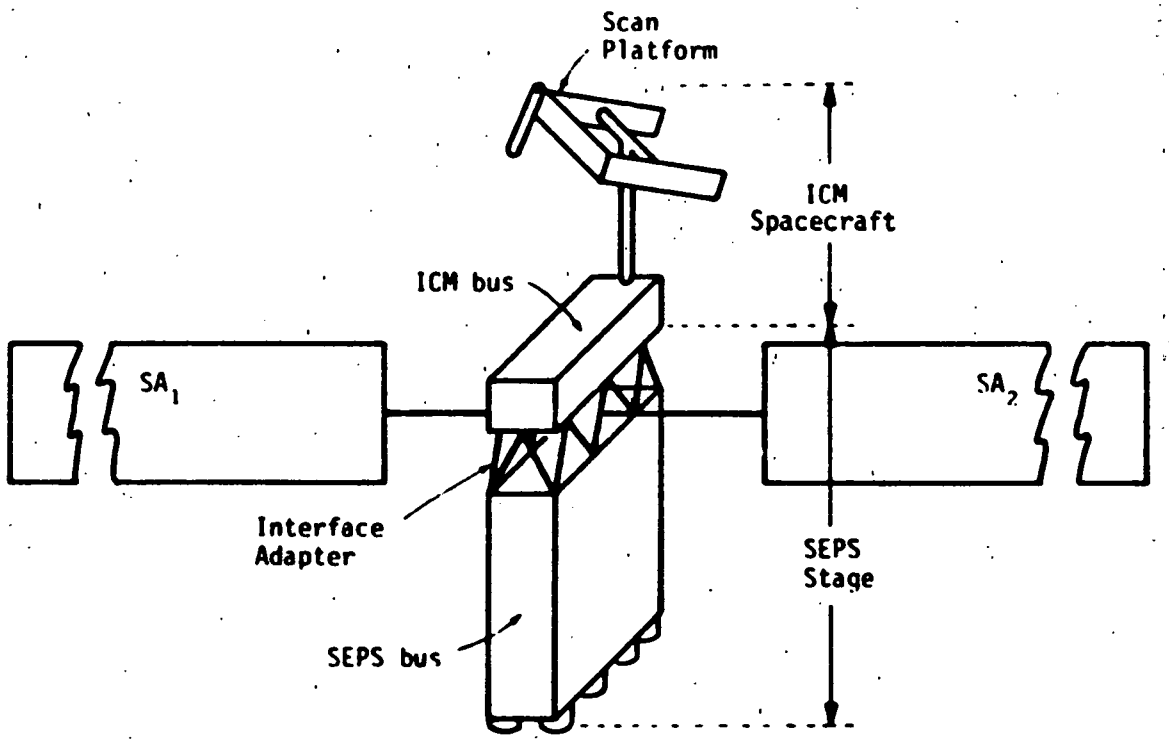

Fig. 2-1. SEPS/ICM Components

For the purposes of this analysis, we will lump the SEPS bus, interface adapter, and ICM bus into one single rigid body b_0 which will, henceforth, be designated as the "vehicle bus" or, simply, "bus". Under these assumptions, the SEPS/ICM vehicle will be modeled as shown in Figure 2-2. The model consists of the following four substructures.

1) A rigid vehicle bus (b_0) (made up of the SEPS bus, interface adapter, and the ICM bus).
2) Two independently articulated flexible Lockheed/MSFC solar arrays. (Flexible model is described in 2.2.)
3) A two-degree-of-freedom articulated Science Scan Platform (SP).

2.1.1 Coordinate Systems

A total of four dextral coordinate systems are necessary to describe the SEPS/ICM as shown in Figure 2-2: one for the bus, one for each solar panel, and one for the scan platform. Throughout this study we will use the following definitions for these coordinate systems.

Bus Coordinate System ($X_B Y_B Z_B$)

The bus coordinate system consists of three mutually perpendicular reference axes embedded in the vehicle bus: bus pitch (X_B), bus yaw (Y_B), and bus roll (Z_B), and is defined as follows: Let the "interface plane" be defined as the imaginary plane formed by the mating surfaces of the SEPS interface adapter with the base of the ICM spacecraft, then

The bus roll axis ($+Z_B$) is the normal to the interface plane passing through the geometric center of the 8 thruster array, with $+Z_B$ in the direction of the exhausting propellant. The intersection of the Z_B axis with the interface plane defines the origin of the bus coordinate system.

The bus pitch axis ($+X_B$) lies in the interface plane and is parallel to the thermal radiator surfaces, with $-X_B$ in the hemisphere containing the scan platform.

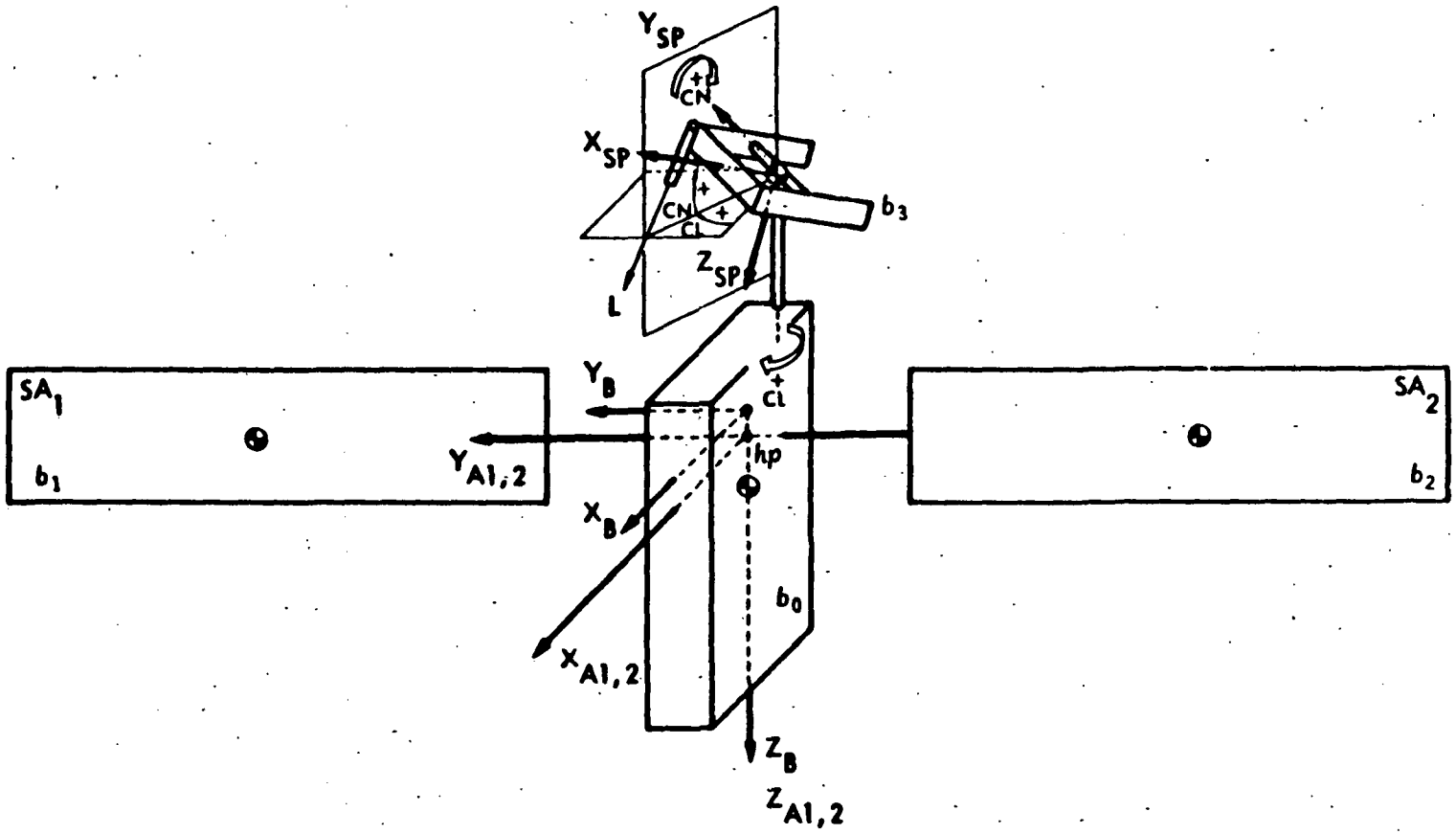

Figure 2-2. SEPS/ICM Model and Coordinates

The bus yaw axis ($+Y_B$) lies in the interface plane and completes the dextral coordinate system.

Solar Array Coordinate Systems ($X_{A1}Y_{A1}Z_{A1}$) and ($X_{A2}Y_{A2}Z_{A2}$)

The solar array panel located in the $+Y_B$ hemisphere (Figure 2-2) will be here designated as "SA_1." Similarly, the $-Y_B$ solar panel will be designated "SA_2." Since each panel will be articulated independently in this study, each of the two solar panels will have a separate coordinate system embedded in it - (X_{A1} Y_{A1} Z_{A1}) and (X_{A2} Y_{A2} Z_{A2}), respectively. Both panels will be articulated about a common hinge line parallel to the Y_B direction but displaced 0.2 m below the interface plane in the $+Z_B$ direction. The point of intersection of the solar array common hinge line and the $+Z_B$ axis will be termed the solar array (SA) hinge point, and its location is (0, 0, +0.2)m in bus coordinates.

The origin of coordinates for (X_{A1} Y_{A1} Z_{A1}) and (X_{A2} Y_{A2} Z_{A2}) is common and will be taken at the "SA hinge point" defined above, with

$+Y_{A1}$ and $+Y_{A2}$ both coincident and parallel to $+Y_B$

$+Z_{A1}$ and $+Z_{A2}$ are defined by the normals to the sensitive (solar cell) sides of the undeformed solar cell blankets

$+X_{A1}$ and $+X_{A2}$ are defined to complete the two dextral systems.

Scan Platform Coordinate Systems (CL CN) and ($X_{SP}Y_{SP}Z_{SP}$)

Two coordinate systems will be useful in the description of the scan platform, which is a two degree of freedom platform articulated by means of "clock" (CL) and "cone" (CN) actuators, as shown in Figure 2-2. The platform coordinates are defined in terms of the look direction L of an imaging instrument mounted on it, as follows

(0° CL, +90° CN) corresponds to L looking in the $+X_B$ direction

(+90° CL, +90° CN) corresponds to L looking in the $+Y_B$ direction.

The $(X_{SP}\ Y_{SP}\ Z_{SP})$ dextral coordinate system has its origin at the intersection of the clock and cone hinge lines and is such that it is parallel to $(X_B\ Y_B\ Z_B)$ when the scan platform is at (0° CL 0° CN).

2.1.2 Assumed Nominal Configuration

Since the solar panels and scan platform orientations relative to the bus change throughout the mission, the SEPS/ICM vehicle exhibits a variable configuration throughout the mission. For the purposes of this study, we have selected a nominal configuration which is defined as shown in Figure 2-3.

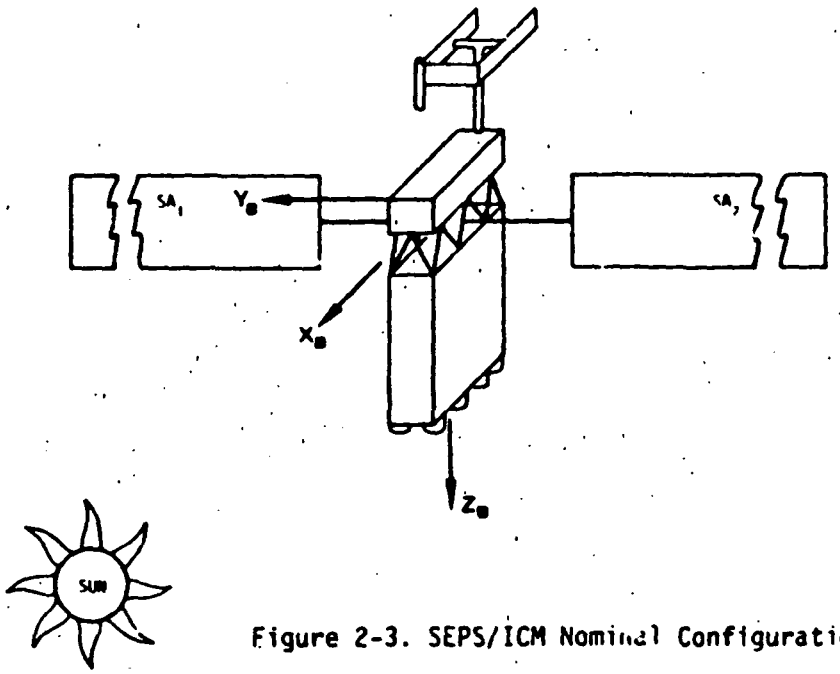

Figure 2-3. SEPS/ICM Nominal Configuration

The selected nominal configuration has the SEPS thrusting normal to the sunline with $+X_B$, $+Z_{A1}$, and $+Z_{A2}$ looking at the sun and the scan platform at (0° CL, 0° CN). The orientation of the Y_B axis in inertial space is arbitrary.

2.1.3 Solar Pressure Disturbance Torques at Tempel 2

Solar pressure disturbance torques can be calculated from

$$T_{dist} = 4.64\ 10^{-6}\ (1+\epsilon)\ \frac{A\ell}{r^2}\ ,\ N\text{-}m$$

where ε = surface reflectivity

A = area, m^2

ℓ = offset between center of pressure and center of mass, m

r = distance from the sun, AU.

Using two 32 x 4 m panels yields $A = 256\ m^2$. Assuming the center of pressure to be at the geometric center of the two solar panels, i.e. at the SA "hinge point" located at (0, 0, +0.2)m in bus coordinates, yields $\ell = 0.3$ m since the vehicle center of mass is at (0, 0, +0.5)m in bus coordinates. Using a reflectivity of $\varepsilon = 0.2$ and an average sun distance r of 1.43 AU at Temple 2, yields

$$T_{dist} = +2.09\ 10^{-4}\ \text{N-m about } Y_B.$$

Solar pressure torques about the other two axes are zero. The effect of this solar pressure disturbance torque is the following:

Thrust Vector Control Mode. Assuming n operating thrusters with a thrust of 0.125 N each, all simultaneously gimballed by an angle α and located in a plane 2.71 m away from the vehicle CM, results in a steady state gimbal angle $\bar{\alpha}$ required to offset the solar torques which can be obtained from

$$0.125\ n\ \ell \sin \bar{\alpha} = 2.09\ 10^{-4}$$

i.e.

$$\bar{\alpha} = \arcsin\left(\frac{2.09\ 10^{-4}}{0.125\ n\ \ell}\right)$$

which gives, with $\ell = 2.71$ m,

$$\bar{\alpha} = \begin{cases} 0.0044 \text{ degrees for } n = 8 \text{ operating thrusters} \\ 0.0176 \text{ degrees for } n = 2 \text{ operating thrusters} \end{cases}$$

for the gimbal angles required to offset solar pressure torques.

Reaction Wheel Control Mode. If we assume the use of a NASA Standard Reaction Wheel (SRW) having a momentum storage capacity of 20 N-m-s @ 2200 rpm, the Y-axis SRW will speed up continuously from 0 rpm to saturation (2200 rpm) in a time T given by

$$T = \frac{20}{2.09\ 10^{-4}} = 95693 \text{ seconds},$$

that is, the Y-axis SRW will saturate in 26.58 hours due to solar pressure, at which time it must be unloaded. Note that the only way to reduce the frequency of unloadings is to reduce the center of mass to center of pressure offset by bringing the two closer together.

Reaction Control System Mode. In a 24 hr. period the gas jets must overcome a one sided solar pressure torque producing a total angular impulse of

$$H = 2.09\ 10^{-4} \times 24 \times 60 \times 60 = 18.0576\ \text{N-m-s}$$

If we assume that the gas jets - center of mass lever arm is $\ell = 2.71$ m, the mass consumed to offset the solar pressure can be computed from

$$m = \frac{1000}{9.81\ I_{sp}} \frac{H}{\ell} = 9.06\ \text{gr/day}$$

where we have used $I_{sp} = 75$ sec (N_e gas). Note that the only way to reduce this consumption is to bring the centers of mass and pressure closer together.

2.1.4 Mass Properties

The total vehicle mass properties assumed in this study are as follows:

Total mass	2200.3 kg
CM location in $(X_B Y_B Z_B)$ coordinates	(0, 0, +0.5)m
Self inertia matrix in nominal configuration	$\begin{bmatrix} 179000. & 0. & -60. \\ 0. & 3500. & 0. \\ -60. & 0. & 178500. \end{bmatrix}$ kg-m^2

The mass breakdown for each component is as shown in Table 2-1.

The solar arrays are assumed to be connected to the bus through a 1 dof line hinge located at (0, 0, +0.2) m in bus coordinates. The scan platform is connected to the bus through a 2 dof hinge located at (-1.3691, -0.37, -0.7893)m in bus coordinates; this implies that the center of mass of the scan platform is located coincident with the intersection point of its two hinges.

TABLE 2-1. SEPS/ICM Mass Properties (Nominal Configuration)

Mass, kg	CM Location[1] (X,Y,Z), m	Self-inertia Matrix[2] kg-m²		
BUS b_0				
	+0.0703	1824.304	+50.133	+114.634
1756.474	+0.0190	+50.133	2635.642	+46.249
	+0.6266	+114.634	+46.249	1769.269
SCAN PLATFORM b_3				
	-1.3691	13.300	-2.100	+0.200
90.190	-0.3700	-2.100	7.500	+1.000
	-0.7893	+0.200	+1.000	16.500
+ Y SOLAR ARRAY b_1				
	0.0000	22084.000	-158.020	0.0
176.818	+19.3764	-158.020	234.610	0.0
	+ 0.2000	0.0	0.0	21876.000
-Y SOLAR ARRAY b_2				
	0.0000	22084.000	+158.020	0.0
176.818	-19.3764	+158.020	234.610	0.0
	+ 0.2000	0.0	0.0	21876.000
TOTAL VEHICLE				
	0.0000	179000.000	0.000	-60.000
2200.3	0.0000	0.000	3500.000	0.000
	+0.5000	-60.000	0.000	178500.000

(1) referenced to (X_B Y_B Z_B) system

(2) reference to a coordinate system parallel to (X_B Y_B Z_B) but centered at the center of mass of each structure

2.2 LOCKHEED/MSFC SOLAR ARRAY FLEXIBLE MODEL

This subsection describes the hybrid modal model used to represent the flexible solar arrays in the computer simulations performed in this study. The hybrid-mode approach [4] is a cross between the free-free approach and the cantilever mode approach in that the rigid base of each solar array wing is considered free in translation but fixed in rotation. For the translational equations of each array, the free rigid base includes the mass of the remainder of the vehicle (as if it were rigid, including the other solar array wing).

A hybrid modal model of each array was generated [5] using the finite element discrete model shown in Figure 2-4. This figure shows the +Y solar panel (SA_1) in the cruise configuration, attached to the vehicle bus at node 1 through a rigid link RL. The mass of the rest of the vehicle was lumped at that node, which in turn was connected to the center of mass of the panel by a massless rigid link. Node 1 was allowed to have translational motion only, the rotational degrees of freedom being set to zero. Both pre-stressed membrane and line elements have been used for the discretization. The associated geometrical stiffness matrices K_G for the solar panel membrane elements were derived by applying pre-stressing along the length of the panel (Y direction), while restraining the two longitudinal edges ($Z = \pm 2$ meters) from any possible lateral movement. Such a measure was necessary to prevent any numerical instability caused by the Poisson's ratio effect, resulting in small or negative diagonal elements in the geometrical stiffness matrix terms pertaining to the lateral (Z direction) motion of the panel. The program EISI/SPAR utilized for the analysis was then found to be effective for the solution of the problem, although the frequency values obtained are slightly higher than expected.

---

[4] Likins, P.W., Dynamics and Control of Flexible Space Vehicles, Technical Report 32-1329, Jet Propulsion Laboratory, Pasadena, Calif., Jan. 15, 1970

[5] Gupta, K.K., SEPS Solar Array Panel Natural Frequency Analysis, Interoffice Memorandum 3545:79:167, Jet Propulsion Laboratory, Pasadena, Calif., May 30, 1979 (JPL internal document).

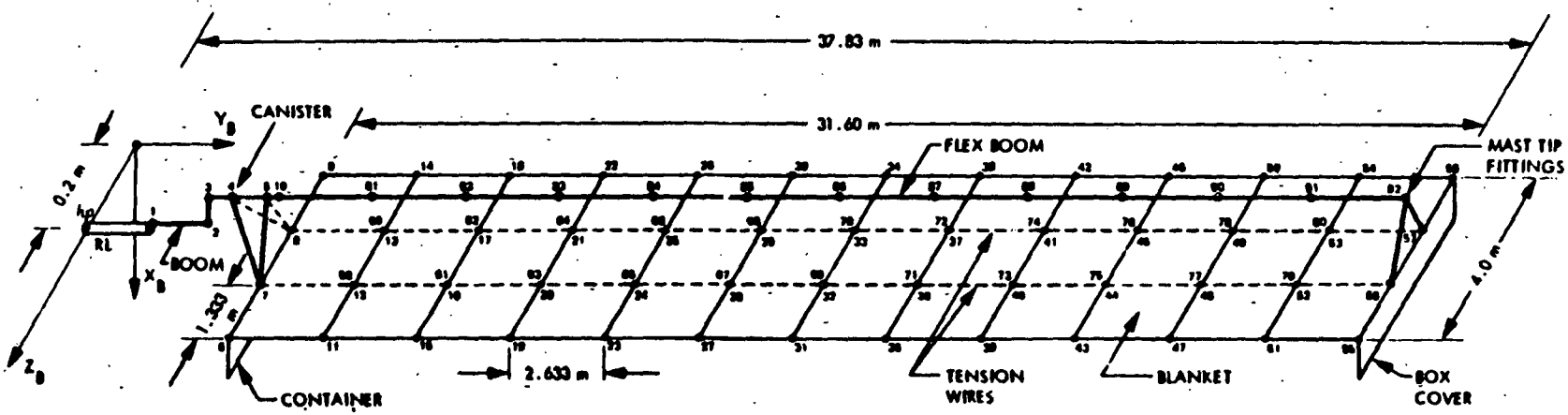

NOTE: TENSION EACH WIRE, 4.45 N (1 lb)
BLANKET TENSION, 88.9 N (20 lb)

Figure 2-4. SA_1 Finite Element Model

The mass breakdown assumed for solar array wing is given in Table 2-2. This model has blanket dimensions of 4.0 x 31.6 meters with a total wing structure length of 35.0 m from node 1 to node 92, and a center of mass for the wing located at

(+0.1242, +16.5474, 0.0) meters

Table 2-2. Mass Summary - Solar Array

Item	kg	lb
Flexible boom	18.05	39.80
Canister	18.73	41.29
Container	11.62	25.62
Position boom	3.18	7.01
Blanket*	115.83	255.36
Box cover	8.57	18.89
Tip fitting (Mast)	0.84	1.85
TOTAL	176.82	389.82

*Array Guidance Mechanism and Tension Mechanism were assumed to be uniformly distributed along blanket.

with respect to node 1. The rigid link RL is used to connect node 1 to the SA hinge point *hp* (0, 0, +0.2) so that the total length from *hp* to the SA_1 wing tip increases to 37.829 m and the center of mass of the SA_1 structure is positioned at

(0., +19.3764, 0.) m with respect to *hp*.

This places the CM of the SA's on the hinge line. The resulting hybrid modal data for SA_1 is given in Table 2-3 which lists the frequency and the rigid elastic coupling coefficients. The corresponding mode shapes (eigenvectors) are shown in Figure 2-5. The data for SA_2 was obtained by rotating the rigid elastic coupling coefficients and the mode shapes by a 180° rotation about a line parallel to X_B passing through *hp*. This simply changes the sign of the Y and Z translations and rotations.

TABLE 2-3. Lockheed/MSFC SA Hybrid Model Data (2200.3 kg vehicle)

Mode No.	Type*	Frequency, Hz	Rigid-elastic Coupling Coefficients μ_x, $kg^{\frac{1}{2}}$	μ_y	μ_z	δ_x, $kg^{\frac{1}{2}}m$	δ_y	δ_z
1	OPB	0.065226	-11.18700	.06995	-.04629	-.55239	.03969	68.5260
2	OPB	0.126145	-.51909	-.09919	.08782	1.02460	-.04128	-88.9900
3	OPB	0.192507	-3.13980	.08922	-.19752	-2.21670	.03269	-8.5395
4	IPB	0.226612	-.13282	-.01158	9.57620	104.93000	-.65980	.7618
5	OPB	0.261074	.80208	.06203	.11783	1.25900	.04004	25.2850
6	OPB	0.329296	1.66380	-.04164	-.02503	-.24815	-1.37720	10.3960
7	T	0.333713	.15877	-.00148	.00885	.05069	12.17000	1.1211
8	T	0.351529	.06603	.00457	.01928	.11299	.13019	.5457
9	T	0.378027	.07672	.00979	.02564	.13027	9.03850	1.1520
10	OPB	0.393748	.54915	.02260	.00615	.06512	-.07812	11.2490
11	T	0.410395	-.07393	.00837	.02850	.10434	.26855	-1.5188
12	T	0.443883	-.23045	.01450	.03038	.08424	2.25460	-2.3978
13	OPB+T	0.453118	.81469	-.00625	.00957	.03618	.87656	7.3644
14	OPB+T	0.478315	-.11917	-.01331	-.03352	-.05150	-.33515	-1.1371
15	OPB	0.501820	.29823	.00182	.00037	.00137	.23342	5.3599

*OPB=OUT OF PLANE BENDING
IPB=IN PLANE BENDING
T =TORSION

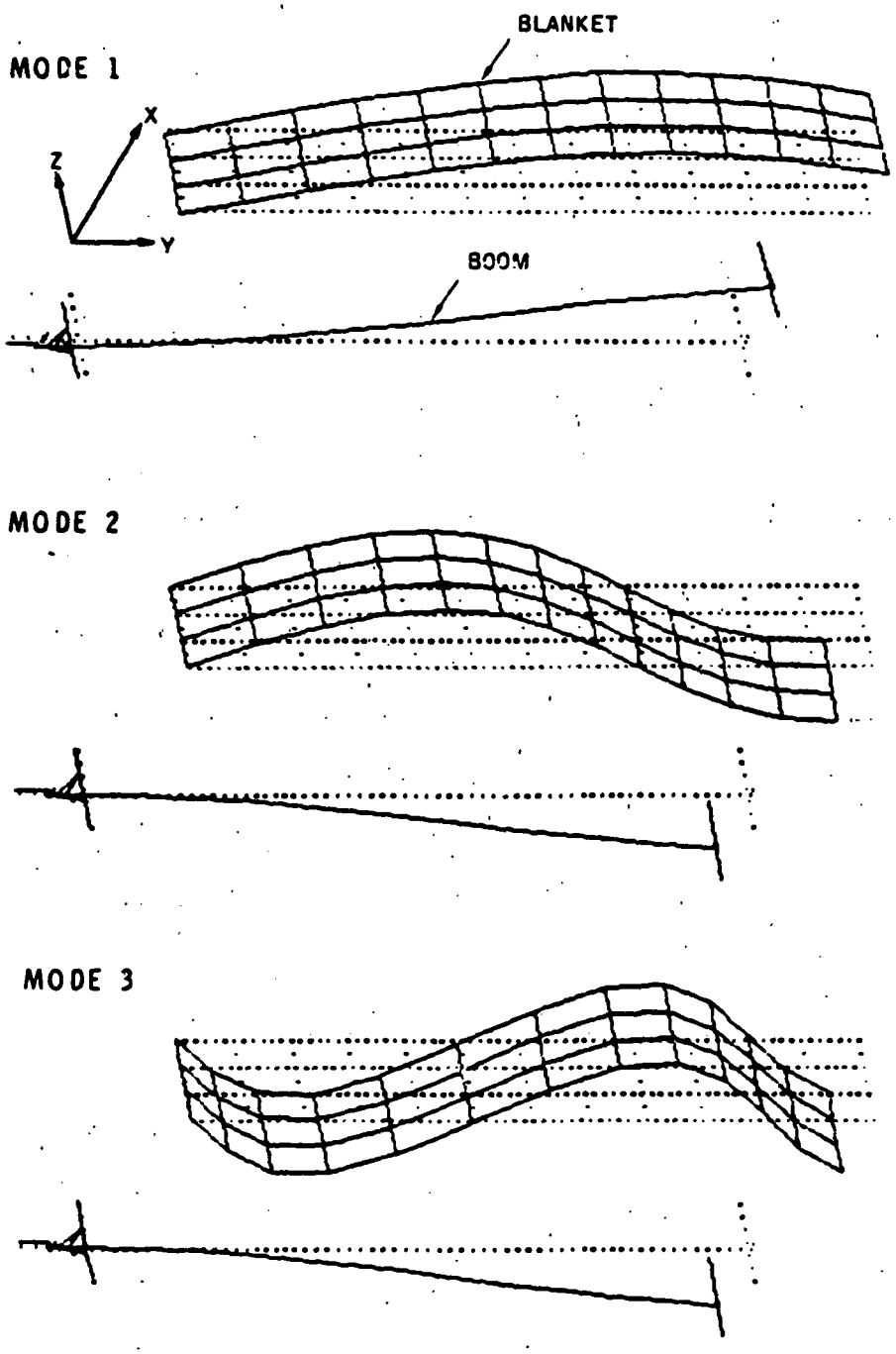

Figure 2-5. Solar Array Eigenvectors (Mode-shapes) - Exploded View
(Motion of blanket and boom not to same scale)

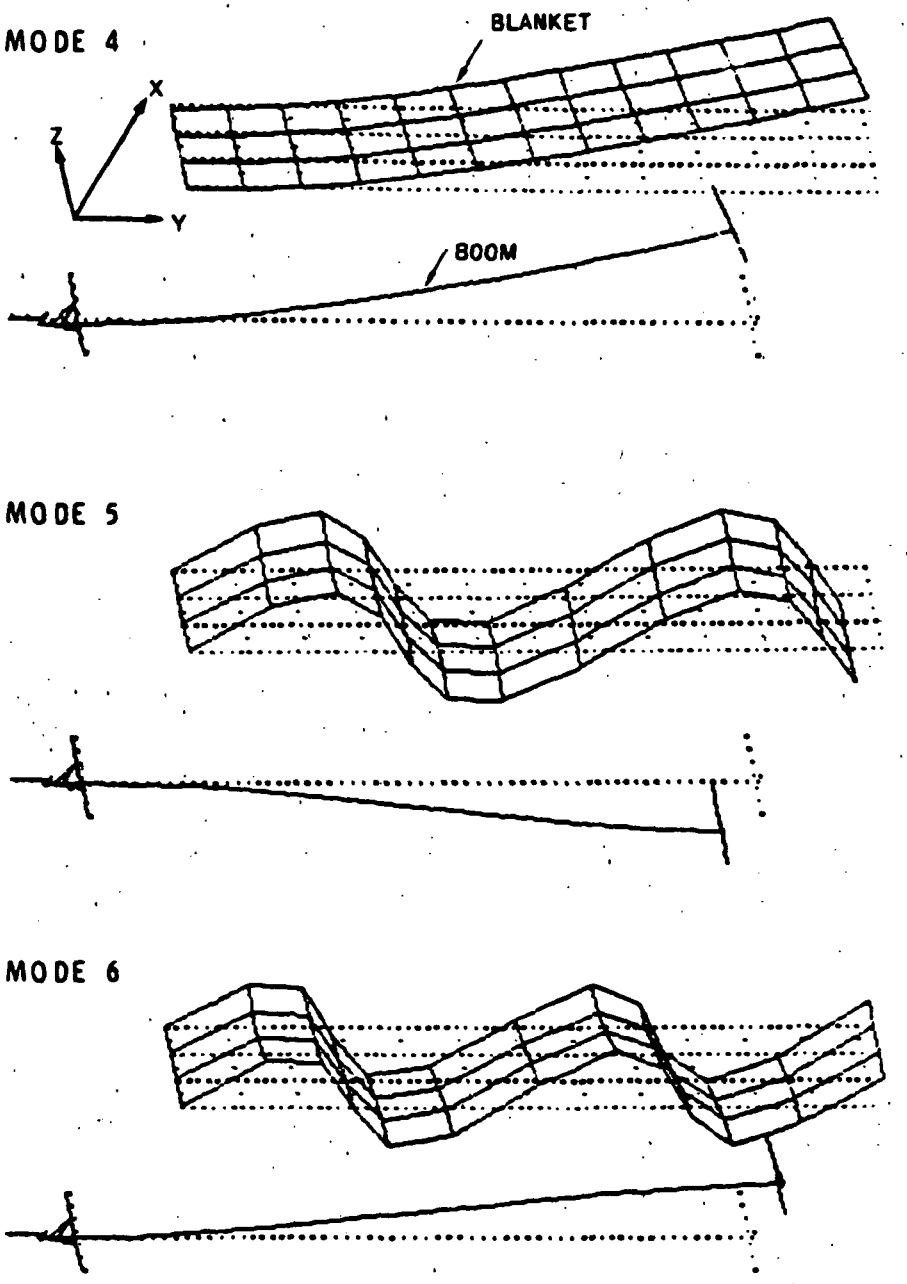

Figure 2-5 (contd)

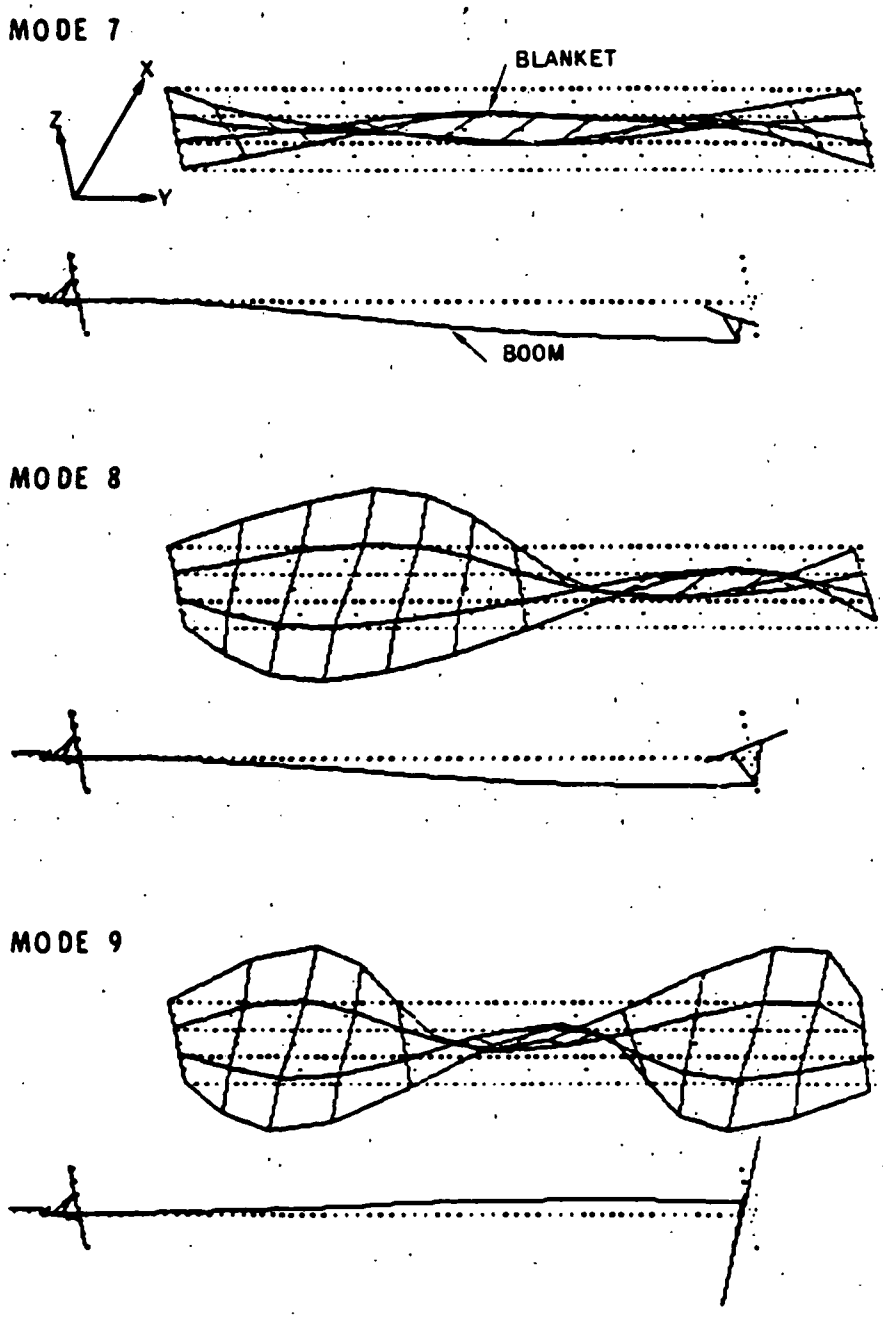

Figure 2-5 (contd)

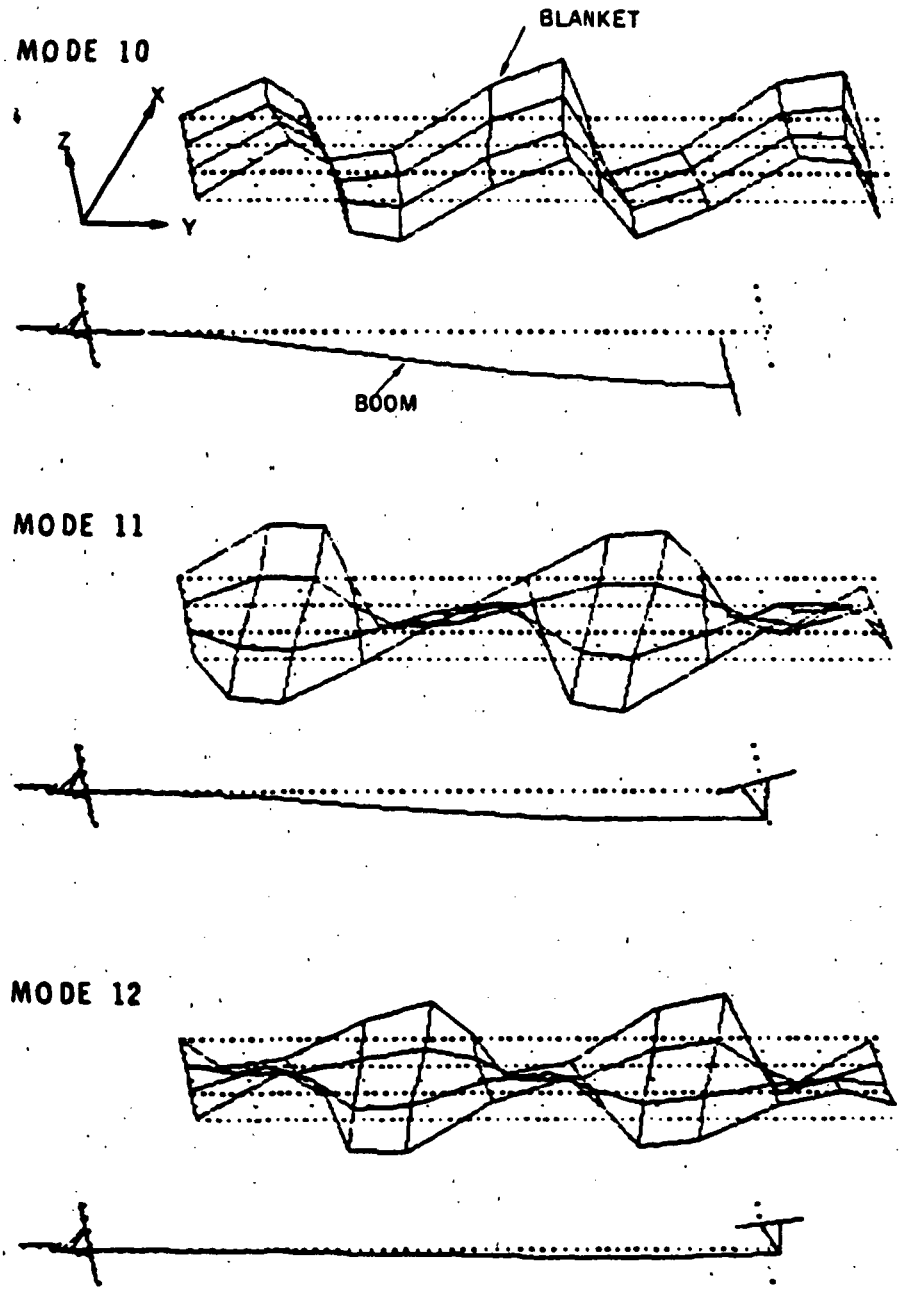

Figure 2-5 (contd)

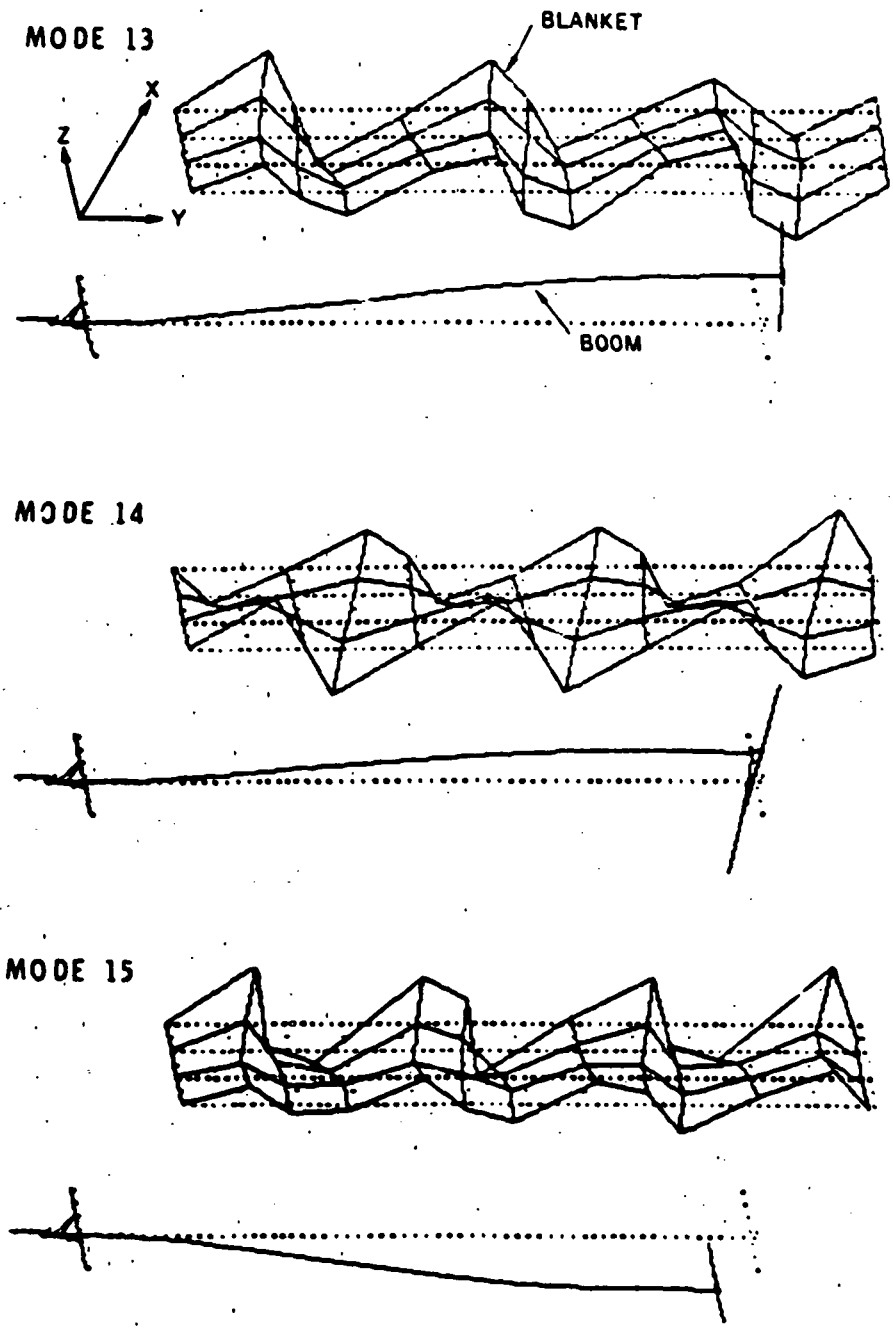

Figure 2-5 (contd)

2.3 SOLAR ARRAY AND SCAN PLATFORM ARTICULATION AND CONTROL

Each wing of the solar array is assumed to be independently articulated about Y_{A1} and Y_{A2} by means of independent actuators. The details on the various actuator characteristics and control schemes for the SA considered in this study can be found in subsections 3.2.4, 4.2, 4.3, and 5.3.3.

The scan platform model and control method, on the other hand, have been constant throughout this stud and will be described here.

Each of the two SP axes (CL and CN) will be controlled by the simple scheme shown in Figure 2-6.

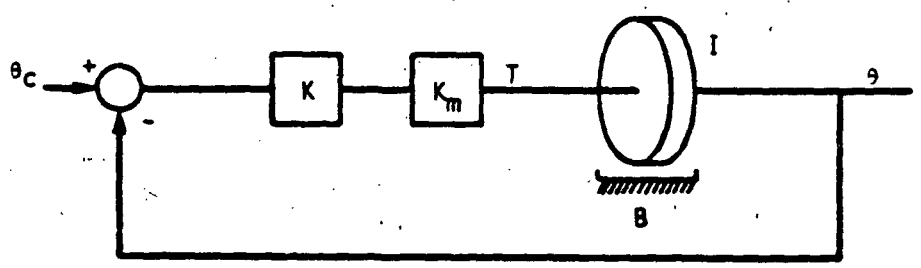

Figure 2-6. Scan Platform Block Diagram

The torque on the scan platform is given by

$$T = -\bar{K}(\theta - \theta_c) - B\dot{\theta}$$

where $\bar{K} = K K_m$.

Such a block diagram can be thought to arise from an actuator drive mechanism having control gain K, motor torque constant K_m, and a viscous damper at the output shaft having a damping constant of B N-m per rad/s.

The pertinent constants are:

	CL	CN	
I	16.5	7.5	kg-m²
$\bar{K}$	1500	1500	N-m/rad
B	220.25	148.50	N-m-s/rad

The high value of $\bar{K}$ is typical of scan platforms flown on earlier missions (Viking, Voyager, etc.) and is required to meet pointing accuracy requirements in the presence of frictional forces, although such forces have been neglected in this study. The choices for B provide 0.7 damping. With these values, the natural frequencies for the scan platform are

$$\omega_{CL} = 9.53 \text{ rad/s} \qquad \xi_{CL} = 0.7$$

$$\omega_{CN} = 14.14 \text{ rad/s} \qquad \xi_{CN} = 0.7$$

2.4 DESCRIPTION OF TEST MANEUVERS

In this study, we will use the following four (typical) maneuvers for evaluation of the control schemes:

i) X TURN: Starting with the vehicle in the nominal configuration of Figure 2-3, the complete vehicle is commanded to turn about the sun line (pitch). The command is a position ramp with a slope of 0.005°/s. The solar arrays are commanded to hold their position relative to the bus.

ii) BUS YAW TURN. The vehicle is commanded to turn about Y_B, while the solar arrays are commanded to remain pointed at the sun, as the bus moves. The command to the bus is a position ramp with a slope of 0.25°/s.

iii) MULTIAXIS ACQUISITION. The attitude control system is enabled at a time when the vehicle has the following initial position errors and rates:

Axis	Initial Position Error	Initial Rate
pitch	+1.0°	+0.005°/s
yaw	+2.0°	+0.250°/s
roll	0.0°	-0.005°/s

iv) SCAN SLEWING. The dynamic disturbance caused by scan platform slewing depends on many factors such as the geometry and mass properties of the platform and vehicle, the size and direction of the slew, the slew rate, and the initial clock and cone orientation of the platform before slewing. In particular, these factors determine the angular rates and momentum imparted by the slew and which must be controlled and absorbed by the attitude control system - whether it is based on reaction wheels, thrust vector gimballing, or on a gas jet system.

Since it is impossible to study all possible sets of scan slewing conditions, we have assumed a slew test sequence. This is a 9°x2° box or raster type slew, at 1°/s. It consists of four 9°-clock slews interspersed with four 2°-cone slews and 2 second wait periods in between each slew; this 8 slew sequence takes 58 seconds to complete. For a graphical description of the sequence, the reader is referred to figure 3-14 v), in the next section.

2.5 COMPUTER SIMULATION PROGRAMS

Three separate flexible dynamics simulation programs were developed, named "TVC," "RCS," and "RWH." The programs are tailored to simulate each of the three control systems considered in this study: thrust vector control (TVC), gas jets (GAS), and reaction wheels (RWH). Each program incorporates the corresponding control system and hardware models described in Sections 3, 4, and 5.

The three simulation programs have several similarities such as the use of a powerful subroutine called FBDYFL. This hybrid-mode subroutine written by Fleischer and Likins [6] solves the equations of rotational motion for a system of hinge-connected rigid bodies with

[6] Fleischer, G.E., and Likins, P.W., Attitude Dynamics Simulation Subroutines for Systems of Hinge-Connected Rigid Bodies with Nonrigid Appendages, Technical Report 32-1598, JPL, Pasadena, CA, Aug. 15, 1975.

flexible appendages. For inputs, the subroutine uses the mass properties and vehicle configuration described in 2.1, as well as the hybrid SA model of 2.2. Each SA panel was modeled by its first 15 hybrid modes and corresponding frequencies, yielding a 30-mode flexible model for the complete SEPS/ICM vehicle.

The simulation programs were all written in the "Continuous System Simulation Language" (CSSL III). As the name implies that language is used to digitally simulate continuous systems. A complete listing of the three programs appear in appendices A (TVC), B (GAS), and C (RWH). The four maneuvers simulated by each program were described in 2.4, and the results of each are given in sections 3 (TVC), 4 (GAS), and 5 (RWH).

SECTION 3

THRUST VECTOR CONTROL

The thrust vector control "TVC" system is a three axis active controller to be used for vehicle control during powered flight. The TVC system utilizes the ion engines to generate vehicle control torques. This is accomplished by gimbaling each engine on a two degree of freedom gimbal. Because of the low thrust provided by the ion engines the control torques are in general small. This coupled with the fact that the vehicle has large rotational inertias results in slow response and lengthy maneuver times. With suitable control laws though, these small control torques provide very smooth vehicle maneuvering and minimal excitation of the vehicle's flexible solar panels.

This section will discuss the TVC attitude control system for the SEPS/ICM vehicle. The performance of this system is also detailed and evaluated. The section is organized as follows:

3.1 DESCRIPTION OF THE TVC HARDWARE

The SEPS/ICM vehicle will use a thrust vector control system for attitude control during powered flight.

The proposed TVC hardware configuration is shown in Figure 3-1. Thrust is provided by eight 30 centimeter mercury ion engines. In this study we have assumed that all eight engines are on and at full thrust, yielding a sum total thrust force F_c = 1 Newton. Vehicle control is accomplished by gimbaling each engine on its own 2 degree of freedom set of gimbals, as shown in Figure 3-2. Each set of gimbals is assumed to have two actuators and two sensors.

Since each engine is gimbaled individually, it is possible to control each engine independently of the others by issuing a total of 8 gimbal angle command pairs. This approach leads to complex control logic. In an effort to reduce this complexity, it is desirable to design a system which issues the same commands to as many thrusters as possible. In this study we have made use of a scheme which reduces the number of different gimbal angle command pairs to the minimum, which is two pairs. This is done as follows. In reference to Figure 3-1, let the four engines labeled 1, 2, 3, and 4 be known collectively as Engine Bank #1 or, simply, Bank 1. Similarly, engines 5, 6, 7, and 8 become Bank 2. We will assume that all eight engines, gimbal hardware, controllers and associated sensors and actuators are identical. Then, it is possible to control the vehicle attitude by simply issuing two pairs of command gimbal angles $(\alpha_{c1}, \beta_{c1})$ and $(\alpha_{c2}, \beta_{c2})$ to the engines in Bank 1 and Bank 2, respectively. Since all four engines in each Bank receive the same command pair and since the controllers and hardware are identical, all four engines in each bank will move simultaneously and undistinguishably from each other - as a bank indeed.

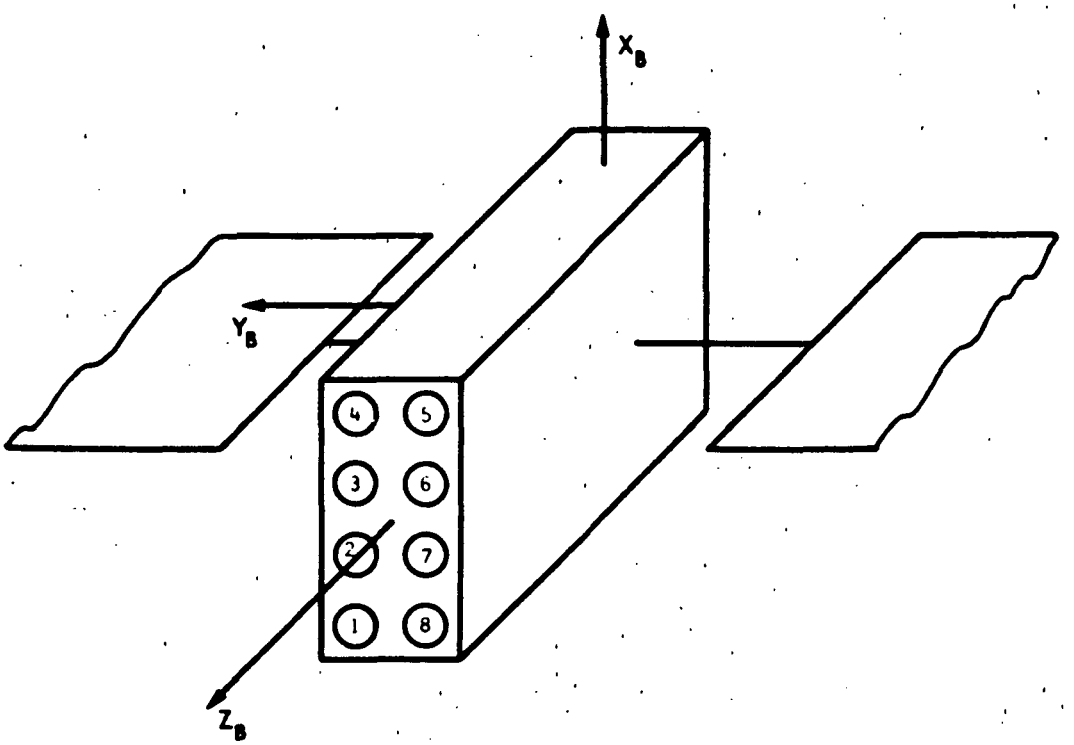

Figure 3-1. Location of the Ion Engines

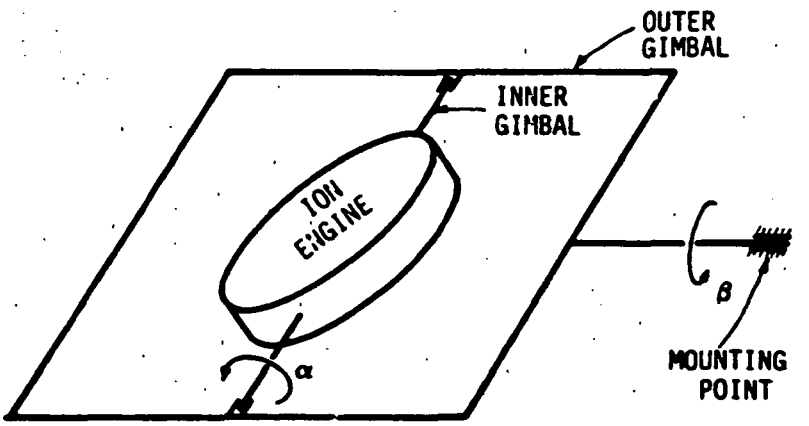

Figure 3-2. 2 dof Gimbaled Engine

3.2 TVC LEAD-LAG CONTROL SYSTEM

A very simplified schematic of the TVC control system used in this study is shown in Figure 3-3. This schematic illustrates the basic control loop configuration which was provided to JPL by MSFC for analysis and evaluation.*

The proposed controller is of the "lead-lag" type and it achieves three-axis control as follows. The position error e is obtained by subtracting the (celestial sensor) position θ_s from the commanded position θ_c. The position error is then filtered. This filter is included to provide some isolation of the loop from the higher frequency gimbal dynamics which might be sensed and fed back through the celestial sensor. The output of the filter e_f is then put through a lead-lag compensating network to derive the control error e_c. The lead-lag network $\frac{\tau_1 s+1}{\tau_2 s+1}$ can be thought to consist of a filter $(\tau_2 s+1)^{-1}$ yielding a "doubly filtered position error signal" e_{ff} followed by a "signal plus derivative" compensator $1+\tau_1 s$ so that e_c can be thought of as the "position plus rate" of the twice-filtered position error e_{ff}. The control error e_c is then multiplied by a gain K to obtain γ_c, the "thrust vector (TV) command angle." The three TV command angles (one per axis) are then fed into a "Gimbal Angle Commander" black box which generates two pairs of gimbal angle commands (α_{c1},β_{c1}) and (α_{c2},β_{c2}) for each of the two banks of engines. Each engine has two controller subloops (one per gimbal) and associated actuators and sensors to move the gimbals to the commanded angular positions, thus, as the engine banks move, control torques are applied to the vehicle, as indicated by the "force and torque" block, which cause the desired attitude control.

We shall explain next how the control torques are obtained from the γ_c's by describing in detail the 3 black boxes labeled "Gimbal Angle Commander," "Gimbal Control Subloops," and "Force and Torques."

---

*A complete block diagram is shown in Figure 3-10, page 3-18.

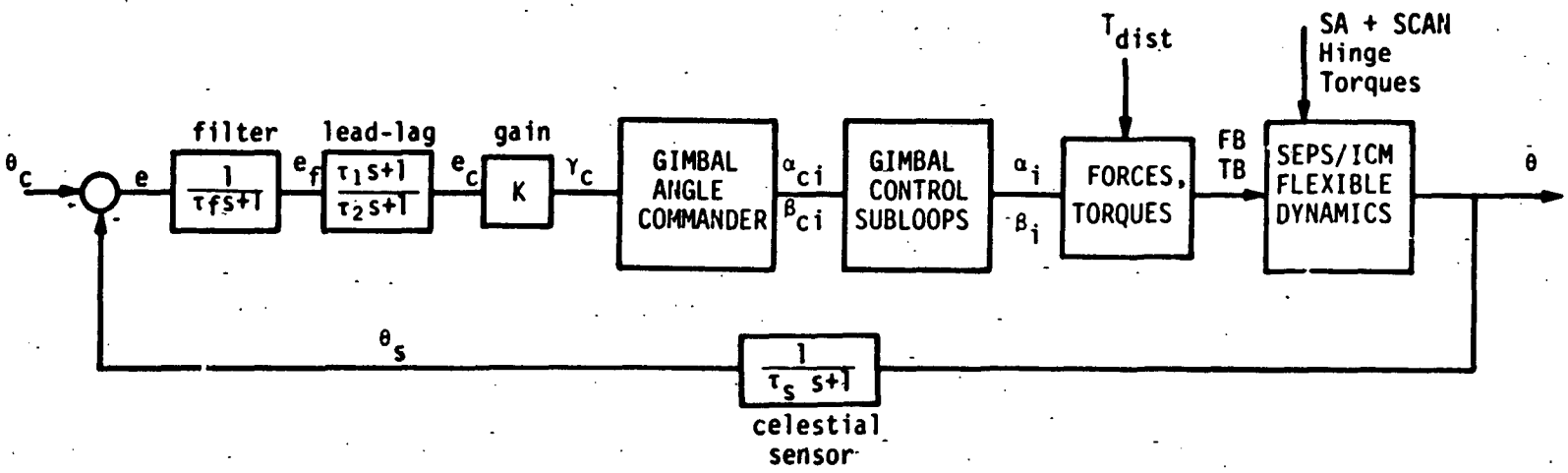

Figure 3-3. Simplified TVC System Schematic

3.2.1 Gimbal Angle Commander

As we have described earlier, we made the decision to gimbal the 8 engines as two banks of 4, called Bank 1 and Bank 2, because of its attractive simplicity. As it turns out, such gimbaling philosophy results in even further simplification of the analysis, since the resultant thrust of the four engines in, say, Bank 1 can be thought as arising from an imaginary "Equivalent Engine (EE) 1" having a thrust of 0.5 N, i.e., 4 times that of a single thruster (f = 0.125 N), and located at the geometric center of the Bank 1 thruster pattern. Similarly, "Equivalent Engine (EE) 2" arises from Bank 2 and has analogous characteristics. This simplification is shown in Figure 3-4.

Also shown in Figure 3-4 are the coordinate frames and gimbal angle conventions used for each bank. Note that the frames for EE1 and EE2 are related to each other through a 180° rotation about Z_B.

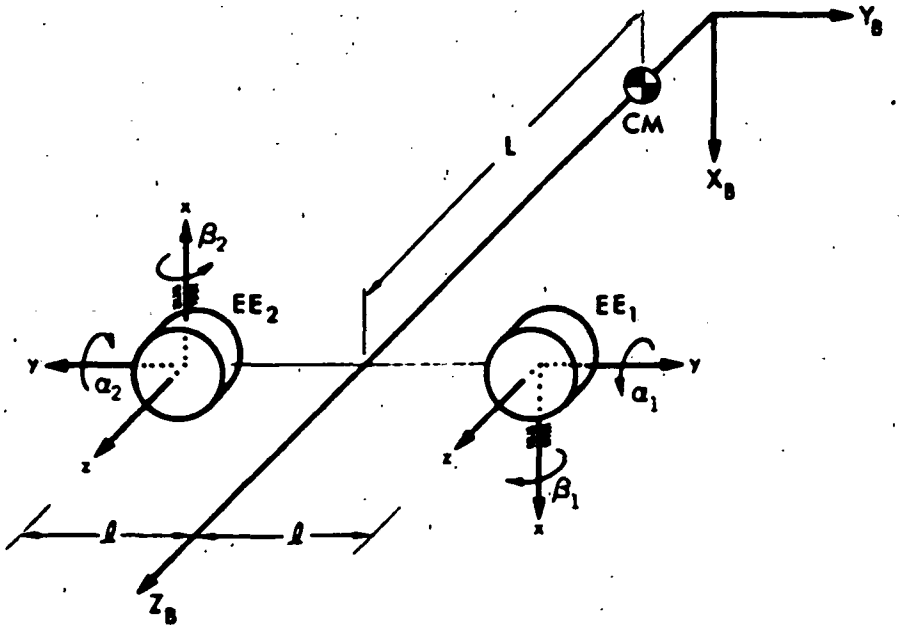

Figure 3-4. Bank Gimbaling Conventions

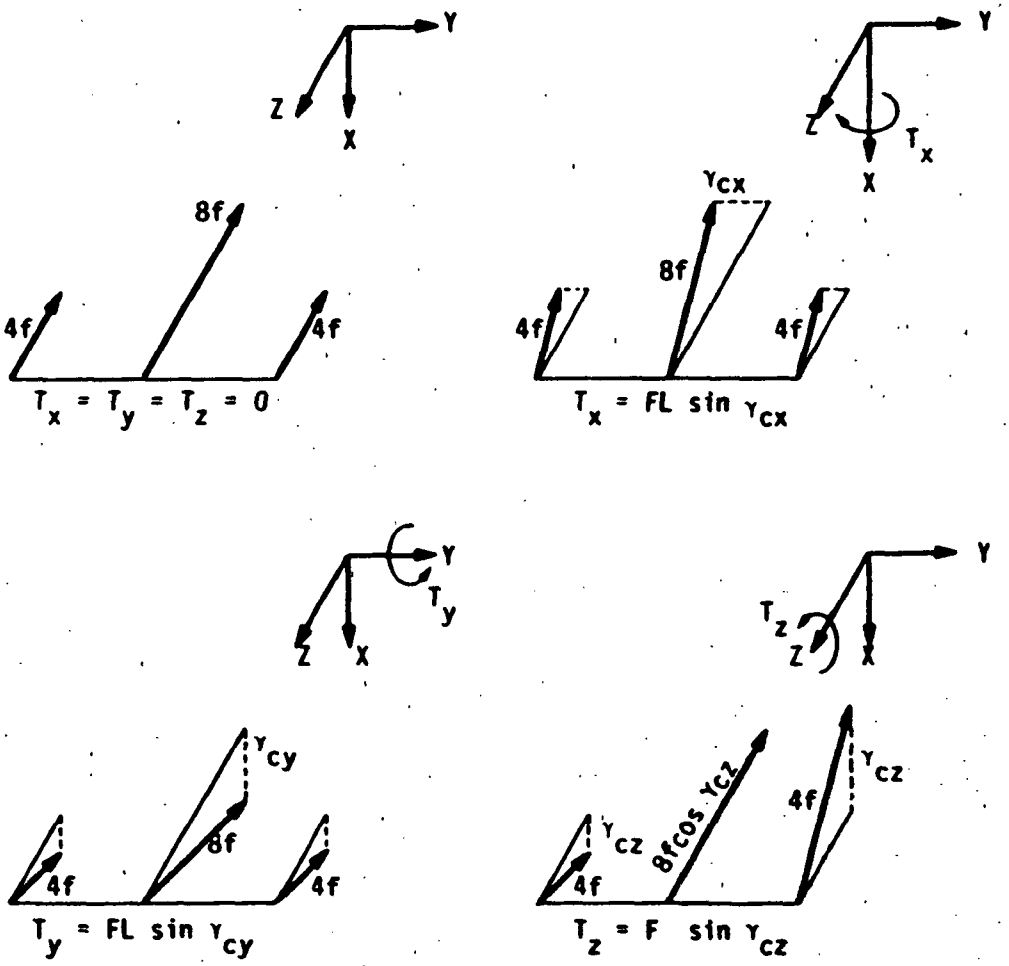

Figure 3-5. Method of Obtaining Pure Positive Torques about each of the 3 axes

Figure 3-5 shows how the gimbals can be moved to produce pure torques about each axis. Thus, if we wish to obtain a positive control torque about X we can command a positive TV control angle γ_{cx} by gimbaling banks 1 and 2 by that angle, as shown. The resultant thrust vector forms an angle with the Z_B X_B - plane of γ_{cx} and results in a torque about X of

$$T_x = + F L \sin \gamma_{cx} \ (\simeq + F L \gamma_{cx} \ , \text{ for small } \gamma_{cx}).$$

Similarly if we command a positive γ_{cy}, we obtain

$$T_y = + F L \sin \gamma_{cy} \; (\simeq + F L \gamma_{cy} \;, \text{ for small } \gamma_{cy})$$

and by commanding a positive γ_{cz}, we obtain

$$T_z = + F \ell \sin \gamma_{cz} \; (\simeq + F L \gamma_{cz} \;, \text{ for small } \gamma_{cz})$$

By using Figures 3-4 and 3-5 we can, by inspection, obtain the polarity of the gimbal angle commands $(\alpha_{c1}, \beta_{c1})$ $(\alpha_{c2}, \beta_{c2})$ necessary to produce each pure torque commanded by γ_{cx}, γ_{cy}, γ_{cz}. This relationship is summarized in Table 3-1.

TABLE 3-1

GIMBAL COMMANDS TO PRODUCE PURE POSITIVE TORQUES

Desired Torque	Desired TV Command Angle	Gimbal Commands Needed			
		α_{c1}	α_{c2}	β_{c1}	β_{c2}
about X	$+\gamma_{cx}$	0	0	$-\gamma_{cx}$	$+\gamma_{cx}$
about Y	$+\gamma_{cy}$	$-\gamma_{cy}$	$+\gamma_{cy}$	0	0
about Z	$+\gamma_{cz}$	$+\gamma_{cz}$	$+\gamma_{cz}$	0	0

It can be observed that β-gimbaling (the outer gimbal) is used to provide pitch control, while α-gimbaling (the inner gimbal) is used for both yaw and roll control. Since, in general, we will need simultaneous control in all three axes, it becomes necessary to "mix" the γ_{cx}, γ_{cy}, and γ_{cz} commands. This can be done, simply, by superposition so that

$$\alpha_{c1} = - \gamma_{cy} + \gamma_{cz}$$

$$\alpha_{c2} = + \gamma_{cy} + \gamma_{cz}$$

$$\beta_{c1} = - \gamma_{cx}$$

$$\beta_{c2} = + \gamma_{cx}$$

This "gimbal angle commander" logic can be equivalently described by the schematic shown in Figure 3-6.

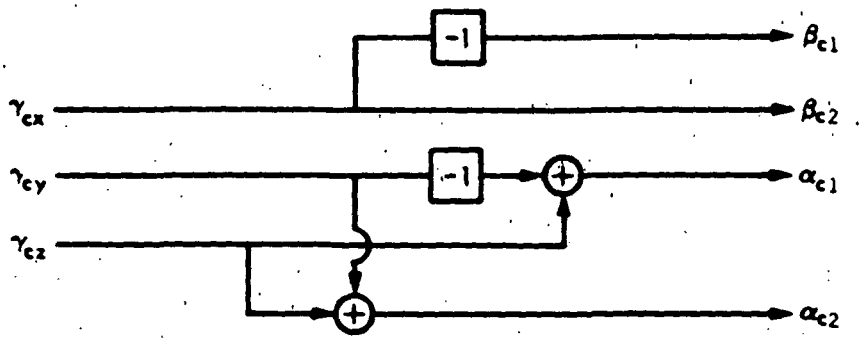

Figure 3-6. Gimbal Angle Commander

3.2.2 Gimbal Controller Subloops

The 2-gimbal command pairs just generated are then fed into the 16 gimbal controllers (2 per thruster). The controllers energize the gimbal drive motors causing the inner and outer gimbals to move to the commanded positions. Each gimbal axis will be assumed to be driven by a controller of the type shown in Figure 3-7. This scheme applies a torque to the gimbal T = Ke which is proportional to the gimbal position error. The rate feedback path provides damping. In reality the system need not use actual gimbal rate feedback, the same damping can be achieved if a suitable viscous damper is included. The limits of $\pm$ 30 degrees for position and $\pm$ 10 degrees/sec for rate are included to model expected gimbal hardware limitations.

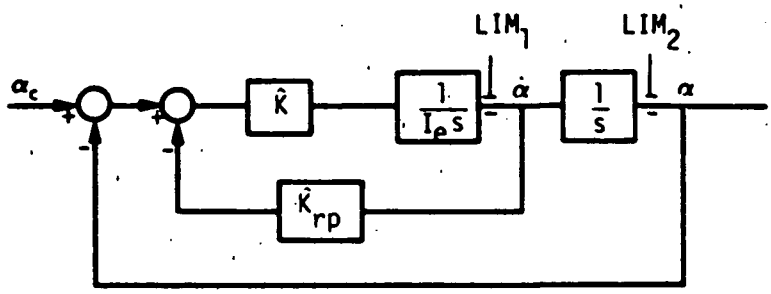

Figure 3-7. Gimbal Control Subloop (1 of 16)

In the non-saturating region the gimbal control loop behaves as a simple second order system with natural frequency and damping

$$\omega_n^2 = \frac{\hat{K}}{I_e} \quad \text{and} \quad \zeta = \frac{1}{2}\,\hat{K}_{rp}\,\omega_n \,.$$

The frequency ω_n should be chosen high enough so that the gimbals track the commands α_{ci} or β_{ci} properly but, at the same time, not so high that gimbal dynamic transients cause unwanted excitation of the flexible structure. We have chosen

$$\omega_n = 0.2 \text{ rad/s} \quad (0.032 \text{ Hz}) \,.$$

which is approximately one octave below the lowest flexible mode of the structure. This results in $\hat{K} = 0.2^2\, I_e$.

Each thruster will be assumed to have an inertia $I_e = 0.475$ kg-m^2 about its gimbaling axes (the gimbals themselves are assumed to have negligible mass). This results in a control gain of $\hat{K} = 0.019$ N-m/rad. Selecting $\zeta = 0.707$ for damping implies a rate to position gain of $\hat{K}_{rp} = 7.07$ s. This completes the description of the the gimbal controllers.

3.2.3 Generation of Forces and Torques

The total force acting on the bus due to the gimbaled thrusters can be computed, simply, as the vector sum of the forces produced by each thruster.

The total torque produced by the thrusters on the bus, on the other hand, is somewhat more difficult to obtain. It must be recognized that the gimbaling of the thrusters produces torques on the bus which arise from two inherently different sources:

> PRIMARY CONTROL TORQUES. In the case of pitch and yaw these are the torques which cause vehicle rotations when the resultant thrust vector does not pass through the vehicle center of mass, C.M. For roll these torques are produced by unbalanced force components in the X Y plane even if the net thrust passes through the CM. Note that these torques are a function of the instantaneous pointing (position) of the engine thrust axes.
>
> DYNAMIC REACTION TORQUES. These torques reflect the transient torques that are experienced by the bus as we rotate the gimbals. They are a consequence of the engine inertial reaction to rotation, and depend on the gimbal accelerations and velocities.

In order to compute the resultant forces and torques we must first obtain the set of coordinate transformations between bus coordinates and each set of thruster-fixed coordinates.

Thruster Coordinate Transformations

The gimbal coordinates and configuration shown in Figure 3-8, will be assumed to be common for the 4 engines in Bank 1.

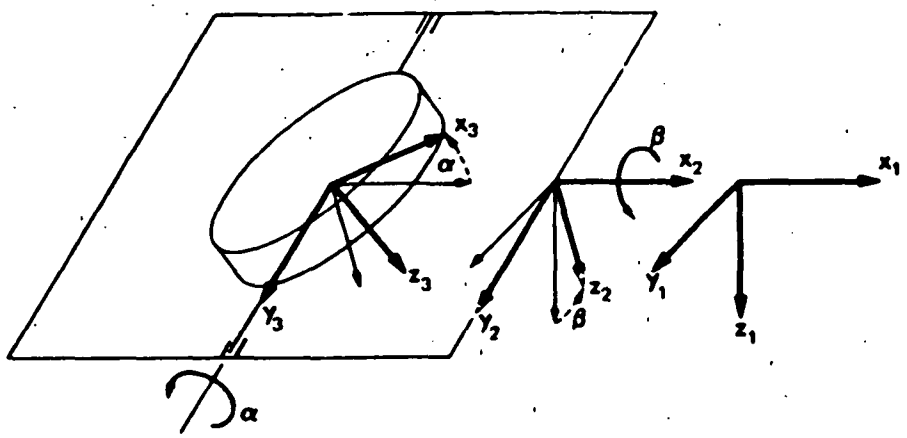

Figure 3-8. Bank 1 Gimbal Coordinates

As shown in the figure, let $\{b^1\}$, $\{b^2\}$, $\{b^3\}$ denote three reference frames defined by triads of unit vectors x_i, y_i, z_i, i=1,2,3 embedded on the bus, the outer gimbal and the thruster (i.e. the inner gimbal), respectively. The gimbal angles of all the engines in Bank 1 is (α_1,β_1), so that frames $\{b^1\}$ and $\{b^3\}$ are related to each other through a rotation about x_1 followed by a α_1 rotation about y_2 so that the transformation T relating both frames can be expressed as

$$\{b^3\} = T\{b^1\} = \begin{bmatrix} \cos\alpha & 0 & -\sin\alpha \\ 0 & 1 & 0 \\ \sin\alpha & 0 & \cos\alpha \end{bmatrix} \begin{bmatrix} 1 & 0 & 0 \\ 0 & \cos\beta & \sin\beta \\ 0 & -\sin\beta & \cos\beta \end{bmatrix} \{b^1\}$$

and

$$\{b^1\} = T^t\{b^3\} = \begin{bmatrix} \cos\alpha & 0 & \sin\alpha \\ \sin\alpha\cos\beta & \cos\beta & -\cos\alpha\sin\beta \\ -\sin\alpha\cos\beta & -\cos\alpha\sin\beta & \cos\alpha\cos\beta \end{bmatrix} \{b^3\}$$

Force Computations

Let f_o denote the magnitude of the force produced by one single thruster. Then, this force, expressed in vector form, is given by

$$F_o = \{b^3\}^t \begin{bmatrix} 0 \\ 0 \\ -f_o \end{bmatrix}$$

for each of the thrusters in Bank 1. Letting F_1 denote the resultant force vector for all 4 engines of Bank 1 yields

$$F = \{b^3\}^t \begin{bmatrix} 0 \\ 0 \\ -4f_o \end{bmatrix} \quad \text{in frame } \{b^3\}.$$

The components of this equivalent engine 1 thrust, expressed in bus frame $\{b^1\}$ are then

$$F_{E1} = \{b^1\}^t \begin{bmatrix} F_{E1x} \\ F_{E1y} \\ F_{E1z} \end{bmatrix} = \{b_1\}^t T^t \begin{bmatrix} 0 \\ 0 \\ -4f_o \end{bmatrix} = \{b^1\}^t 4f_o \begin{bmatrix} -\sin\alpha_1 \\ +\cos\alpha_1 \sin\beta_1 \\ -\cos\alpha_1 \cos\beta_1 \end{bmatrix}$$

For thruster Bank 2 the whole thruster assemblies are rotated 180° about Z_B, as shown in Figure 3-4, so that the resultant thrust vector F_{E2} from Bank 2 can be obtained simply by taking F_{E1} evaluated at (α_2, β_2) and changing the sign of the x and y components:

$$F_{E2} = \{b^1\}^t \begin{bmatrix} F_{E2x} \\ F_{E2y} \\ F_{E2z} \end{bmatrix} = \{b^1\}^t 4f_o \begin{bmatrix} +\sin\alpha_2 \\ -\cos\alpha_2 \sin\beta_2 \\ -\cos\alpha_2 \cos\beta_2 \end{bmatrix}$$

so that the net force acting on the bus due to the thrusters is

$$FB = F_{E1} + F_{E2} = \{b^1\}^T 4f_o \begin{bmatrix} -\sin\alpha_1 + \sin\alpha_2 \\ \cos\alpha_1 \sin\beta_1 - \cos\alpha_2 \sin\beta_2 \\ -(\cos\alpha_1 \cos\beta_1 + \cos\alpha_2 \cos\beta_2) \end{bmatrix}$$

Primary Control Torques TB_c

The primary control torque about the bus center of mass (CM_B) can be obtained as follows: Let R_{E1} and R_{E2} denote the vectors from CM_B to equivalent engines 1 and 2, respectively. Then the primary control torque is given by

$$TB_c = R_{E1} \times F_{E1} + R_{E2} \times F_{E2}$$

Dynamic Reaction Torques

Here we shall compute those torques experienced by the bus as we rotate the gimbals. They are caused by the inertial resistance to rotation of the engines.

We shall assume that each thruster is seated on the gimbals in such a manner that its center of mass is coincident with the cross-point of the gimbal axes, so that gimbaling of the thrusters does not produce any translation of their centers of mass. It will also be assumed that the gimbals themselves have negligible mass so that the inertia of each engine/gimbals assembly is equal to the self-inertia matrix of the engine itself, which will be assumed to be

$$I = \begin{bmatrix} I_e & 0 & 0 \\ 0 & I_e & 0 \\ 0 & 0 & I_e \end{bmatrix} \quad \text{in frame } \{b^3\},$$

That is, the inertia for the center of mass of the thruster is I_e about axes x_3, y_3, and z_3. This assumption results in the interesting fact that the self-inertia of the thruster with respect to any other frame has the same diagonal (I_e, I_e, I_e) form.

Let ω denote the angular velocity of, say, thruster #1 with respect to inertial space and let $\mathscr{I}$ denote the inertia dyadic of the thruster. Then, the angular momentum of the thruster about its CM is given by

$$H = \mathscr{I} \cdot \omega$$

The external moment on the thruster T can then be computed from

$$T = \dot{H}$$

Let $\{b^0\}$ denote an inertial frame of reference. Let $\{b^1\}$, $\{b^2\}$, and $\{b^3\}$ denote the frames defined earlier. Let ω^{ij} denote the angular velocity of frame i relative to frame j, then the inertial angular velocity of the thruster $\omega = \omega^{30}$ can be computed by the chain rule

$$\omega = \omega^{30} = \omega^{32} + \omega^{21} + \omega^{10} ,$$

where the superscripts refer to the frames $\{b^i\}$, i = 0,1,2,3. The term ω^{10} represents the inertial angular velocity of the bus. Since the bus moves extremely slow when compared to the gimbal velocities

and accelerations, we will make the simplifying assumption that the velocity ω^{10} can be neglected, that is, the torques produced on the gimbals as a consequence of the bus rotations in inertial space can be neglected. Thus, we can assume that $\{b^1\}$ itself is fixed in inertial space and, therefore,

$$\omega = \omega^{31} = \omega^{32} + \omega^{21}$$

By inspection of Figure 3-8, we can write

$$\omega^{32} = \dot{\alpha}_1 y_3 = \dot{\alpha}_1 y_2$$

$$\omega^{21} = \dot{\beta}_1 x_2 = \dot{\beta}_1 x_1$$

so that

$$\omega^{31} = \dot{\beta}_1 x_1 + \dot{\alpha}_1 y_2 \ .$$

Making use of the fact that

$$y_2 = \cos\beta_1 y_1 + \sin\beta_1 z_1 \ ,$$

we can write

$$\omega = \omega^{31} = \dot{\beta}_1 x_1 + \dot{\alpha}_1 \cos\beta \ y_1 + \dot{\alpha}_1 \sin\beta \ z_1$$

letting ω_1^{31} denote the components of ω^{31} expressed in frame 1 we can write

$$\omega_1^{31} = \begin{bmatrix} \dot{\beta}_1 \\ \dot{\alpha}_1 \cos\beta \\ \dot{\alpha}_1 \cos\beta \end{bmatrix} \quad \text{and} \quad \omega = \omega^{31} = \{b^1\}^t \ \omega_1^{31}$$

The angular momentum can be expressed as

$$H = \mathscr{I} \cdot \omega = \{b^1\}^t I \{b^1\} \cdot \{b^1\}^t \omega_1^{31} = \{b^1\}^t \ I \ \omega_1^{31}$$

since I is the thruster inertia matrix in all frames. The external torque is given by

$$T = \frac{d}{dt} (\mathscr{I} \cdot \omega) = \{b^1\}^T \ I \ \dot{\omega}_1^{31} = \{b^1\}^t \ I_e \begin{bmatrix} \ddot{\beta}_1 \\ \ddot{\alpha}_1 \cos\beta_1 - \dot{\alpha}_1 \dot{\beta}_1 \sin\beta_1 \\ \ddot{\alpha}_1 \sin\beta_1 + \dot{\alpha}_1 \dot{\beta}_1 \cos\beta_1 \end{bmatrix}$$

The reaction torque exerted on the bus by the 4 engines of Bank 1 is then, simply

$$TB_{g1} = -4T = \{b^1\}^t\, 4I_e \begin{bmatrix} -\ddot{\beta}_1 \\ -\ddot{\alpha}_1 \cos\beta_1 + \dot{\alpha}_1\dot{\beta}_1 \sin\beta_1 \\ -\ddot{\alpha}_1 \sin\beta_1 - \dot{\alpha}_1\dot{\beta}_1 \cos\beta_1 \end{bmatrix}$$

By an analogous procedure, the reaction torque exerted on the bus by the four engines of Bank 2 is given by

$$TB_{g2} = \{b^1\}^t\, 4I_e \begin{bmatrix} \ddot{\beta}_2 \\ \ddot{\alpha}_2 \cos\beta_2 - \dot{\alpha}_2\dot{\beta}_2 \sin\beta_2 \\ -\ddot{\alpha}_2 \sin\beta_2 - \dot{\alpha}_2\dot{\beta}_2 \cos\beta_2 \end{bmatrix}$$

and the total dynamic reaction torques on the bus are

$$TB_g = TB_{g1} + TB_{g2} .$$

The total external torque acting on the bus is

$$TB = TB_c + TB_g + T_{dist}$$

i.e., the sum of the primary control torques, the dynamic reaction torques, and the external disturbances.

This completes the description of the TVC loop. We shall next describe the Scan Platform and Solar Array Controllers.

3.2.4 Solar Array and Scan Platform Controllers

Each solar array wing has its own separate control loop to articulate it relative to the bus. Since each solar array wing controller is an independent system, the wings can be made to rotate separately or together. They can also be made to follow the bus as it rotates, or not to follow yaw bus rotations θ_2 by commanding $-\theta_2$ into the solar array wing controllers (this is what has to be done, for example, when we wish to reorient the bus in yaw without moving the solar panels from the sun).

The controller assumes that suitable actuators are provided between the bus and each wing of the solar array to control their relative positions.

The actuators will be controlled by another lead-lag type controller as shown in Figure 3-9.

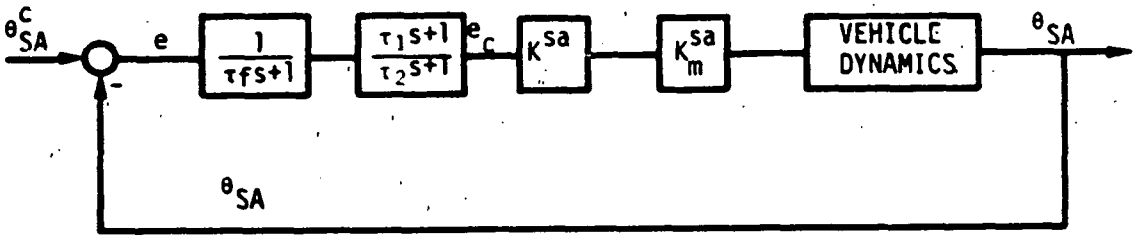

Figure 3-9. Solar Array Lead-Lag Controller (1 of 2)

The position of the solar array θ_{SA} relative to the bus (as measured by a potentiometer or encoder) is subtracted from the command to obtain the position error e which is then put through a filter and a lead-lag compensation network to obtain the control error e_c. This is similar to the TVC loop controller described earlier. The control error is then multiplied by a gain K^{sa} and by means of the motor torque constant K^{sa}_m we apply a torque to the solar array wing

$$T_{SA} = \bar{K}^{sa} e_c ,$$

where

$$\bar{K}^{sa} = K^{sa} K^{sa}_m .$$

The scan platform controller used has been described previously. For details the reader is referred to subsection 2.3.

3.2.5 System Block Diagram and Parameters

Assembling the controllers described in the preceding pages together with the ICM scan platform described in 2.3, results in the TVC control system block diagram shown in Figure 3-10. The system parameters are listed in Table 3-2.

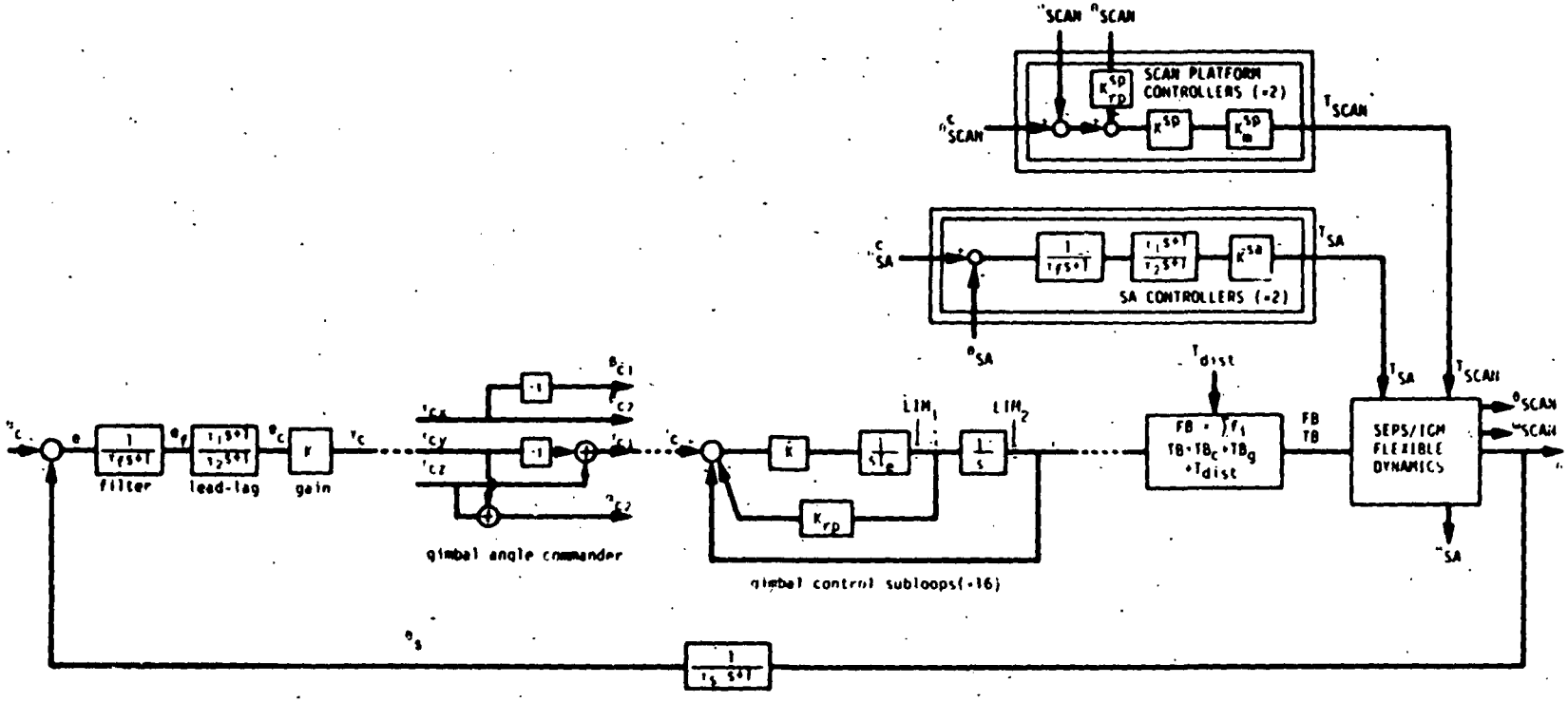

Figure 3-10. TVC "Lead-Lag" System Block Diagram (1 axis shown)

TABLE 3-2. TVC "LEAD-LAG" SYSTEM PARAMETERS
(same for all axes unless otherwise indicated)

PARAMETER	VALUE	UNITS	DESCRIPTION
I. LEAD-LAG CONTROLLER			
τ_s	1.0	s	Celestial sensor time constant
τ_f	15.0	s	Filter time constant
τ_1	200.0	s	Lead-lag
τ_2	10.0	s	Lead-lag
K	3.52	dimensionless	X-axis position-to-TV angle gain
	0.11	dimensionless	Y-axis position-to-TV angle gain
	15.70	dimensionless	Z-axis position-to-TV angle gain
II. GIMBAL CONTROL SUBLOOPS			
$\dot{K}$	0.019	N-m/rad	Position-to-torque gain
$\dot{K}_{rp}$	7.07	s	Rate-to-position gain
I_e	0.475	Kg-m^2	Single thruster inertia
LIM_1	$\pm$10.0	deg/s	Gimbal rate limit
LIM_2	$\pm$30.0	deg	Gimbal position limit
III. SOLAR ARRAY AND SCAN PLATFORM CONTROL			
K^{sa}	0.02557	N-m/rad	Position-to-torque gain
τ_f	15.0	s	Filter time constant
τ_1	200.0	s	Lead-lag
τ_2	20.0	s	Lead-lag
$K^{sp}K_m^{sp}$	1500.0	N-m/rad	Scan position-to-torque gain
K_{rp}^{sp}	0.14683	s	Scan rate-to-position gain(clock)
	0.09901	s	Scan rate-to-position gain(cone)

3.3 TVC PERFORMANCE

The performance of the TVC lead-lag system just described was evaluated through computer simulation of the four test maneuvers described in 2.4. Full details of the flexible dynamics models, simulation programs and assumptions can be found in Section 2.

The results of the simulations are shown in Figures 3-11 through 3-14 and discussed below in some detail. The figures themselves are also captioned with pertinent explanations and commentary. The nomenclature used in these figures is listed in Table 3-3.

The simulation program was written in such a way that it assumes the vehicle to be initially moving in a steady state (constant linear or angular velocities). As the simulation starts and the ion engines provide thrust, the vehicle experiences a change to a state of constant linear acceleration, which brings about a constant deformation of the solar panels and possible shifts of the center of mass (and accompanying rotations). This dynamic transient is due to what we might call the "engine turn-on transient." It is, generally, very small but was found to be large enough to mask the vehicle response for some of the planned maneuvers. In an effort to reduce this undesirable turn-on-transient effect, all TVC simulation programs were modified to ramp up the thrust in a very smooth fashion during the first 20 seconds of the simulation. The thrust is assumed to increase smoothly from 0 to 1 Newton as follows:

$$F = \begin{cases} \frac{1}{2}\left(1 - \cos\frac{\pi t}{20}\right), & \text{for } 0 \leq t \leq 20 \text{ s} \\ 1 \quad , & \text{for } t \leq 20\text{s} \ . \end{cases}$$

This ramping up is so smooth compared to the solar panel resonances that it produces practically no significant oscillatory transients in the solar panels.

The 1 degree pitch turn maneuver simulation (Figure 3-11) demonstrated the TVC system's capability to make smooth turns with minimal excitation of the vehicle's flexible dynamics. The vehicle achieved the turn rate of .005°/ s in approximately 150 seconds and completed the maneuver in 800 seconds. There is a small amount of cross

axis motion in yaw and roll for this maneuver, as is for most maneuvers. This is a result of the vehicle dynamics and not a controller generated problem. The maximum gimbal angle was 3.72° in β while the maximum gimbal rate was .12°/s also in β. The solar array panels experienced a small rotation due to the cross coupled motion of the bus in yaw but the controller was able to correct this condition. The generalized coordinates plots of SA modal deformation indicate that their flexible body motion was smooth and non-vibratory. All coordinates settled to some non-zero steady-state value as a result of thrusting in the -Z direction throughout the length of the maneuver. Note that most of the modal deformations occurred within the first 20 seconds of the simulation.

The bus yaw turn simulation (Figure 3-12) shows again that the TVC system can make smooth turns. The bus position has one overshoot and settles to the final 30° command position in about 800 seconds. Pitch and roll exhibit very small cross-coupled motion for this maneuver. The bus achieved the commanded turn rate of .25°/s in 120 seconds then continued to increase until it reached a peak value of .34°/s. The yaw control torque was amooth and the gimbal subloop tracked the desired torque very well. The roll torque had a small transient due to thruster turn-on effects during the first 20 seconds. The maximum gimbal angle during the maneuver was about 6.3° in α and the maximum gimbal rate was .22°/s also in α. During this maneuver the SA wings were commanded to remain in their initial position (normal to the sun line) while the bus was turning. They performed as commanded with negligible error. The modal deformations in the SA panels were primarily due to the linear acceleration of the vehicle in the -Z direction.

The performance of the acquisition maneuver is highly dependent upon the initial conditions specified, but for the set used in this simulation the performance was very good (Figure 3-13) The set of initial conditions is listed below:

Axis	Initial Position	Initial Rate
pitch	+1.0°	+0.005°/s
yaw	+2.0°	+0.250°/s
roll	0.0°	-0.005°/s

The vehicle was stabilized to a zero final condition in approximately 700 seconds. The maximum position error, 13.3°, occurred in yaw (the axis of least inertia) at 88 seconds. Since pitch and roll axes have higher inertias their positions did not drift as much as yaw. The maximum pitch and roll angles were 1.2° and 0.4° respectively. The engine gimbal subloops tracked the desired torques very well and exercised maximum gimbal angles of 21° in α and 7° in β. As the vehicle moved predominantly in yaw, the SA wings also experienced large angular rotations since the SA actuators have very low control authority (low position-to-torque gain). The modal deformations reflect most the response in yaw while constant deformations due to engine thrusting are also present.

For the scan slewing simulation (Figure 3-14), the TVC system was commanded to maintain the vehicle in its initial zero state while the science platform was scanning. The box slew sequence introduces high frequency disturbances into the vehicle, with yaw being the axis most affected. The engine gimbals reached a maximum angle of .11° in α to compensate for the .014° movement in yaw. The most noticeable characteristic of the controller during this maneuver is its low pass filtering of the input disturbances. The roll torque (plot n) shows that the controller tracks the low frequency components of the input well but filters out the high frequency transients. For this maneuver the SA actuators were commanded to hold the wings in place. The solar panel vibration observed in the generalized modal coordinates is by in large due to the impulsive type disturbances transmitted to the vehicle during science platform slewing.

In summary, the TVC control system provided very smooth proportional control of the vehicle for the four maneuvers studied, with negligible excitation of the vehicle flexibility. The required gimbal angles were acceptable.

TABLE 3-3. KEY TO VARIABLE NAMES FOR FIGURES 3-11 to 3-14

ALPH1,2,3*	Angular position of the bus (b_o), rad
ANGM	System angular momentum magnitude, N-m-s
COERR1,2,3	Control error e_c, rad
COMCL, COMCN	Position commands into Scan Platform, rad
COMSA1,2	Position commands into SA wings, rad
ERROR1,2,3	Sensed position error e, rad
ETA11 to ETA18	Panel deformation generalized coordinates (panel 1, first 8 modes)
GIMA1,2 & GIMB1,2	Gimbal angles α_1, α_2, β_1, β_2, respectively, rad
GIMA1D,2D & GIMB1D,2D	Gimbal angle rates $\dot{\alpha}_1$, $\dot{\alpha}_2$, $\dot{\beta}_1$, $\dot{\beta}_2$, respectively, rad/s
GM1,2,3,4	Hinge rotation angles for Solar Array Panels 1,2, and Scan Clock, and Cone, respectively, rad
RATE1,2,3	Bus angular rates, rad/s
TDESR1,2,3	Desired control torques, N-m
TH1,2,3,4	Hinge torques for Solar Array Panels 1,2, and Scan Clock, and Cone, respectively, rad
TRNCOM	θ_c position input (turn command), rad
TSC1,2,3	External torques about vehicle CM, N-m

*1,2,3, denote the pertinent axis: X,Y,Z, respectively.

FULL FLEX MODEL WITH TVC-LL200/1C

FIGURE 3-11
1° X TURN

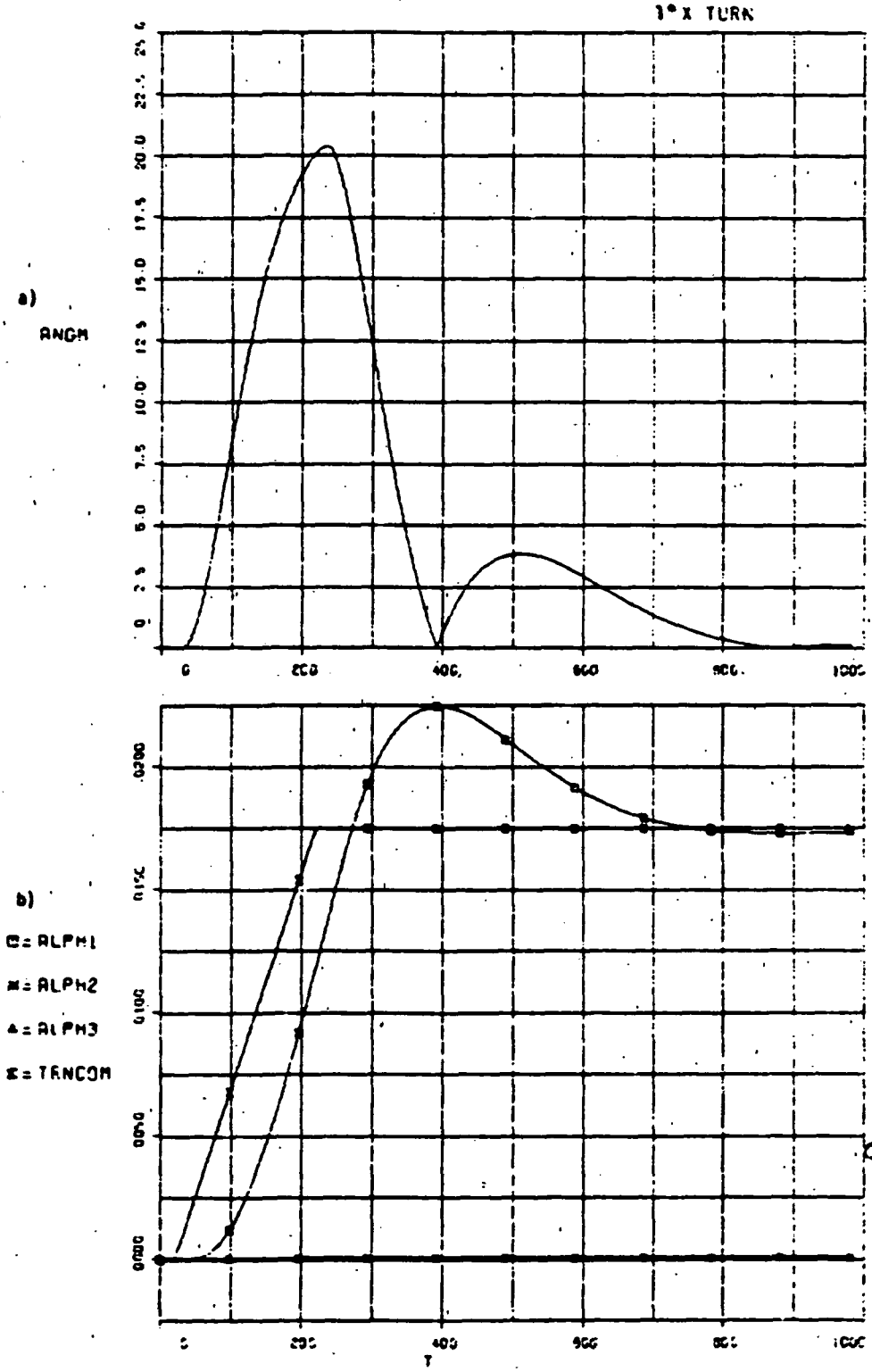

1° turn with approximately 28% overshoot (highly dependent on command final position). Smooth transient with no signs of excitation of flexible dynamics.

FULL FLEX MODEL WITH TVC-LL200/10 **FIGURE 3-11**

1° X TURN

c)

ALPHI

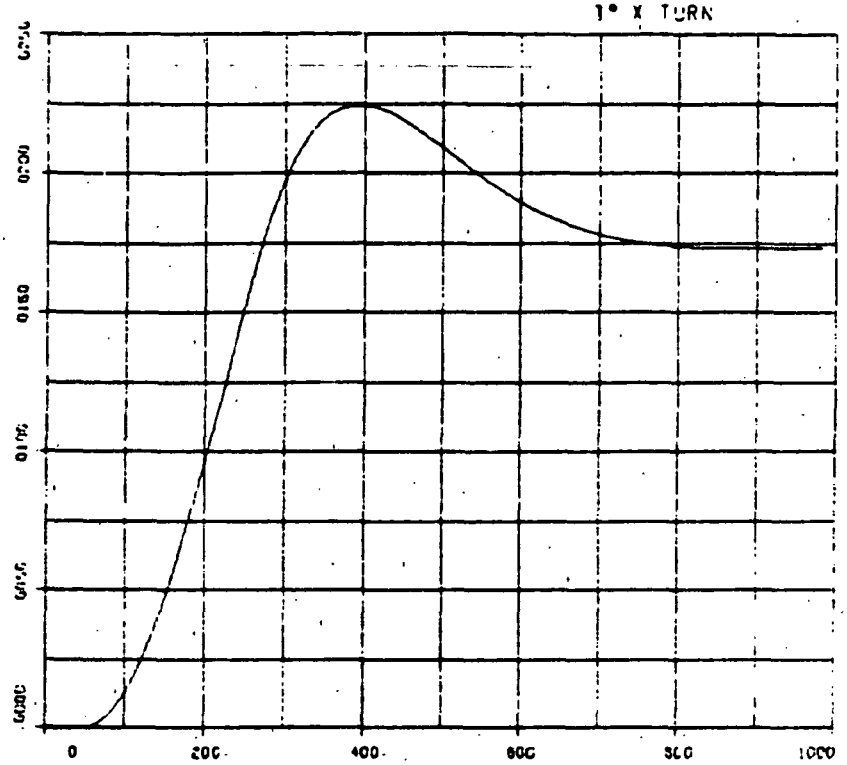

d)

RATE1

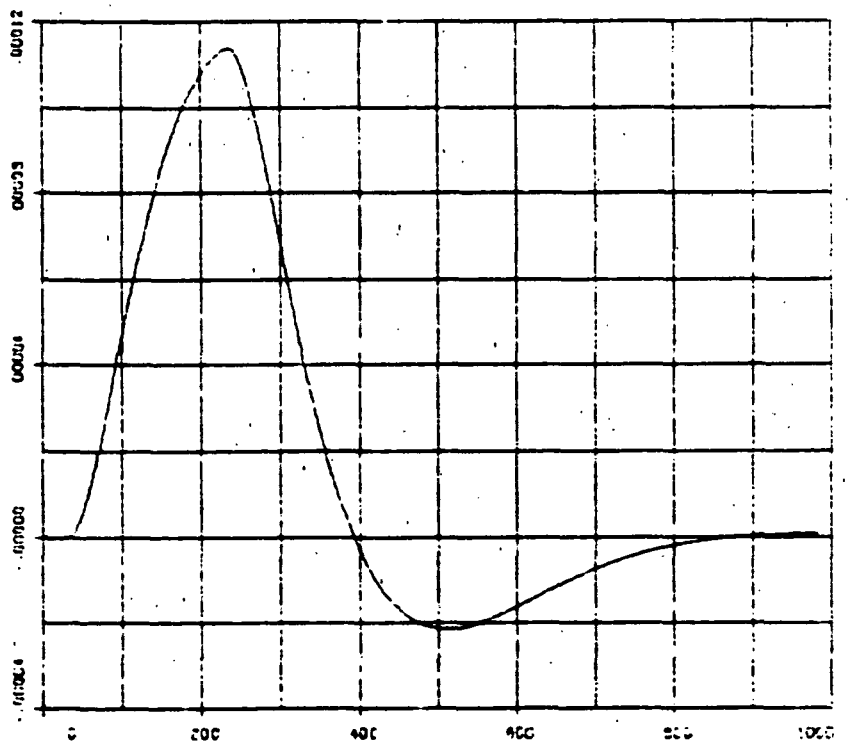

This pitch turn took about 800 s to complete. c) Position reaches commanded position in about 260 s, then overshoots it by -28%. d) Rate takes about 150 s to accelerate to command turn rate (0.005°/s), then overshoots by -32%.

FULL FLEX MODEL WITH TVC-LL200/10 FIGURE 3-11
1°x TURN

e)

ALPH2

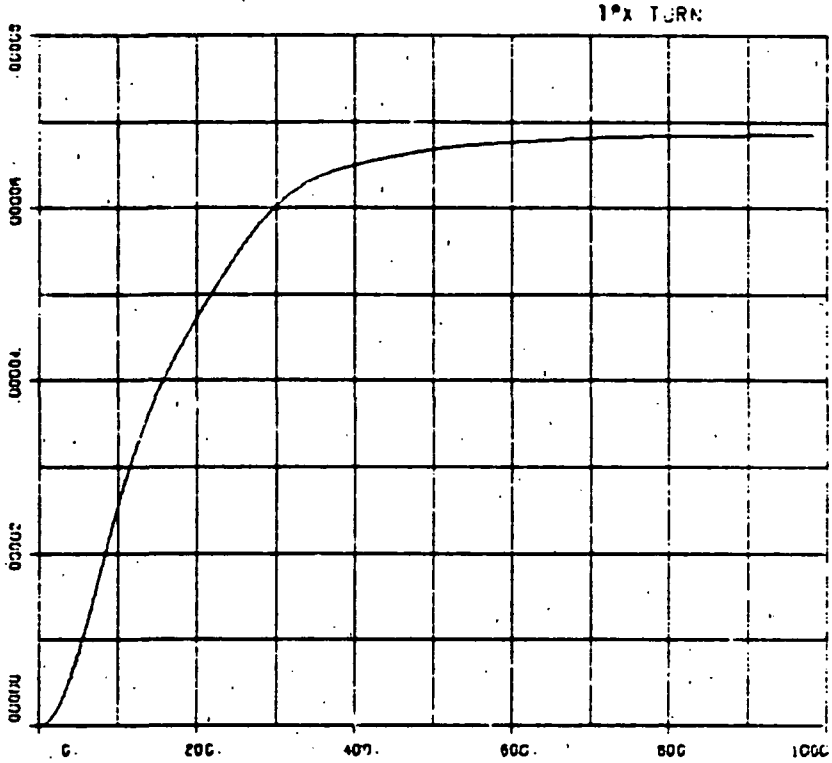

f)

RATE2

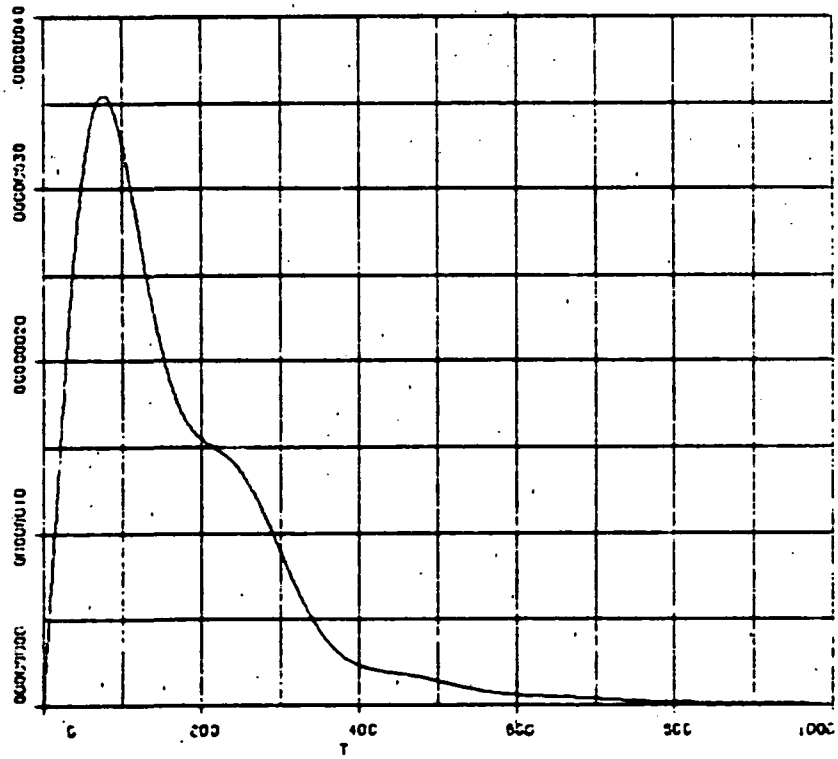

e) Yaw axis motion is mostly the result of cross-coupling between axes and a small shift in the instantaneous center of mass of the vehicle due to out-of-plane motion of solar panels.

FIGURE 3-11

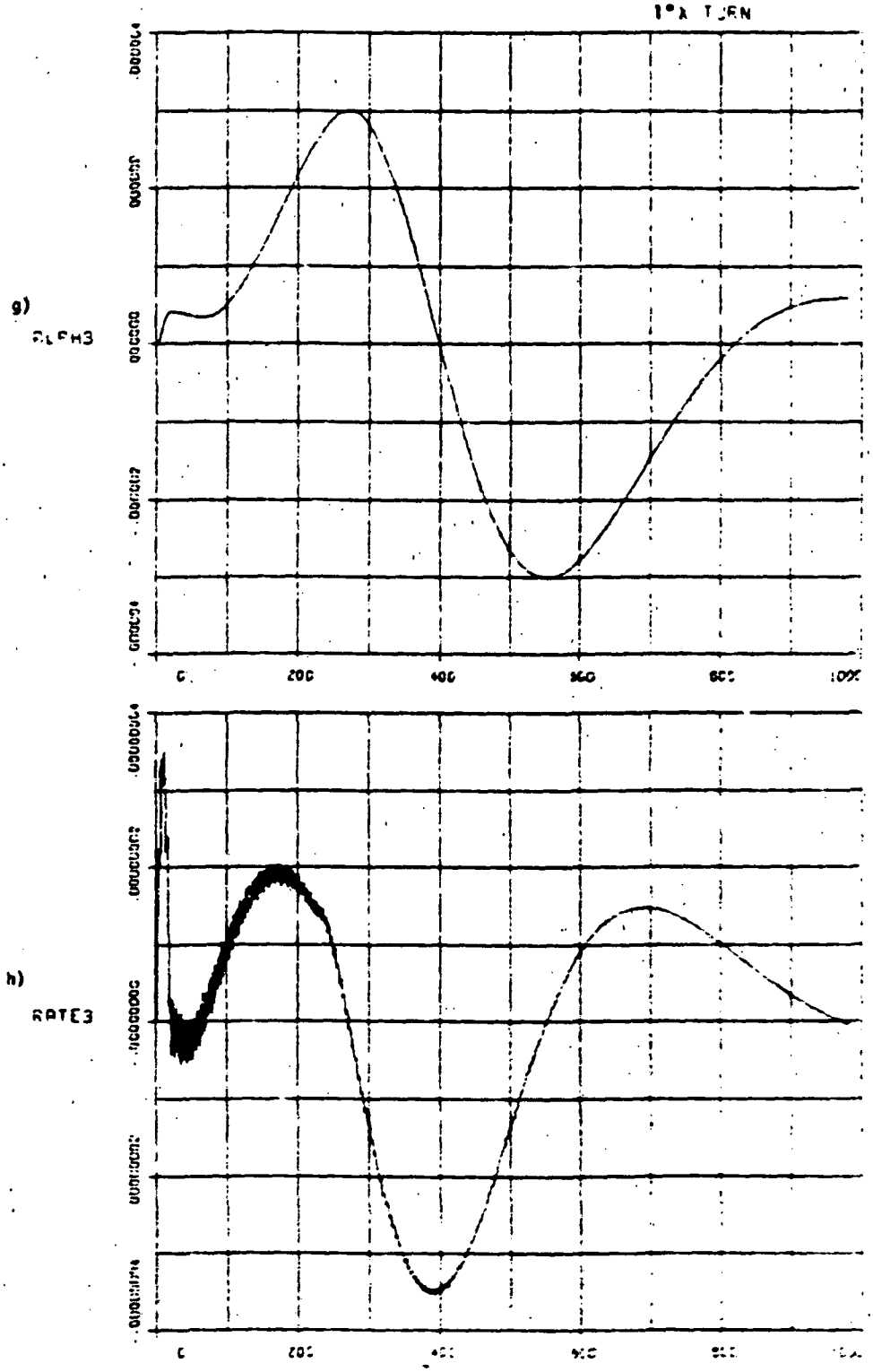

g) Some small cross-coupling can be observed in the roll axis.

FIGURE 3-11

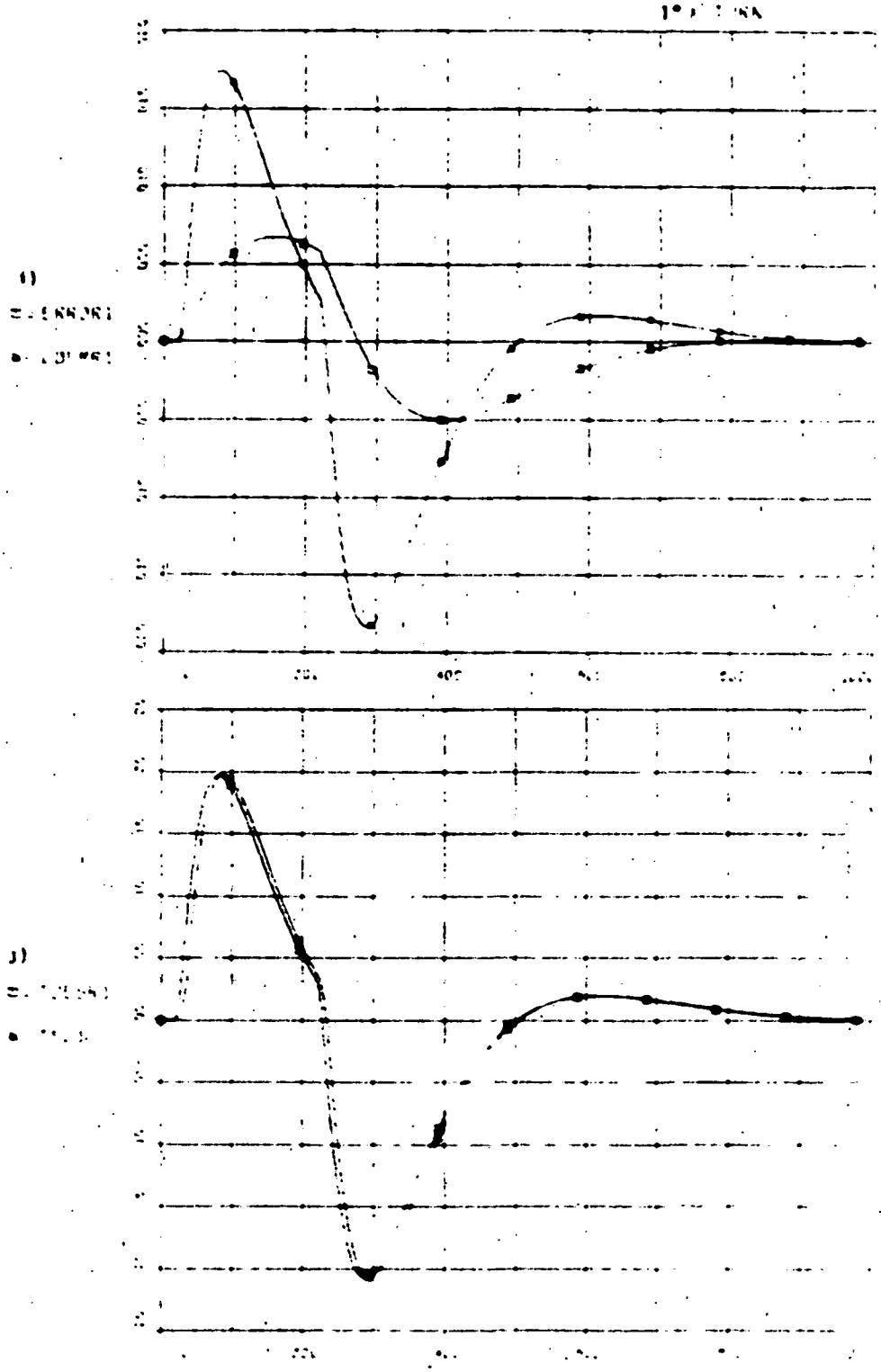

j) Torque generated by engines tracks desired torque quite well. Observe the smooth, slowly varying torques produced by TVC, their low frequency content causes vehicle to turn without exciting appreciable vibrations in solar panels.

FIGURE 3-11

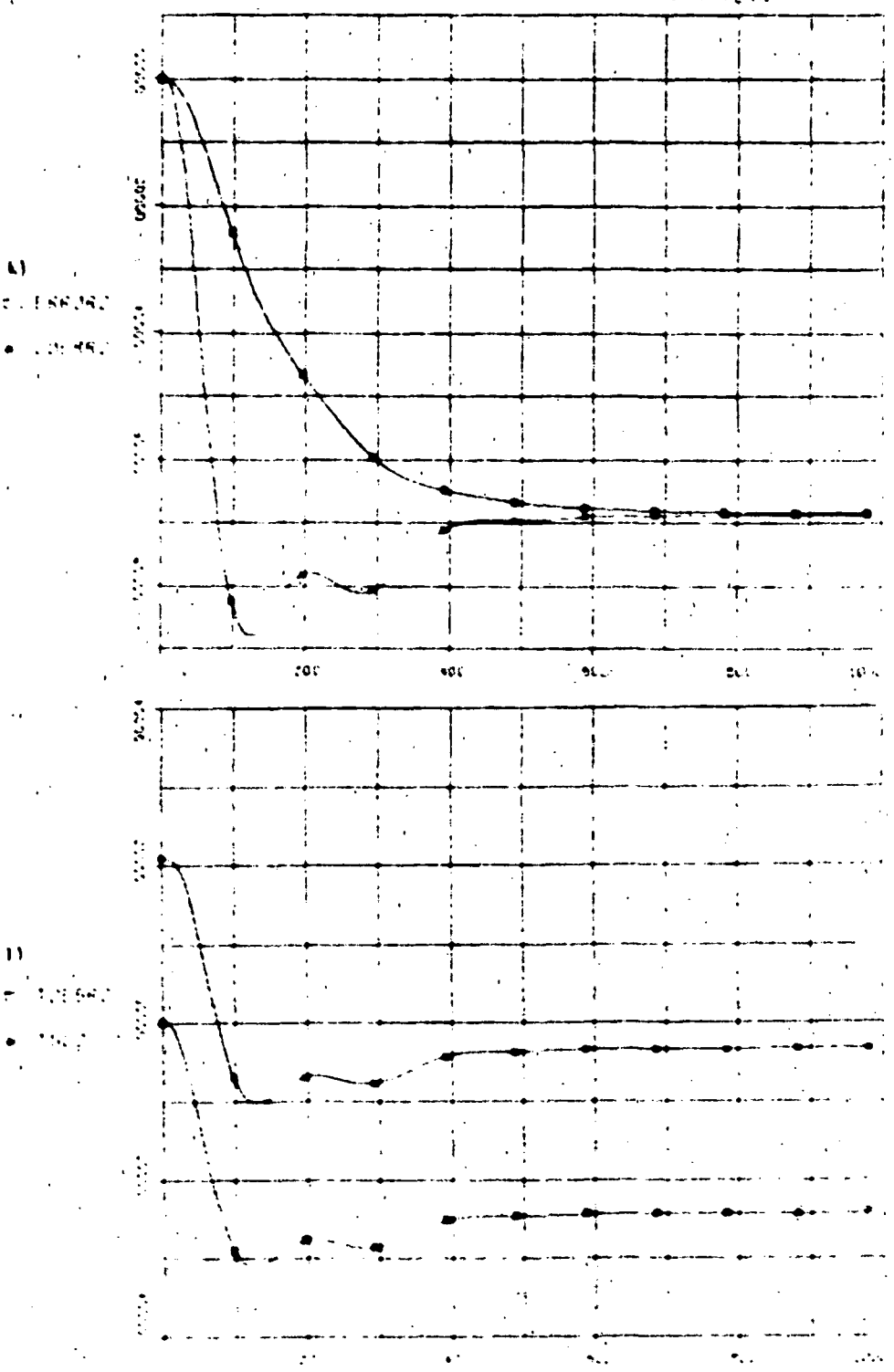

1) TSC 2 includes external solar pressure torque of $0.209\ 10^{-6}$ N-m.

FULL FLEX MODEL WITH TVC-L200/10 FIGURE 3-11
1°X TURN

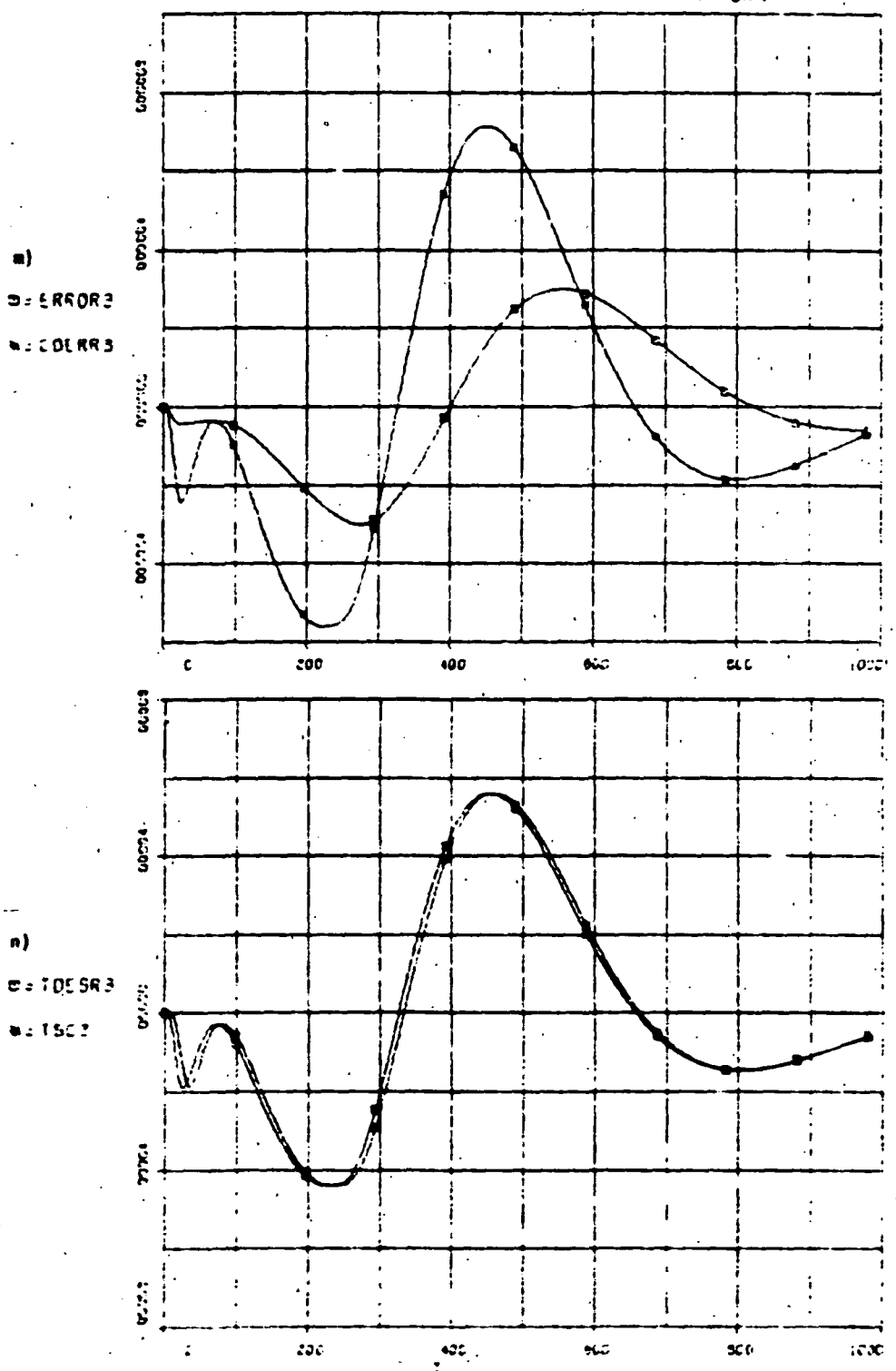

b) Small roll torques to control motion due to cross axis coupling.

FULL FLEX MODEL WITH TVC-(L200-1C

FIGURE 3-11
1° X TURN

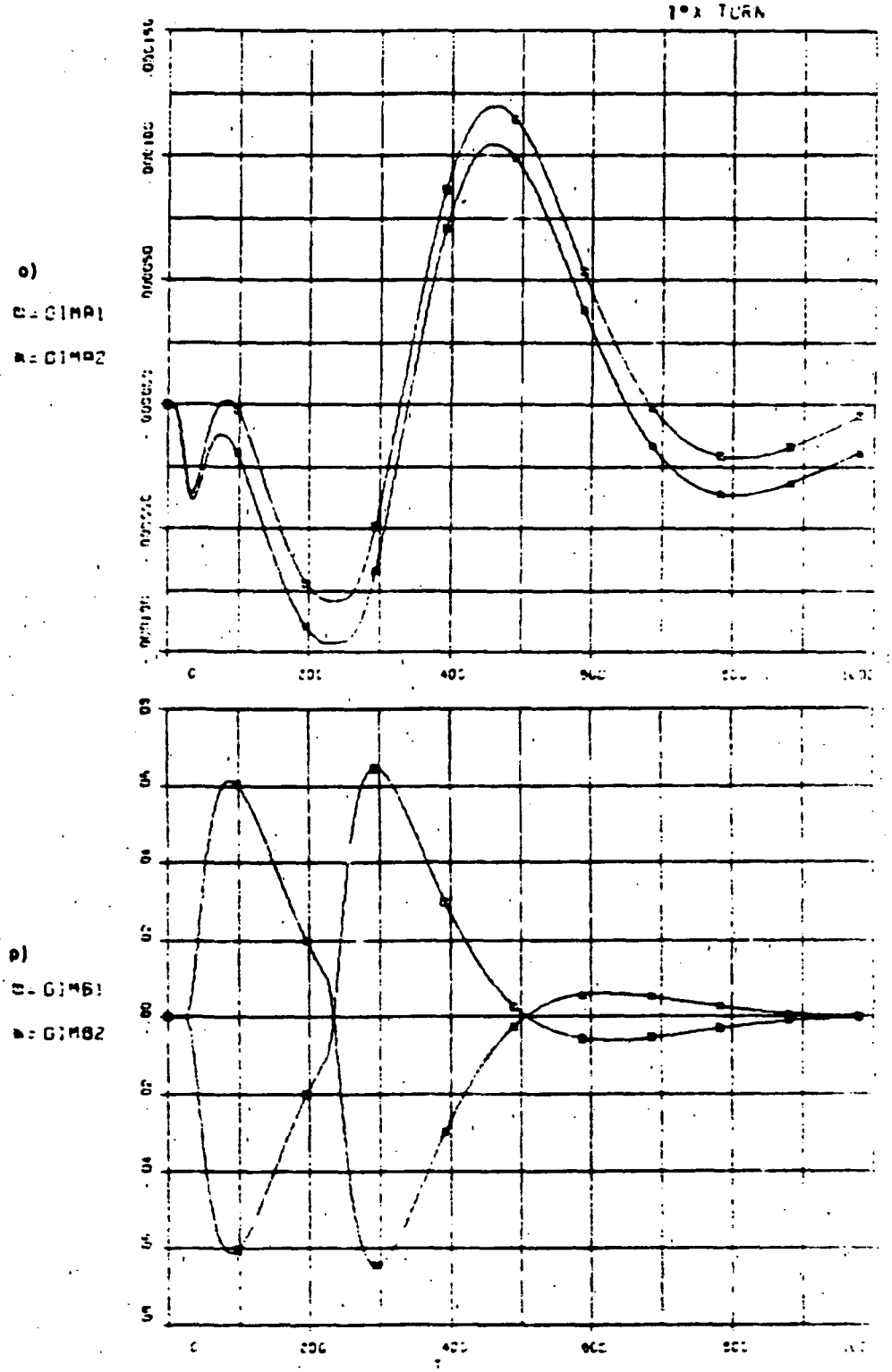

a) The engines are being gimbaled in α in order to control yaw and roll transients.
p) The engines are being gimbaled in β to provide the turning torque for the 1° pitch turn, MAX gimbal angle reached 0.065 rad (3.7°). Max gimbal rates of 0.12°/s as shown on r).

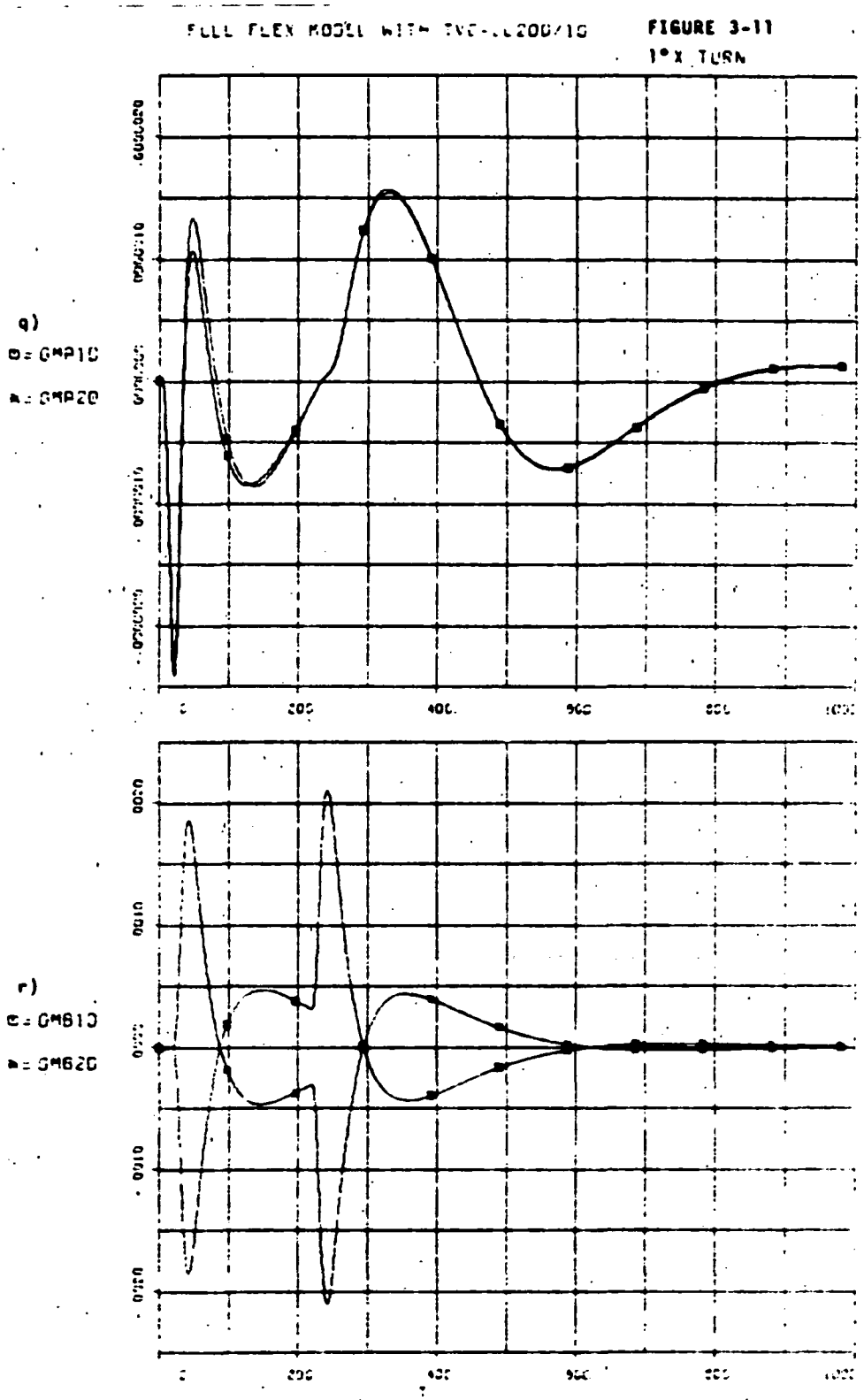

FIGURE 3-11

FULL FLEX MODEL WITH TVC-LL200/10

FIGURE 3-11

1°X TURN

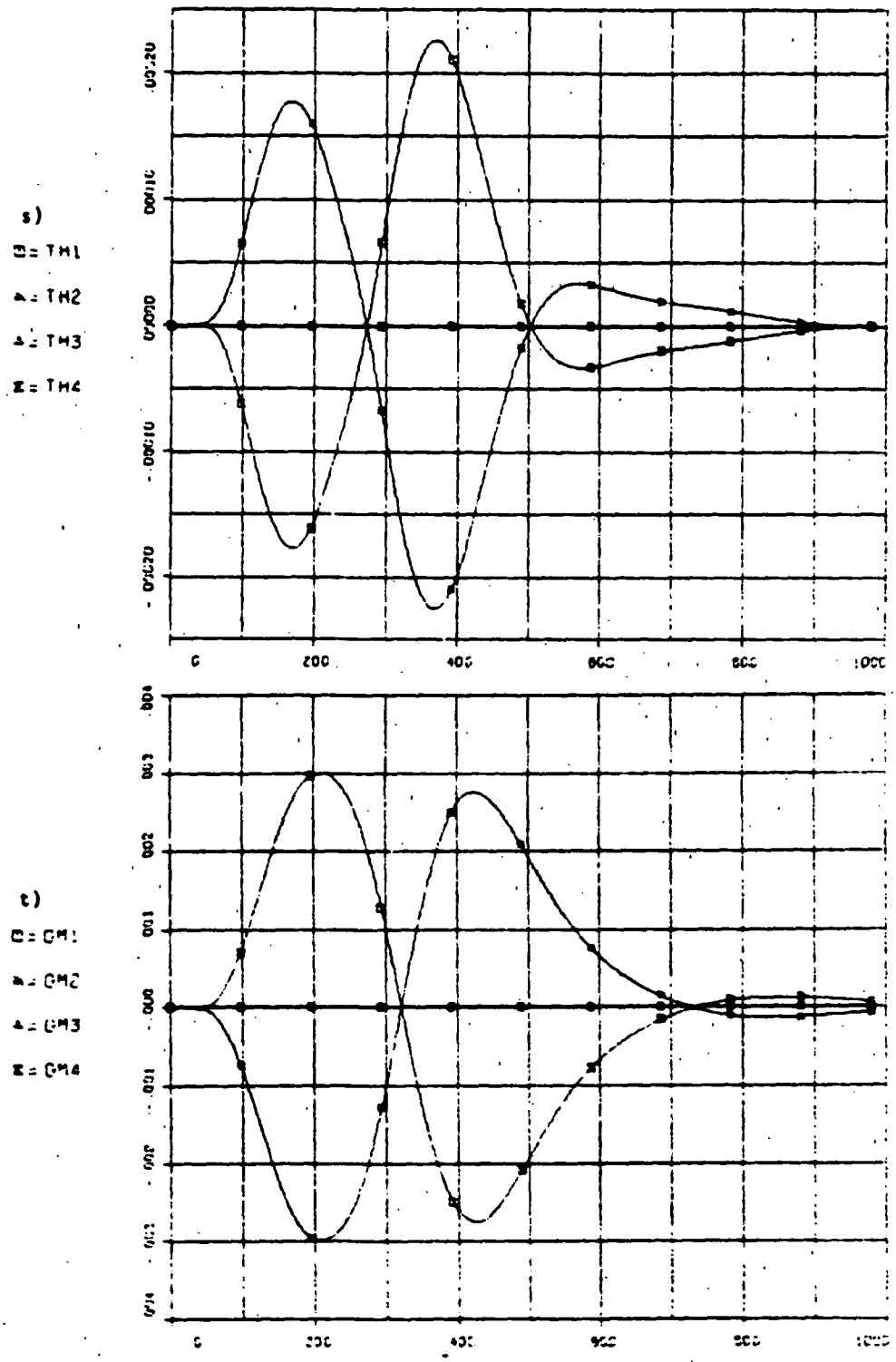

Note small SA torques, with max SA rotation of 0.17°.

FULL FLEX MODEL WITH [illegible]

FIGURE 3-11

1ST TDRS

u)

□ = GM1

+ = COMSR1

△ = GM2

✕ = COMSR2

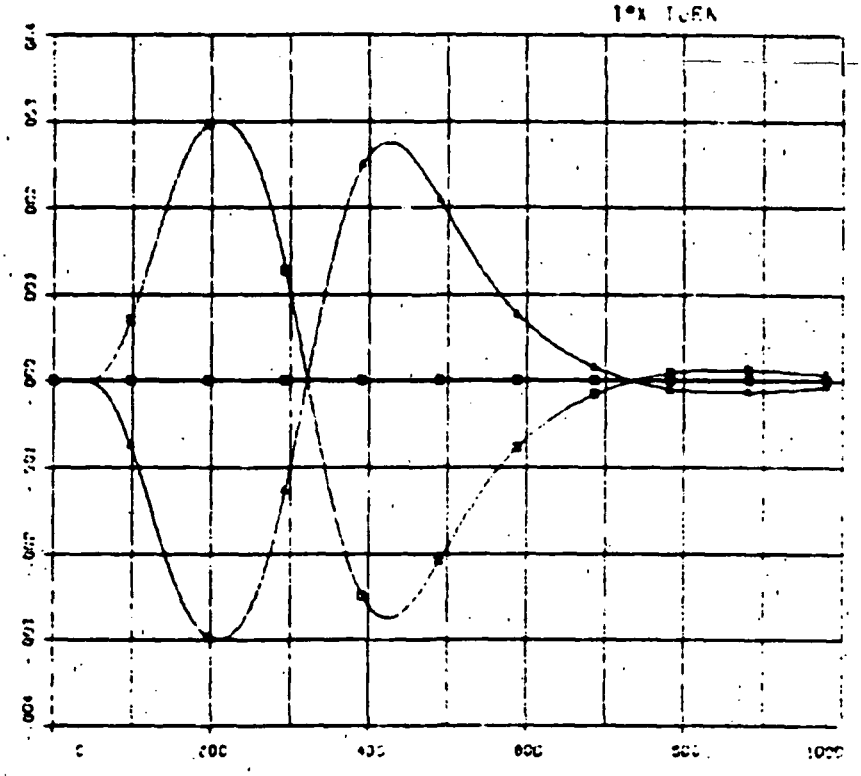

v)

□ = GM3

✕ = COMCL

△ = GM4

✕ = COMCN

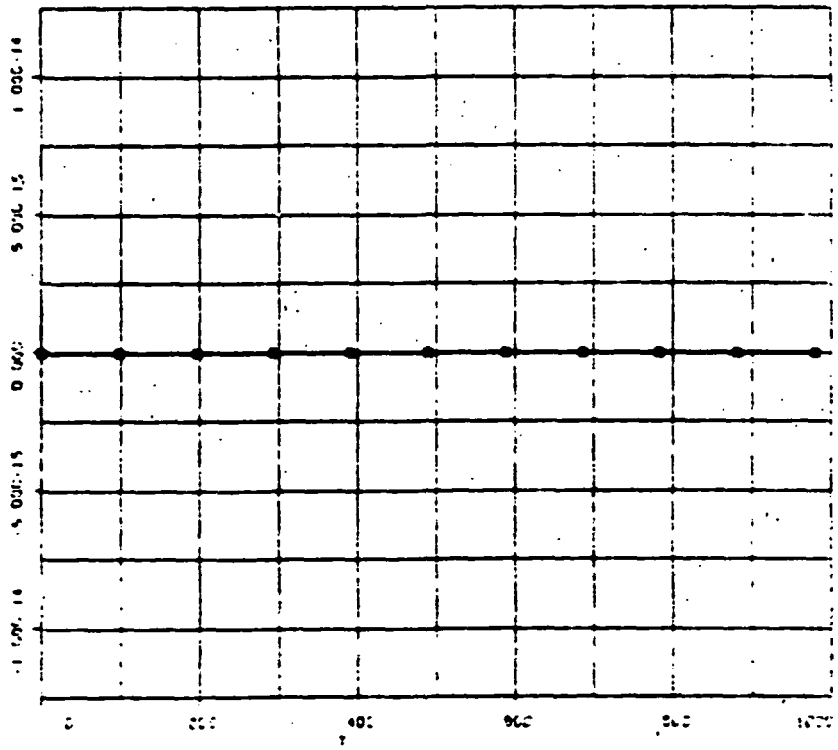

v) Scan platform was locked in place for this maneuver.

FULL FLEX MODEL WITH TVC-LL200/10 FIGURE 3-11
1°X TURN

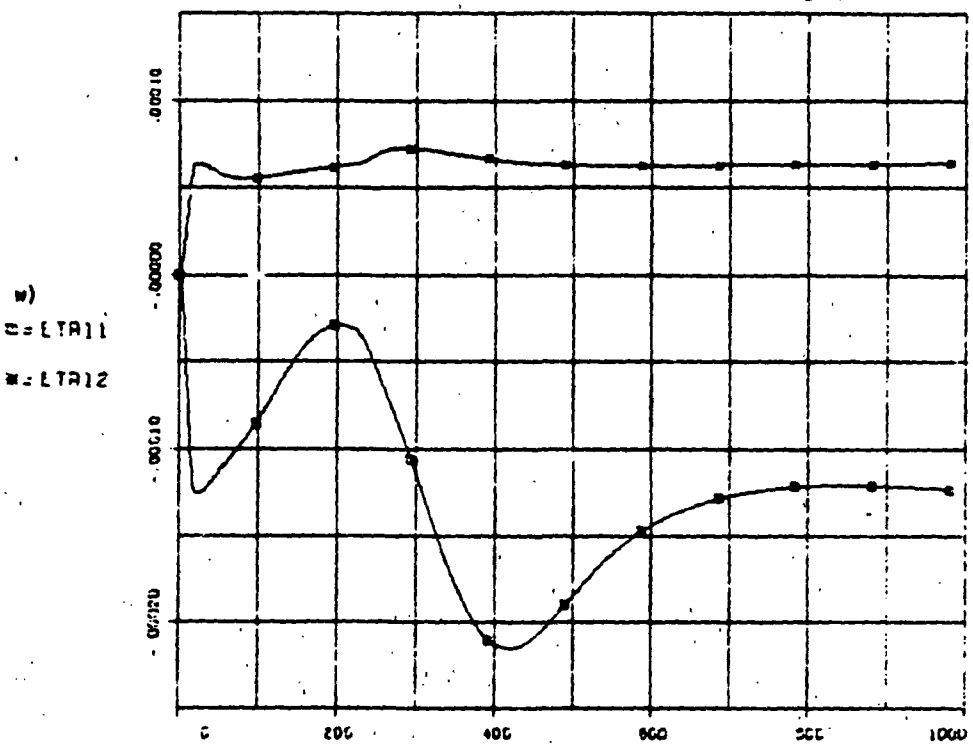

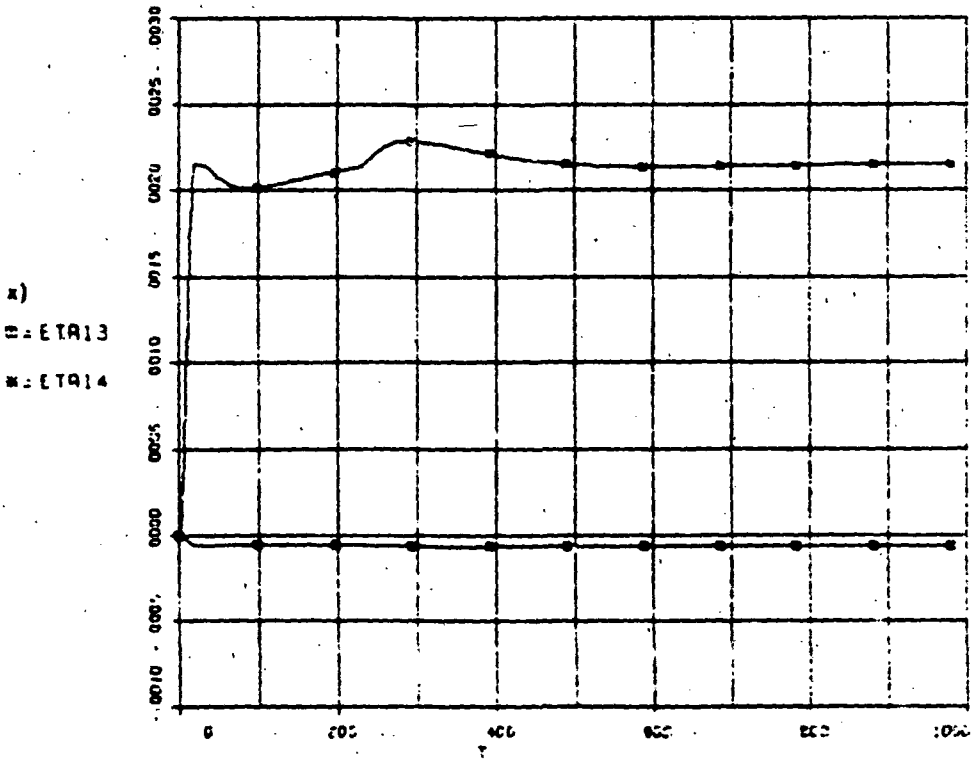

w) through z)
SA deformation in generalized coordinates showing predominant (and expected) mode 4 in-plane deformation of SA, and some small coupled out-of-plane motion. Note steady state panel deformation due to constant linear acceleration of vehicle produced by ion thrusters. Extremely low residual vibration levels.

FULL FLEX MODEL WITH TVC-LL200 10

FIGURE 3-11

1°x TURN

y)

D = ETA15

A = ETA16

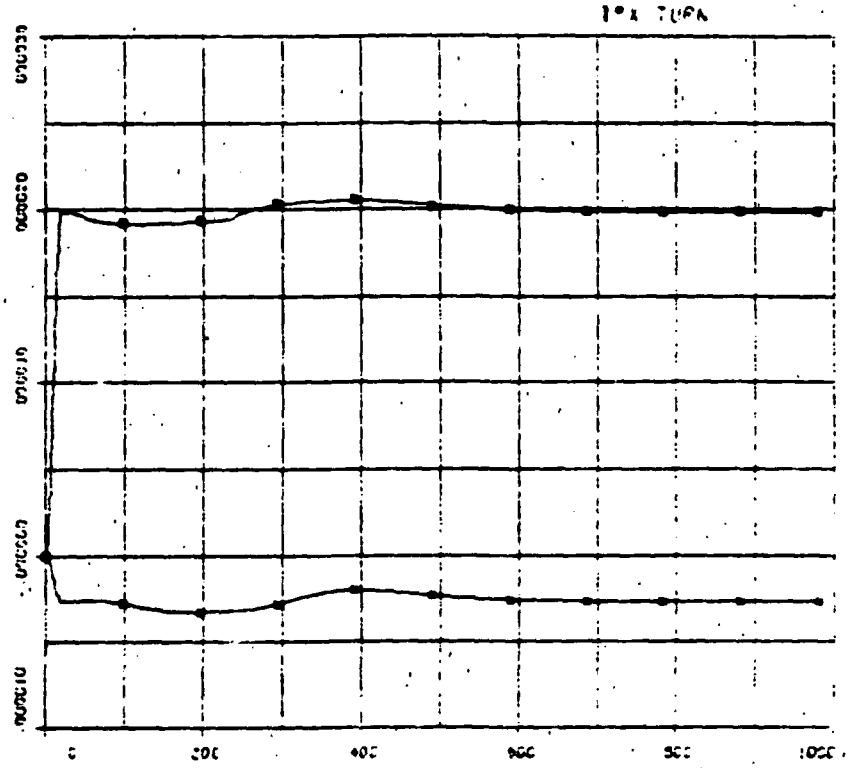

z)

D = ETA17

A = ETA18

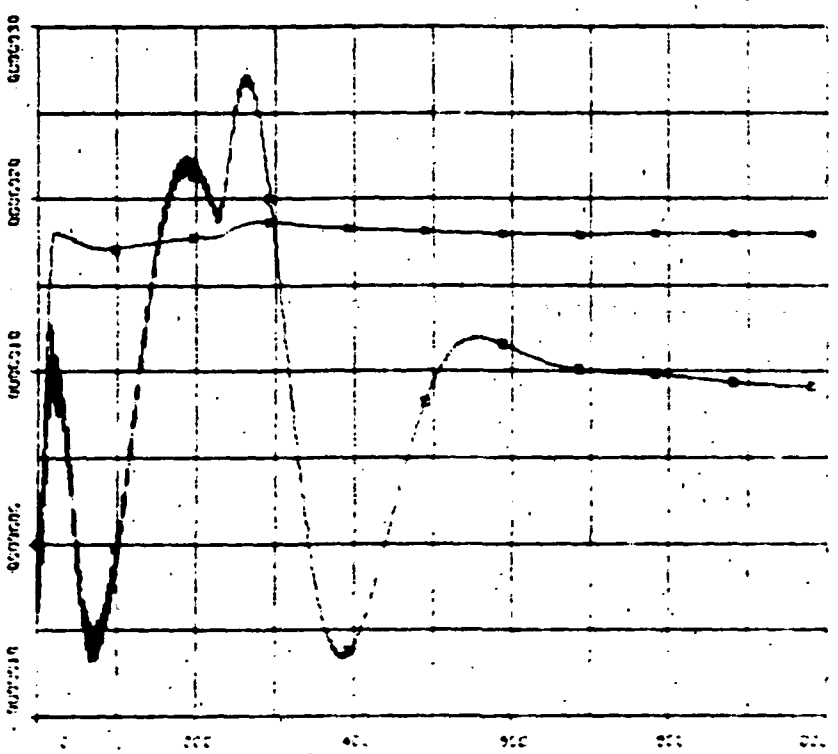

FIGURE 3-12

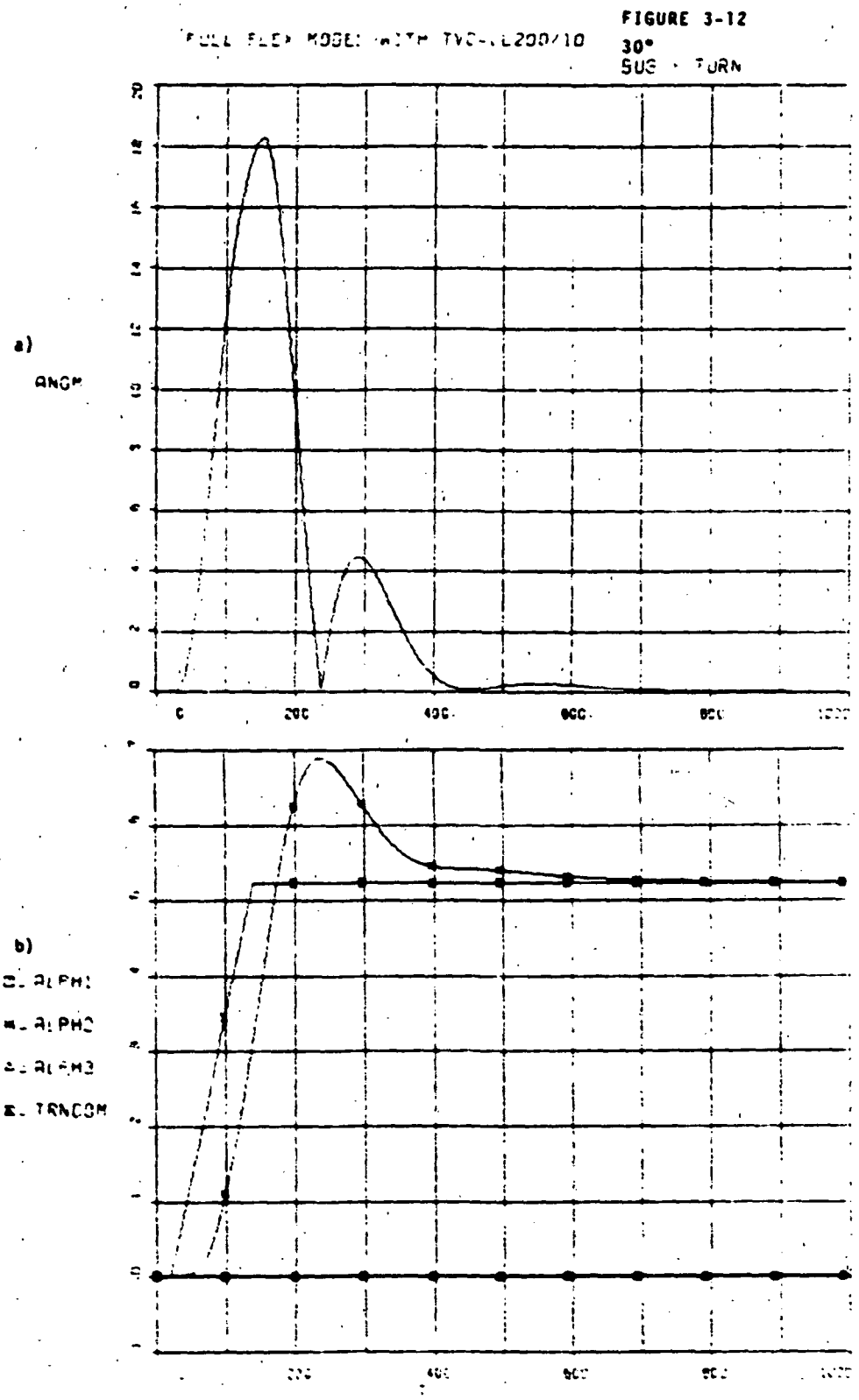

30° bus turn with solar arrays remaining pointed to the sun. Overshoot -30% (highly dependent on commanded final position). Smooth transient with no signs of excitation of flexible dynamics.

FIGURE 3-12

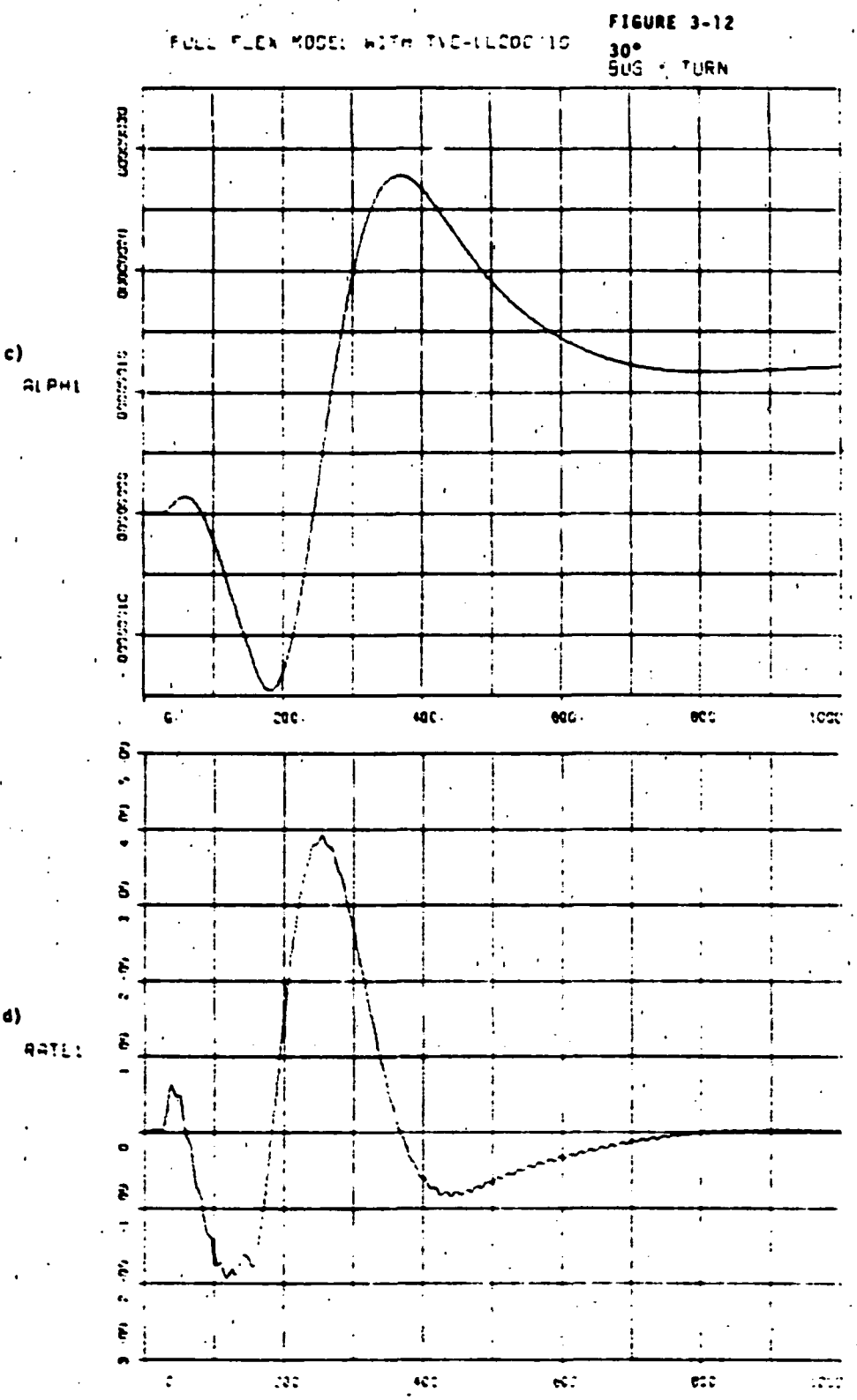

Negligible cross-coupled motion in pitch.

FIGURE 3-12

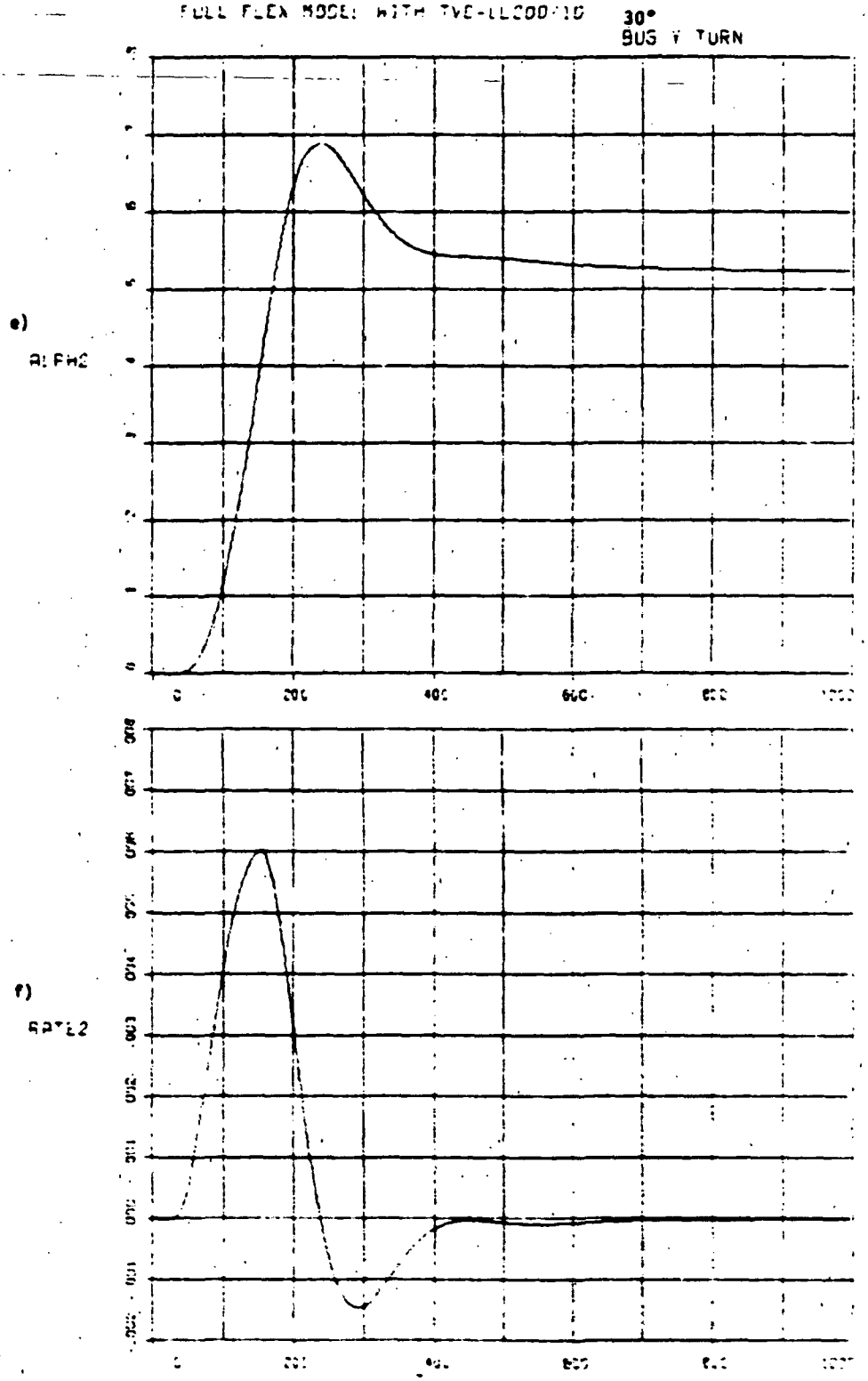

This yaw turn took about 450 seconds. e) Position reaches commanded position in about 180 s, then overshoots it by -31%. f) Rate reaches command rate (0.25°/s) in about 100 s, then overshoots it by -37%.

FIGURE 3-12
30°
BUS Y TURN

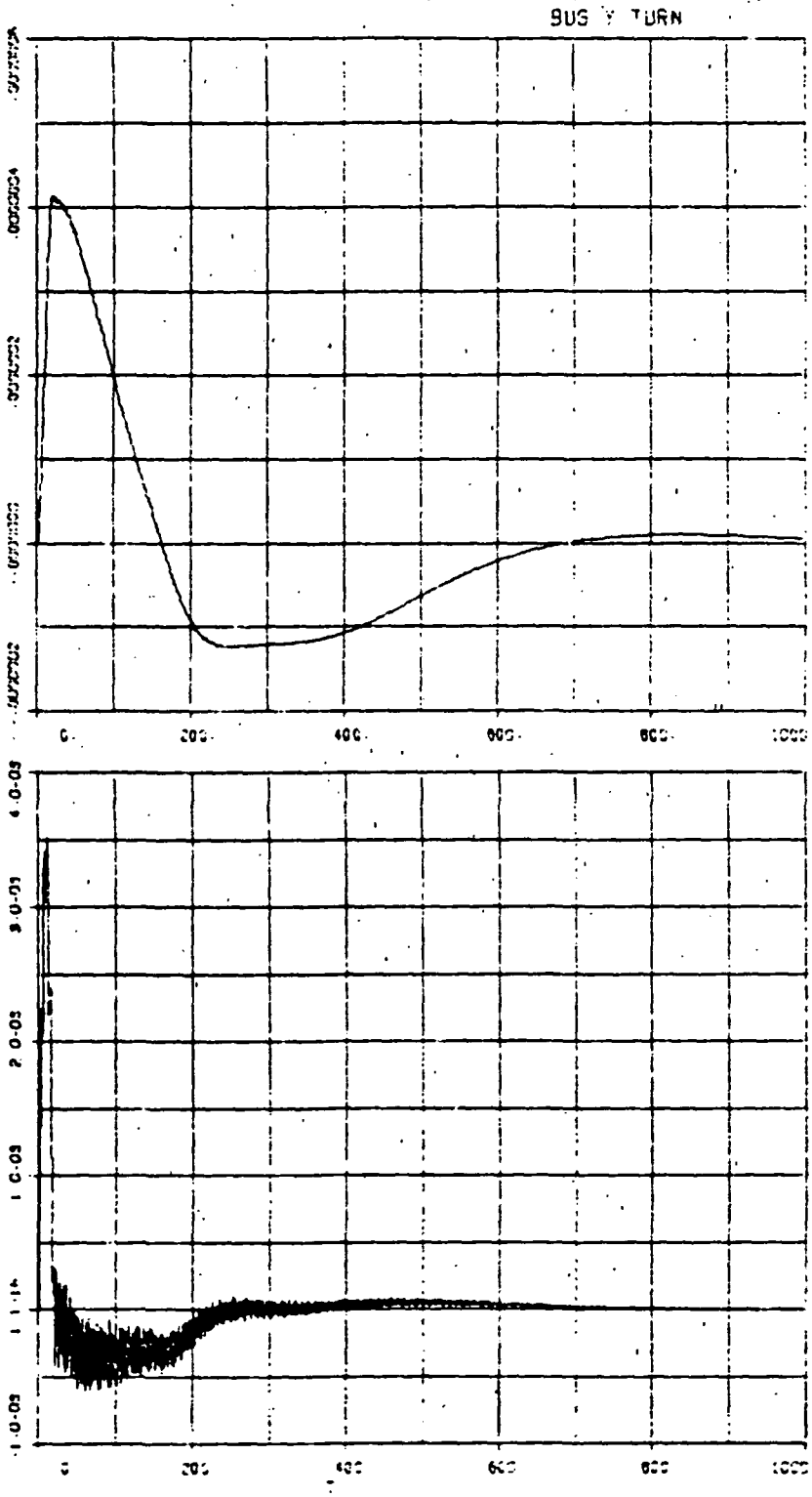

Negligible cross-coupled motion in roll.

FIGURE 3-12

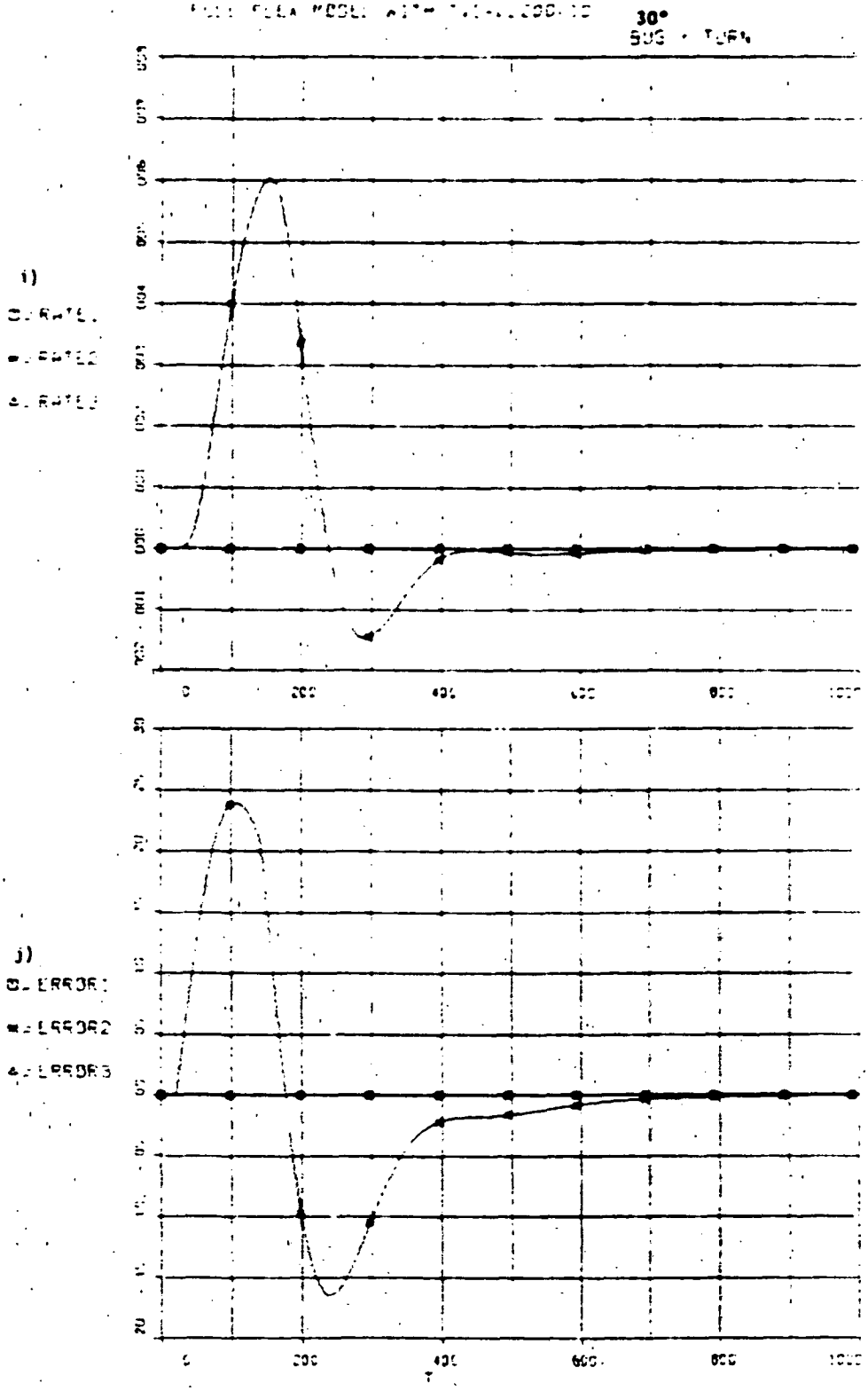

FIGURE 3-12

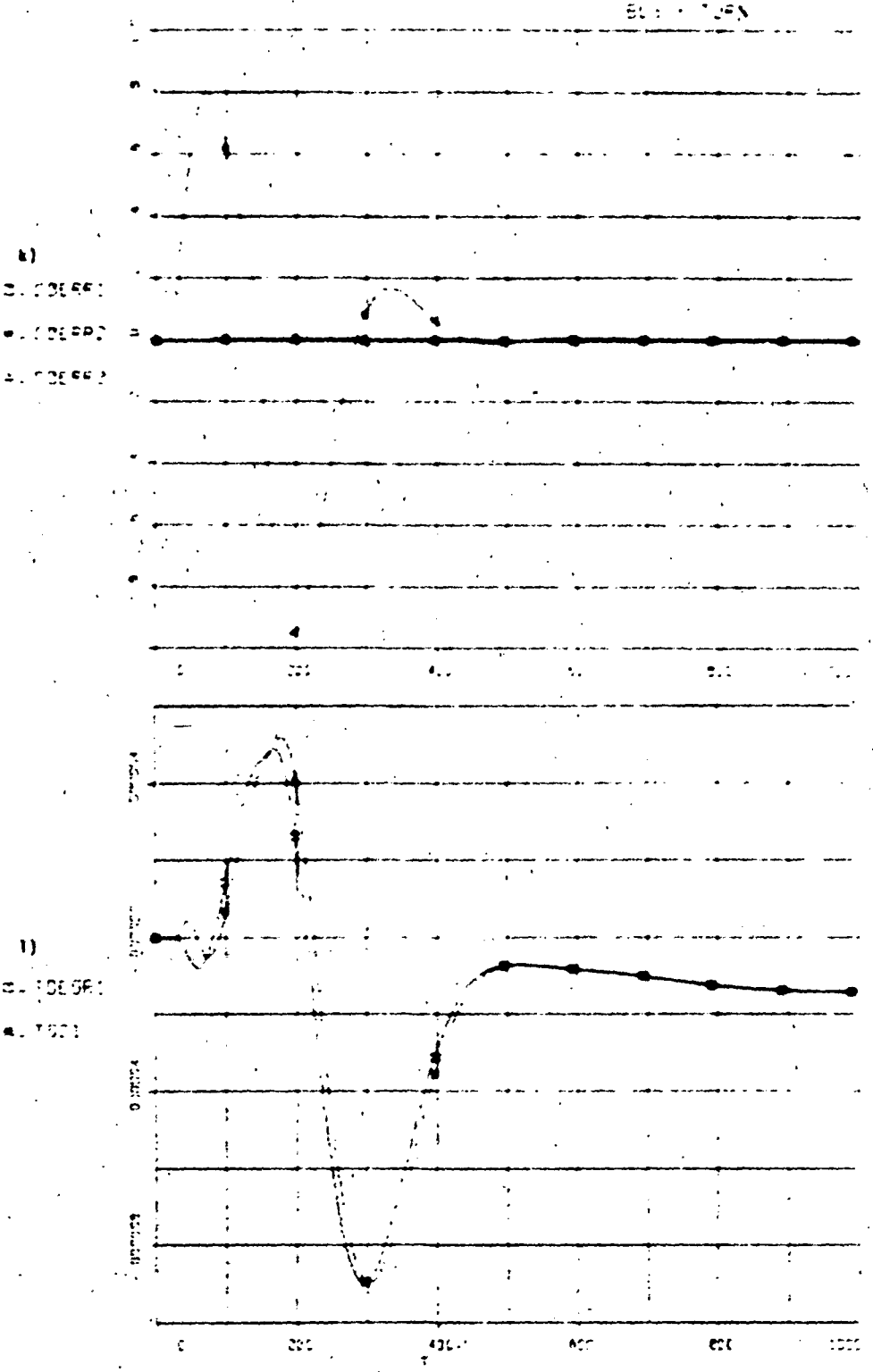

1) Negligible torques on pitch axis.

FIGURE 3-12

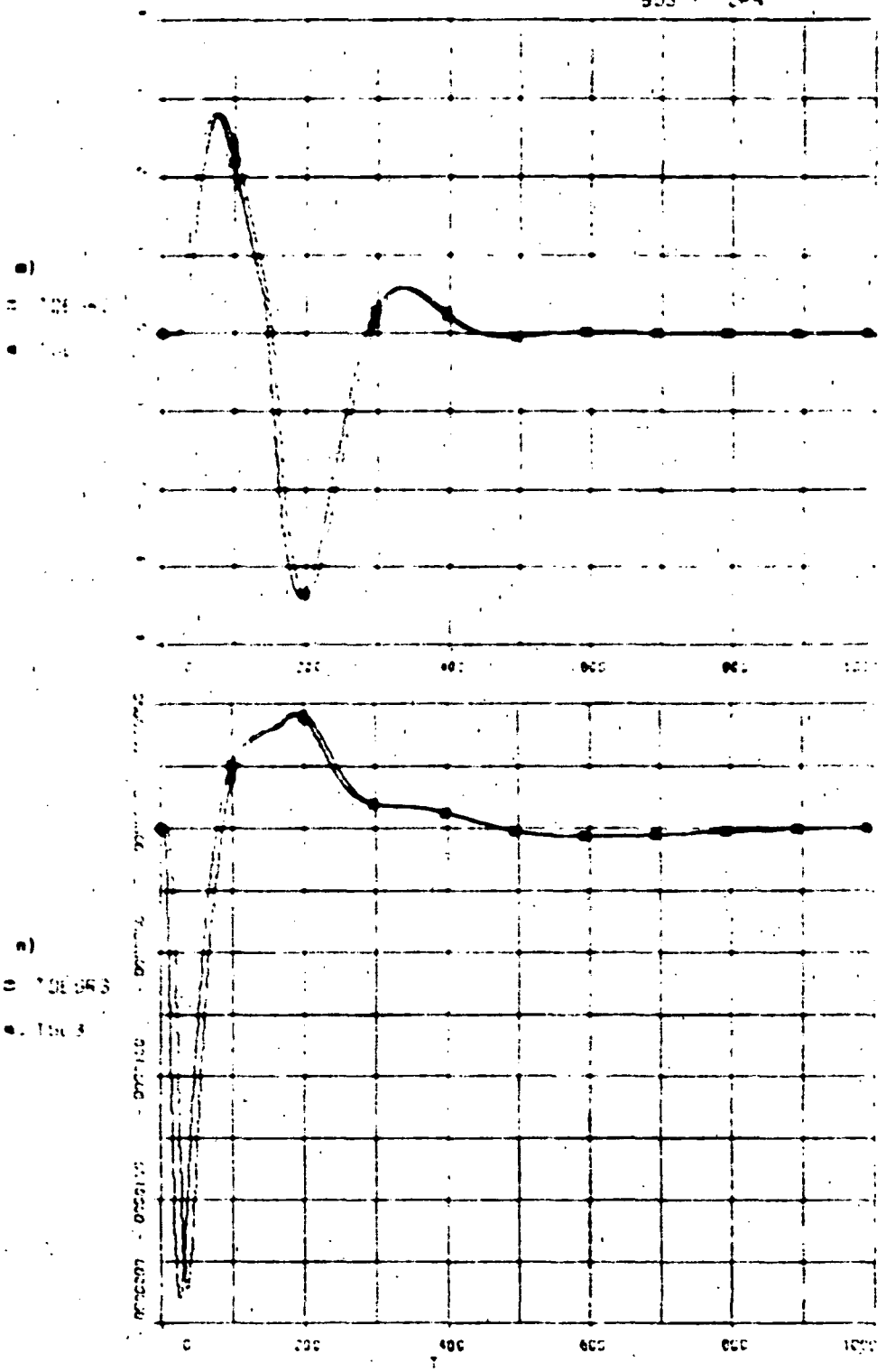

m) Yaw control torques are smooth (low-frequency content) do not excite solar panel vibrations. n) Very small roll transient appears to be due to thruster turn-on transient.

FIGURE 3-12
30°
SUS - TURN

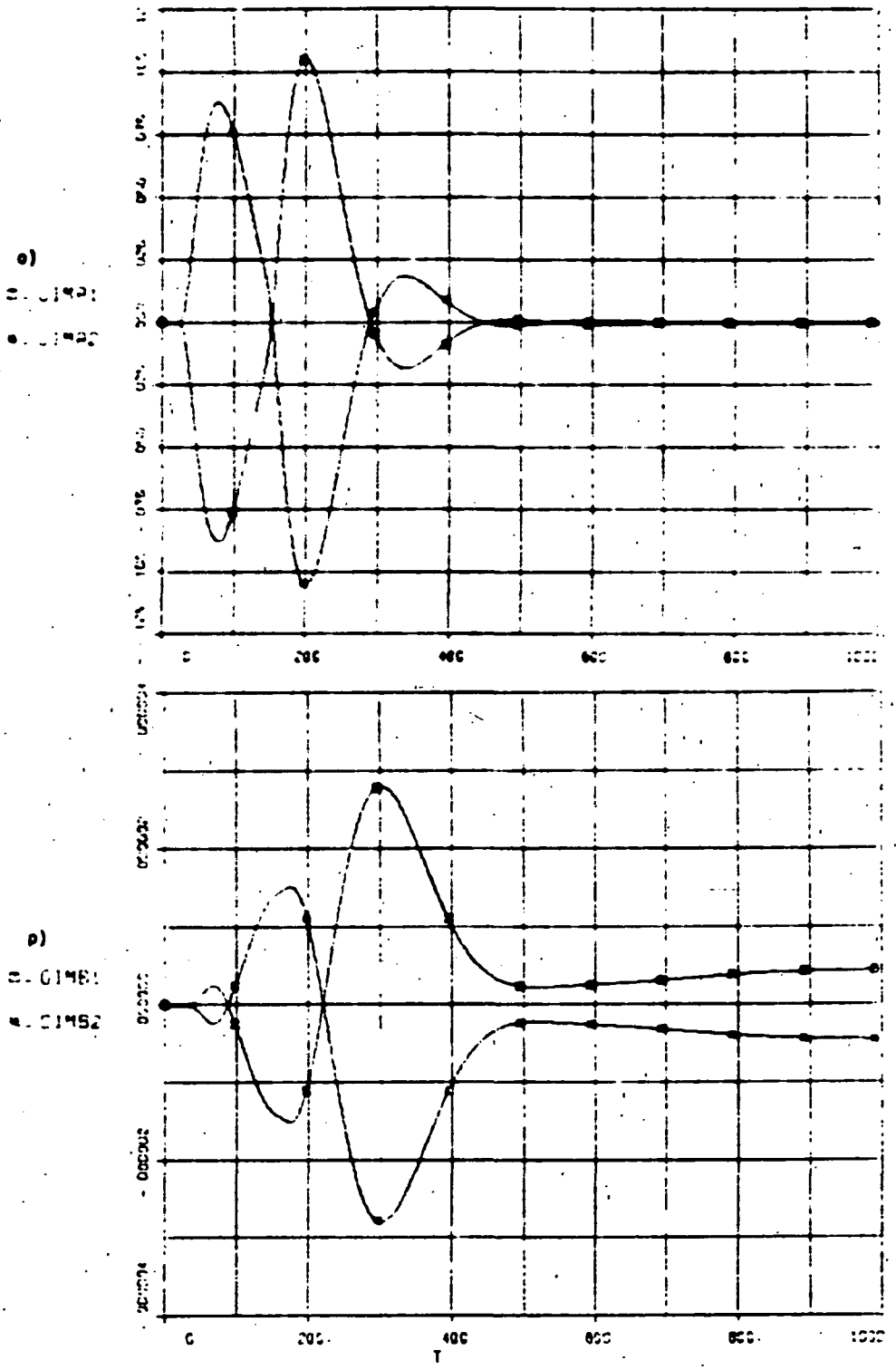

Predominant α-gimbaling o) produces yaw turning torques for 30° turn. Max gimbal angle -6.3°. Max gimbal rate 0.22°/s, see q).

FIGURE 3-12
30°
SOS

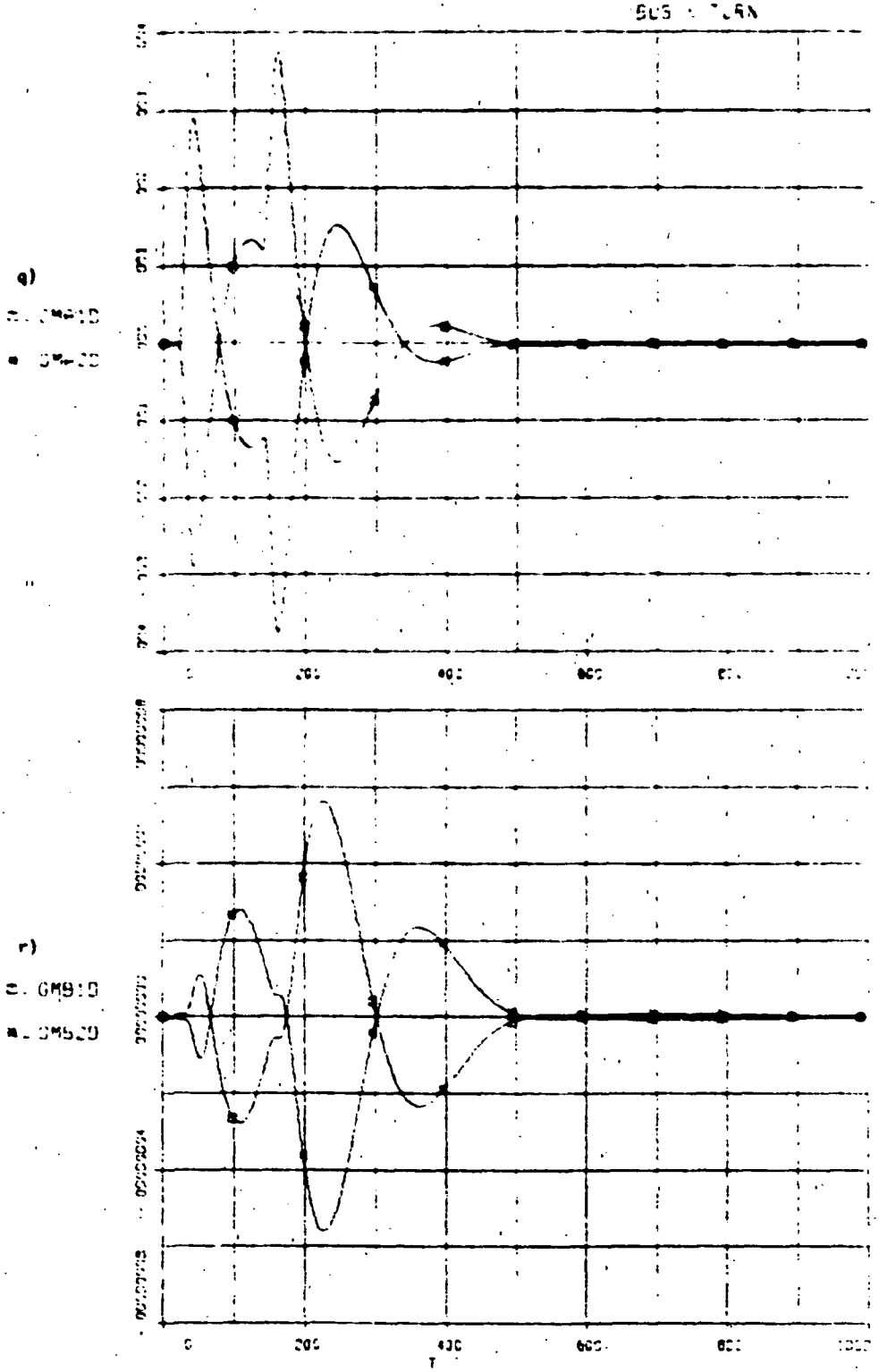

FIGURE 3-12

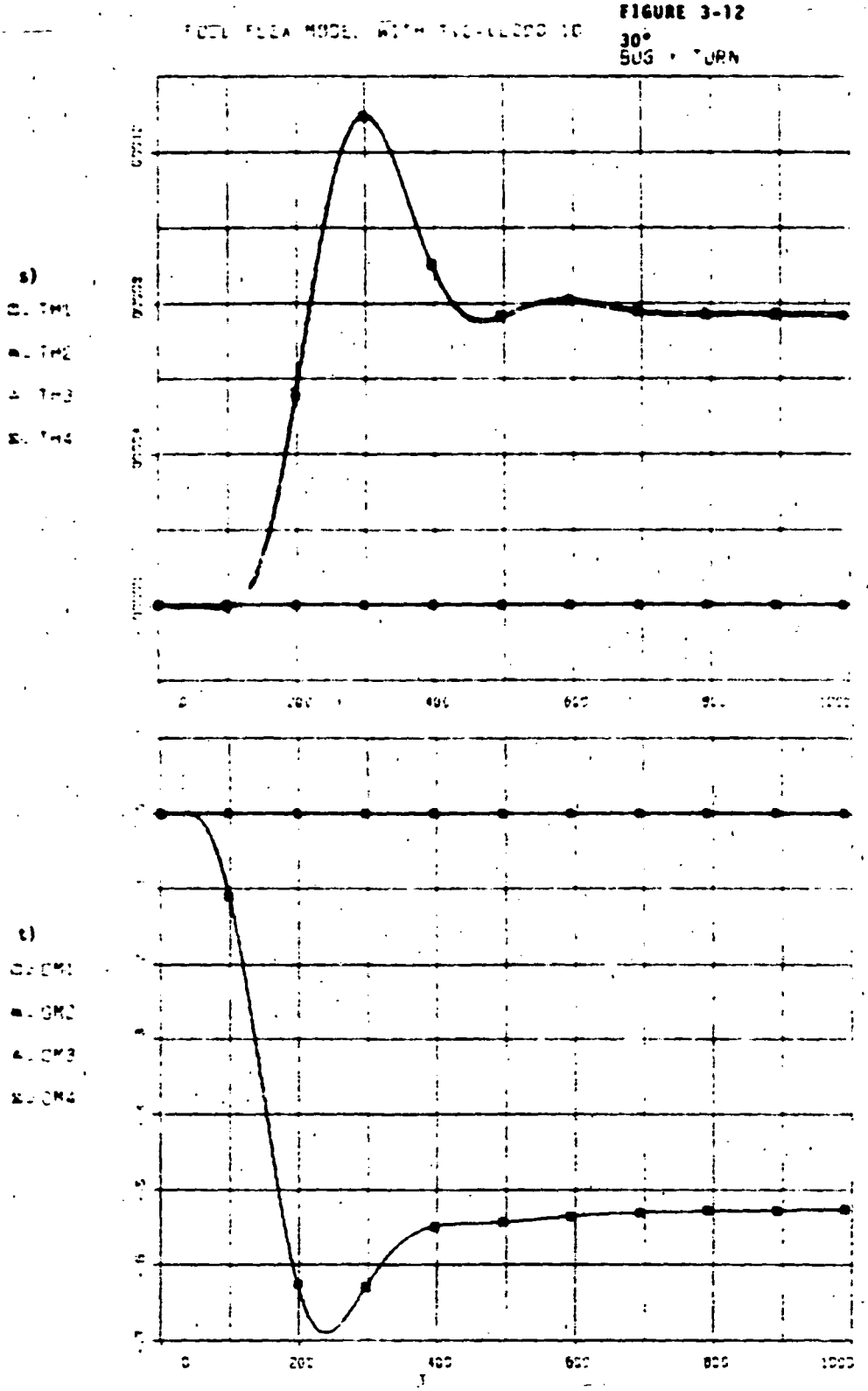

s) Small SA hinge torques. t) SA wings turn -30° with respect to bus so as to stay on sun as bus turns.

FIGURE 3-12
30°
SUS - TURN

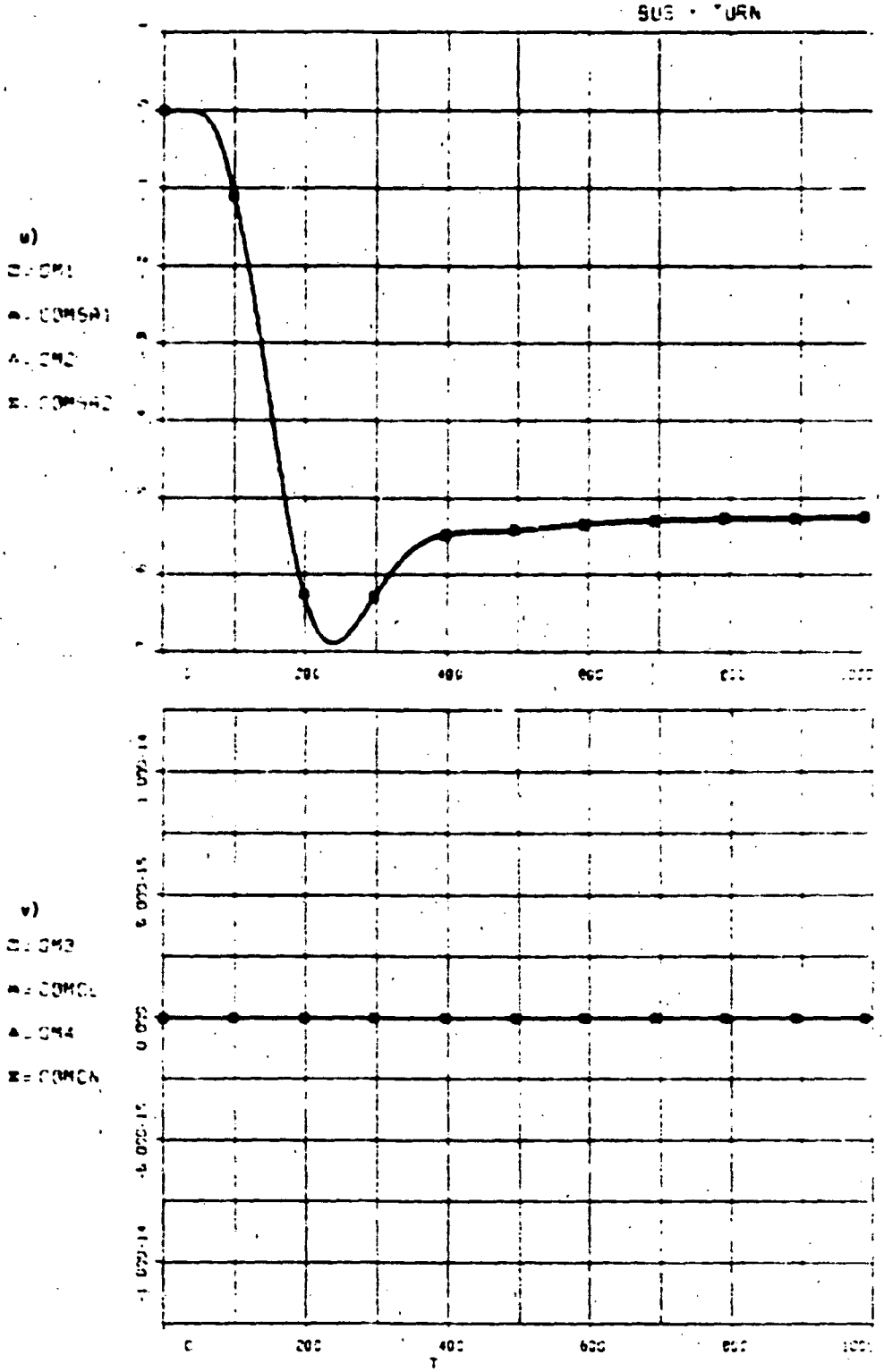

u) SA wings track their commands to -30°, with respect to bus. v) Scan platform locked in place for this maneuver.

FIGURE 3-12

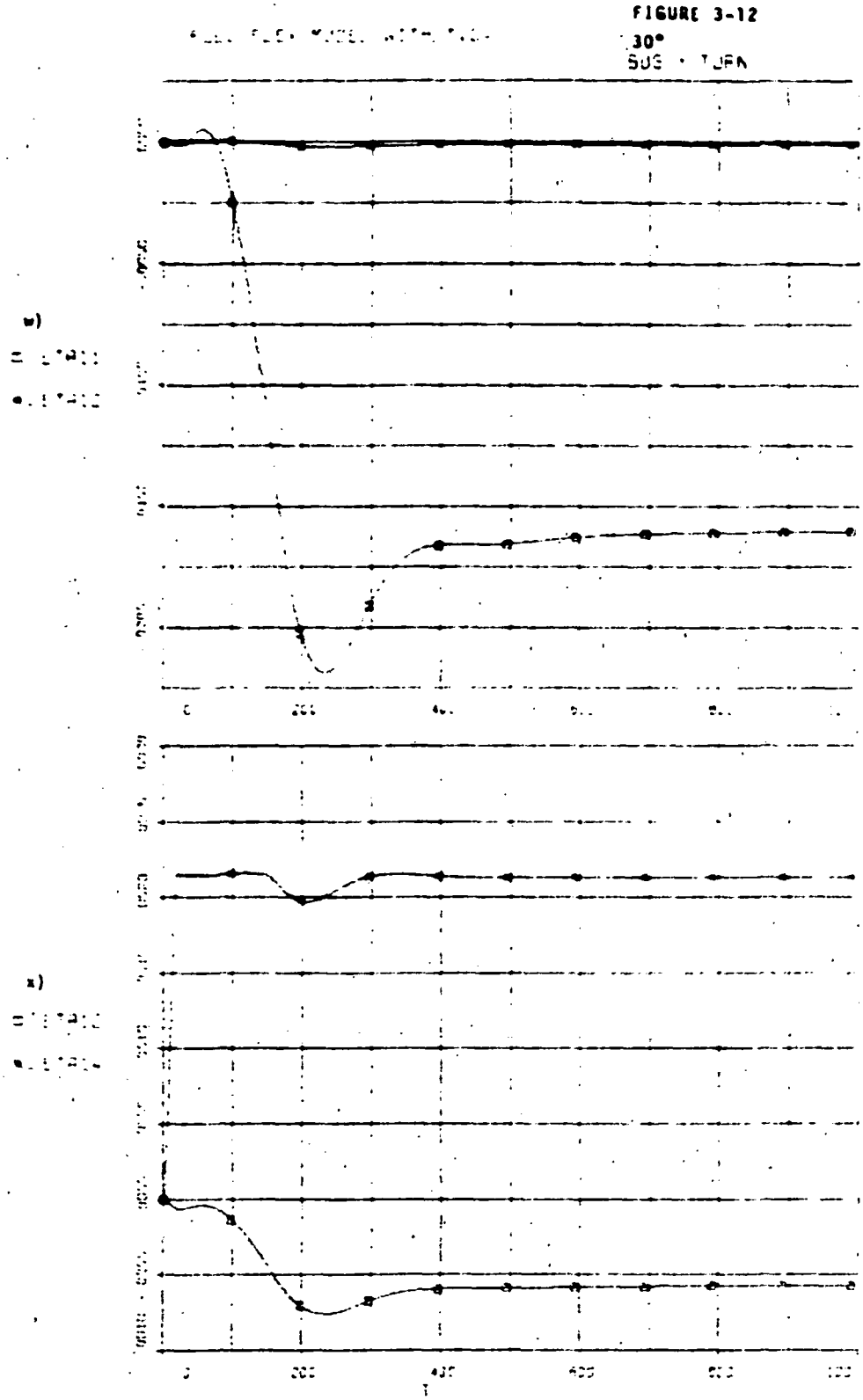

w) through z)
Note steady state solar panel deformation due to constant linear acceleration of venicle due to ion thrusters. Very low residual vibration levels.

FIGURE 3-12

30°
SUS : TURN

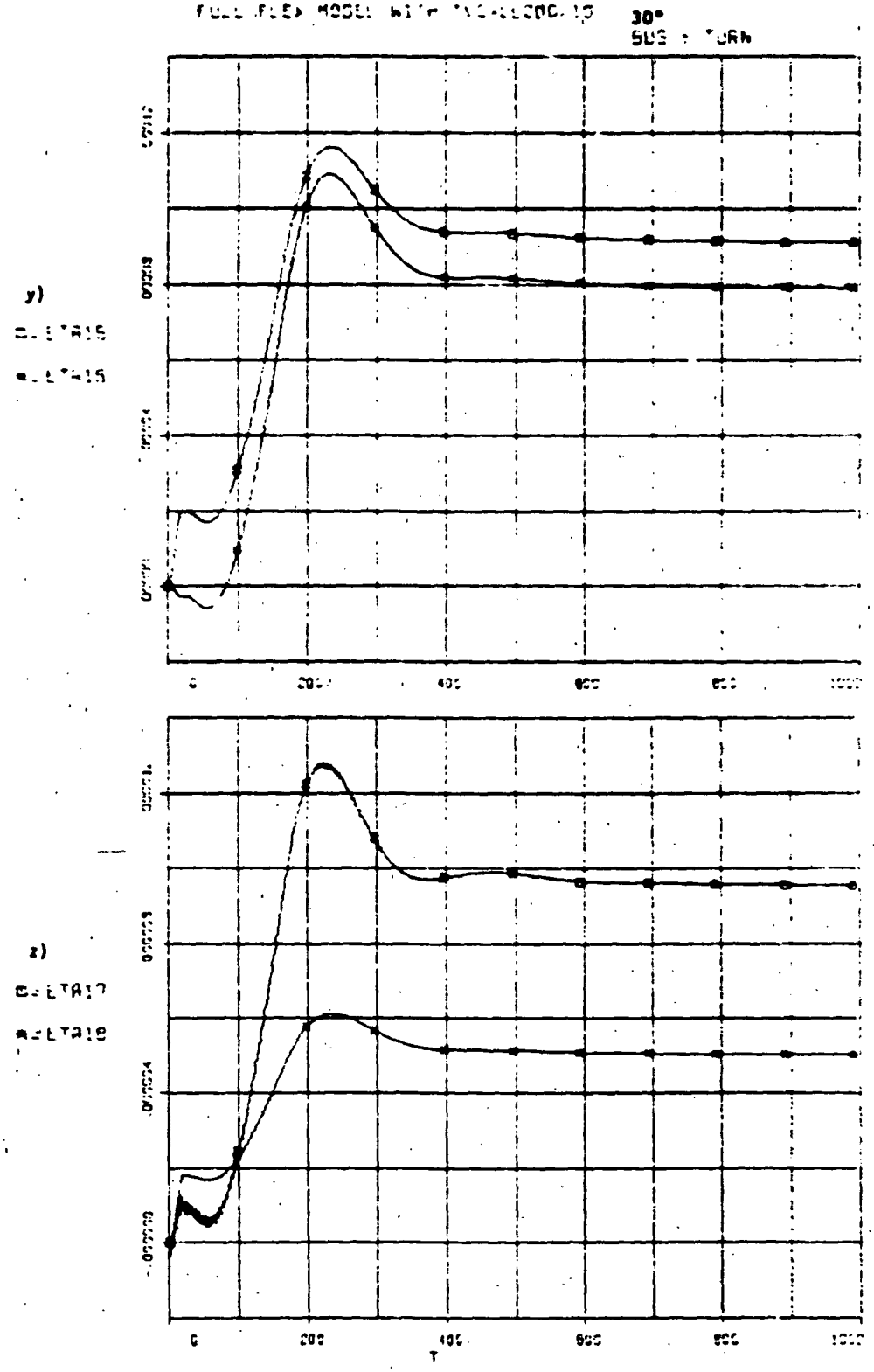

FIGURE 3-13

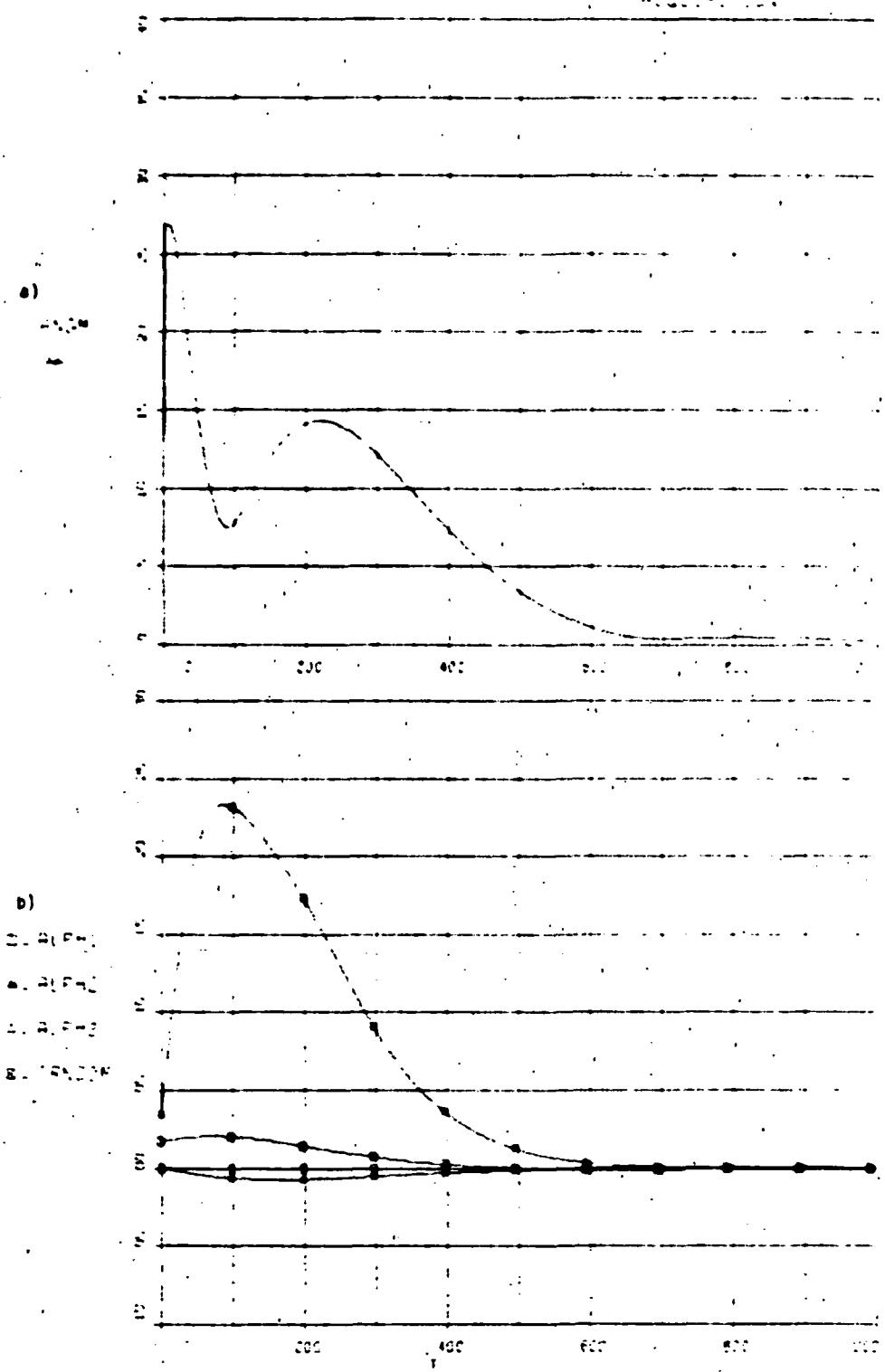

-700 seconds required for this particular set of acquisition initial conditions.

FIGURE 3-13

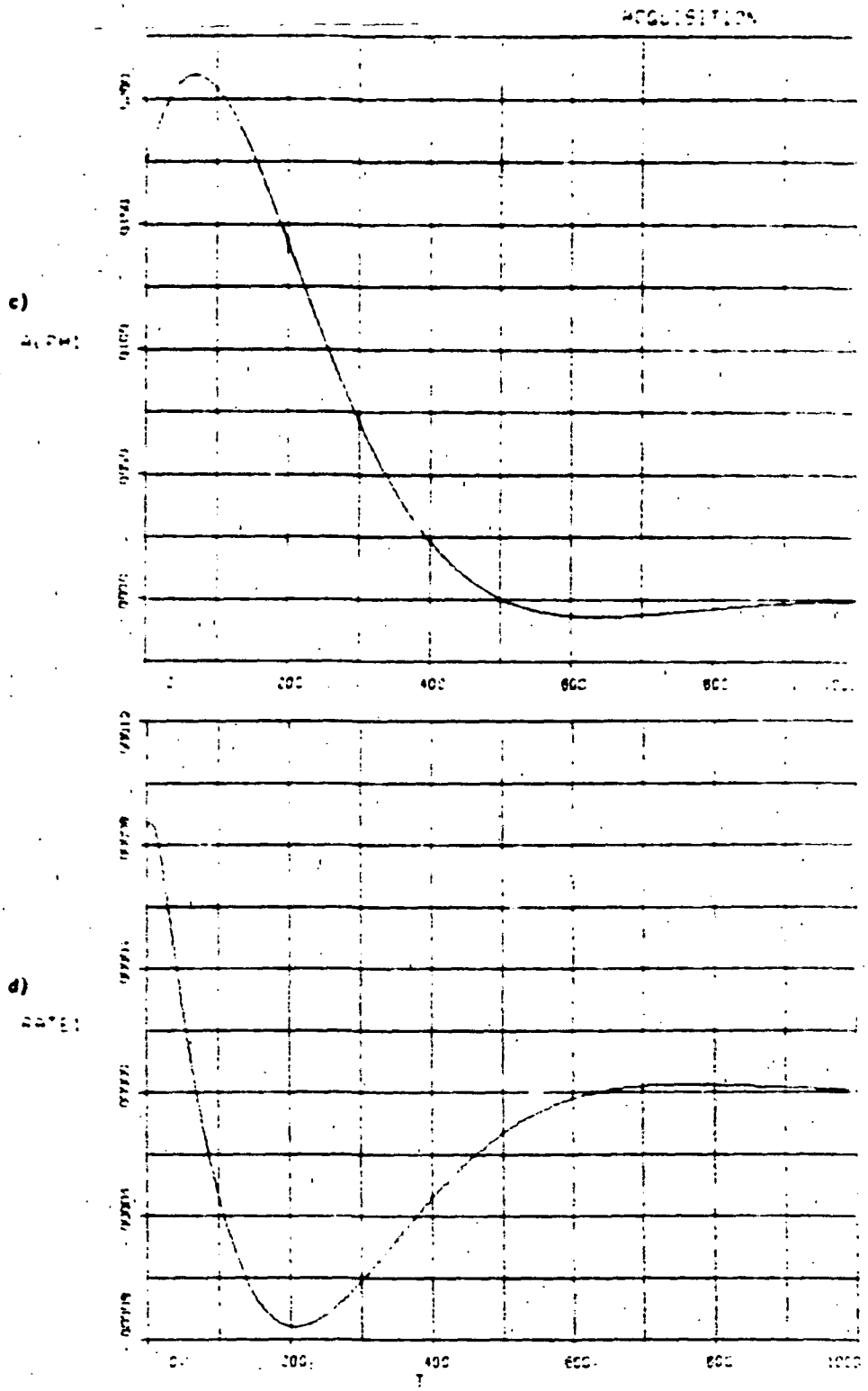

Pitch overshoots -0.18° before being turned around.

FIGURE 3-13

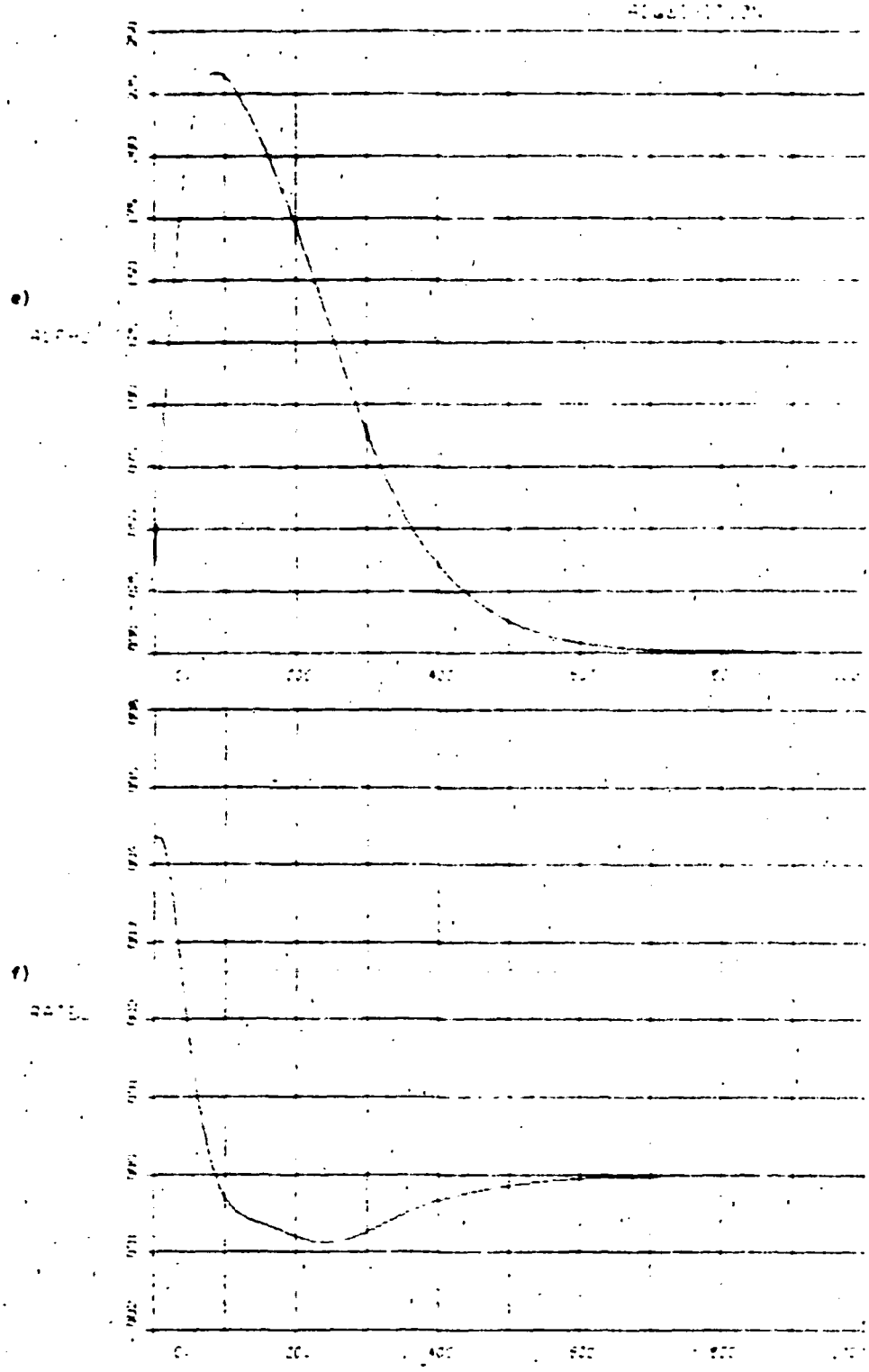

Yaw overshoots initial position by -11.3° before being turned around.

FULL FLEX MODE, WITH TVC-1200 IC **FIGURE 3-13**
ACQUISITION

g)
ALPH3

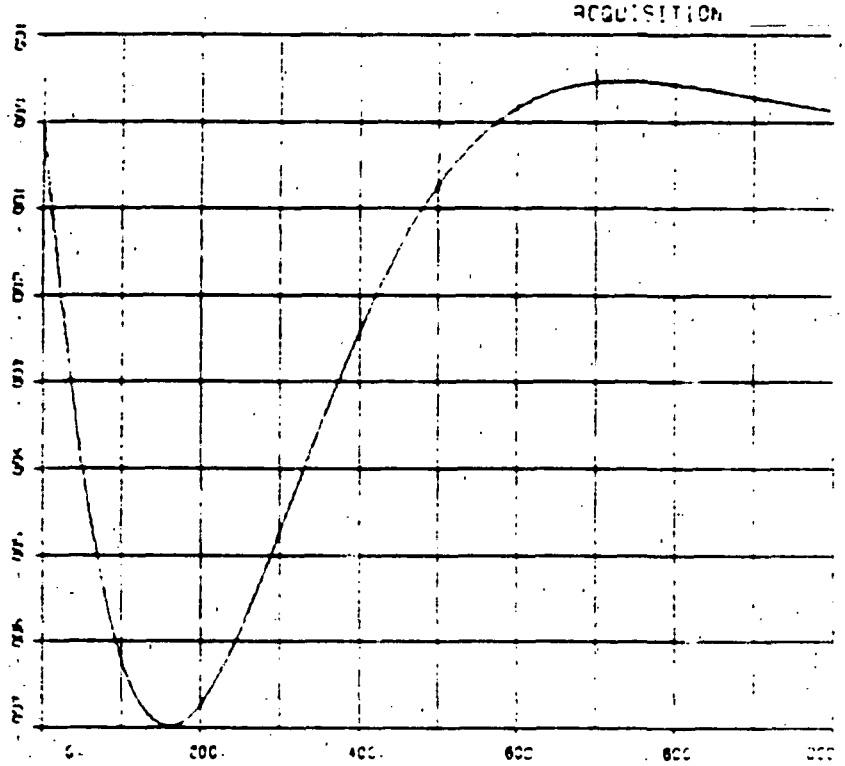

h)
RATE3

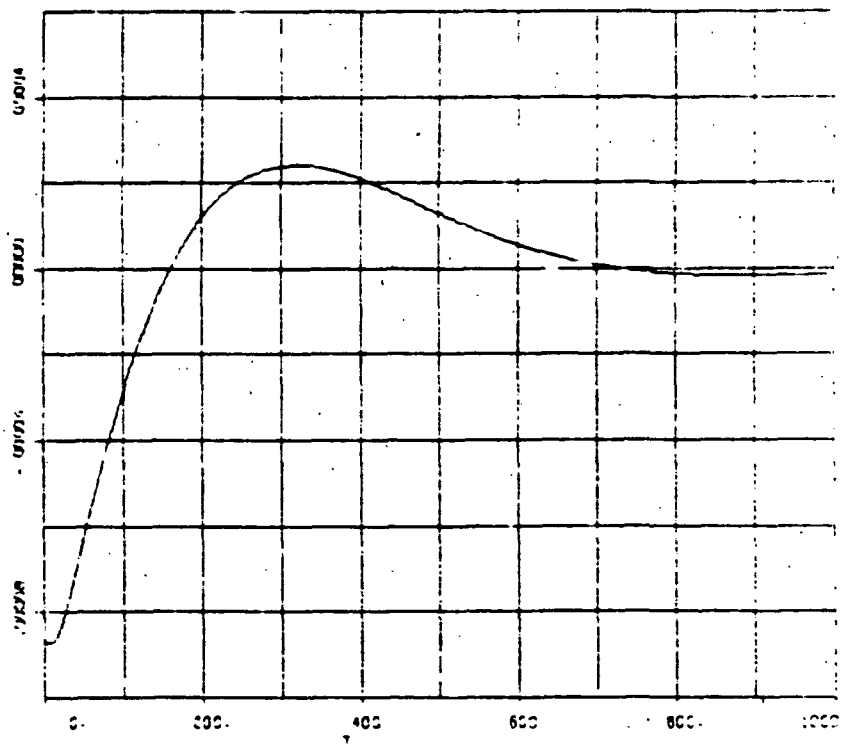

Roll overshoots by 0.4° before being turned around.

FIGURE 3-13

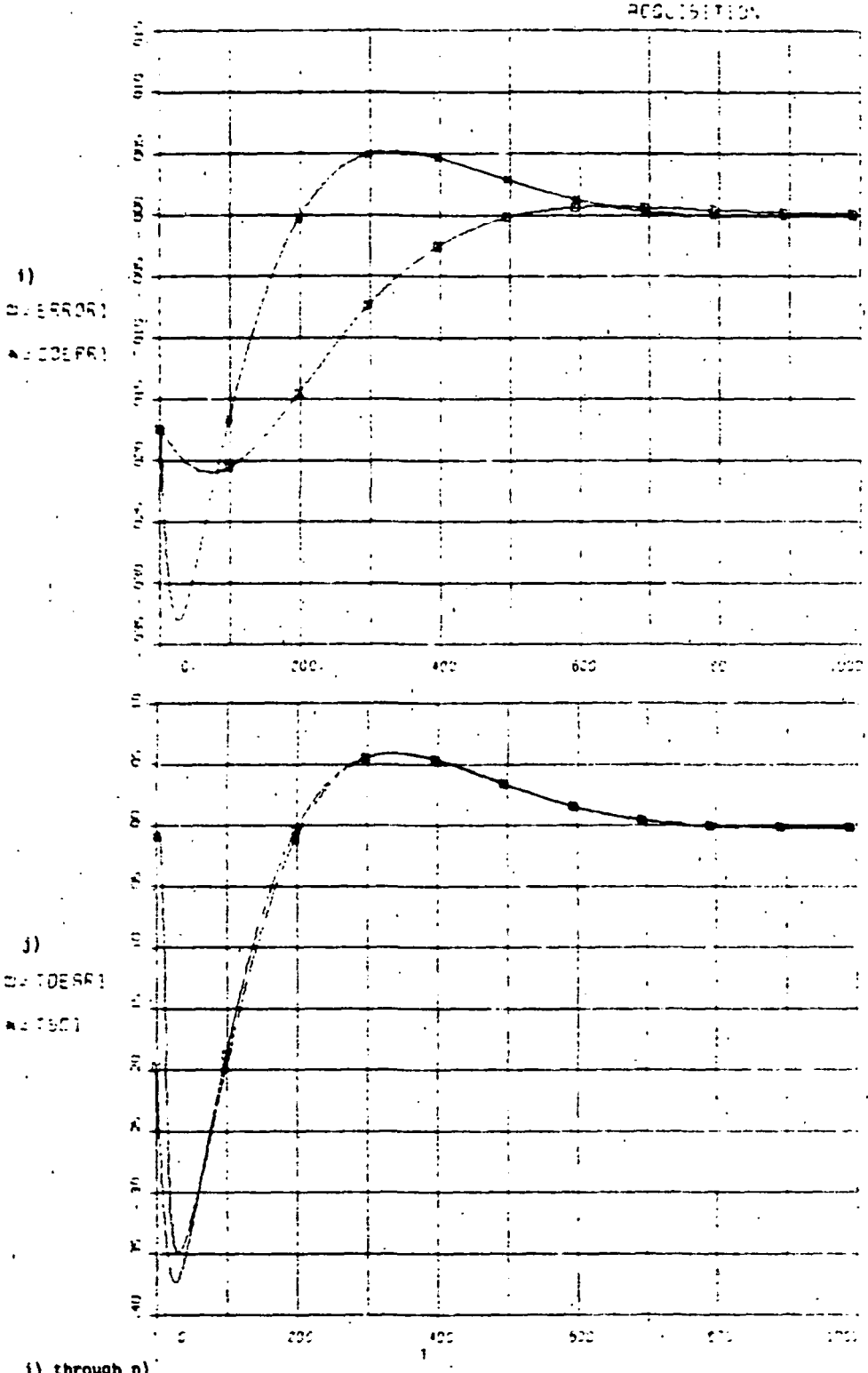

i) through n)
Control system on gimbals tracks desired torque quite well. Observe the smooth, slowly varying torques produced by gimbaling; their low frequency content causes vehicle to turn smoothly without exciting significant solar panel vibrations.

Page intentionally left blank

Page intentionally left blank

FULL FLEX MODEL WITH TVC-LL20C/10 **FIGURE 3-13**
ACQUISITION

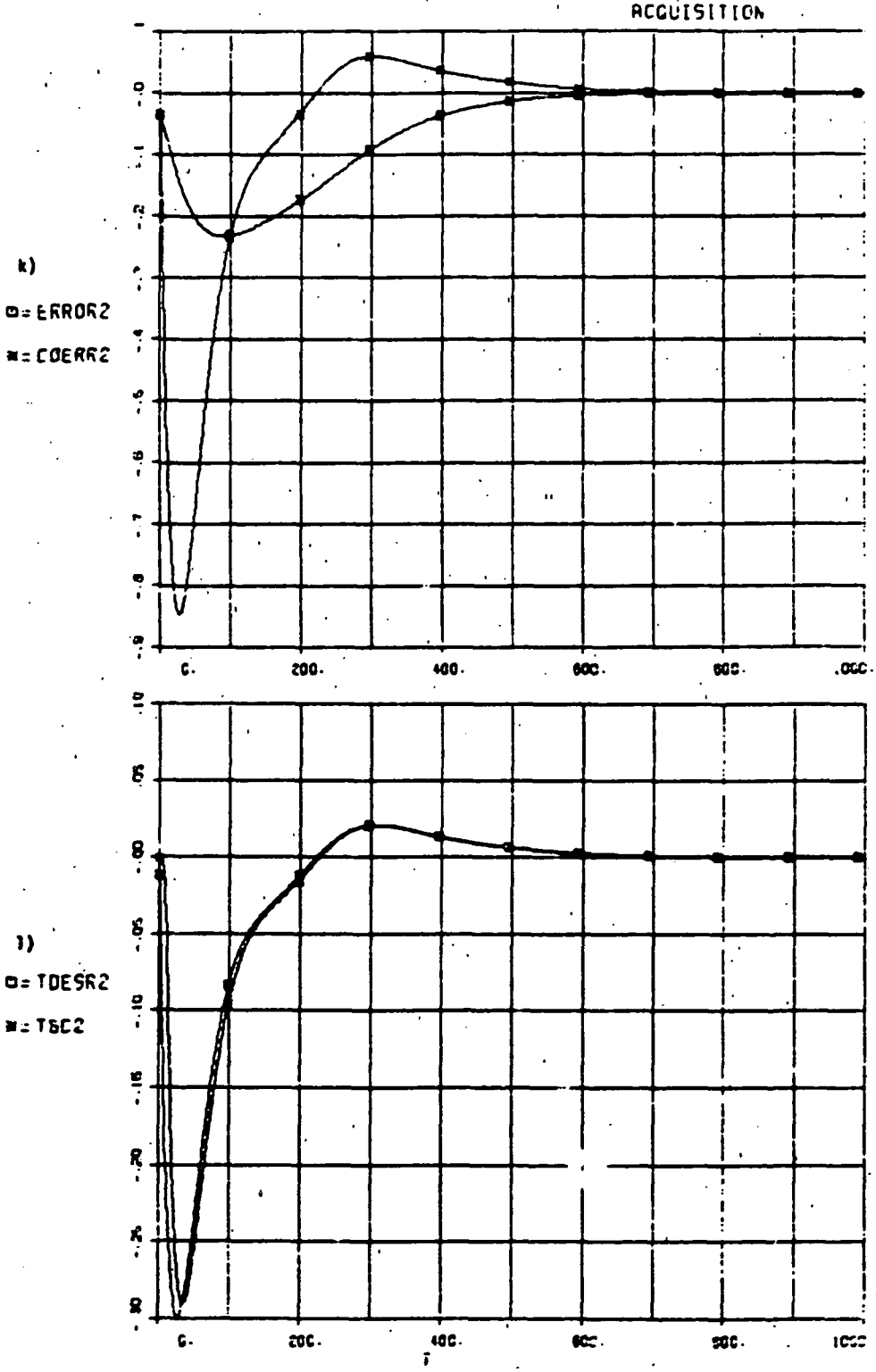

C-2

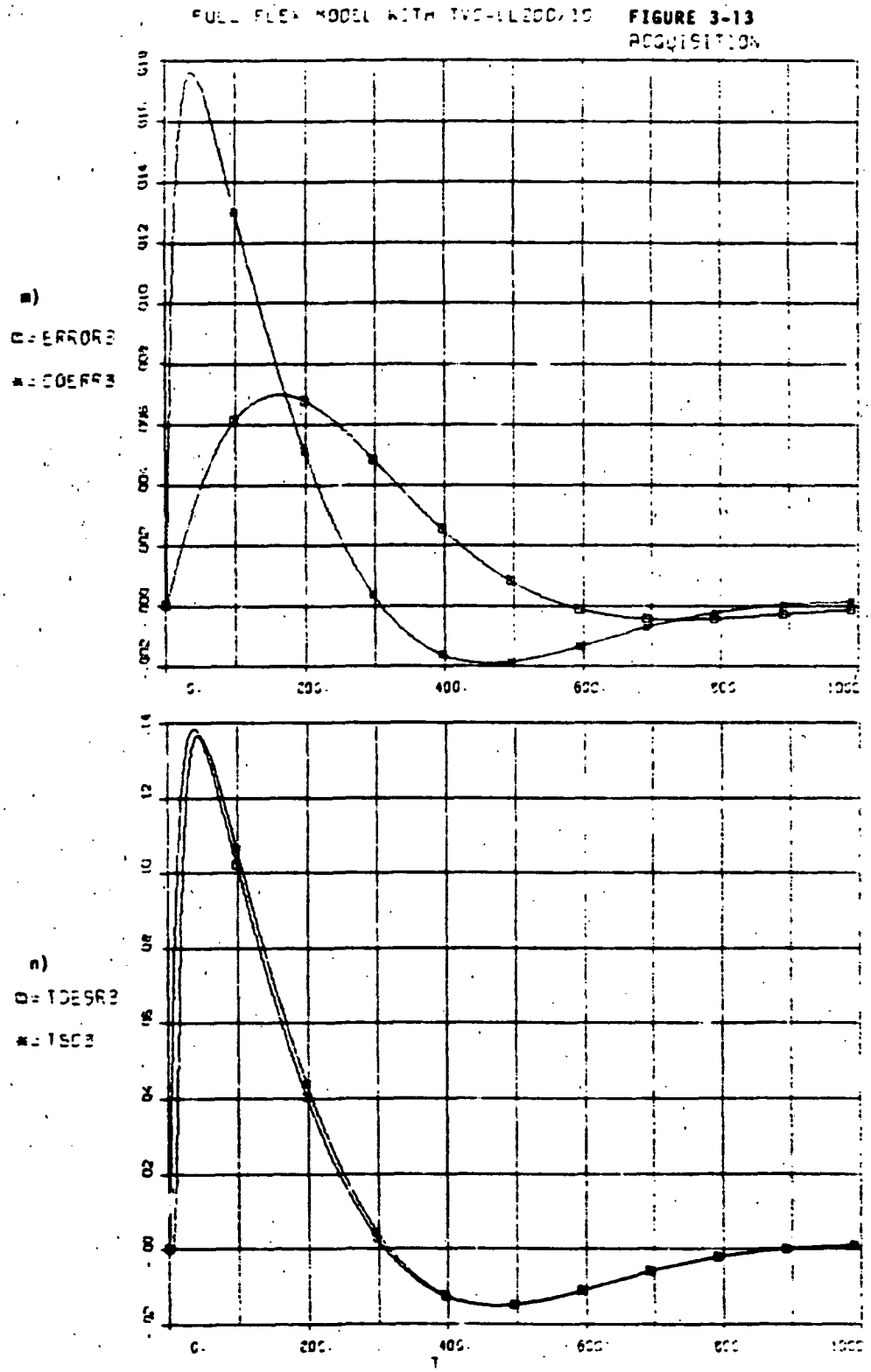
FULL FLEX MODEL WITH TVC-ILQGDC/IC
ACQUISITION
a)
□ = ERROR3
* = DERR3
b)
□ = TDESR3
* = TSC3
T

FIGURE 3-13

FULL FLEX MODEL WITH TVC-FEEDBACK

FIGURE 3-13
ACQUISITION

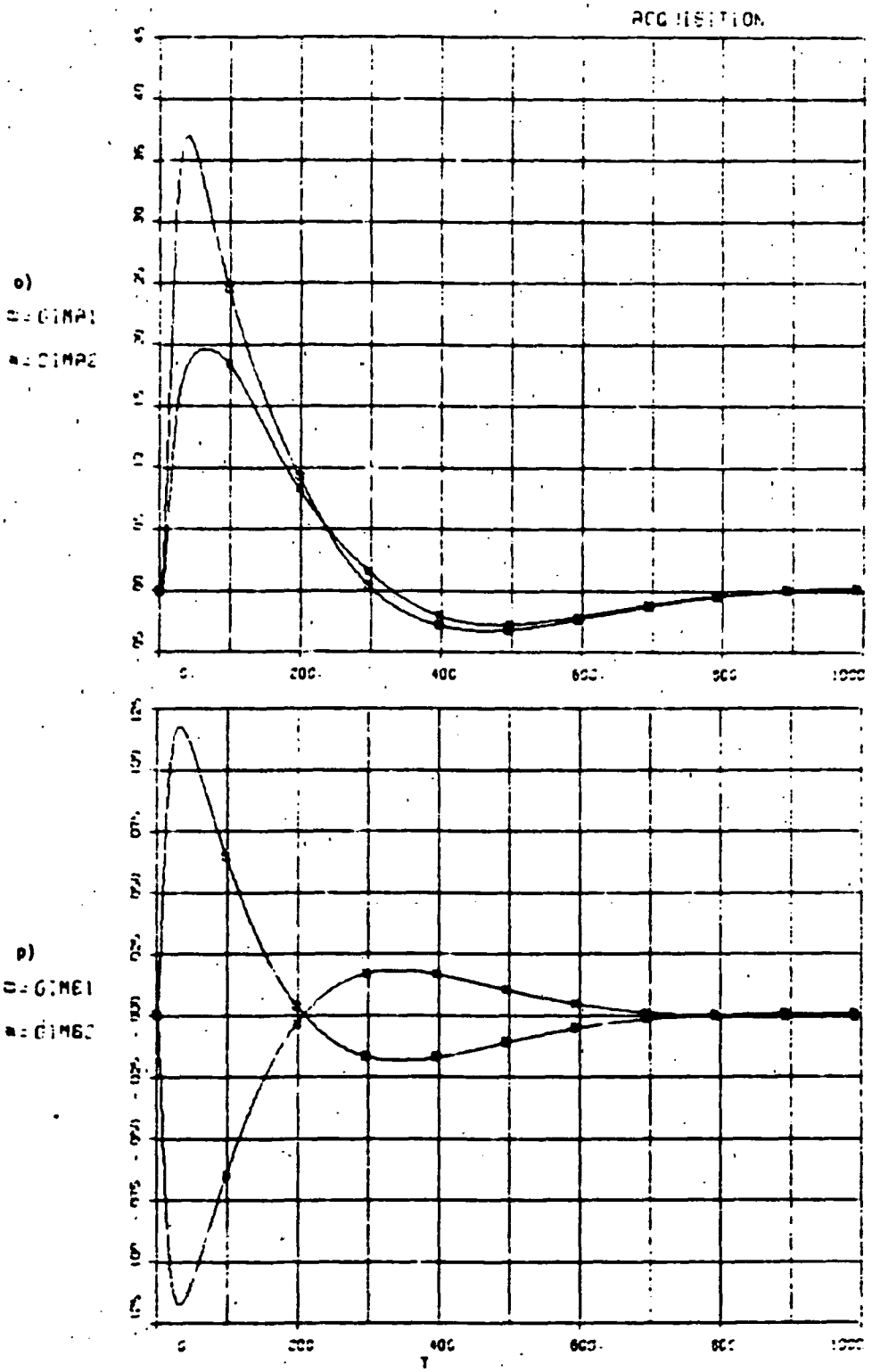

...gimbals move to control yaw and roll. Maximum α-gimbal angle -21°, max rate 1.08°/s, ...q). β gimbals move to control pitch transient. Max β-gimbal angle -7°, max rate 0.42°/s.

FULL FLEX MODEL WITH TWO-BLOCK IC

FIGURE 3-13
ACQUISITION

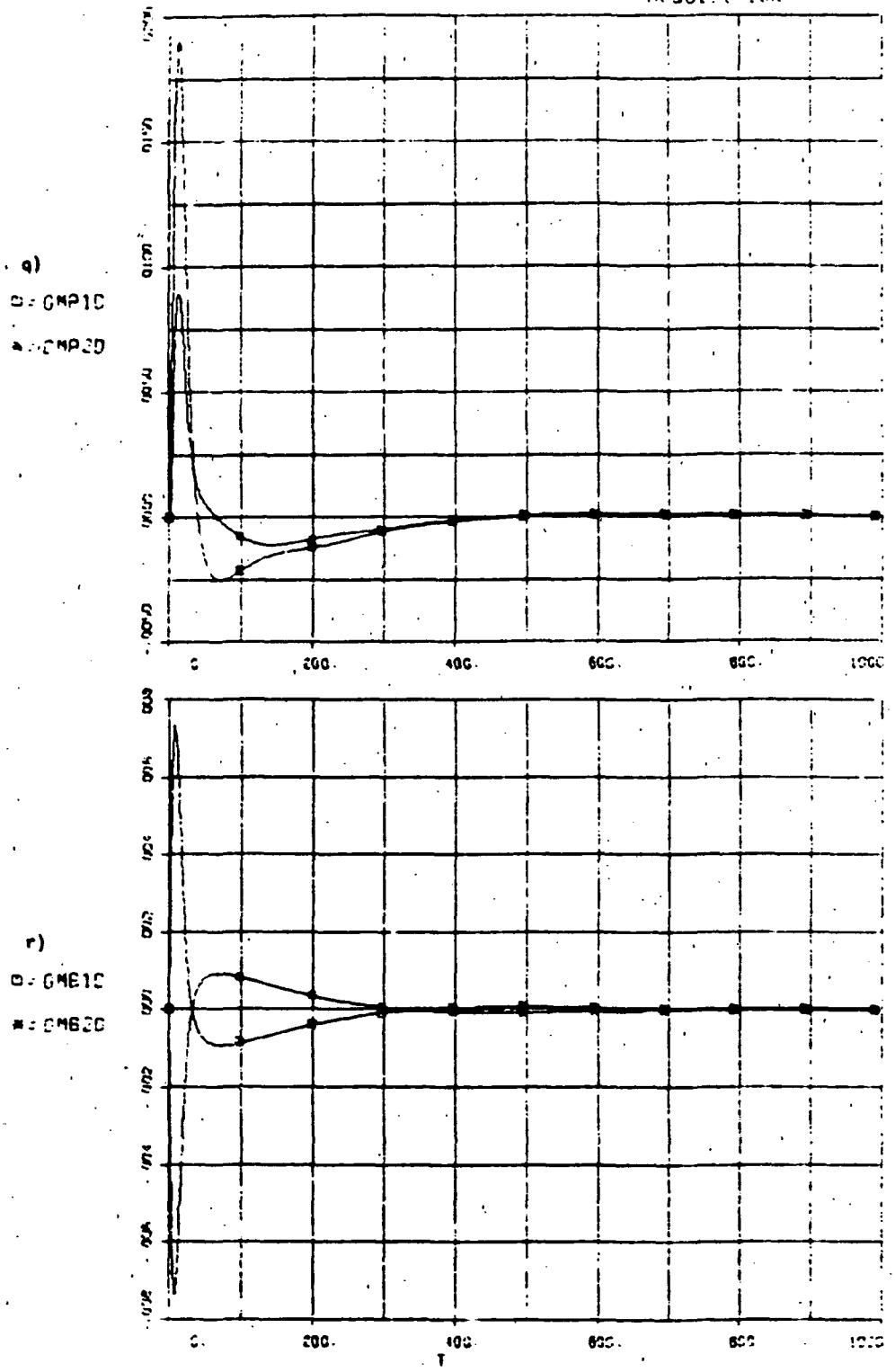

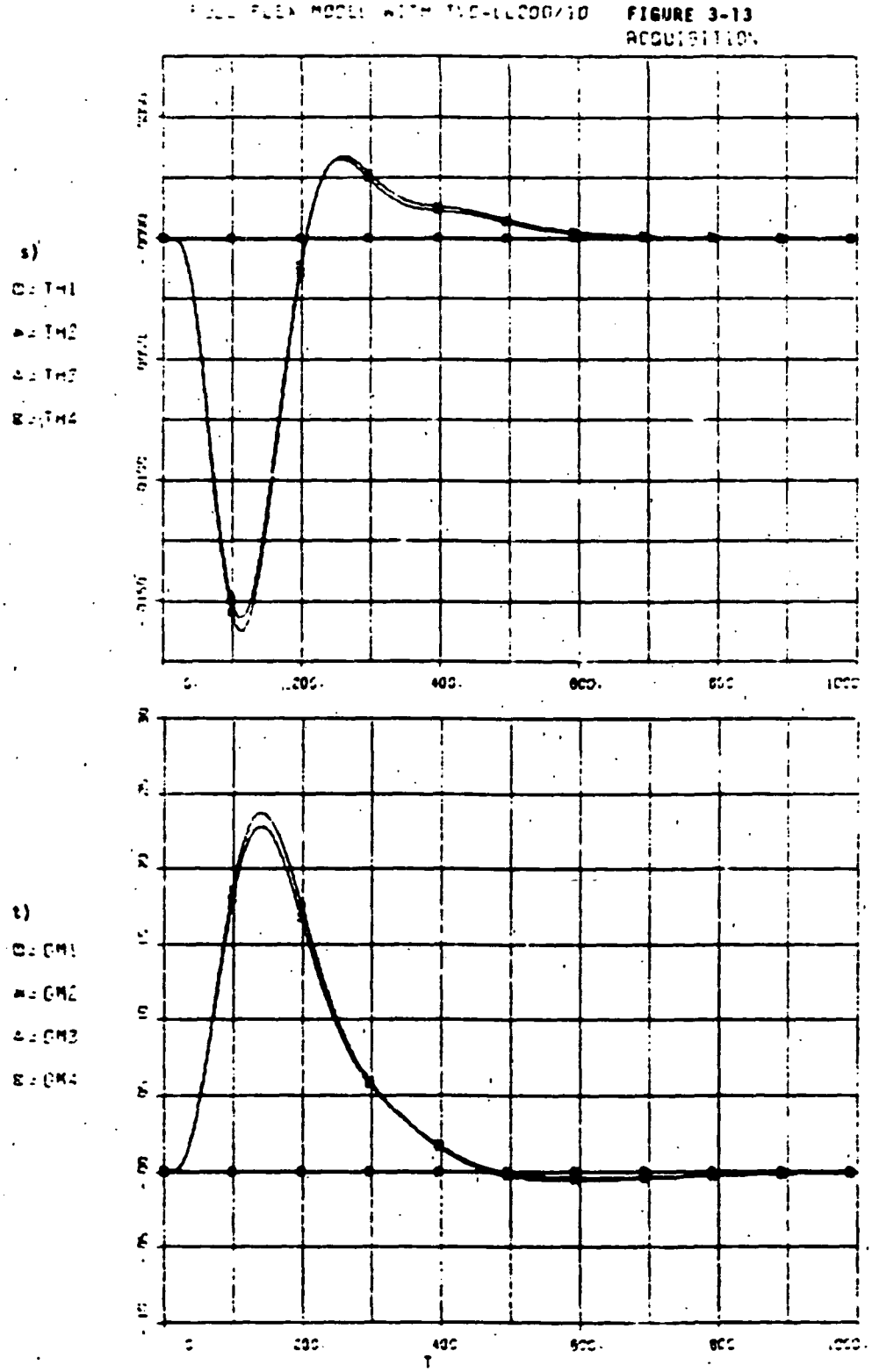

FIGURE 3-13
ACQUISITION

s) Small SA hinge torques. t) SA hinge rotation transient of -13.7°.

FULL FLEX MODEL WITH TVC-LL200/1G FIGURE 3-13
ACQUISITION

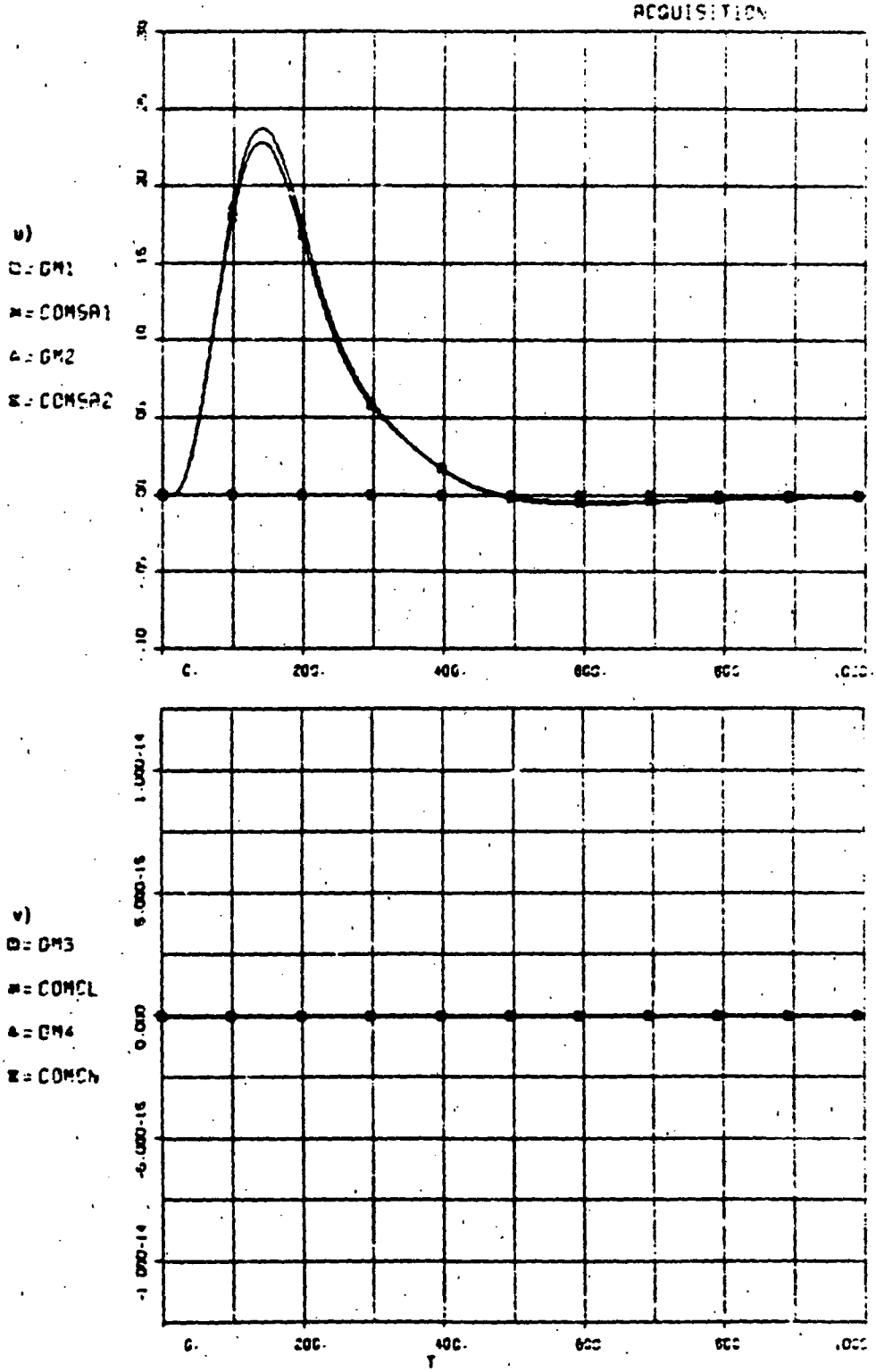

v) Scan platform locked in place for this maneuver.

FULL FLEX MODEL WITH TVC-LL200-10 **FIGURE 3-13**
ACQUISITION

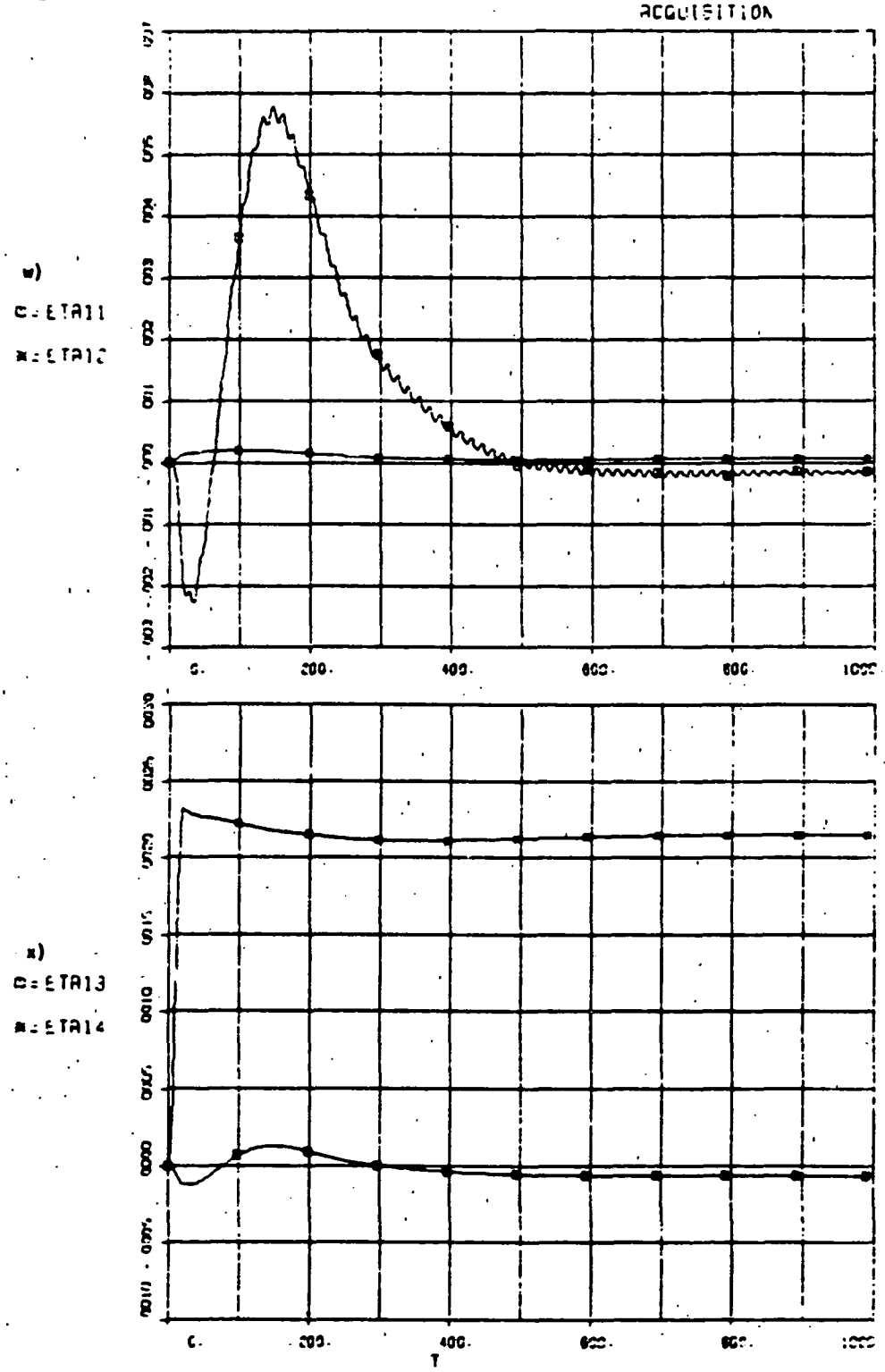

w) through z)
Note steady state solar panel deformation due to linear vehicle acceleration due to thrusting. Very low residual vibration levels.

FULL FLEX MODEL WITH TVC-LL200/15 **FIGURE 3-13**
ACQUISITION.

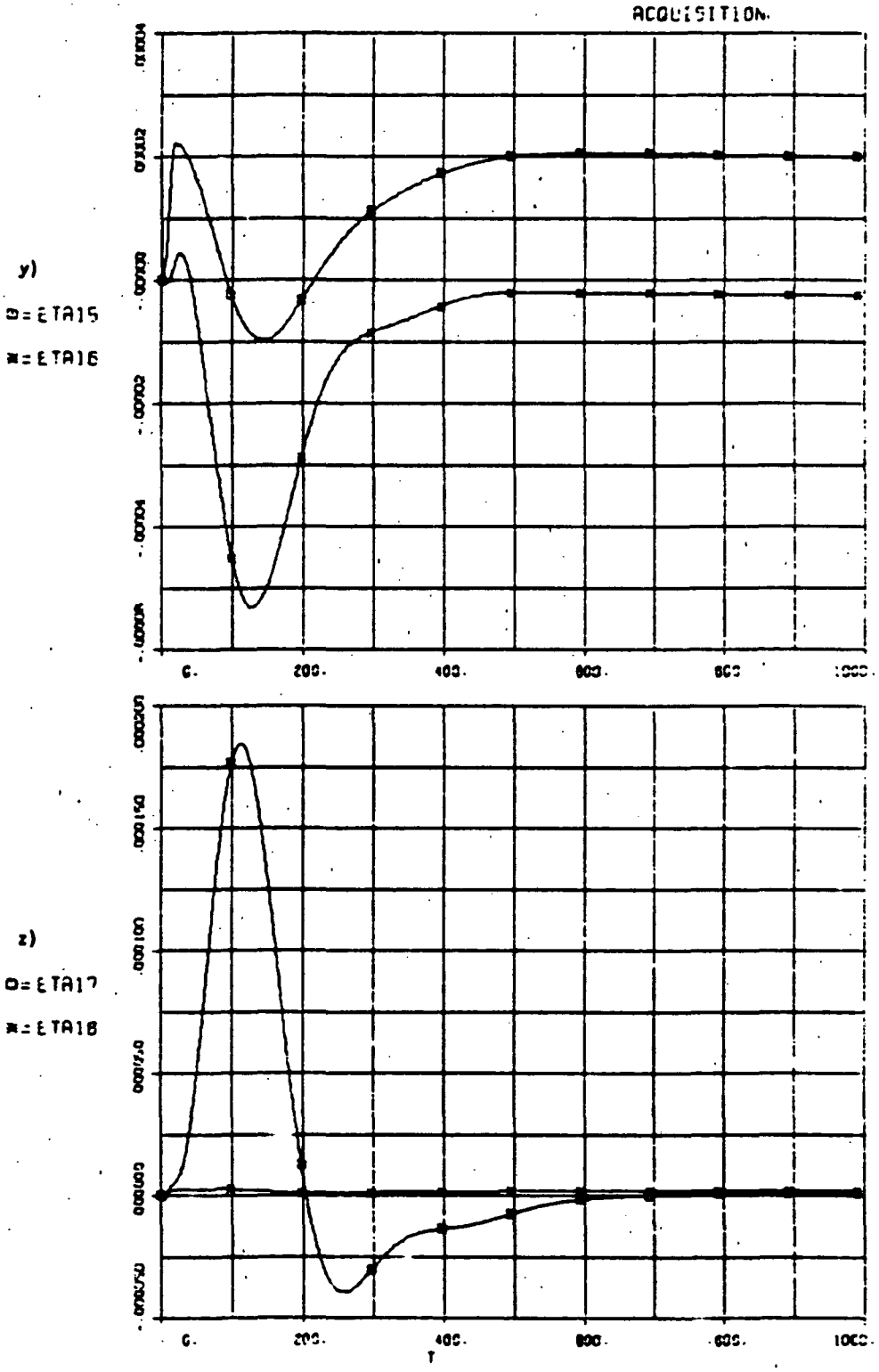

FULL FLEX MODEL WITH TVC-ILLEGIBLE

FIGURE 3-14
BOX SCAN

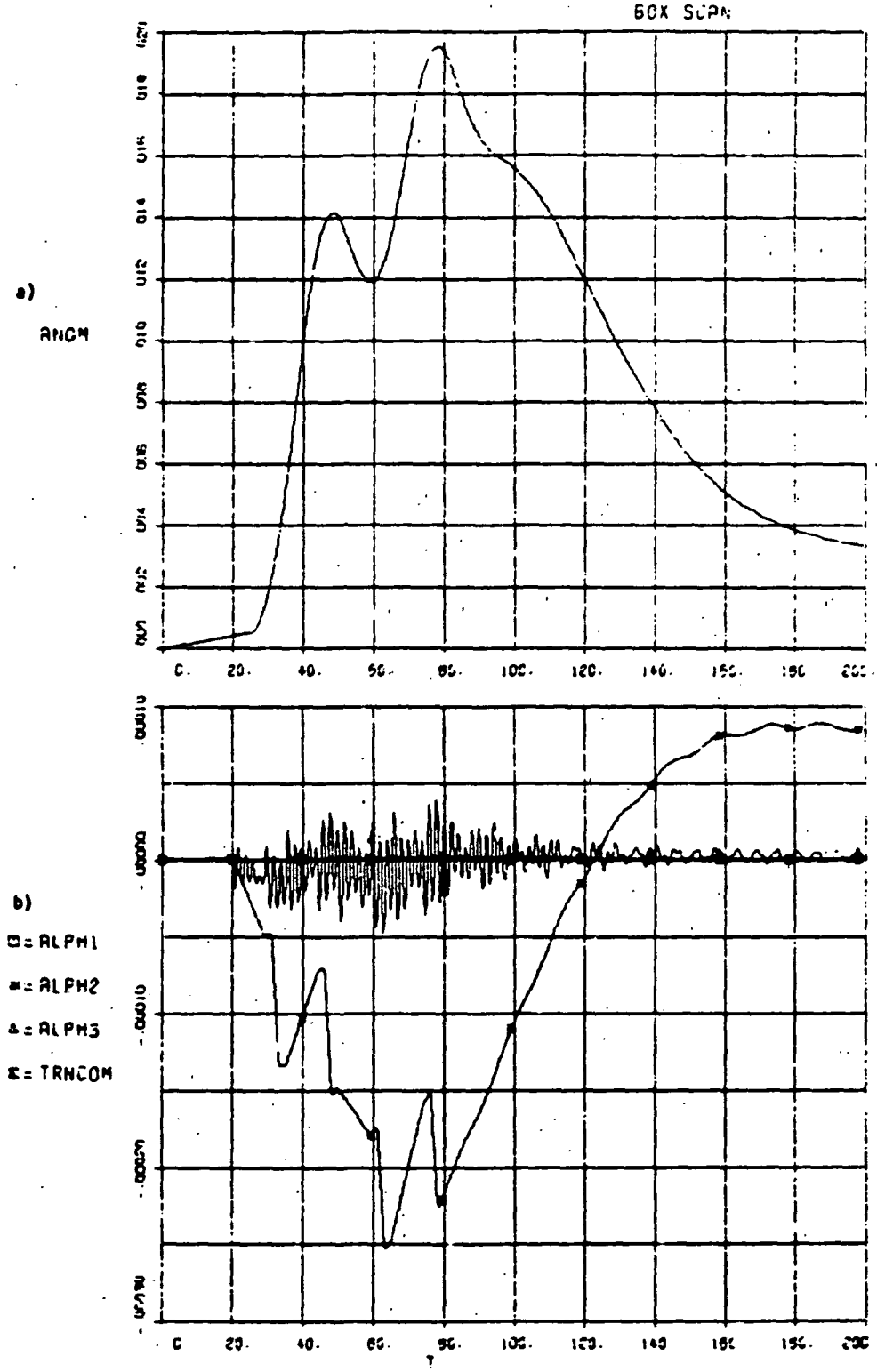

TVC keeps vehicle attitude within 250 urad of initial position under the disturbance created by the box slew sequence considered.

FULL FLEX MODEL WITH TVC-LL200/10 FIGURE 3-14
60X SCAN

c)
ALPH1

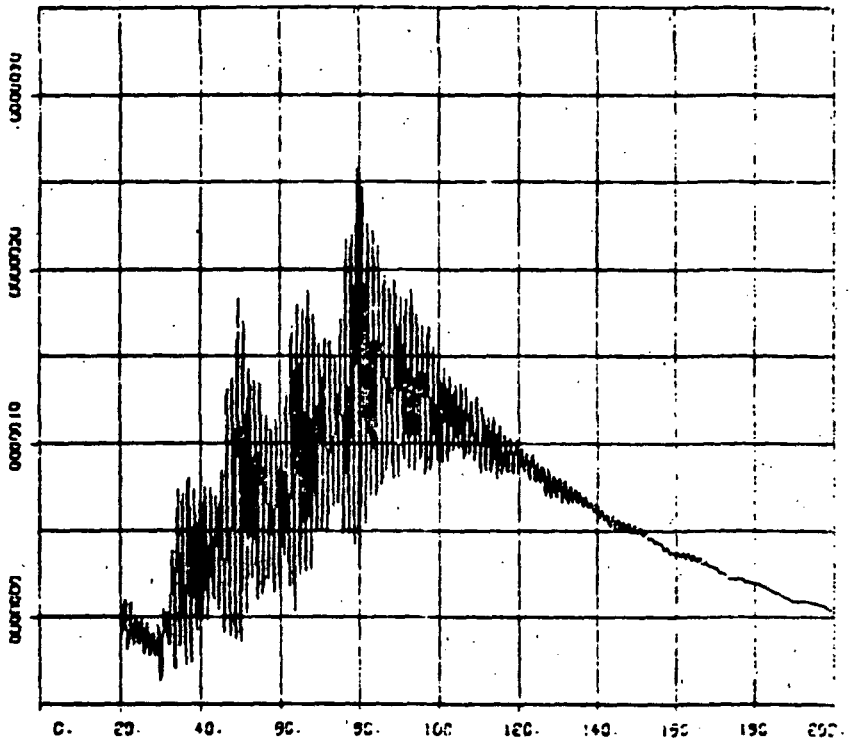

d)
RATE1

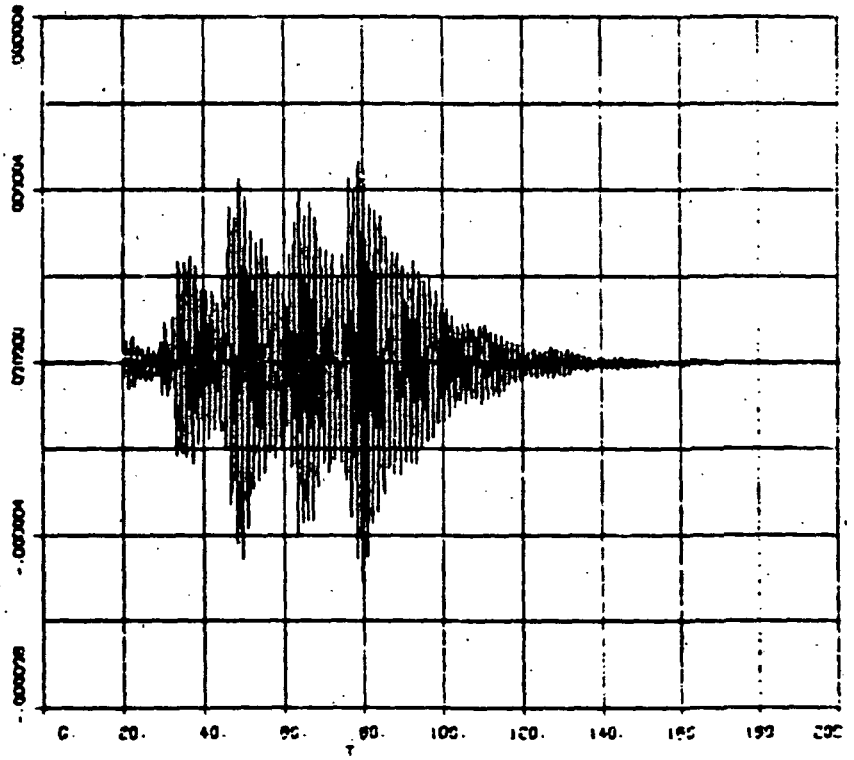

Induced pitch position and rate errors are very small (<2.5 urad and < ± 4.5 urad/s).

FULL FLEX MODEL WITH [illegible]

FIGURE 3-14
50X SCAN

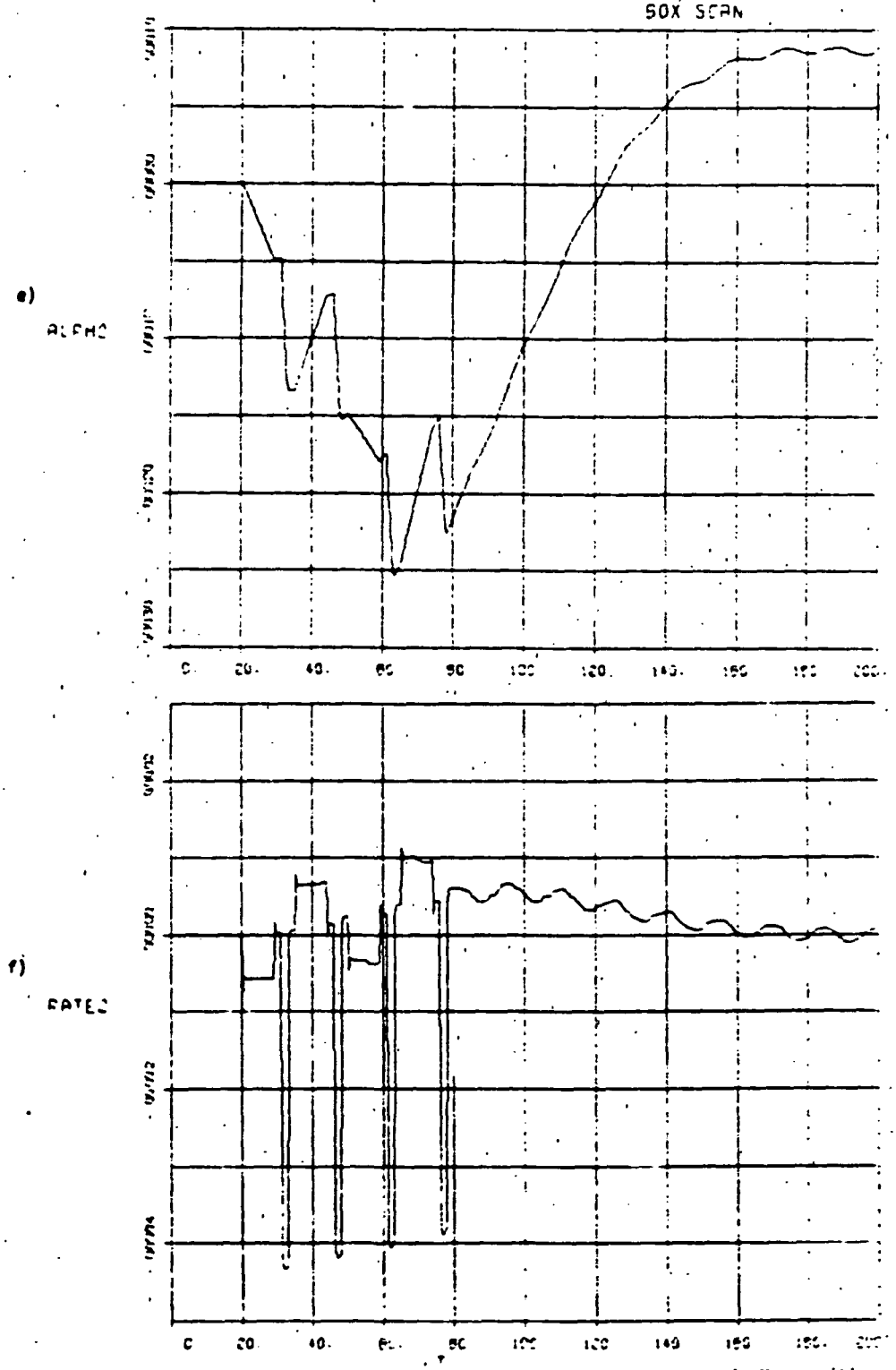

Predictably, the largest disturbance is in yaw (the axis of least inertia). Max position error of -250 urad. Max rate of -43 urad/s (due predominantly to scan start-stops, not to A/C).

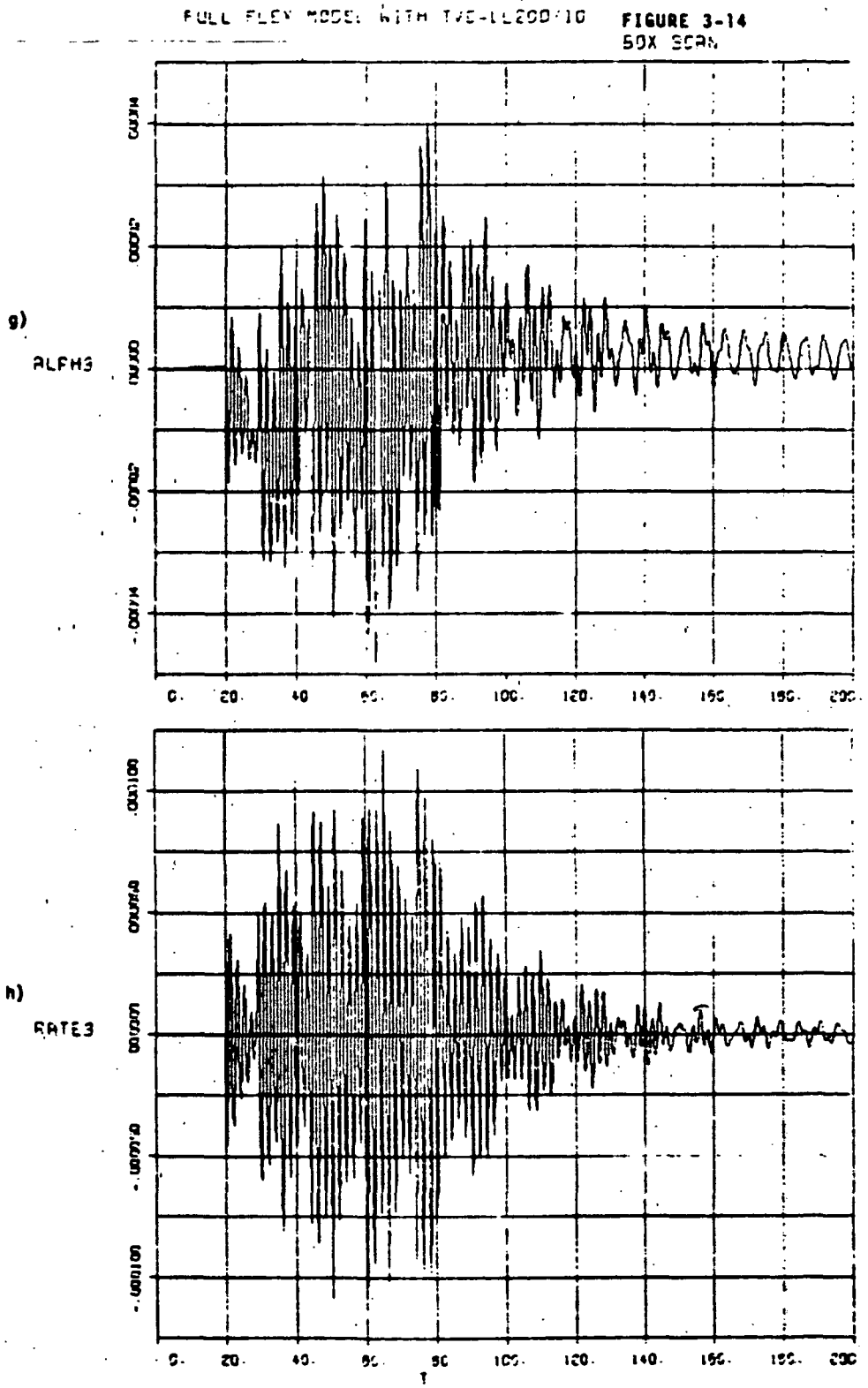

FIGURE 3-14

Induced roll position and rate errors of 50 urad and 120 urad/s, respectively, mostly due to scan start-stops.

FIGURE 3-14

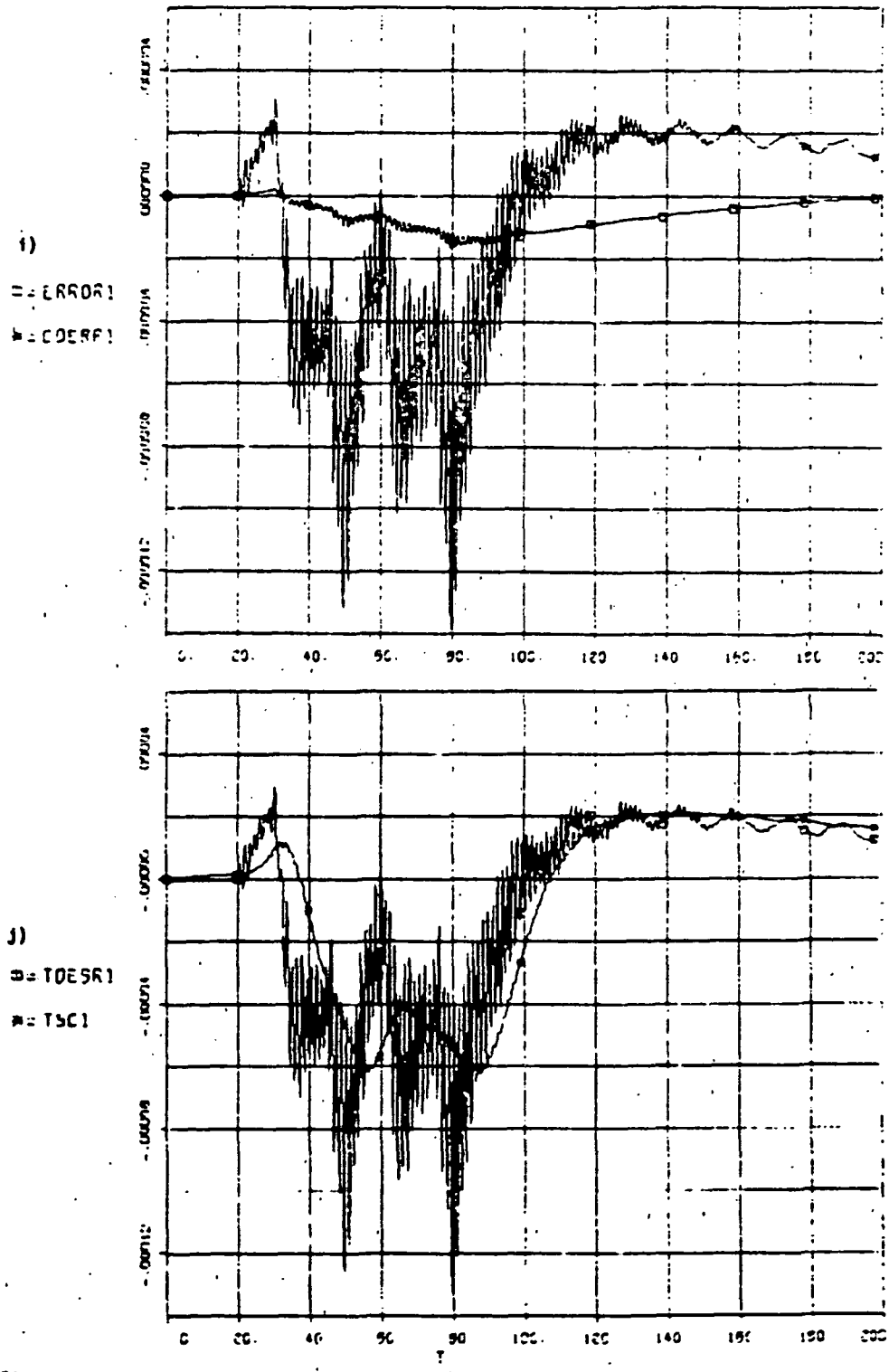

Pitch control error shows structural vibrations. The noisy control error causes dither in gimbals (see r) which, in turn, results in a somewhat noisy torque, j).

FULL FLEX MODEL WITH TVC-FLEX(1) **FIGURE 3-14**
SOX SCAN

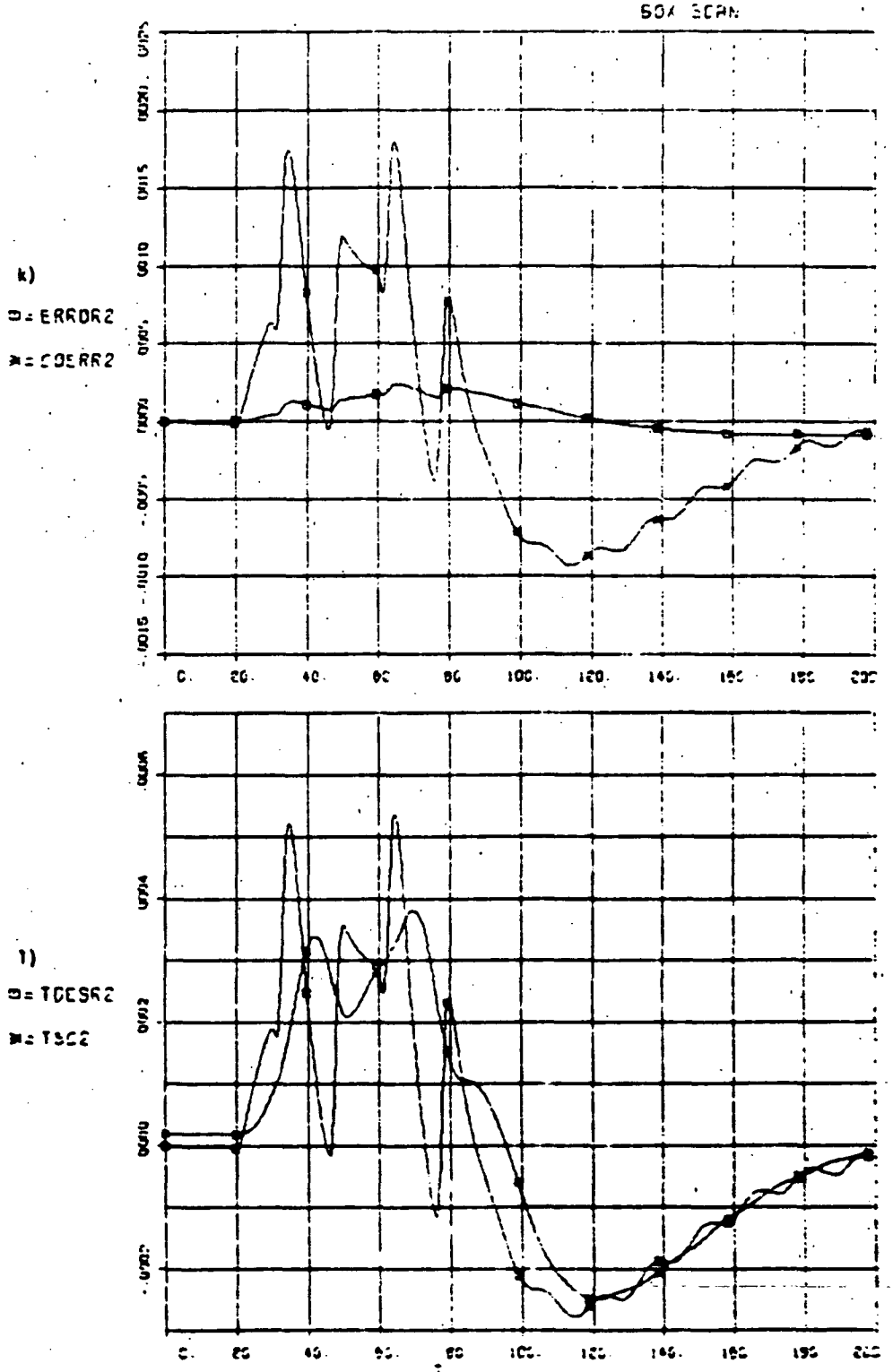

1) Note gimbals track desired torque trends but not high frequency transients.

FIGURE 3-14

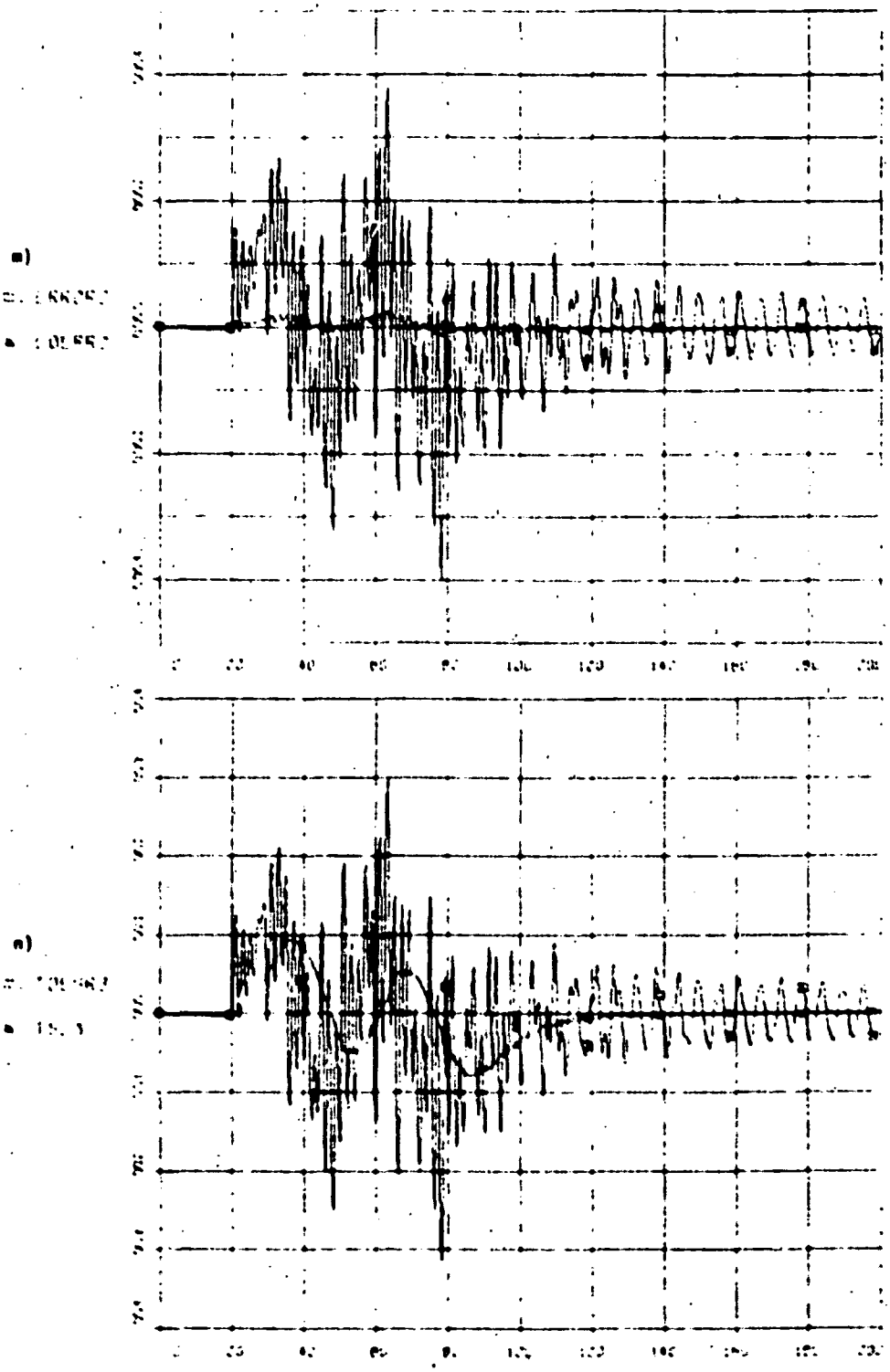

Roll control error shows presence of structural vibration. Noisy control error causes dither in gimbals (see q) which, in turn, results in a somewhat noisy torque, n).

FIGURE 3-14

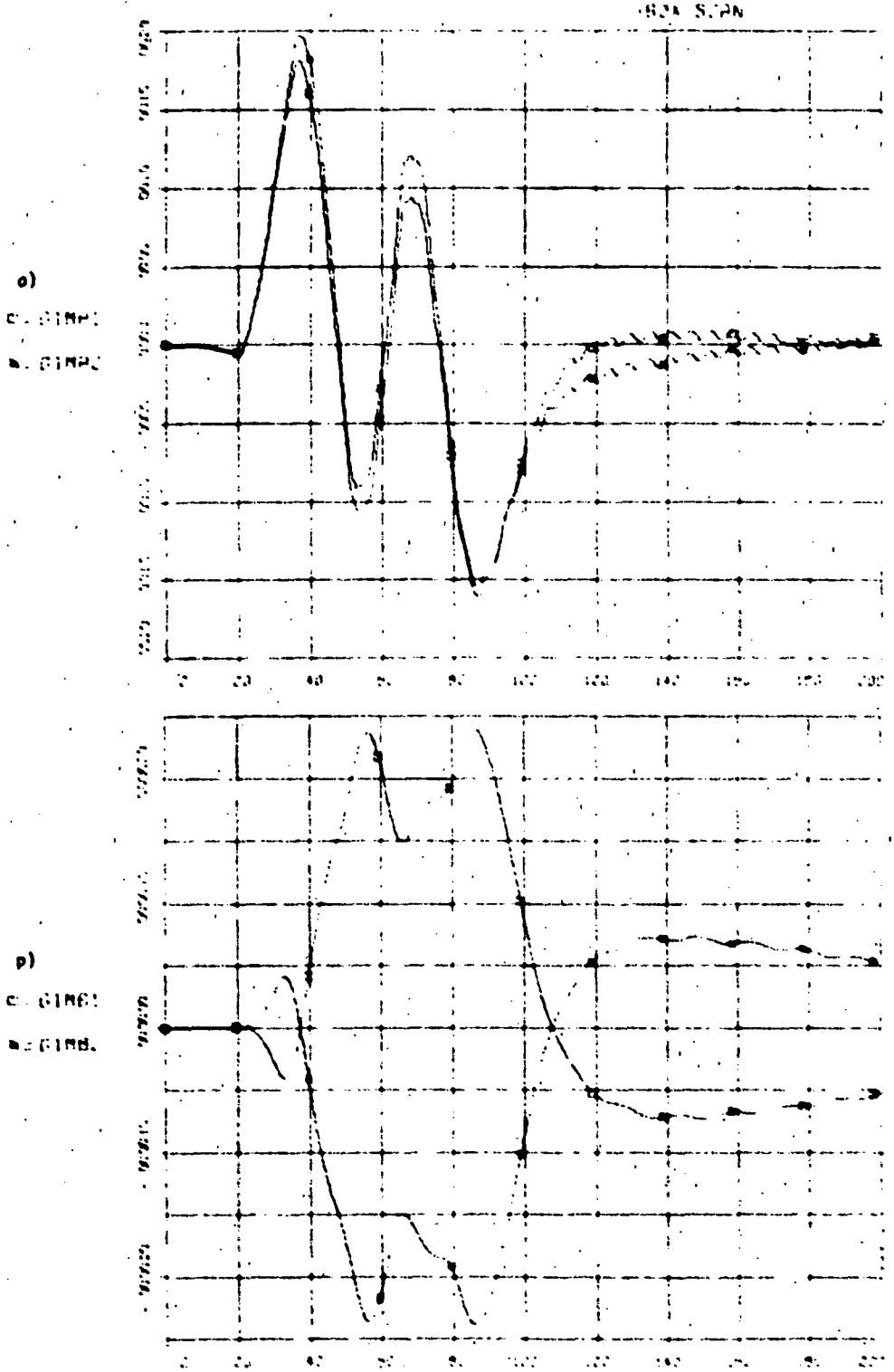

Predominant a-gimbaling to control yaw. Max gimbal angle of .11°, max rate of 0.02°/s.

FULL FLEX MODEL WITH [illegible] IC FIGURE 3-14
BOX SCAN

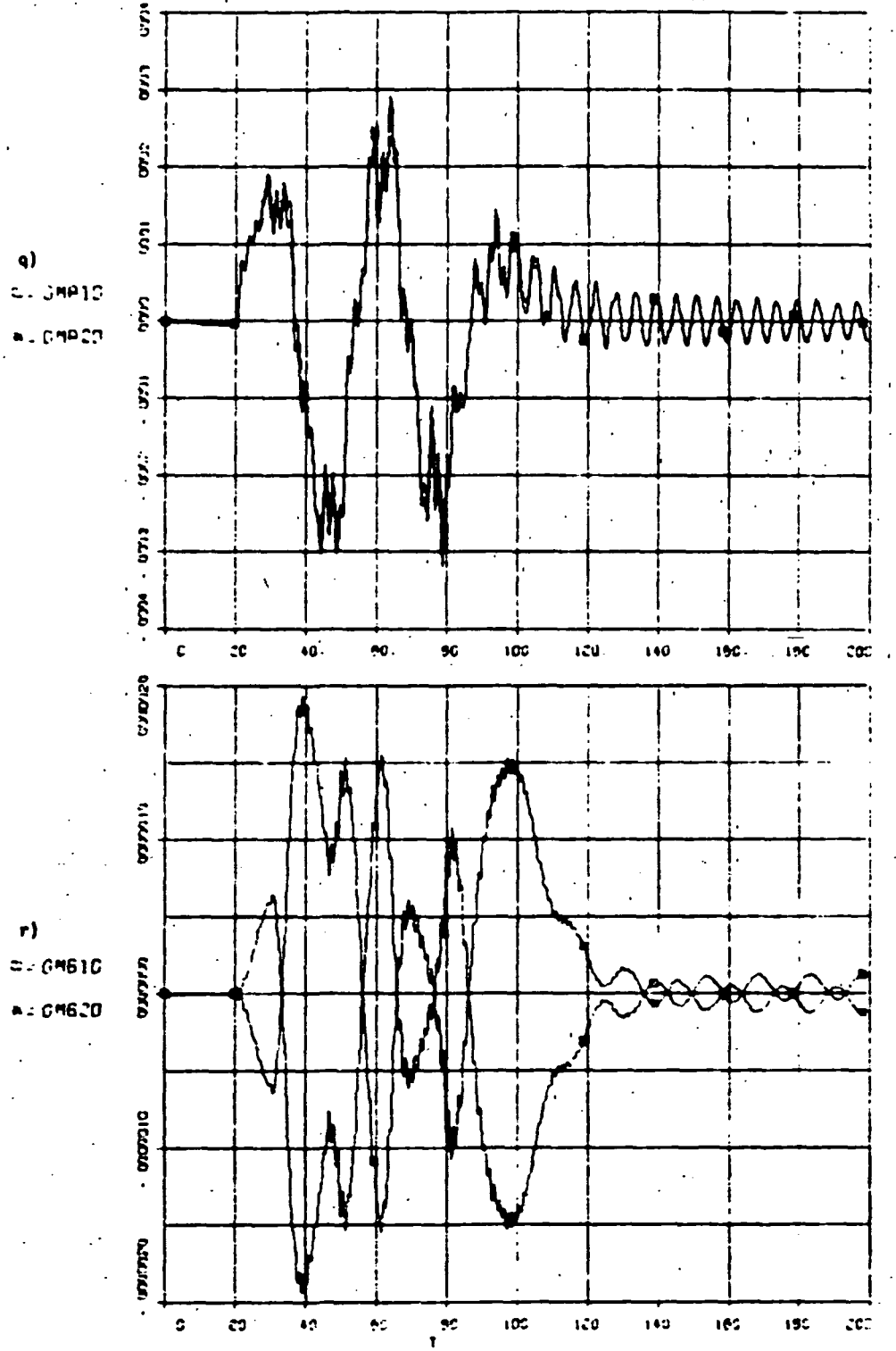

Note dither in gimbals.

FULL FLEX MODEL, WITH TV[illegible] 10

FIGURE 3-14
BOX SCAN

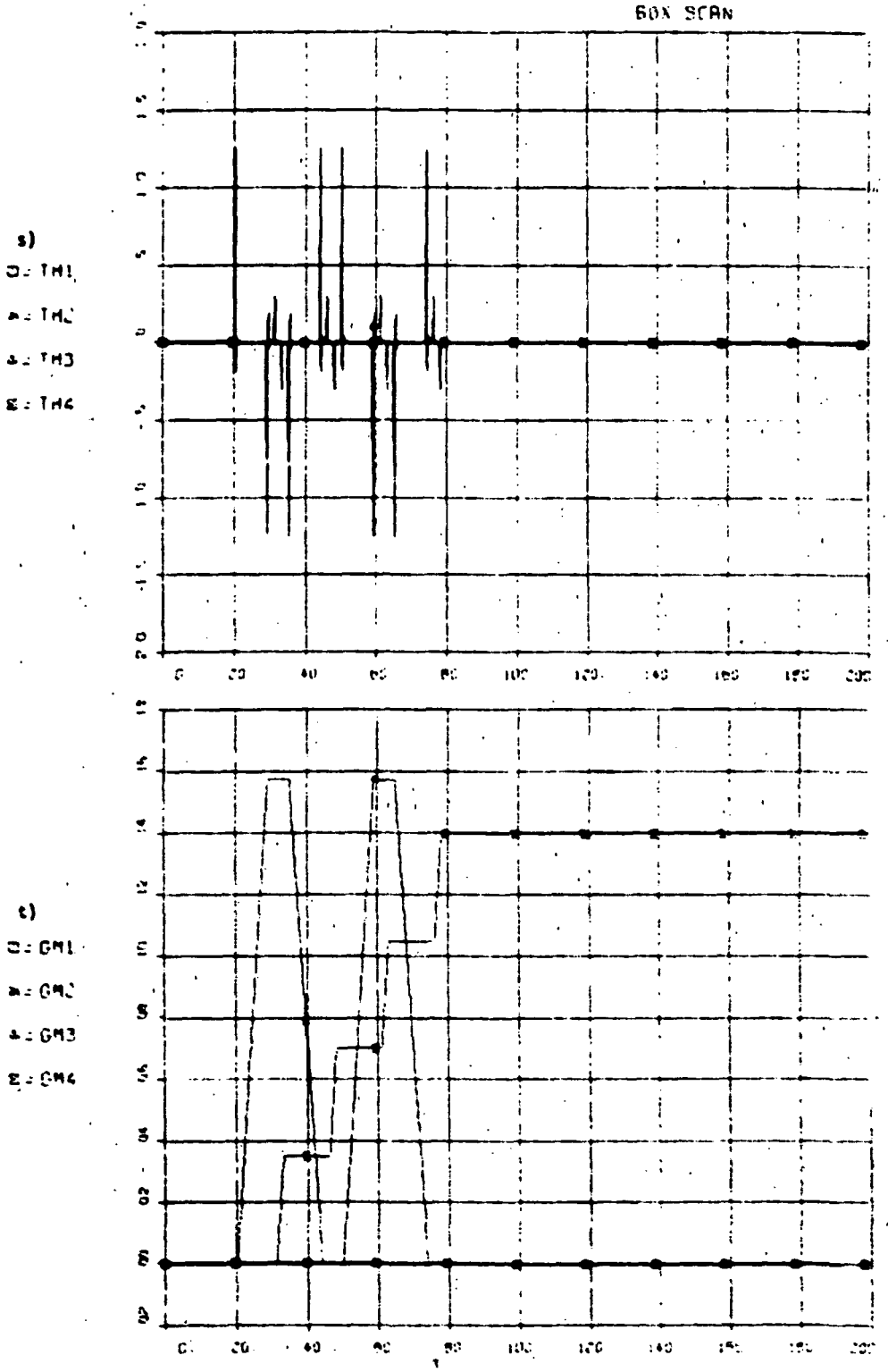

s) Note predominant scan hinge torque spikes at scan start-stops, r).

FULL FLEX MODEL WITH TVC-LLADC 10 **FIGURE 3-14**
60A SCAN

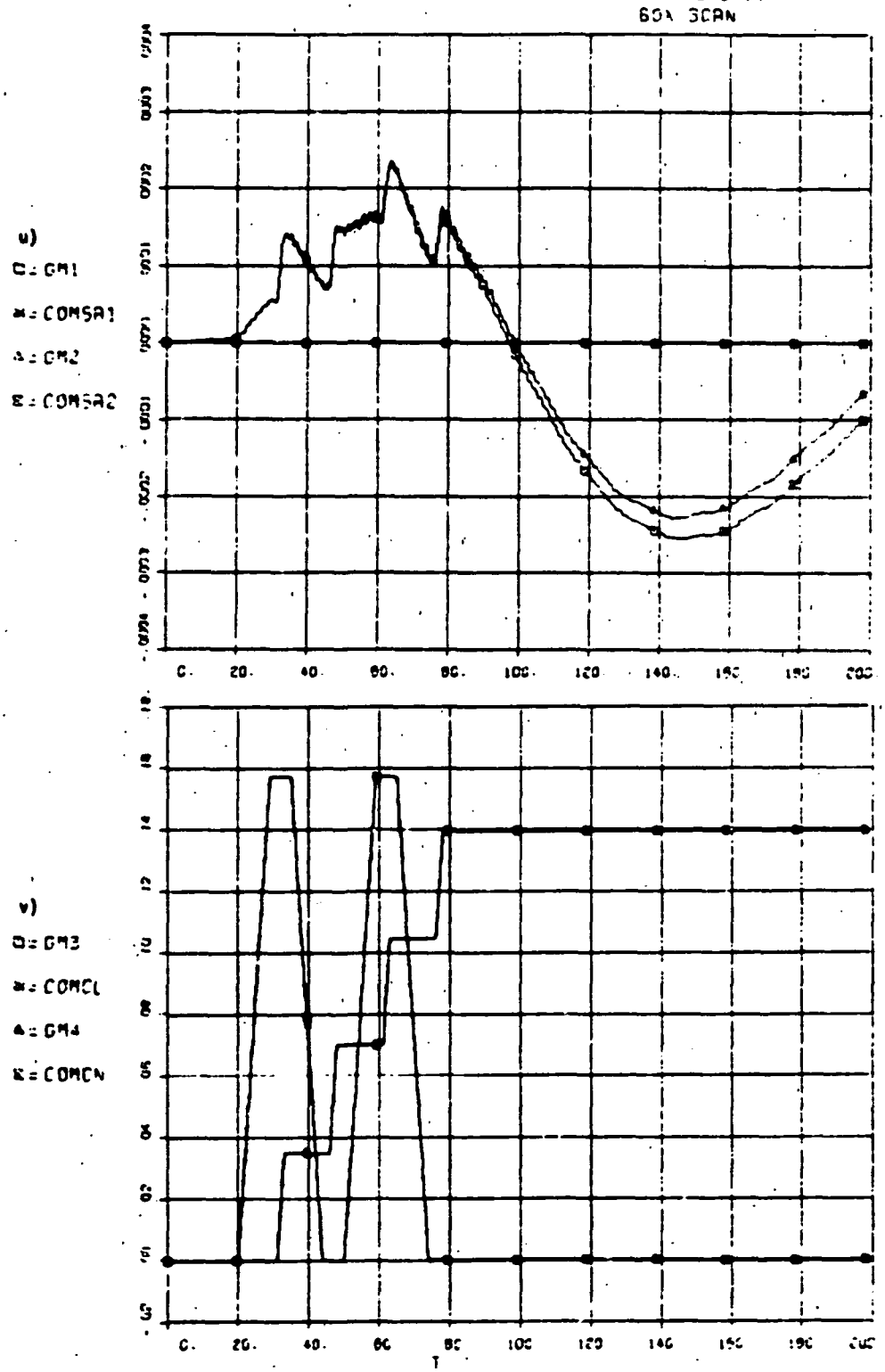

u) Solar panel transient hinge rotation of -0.015°.

FULL FLEX MODEL WITH TVC-ILOOP/IC **FIGURE 3-14**
BOX SCAN

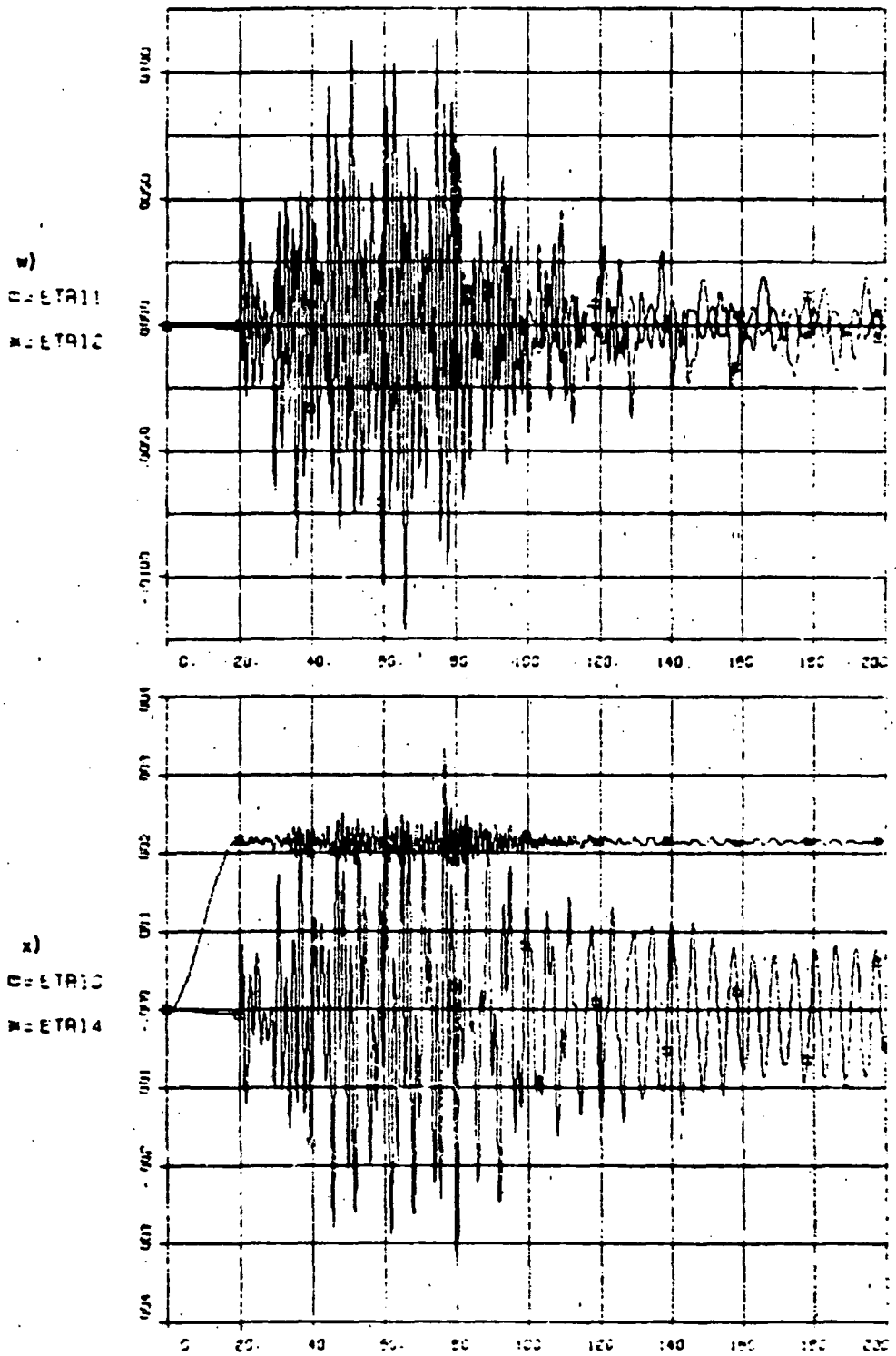

w) through z)
Solar panel vibration is mostly due to scan start-stops. Note a significant amount of residual vibration.

FIGURE 3-14
50X SCAN

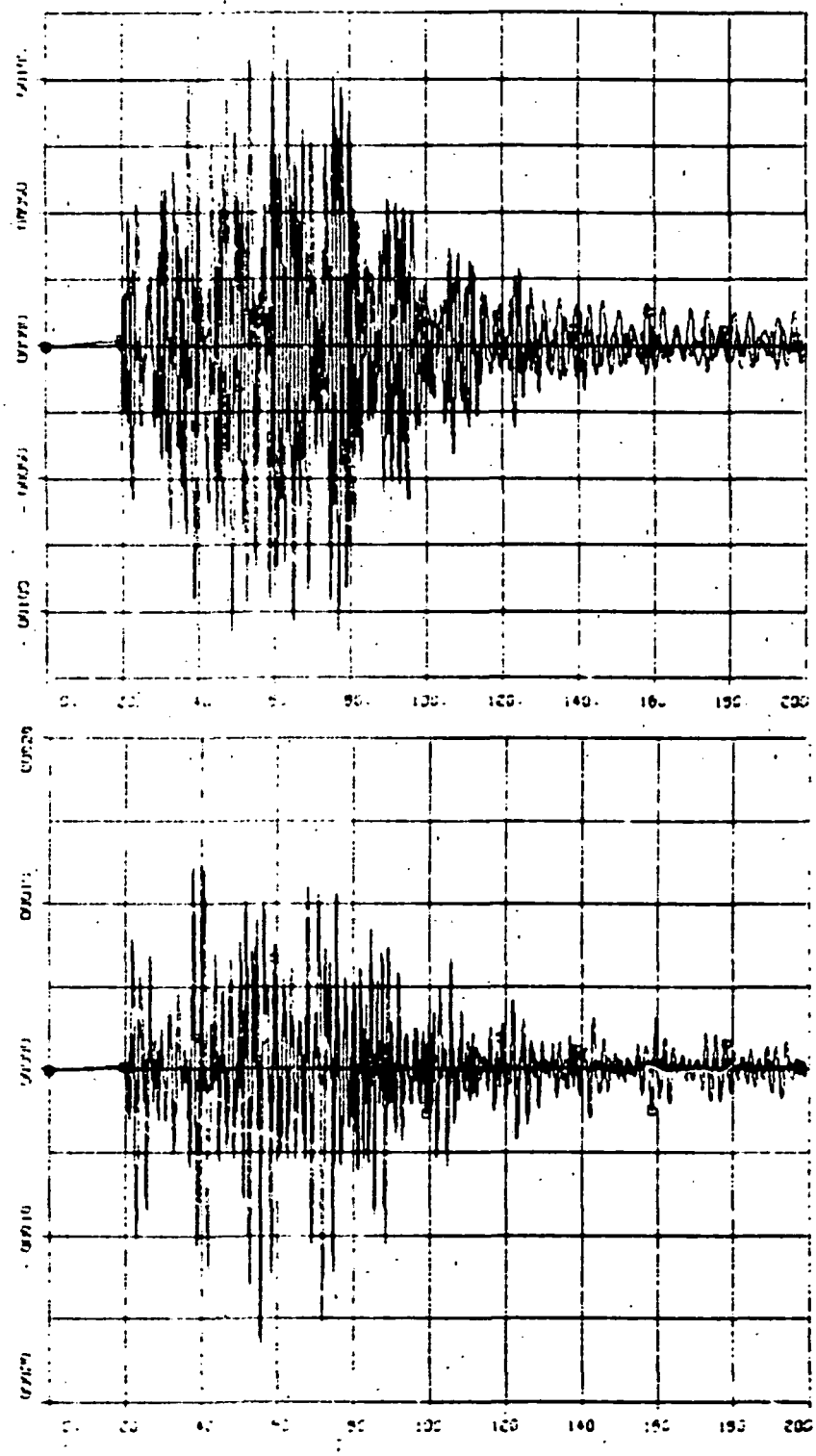

SECTION 4

GAS JET REACTION CONTROL

A Gas Jet Reaction Control System (RCS) achieves attitude control by selective firing of tiny gas jets suitably located on the vehicle.

RCS systems can provide high control authority at the cost of mass expenditures (system weight). As a class, however, they are, generally, undesirable for the control of flexible spacecraft because their nature is to impart impulsive loads to the structure. These loads are, essentially, square pulses having very high frequency content and, thus, all structural resonant frequencies tend to be excited. Because of this, RCS systems frequently exhibit undesirable interactions of the control system and the structure, resulting in degraded performance.

In this section we will discuss two RCS control systems for the SEPS/ICM vehicle and will analyze their performance. The section is organized as follows:

4.1 DESCRIPTION OF THE RCS HARDWARE

To obtain control torques on the vehicle two clusters of gas jets will be used as shown in Figure 4-1.

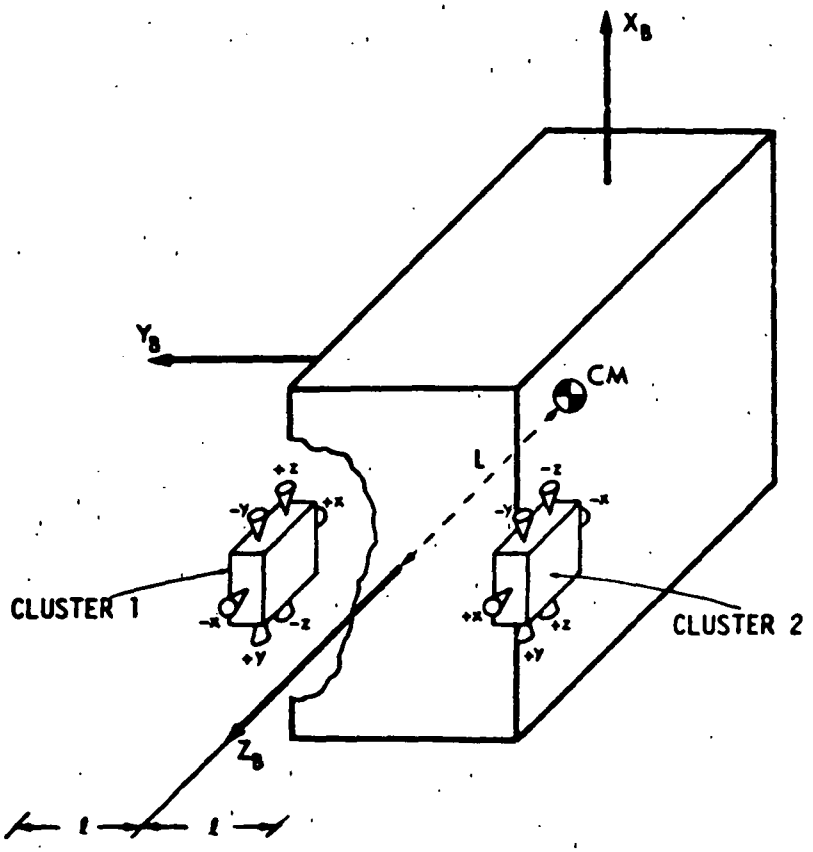

Figure 4-1. Location of Attitude Control Jets and Firing Polarities

With the above arrangement of jets, it is possible to obtain independent control torques about the three axes by selective firing of the gas jets as indicated in the figure. Note that for pitch (or roll) two gas jets are fired providing a pure torque couple on the vehicle, while for yaw two thrusters are fired which provide torque as well as a translational impulse to the vehicle. This configuration of thrusters has the advantage of clustering the gas jets and, thus, minimizing plumbing problems. It also has some inheren' disadvantages, for example,

the yaw jets provide the maximum torque about Y, the axis of least inertia, while at the same time producing a translational impulse along X which will induce out-of-plane deformation of the solar panels and, thus, tend to aggravate the structure/control system interaction problem. This configuration may also have plume impingement problems. It is thus recognized that this approach may not be the best and, although it will be assumed in this study, further analysis and trade-offs should be made in the future, to determine if further improvement can be attained by trading plumbing complexity against improved performance.

The gas jets considered in this study were assumed to provide a thrust of 0.0675N (15 mlb) with a minimum-on-time (MOT) of 20 ms, providing a minimum impulse bit of $1.35\ 10^{-3}$ N-s. The jet clusters will be assumed to be located at (0, $\pm$ 1.27, +3.21) m in bus coordinates as shown in Fig. 4-1. Since the vehicle center of mass is located at (0, 0, + 0.5) m the lever arms for each cluster, in m, are

	Cluster 1	Cluster 2
ℓ_x	1.27	1.27
ℓ_y	2.71	2.71
ℓ_z	1.27	1.27

4.1.1 Criteria for Selection of Attitude Control Propellant

The scientific objectives of the SEPS/ICM mission of determining the chemical nature and physical structure of the nuclei, atmosphere, and ionisphere of comets places very severe limitations on the chemical composition of the propellants which may be used for attitude control. For example, we cannot use propellants which (in either pure form or by forming other compounds) would compromise the scientific objectives of the mission by confusing the background concentration ratios.[7]

Table 4.1 is a list of materials expected to be present in the vicinity of a comet. These species are tabulated by mass, and their

[7] McMinimy, W., Reaction Control Gases for the HFB/T2R Comet Mission, IOM 3136-79-167, July 6, 1979, JPL Internal Document.

TABLE 4-1. A Search List for Cometary Gases[1]

Species ($\log_{10}$ of Abundance, Normalized to $\log_{10}(H_2O)=10$)

Mass	Species (abundance)	Mass	Species (abundance)
1	H(10)	38	
2	H_2(8), D(6)	39	K(6)
3		40	CH_3·C·CH(7), Ca(7), Ar(6)
4	He(4)	41	CH_3CH(7)
5		42	CH_2CO(5), NH_2CH(5)
6		43	HNCO(7), H_2NCH(7)
7		44	CS(7), CO_2(8), CH_3·CH·O(7)
8		45	NH_2·CH·O(6), CH_3·NH·CH_3(6)
9		46	HCO·OH(7), H_2CS(8), CH_3·NH·NH_2(6), NS(8), C_2H_5OH(7), CH_3OCH_3(7)
10			
11		47	
12	^{12}C(8)	48	C_4(6), SiO(6)
13	CH(7), ^{13}C(6)	49	C_4H(6)
14	N(7), CH_2(8)	50	C_3N(6)
15	NH(7), ^{15}N(5), CH_3(7)	51	CH·C·CH(6)
16	O(10), CH_4(9), NH_2(7)	52	Cr(4)
17	NH_3(9), OH(10)	53	CH_2·CH·CH(6)
18	H_2O(10), ^{18}O(7)	54	
19		55	Mn(4), CH_3·CH_2·CH(6)
20	Ne(4)	56	Fe(5), C_4H_8(6)
21		57	
22		58	Ni(4)
23	Na(7)	59	Co(4)
24	C_2(8)	60	OCS(5), $CO(NH_2)_2$(4), CH_3OOCH(5)
25	$^{12}C^{13}C$(6), CCH(6)	61	NH_2·CO·OH(6)
26	CN(8), C_2H_2(6)	62	
27	HCN(8)	63	
28	CO(10), N_2(9), C_2H_4(6)	64	S_2(8), SO_2(7)
29	CH_2NH(7), HCO(6)	65	Cu(4)
30	H_2CO(8), NO(7), C_2H_6(5)	66	$^{34}SO_2$(5)
31	CH_3NH_2(7), HNO(6)	72	C_5H_{12}(5)
32	S(8), CH_3OH(7), NH_2·NH_2(?), O_2(6)	75	NH_2acid(5), HC_3N(6)
33		84	Kr(6)
34	H_2S(8)	99	HC_4N(6)
35		123	HC_9N(6)
36	C_3(7)	132	Xe(7)
37			

[1] See reference in page 1-1

expected relative abundances to water are shown. In order to not compromise the aforementioned scientific objectives, it is necessary that the propellant gases do not introduce into the environment species having a relative abundance higher than 7, following rendezvous with Tempel 2.

Examination of the table shows that all gases containing Carbon, Nitrogen, or Oxygen are not acceptable for attitude control after Tempel 2 rendezvous. The noble gases (Helium - He, Neon - Ne, Argon - Ar, Krypton - Kr, and Xenon - Xe) all satisfy the concentration constraint. However, there are certain restrictions in their use. In particular, if the proposed Gamma Ray Spectrometer is included in the ICM science payload, Kr would not be used because Kr^{85} produces 0.514 MeV γ photons which could alias the γ ray observations. The remaining gases could be used, although Xe is less desirable because of its higher expected abundance (7), and He is also less desirable because of its small molecular size which makes it difficult to prevent from leaking.

In view of the above, Ne and Ar would be optimum from the standpoint of being about 6 orders of magnitude down from water in abundance, and are more easily maintained in storage. Neon appears to be a good choice because it provides a specific impulse of I_{sp}=75 s which is twice the I_{sp} of Argon. It should be noted, however, that the optimum choice depends also on other factors besides I_{sp} (such as gas densities, tankage and plumbing weight and, ultimately in total system weight). From a systems viewpoint, therefore, Ne may not be such an obvious best choice. In fact, it may turn out that the best choice will vary from mission to mission depending on whether the total RCS system weight is dominated by tankage weight or by propellant mass requirements for the mission.

For the purposes of this study we will assume a Ne system for gas consumption calculations. It should be noted that this assumption in no way affects the applicability of other results shown herein should another gas be decided upon. Change of propellant will only change propellant consumption.

4.2 RCS LEAD-LAG CONTROL SYSTEM

The Lead-Lag RCS control system block diagram (based on loop configuration and data supplied by MSFC) is shown in Figure 4.2. It is similar to the lead lag controller described in Section 3 for TVC except that the TVC hardware has been replaced by RCS hardware. Also, the control gains have been replaced by deadband logic to fire the thrusters. The filtering of the error has been eliminated since it was intended to filter the gimbal high harmonics which are no longer present. The scan platform and solar array controllers are exactly the same as those described in the preceding section for TVC. A list of the pertinent system parameters is given in Table 4-2. Most of them were described in Section 3, a few new ones, such as the deadband characteristics, will be described herein.

The block diagram shows the position error being put through a lead-lag network to generate the control error e_c. This control error is then fed into the deadband logic which determines how the gas jets are to be fired: If the control error is less than 0.5° no action is taken. If the error exceeds 0.5° the gas jets are fired to bring the vehicle back into the deadband. The scheme proposed by MSFC uses the following deadband logic in an attempt to make the system a pseudo-proportional bang-bang system. If the control error exceeds 0.5° the gas jets are turned on for an amount of time t_{ON} which is proportional to the control error as shown in Figure 4-3. For example, at $e_c = 0.5°$ $t_{ON} = 20$ ms, at $e_c = 0.6°$ $t_{ON} = 36$ ms, and at $e_c = 1°$ $t_{ON} = 100$ ms.

In this study we have assumed that the RCS logic is implemented in an onboard computer as a routine having a frametime of 50 milliseconds, so that every 50 ms a decision will be made by the routine as to how long the thrusters will be on during the next 50 milliseconds. Thus, if at some instant of time the error is 1.5°, for example, the logic would say "fire for 180 ms;" in reality, the controller would leave the jets on for 50 ms and then perform another logic decision at the next 50 ms frametime. If the error still exceeded the deadband we would continue firing, if, on the other hand, it had returned into the deadband, then no further firings would take place. Therefore, the 50 ms frametime decisions override decisions made previously.

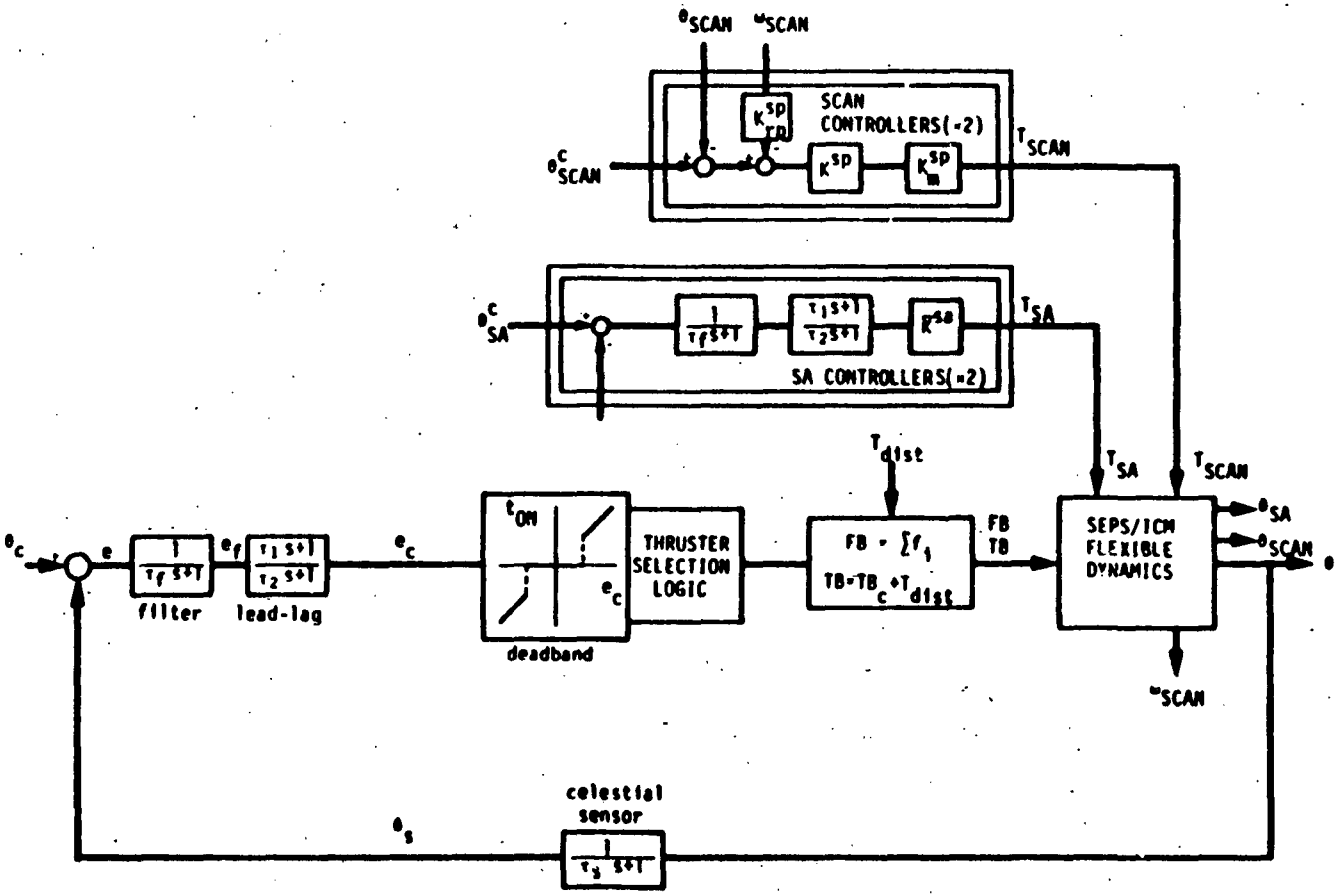

Figure 4-2. RCS "Lead-Lag" System Block Diagram (1 axis shown)

TABLE 4-2. RCS "LEAD-LAG" SYSTEM PARAMETERS
(same for all axes unless otherwise indicated)

PARAMETER	VALUE	UNITS	DESCRIPTION
I. LEAD-LAG CONTROLLER			
τ_s	1.0	s	Celestial sensor time constant
τ_f	15.0	s	Filter time constant
τ_1	200.0	s	Lead-lag
τ_2	10.0	s	Lead-lag
II. DEADBAND AND GAS JET CHARACTERISTICS			
DB	$\pm$0.5	deg	Deadband size
PWM	160.0	ms/deg	Pulse-width modulation slope: $t_{ON} = 20 + 160\|e_c\|$ for $\|e_c\|>0.5°$
FTIME	50.0	ms	Frequency of execution of jet firing decision routine
MOT	20.0	ms	Gas jet minimum-on-time
f	0.0675	N	Single jet force (15 mlb_f)
L_1	(0,+1.27,2.71)	m	CM to jet cluster 1 vector
L_2	(0,-1.27,2.71)	m	CM to jet cluster 2 vector
III. SOLAR ARRAY AND SCAN PLATFORM CONTROL			
R^{sa}	0.02557	N-m/rad	Position-to-torque gain
τ_f	15.0	s	Filter time constant
τ_1	200.0	s	Lead-lag
τ_2	20.0	s	Lead-lag
$K^{sp}K^{sp}_m$	1500.0	N-m/rad	Scan position-to-torque gain
K^{sp}_{rp}	0.14683 0.09901	s s	Clock rate-to-position gain Cone rate-to-position gain

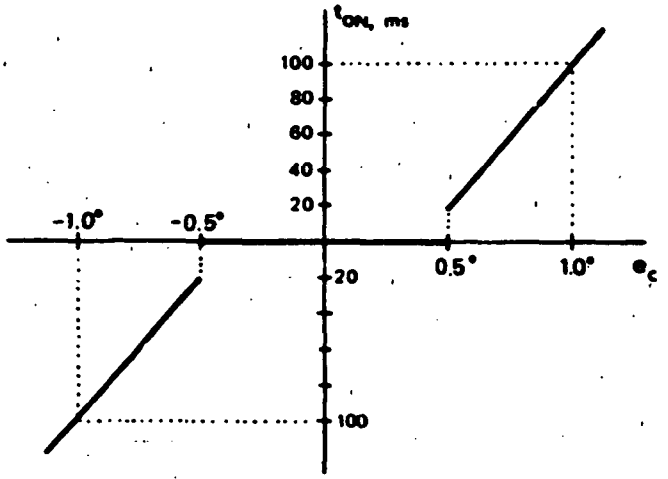

Figure 4-3. Deadband Logic with 20 ms MOT

The t_{ON} signals coming out of the deadband logic, are then fed into the Thruster Selection Logic which selects the appropriate gas jet thrusters to be fired as shown in Figure 4-1. It also generates the necessary electrical signals to open and close the valves of those gas jets.

The force and torque acting on the bus can then be computed as follows. Let $f_i^1(t)$ and $f_i^2(t), i = 1,2,...6$ denote the vector force pulses produced by each of the 6 jets of clusters 1 and 2 respectively, all expressed in some common coordinates, say bus coordinates. Let R_1 and R_2 denote the vector from the bus center of mass CM_B to clusters 1 and 2 respectively, in bus coordinates. The total force and torque produced by the jets on the bus are then given by

$$FB(t) = \sum_{i=1}^{6} f_i^1(t) + \sum_{i=1}^{6} f_i^2(t)$$

$$TB_C(t) = R_1 \times \sum_{i=1}^{6} f_i^1(t) + R_2 \times \sum_{i=1}^{6} f_i^2(t)$$

In order for the simulation program to integrate accurately this pulse-width-modulated train of torques, one has to use an extremely small integration step. This poses serious numerical and cost problems if we consider that simulation times of 500 - 1000 seconds are typical due to the slow response of this large vehicle. Because of this, the pulse width modulation logic was not simulated directly in that form but converted to an amplitude-modulation scheme, such that the amplitude of the pulse was made constant over the 50 ms and proportional to the error. Thus, instead of firing 15 mlb for the first, say, 27 ms of a 50 ms interval, we implemented the proportional logic by firing for the full 50 ms with a force of

$$\frac{27}{50} \times 15 \text{ mlb} .$$

This amplitude modulation approximation makes sense because during each 50 ms interval it imparts the same momentum to the vehicle as the pulse width modulation approach it simulates.

This completes the description of the RCS lead-lag control system.

4.3 RCS RATE + POSITION CONTROL SYSTEM

As we will see in the following subsection, some of the RCS maneuvers simulated with the lead-lag controller scheme produced unsatisfactory results. In an effort to determine if this poor performance could be improved, a second control scheme has been considered. This is the so called rate plus position system in which the control signal e_c is obtained as the negative of the weighted sum of the position error and the actual vehicle rate

$$e_c = -((\theta_s - \theta_c) + K_{rp}\,\omega)$$

The "rate to position" gain K_{rp} provides damping. This scheme is similar to the lead-lag system in that the lead-lag produces a control error based on the position error plus the rate of the error. Our present controller, however, uses the vehicle rate itself rather than the rate of the position error. The Solar Array controllers were also changed to rate + position systems.

The resulting block diagram is shown in Figure 4-4. It is similar to the block diagram shown in Figure 4-2 but the lead-lags have been replaced with "rate plus position" signals. The system parameters are given in Table 4-3 which reflects a change from the lead-lag controllers to rate plus position control systems.

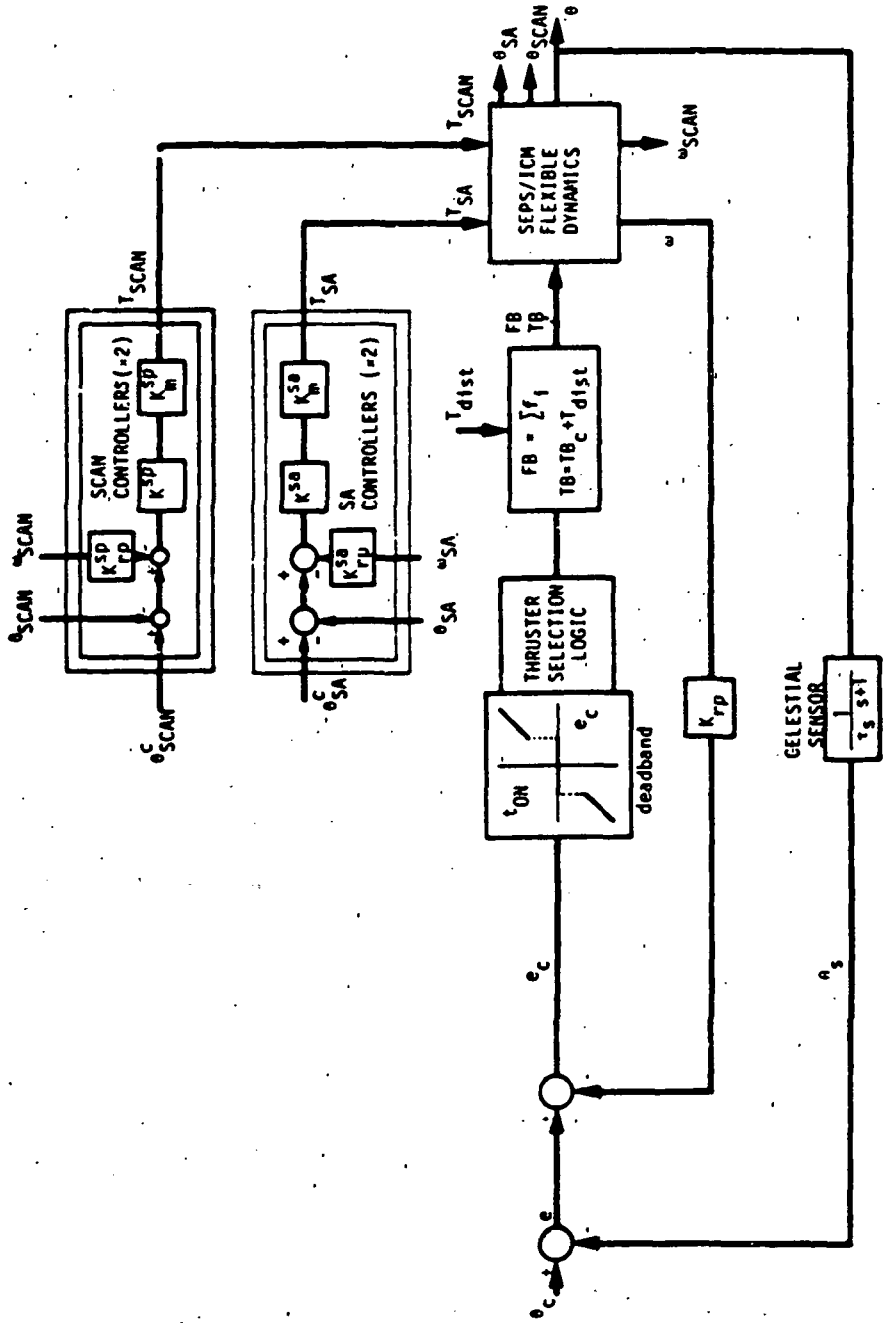

Figure 4-4. RCS "Rate + Position" System Block Diagram (1 axis shown)

TABLE 4-3. RCS "RATE + POSITION" SYSTEM PARAMETERS
(same for all axes unless otherwise indicated)

PARAMETER	VALUE	UNITS	DESCRIPTION
I. RATE + POSITION CONTROLLER			
K_{rp}	49.96142	s	Rate-to-position gain
τ	1.0	s	Celestial sensor time constant
II. DEADBAND AND GAS JET CHARACTERISTICS			
DB	$\pm$0.5	deg	Deadband size
PWM	160.0	ms/deg	Pulse-width modulation slope: $t_{ON} = 20 + 160\|e_c\|$ for $\|e_c\|>0.5°$
FTIME	50.0	ms	Frequency of execution of jet firing decision routine
MOT	20.0	ms	Gas jet minimum-on-time
f	0.0675	N	Single jet force (15 mlb_f)
L_1	(0,+1.27,2.71)	m	CM to jet cluster 1 vector
L_2	(0,-1.27,2.71)	m	CM to jet cluster 2 vector
III. SOLAR ARRAY AND SCAN PLATFORM CONTROLLERS			
$K^{sa}K_m^{sa}$	15.0	N-m/rad	SA position-to-torque gain
K_{rp}^{sa}	5.53676	s	SA rate-to-position gain
$K^{sp}K_m^{sp}$	1500.0	N-m/rad	Scan position-to-torque gain
K_{rp}^{sp}	0.14683	s	Rate-to-position gain
	0.09901	s	Rate-to-position gain

4.4 RCS PERFORMANCE

The performance of the lead-lag control systems described above was evaluated through computer simulation of the four test maneuvers described in 2.4. The bus yaw turn and scan slewing maneuvers were simulated also with the rate + position controller described in 4.3. Full details of the flexible dynamics models, simulation programs, and assumptions can be found in Section 2.

The results of the simulations are shown in Figures 4-5 through 4-10, and are discussed below in some detail. The figures themselves are also captioned with pertinent explanations and commentary. The nomenclature used in these figures is listed in Table 4-4.

The 1° pitch turn maneuver simulation (Figure 4-5) shows acceptable performance for this type of maneuver. Some structural vibration is evident in the rate plots d), h), and, especially, in the solar panel deformation coordinate plots u) through x). Note structural vibrations to be coincident with gas jet firings.

The 30° bus yaw turn (Figure 4-6), on the other hand, exhibits totally unacceptable performance characterized by uncontrolled, undamped limit cycling resulting in a steady state limit cycle gas consumption of 540 gr/hour (~1.19 lb/hr) following turn stop. This serious situation is not an uncommon one. Several spacecraft have exhibited this type of behavior in flight. The Voyagers 1 and 2 are a recent example of exactly this type of situation [8]. This phenomenon is thought to occur as a consequence of structure/control interactions, where the solar arrays are excited into oscillation and their motion causes (phase-shifted) gas jet firings which sustain the oscillations indefinitely. In an effort to determine if this poor performance could be improved upon, this same bus yaw maneuver was simulated a second time, this time after changing the lead-lag (LL) controller to the "rate-plus-position" (R+P) controller described in 4.3. The R+P system provided a very clean and reasonable bus yaw turn (Figure 4-7) with RCS-typical vibration levels but no evidence of

[8] Tolivar, A.F., "Voyager Oscillations - Some Data and Comments" Interoffice Memorandum 343-319, Nov. 16, 1977, JPL Internal Document.

control/structure interaction. Gas consumption was much smaller than before and the residual limit cycle rates after the turn are very small.

The multi-axis acquisition maneuver was simulated with the baseline lead-lag controller and the resulting plots are shown in Figure 4-8. Acquisition (for the particular set of initial conditions considered here) takes about 700 seconds and results in unacceptable, undamped, high limit cycle rates in yaw, entirely analogous to the situation observed for the bus yaw turn.

Simulation plots for the scan platform slewing test are given in Figures 4-9 for the LL controller, and in Figure 4-10, for the R+P controller. In both cases, the vehicle was assumed to be initially just "sitting" on the edge of the deadband on all 3 axes. Both sets of simulation plots appear quite similar, in the sense that most of the dynamic disturbance experienced by the vehicle is caused by the slewing of the platform, not by the gas jet firings. However, a very significant difference is the amount of (Ne) attitude control gas consumed for the slew sequence considered; the LL system used 0.63 gr, while the R+P system used 2.25 gr (almost four times as much). This is because the R+P system considered here is more sensitive to the rate spikes (produced by the scan slewing and jet firings) and results in considerably more multipulsing when at the edge of the deadband.

In summary, the RCS system has been shown to produce vehicle attitude control characterized by high vibration levels and excitation of the vehicle flexible appendages. These high vibration levels are due to the impulsive nature of the loads produced by the nearly-square gas jet pulses. Such loads have a very high frequency content and, thus, tend to excite all resonant frequencies in the structure. The higher vibration levels are very dangerous and, in fact, in 2 out of the 6 simulations, have been shown to lead to severe control/structure interaction resulting in exceedingly high limit cycle rates, and unacceptable propellant consumption.

TABLE 4-4. KEY TO VARIABLE NAMES FOR FIGURES 4-5 to 4-10

ALPH1,2,3*	Angular position of the bus (b_0), rad
ANGM	System angular momentum magnitude, N-m-s
COERR1,2,3	Control error e_c, rad
COMCL, COMCN	Position commands into Scan Platform, rad
COMSA1,2	Position commands into SA wings, rad
ERROR1,2,3	Sensed position error e, rad
ETA11 to ETA18	Panel deformation generalized coordinates (panel 1, first 8 modes)
GM1,2,3,4	Hinge rotation for Solar Array Panels 1,2, and Scan Clock, and Cone, respectively, rad
RATE1,2,3	Bus angular rates, rad/s
TH1,2,3,4	Hinge torques for Solar Array Panels 1,2, and Scan Clock, and Cone, respectively, rad
TPONX,Y,Z*	Gas jet on polarities
TRKCOM	θ_c position input (turn command), rad
TSC1,2,3	External torques about vehicle CM, N-m
X,Y,ZGASGR & TGASGR	Neon gas consumption in grams (X,Y,Z, and total)

*1,2,3, or (equivalently) X,Y,Z, denote the pertinent axis.

FULL FLEX MODEL WITH RCS-CL200/10 FIGURE 4-5
1°X TURN

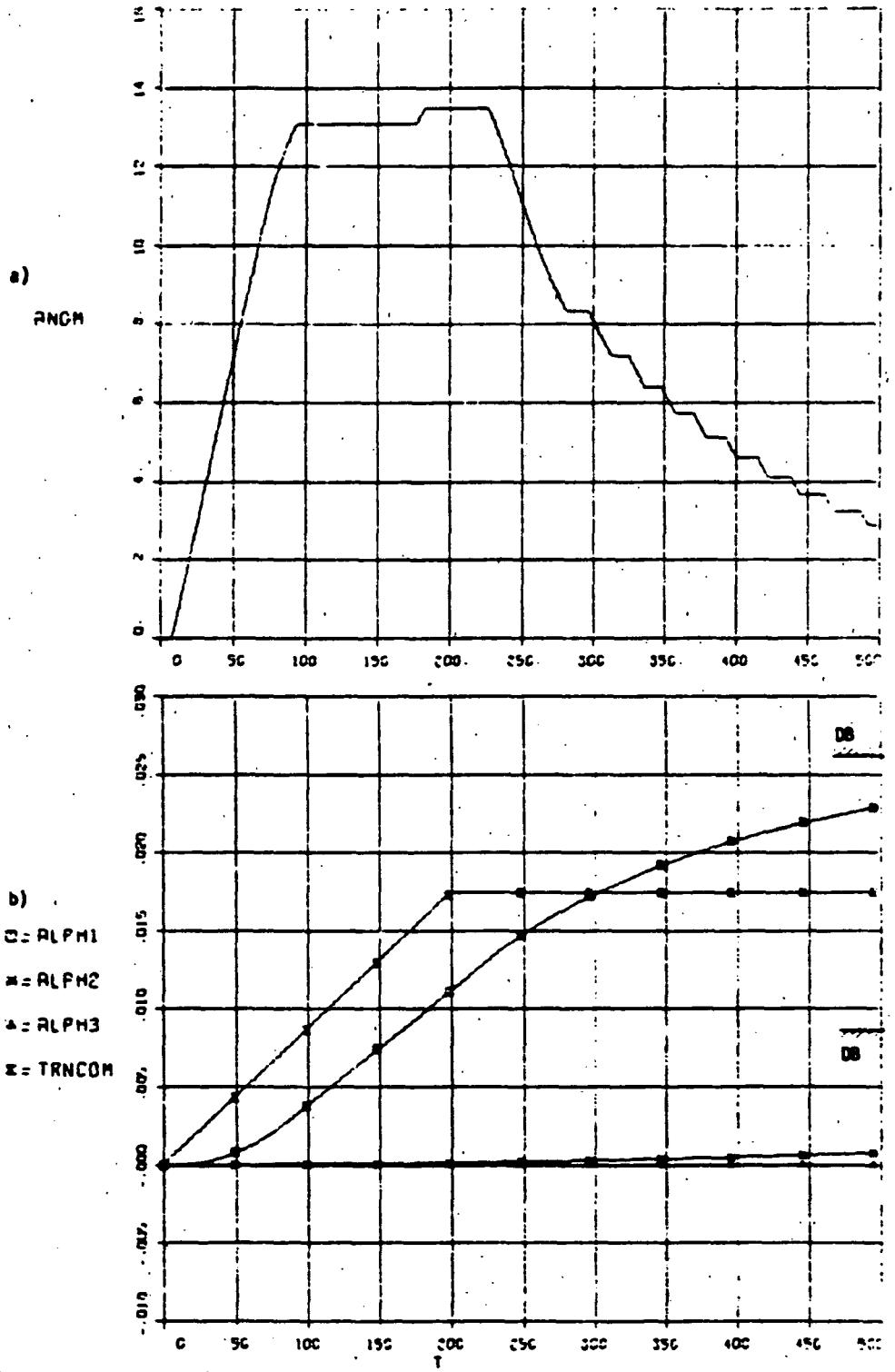

Well damped turn response. At end of simulation vehicle is approaching upper deadband.

FULL FLEX MODEL WITH RCS-LL200/10 FIGURE 4-5
1° X TURN

c)

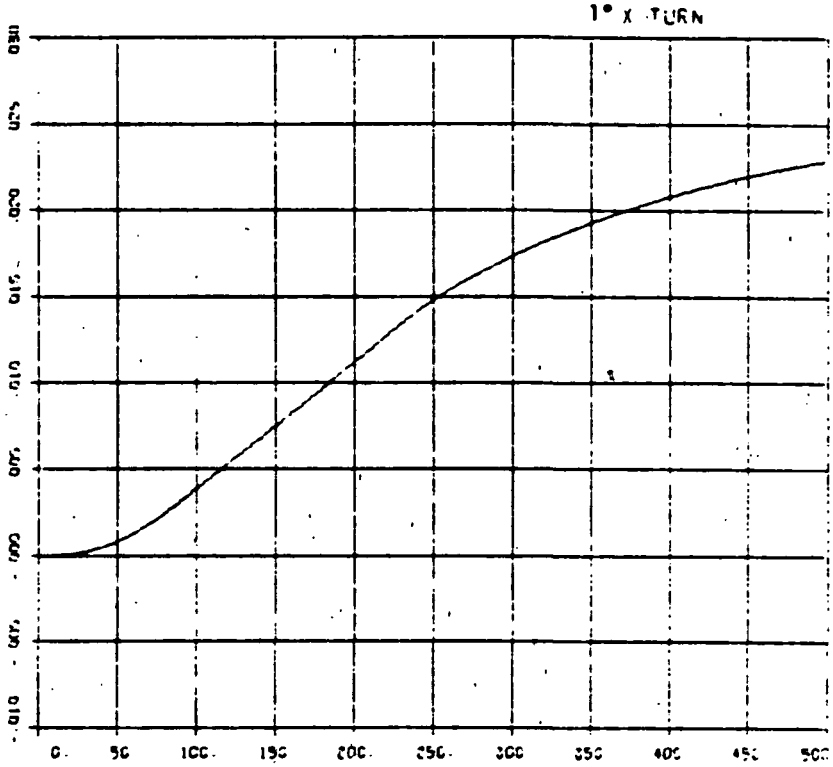

d)

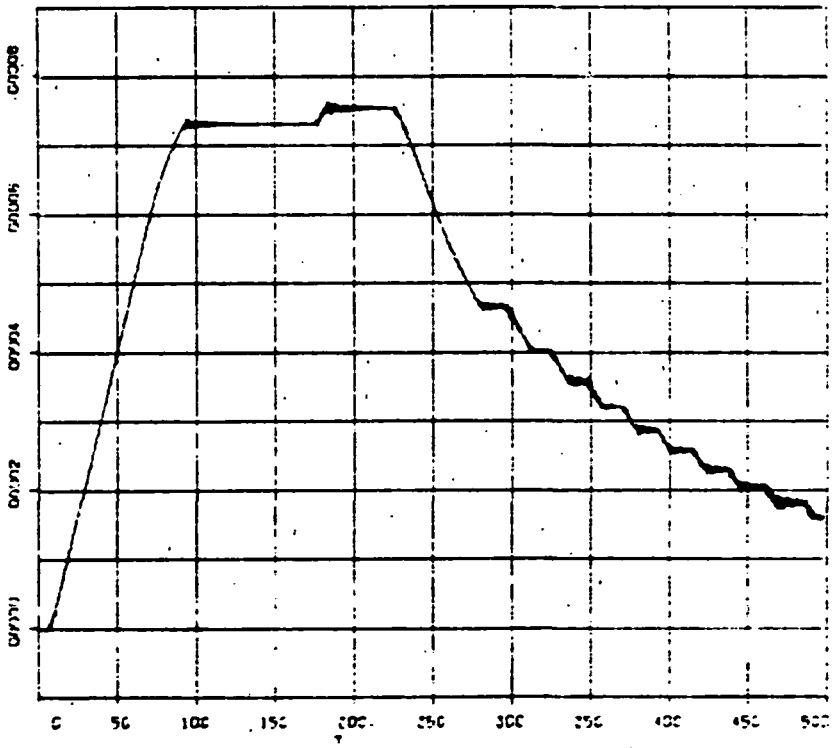

d) Pitch takes -90 s to accelerate to turn rate (0.005°/s) and holds it until turn command stop (T=200) at which time jets fire to slow vehicle down. Note rate vibrations coincident with jet firings.

FULL FLEX MODEL WITH RCS-LLCDC/1D FIGURE 4-5
1°X TURN

e)

PLPH2

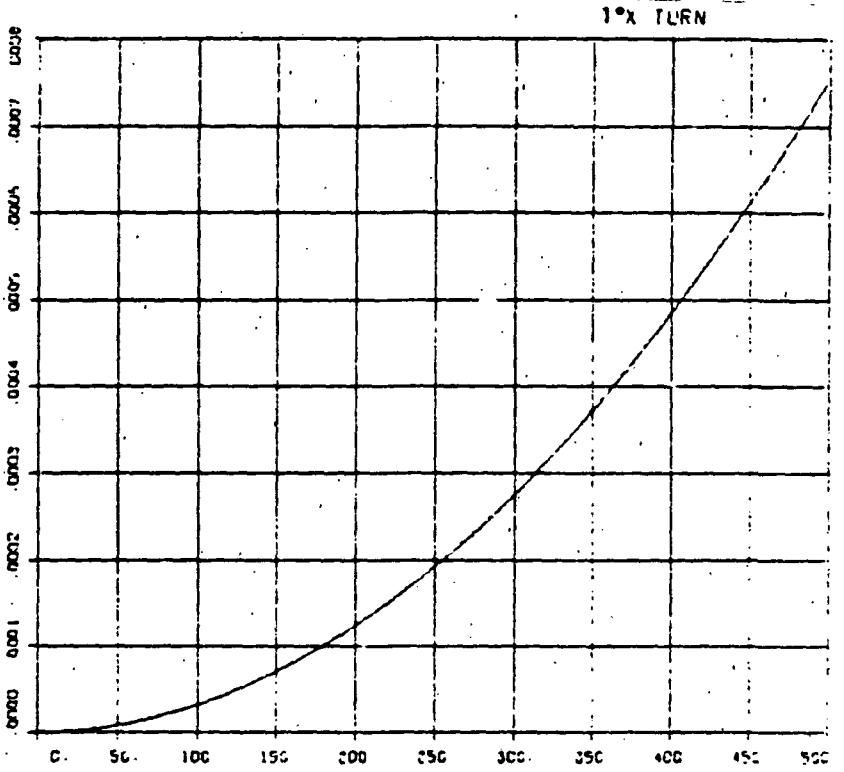

f)

RATE2

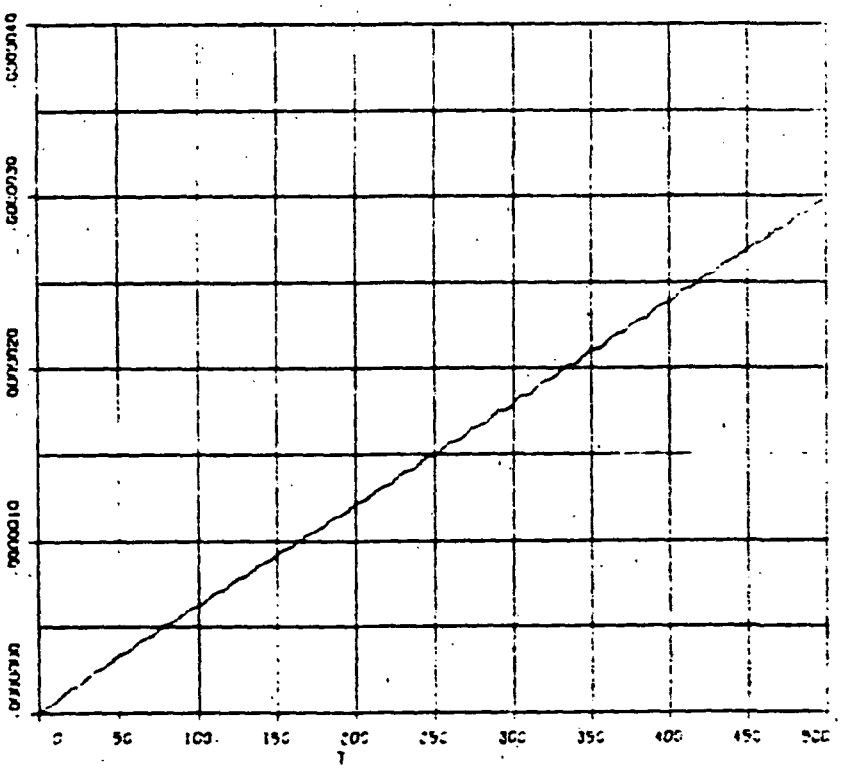

Yaw axis moving within deadband under effect of solar pressure torque ($0.209\ 10^{-4}$ N-m).

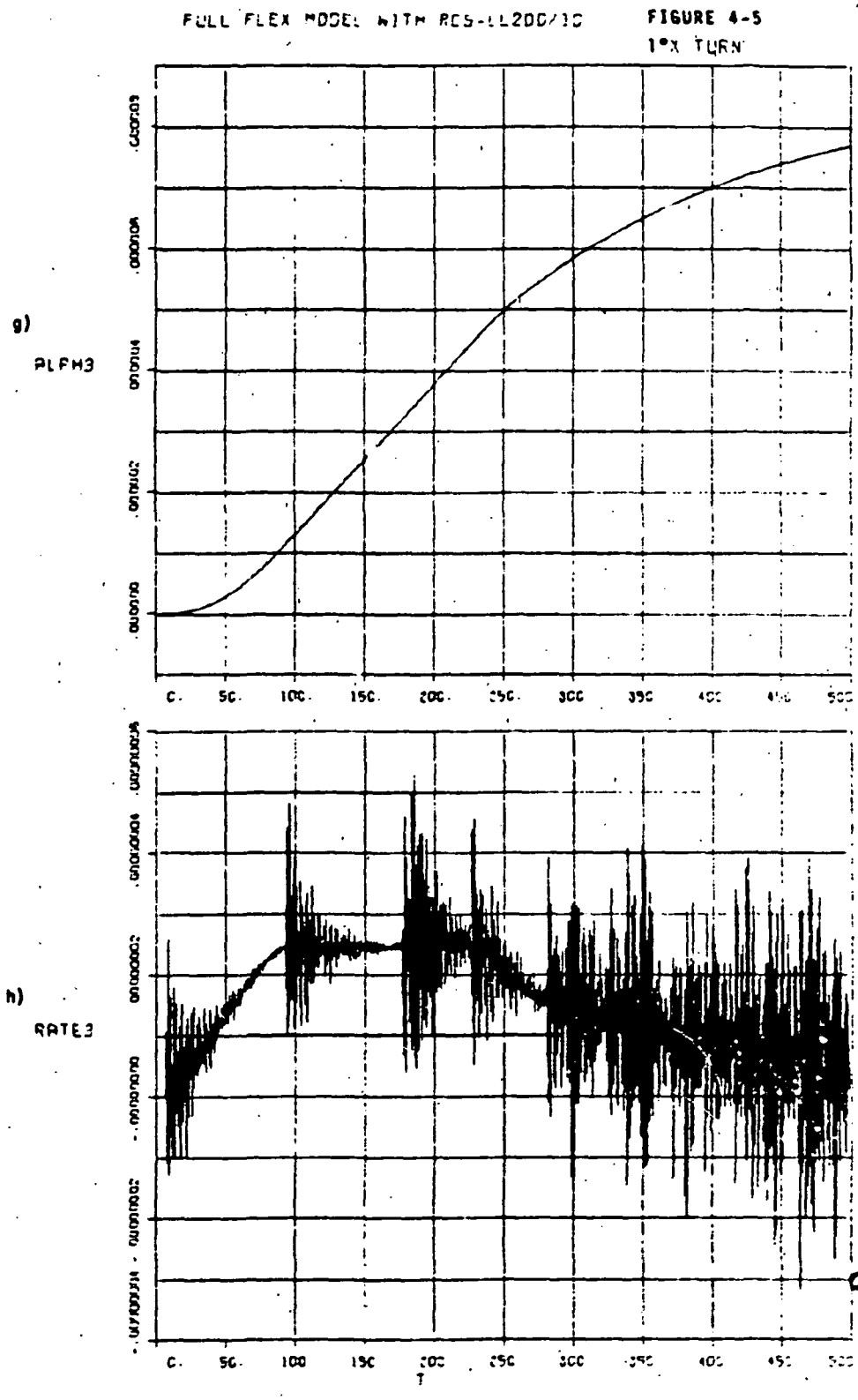

FIGURE 4-5

Motion in roll due to cross-coupling from pitch. Roll jets are not firing. Roll rate spikes due to vibrations in the solar panels caused by pitch firings.

FULL FLEX MODEL WITH ROD-FLEX/ID

FIGURE 4-5

1°X TURN

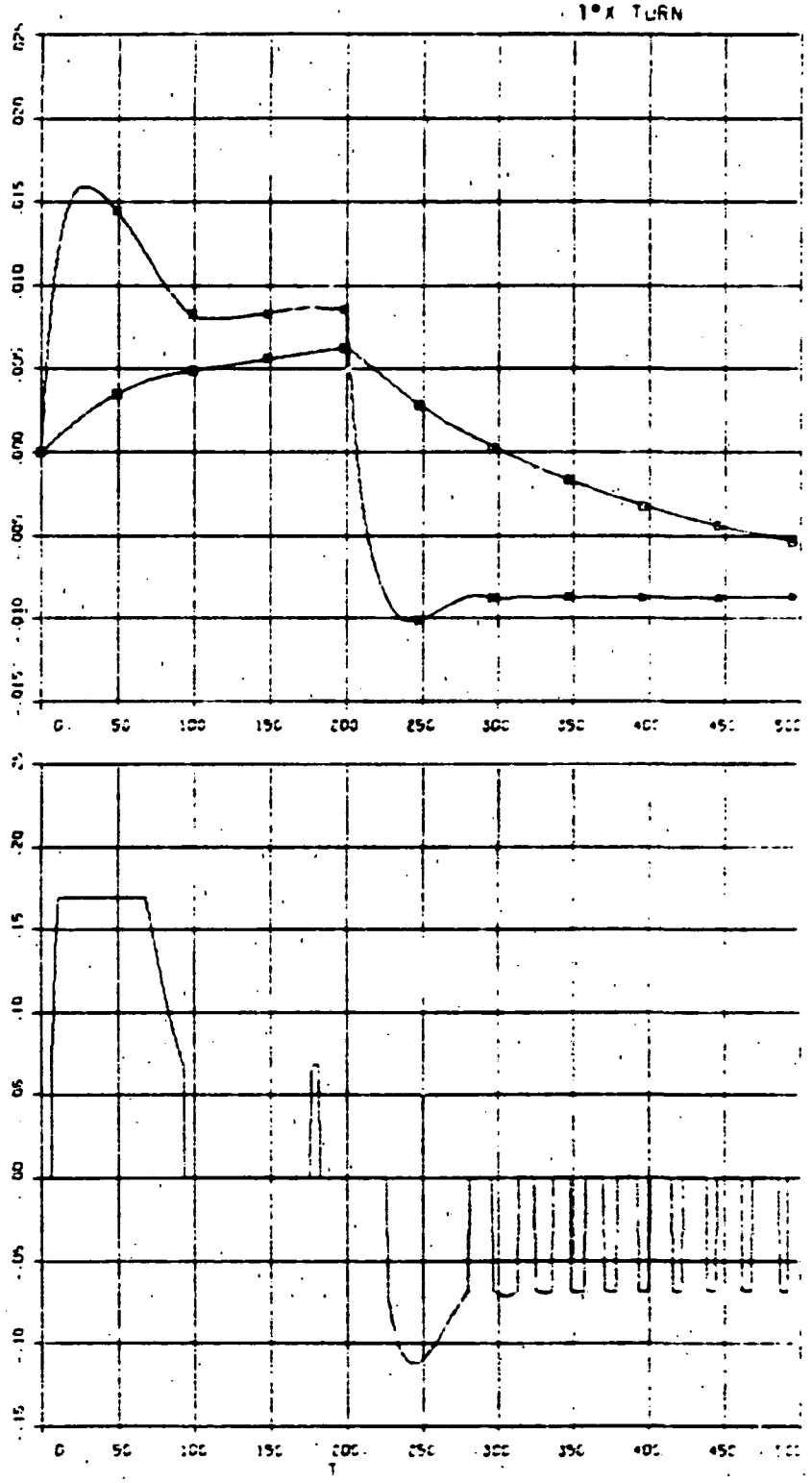

Note impulsive nature of control torques. By comparing with panel deformation plots u) - x) one can observe excitation of structure coincident with on-off edges of torque pulses.

FIGURE 4-5

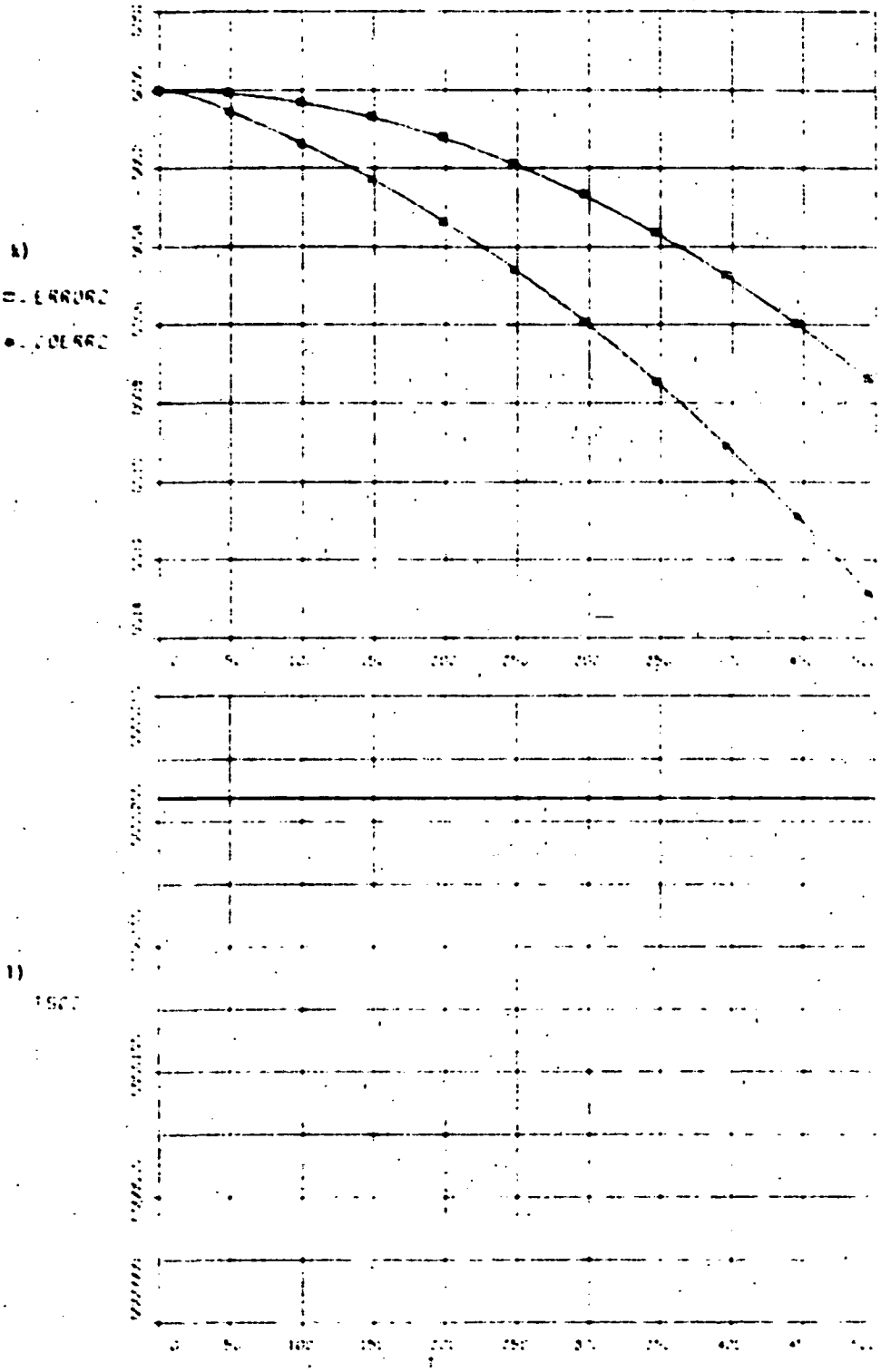

k) Yaw motion is within deadband. l) Shows disturbance torque is the only external torque acting on yaw.

FULL FLEX MODEL WITH RCS-LLCDG/ID

FIGURE 4-5
1°X TURN

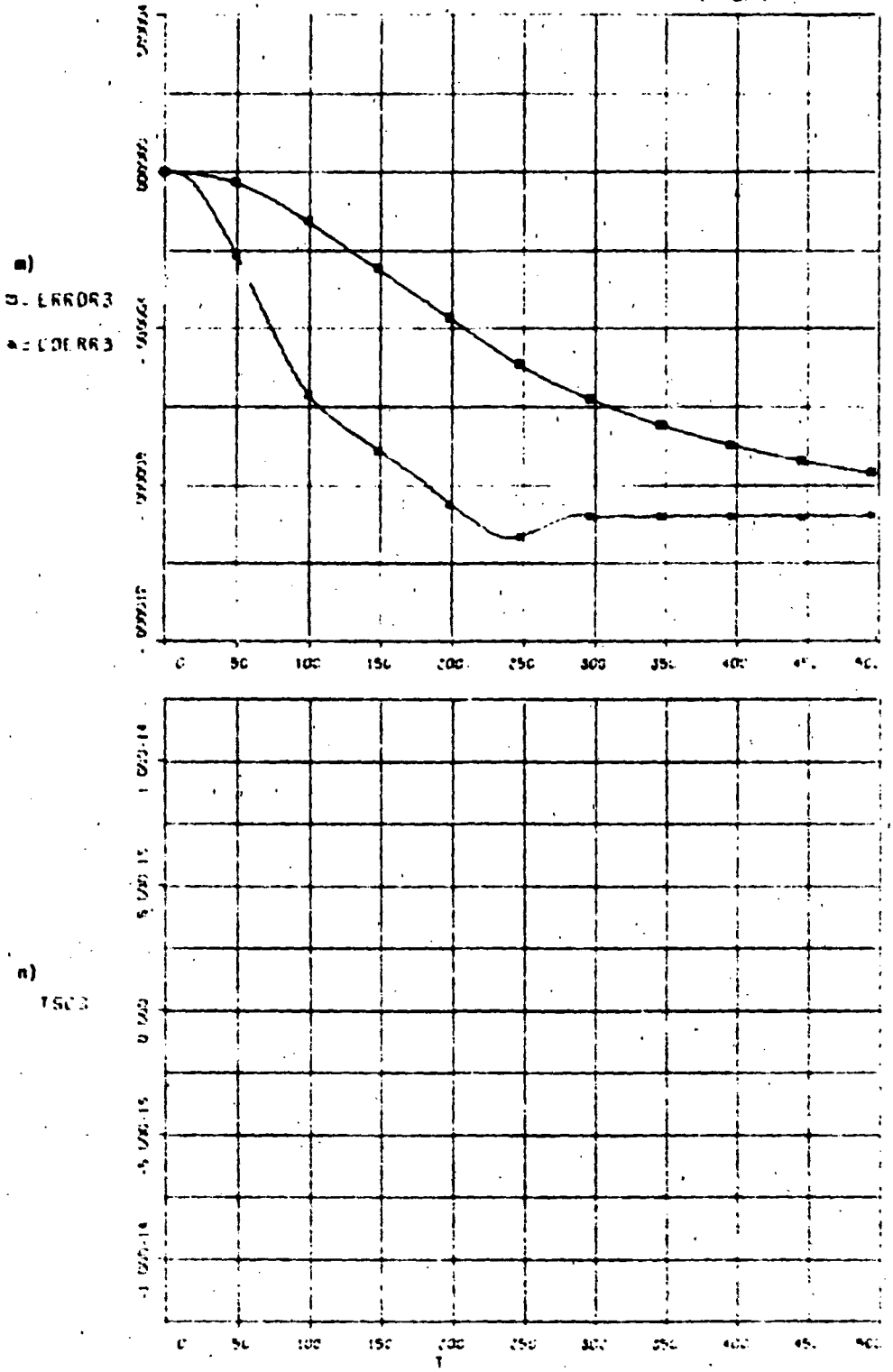

m) Roll motion within deadband. n) No external torques on roll.

FULL FLEX MODEL WITH RCS-LL200/10 FIGURE 4-5
1°X TURN

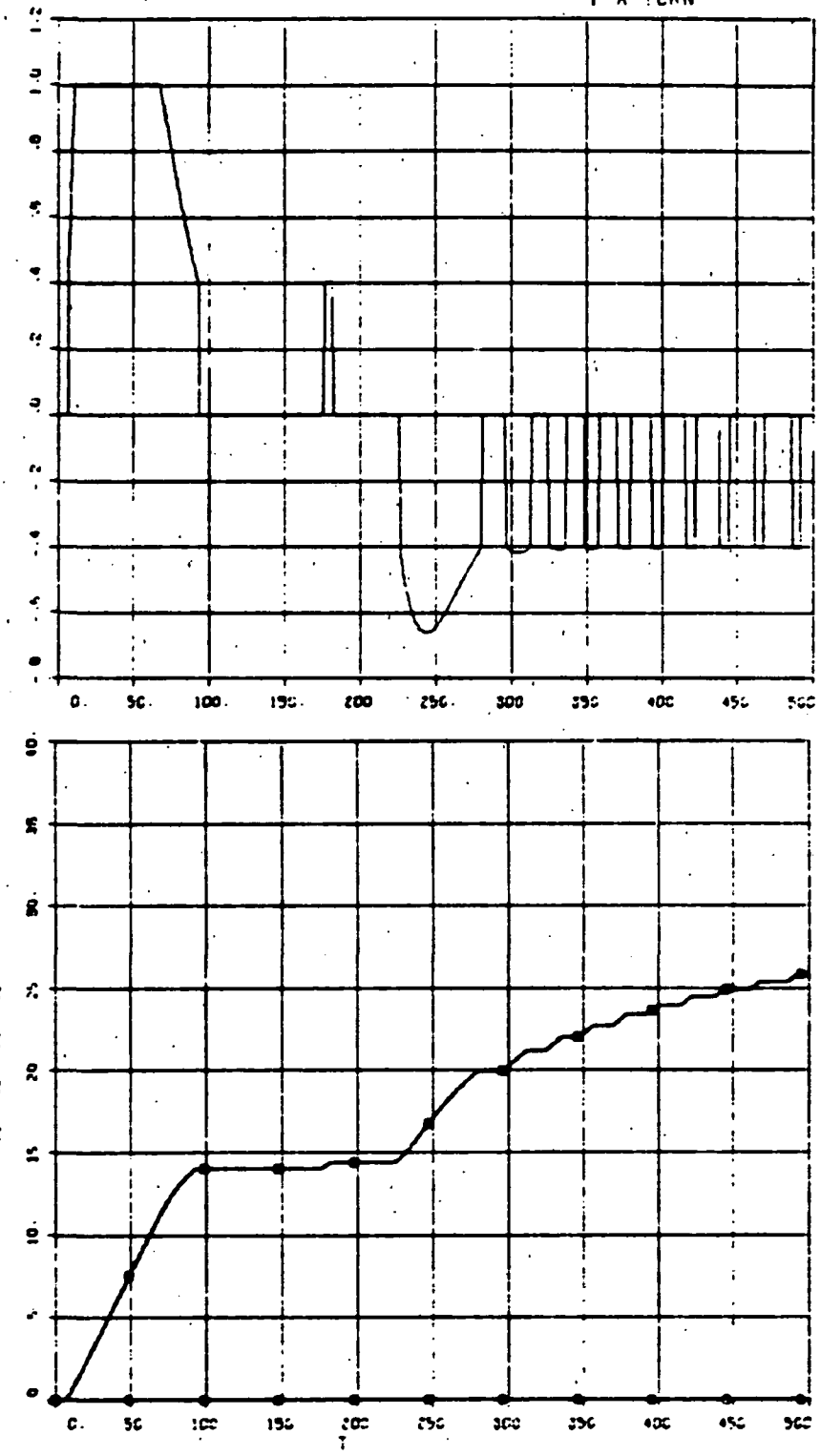

a) Expected gas consumption to come to a complete stop -29 gr.

FULL FLEX MODEL WITH RCS-LL200-10

FIGURE 4-5
1°X TURN

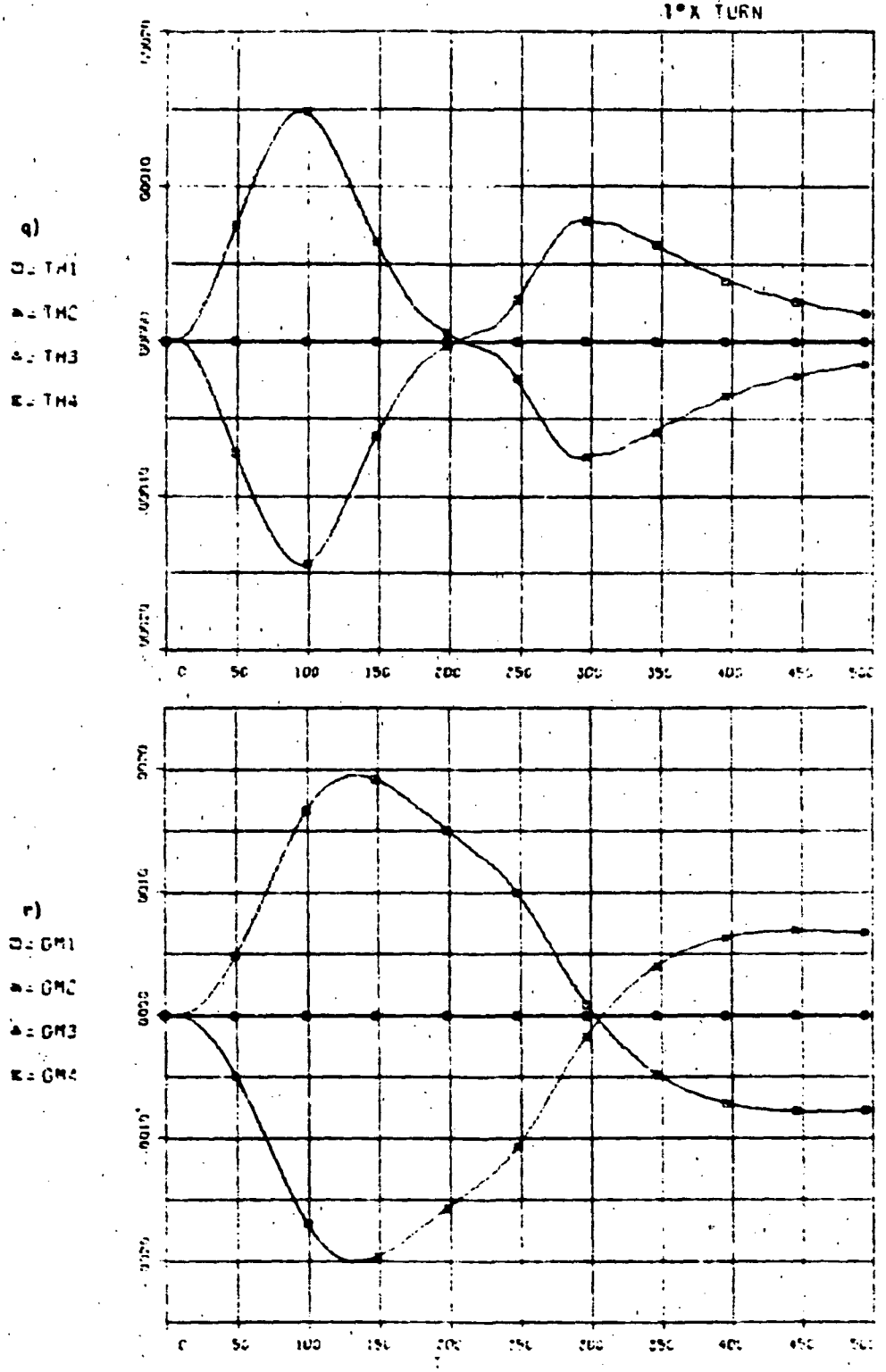

Small hinge torques and deflections.

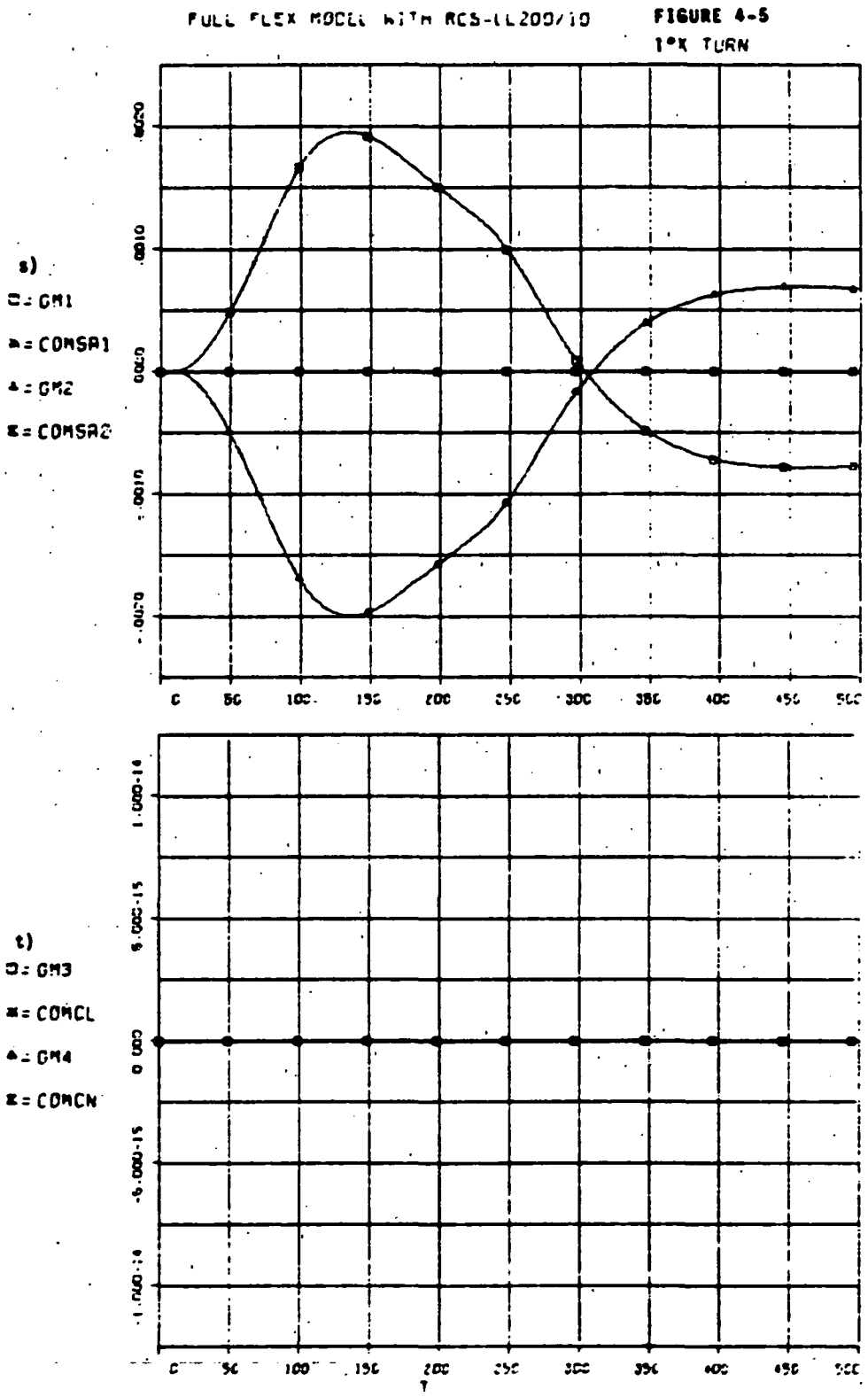

FIGURE 4-5

t) Shows scan platform locked in place for this maneuver.

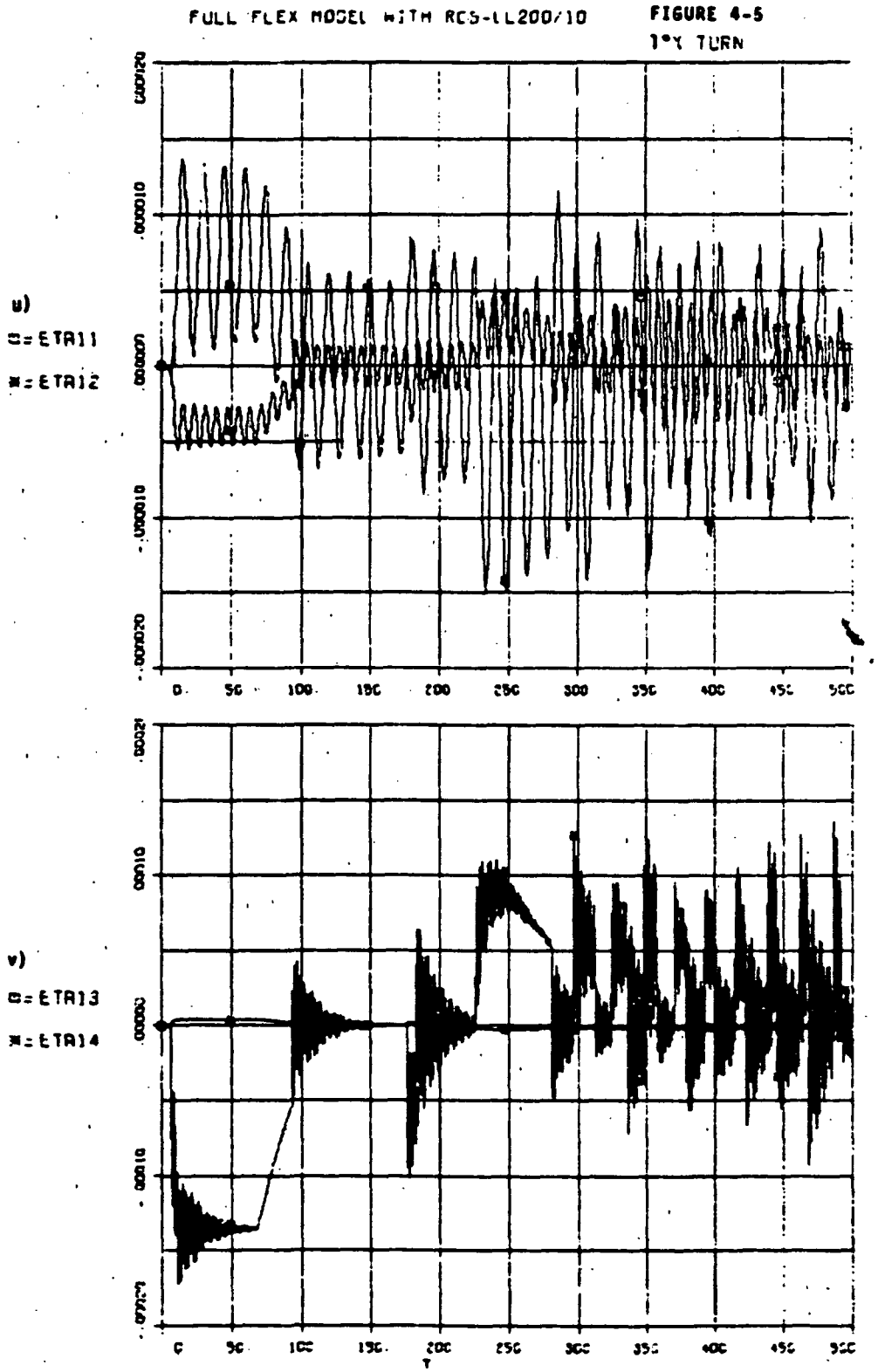

FIGURE 4-5

u) through x)
Solar array generalized deformation coordinates showing excitation of the vibrational modes coincidently with jet pulses. Predictably, in-plane excitation is predominant for this maneuver. Residual vibration levels are high.

FULL FLEX MODEL WITH RCS-LOOP 10

FIGURE 4-5

1ST TURN

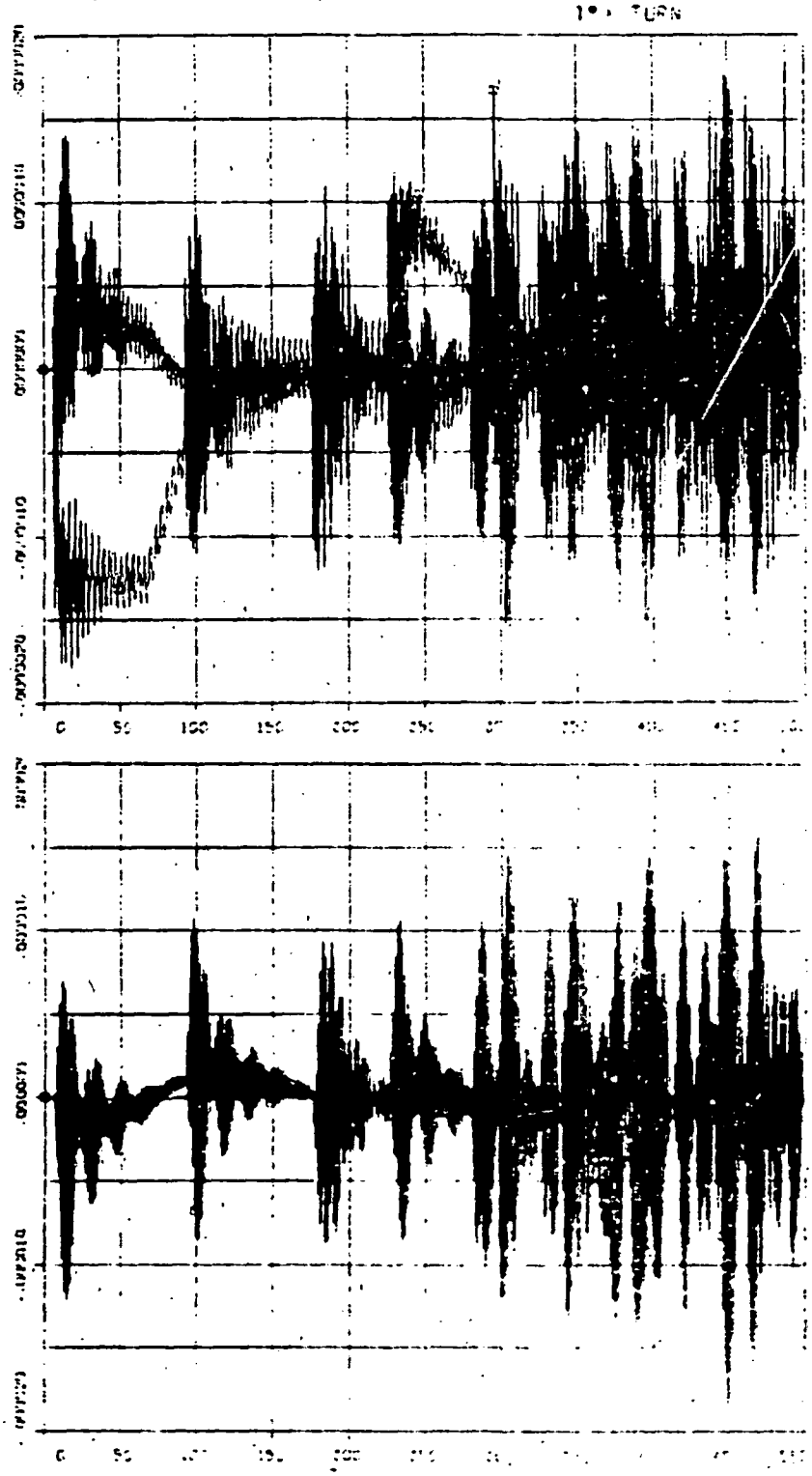

w)

□ ELTR15

▲ ELTR16

x)

□ ELTR17

▲ ELTR18

FIGURE 4-6

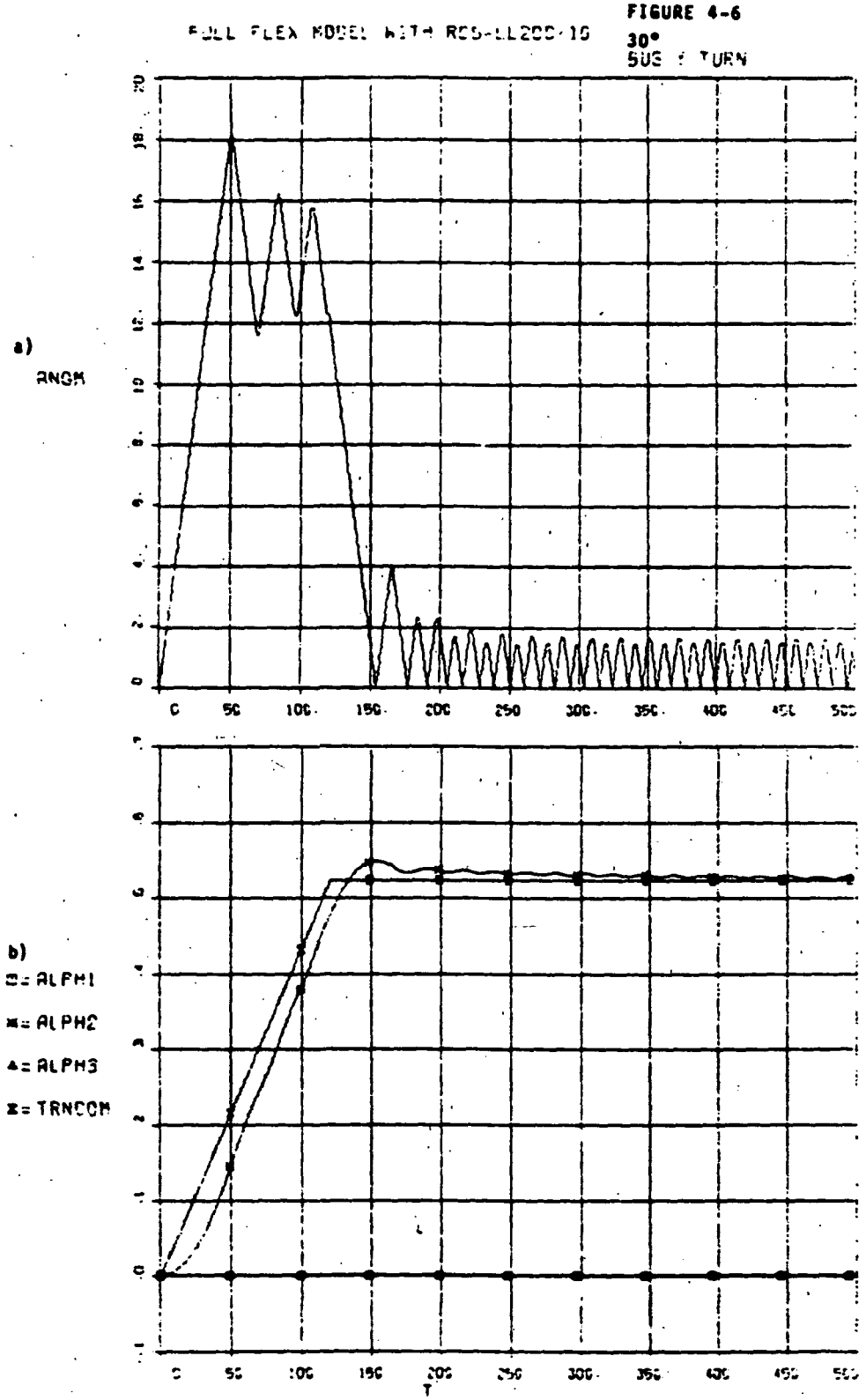

Poor turn performance with excessive (undamped) limit cycling. Results in unacceptable gas consumption of -9 gr/minute after turn is supposed to have ended.

FIGURE 4-6

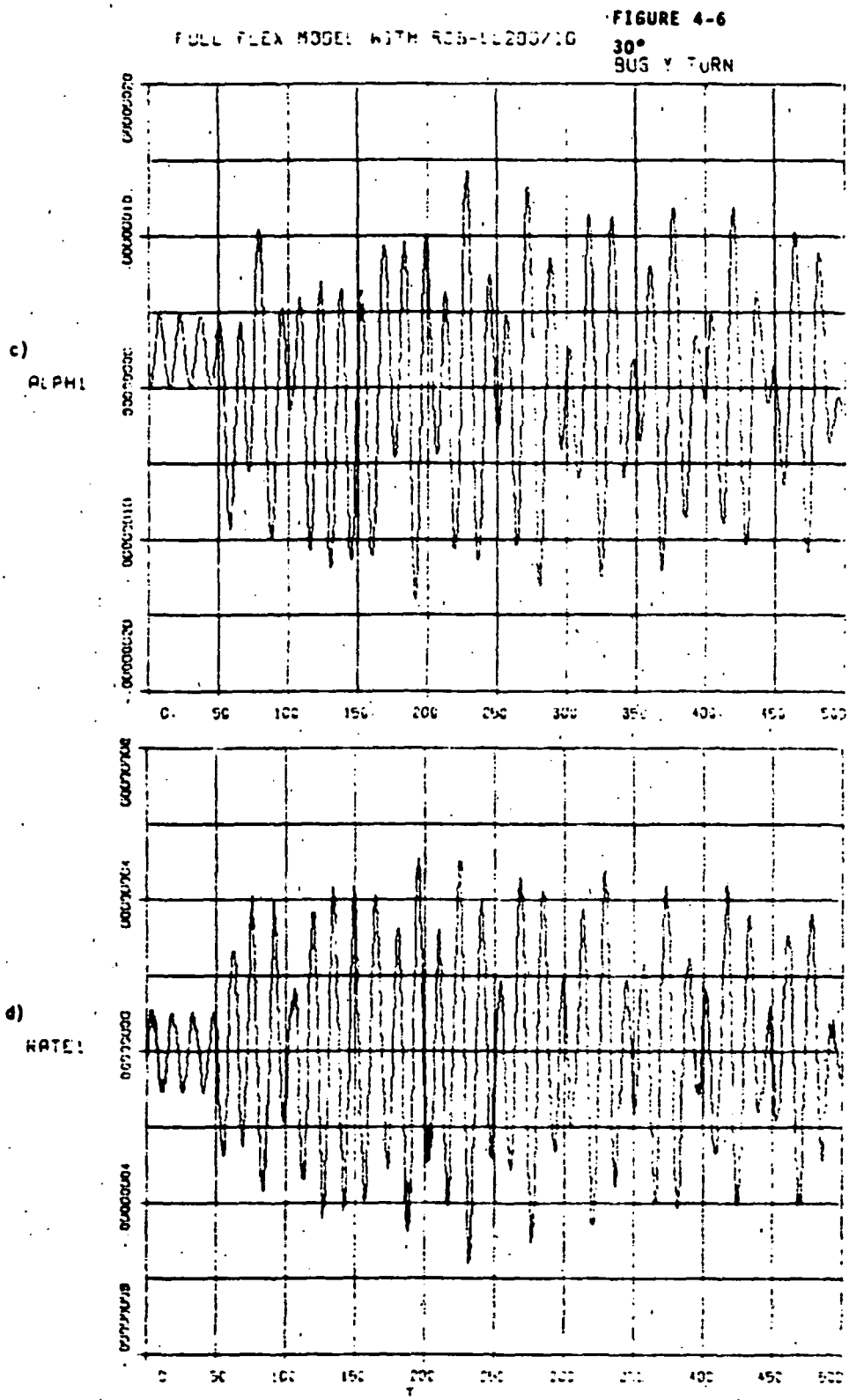

Small pitch oscillations due to flexibility, within deadband.

FIGURE 4-6

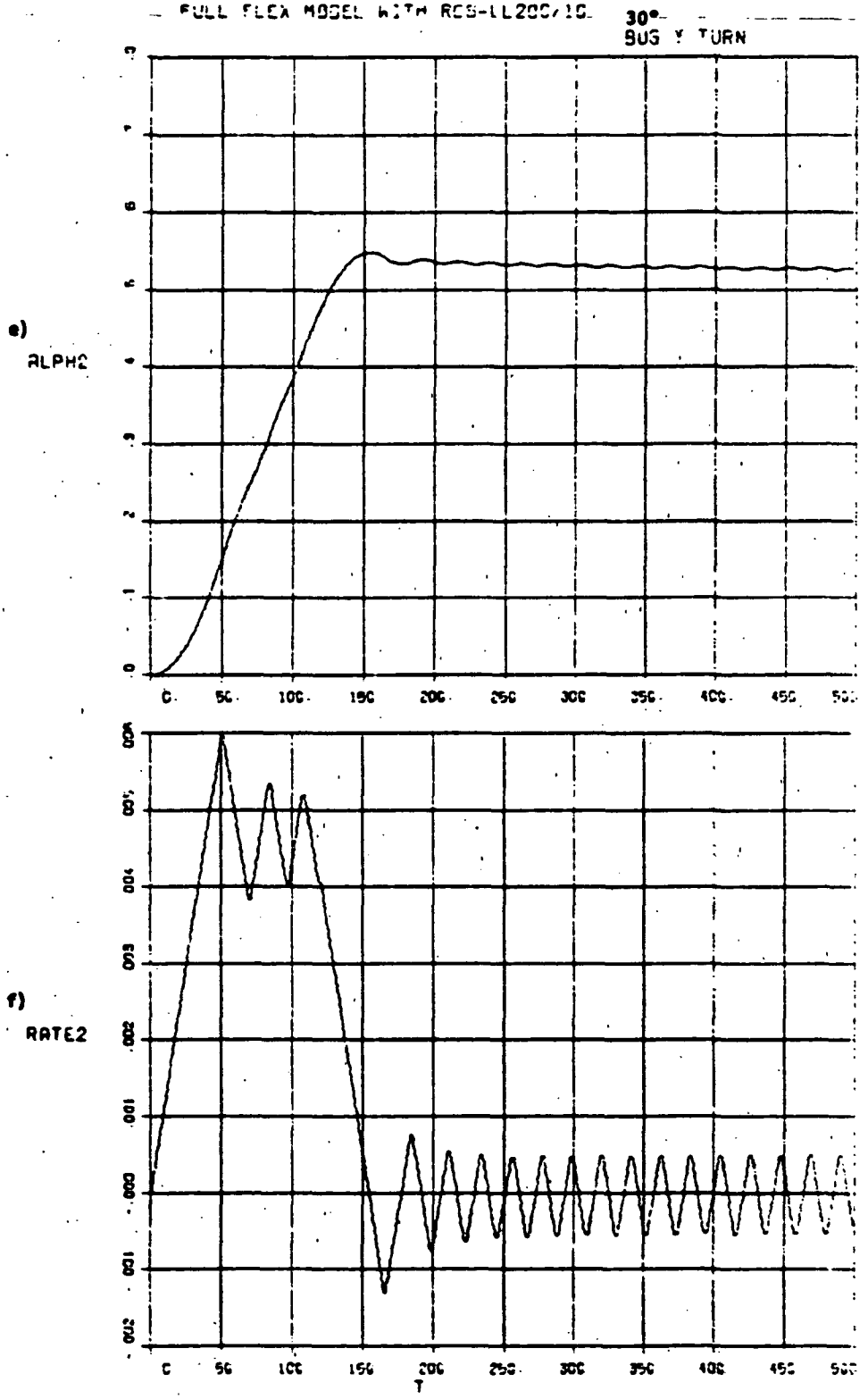

Yaw undamped limit cycling.

FIGURE 4-6

30°

g)

ALPH3

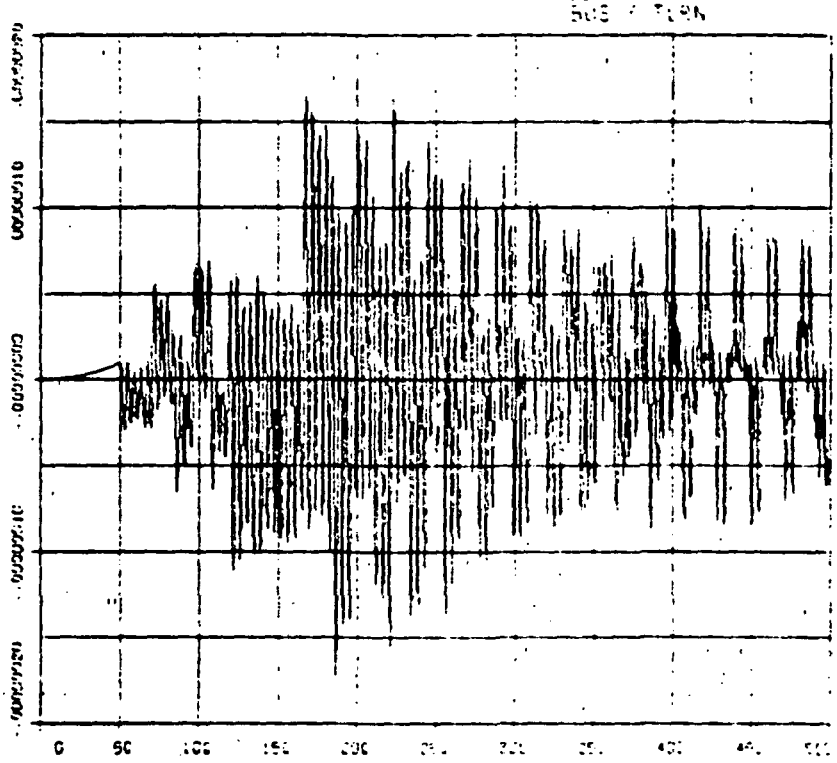

h)

RATE3

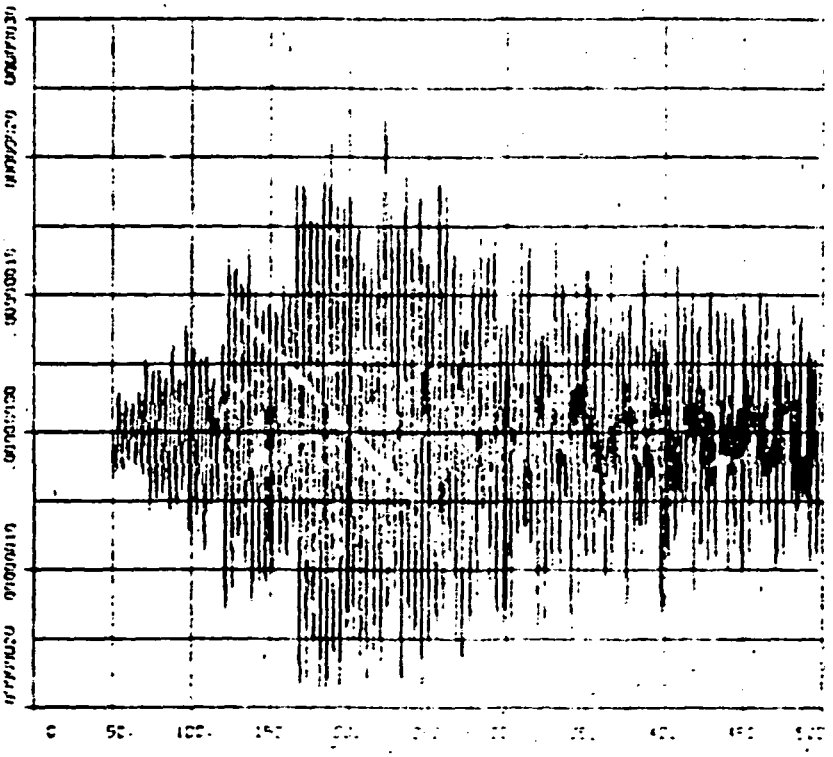

Small roll oscillations due to flexibility, within deadband

FIGURE 4-6
30°
SUS Y TURN

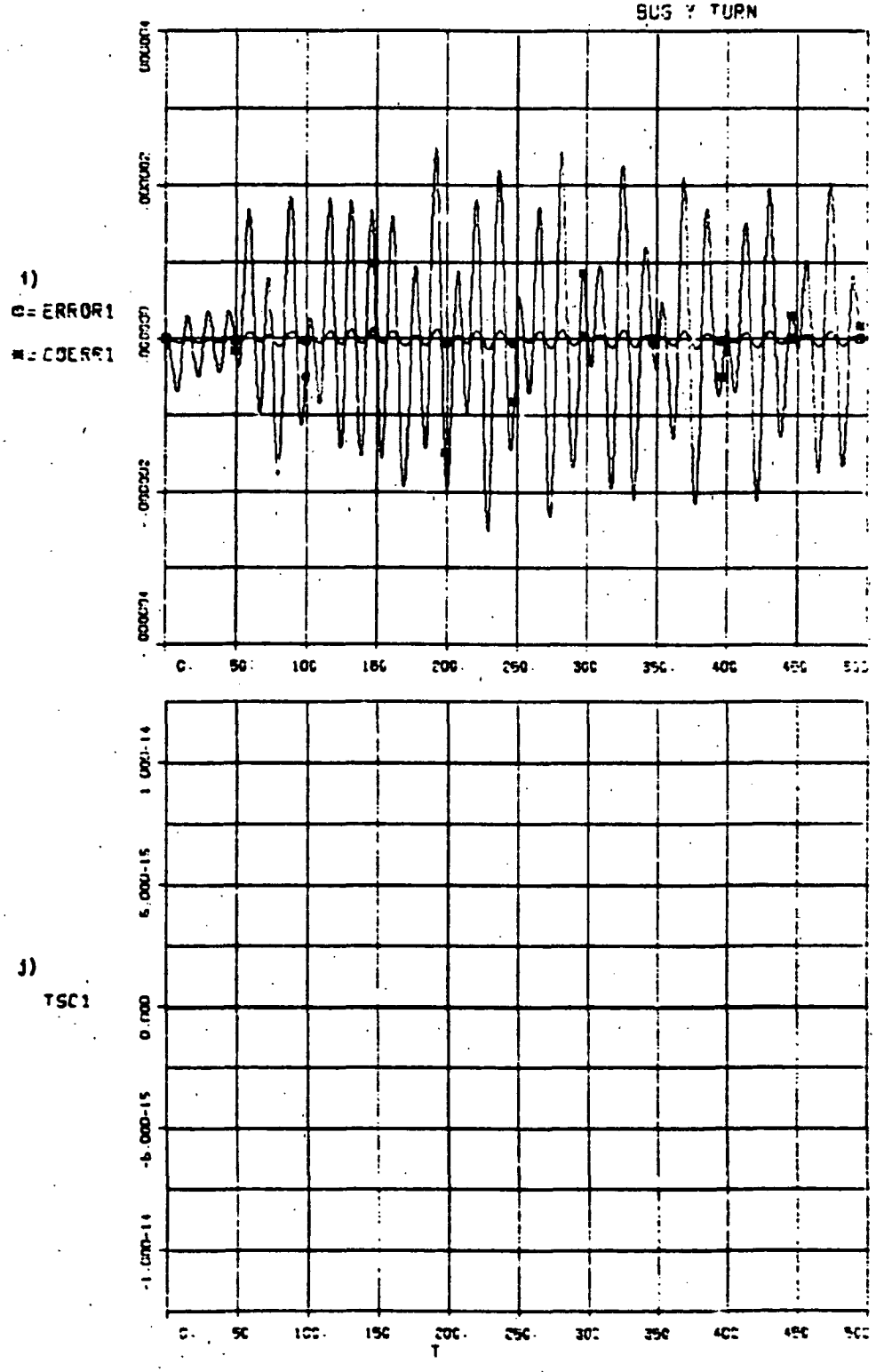

FIGURE 4-6

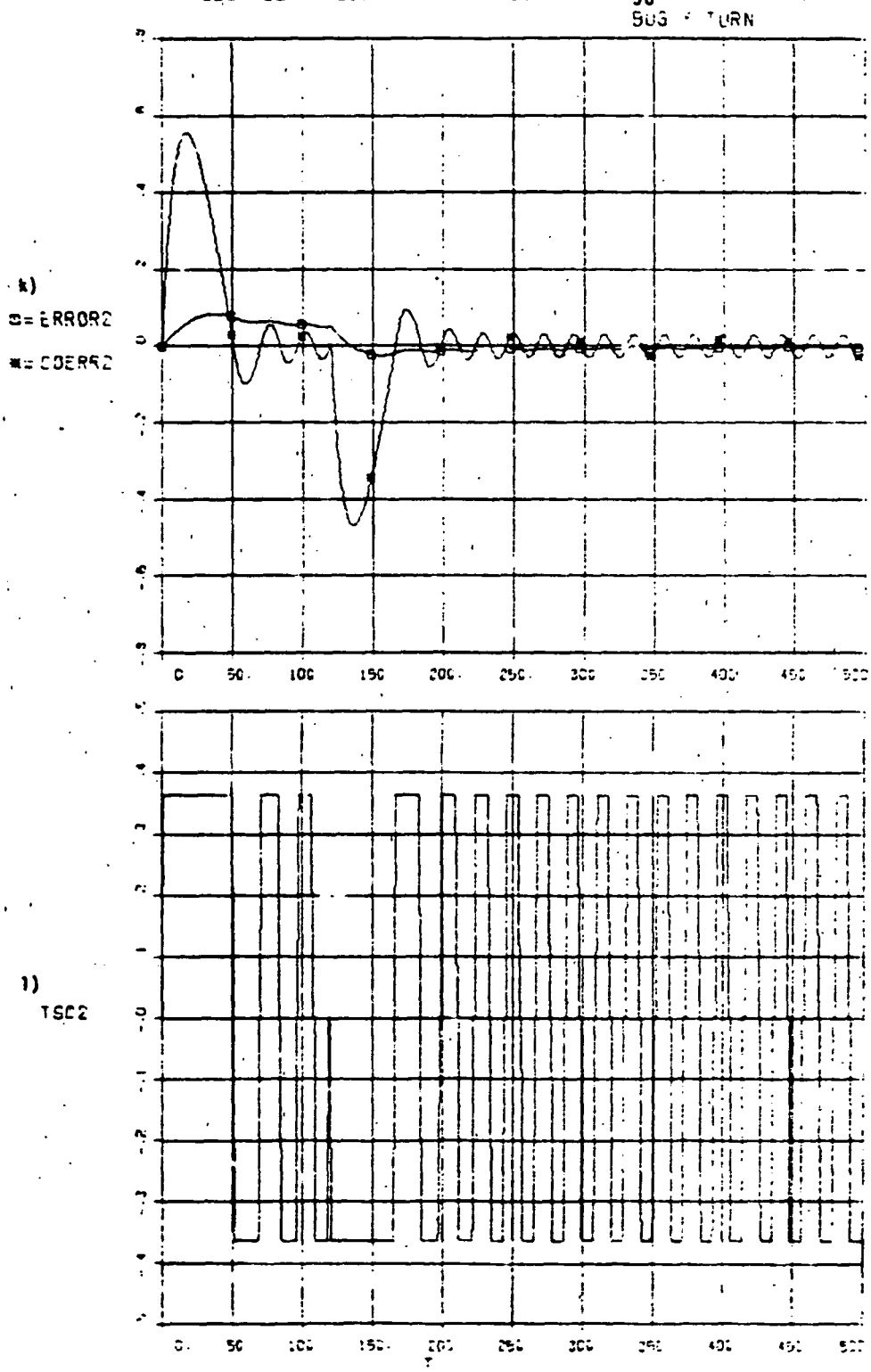

Undamped oscillating yaw control error and resulting gas jet firings.

FIGURE 4-6

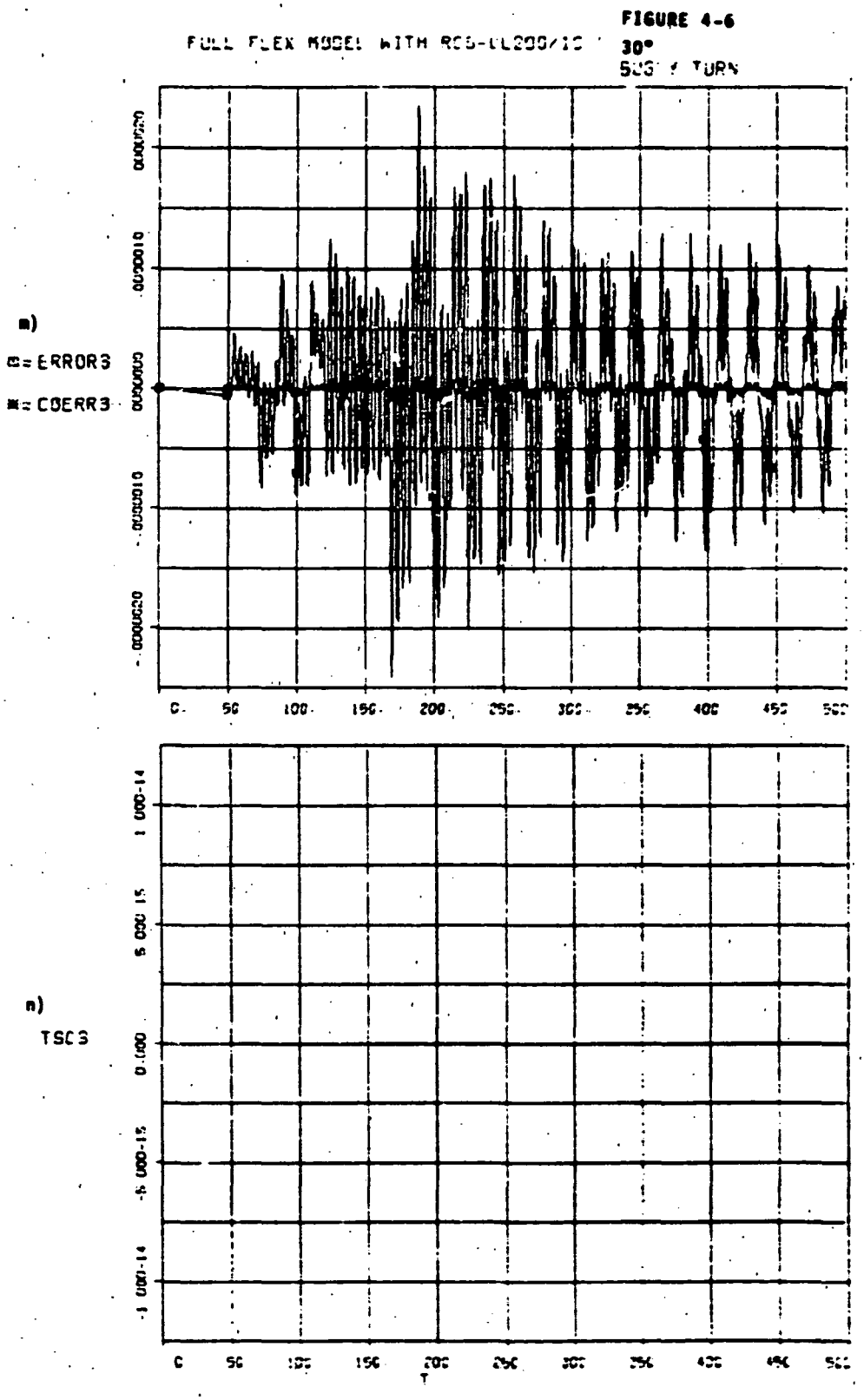
FULL FLEX MODEL WITH RCS-UL200/10
30°
SEC / TURN
a)
□ = ERROR3
* = COERR3
0.000020
0.000010
0.000000
-0.000010
-0.000020
0
50
100
150
200
250
300
350
400
450
500
b)
TSC3
1.000-14
5.000-15
0.000
-5.000-15
-1.000-14
0
50
100
150
200
250
300
350
400
450
500
T

FIGURE 4-6

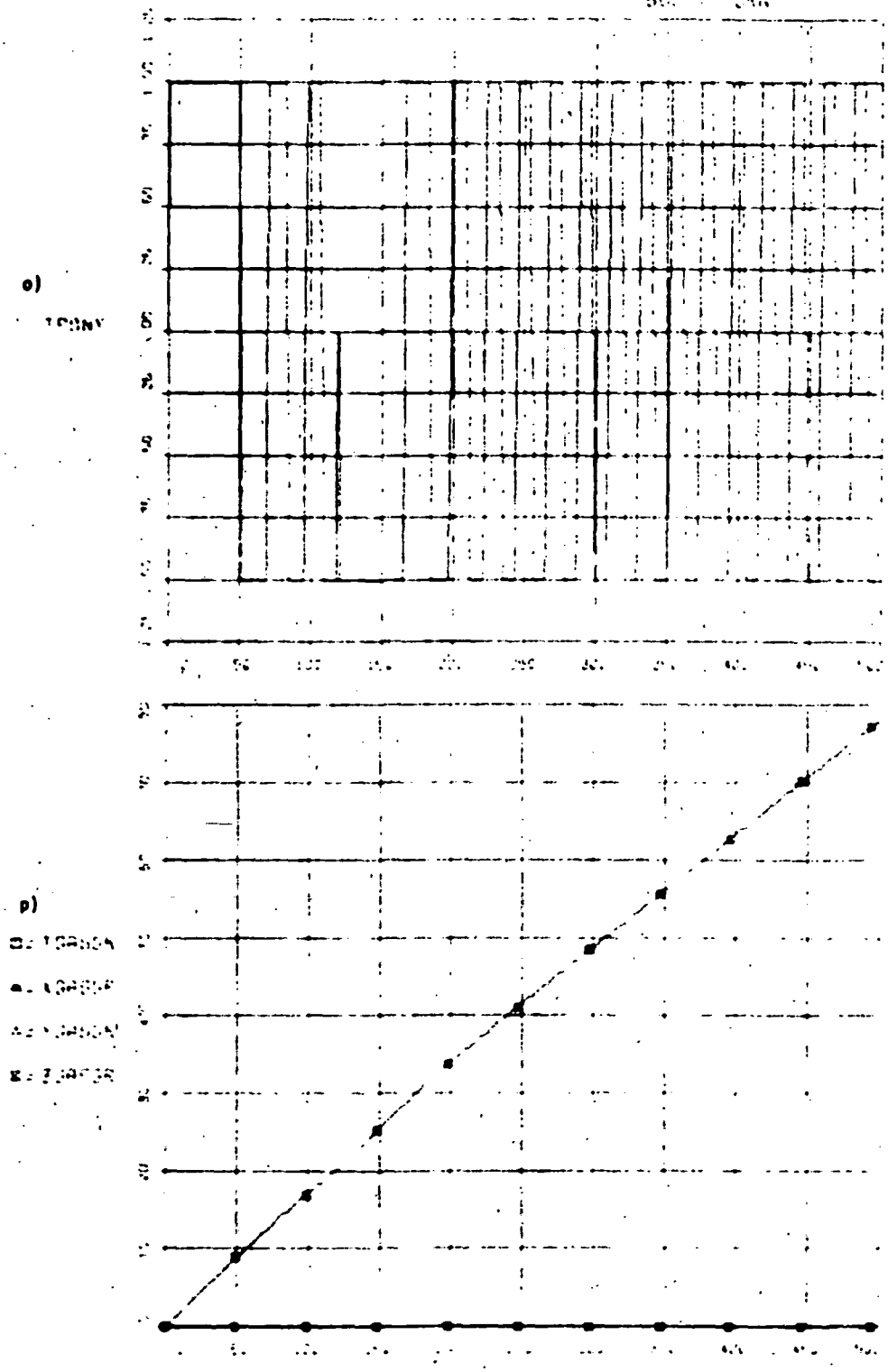

Excessive gas consumption.

FIGURE 4-6

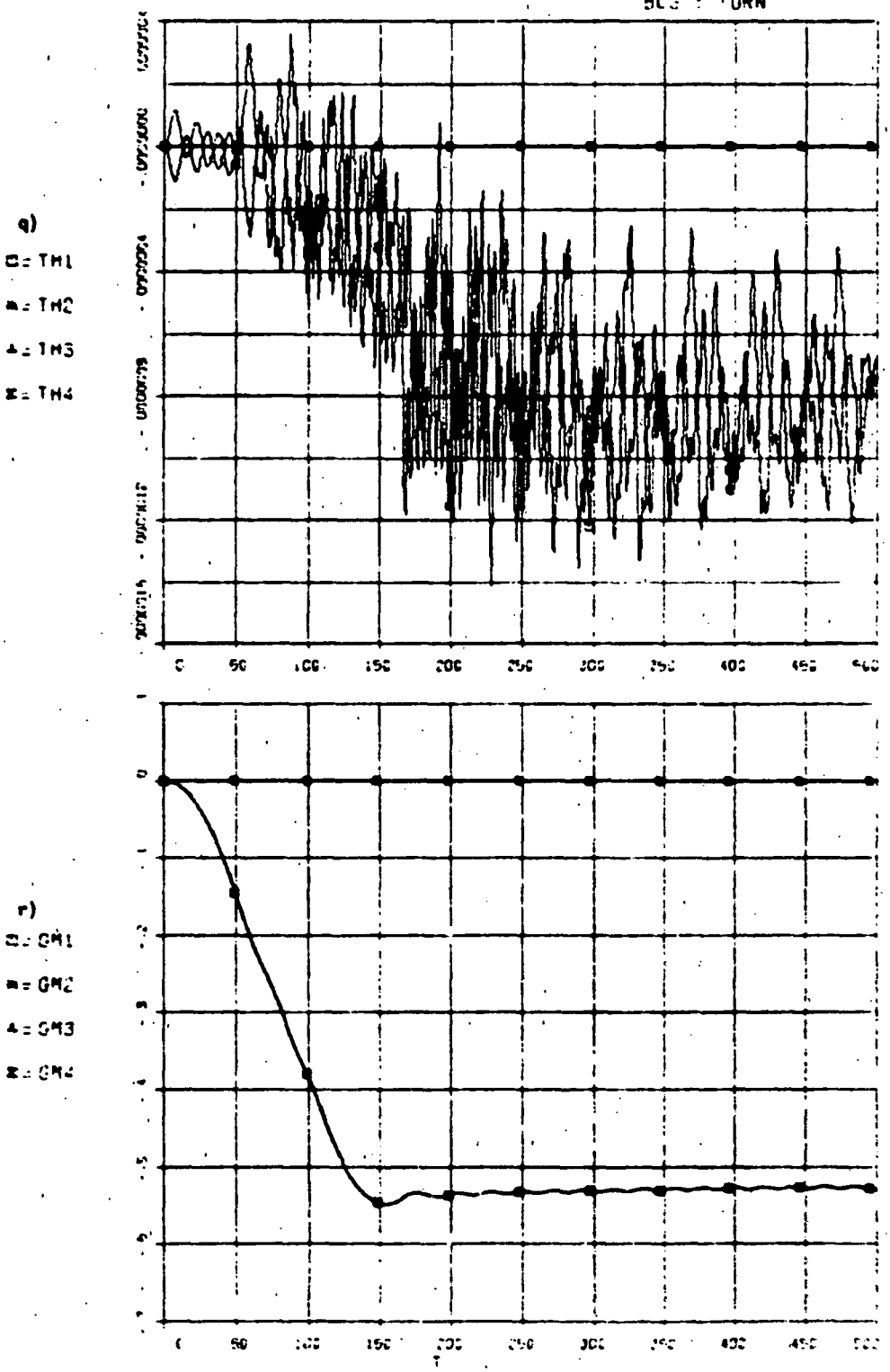

q) Small hinge torques on SA. r) SA wings turn -30° with respect to the bus so as to stay on the sun as the bus turns.

FIGURE 4-6

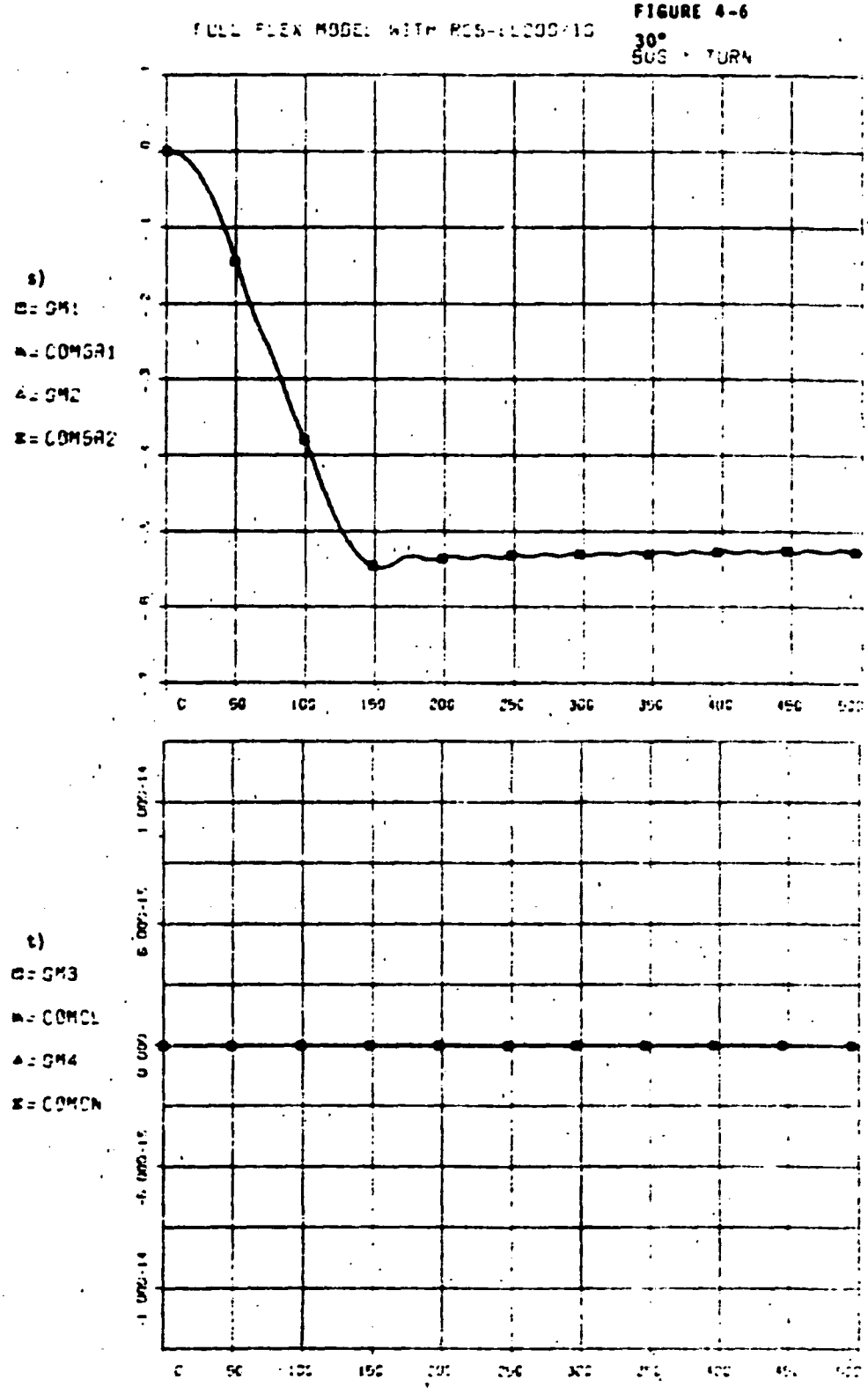

s) SA wings track their commands to -30° with respect to bus. t) Scan platform locked in place for this maneuver.

FIGURE 4-6

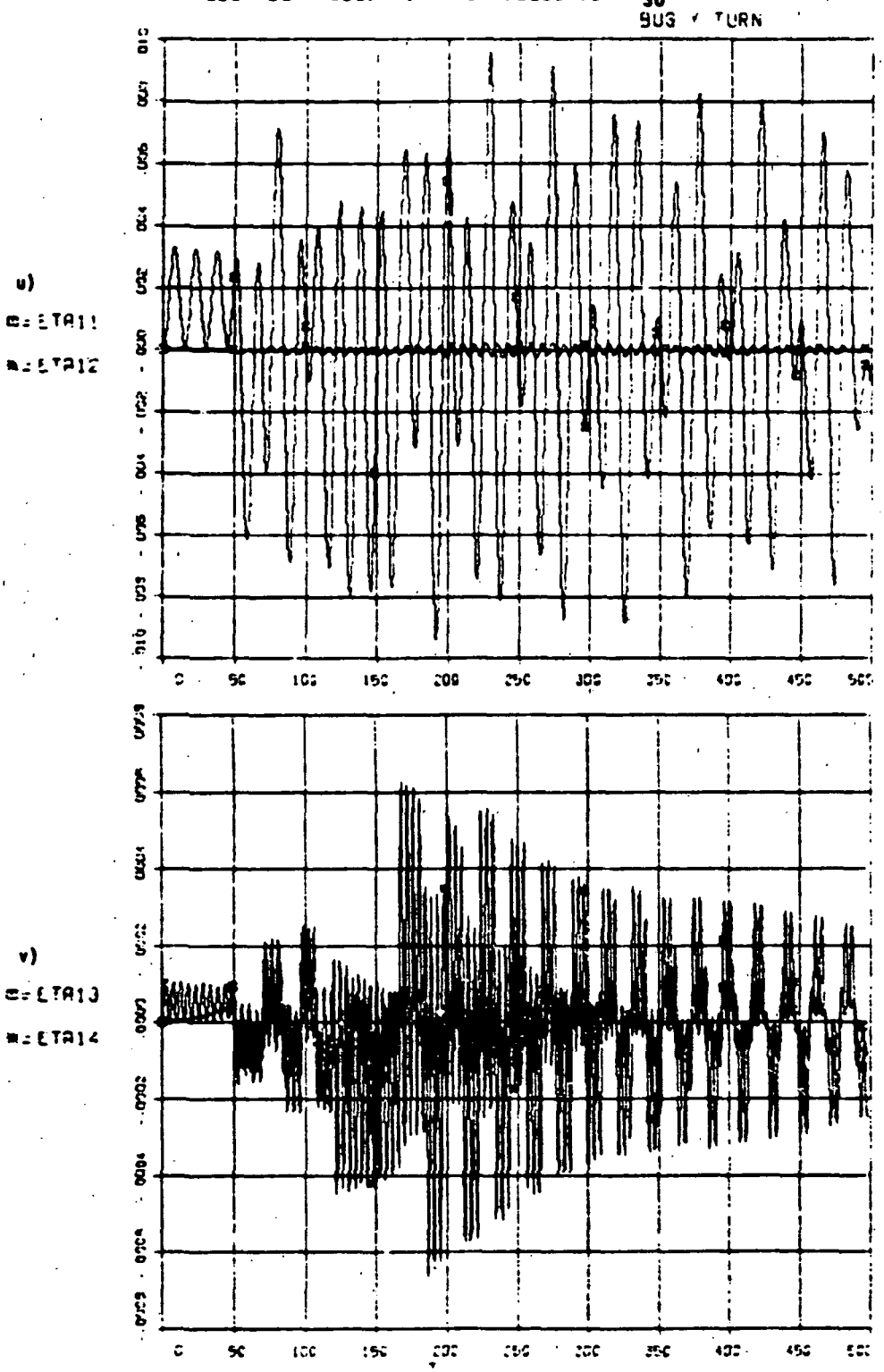

u) through x)
Solar array generalized deformation coordinates showing excitation of the vibrational modes coincidently with jet pulses. Predictably, out-of-plane excitation is predominant for this maneuver. Note high residual vibration.

FIGURE 4-6

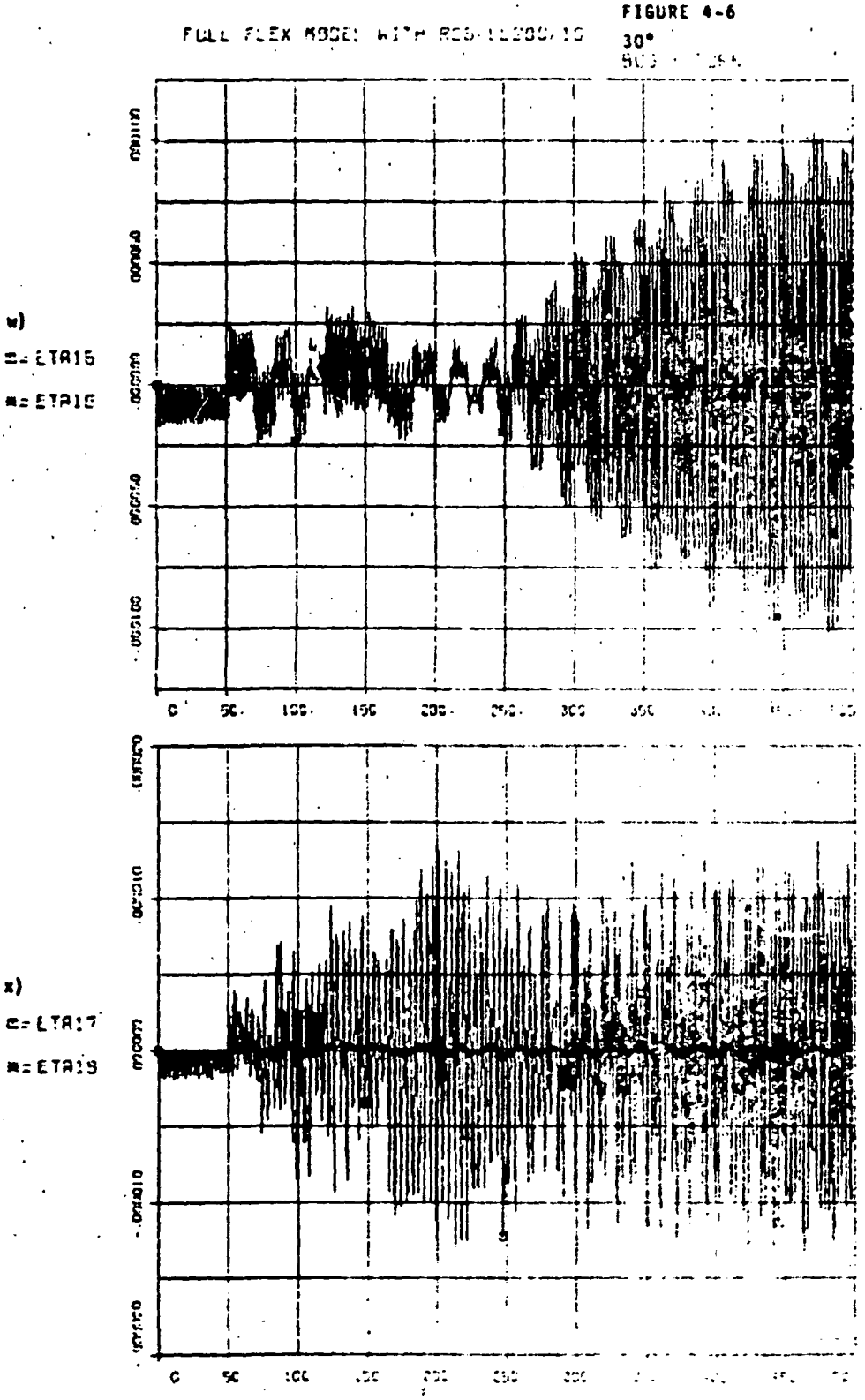
FULL FLEX MODEL WITH RCS-112000-10
30°
w)
E= ETA15
M= ETA16
x)
E= ETA17
M= ETA18
0
50
100
150
200
250
300
350

FIGURE 4-7

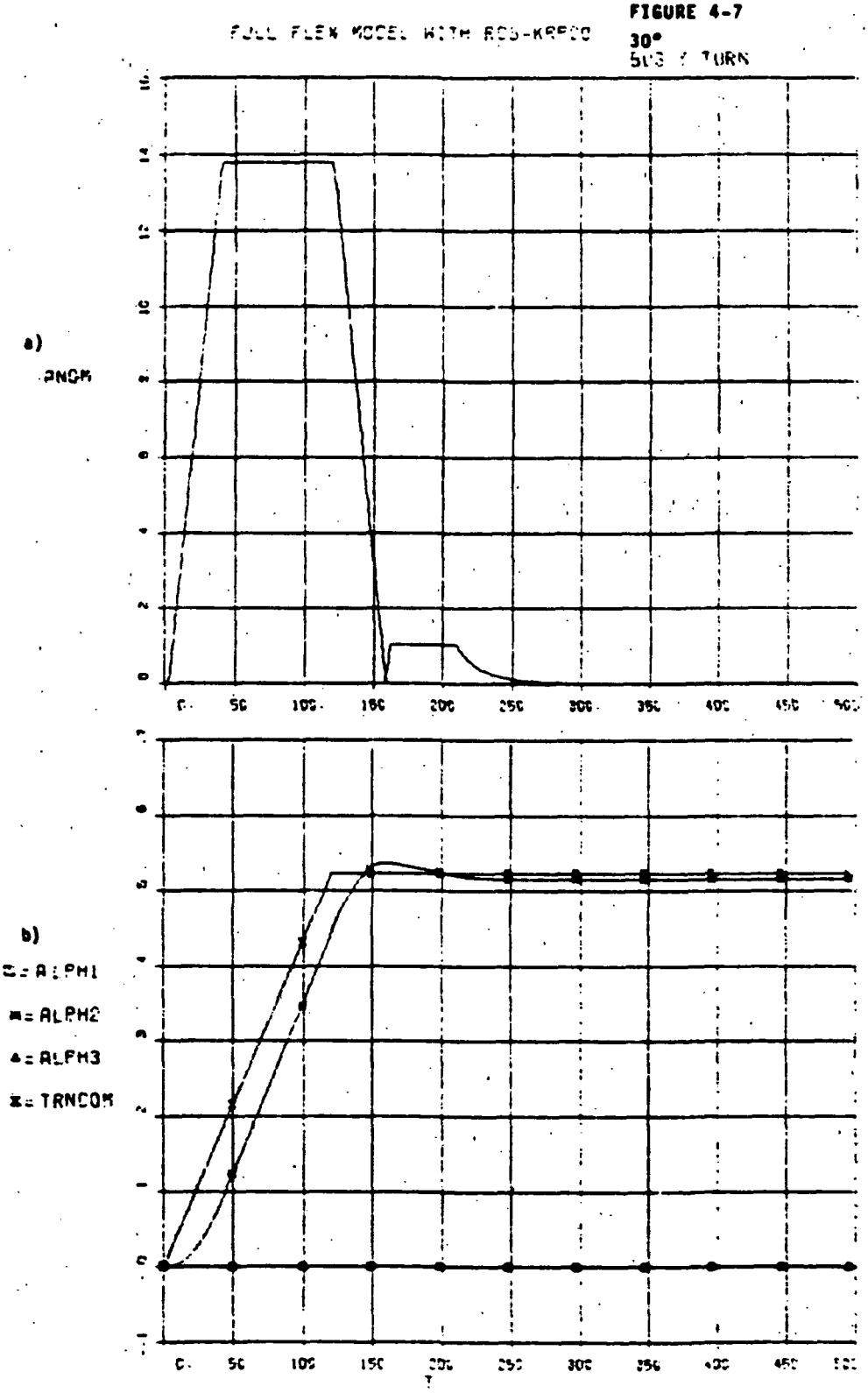

Good turn performance with a slight overshoot.

FIGURE 4-7
30°

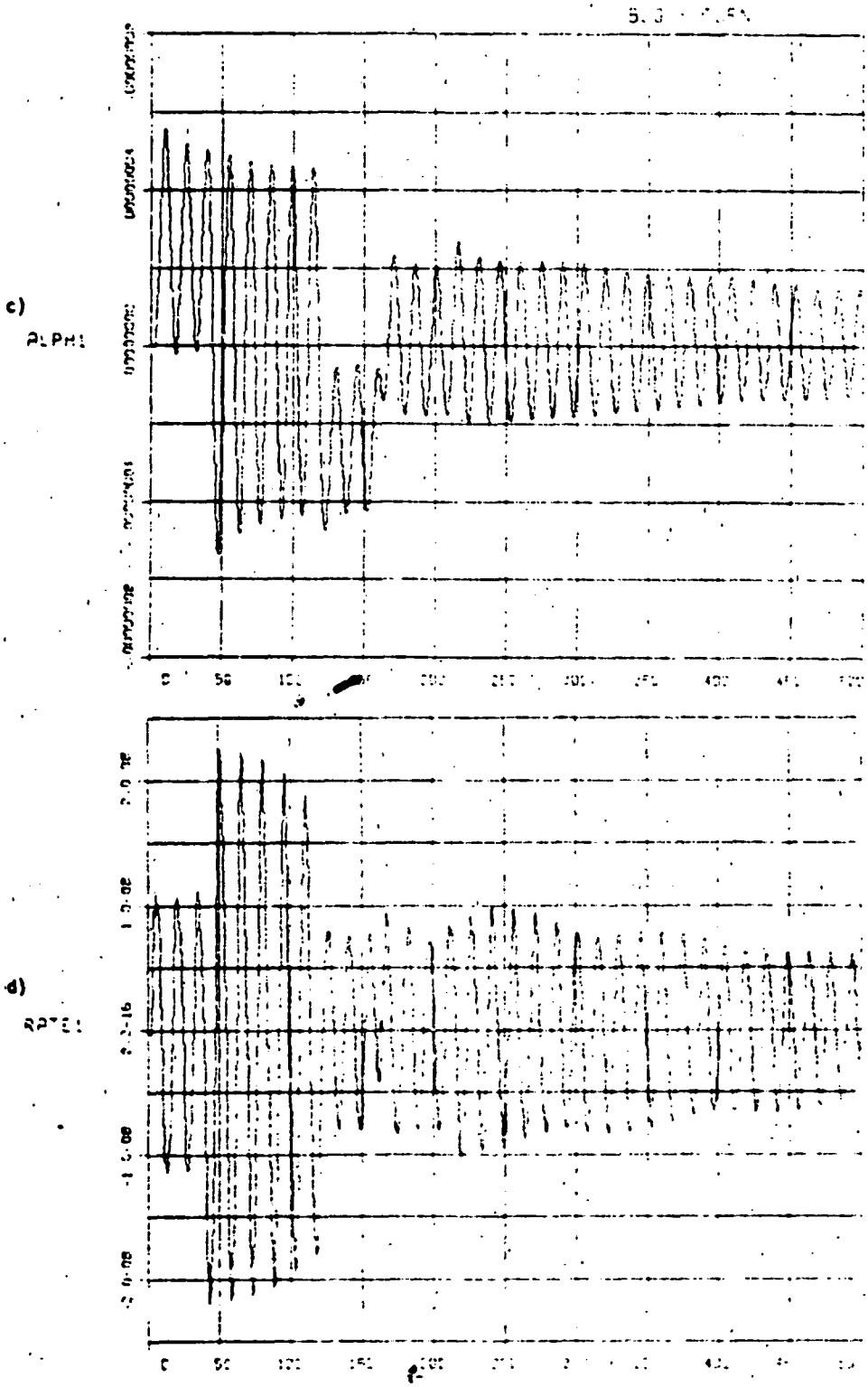

Small pitch oscillations within deadband, due to flexibility

FIGURE 4-7

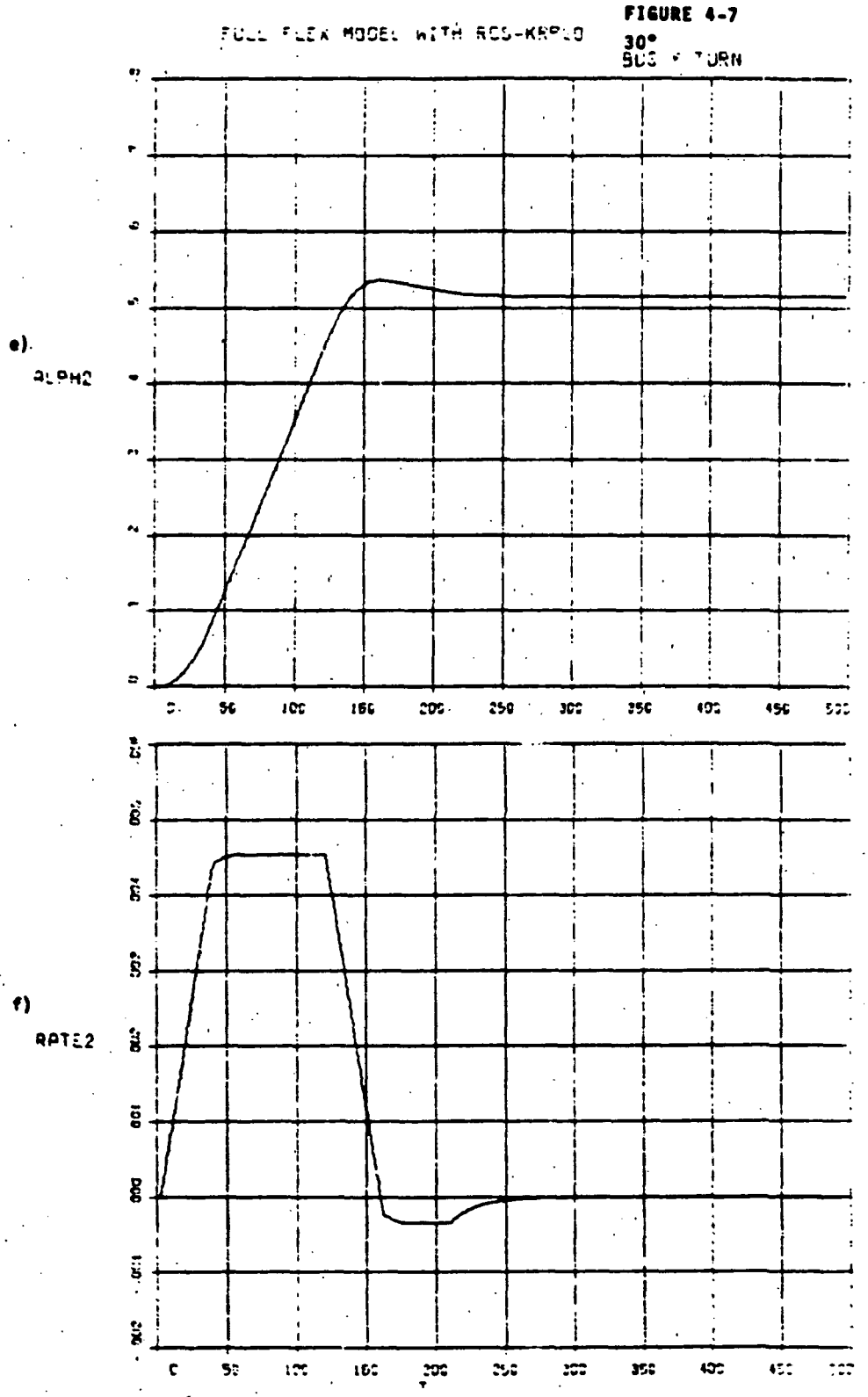

Slight overshoot in position and rate.

FIGURE 4-7

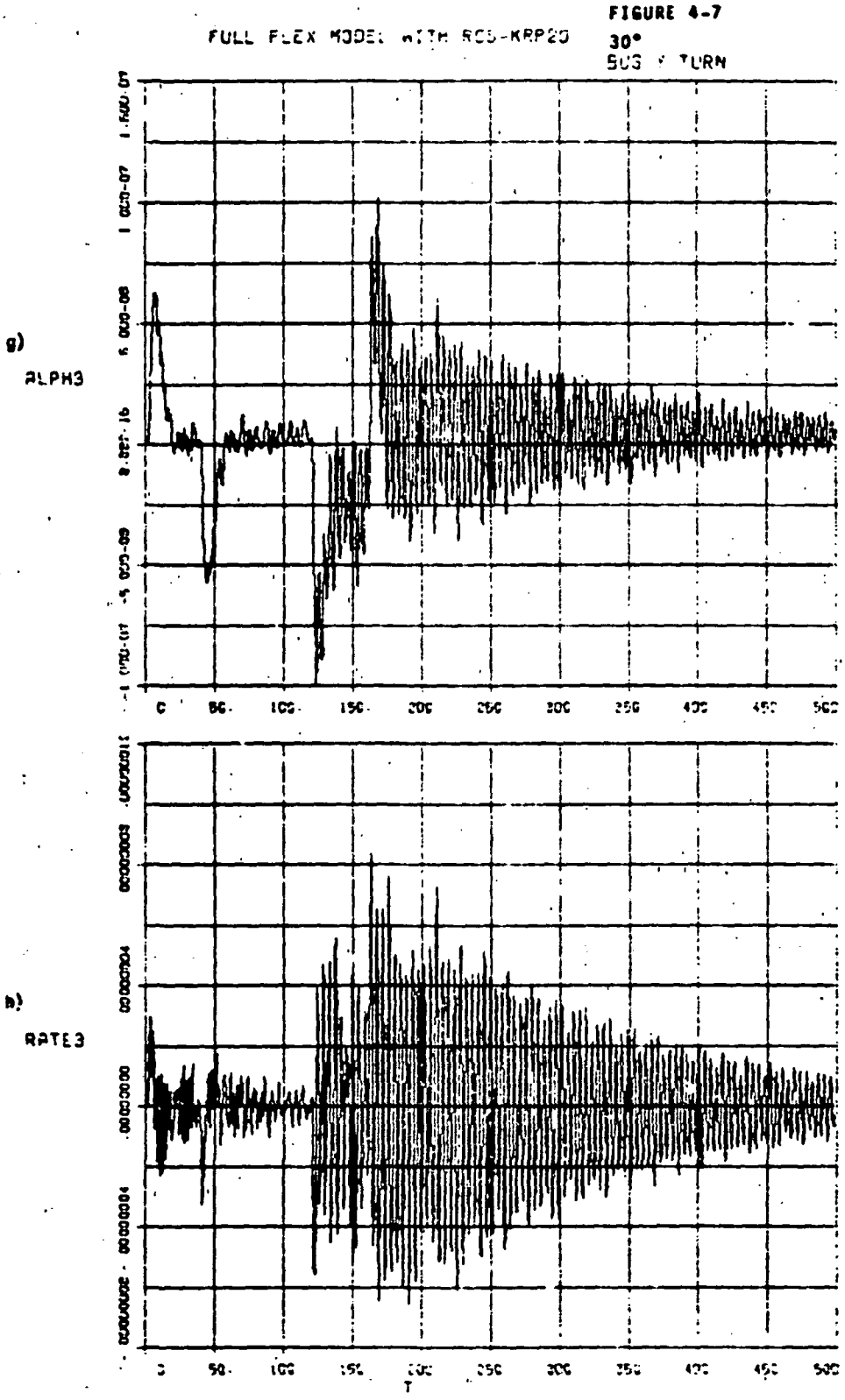

Small roll oscillations within deadband; due to flexibility.

FIGURE 4-7

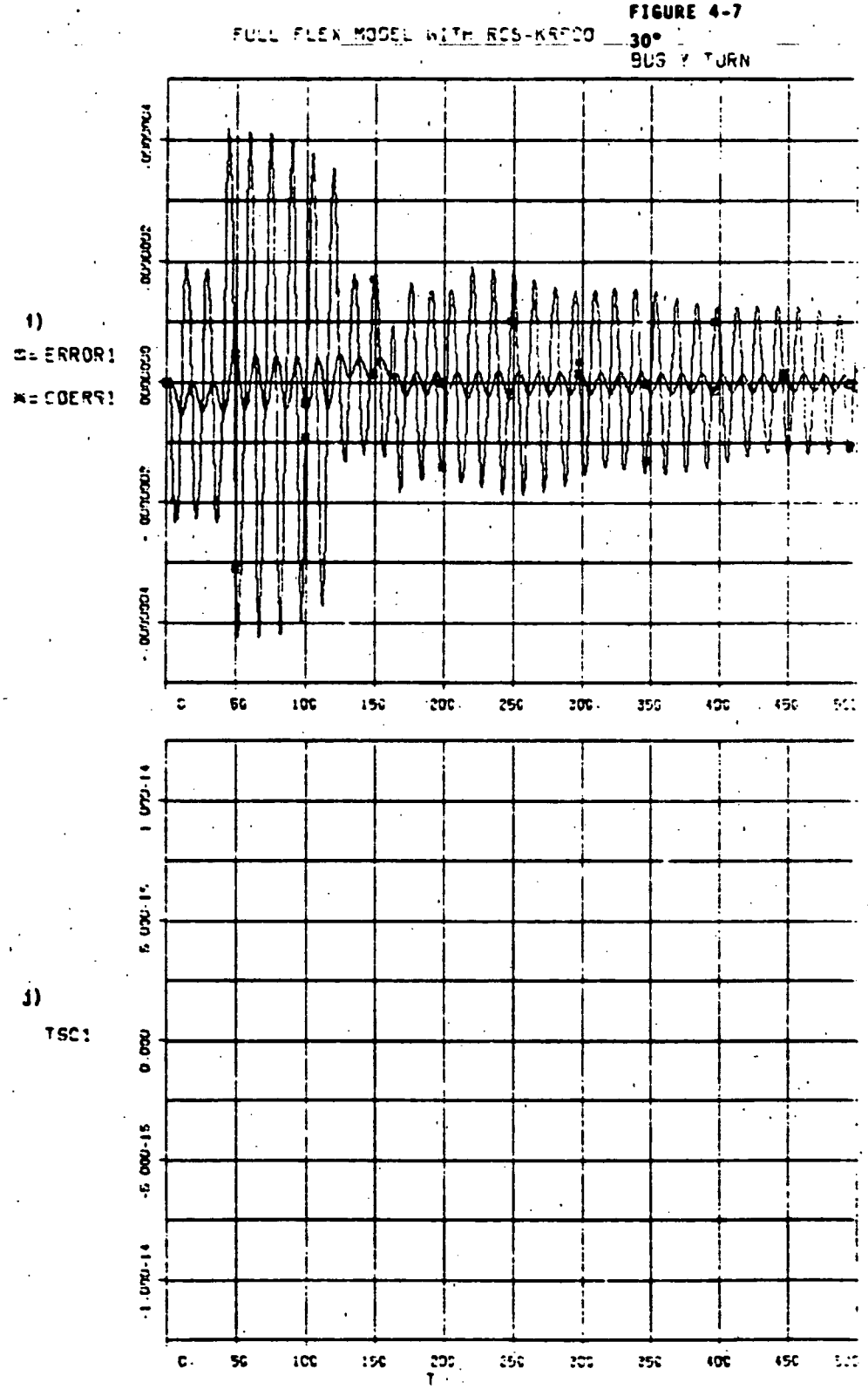
FULL FLEX MODEL WITH RCS-KRCC0 30°
BUS Y TURN
1)
□= ERROR1
*= CDERR1
0
50
100
150
200
250
300
350
400
450
J)
TSC1
T

FIGURE 4-7

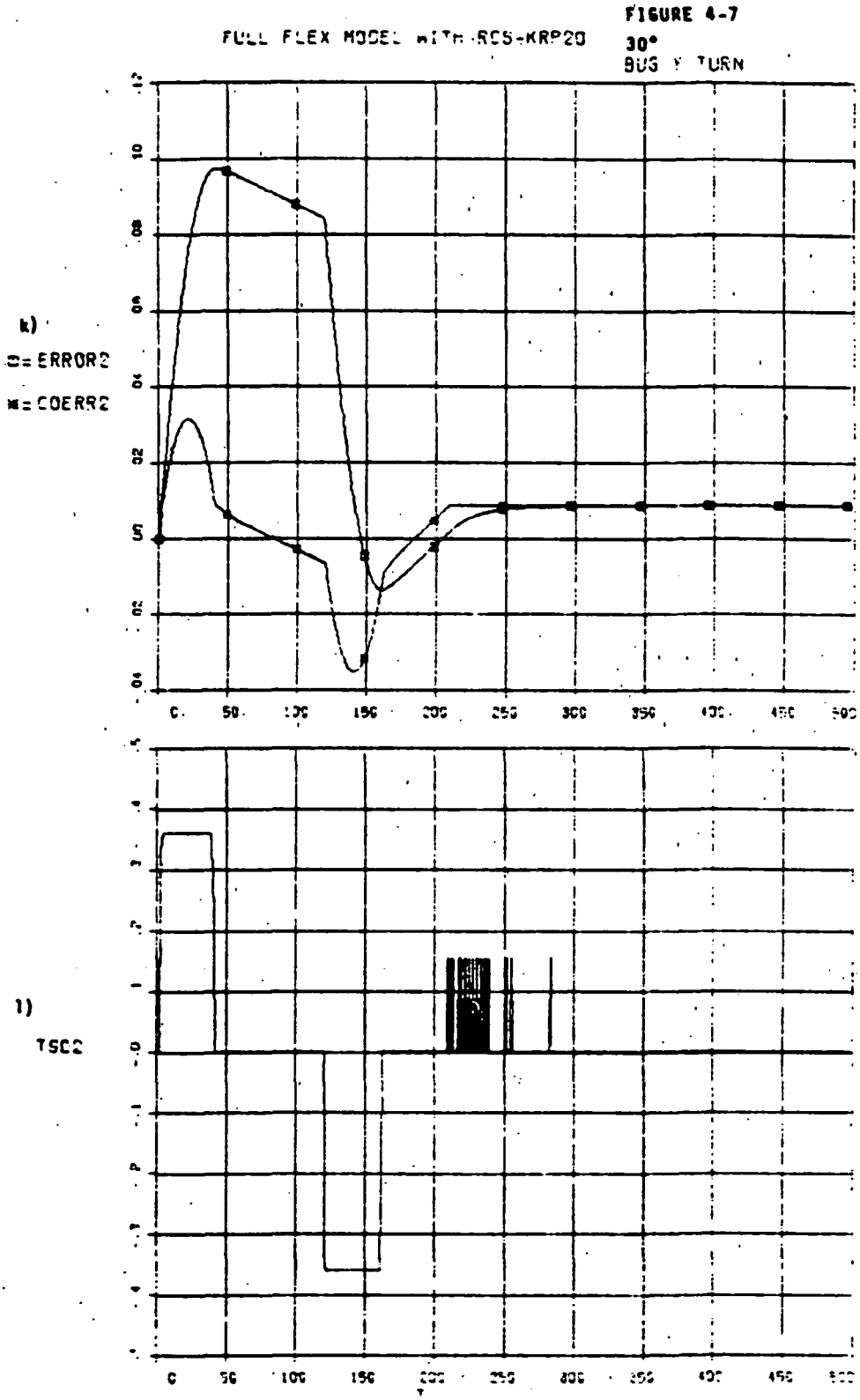
FULL FLEX MODEL WITH RCS-KRP20
30°
90S Y TURN
k)
□= ERROR2
×= COERR2
1)
TSC2

FIGURE 4-7

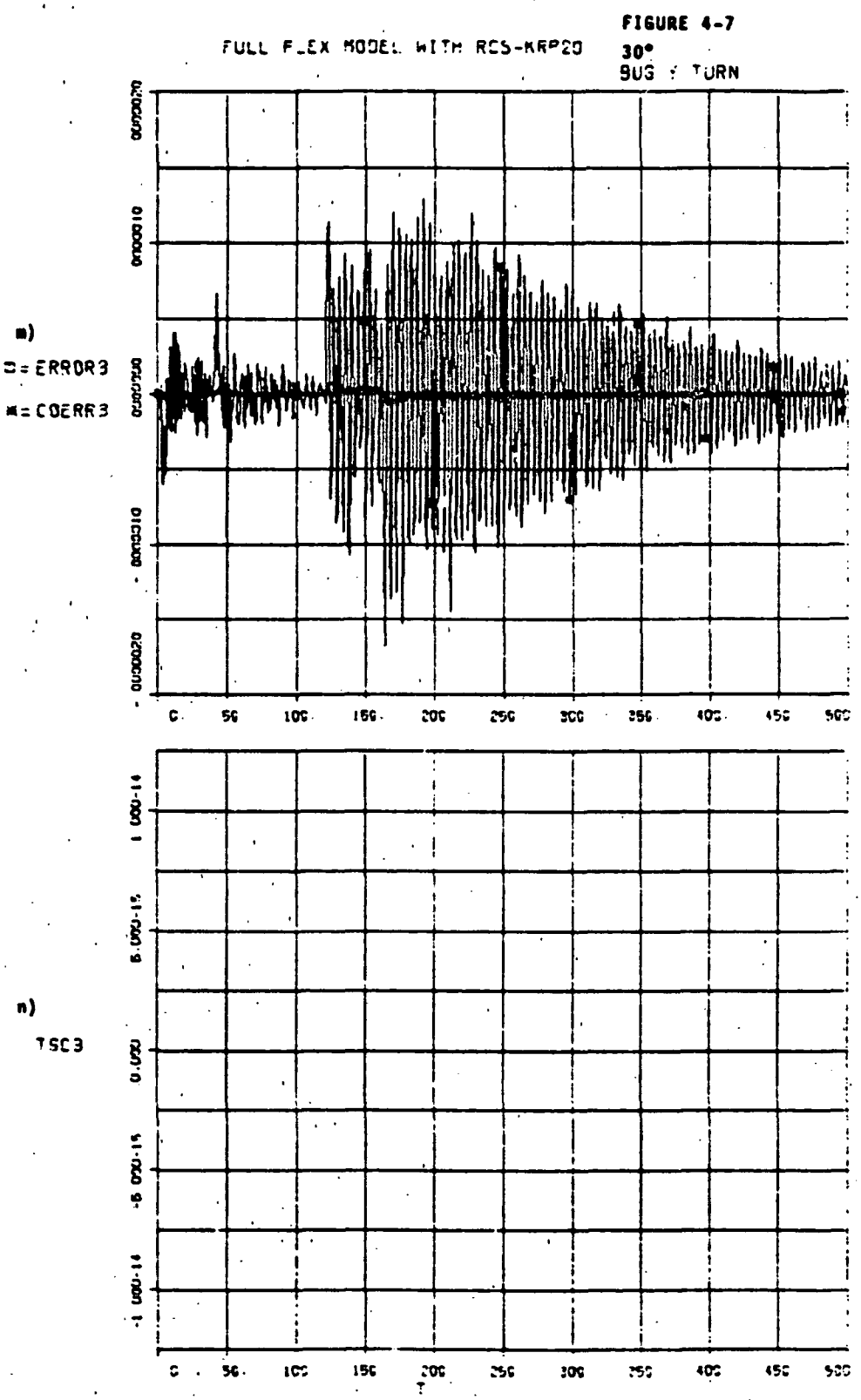
FULL FLEX MODEL WITH RCS-KRP20
30°
SUG Y TURN
m)
□ = ERROR3
× = COERR3
0.000020
0.000010
0.000000
-0.000010
-0.000020
0
50
100
150
200
250
300
350
400
450
500
n)
TSC3
1.000-14
5.000-15
0.000
-5.000-15
-1.000-14
T

FIGURE 4-7
30°
BUS Y TURN

FULL FLEX MODEL WITH RCS-KR420

o)
TPONY

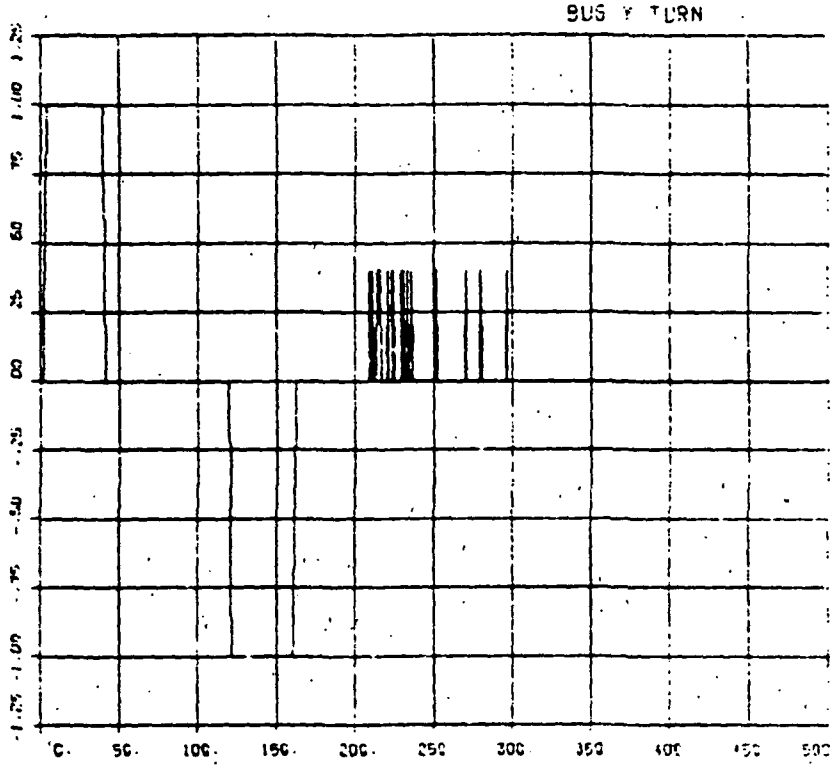

p)
□= TGASOR
×= XGASOR
△= YGASOR
⧗= ZGASOR

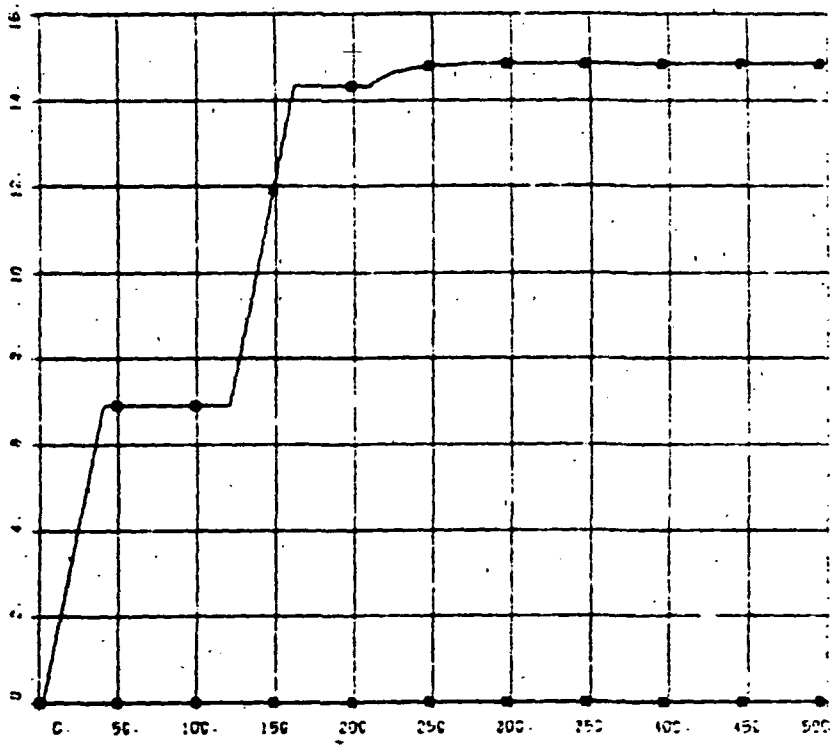

Total gas consumption -15 gr.

FIGURE 4-7

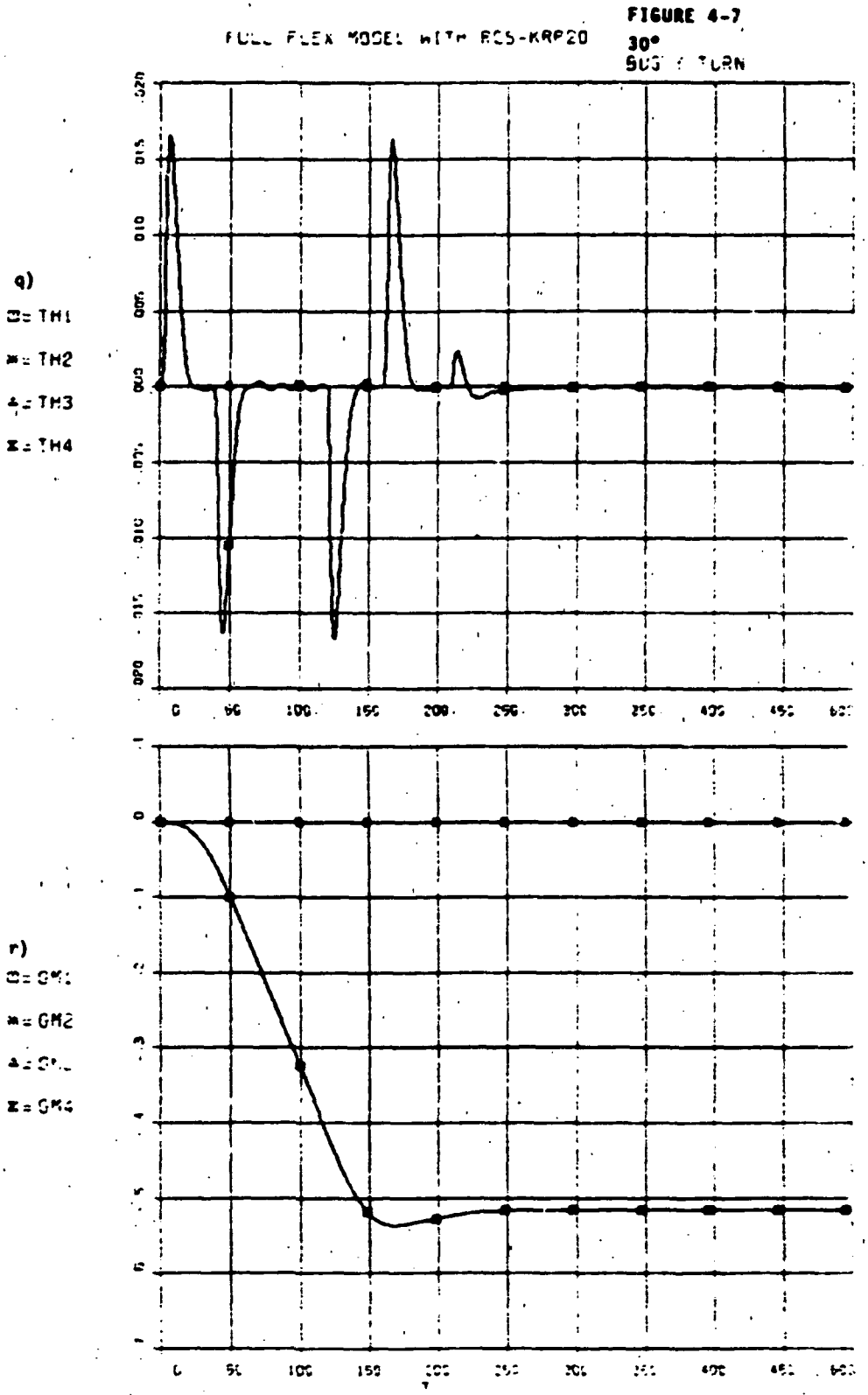

q) Small hinge torques. r) SA wings turn -30° with respect to the bus so as to stay on the sun as the bus rotates.

FIGURE 4-7

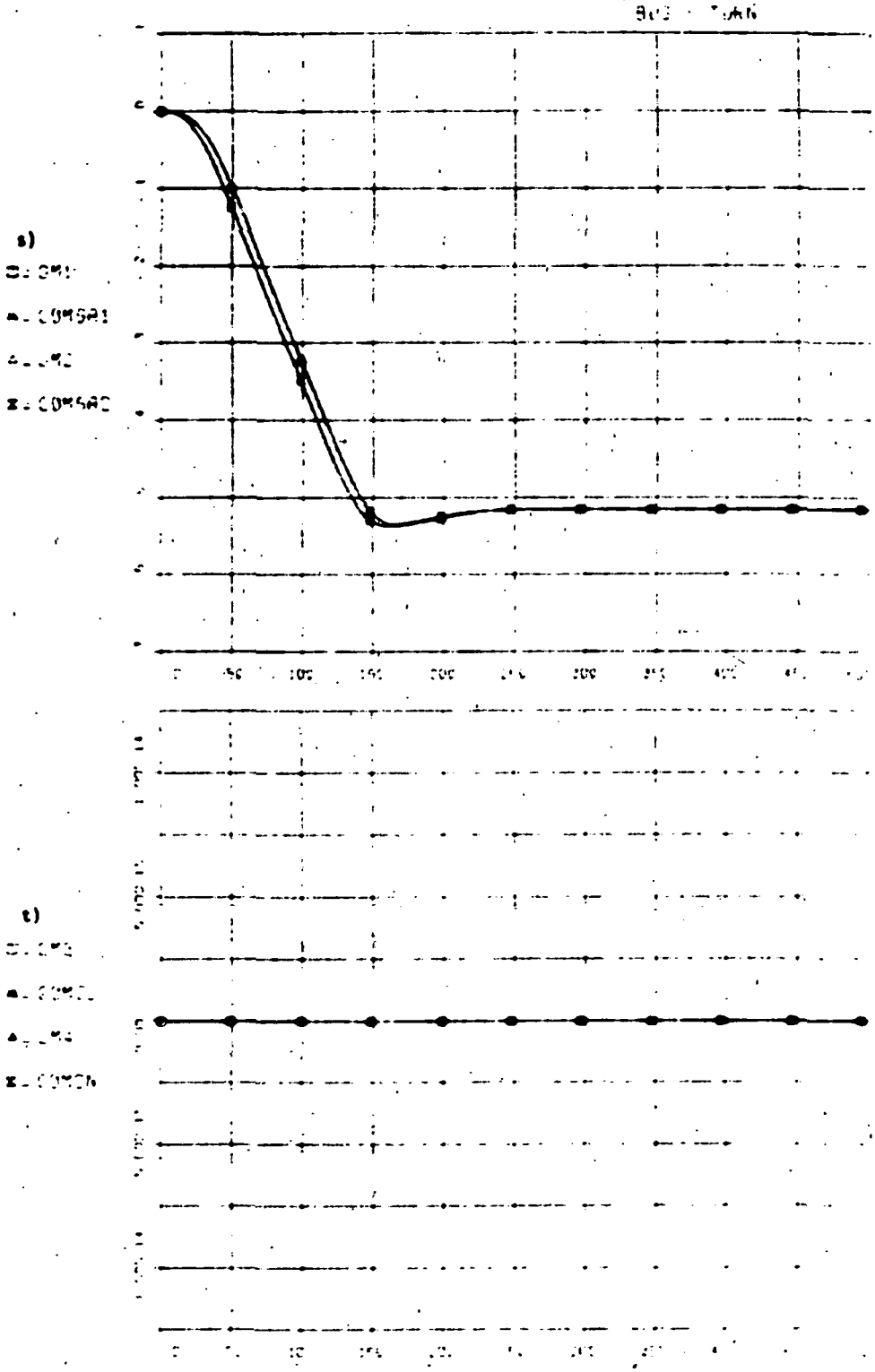

s) SA wings track their commands to -30° with respect to bus t, Scan platform locked in place for this maneuver.

FIGURE 4-7

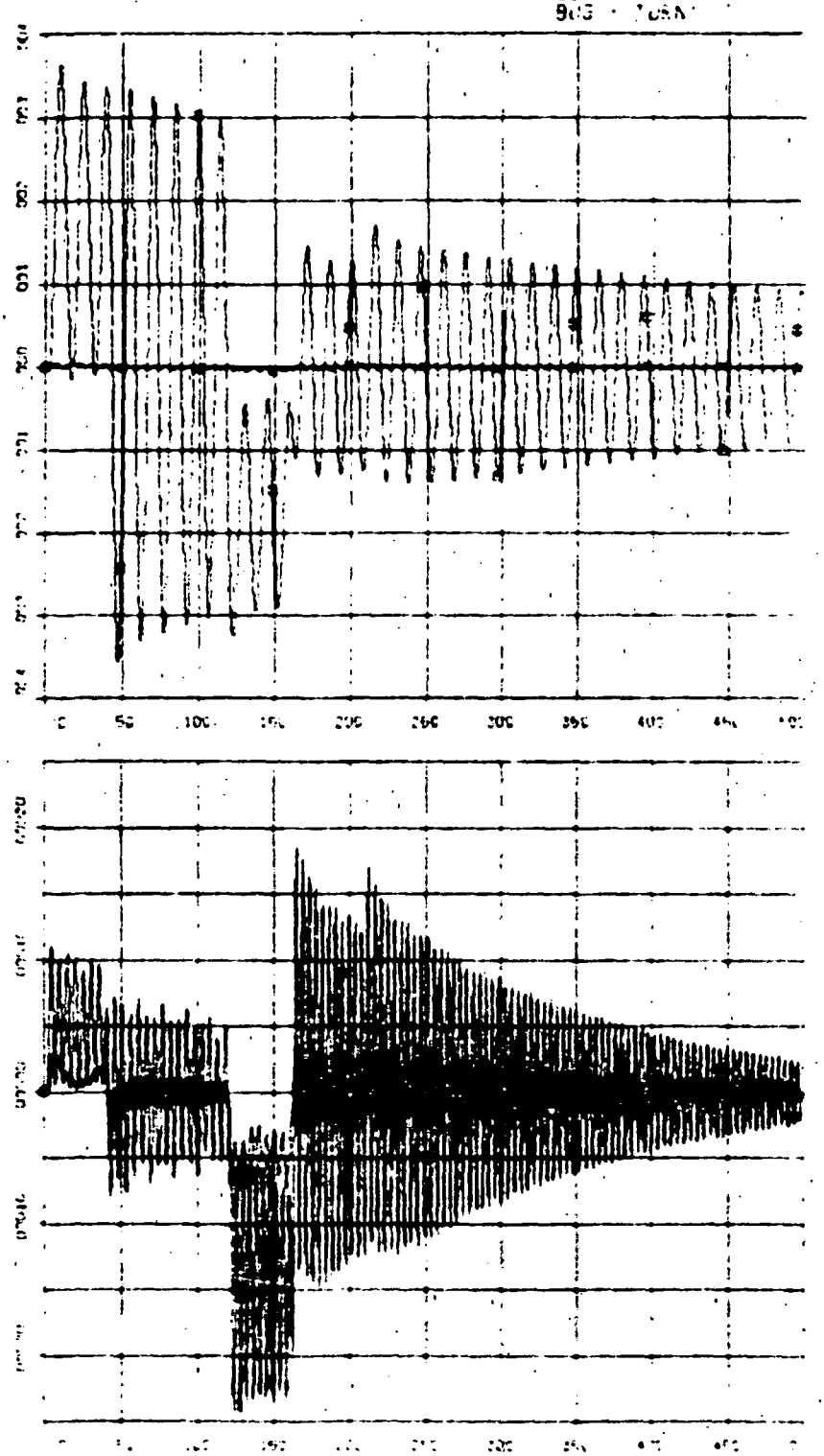

u) through z)
Solar array generalized deformation coordinates showing excitation of the modes coincidently with jet pulses. Predominant out-of-plane excitation. Note vibration levels damping out towards end of plot.

FIGURE 4-7

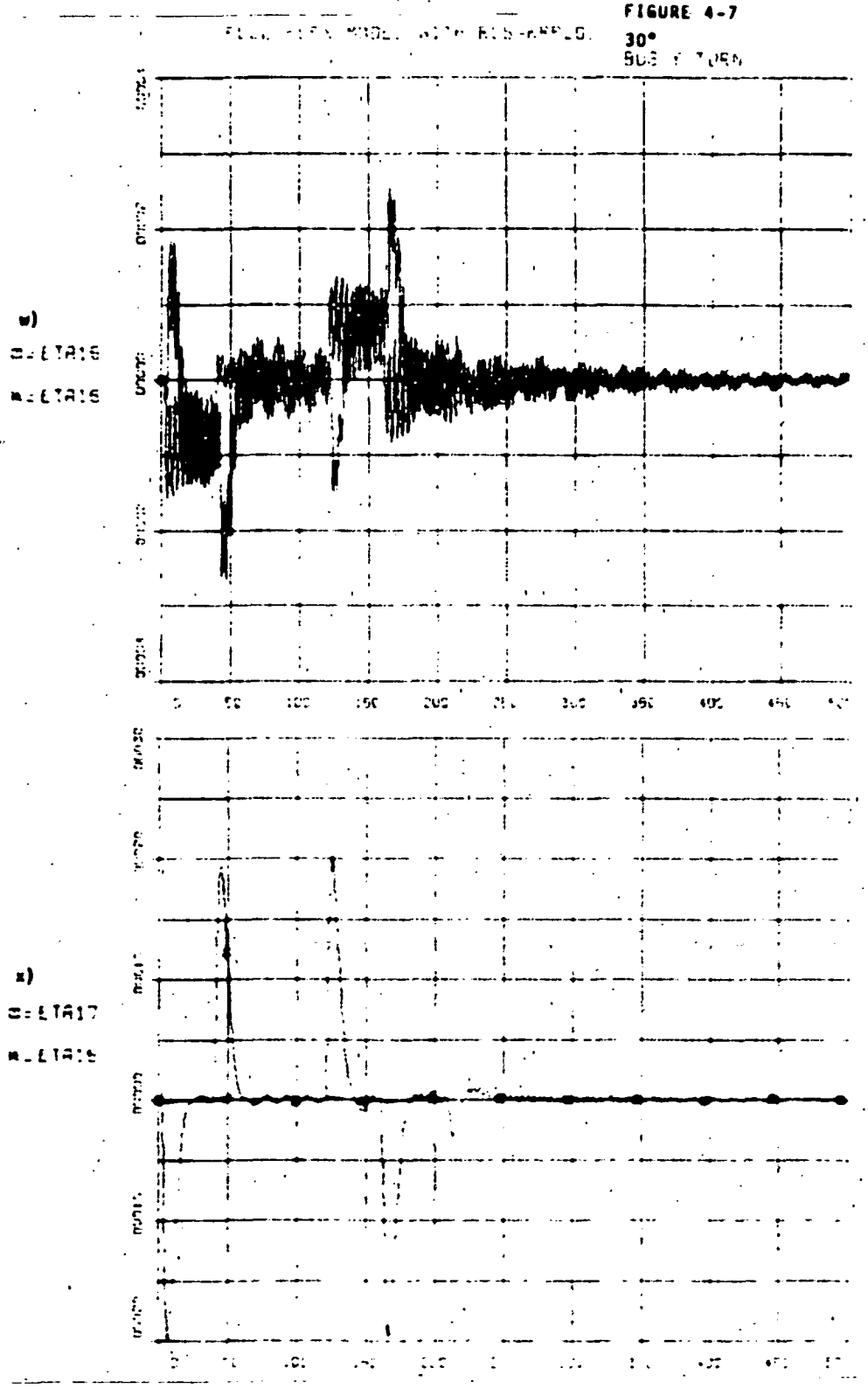

ORIGINAL PAGE IS
OF POOR QUALITY

FULL FLEX MODEL WITH RCS-LL200/1C **FIGURE 4-8**
ACQUISITION

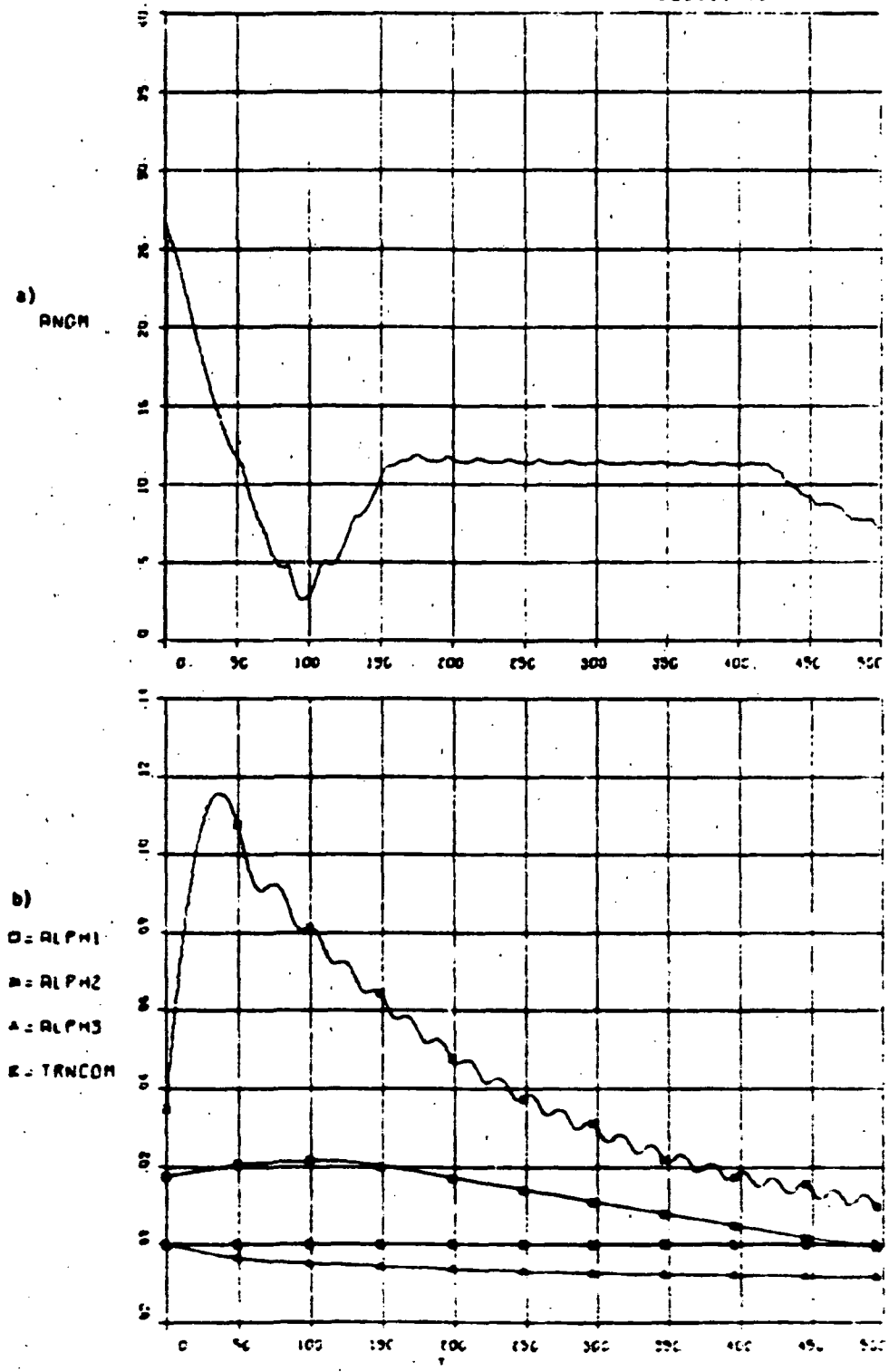

An estimated 700 seconds will be required for this particular set of acquisition initial conditions. Note excessive undamped yaw limit cycling which results in unacceptably high gas consumption. Similar to the behavior seen in Figure 4-6 for a bus yaw turn with the lead-lag controller.

FULL FLEX MODEL WITH RCS-LL200/10 **FIGURE 4-8**
ACQUISITION

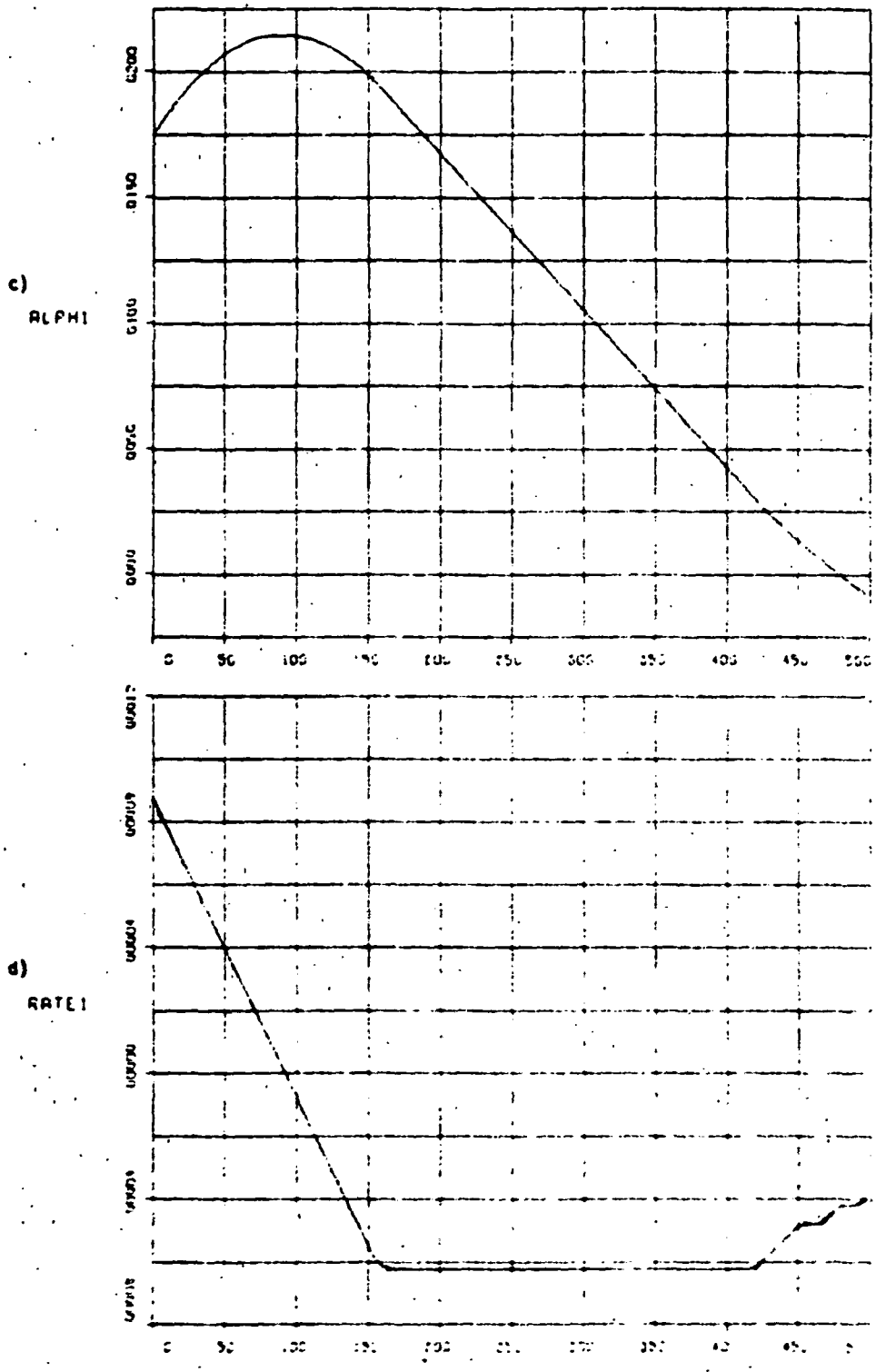

Pitch overshoots -4 mrad (0.25°) before being stopped and brought back into the deadband.

FULL FLEX MODEL WITH RCS-LL200/10 **FIGURE 4-8**
ACQUISITION

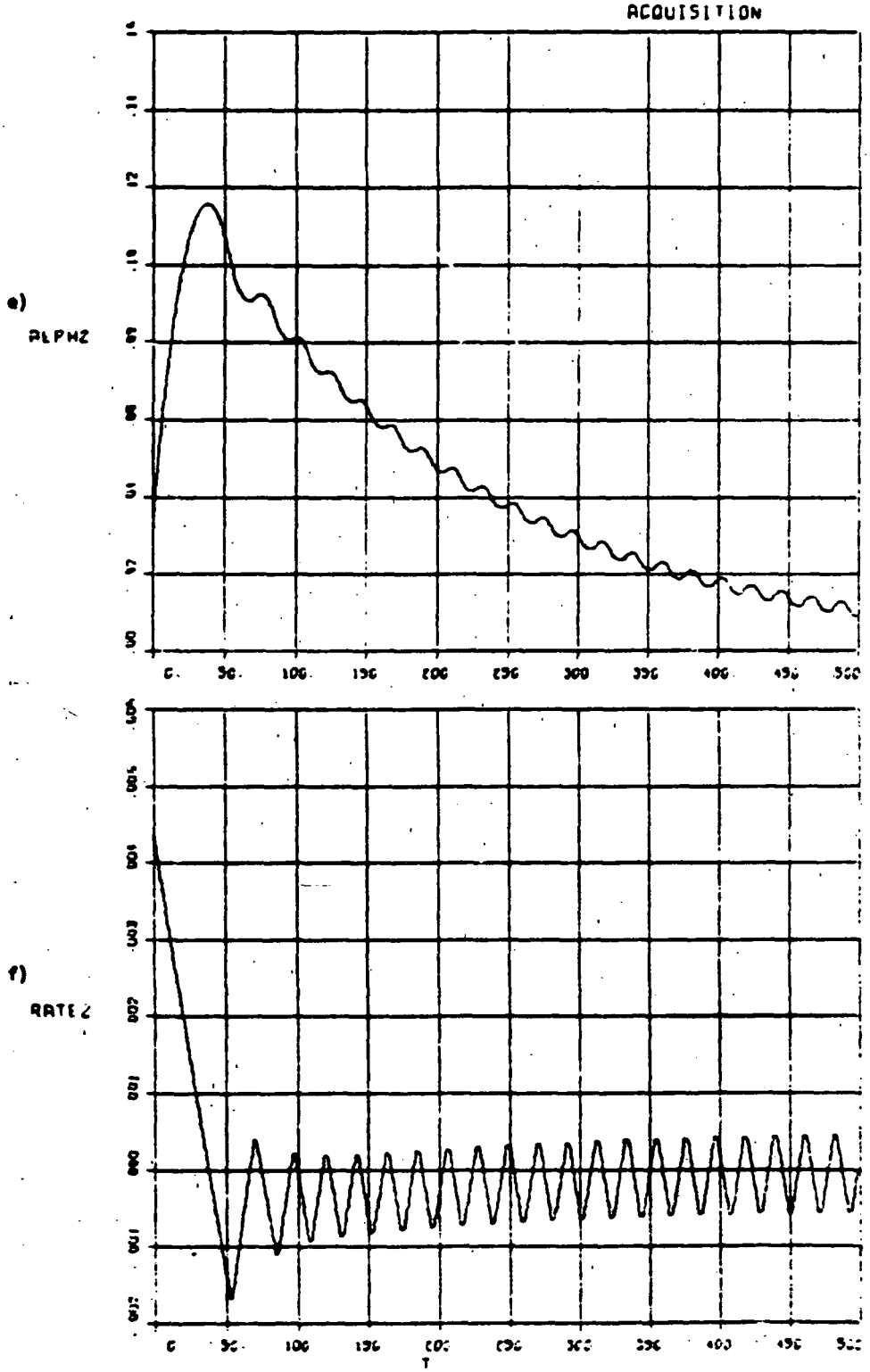

Yaw overshoots 80 mrad (4.6°) before being stopped and reversed towards null. Note excessive undamped limit cycling after T=100 seconds. (Compare with 4-6 f)

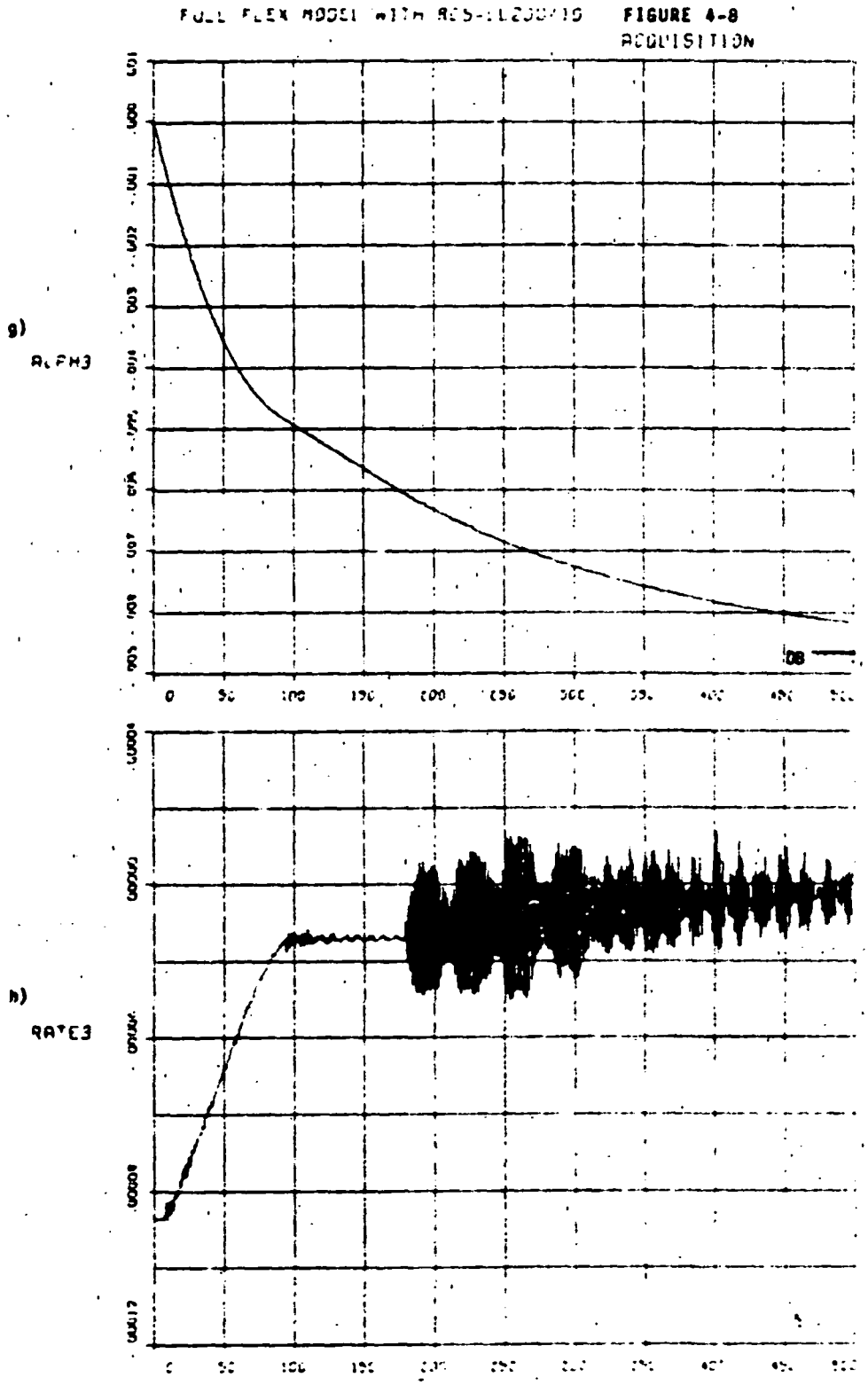

FIGURE 4-8

g) Roll rate being slowed down (within the position deadband). h) Rate spikes starting at T=180 are due to high frequency multipulsing as roll encounters the deadband.

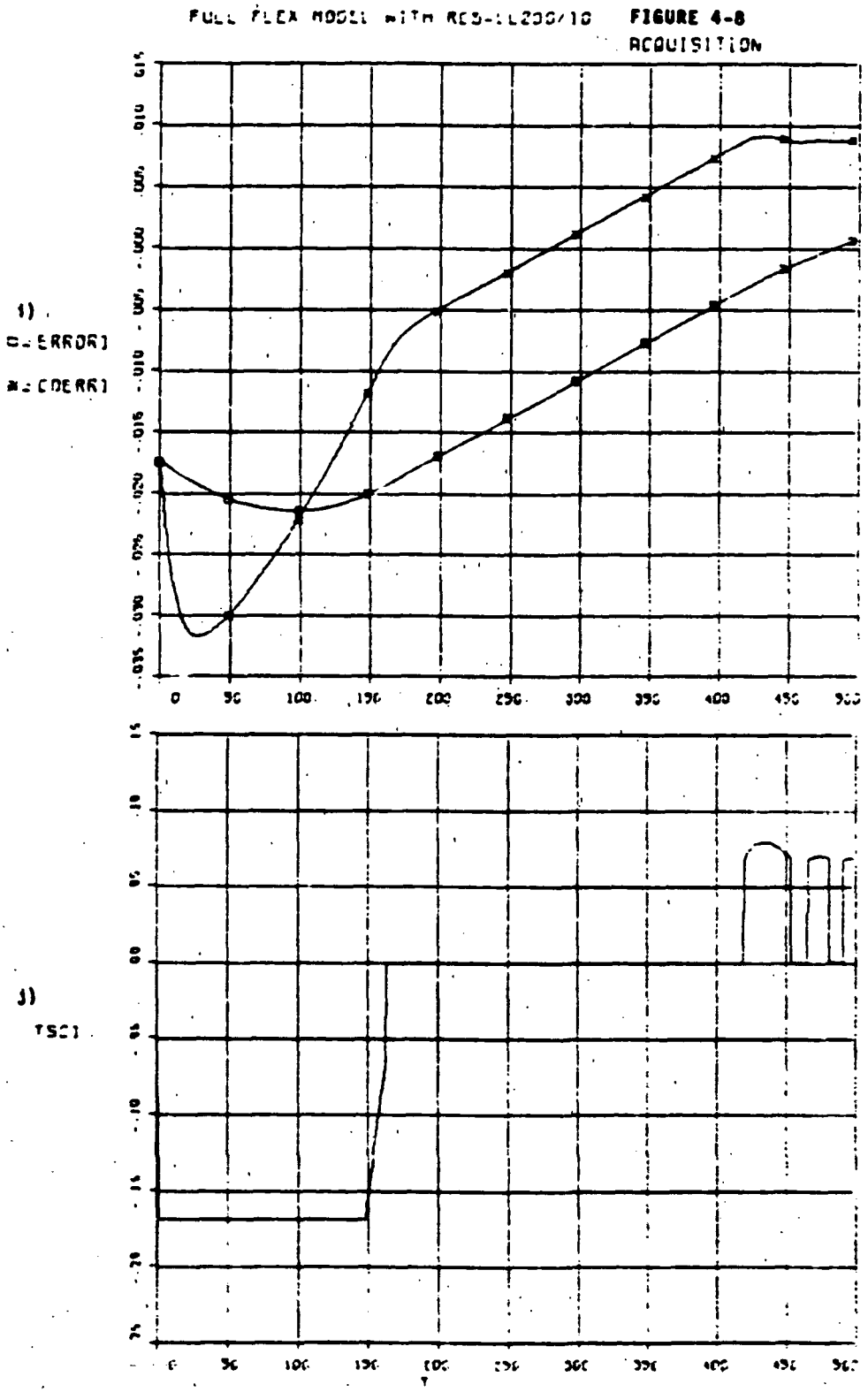

Pitch control errors and jet torques.

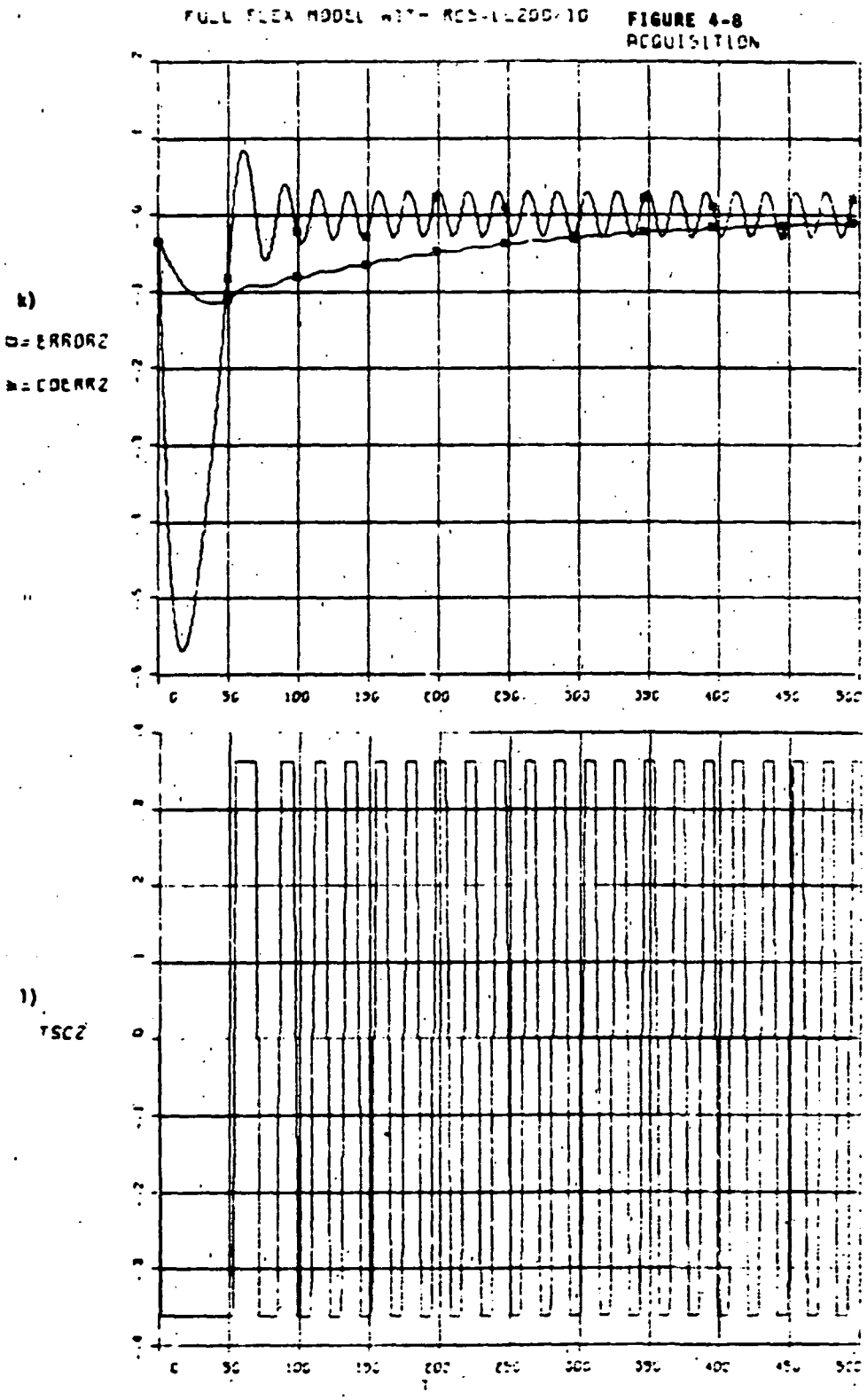

FIGURE 4-8
ACQUISITION

Undamped yaw oscillations in control error and resulting gas jet firings.

FULL FLEX MODEL WITH RCS-11200/10 **FIGURE 4-8**
ACQUISITION

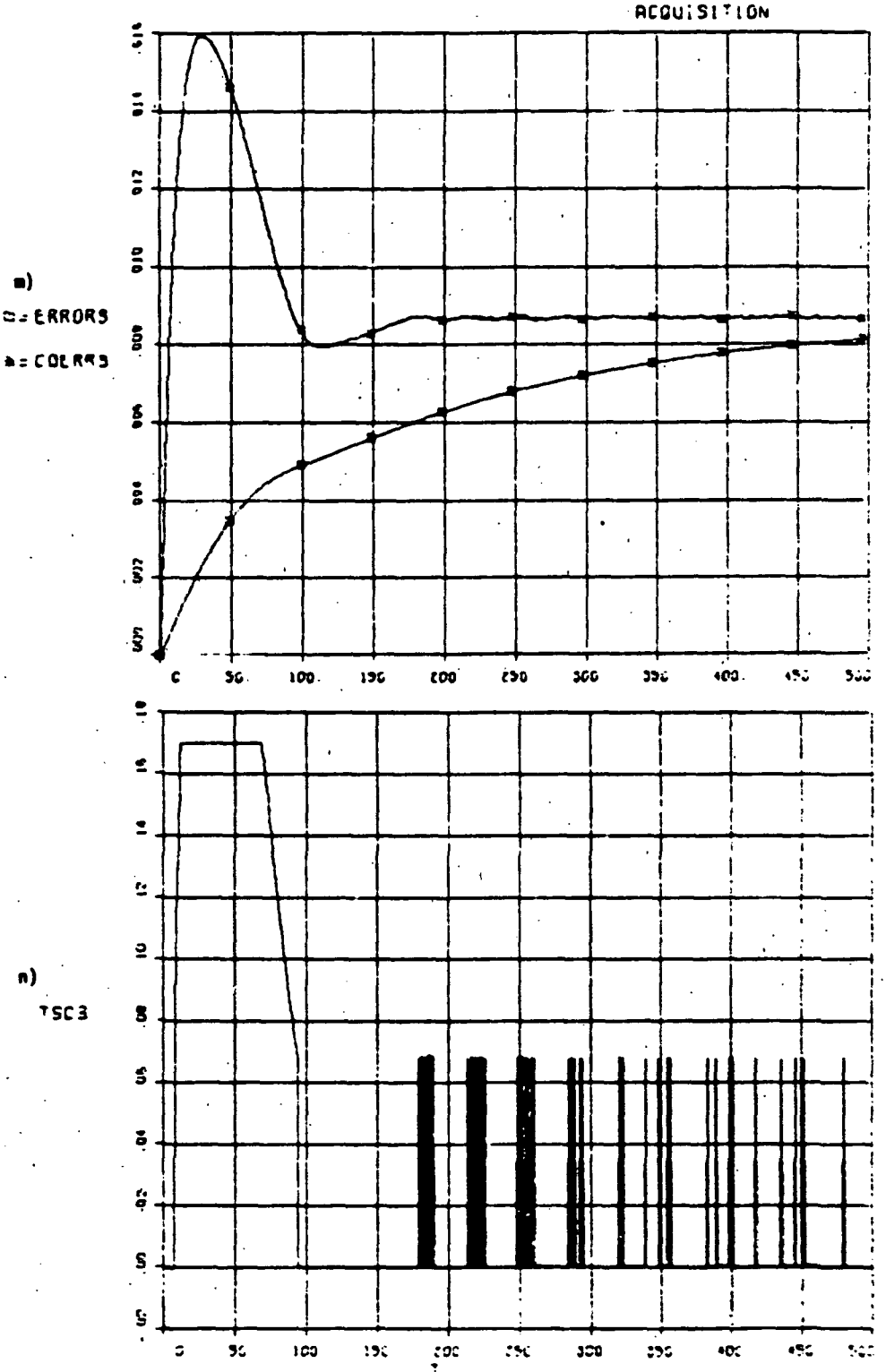

Note multipulsing starting at T=180 s as roll "sits" on the edge of the deadband

FULL FLEX MODEL WITH RCS-LL200/10 **FIGURE 4-8**
ACQUISITION

o)
XCGSCR

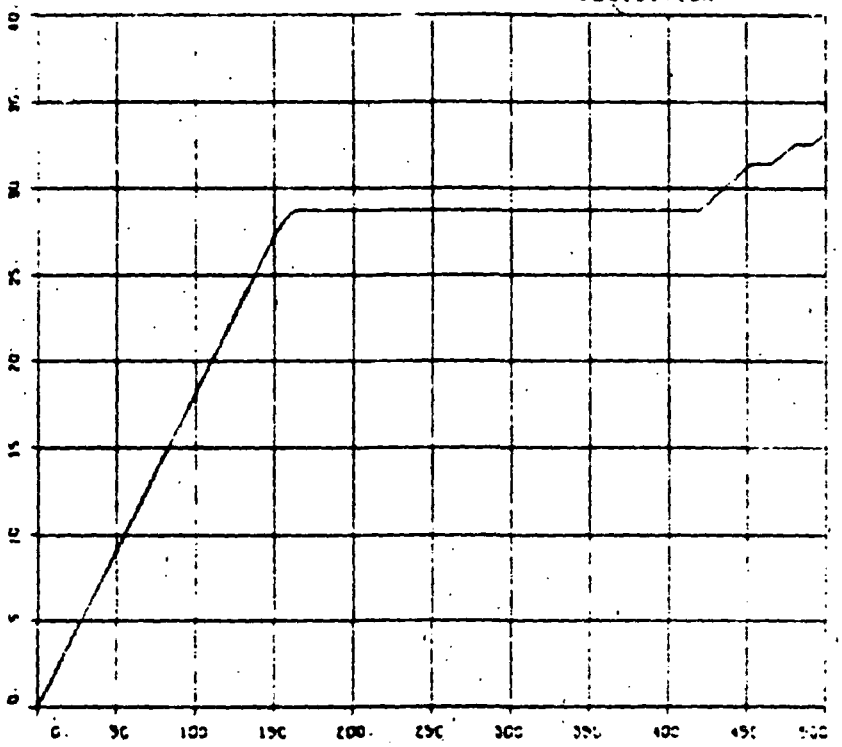

p)
YCGSCR

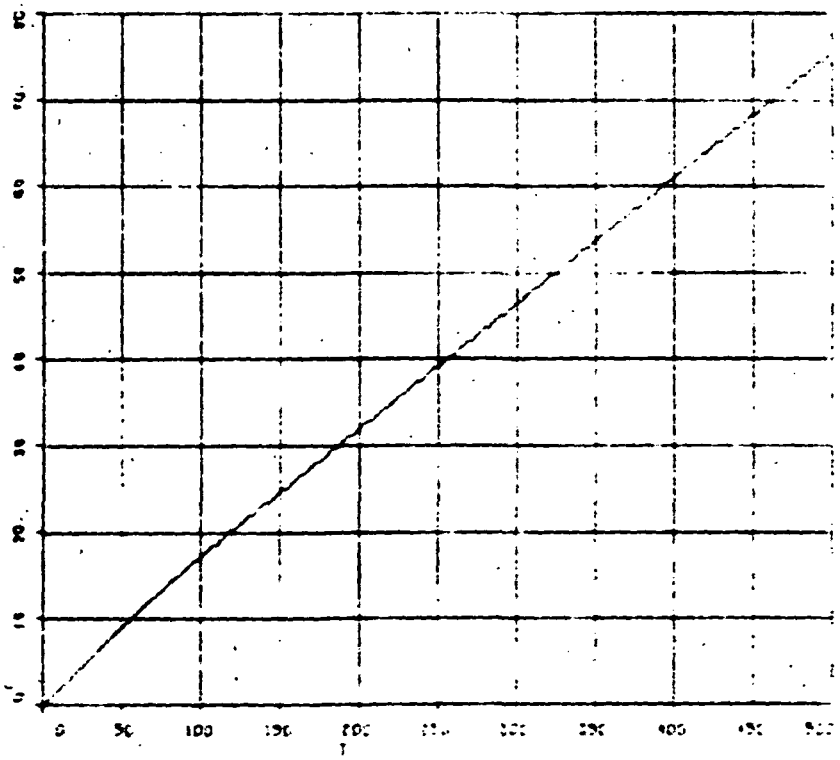

o) through r)
Gas consumption. Note an excessive total of 122 gr at end of simulation, and still firing.

FULL FLEX MODEL WITH RCS-LL200/.) FIGURE 4-8
ACQUISITION

q)
ZGPSCR

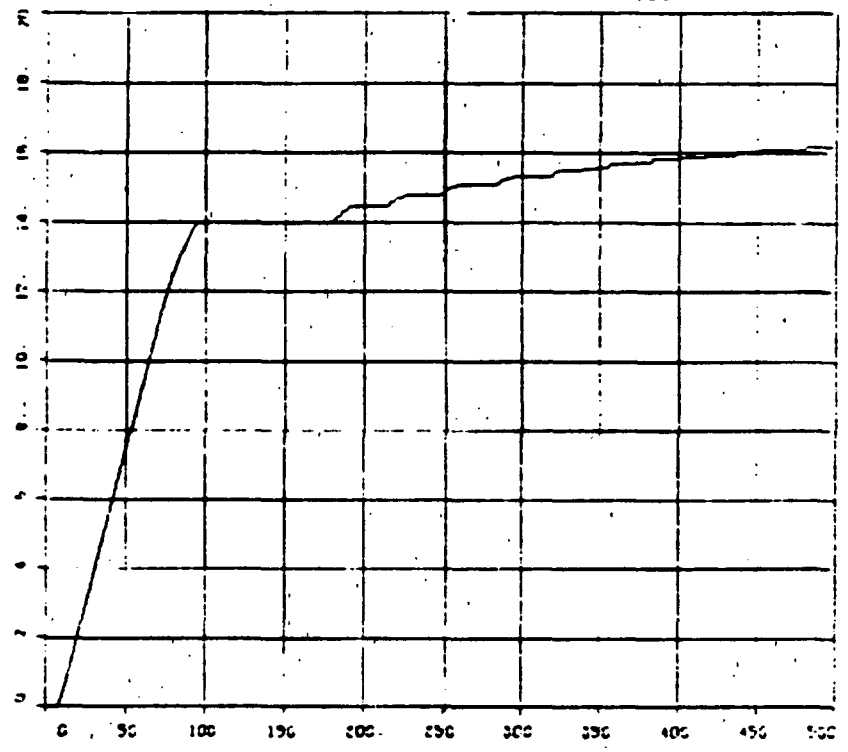

r)
□ = YGPSCR
▲ = XGPSCR
◆ = YGPSCR
✱ = ZGPSCR

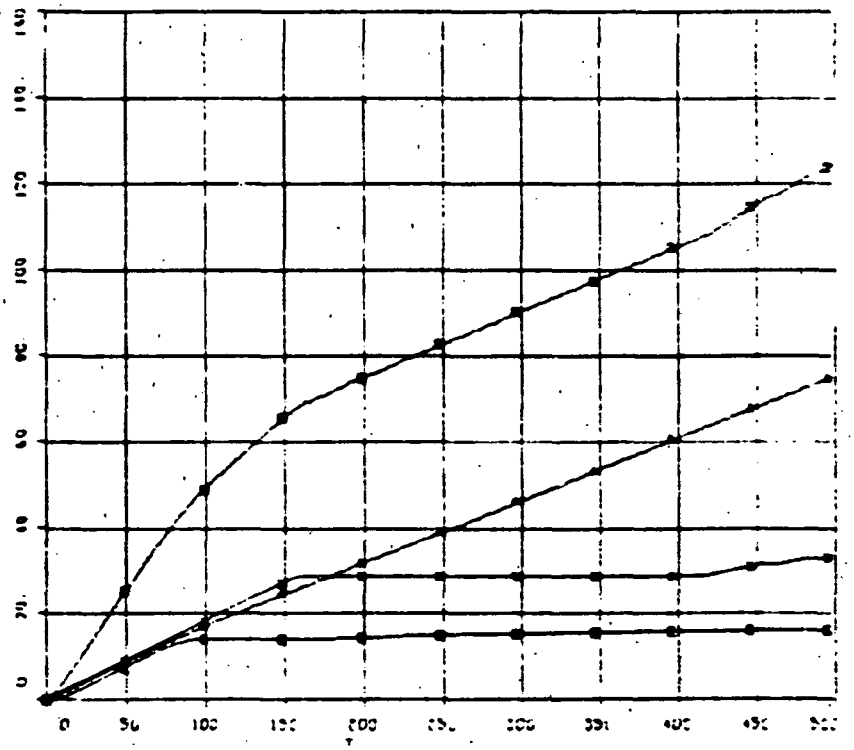

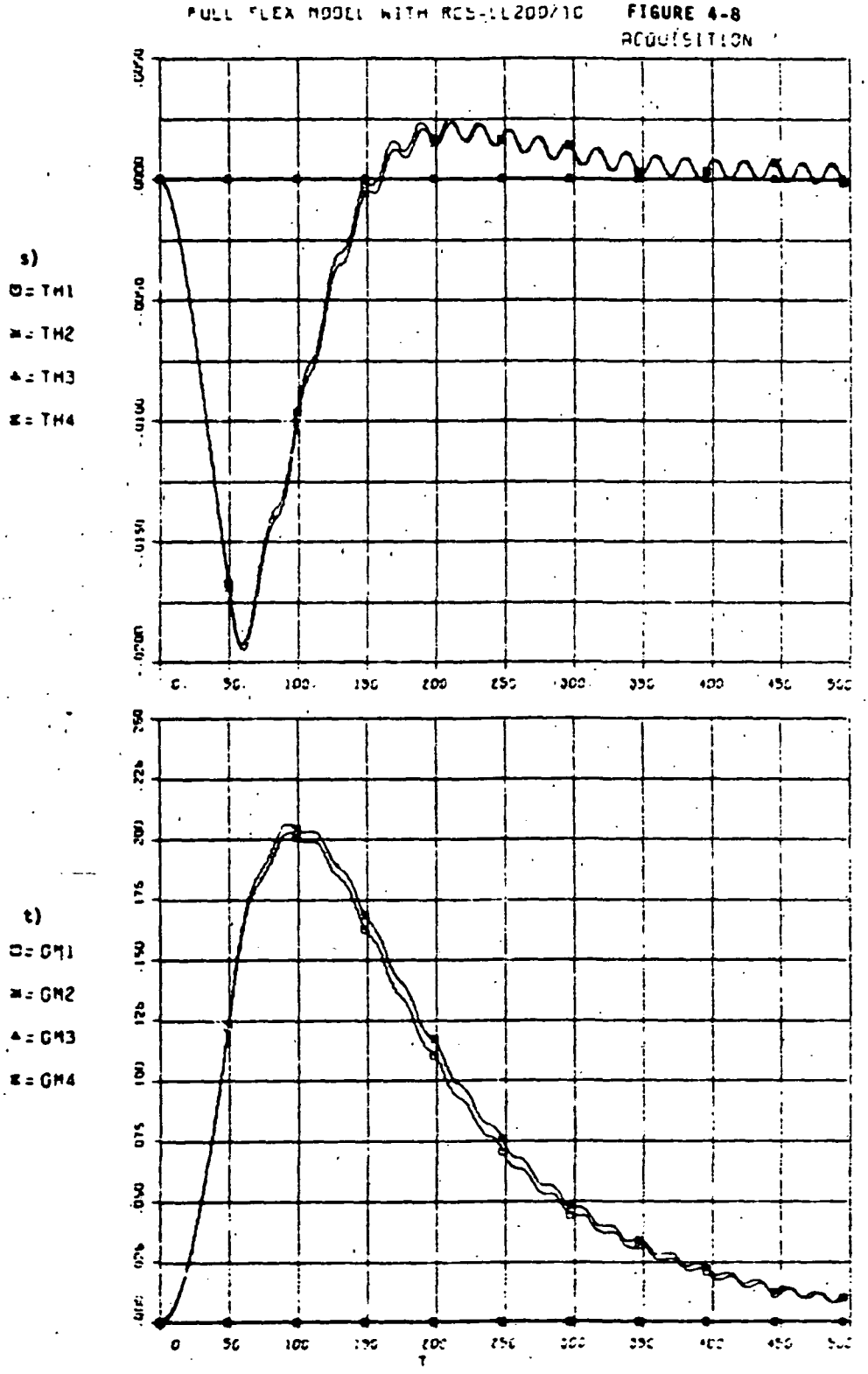

FIGURE 4-8

t) Solar array is moving with bus yaw initially at 0.25°/s. As the bus slows down, SA overshoots bus by -0.2 rad (11.5°) before the SA actuators stop it and bring it back. This is due to low SA control torques as shown in s).

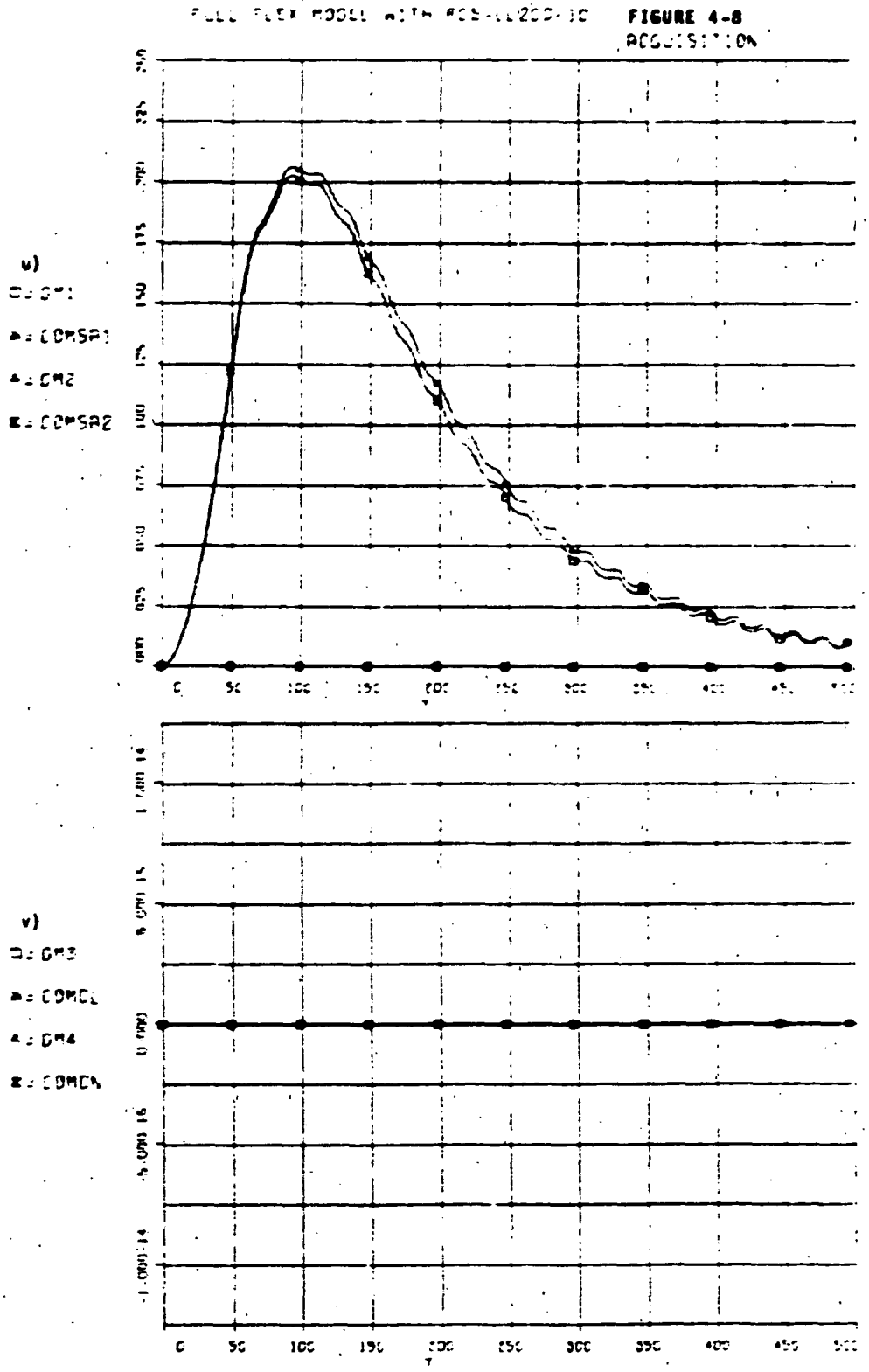

FIGURE 4-8

u) SA overshoot. v) Scan platform locked in-place for this maneuver.

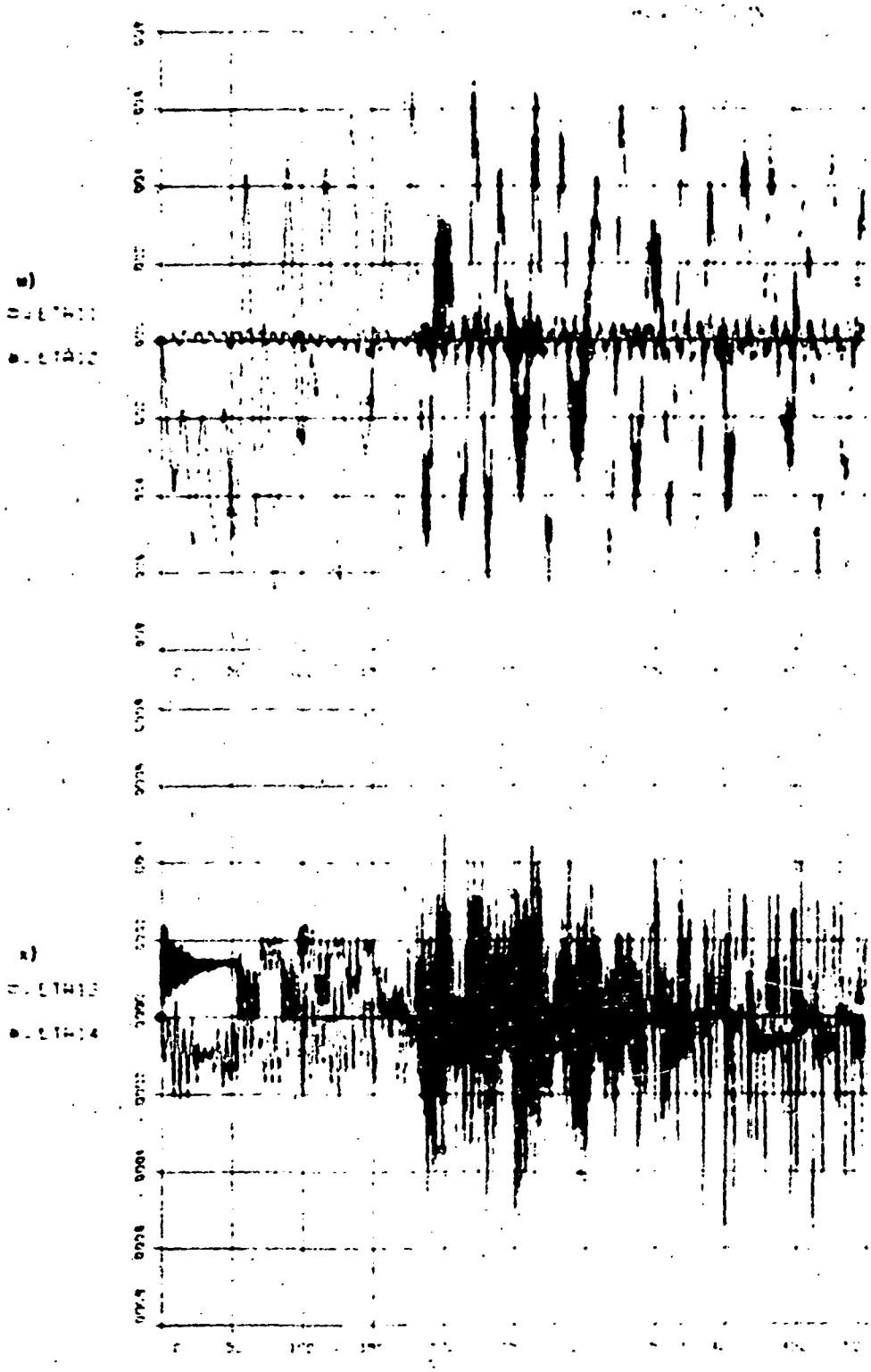

w) through z)
Solar array generalized deformation coordinates showing excitation of flexible structure coincidently with jet pulses. Note high residual vibration

FIGURE 4-8

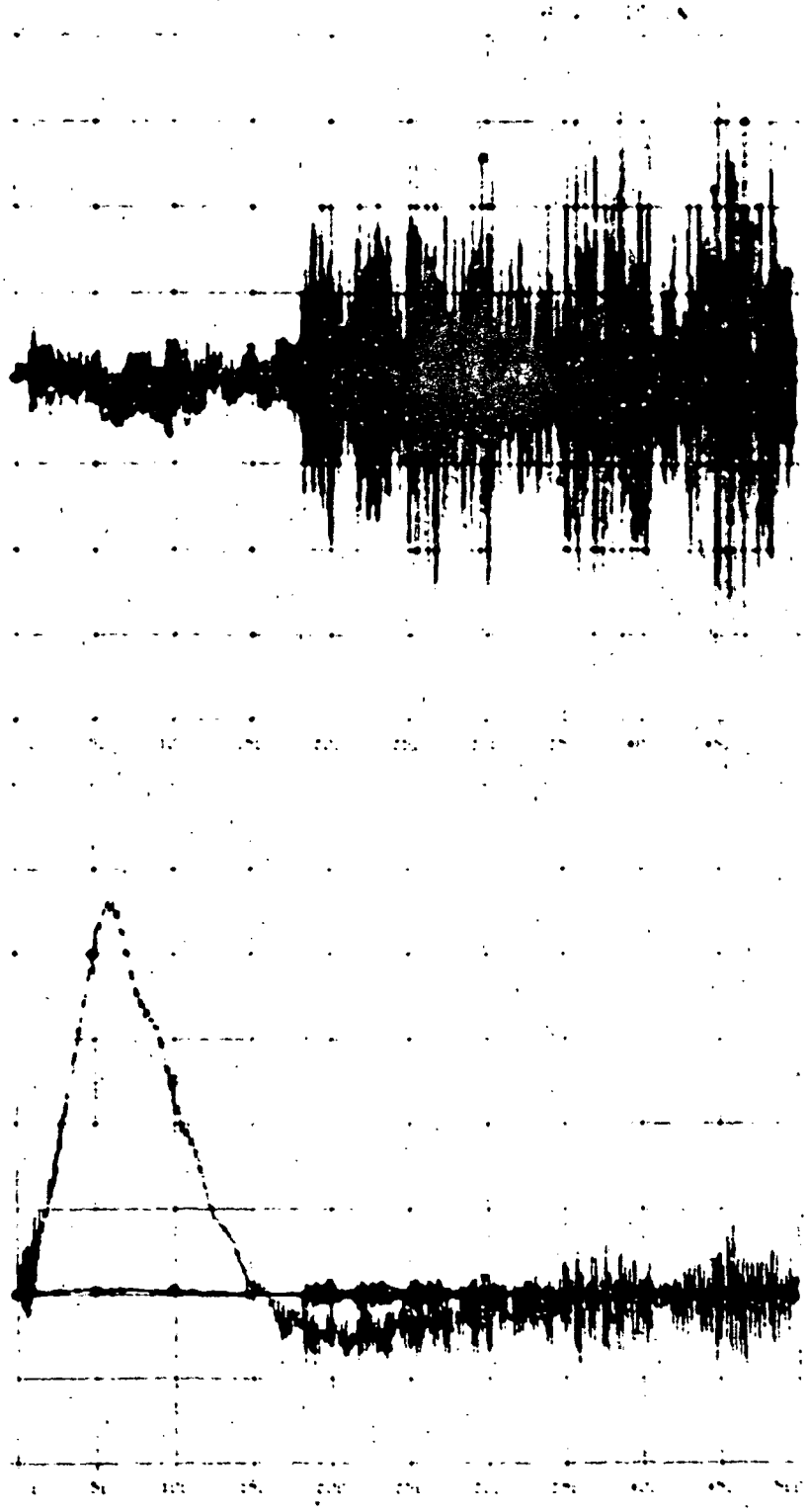

FIGURE 4-9

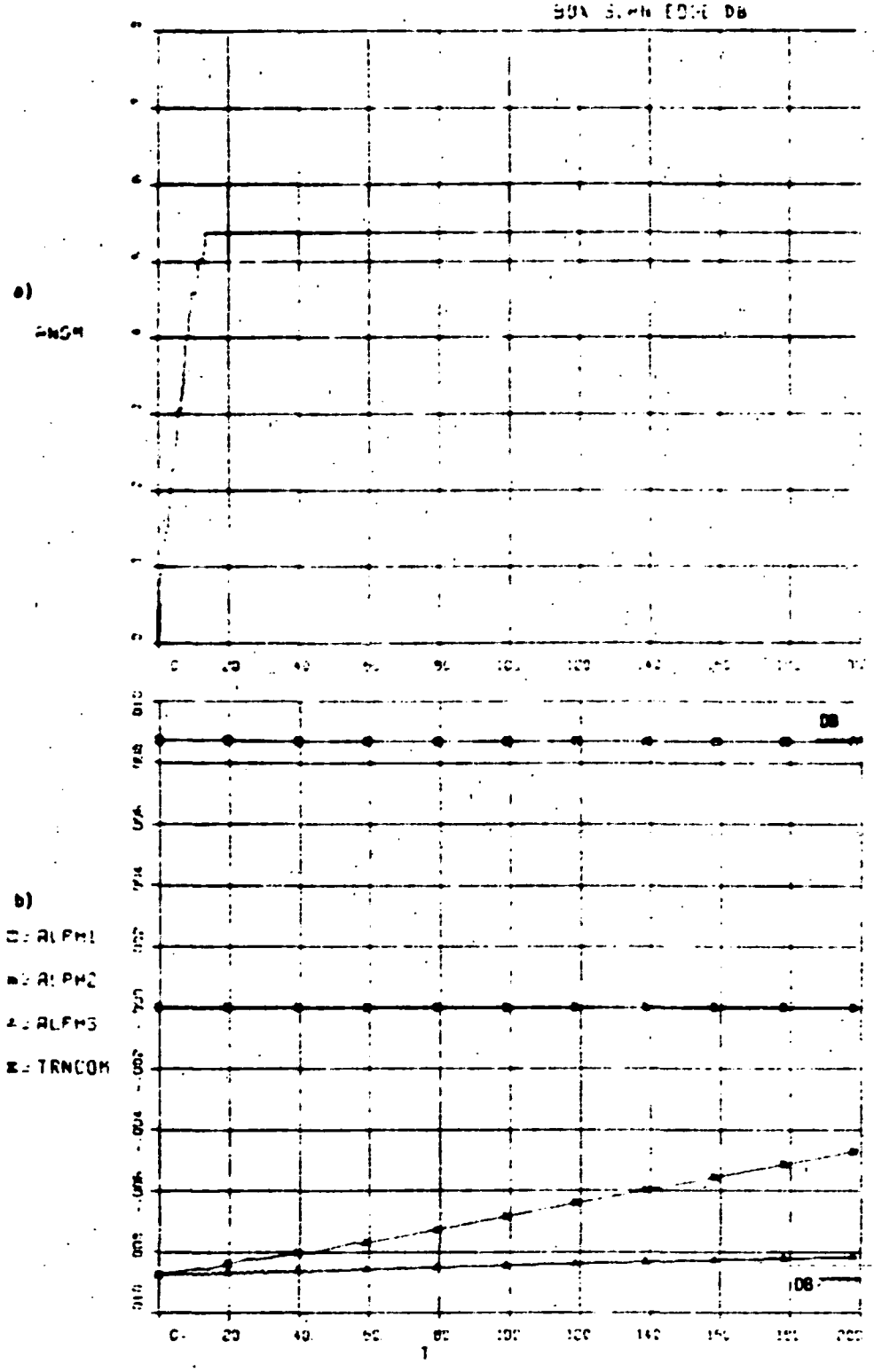

Vehicle is initially on the edge of the deadband on all 3 axes. Slewing causes jet firings which move it back into the deadband.

FIGURE 4-9

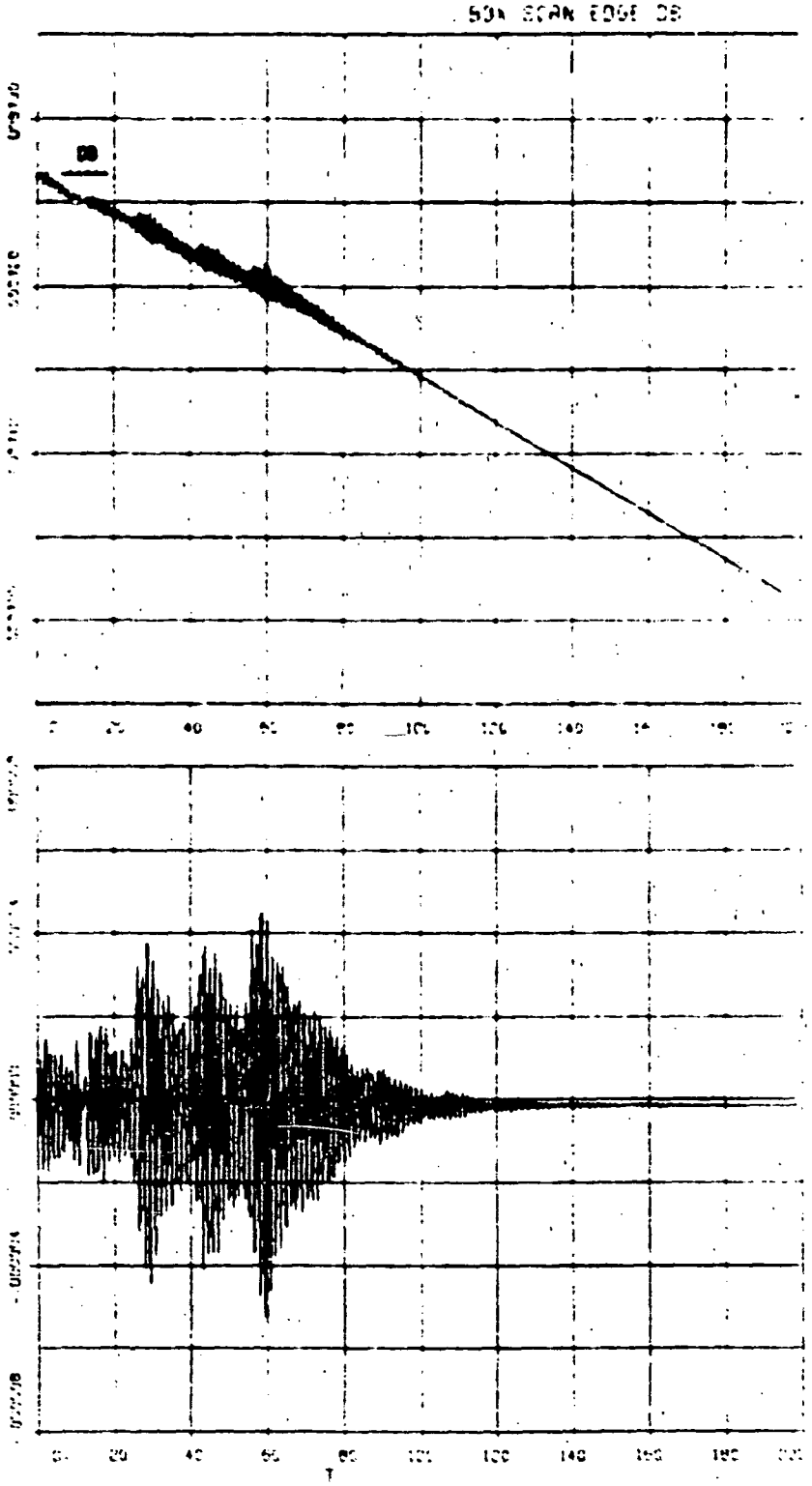

Pitch jet firings take place during the first 2 seconds (see j) moving vehicle away from deadband at a very small average rate of 0.16 urad/s. Max peak rates -5 urad/s. The oscillations after T=15 are due to scan platform slewing not to jet firings.

FIGURE 4-9

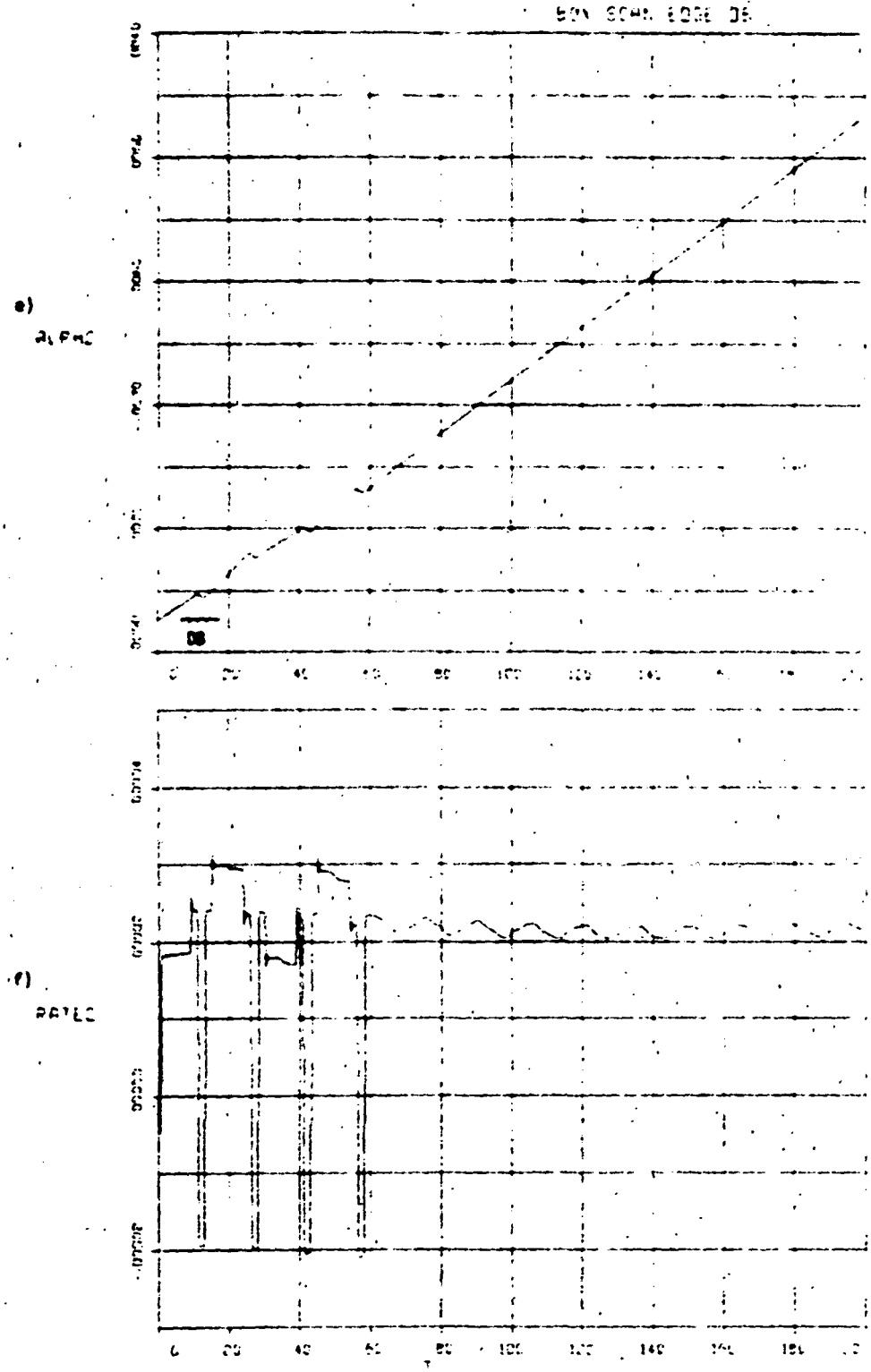

Yaw moving into deadband at average rate of 22 urad/s. Rate spikes are caused primarily by scan slew start-stops. All yaw jet firings occur during the 1st second, see e).

FIGURE 4-9

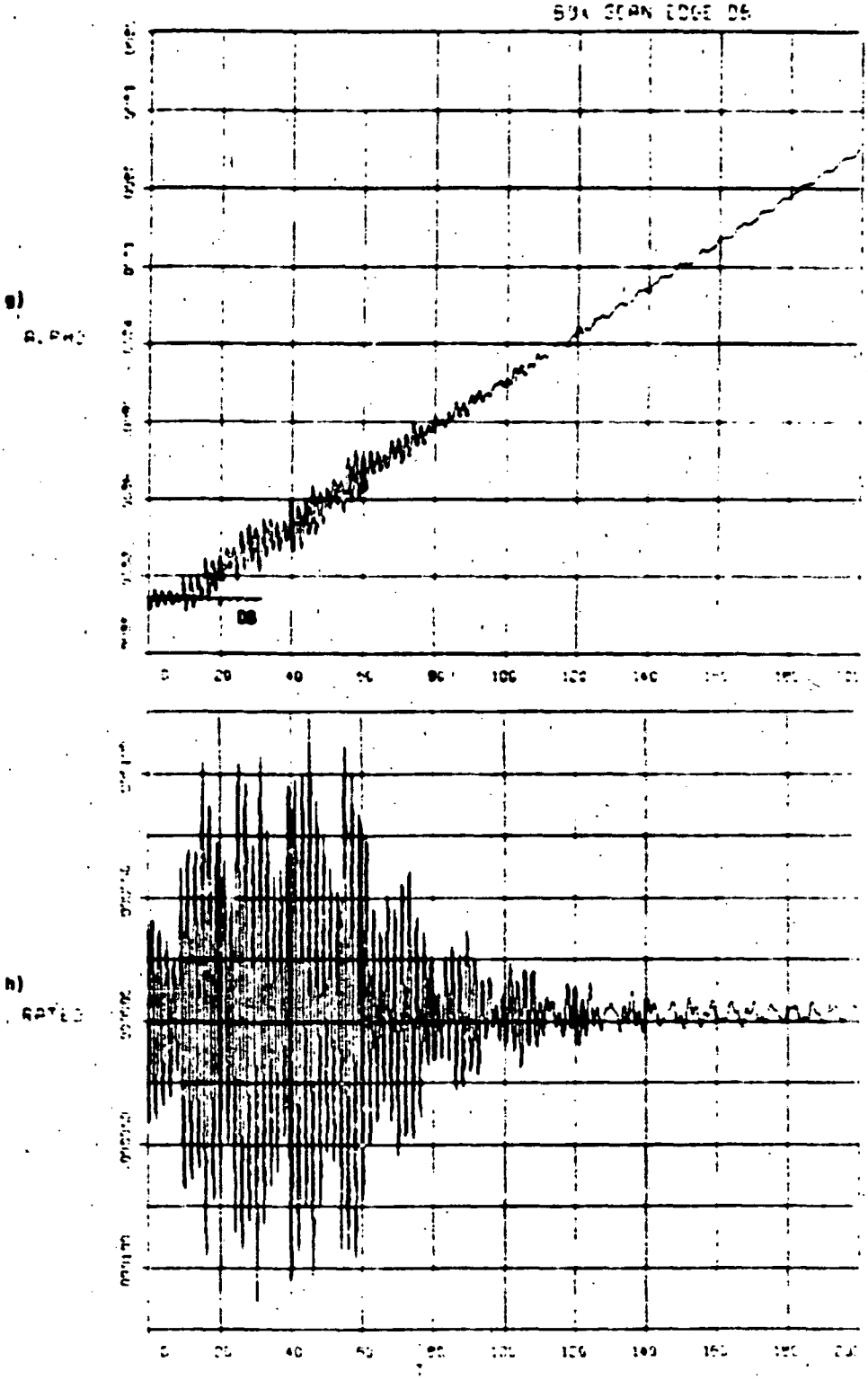

Roll jet firings take place during the first 14 seconds (see n) causing vehicle to move into deadband to a limit-cycle rate of 3 μrad/s. Max peak rates of 100 μrad between T=20 and 60 are due to scan platform start-stop interactions, not to jets.

FIGURE 4-9

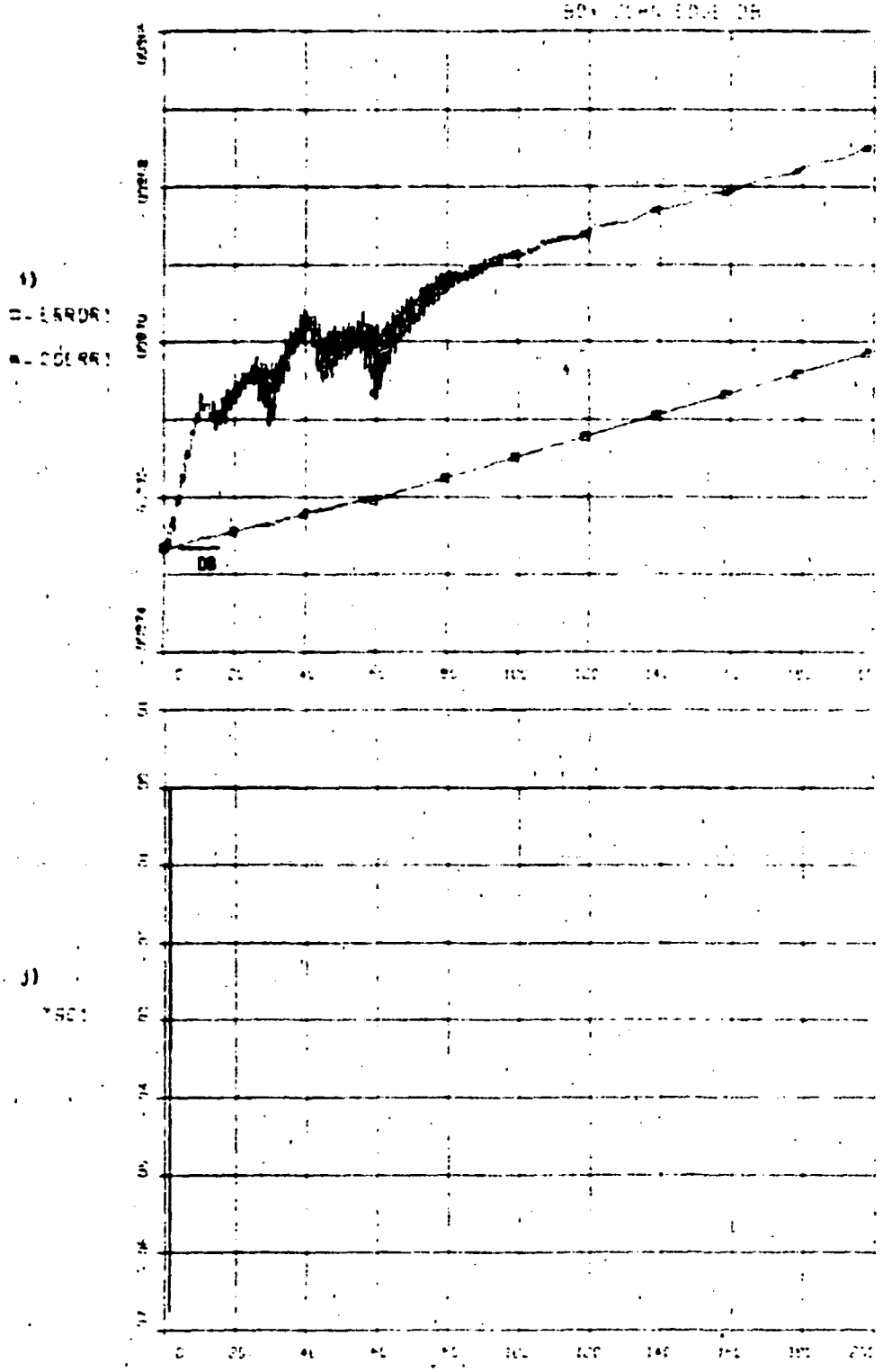

Vehicle leaving pitch deadband edge very cleanly, without multipulsing.

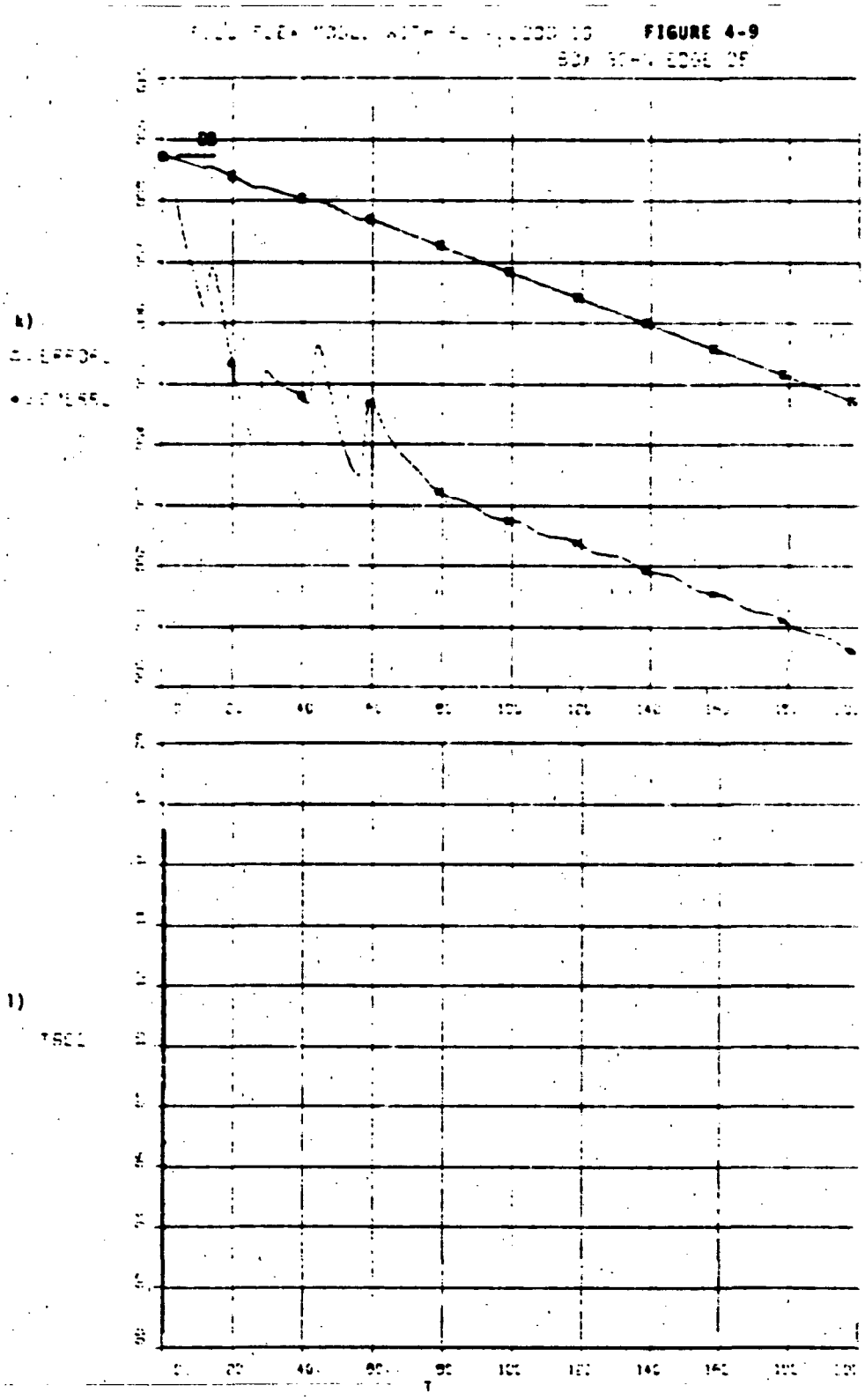

FIGURE 4-9

Vehicle leaving yaw deadband edge very cleanly, without multipulsing.

FIGURE 4-9

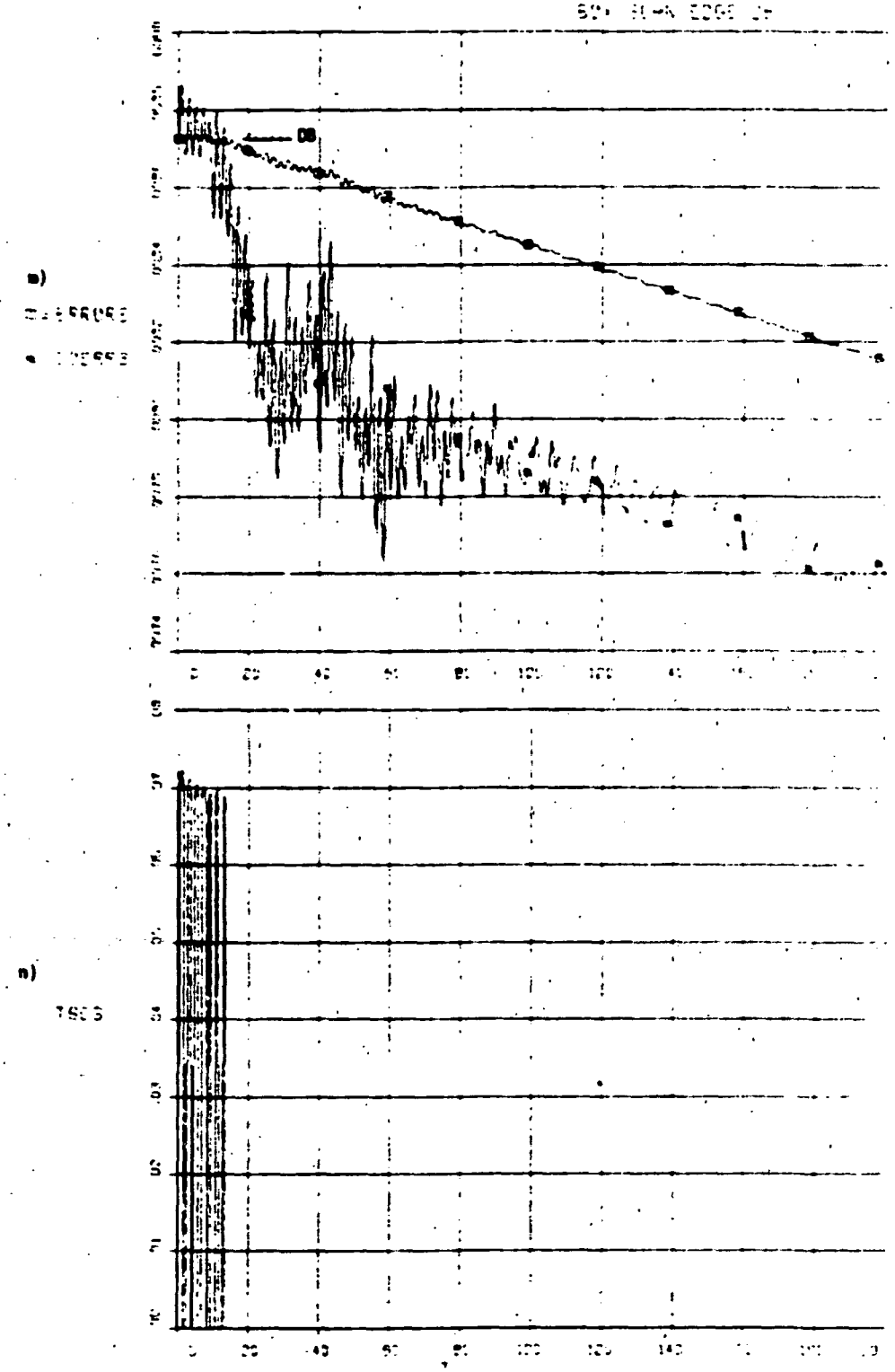

Note multipulsing as roll tries to get away from the edge of the deadband.

FULL FLEX MODEL WITH AERODYNAMIC **FIGURE 4-9**
BOX SCAN EDGE DE

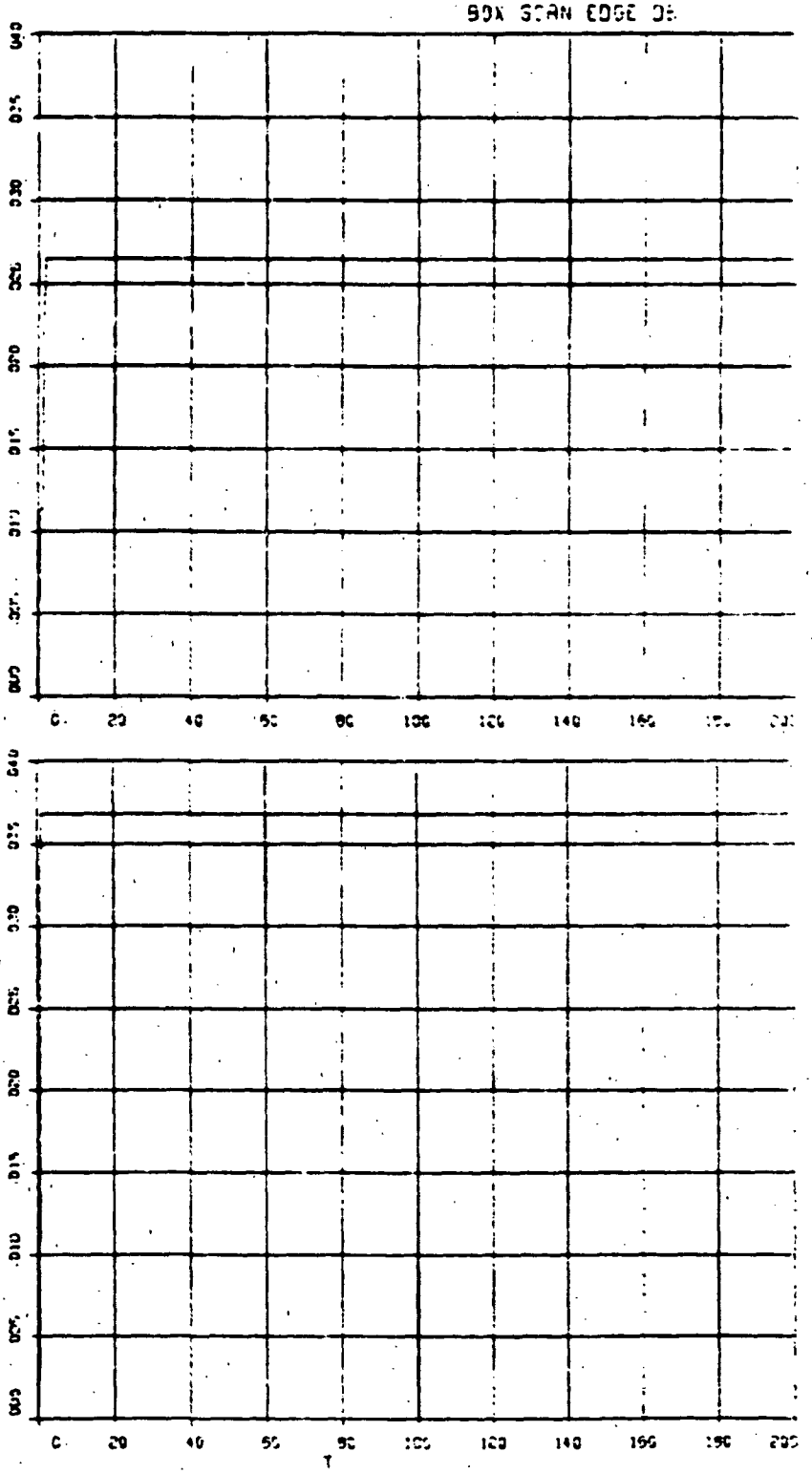

o) through r)
Gas consumption plots. Total consumption fot this box scan sequence: 0.63 gr

FIGURE 4-9

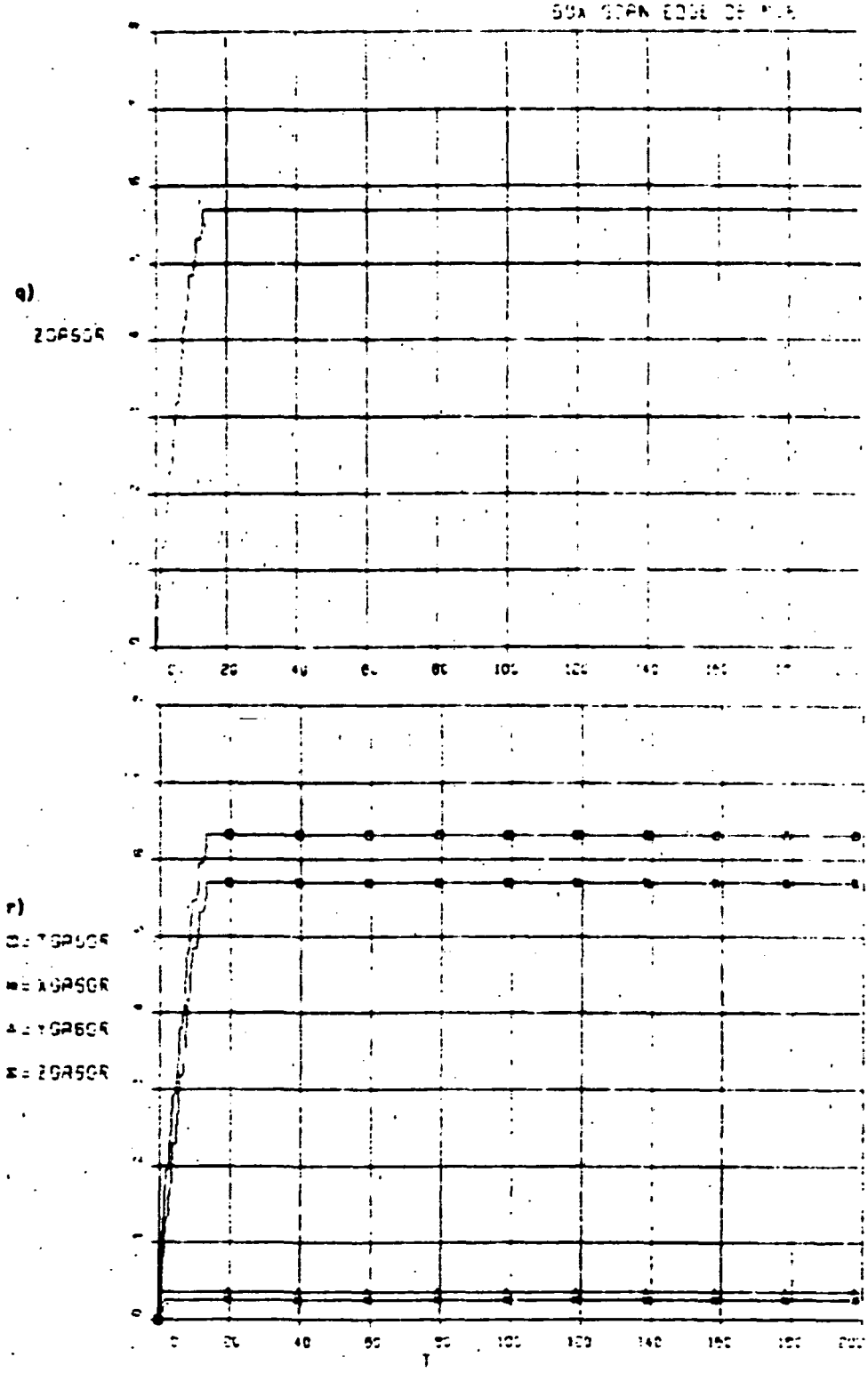

FULL FLEX MODEL WITH RCS-LLOOP.IC **FIGURE 4-9**
60λ SCAN EDGE DS

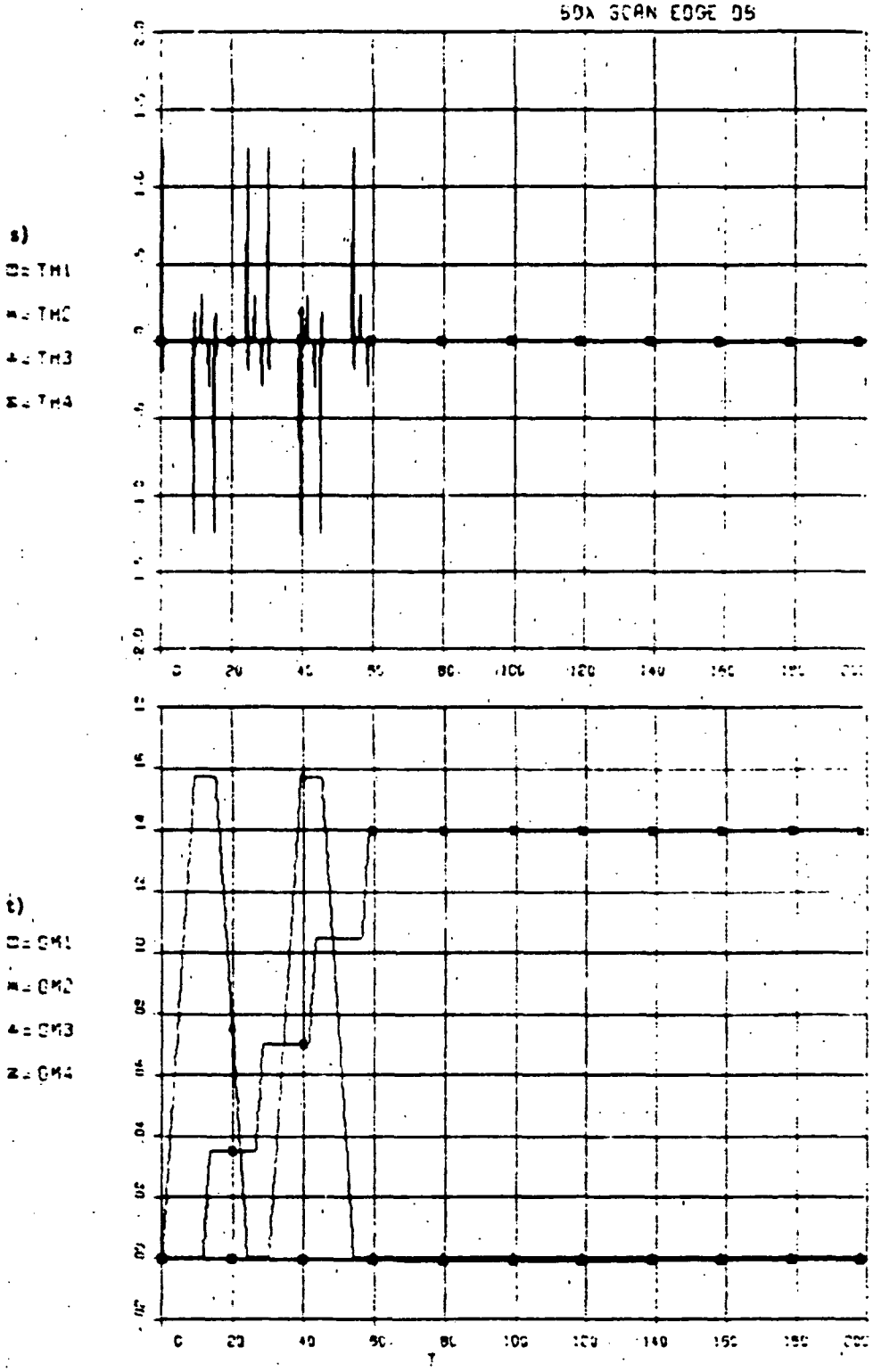

s) Note scan torque spikes at platform start-stops t)

FIGURE 4-9

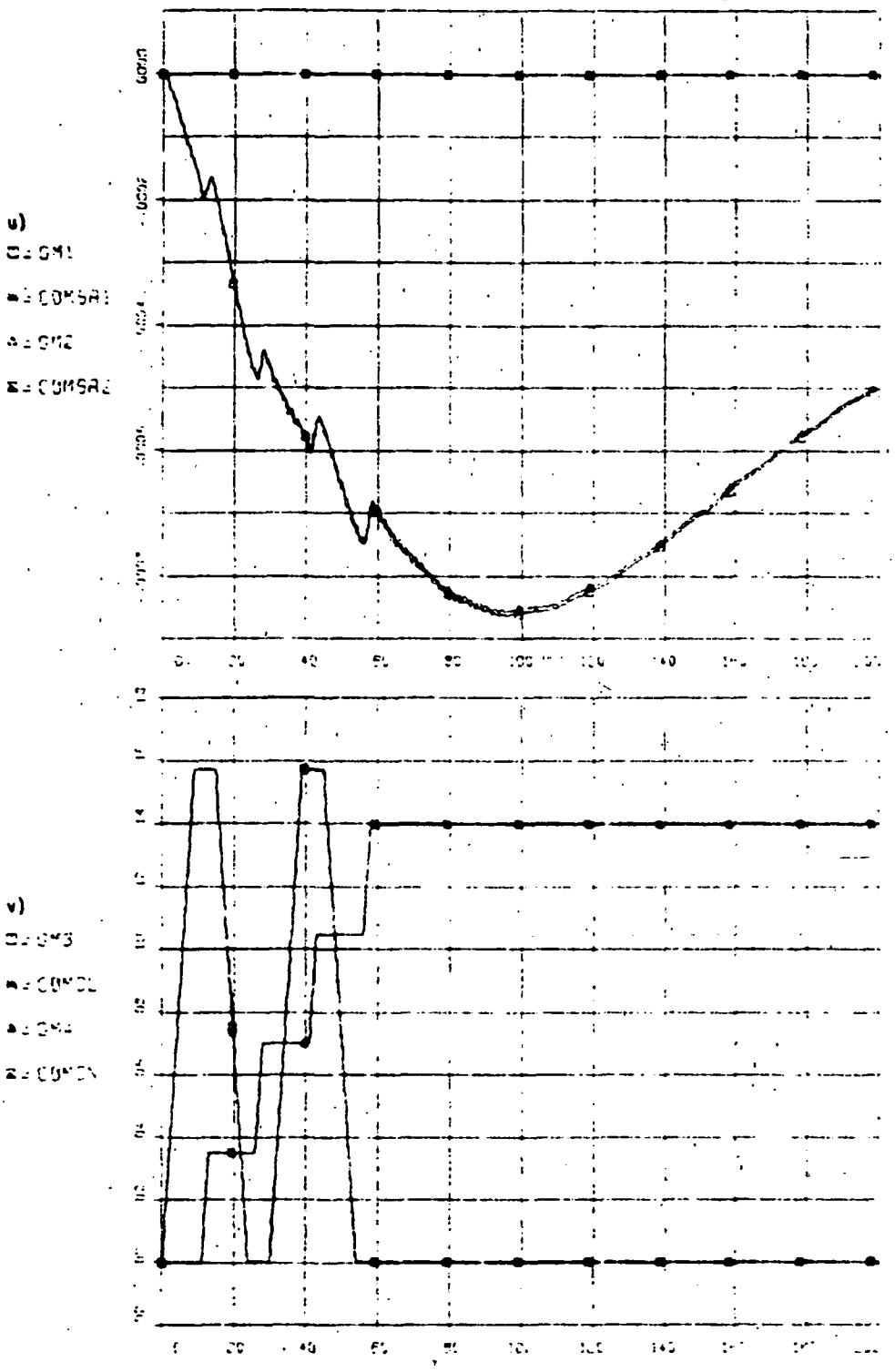

u) Solar array wing transients of 850 μrad.

FULL FLEX MODEL WITH RCS-11L200/10 FIGURE 4-9
90X SCAN EDGE DB

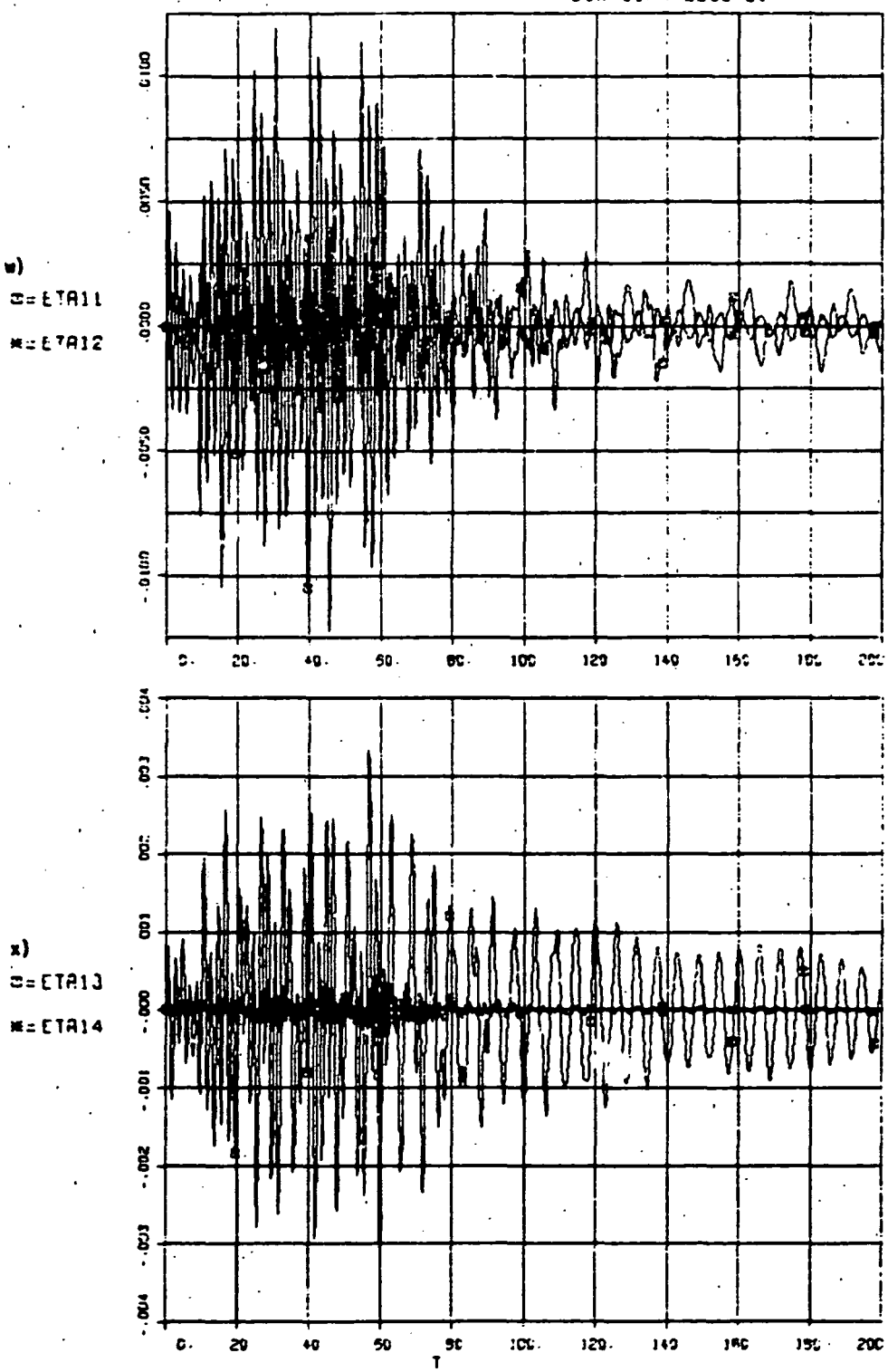

w) through z)
Vibration of the structure due primarily to scan torques, not to jet firings.

FIGURE 4-9

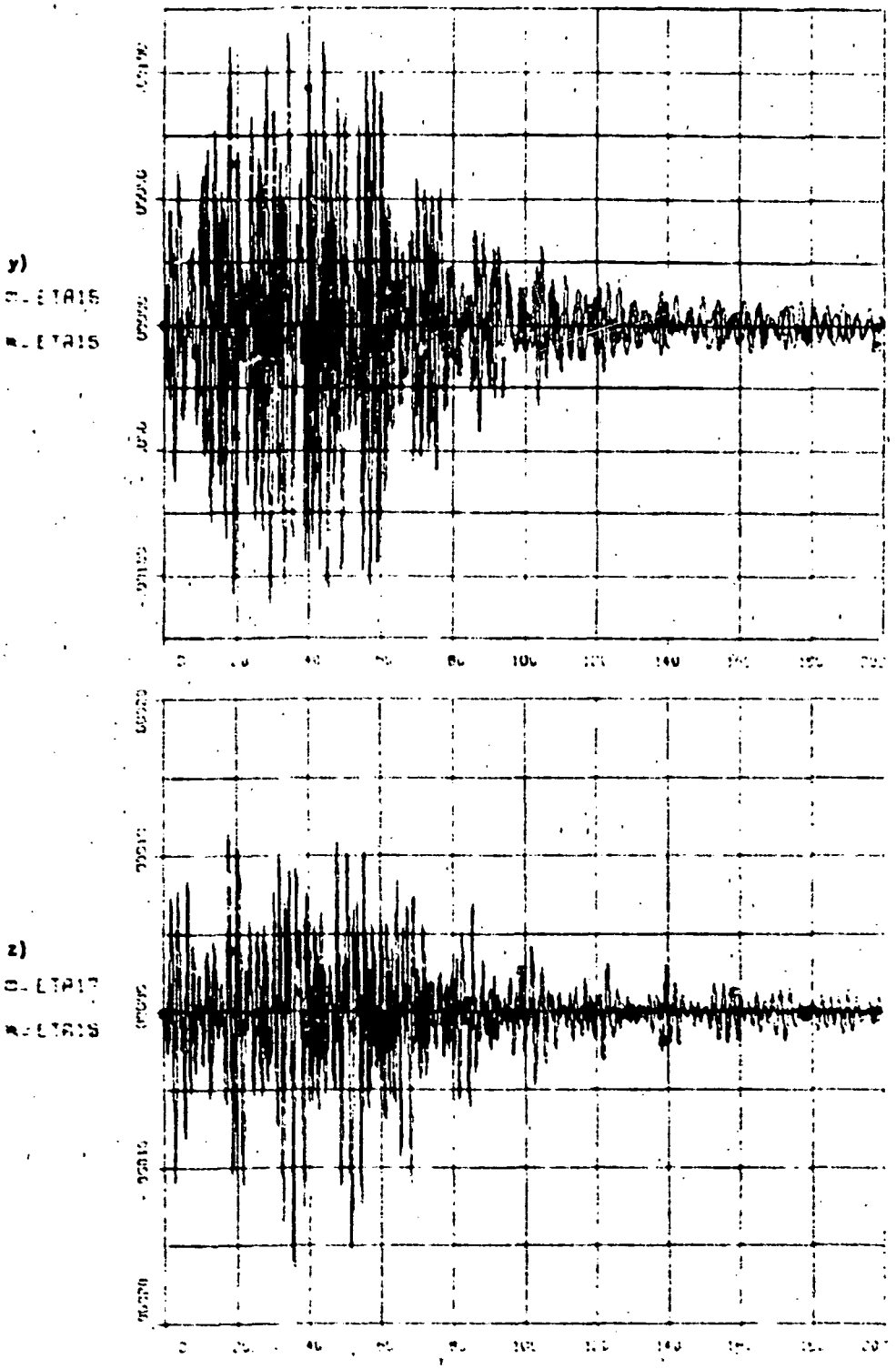

FULL FLEX MODEL WITH ROS-ARPUS **FIGURE 4-10**

80X SCAN EDGE DB

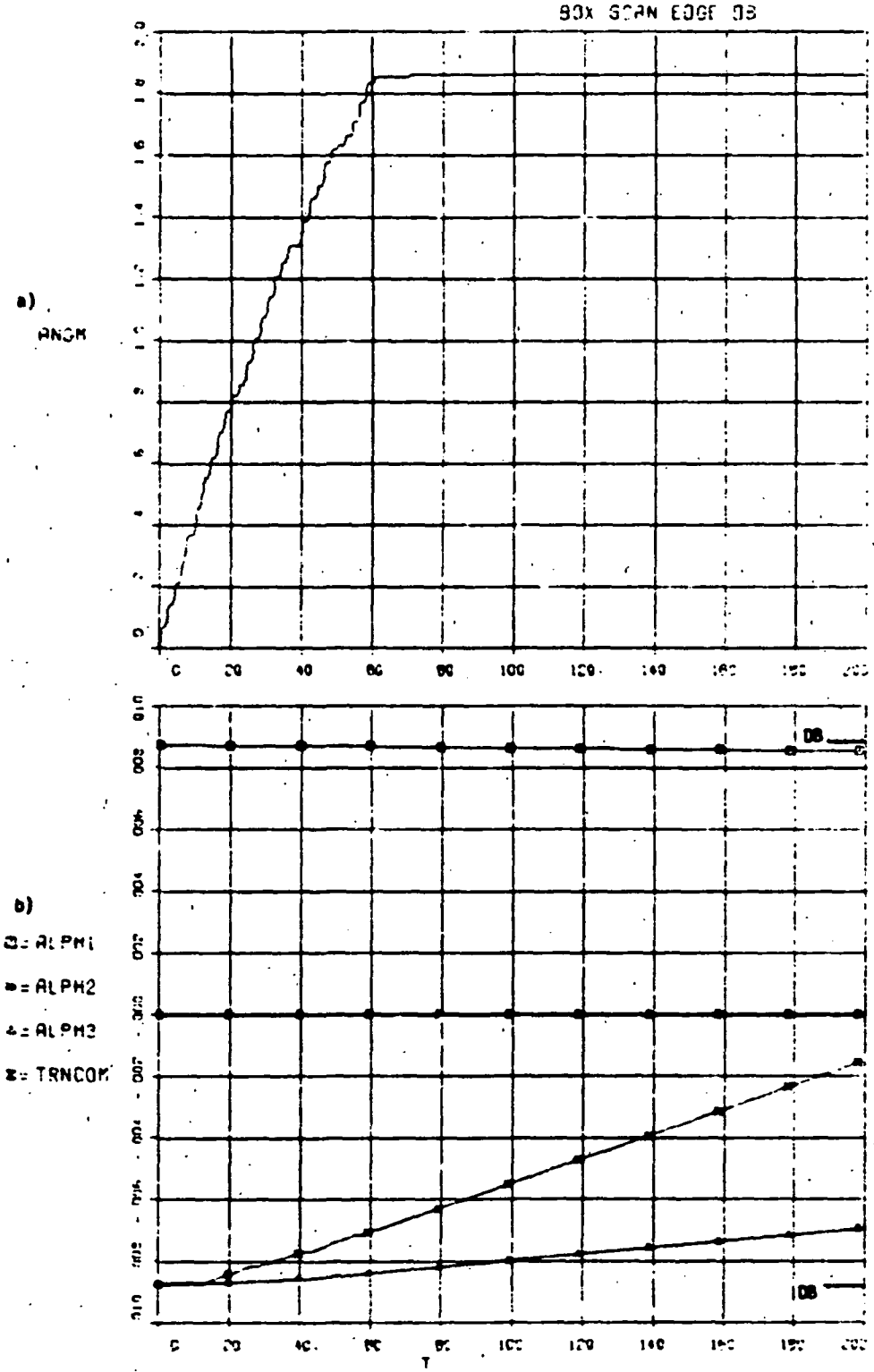

Vehicle is initially on the edge of the deadband on all 3 axes. Slewing causes jet firings which move it back into the deadband. Note that present rate + position controller produces higher limit cycle rates (for this particular slew sequence) than the lead-lag controller of Figure 4-9.

FIGURE 4-10

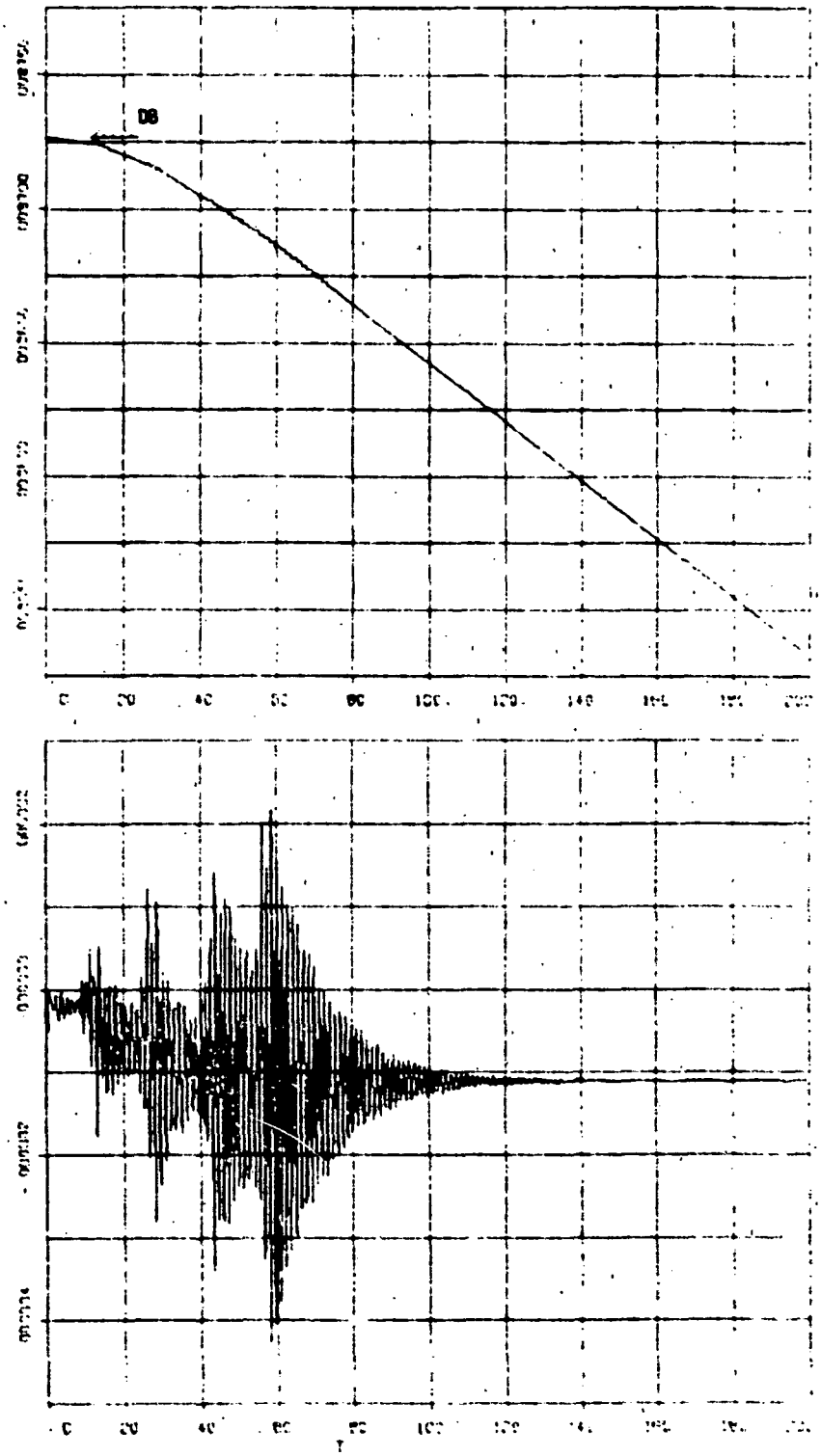

Pitch jet firings take place during the first 60 seconds (see j) moving vehicle into the deadband to an average limit cycle rate of 1.6 μrad/s. Max peak rates of 4 μrad/s due to scan dynamic interaction plus pitch firings.

FULL FLEX MODEL WITH RCS-HRP20 **FIGURE 4-10**

90X SCAN_EDGE 05

e)

ALPH2

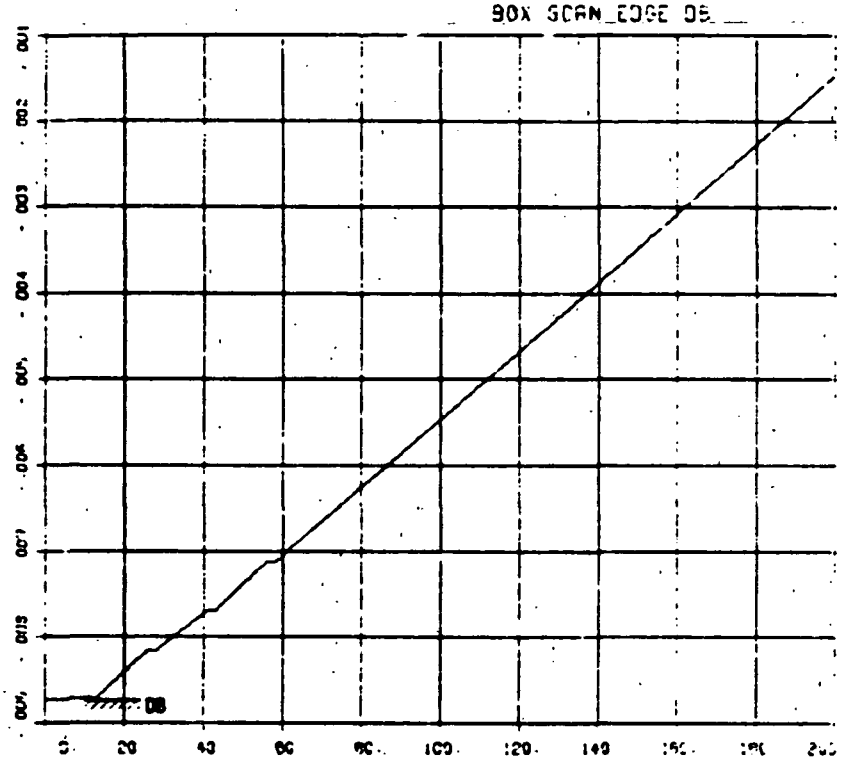

f)

RATE2

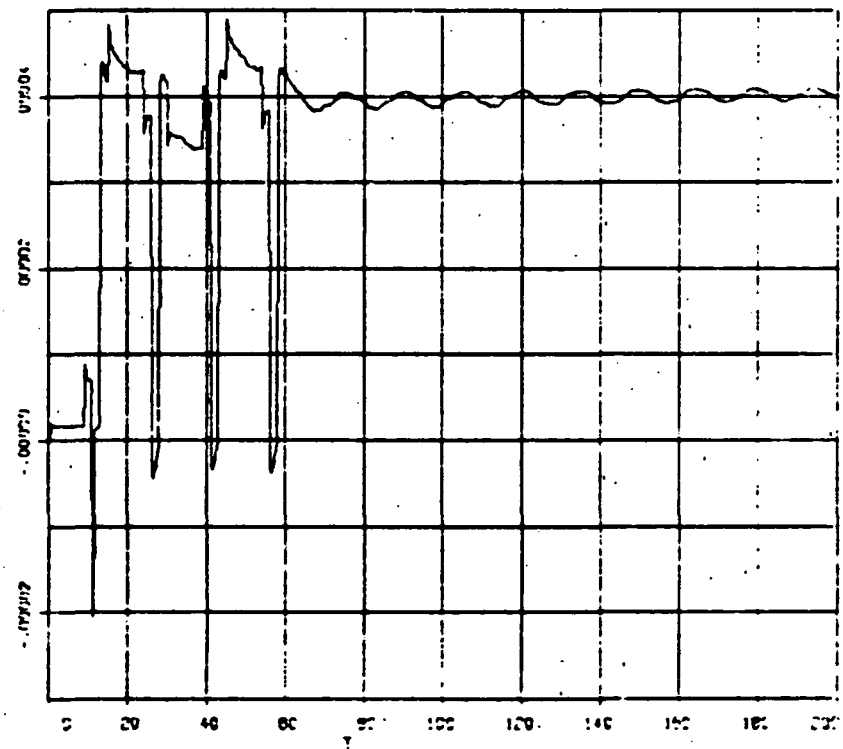

Yaw moving into deadband to an average limit cycle rate of 40 urad/s. Rate spikes are caused primarily by scan slew start-stops. All yaw firings occur during first 13 seconds, see 1).

FULL FLEX MODEL WITH RCS-KPPCD **FIGURE 4-10**

60X SCAN EDGE 06

g)

PLPH2

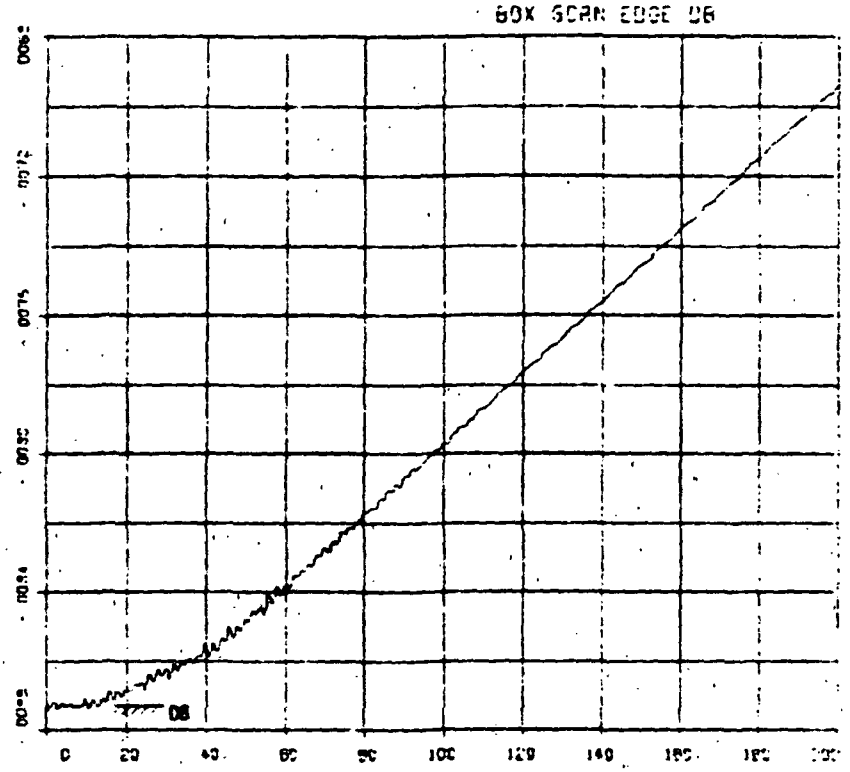

h)

RATE3

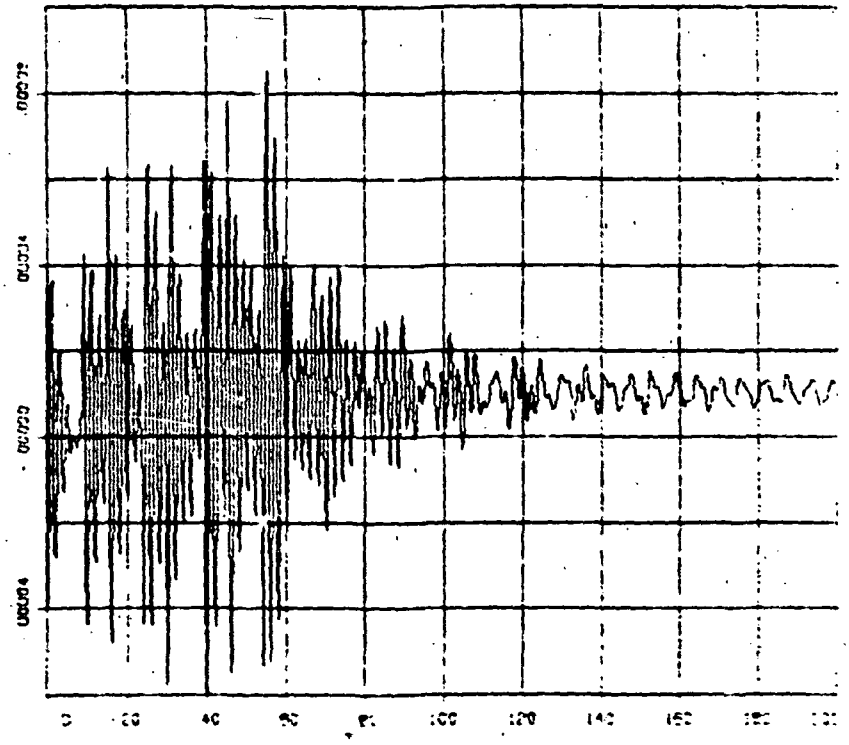

Roll jet firings take place during the first 60 seconds, while slewing, (see n) causing vehicle to multipulse and eventually, get away from deadband (see m) to a limit cycle rate of 20 urad/s. Rate oscillations caused by scan dynamic interaction plus roll firings.

FULL FLEX MODE: WITH RCS-KRP20 FIGURE 4-10
50X SCAN EDGE DB

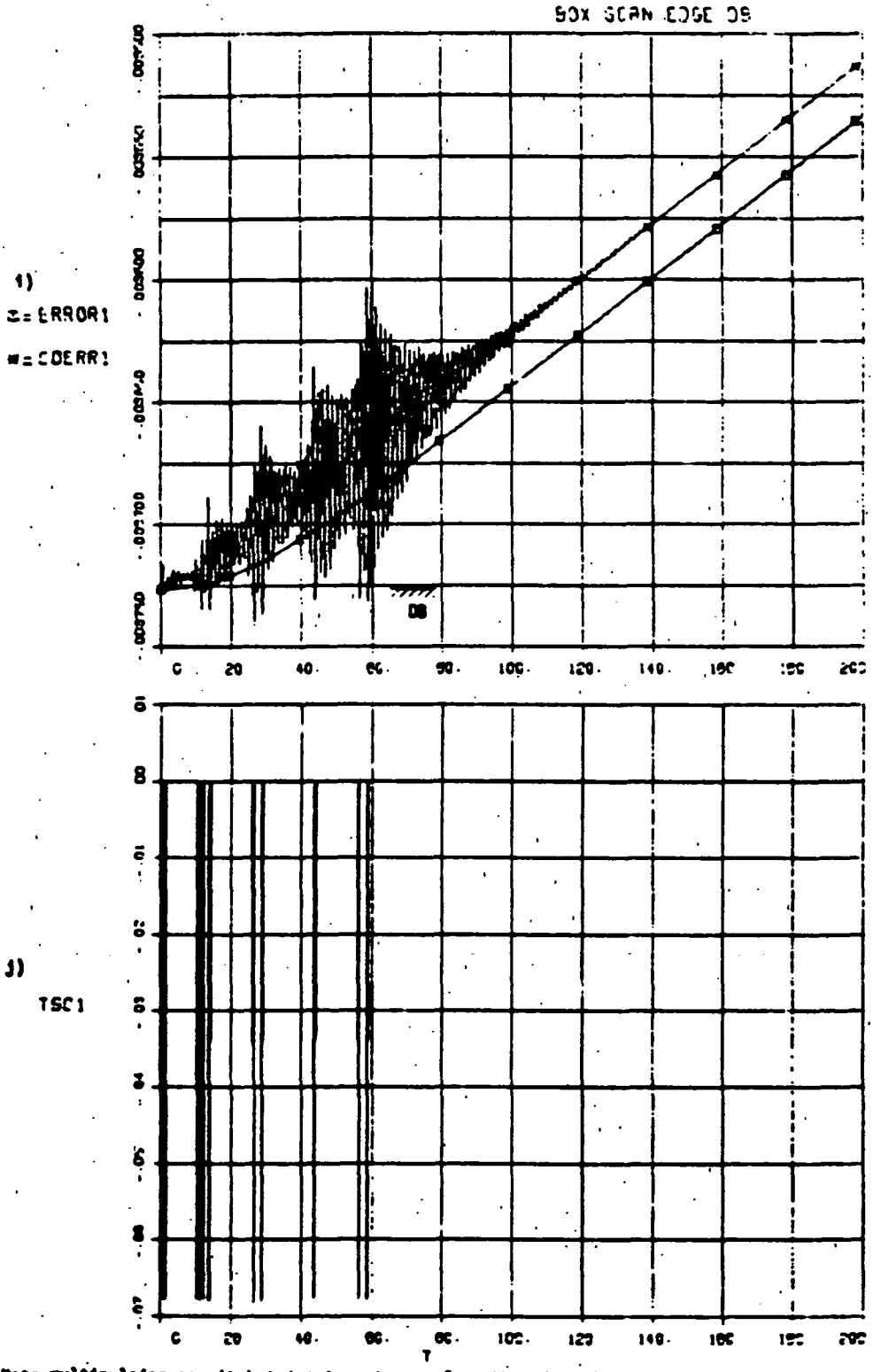

Note multipulsing as pitch tries to get away from the edge of the deadband. Also note large component of vehicle rate in the control error. This is what causes the multipulsing. Multipulsing could be reduced by pre-filtering rate before feeding it into controller.

FULL FLEX MODEL WITH ROS-KRSD FIGURE 4-10
50X SCAN EDGE DB

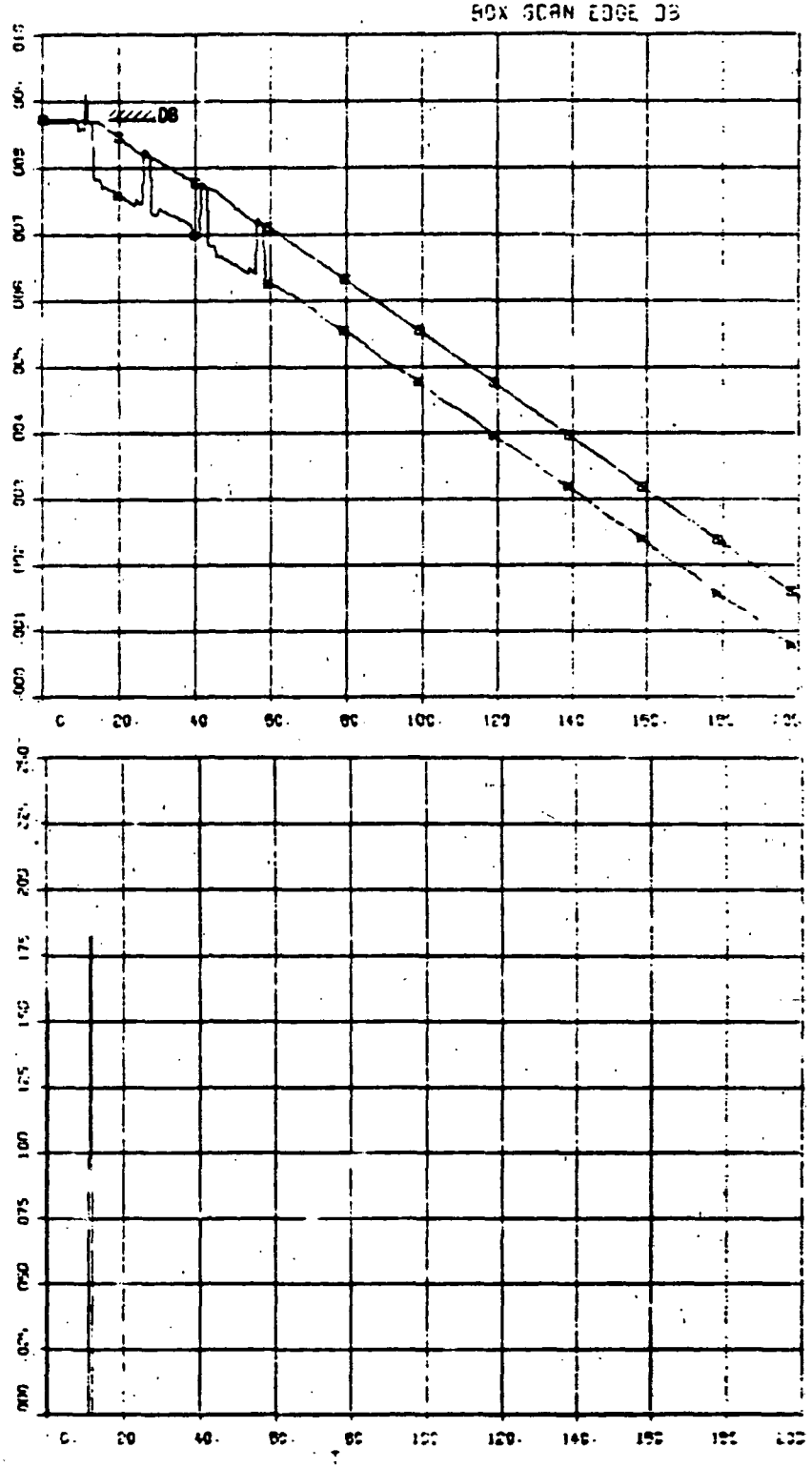

k)
ERROR2
COERR2

l)
TSC2

Yaw leaving deadband very cleanly, without excessive multipulsing.

FULL FLEX MODEL WITH RCS-KRP20 **FIGURE 4-10**

BOX SCAN EDGE DB

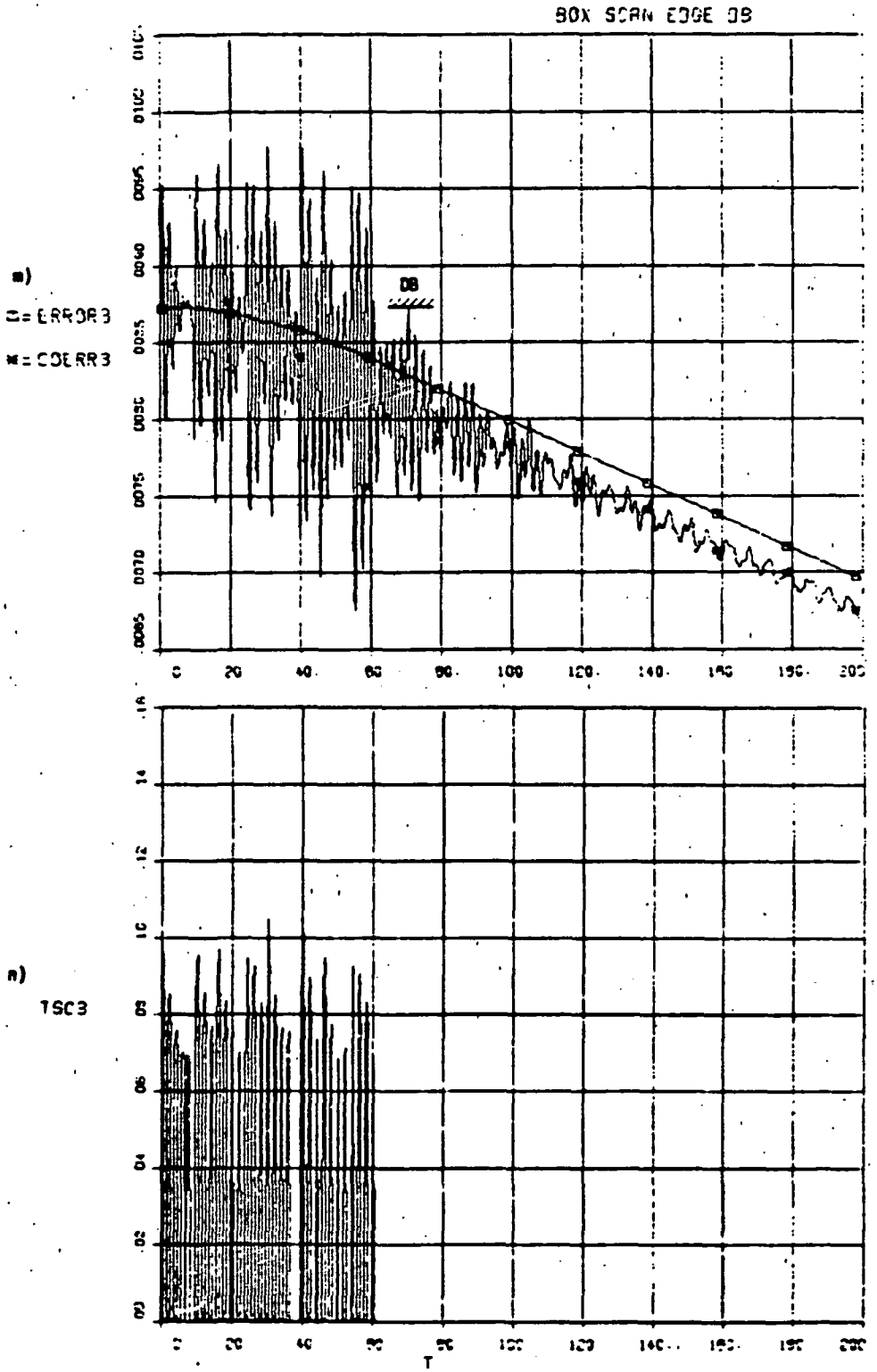

Note multipulsing as roll tries to get away from the edge of the deadband.

FULL FLEX MODEL WITH BOX-KREEP **FIGURE 4-10**

BOX SCAN EDGE 05

o)

XGASGR

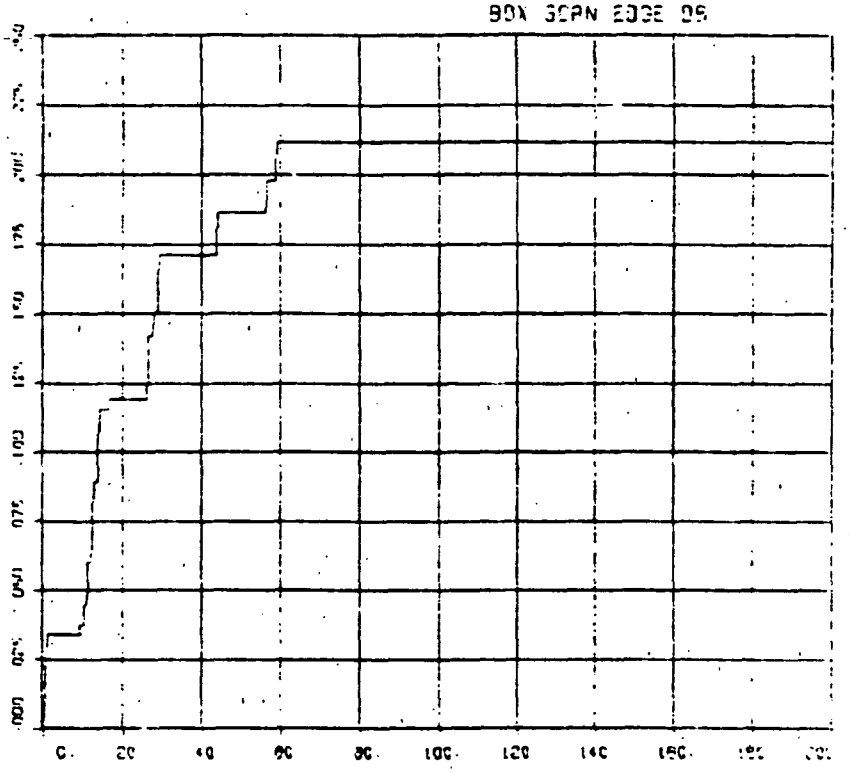

p)

YGASGR

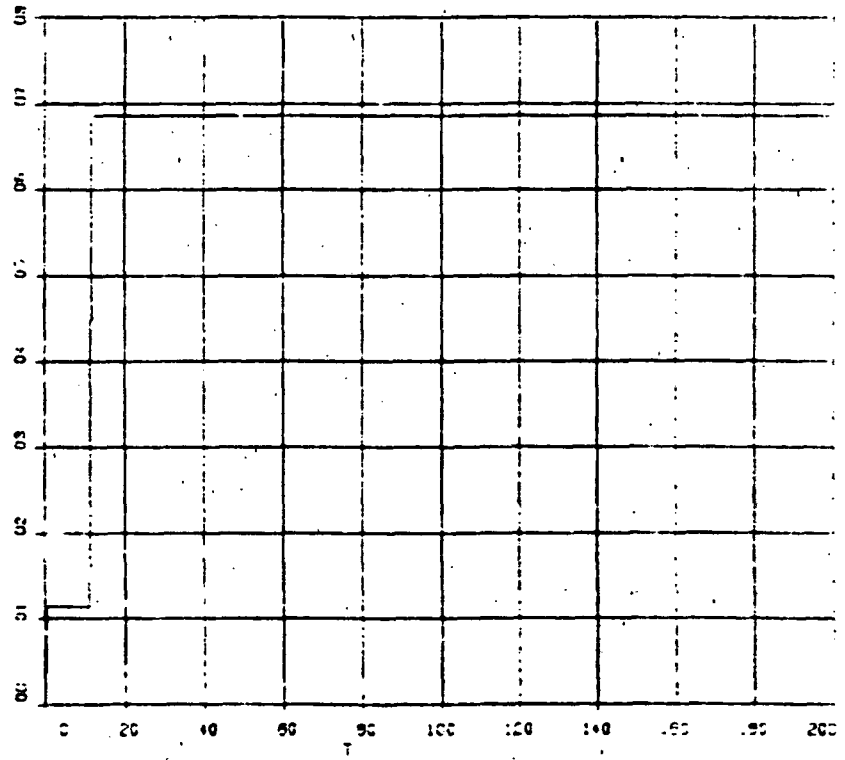

o) through r)
Gas consumption plots. Total consumption for this box scan sequence: 2.25 gr. Note that same sequence with lead-lag controller (Figure 4-9r) only required 0.63 gr, i.e., 3.6 times less gas.

FULL FLEX MODE: WITH SCS-RBF20 **FIGURE 4-10**

SOX SCAN EDGE 05

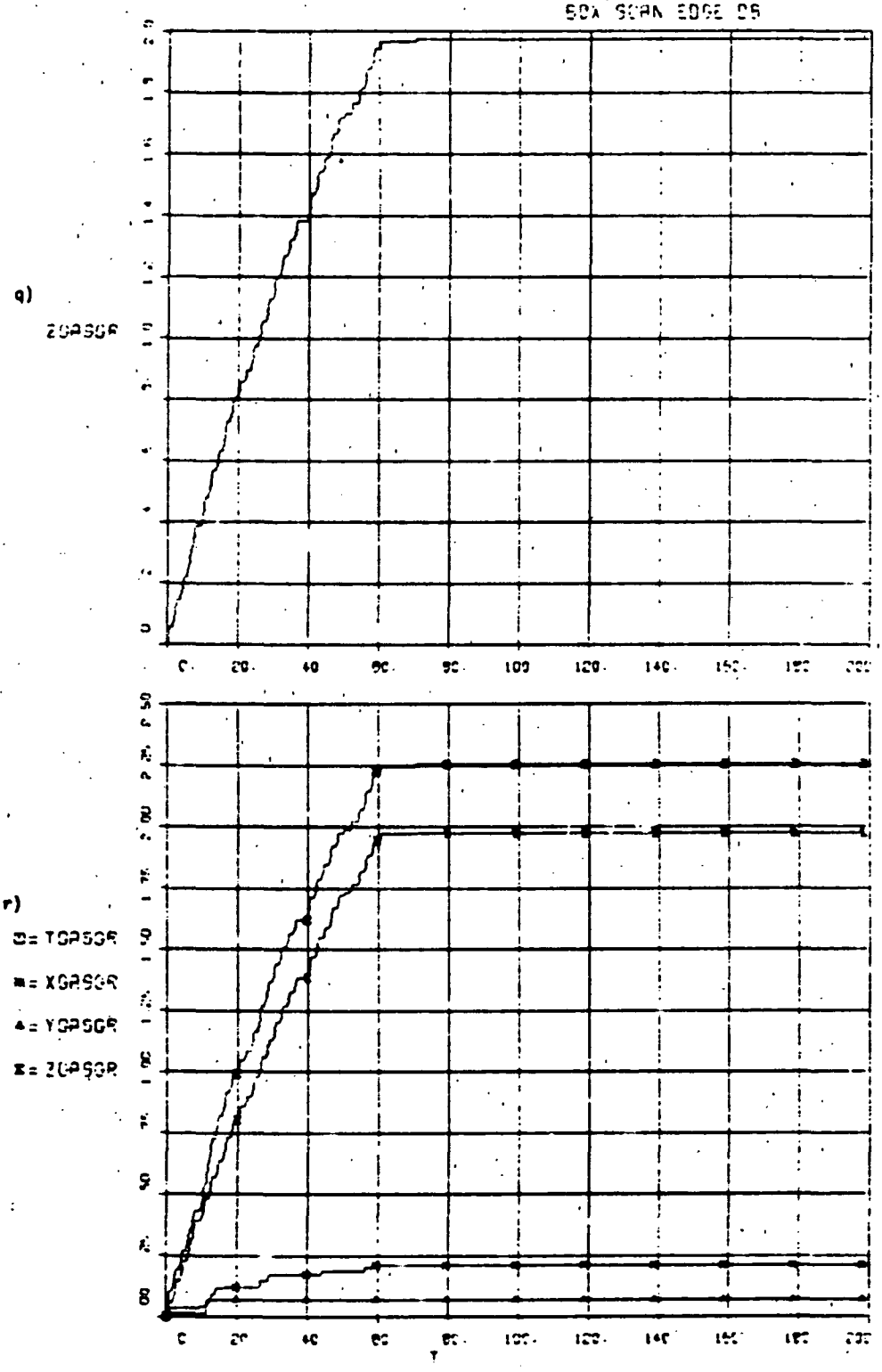

FULL FLEX MODE, WITH RCS-KARSAN **FIGURE 4-10**

BOX SCAN EDGE DB

s)

□ = TH1

✕ = TH2

△ = TH3

⧓ = TH4

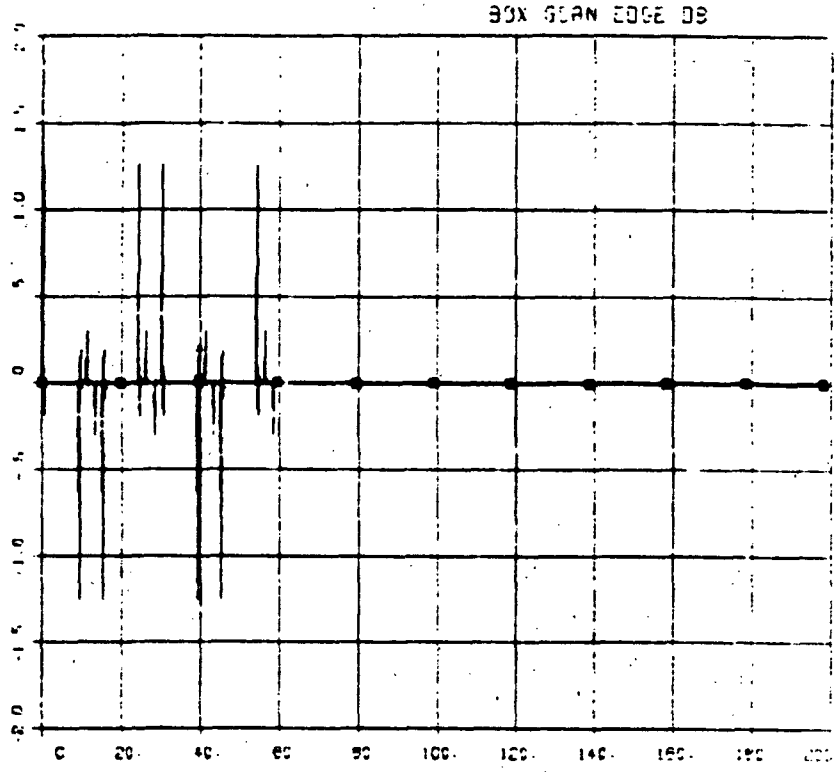

t)

□ = GM1

✕ = GM2

△ = GM3

⧓ = GM4

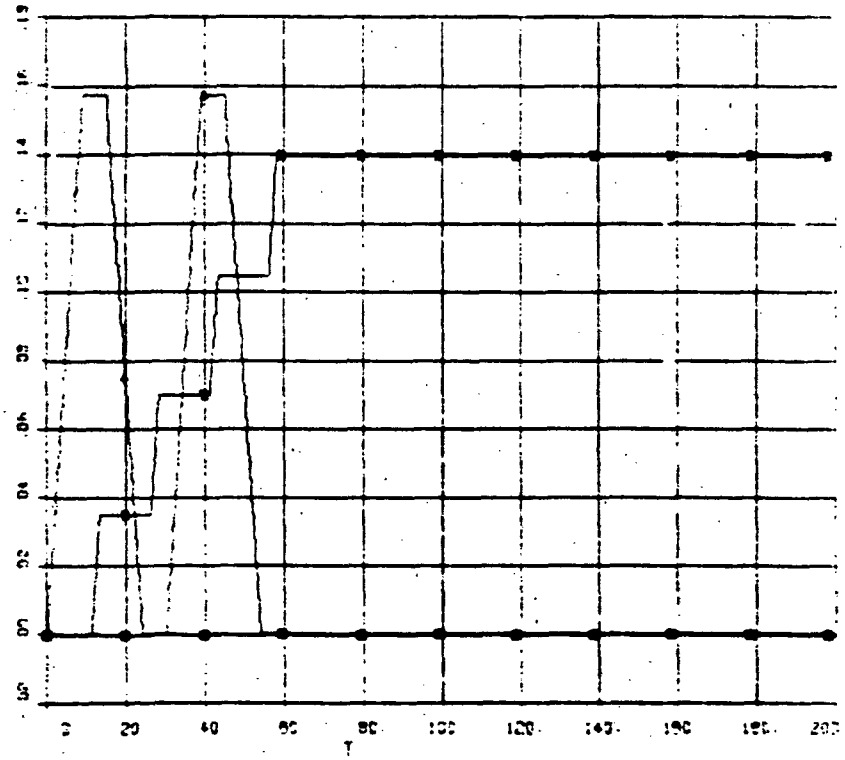

s) Note scan torque spikes at scan platform start-stops t)

FULL FLEX MODE, WITH SCS-KRF2G FIGURE 4-10
50% SCRN EDGE DB

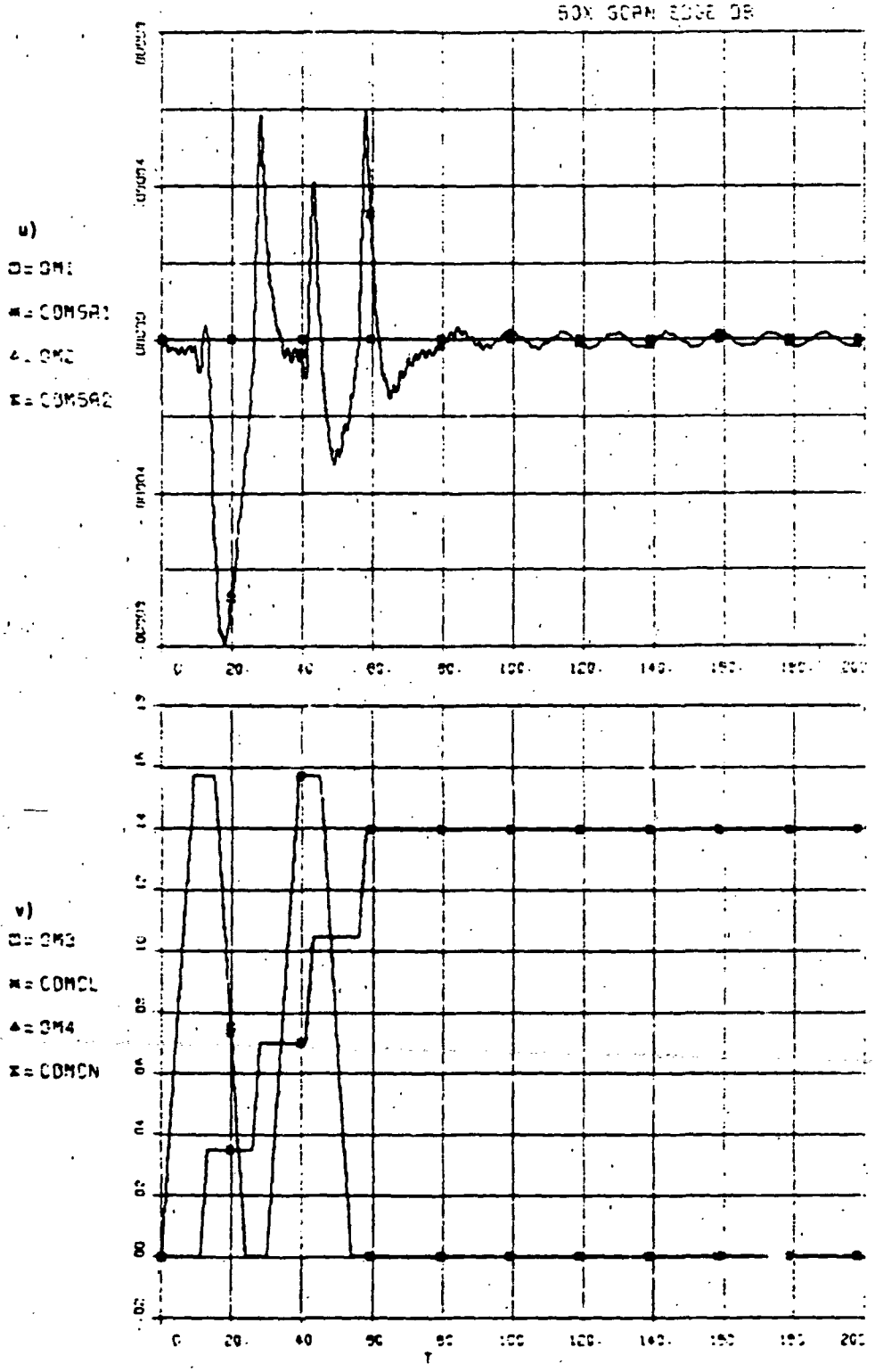

u) Solar array transient of 80 urad (vs. 850 for lead-lag controller).

FULL FLEX MODEL WITH ROS-ARP2B **FIGURE 4-10**
50X SCAN EDGE 98

w)
□=ETR11
*=ETR12

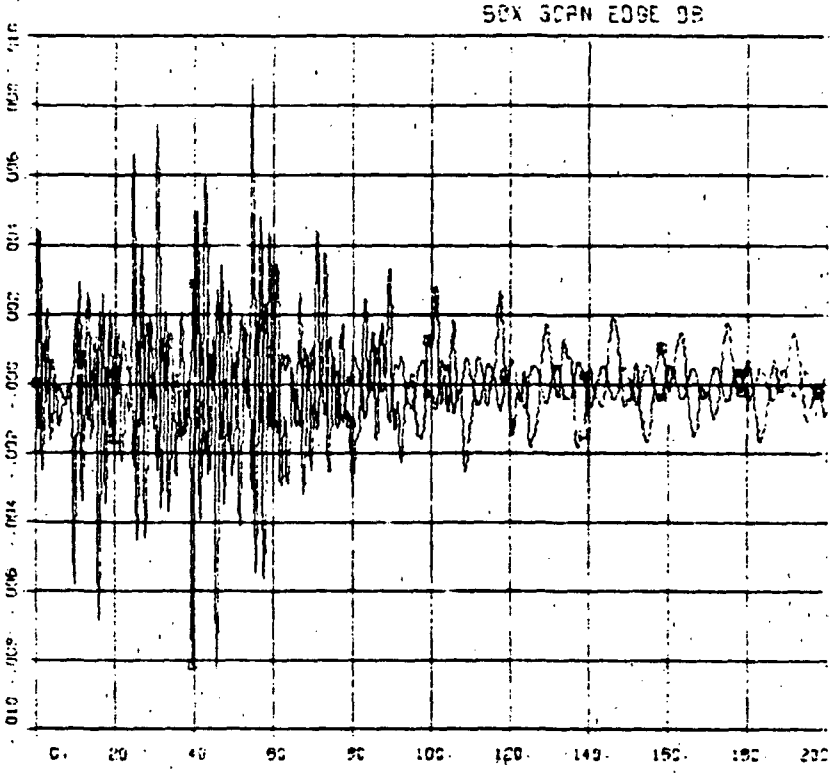

x)
□=ETR13
*=ETR14

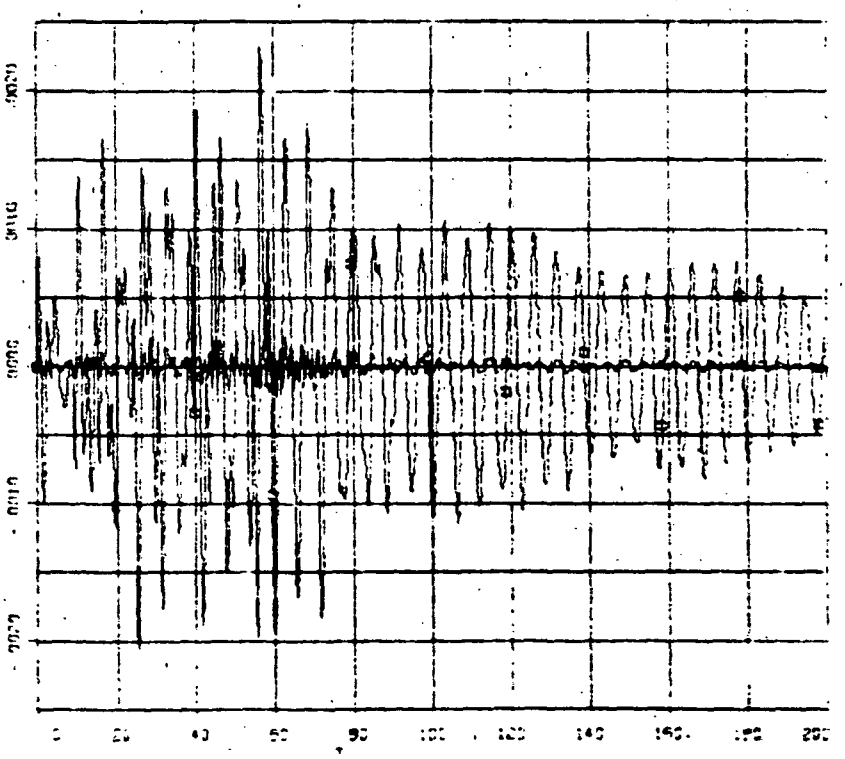

w) through z)
Vibration of the structure due to both scan dynamic interaction and jet firings.
Vibration levels somewhat less than with lead-lag.

FIGURE 4-10

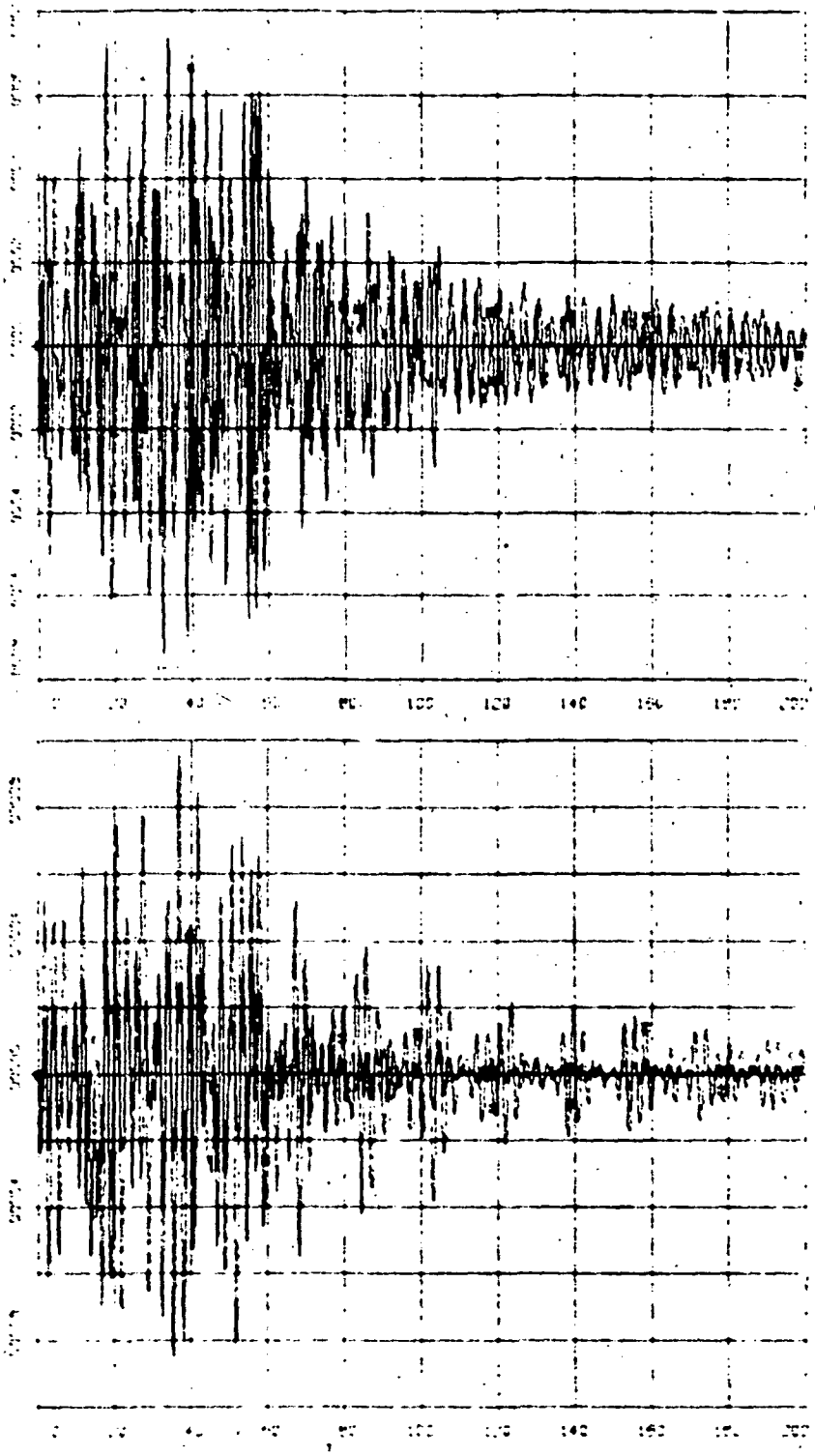

SECTION 5

REACTION WHEEL ATTITUDE CONTROL

A Reaction Wheel Attitude Control System achieves vehicle control through the use of motor driven flywheels. The motors are energized to develop the torques which control the vehicle. These torques are felt by both the vehicle and the wheels causing each to accelerate (in opposite directions) in inverse ratio to their respective moments of inertia.

Reaction wheels with suitable control laws can provide extremely accurate and smooth proportional control. This is a very important asset in the control of flexible vehicles as it reduces significantly the problems of control/structure interactions that one encounters with impulsive type A/C systems, such as the RCS system described in Section 4.

In the present section we will develop an attitude control system for SEPS/ICM using NASA Standard Reaction Wheels. We will also evaluate its performance. The section is organized as follows:

5.1 DESCRIPTION OF THE NASA STANDARD REACTION WHEEL (SRW)

The SRW (Figure 5-1) consists of a flywheel, a two phase induction drive motor, redundant tachometers, a temperature sensor, a pressure transducer and a sealed housing. Table 5-1 lists its performance characteristics.

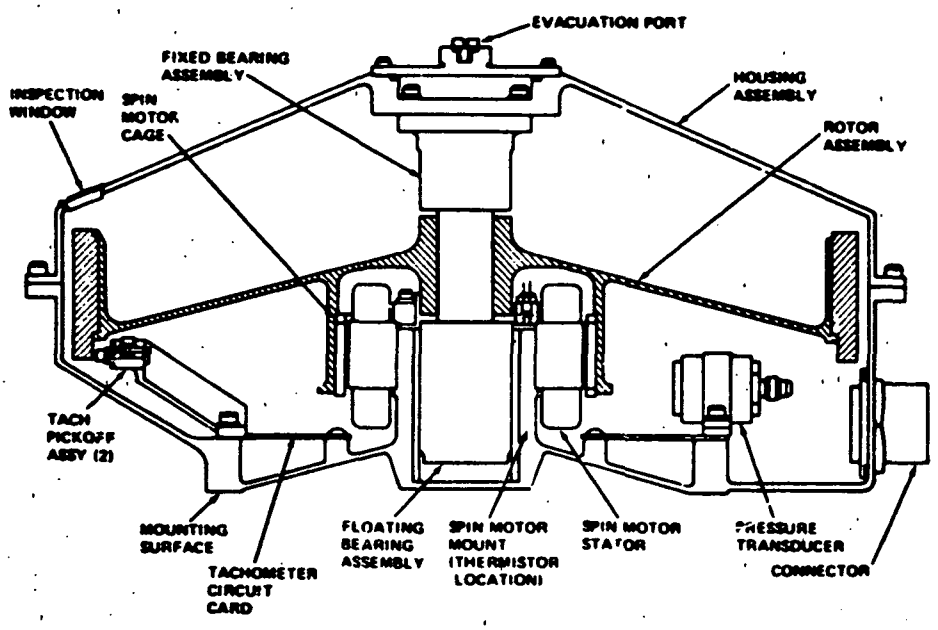

Figure 5-1. NASA SRW Cross Section

Figure 5-2 shows the torques available at various wheel speeds and motor voltages for dual-phase excitation of the motor (this means that, for a given speed, the torque is proportional to the square of the voltage). It can be observed from Figure 5-2 that in the range of $\pm$ 1800 rpm - and for a given applied voltage - the torque is approximately constant.

The synchronous speed of the motor (ω_s) at 400 Hz excitation is 2400 rpm. The wheel, however, loses its torquing capability near this speed and should not be operated above 2200 rpm.* In this study,

*It is possible to drive the SRW at different frequencies and thus alter its momentum storage capability, torque characteristics, and maximum speed.

Table 5-1. PERFORMANCE CHARACTERISTICS

Description	Specification Requirement	Typical Performance at Ambient
Angular Momentum at 24V	20 N-m-s minimum	21.8 N-m-s
Wheel Speed Range at 400 Hz Excitation	Zero to ±2200 rpm	Zero to ±2200 rpm
Reaction Torque		
Normal Mode at 24V	.15 N-m minimum	.175 N-m
High Mode at 33V	.30 N-m minimum	.339 N-m
Tachometer Output	240 Pulses per revolution with rotation direction indication	240 Pulses per revolution with rotation direction indication
Momentum Vector Misalignment	15 arc minute maximum	2.48 arc minute
Torque Noise	±1.5° maximum above .1 rad/s	±1.0° above .1 rad/s
Wheel Breakaway Torque	.003 N-m maximum	.0023 N-m
Power Consumption		
Maximum Torquing at 24 V	75 watts maximum	62.4 watts
Constant Speed (at .9 Synchronous Speed)	10 watts maximum	6.6 watts

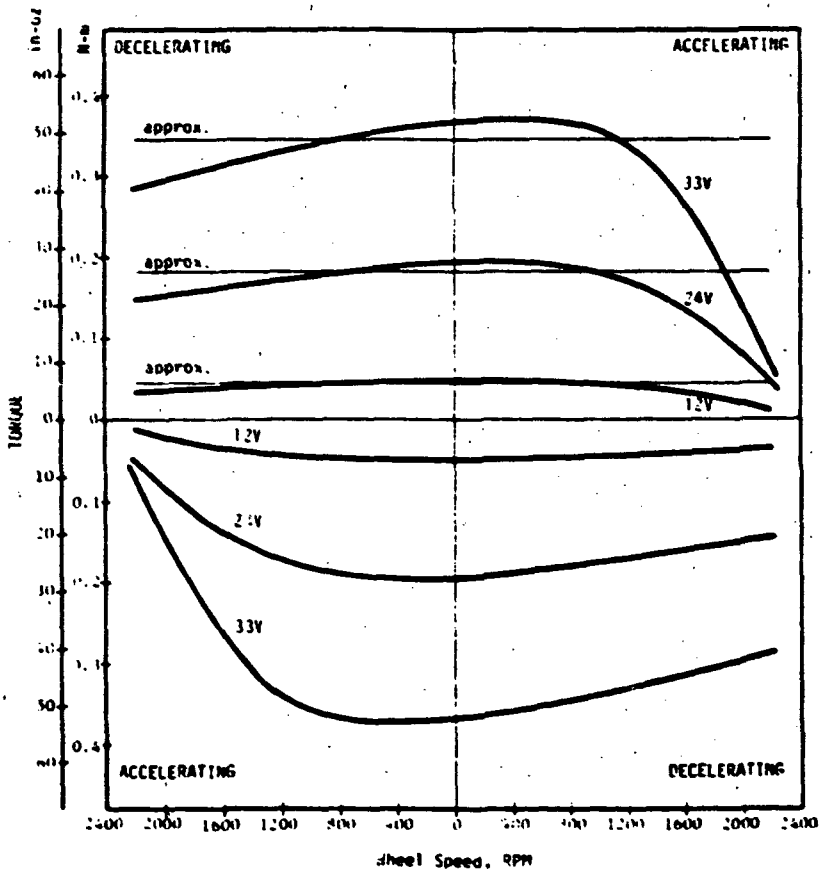

Figure 5-2. Torque-speed characteristics

we have aimed at using the SRW at less than 2200 rpm (92% of ω_s) and have taken advantage of a constant torque approximation over this range of speeds, as shown in Figure 5-2. This approximation is given by

$$T_r = K_m V_m^2 \text{ sign } (V_m) \qquad (5\text{-}1)$$

where

K_m = 0.045 in-oz/V^2 (0.3177 N-m/V^2) is the "motor torque constant,"

V_m = the voltage applied to the motor, in volts,

sign(V_m) = the "sign of V_m ".

Neglecting frictional torques, the SRW can then be modelled as shown in Figure 5-3,

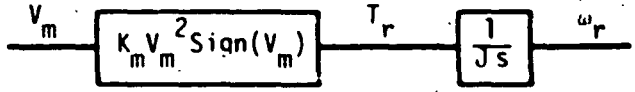

Figure 5-3. SRW model

where K_m = 0.3177 N-m/V^2 is the motor torque constant,

J = 0.0868117 kg-m^2 is the flywheel and motor rotor inertia,

ω_r = the inertial spin rate of the SRW, in rad/s.

5.2 THREE-AXES CONTROL IMPLEMENTATION USING SRW'S

To obtain control torques on the vehicle three SRW's will be used. They are mounted on the bus (b_o) with their spin axes parallel to the bus XYZ axes as shown in Figure 5-4. Note that their actual location within the bus is immaterial, they can be placed anywhere they fit.

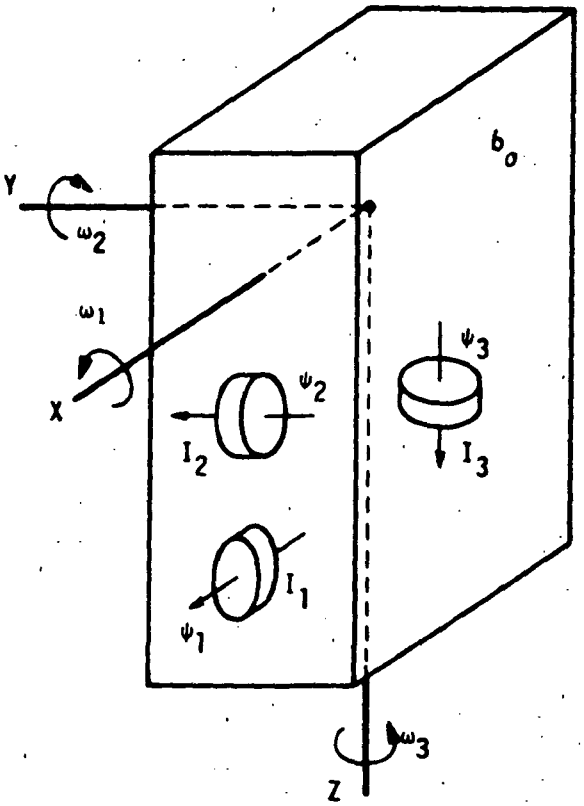

Figure 5-4. Bus with 3 SRW's

Let

$\omega = (\omega_1\ \omega_2\ \omega_3)^T$ denote the body fixed angular rates of the bus b_o

$\psi = (\psi_1\ \psi_2\ \psi_3)^T$ denote the spin angle of SRW's relative to b_o

$I = \text{diagonal}\ (I_1\ I_2\ I_3)$ with I_i the spin axis inertia of rotor i

$T_r = (T_{r1}\ T_{r2}\ T_{r3})^T$ denote the vector of applied torques to rotors

$TB_r = (TB_{r1}\ TB_{r2}\ TB_{r3})^T$ denote the vector of torques on the bus b_o due to SRW's

The torques on the rotors and on the bus are given by

$$T_r = \hat{I}(\ddot{\psi} + \dot{\omega}) \tag{5-2}$$

$$TB_r = -[\hat{I}(\ddot{\psi} + \dot{\omega}) + \omega \times \hat{I}(\dot{\psi} + \omega)] \tag{5-3}$$

In our case, for three identical wheels $I_1 = I_2 = I_3 = J$, these equations yield

$$T_{r1} = J(\ddot{\psi}_1 + \dot{\omega}_1) \quad , \quad TB_{r1} = -T_{r1} - J(-\omega_3\dot{\psi}_2 + \omega_2\dot{\psi}_3) \tag{5-4a}$$

$$T_{r2} = J(\ddot{\psi}_2 + \dot{\omega}_2) \quad , \quad TB_{r2} = -T_{r2} - J(\omega_3\dot{\psi}_1 - \omega_1\dot{\psi}_3) \tag{5-4b}$$

$$T_{r3} = J(\ddot{\psi}_3 + \dot{\omega}_3) \quad , \quad TB_{r3} = -T_{r3} - J(-\omega_2\dot{\psi}_1 + \omega_1\dot{\psi}_2) \tag{5-4c}$$

The terms

$$T_{g1} = J(-\omega_3\dot{\psi}_2 + \omega_2\dot{\psi}_3) \tag{5-5a}$$

$$T_{g2} = J(+\omega_3\dot{\psi}_1 - \omega_1\dot{\psi}_3) \tag{5-5b}$$

$$T_{g3} = J(-\omega_2\dot{\psi}_1 + \omega_1\dot{\psi}_2) \tag{5-5c}$$

represent the gyroscopic cross-coupling reaction torques on each axis caused by the vehicle and wheel spin rates of the other two axes. These gyroscopic terms are very small under normal conditions, becoming noticeable only when the vehicle rates are high and, simultaneously, the wheels are spinning at high velocity.

It should be noted that the tachometers in the SRW's provide measurements of $\dot{\psi}$, the spin rate relative to the SRW housing (i.e., b_o). To obtain the inertial spin rate ω_r all that is needed is to compute $\omega_r = \dot{\psi} + \omega$ where $\dot{\psi}$ is obtained from the tachometer and ω is obtained from the gyros mounted on b_o.

The final SRW model (including gyroscopic torques) is shown in Figure 5-5.

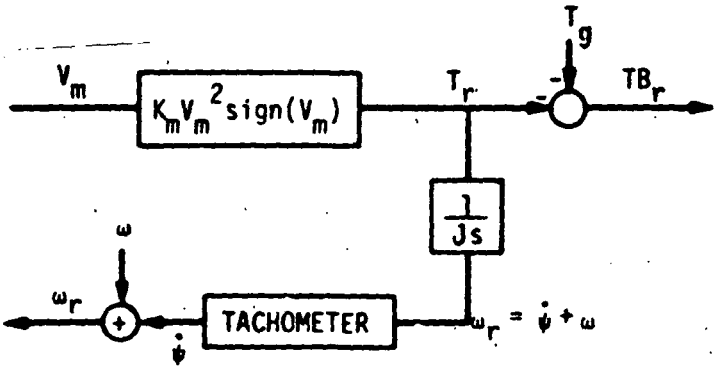

Figure 5-5. SRW model including gyroscopic torques

5.3 DESIGN OF THE ATTITUDE CONTROL SYSTEM

In order to design the Reaction Wheel A/C System for SEPS we will make some simplifying assumptions which will allow us to design the systems as if the vehicle were rigid. This is a temporary assumption which will only be used for the design phase of the A/C loop and the sizing of its parameters. The A/C system developed under these assumptions will then be integrated with a fully flexible dynamics SEPS model. Their joint performance will be evaluated through computer simulation of several maneuvers in subsection 5.4.

Under certain conditions, to be described below, this is a viable and desirable design approach because of its simplicity. It can be justified by the following considerations. If the control loop is designed so as to provide a control frequency well below the lowest flexible mode frequency, then the vehicle will move slowly enough that structural deformations will be minimal and, therefore, vehicle flexibility will not play a significant role; the vehicle will move as an essentially rigid body. In more mundane and graphical terms, this philosophy can be summarized by the following principle: "If moved slowly enough, even a bowl of Jello will behave as a nearly perfect rigid body."

We should, thus, aim for a control frequency Ω_c sufficiently below the lowest modal frequency of the solar panels - so as to not excite the structure significantly - but, at the same time, high enough, so that the speed of response of the vehicle is adequate. The lowest

modal frequency of the panels was given in Section 2 as f_L=0.065226 Hz (0.409827 rad/s, with a period T=15.33 seconds). We will select for Ω_c a frequency 10 to 20 times lower than f_L, i.e., somewhere between 0.0065 and 0.0032 Hz, let us say

$$\Omega_c = 0.004 \text{ Hz} = 0.025 \text{ rad/s} \qquad (T = 250 \text{ seconds}),$$

which is 16 times (4 octaves) below the lowest flexible mode. Such value is considered to be sufficiently below f_L to satisfy the above principle and, yet, high enough to provide adequate response times to meet performance requirements. The adequacy of this choice (on both counts) can be appreciated by examining the A/C performance plots given in subsection 5.4.

The attitude control scheme to be considered here is a "rate-plus-position error" type controller as shown in Figure 5-6. The controller commands the SRW's to apply a torque T_c on the vehicle which is proportional to the weighted sum of the vehicle rate and its position error

$$T_c = - K((\theta_s - \theta_c) + K_{rp}\hat{\omega})$$

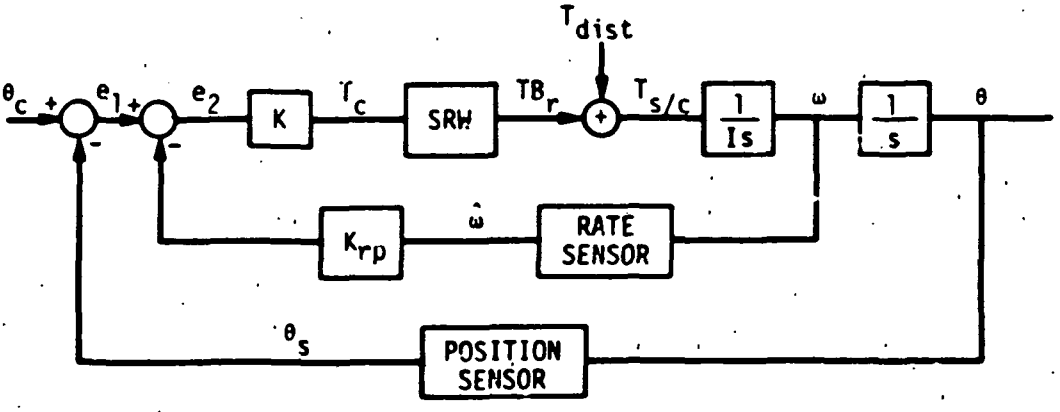

Figure 5-6. A/C loop using "rate + position error" controller

where,

θ_c = position command

θ = vehicle position

θ_s = vehicle position as sensed by a position sensor (here assumed to be $\frac{1}{\tau s+1}$)

e_1 = $\theta_c - \theta_s$. Note that $-e_1$ is the position error.

e_2 = $\theta_c - \theta_s - K_{rp}\hat{\omega}$. Note that $-e_2$ is the "position error plus (weighted) rate error."

K_{rp} = "rate-to-position" gain (determines damping)

K = control gain $T_c = K\, e_2$ (determines control frequency)

T_{dist} = external disturbance torque on vehicle

I = vehicle inertia

In order to make a preliminary evaluation of the control scheme, let us make two simplifying assumptions for the moment:

a) A perfect celestial sensor (τ=0 so that $\theta_s = \theta$)

b) A perfect reaction wheel SRW(s) = 1, so that the SRW can provide a torque equal to its input T_c, whatever it might be.

Under these simplifying assumptions, the closed loop transfer function of Figure 5-6 (with $T_{dist} = 0$ and $\hat{\omega} = \omega$) is given by

$$\frac{\theta(s)}{\theta_c(s)} = \frac{K/I}{s(s + K_{rp}K/I) + K/I} \qquad (5\text{-}6)$$

that is, a simple second order system with characteristic polynomial

$$s^2 + 2\xi\omega_n s + \omega_n^2 = 0 \qquad (5\text{-}7a)$$

where

$$\omega_n = \sqrt{\frac{K}{I}} \quad (= \Omega_c) \qquad (5\text{-}7b)$$

$$\xi = \frac{1}{2} K_{rp}\, \omega_n \qquad (5\text{-}7c)$$

so that a suitable controller can be designed by choice of K and K_{rp}.

In practice, however, SRW(s) is not a "straight wire" but contributes its own non-linear dynamics to the system. Such dynamics are studied next.

5.3.1 Design of SRW Torque Controller

We will begin by designing the SRW Torque Controller, i.e., the controller that takes the desired torque T_c as its input and generates a torque TB_r on the vehicle which is reasonably close to T_c. A method to accomplish this is shown in Figure 5-7. It uses an integrator followed by an accurate speed control loop for the wheel.

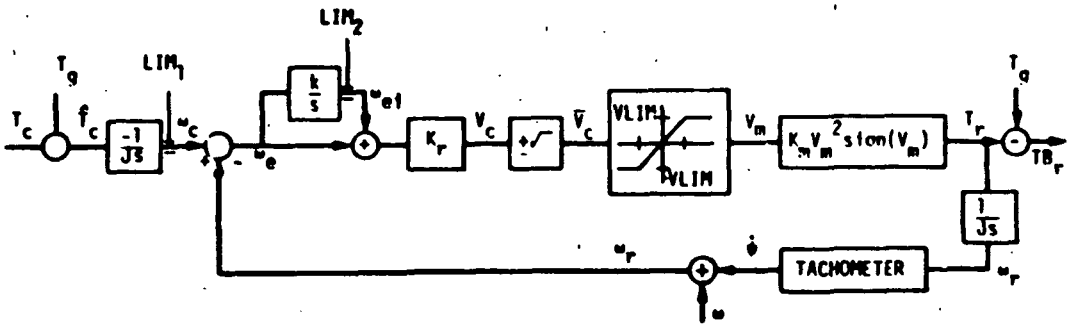

Figure 5-7. SRW torque control loop

The torque command is first converted to a SRW speed command ω_c by integrating $-\hat{T}_c/J$ with a limited integrator. The difference between the commanded and the actual (inertial) speeds is fed through a compensator $K_r(1+k/s)$ to produce a voltage to be applied to the motor. The square root of this voltage is put through a $\pm$ 30 V limiter (protection to the motor) and then applied to the motor. The tachometer output plus the bus gyro rate are added to obtain the SRW inertial spin rate which completes the loop. The square root block included in this loop has the purpose of cancelling the nonlinear square characteristics of the motor. Note that the scheme attempts to compensate for the disturbance-like effects of the gyroscopic torques T_g by commanding, not the "desired" torque T_c, but $\hat{T}_c = T_c + T_g$ into the loop. This causes T_r to track $-\hat{T}_c$, and TB_r to track T_c proper.

There are two "limited integrators" included in the SRW loop. A limited integrator is a device which acts as normal integrator until its state (output) reaches a preset limit (LIM) at which point

it stops accumulating. Its output stays saturated at LIM until the input changes polarity, causing the integrator to come out of saturation instantly.

The first limited integrator in the loop is the one which generates the RW speed command and is limited to $\pm$ LIM$_1$ = $\pm$ 230.38 rad/s (2200 rpm) to avoid generating speed commands greater than the capability of the SRW, and to avoid the lag problem that would occur if such greater commands were generated.

The second limited integrator is in the feedforward path of the compensator. This feedforward path is included so that two problems are taken care of

a) Maintain SRW speed in spite of its frictional forces.
b) Maintain a non-zero accelerating voltage input to the SRW to compensate for external disturbance torques on the vehicle, without the need for a steady state error.

The integrator is limited also to avoid lag problems. Its limit $\pm$ LIM$_2$ will be set so that the output of the saturated integrator will never command more than 30 V at $\bar{V}_c$ (Figure 5-7) i.e.,

$$LIM_2 \times K_r \leq 30 \text{ volts.}$$

This implies

$$|LIM_2| \leq 27.447 \text{ rad/s.}$$

In this study it will be assumed that the vehicle rate sensor (rate estimator or gyro) of Figure 5-6 provides a perfect measurement of the bus rate ω, and that the tachometer provides an exact measurement of the SRW speed $\dot{\psi}$. Then, for the non-saturating region of operation ($|V_c| \leq 30$ volts, $|\omega_c| \leq 230.38$ and $|\omega_{ei}| \leq 27.447$ rad/s), the SRW torque controller can be simplified to that shown in Figure 5-8.

The transfer function of the SRW Torque Controller is given by

$$SRW(s) = \frac{TB_r(s)}{T_c(s)} = \frac{\bar{K}(s+k)}{s^2 + \bar{K}(s+k)}, \quad \bar{K} = \frac{K_r K_m}{J} \qquad (5\text{-}8)$$

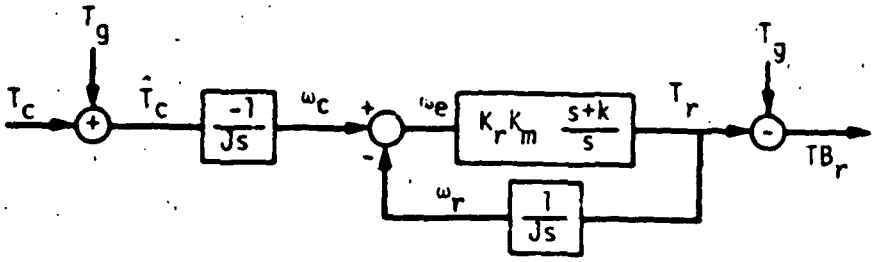

Figure 5-8. Simplified SRW torque controller for non-saturating region

Note that we can place the poles of the SRW loop anywhere we wish by choice of gains K_r and k

$$\phi(s) = s^2 + \frac{K_r K_m}{J}(s+k) = s^2 + 2\bar{\xi}\bar{\omega}_n s + \bar{\omega}_n^2 , \qquad (5\text{-}9a)$$

which implies

$$\bar{\omega}_n^2 = \frac{k\, K_r K_m}{J} , \quad \bar{\xi} = \frac{1}{2}\frac{\bar{\omega}_n}{k} , \qquad (5\text{-}9b)$$

$$K_r = 2\bar{\xi}\bar{\omega}_n \frac{J}{K_m} , \quad k = \frac{\bar{\omega}_n}{2\bar{\xi}} , \qquad (5\text{-}9c)$$

Note that the zero is automatically fixed at $-k$. Also note that $\bar{K} = 2\bar{\xi}\bar{\omega}_n$. By trial and error it was determined that a good choice for the SRW loop parameters is

$$\bar{\omega}_n = 0.06 \text{ rad/s} \quad \text{and} \quad \bar{\xi} = 1$$

That is, a critically damped SRW loop with $\bar{\omega}_n$ about 2.4 times faster than the control frequency $\Omega_c = 0.025$ rad/s. This choice results in

$$k = \frac{\bar{\omega}_n}{2\bar{\xi}} = 0.03$$

$$K_r = 2\bar{\xi}\bar{\omega}_n \frac{J}{K_m} = 32.7990066 \text{ volts/rad/s}$$

where we have used $J = 0.0868117$ kg m^2 and $K_m = 0.3177\ 10^{-3}$ N-m/V^2. This completes the design of the SRW Torque Controller.

5.3.2 Design of Rate + Position Error Controller

Incorporating the SRW Torque Controller transfer function given by equation 5-8 into the block diagram of Figure 5-6, we obtain the linearized A/C loop as shown in Figure 5-9.

The open loop transfer function for the inner loop is

$$G_1(s)\, H_1(s) = \frac{K\, K_{rp}}{I}\, \frac{\bar{K}(s+k)}{s(s^2 + \bar{K}(s+k))} \qquad (5\text{-}10)$$

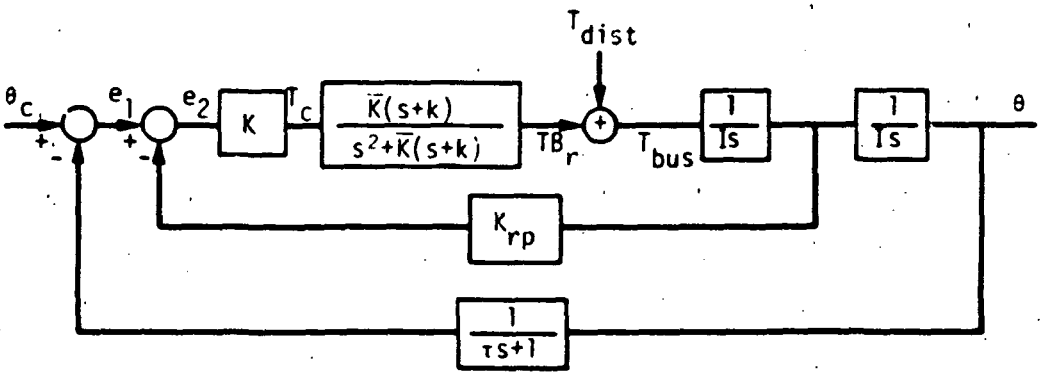

Figure 5-9. Linearized A/C loop

The corresponding root locus is shown in Figure 5-10 (calibrated in terms of the dc-gain

$$K_{dc} = \frac{K\, K_{rp}}{I}\, \frac{\bar{K}\, k}{\bar{K}\, k} = \frac{K\, K_{rp}}{I} \quad . \qquad (5\text{-}11)$$

Selecting $K_{dc} = 0.03$ yields

$$K\, K_{rp} = 0.03\, I \, , \qquad (5\text{-}12)$$

and inner closed loop poles at

$p_1 = -0.021307$ and $-0.04947 \pm 0.05165j$ ($\zeta_1 = 0.6917$, $\omega_1 = 0.071519$),

with an inner loop transfer function

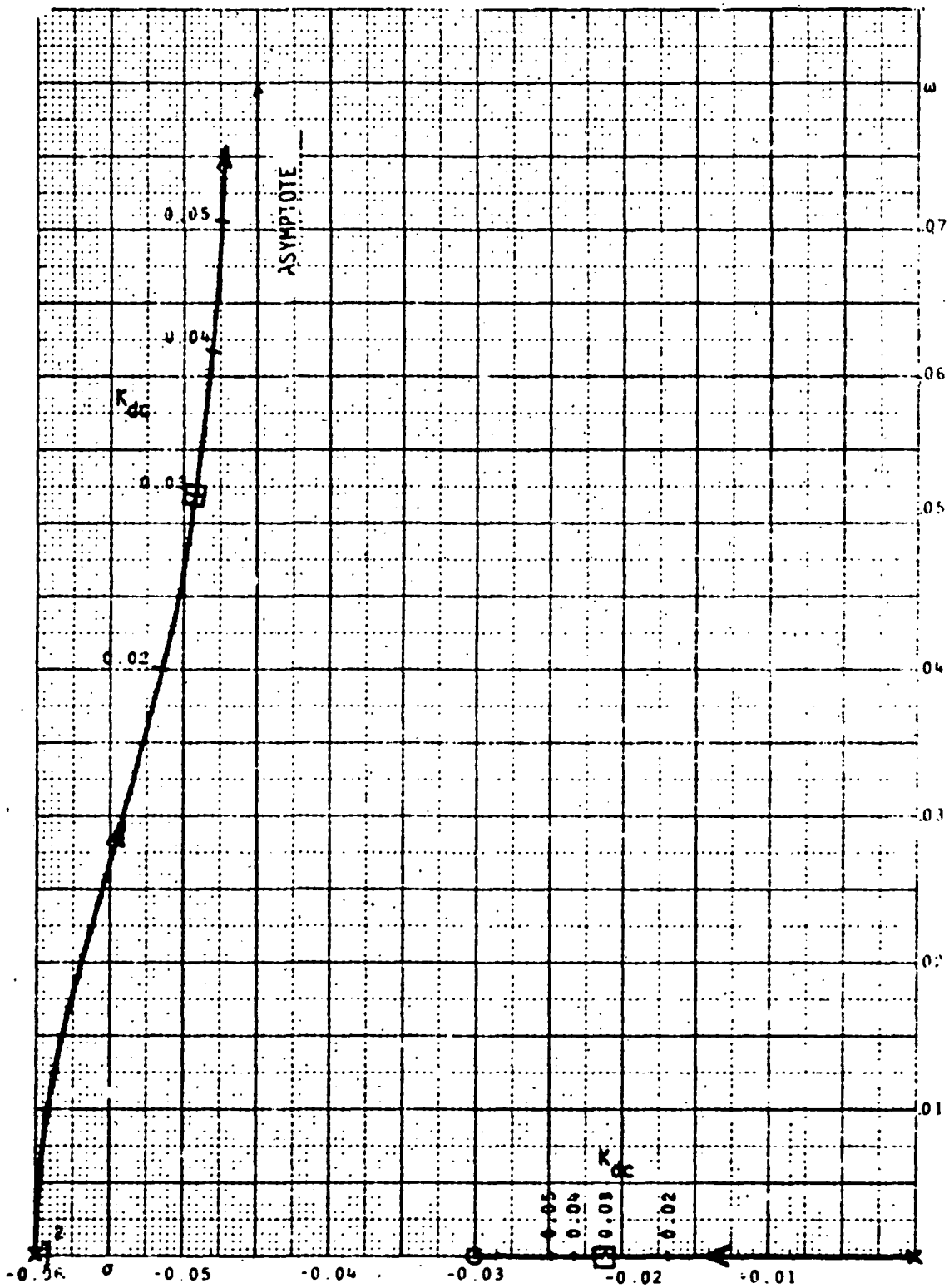

Figure 5-10. Root locus for inner loop

$$\frac{\omega(s)}{e_1(s)} = \frac{\frac{K}{I}\bar{K}(s+k)}{(s + 0.0211307)(s^2 + 2\xi_1\omega_1 s + \omega_1{}^2)} \qquad (5\text{-}13)$$

Note that the inner (rate) loop only determines the product of the gains $K\,K_{rp}$ (which is appropriate, since $K\,K_{rp}$ can be viewed as a "rate to torque" gain).

The outer (position) loop is shown in Figure 5-11.

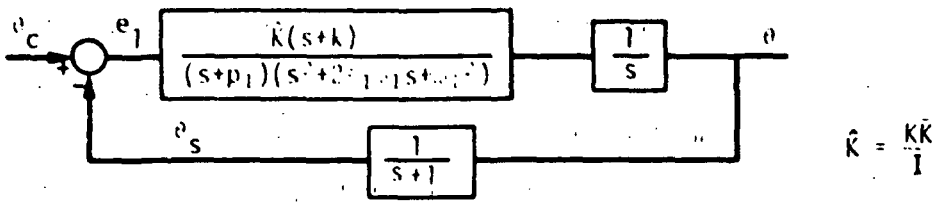

Figure 5-11. Outer loop

The root locus of this system is shown in Figure 5-12 calibrated in terms of the dc-gain

$$\hat{K}_{dc} = \frac{K\,\bar{K}}{J}\,\frac{k}{p_1\omega_1{}^2} \qquad (5\text{-}14)$$

Selecting our operating point at $\hat{K}_{dc} = 0.02$ yields a dominant pole pair (our control frequency ω_c) at

$$-0.0180986 \pm 0.0171644j \quad (\xi_c = 0.725,\ \omega_c = 0.02494 \text{ rad/s})$$

so we do indeed obtain a control frequency of about 0.025 rad/s as was our intent.

The other pole pair is at

$$-0.042 \pm 0.0415j \quad (\xi = 0.711,\ \omega = 0.059 \text{ rad/s})$$

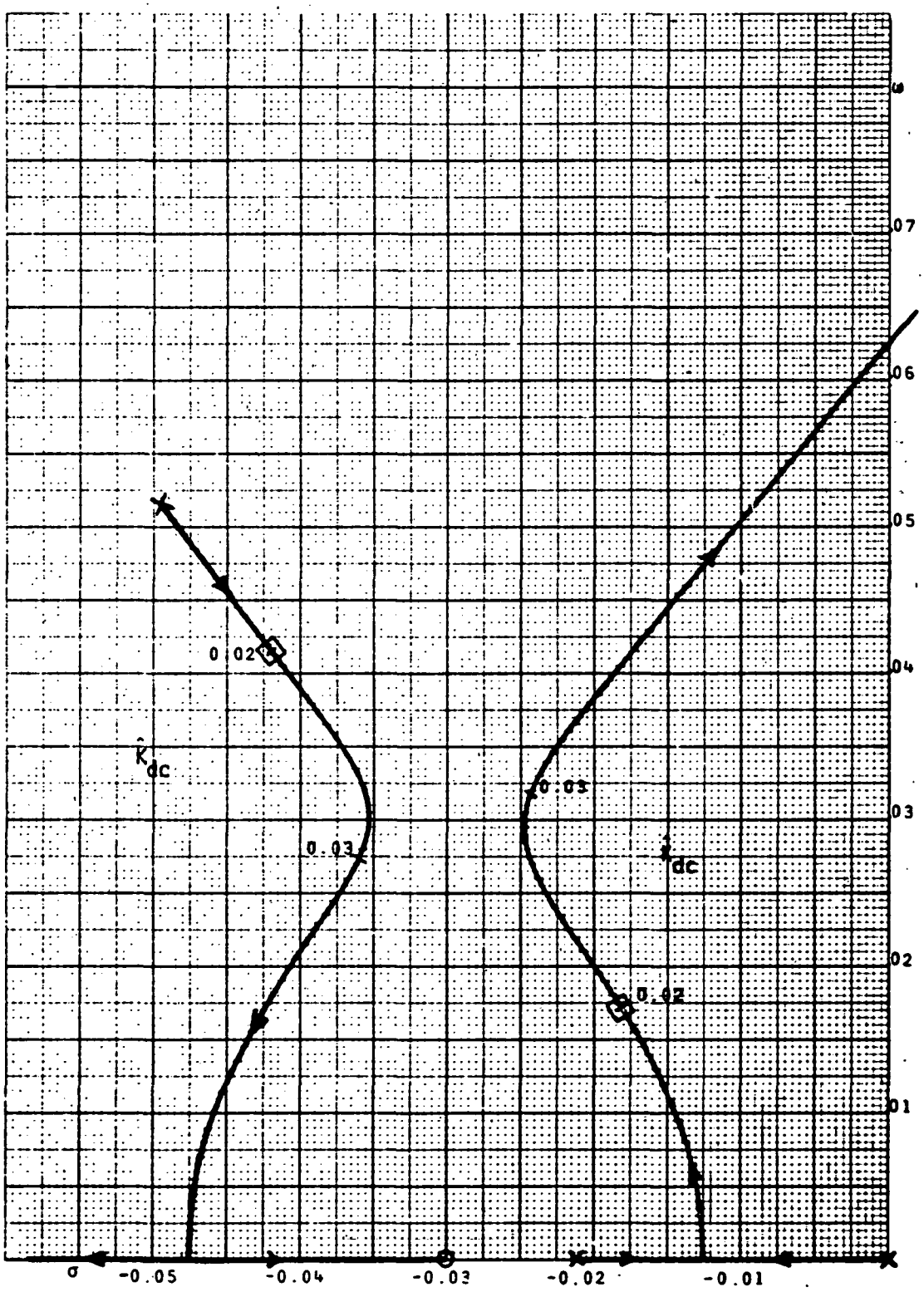

Figure 5-12. Root locus for outer loop

We can now solve for K from equation (5-14), obtaining

$$K = \hat{K}_{dc} \frac{p_1 \omega_1^2}{k \bar{K}} I = (0.02) \frac{0.0211307 \ (0.0715192)^2}{(0.03) \ (0.12)} I$$

i.e.

$$K = 6.0046333 \ 10^{-4} \ I$$

We can solve then for K_{rp} from (5-12)

$$K_{rp} = \frac{0.03I}{K} = \frac{0.03 \ I}{6.0046333 \ 10^{-4} I} = 49.961418$$

(independent of the inertia).

Thus, for $I_x = I_z = 179000$ kg m^2 and $I_y = 3500$ kg m^2 we obtain

$K_x = 107.48293$ for the X axis,

$K_y = 2.10162$ for the Y axis,

$K_z = 107.48293$ for the Z axis,

and

$$K_{rp} = 49.961418$$

for all three axes.

5.3.3 Design of Solar Array Controller

Each of the SA wings will be controlled by the simple scheme shown in Figure 5-13.

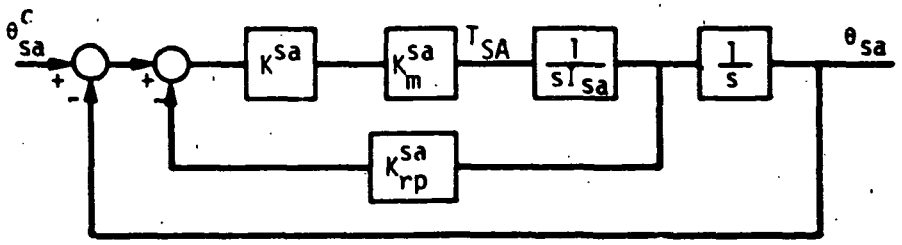

Figure 5-13. Solar array controller block diagram

The torque on each solar array wing is given by

$$T_{sa} = -\bar{K}_{sa}(\theta_{sa} - \theta_{sa}^{c} + K_{rp}^{sa}\ \omega_{sa}),$$

where

$$\bar{K}_{sa} = K^{sa}\ K_{m}^{sa}.$$

Such a system can be thought to arise for either of the following two mechanizations.

MECHANIZATION 1) An actuator drive mechanism having control gain K^{sa}, motor torque constant K_m^{sa}, and a viscous damper at the output shaft having damping constant $B = K^{sa}K_m^{sa}\ K_{rp}^{sa}$ N-m per rad/s.

MECHANIZATION 2) A rate-plus position type controller similar to the one described earlier having position-to-torque gain $\bar{K}_{sa} = K^{sa}K_m^{sa}$ and rate-to-position gain K_{rp}^{sa}. In this case the damping is provided by the control loop and no damping hardware is required; instead, it requires a measurement (or estimate) of the SA rate.

In either case, the controller results in a second order system with ω_{sa} and ξ_{sa} given by

$$\omega_{sa}^2 = \frac{\bar{K}_{sa}}{I_{sa}} \qquad \xi_{sa} = \frac{1}{2} K_{rp}^{sa}\ \omega_{sa}$$

Using $I_{sa} = 234.61$ kg m^2/wing and selecting

$$K_{sa} = 15 \text{ N-m/rad}, \qquad K_{rp}^{sa} = 5.53676 \text{ s},$$

results in

$$\omega_{sa} = 0.2528 \text{ rad/s} \quad (0.0402 \text{ Hz}, T = 24.85 \text{ s period})$$

$$\xi_{sa} = 0.7$$

This frequency was selected because of the following considerations

1) It is about 10 times faster than the vehicle control frequency Ω_c, so that the SA's and their control loops will have minimal effect on the vehicle controller.

2) It is about 1.6 times slower than the lowest modal frequency f_L (which corresponds to the first-out-of-plane bending of the solar array). However, and more importantly, it is 8.3 times slower (~3 octaves) than the frequency of the lowest torsion mode (0.3337 Hz) and, therefore, rotational excitation of the SA at ω_{sa} will result in minimal excitation of the SA structure. Because of this the SA controllers will "see" a SA which appears quite rigid.

5.3.4 System Block Diagram and Parameters

Assembling the controllers designed in the preceding pages together with the ICM Scan Platform described in Section 2, results in the attitude control system block diagram shown in Figure 5-14. The system parameters are listed in Table 5-2.

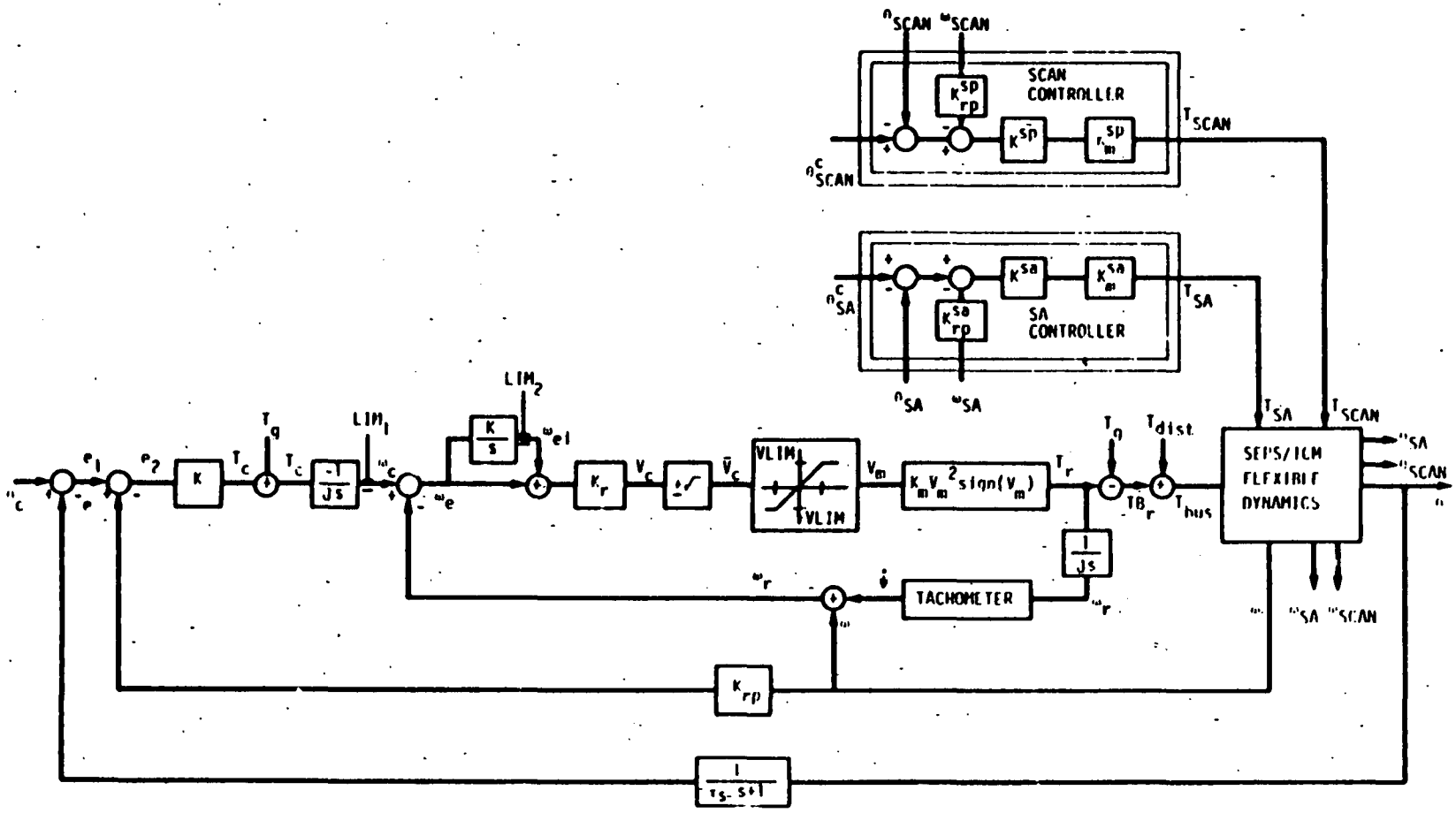

Figure 5-14. Reaction wheel control system block diagram (1 axis shown)

TABLE 5-2. REACTION WHEEL CONTROL SYSTEM PARAMETERS
(same for all axes unless otherwise indicated)

PARAMETER	VALUE	UNITS	DESCRIPTION
I. RATE + POSITION CONTROLLER			
τ	1.0	s	Celestial sensor time constant
K	107.48293	N-m/rad	X-axis position-to-torque gain
	2.101620	N-m/rad	Y-axis position-to-torque gain
	107.48293	N-m/rad	Z-axis position-to-torque gain
K_{rp}	49.96142	s	Rate-to-position gain
II.. SRM TORQUE CONTROLLER			
J	$8.68117\ 10^{-2}$	$kg\text{-}m^2$	SRM inertia
LIM_1	± 230.38	rad/s	SRM speed command limit
k	0.03	s^{-1}	Feedforward integrator gain
LIM_2	± 27.447	rad/s	Feedforward integrator limit
K_r	32.79006	V-s/rad	SRM rate-to-voltage gain
V_{LIM}	± 30.0	V	Motor voltage limiter
K_m	$0.3177\ 10^{-3}$	$N\text{-}m/V^2$	Motor torque constant
III. SOLAR ARRAY AND SCAN PLATFORM CONTROLLERS			
$K^{sa}K_m^{sa}$	15.0	N-m/rad	SA position-to-torque gain
K_{rp}^{sa}	5.53676	s	SA rate-to-position gain
$K^{sp}K_m^{sp}$	1500.0	N-m/rad	Scan position-to-torque gain
K_{rp}^{sp}	0.14683	s	Scan rate-to-position gain(clock)
	0.09901	s	Scan rate-to-position gain(cone)

5.4 SRW ATTITUDE CONTROL PERFORMANCE

The performance of the SRW control system just described was evaluated through computer simulation of the four test maneuvers described in 2.4. Full details of the 30-mode flexible dynamics model, simulation programs, and assumptions can be found in Section 2.

The results of the SRW simulations are shown in figures 5-15 through 5-18, and are discussed below. The figures themselves are also captioned with pertinent explanations and commentary. The nomenclature used in these figures is given in Table 5-3.

Figures 5-15 and 5-16 show the performance for 1° pitch turn and 30° bus yaw turn, respectively. Both of these figures exhibit similar characteristics in that they both serve to illustrate the very smooth proportional control and vehicle response achievable with reaction wheels. Excitation of the flexible appendages is very small.

Figure 5-17 shows the results of the simulation for the multi-axes acquisition maneuver. The initial conditions assumed were:

Axis	Initial Position	Initial Rate	Corresponding Momentum
pitch	+1.0°	+0.005°/s	15.62 N-m-s
yaw	+2.0°	+0.250°/s	15.27 N-m-s
roll	0.0°	-0.005°/s	15.58 N-m-s

The performance plots show a marginally acceptable acquisition performance, because the initial conditions used are near the limit of the SRW momentum storage capability. This causes the wheels to speed up to (or very near to) their saturation point, where they loose their torquing ability. The 20 N-m-s momentum storage capacity of the NASA SRW limits acquisitions to conditions where the initial momentum to be absorbed is $\leq$15 N-m-s.

For the scan slewing simulation (Figure 5-18), the SRW system was commanded to maintain the vehicle attitude in its initial zero state while the scan platform was slewing. The box slew sequence

introduces high frequency disturbances into the vehicle, with yaw being the axis most affected. The control system manages to keep yaw within 165 μrad of the initial position. Note that the control system attempts to preserve the initial attitude by slowly varying, low-frequency smooth nudging of the vehicle towards null, not by trying to react to and control each individual transient caused by platform articulation.

In summary, the SRW system has been shown to provide very smooth proportional attitude control of the vehicle, with very small excitation of the vehicle flexibility. Its excellent dynamic performance is similar to the smooth TVC performance seen in Section 3. It must be remembered, however, that all reaction wheel systems are "momentum management" systems which have the limitations imposed by the momentum storage capacity (size) of the wheels; once the wheels reach their maximum speed (saturation) they become "loaded" and must be unloaded by a secondary torquing method such as TVC or a gas jet system. Thus, even though an SRW system must also have, say, a secondary RCS system, the main (and very significant) advantage of SRW system is the mass savings to be realized. This is because all zero net momentum maneuvers (not exceeding the wheel capacity) may be performed by the wheels without any propellant consumption at all. This is true for turns, as well as for scan platform slewing since the net average momentum on a long sequence of typical slews tends to zero, as the number of slews increases.

TABLE 5-3. KEY TO VARIABLE NAMES FOR FIGURES 5-15 to 5-18

ALPH1,2,3*	Angular position of the bus (b_c), rad
ANGM	System angular momentum magnitude, N-m-s
COERR1,2,3	Control error e_c, rad
COMCL, COMCN	Position commands into SA wings, rad
ERROR1,2,3	Sensed position error e, rad
ETA11 to ETA18	Panel deformation generalized coordinates (panel 1, first 8 modes)
GM1,2,3,4	Hinge rotation angles for Solar Array Panels 1,2, and Scan Clock, and Cone, respectively, rad
RATE1,2,3	Bus angular rates, rad/s
TB1,2,3	External torques about bus CM (from SRW's plus external disturbances), N-m
TDESRX,Y,Z*	Desired control torques $\bar{T}_c$, N-m
TH1,2,3,4	Hinge torques for Solar Array Panels 1,2, and Scan Clock, and Cone, respectively, rad
TRNCOM	θ_c position input (turn command), rad
TRWX,Y,Z	Torques on SRW's, N-m
VWX,Y,Z	SRW motor applied voltage, V
WRWCX,Y,Z	SRW speed command ω_c, rad/s
WRWX,Y,Z	SRW actual speed ω_r, rad/s

*1,2,3, or (equivalently) X,Y,Z, denote the pertinent axis.

FULL FLEX MODEL WITH Rwb

FIGURE 5-15

1° x TURN

a)

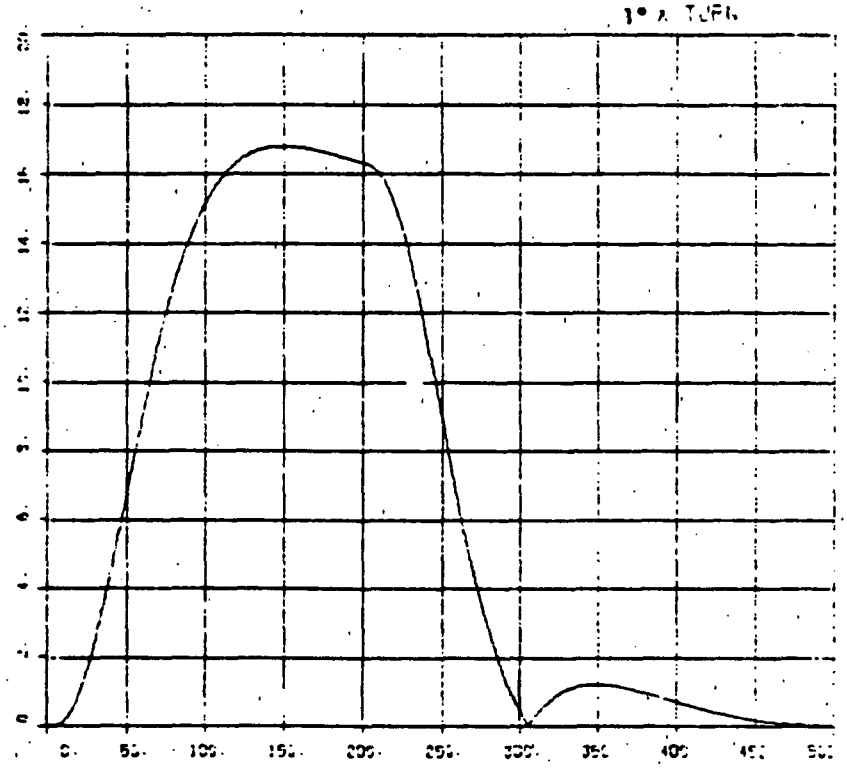

b)

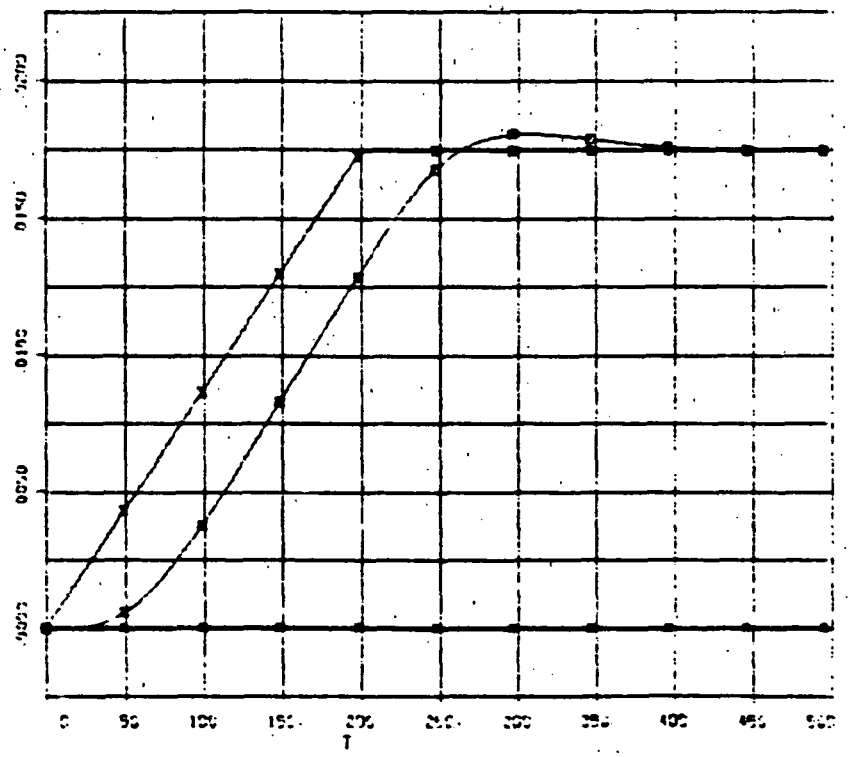

Damped smooth turn transient (ζ=0.6). Excitation of flexible structure is not noticeable.

FULL FLEX MODEL WITH RW

FIGURE 5-15
1° X TURN

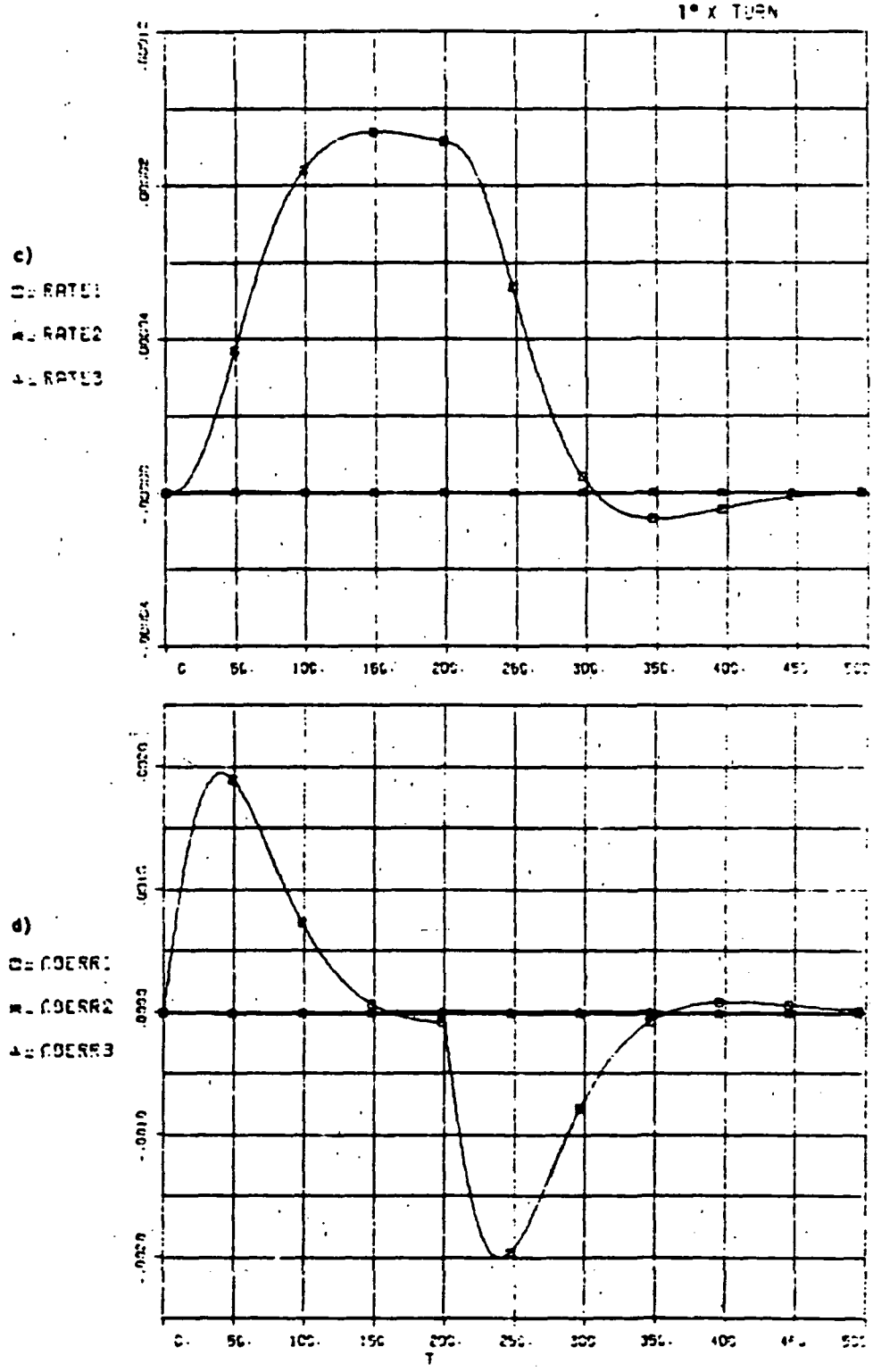

c) Pitch takes -120 s to accelerate to turn rate (0.005°/s) and holds it until turn command stop (T=200). d) Shows control error which commands the vehicle to accelerate (decelerate) at turn start (stop).

FULL FLEX MODEL WITH RW

FIGURE 5-15

1° Y TURN

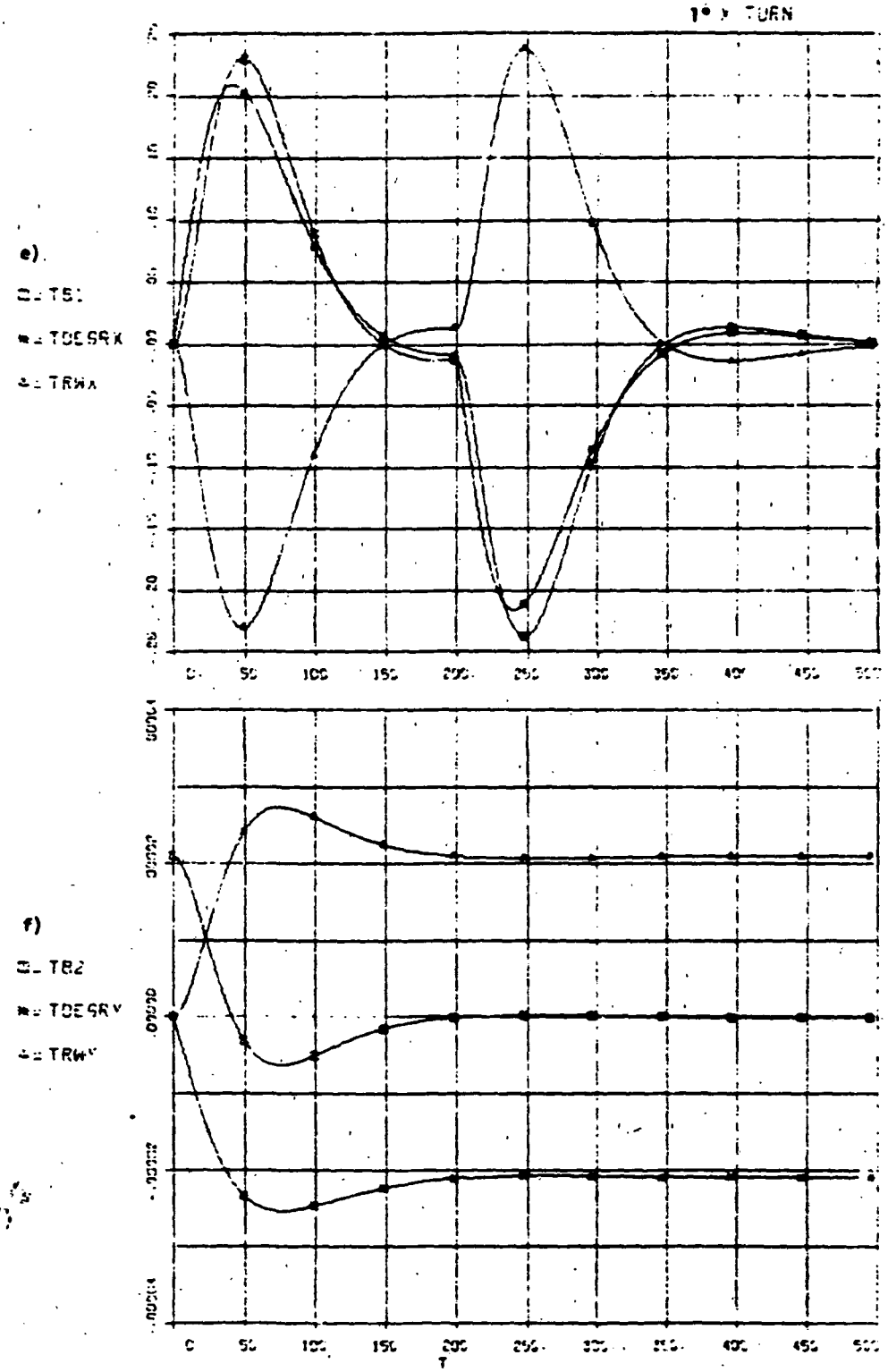

Note smooth, slowly varying torques produced by RW in above two graphs, as well as in TB3 next page. TB2 includes RW torque plus solar pressure disturbance torque of 0.209 10-4 N-m.

FIGURE 5-15

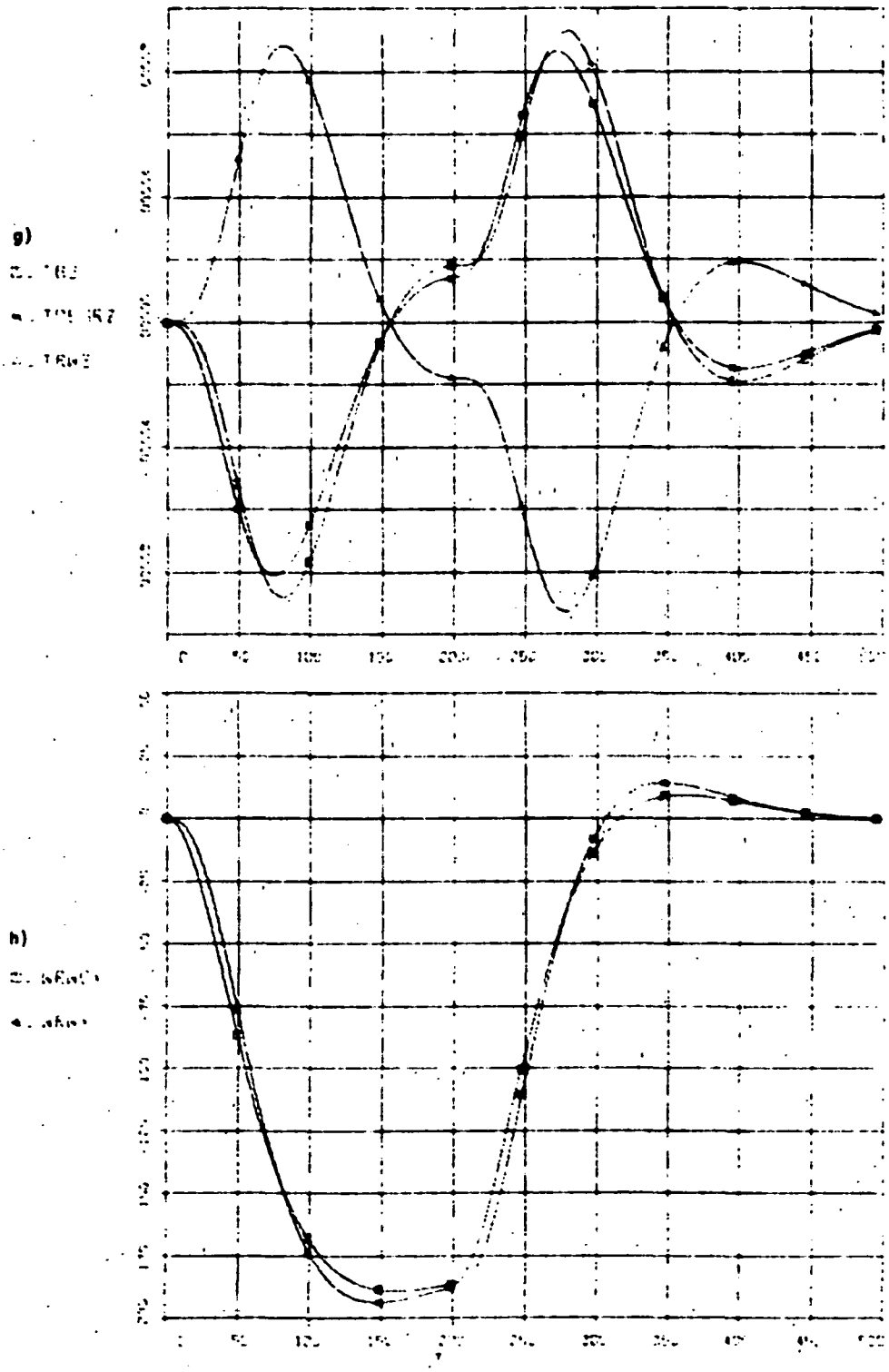

X RW tracks speed command WRWCX reaching a max of -194 r/s (1850 rpm) at t=150. Wheel returns to -0 rpm at t=500.

FIGURE 5-15

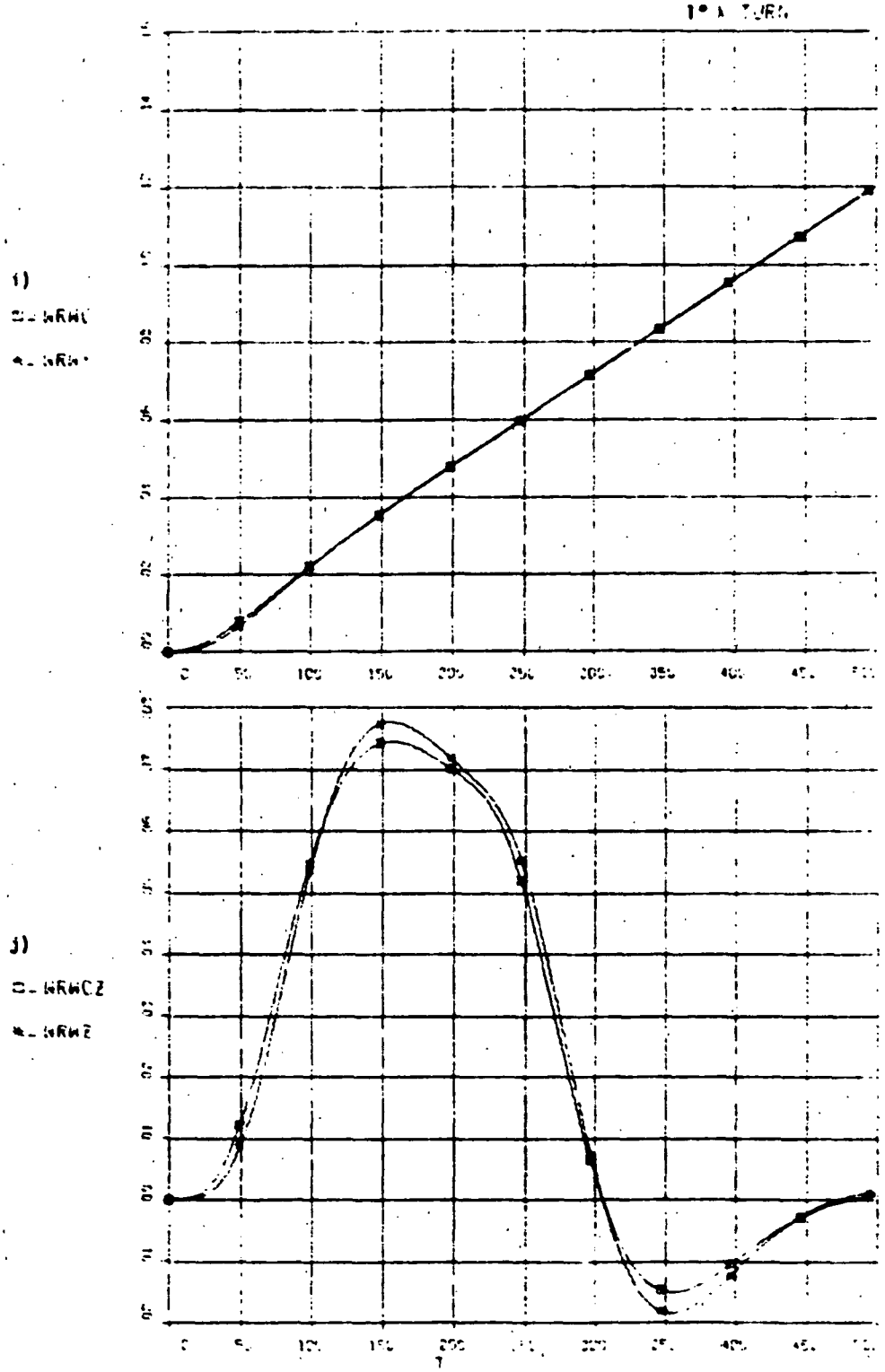

i) Y RW spinning at constant acceleration to overcome solar pressure torque. j) Z RW taking care of disturbance due to cross-coupling reaches a maximum velocity of 0.079 r/s (0.75 rpm).

FIGURE 5-15
1° x TURN

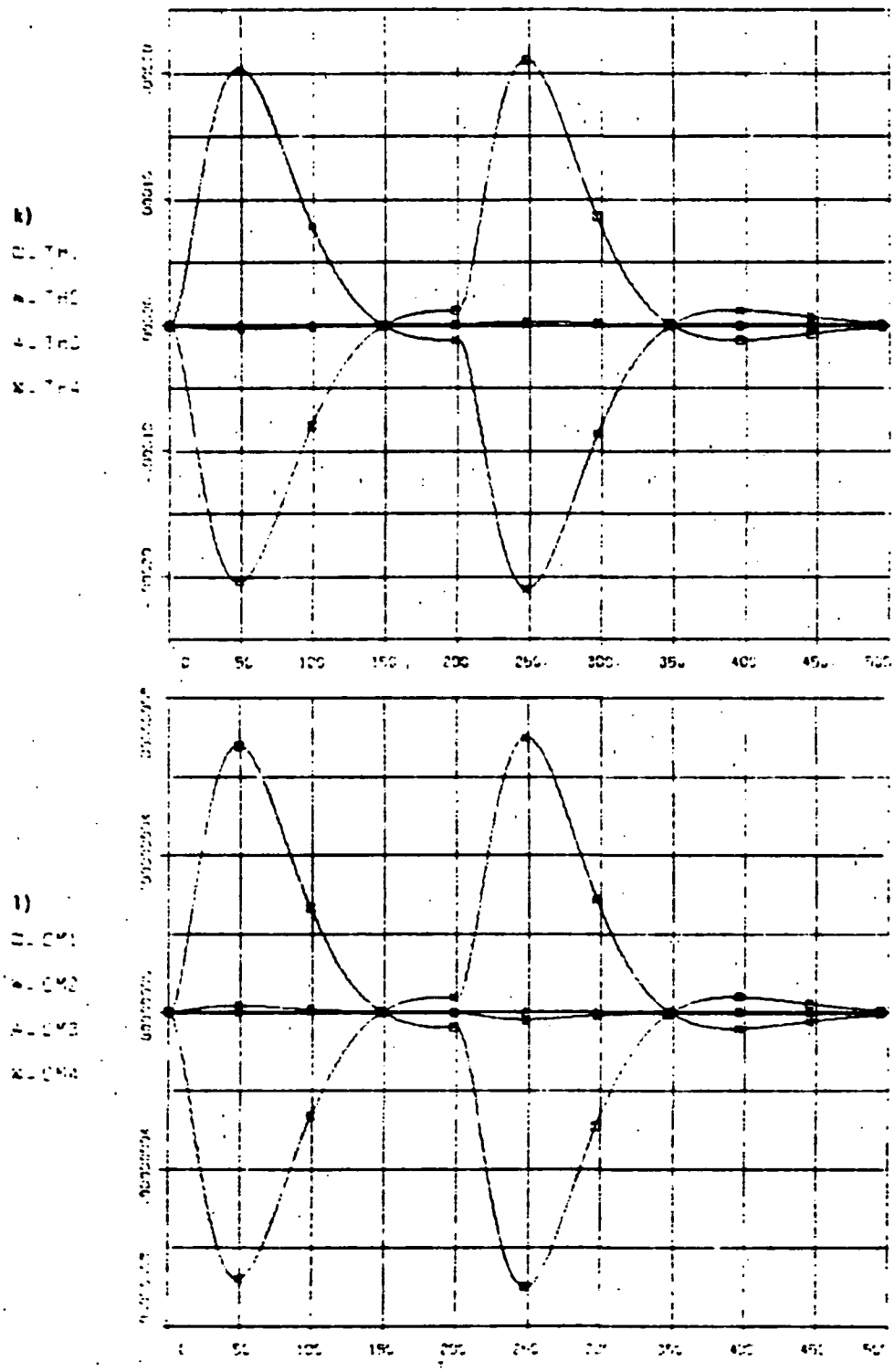

Torques and deflections at hinges (solar array and scan platform) values are negligible.

FULL FLEX MODEL WITH Rwr

FIGURE 5-15
1°X TURN

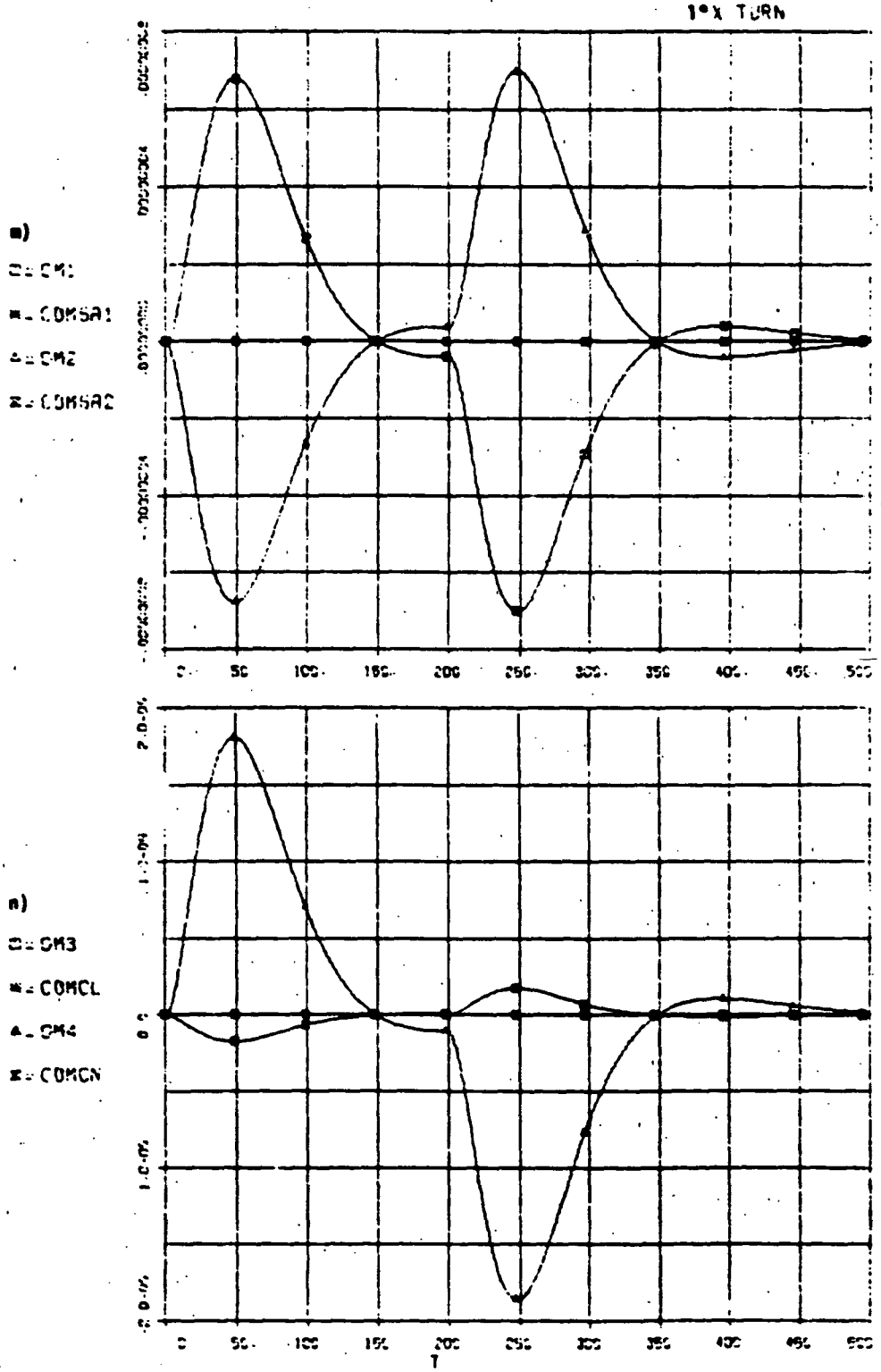

Negligible hinge deflections.

FIGURE 5-15

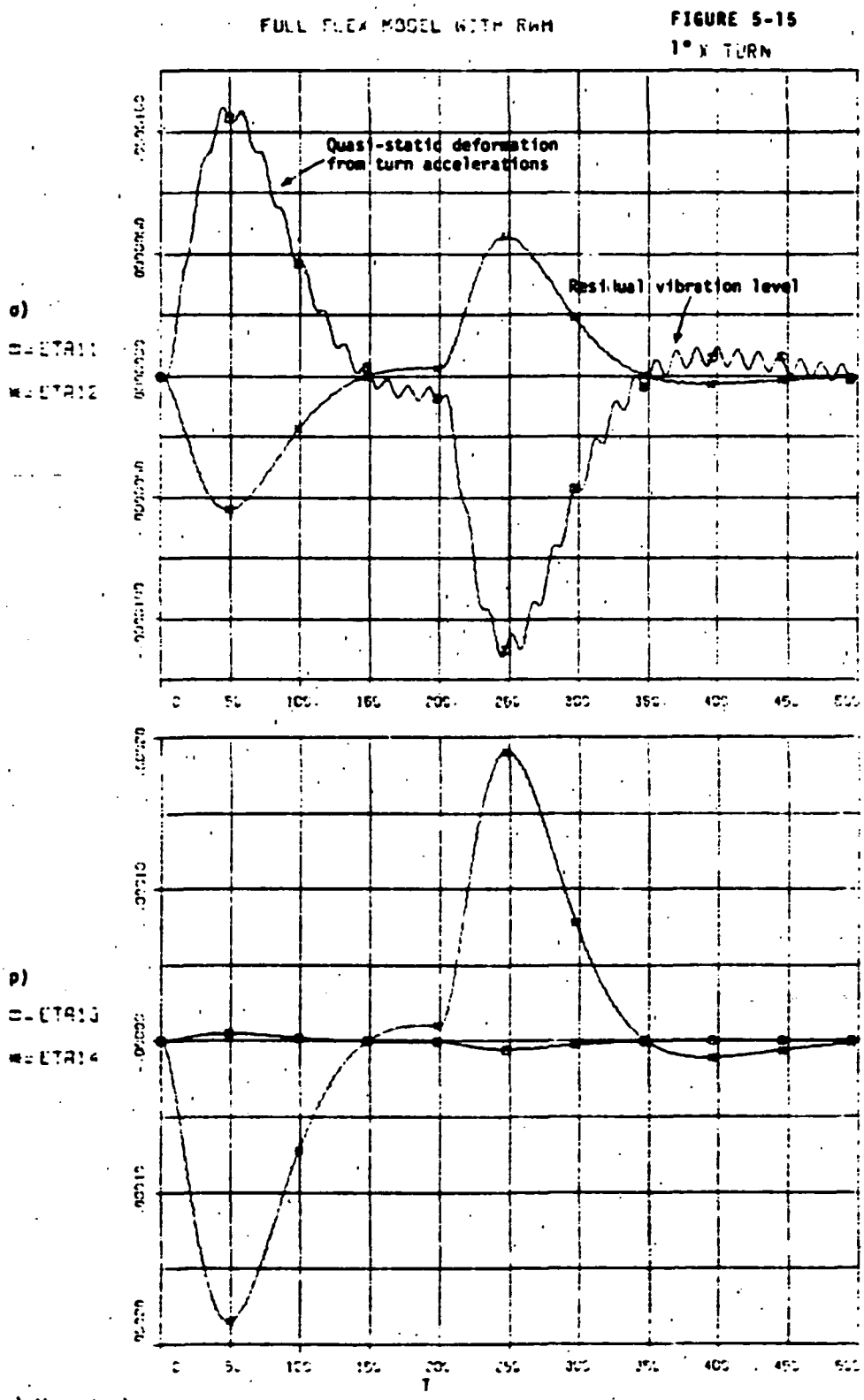

a) through r):
SA deformation generalized coordinates showing predominant (and expected) mode 4 in-plane deformation of SA, with some coupled out-of-plane motion. Note that the residual vibration levels are very small due to the smoothness of the applied torques.

FULL FLEX MODEL WITH RWH

FIGURE 5-15

1° X TURN

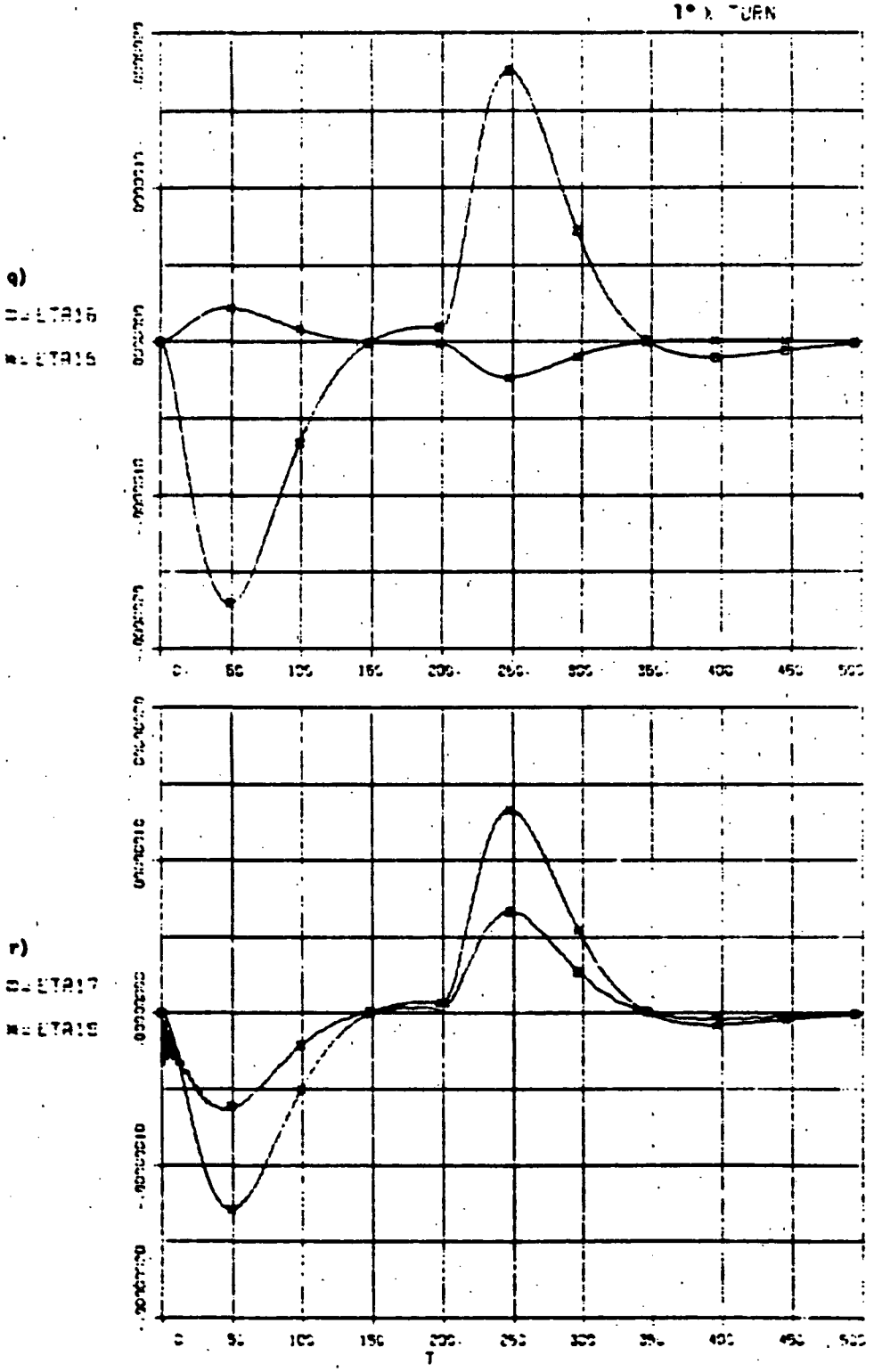

FULL FLEX MODEL WITH RHP **FIGURE 5-16**

30° SCS : TURN

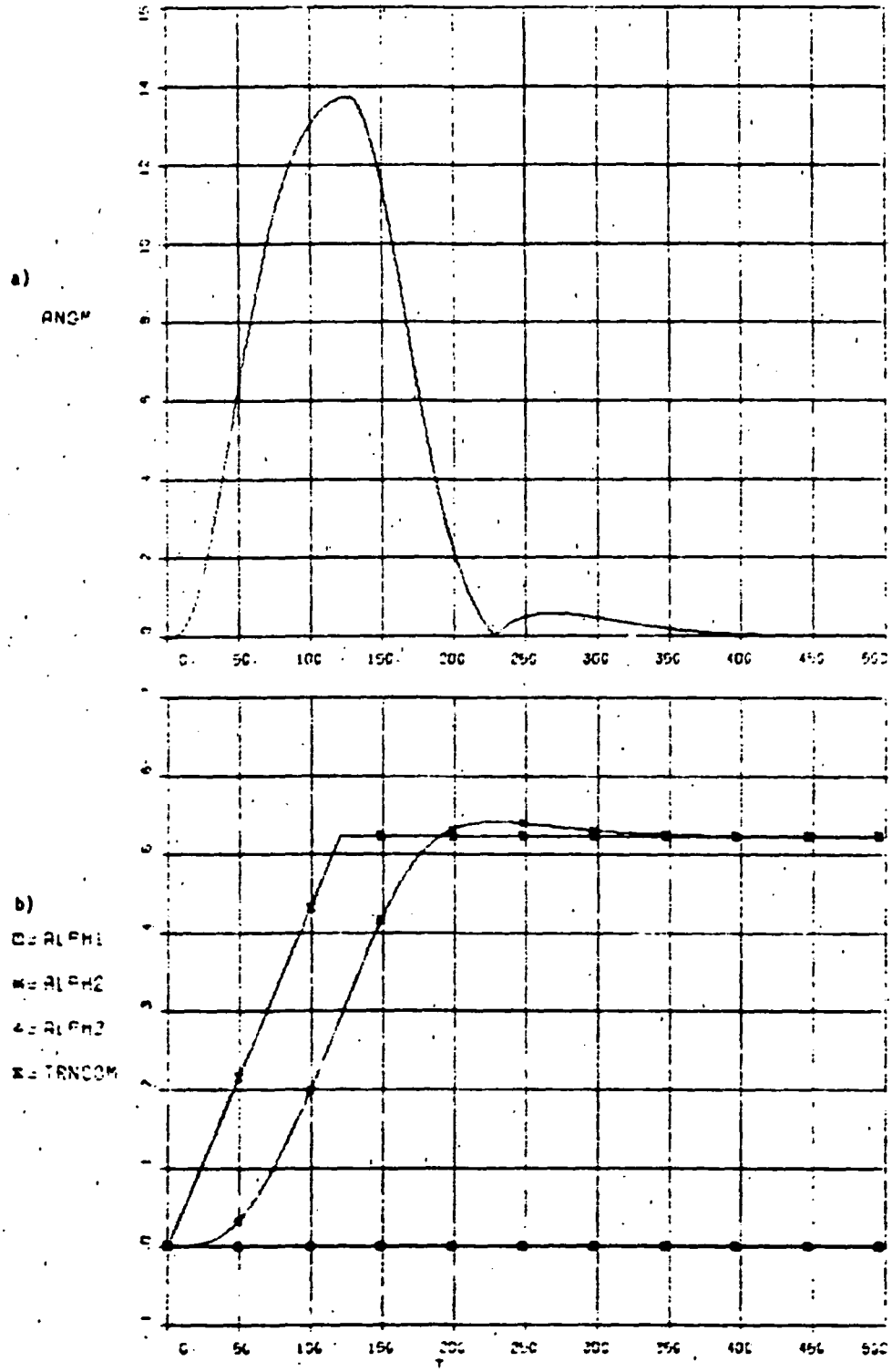

Damped smooth turn transient (ξ=0.6). Excitation of flexible structure is not noticeable.

FULL FLEX MODEL WITH RWH **FIGURE 5-16**

30°BUS : TURN

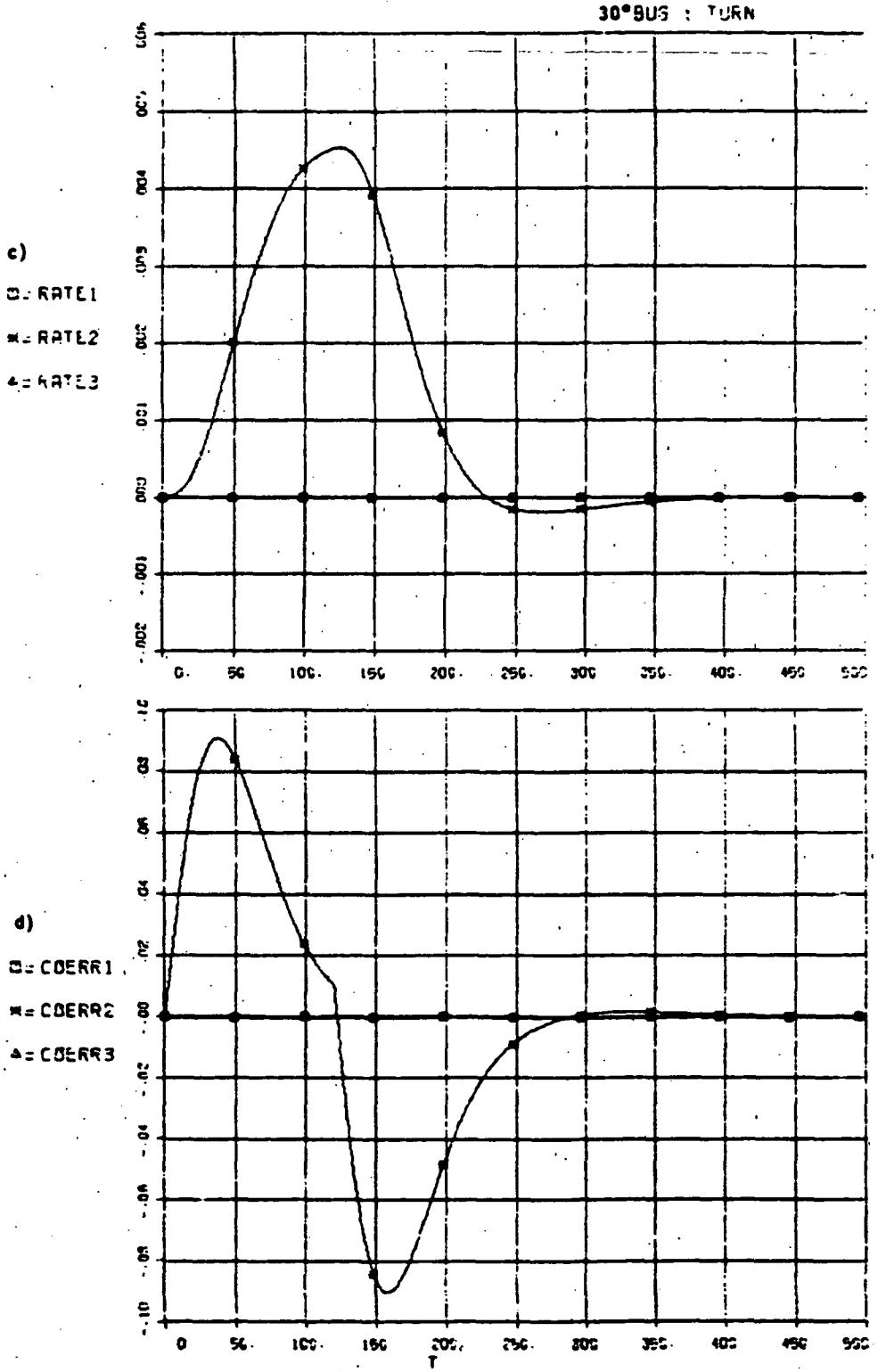

c) Yaw takes -120 s to accelerate to turn rate (0.25°/s) at which time turn is commanded to stop. It takes another 120 s for vehicle to slow down. d) Shows control error commanding the vehicle to accelerate and decelerate.

FULL FLEX MODEL WITH RWH **FIGURE 5-16**

30°SUS Y TURN

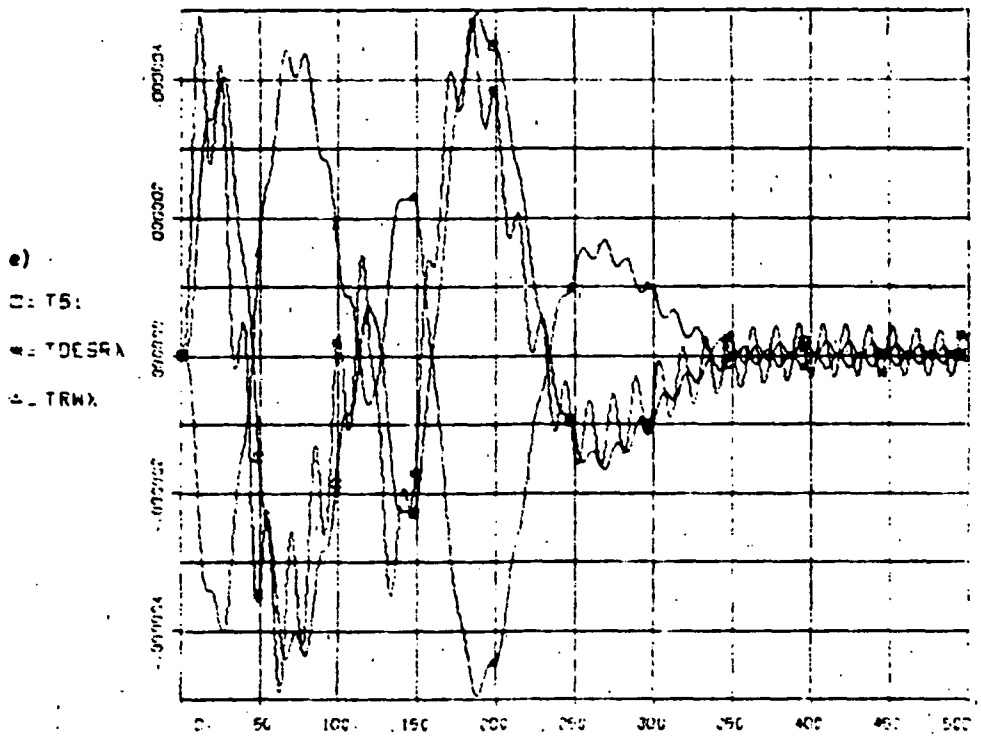

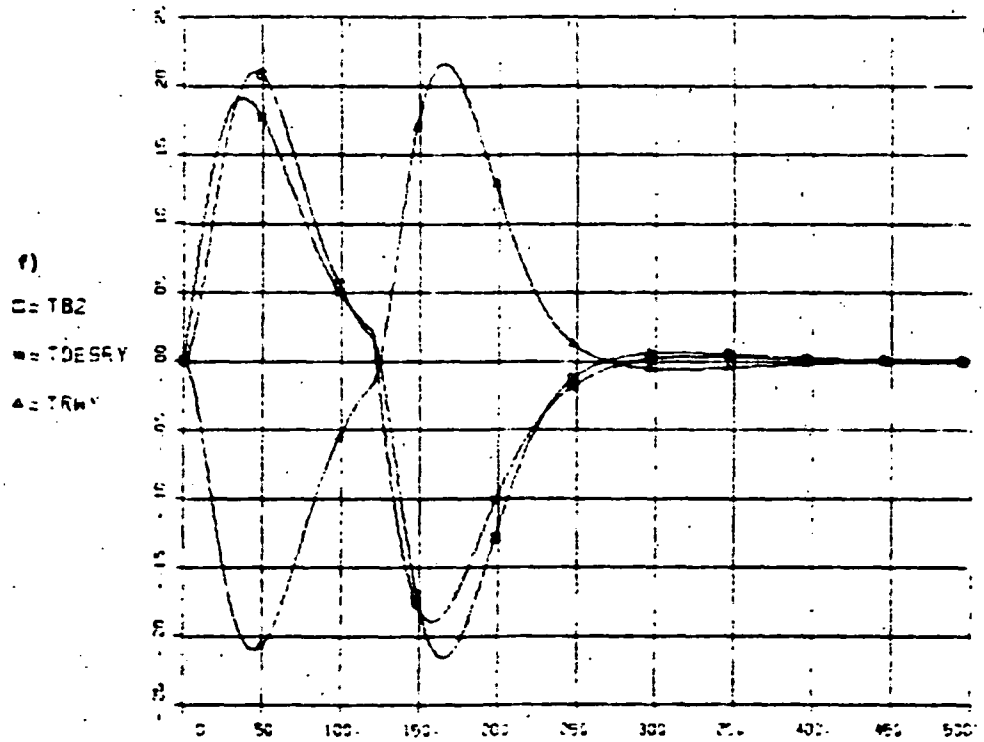

Turning torques are smooth (f). Figures e) and h) show extremely small pitch and roll torques produced by cross-coupling and panel deformation due to the yaw turn.

FULL FLEX MODEL WITH RHH **FIGURE 5-16**

30°SUS r TURN

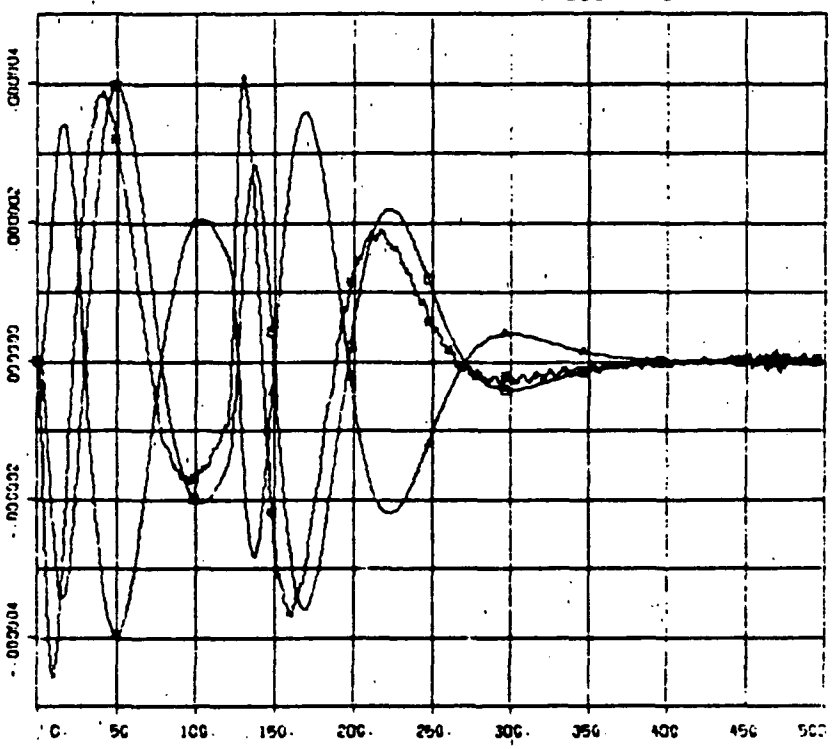

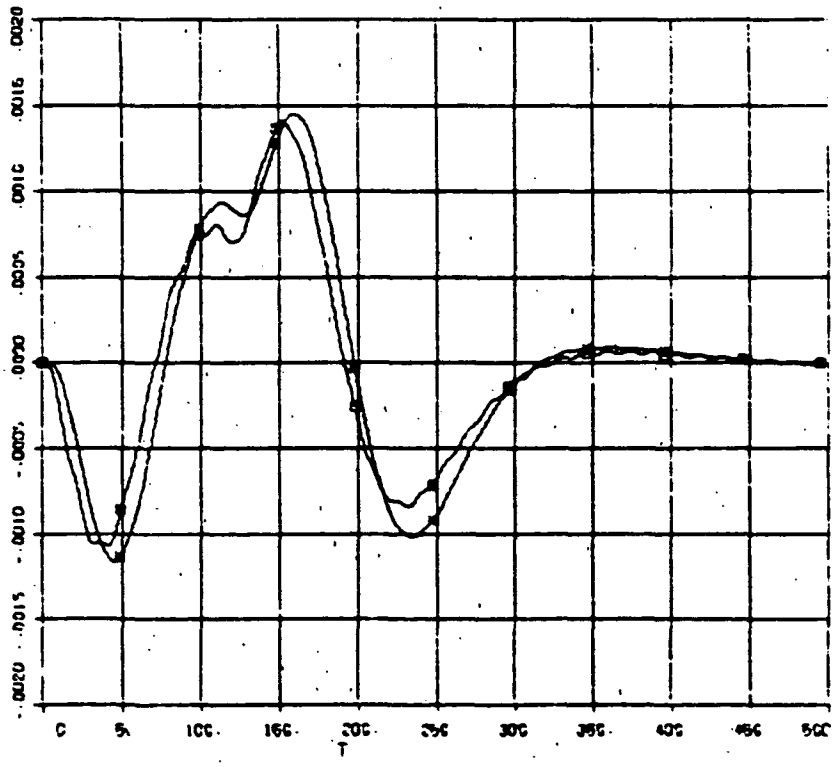

h) Negligible X RH motion at a maximum of -0.0014 r/s (0.01 rpm).

FULL FLEX MODEL WITH RWP **FIGURE 5-16**

30°BUS / TURN

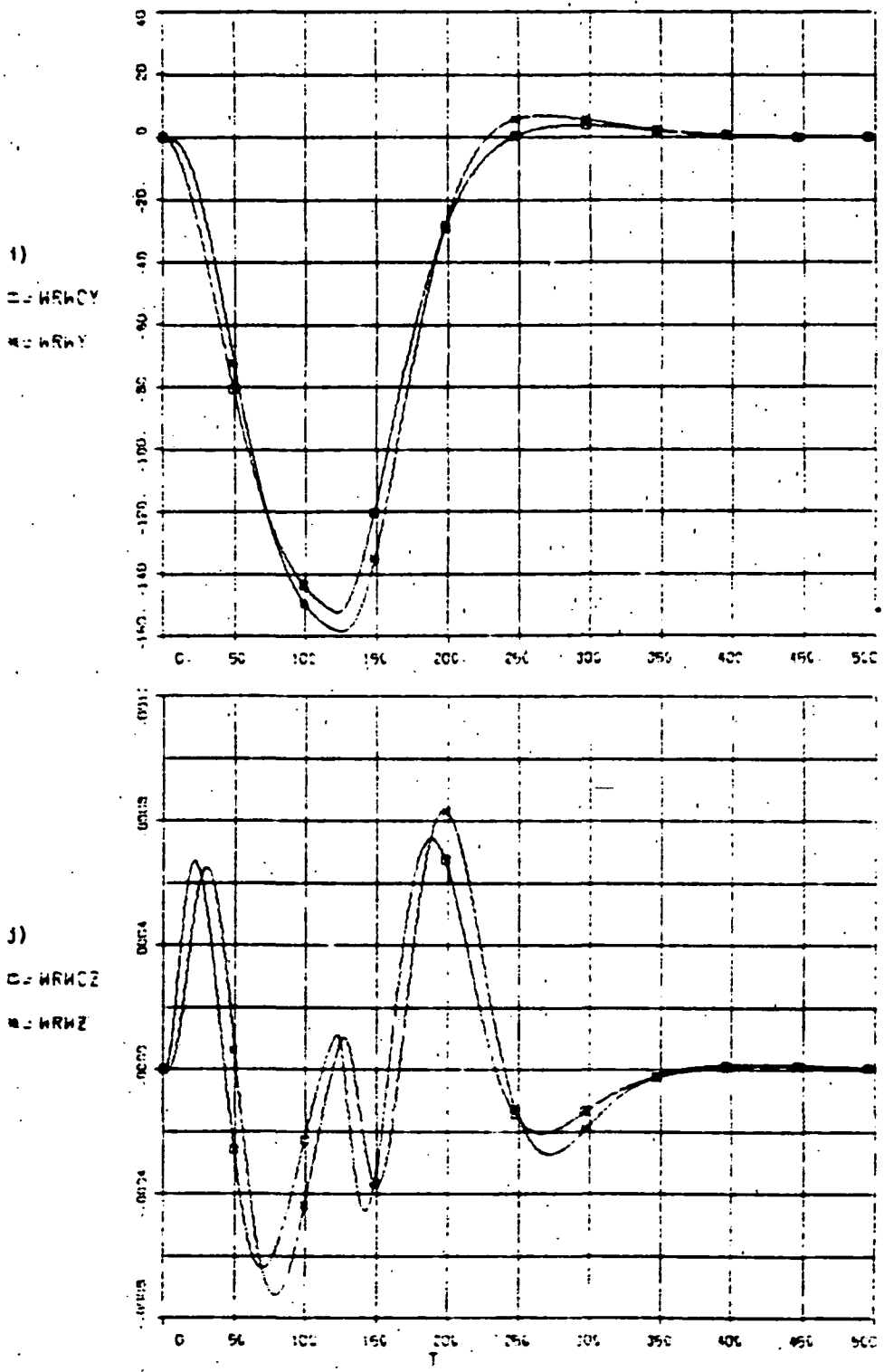

i) Y RW tracks speed command WRWCY reaching a maximum of -159 r/s (1518 rpm) at T=125 s; wheel returns to -0 rpm at t=400. j) Negligible Z RW motion at a maximum of 0.0008 r/s (0.007 rpm).

FULL FLEX MODEL WITH RWH **FIGURE 5-16**

30° SUS / TURN

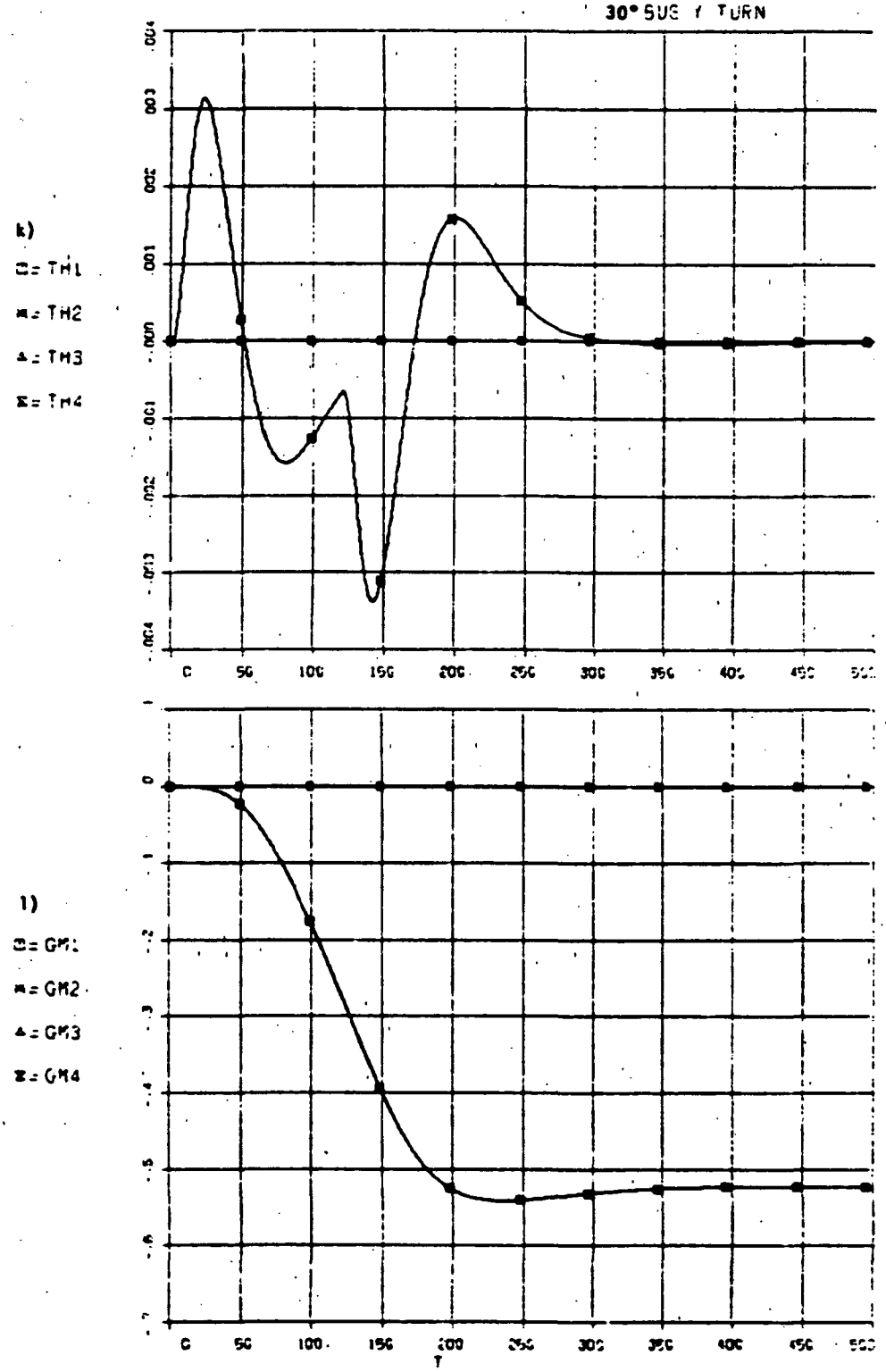

k) Small hinge torques on SA. 1) SA wings turn -30° with respect to the bus so as to stay on the sun as the bus turns.

FULL FLEX MODEL WITH RMS **FIGURE 5-16**
30° BUS Y TURN

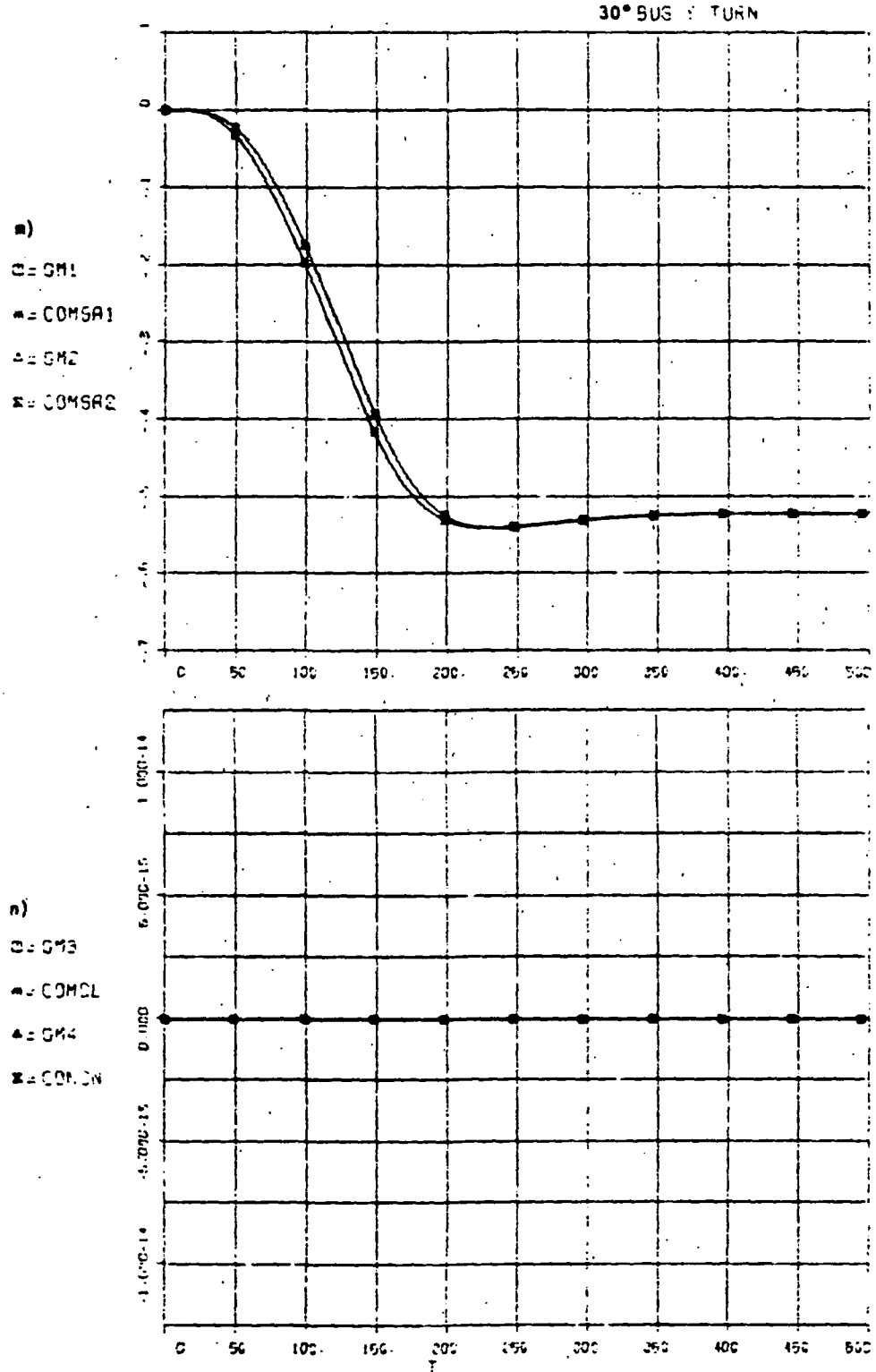

m) SA wings track their commands to -30° with respect to bus. n) Scan platform locked in place for this maneuver.

o)

□ = ETA11

✱ = ETA12

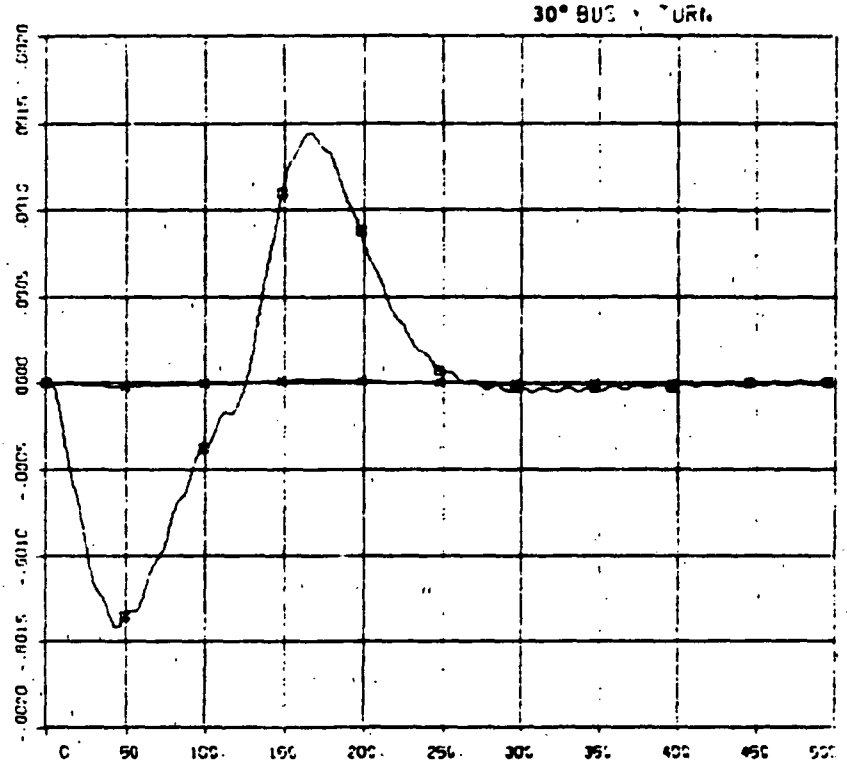

p)

□ = ETA13

✱ = ETA14

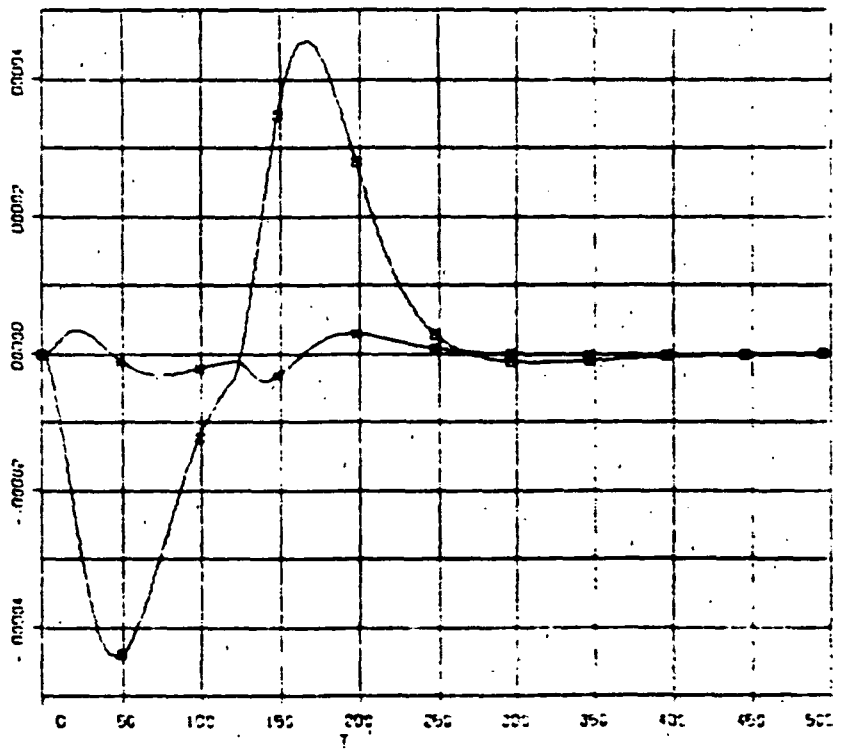

o) through r)
SA deformation generalized coordinates showing predominant mode 1 out-of-plane small deformation with some coupled in-plane and torsion. Residual vibration levels are very small due to the smoothness (low frequency) of the applied torques.

FULL FLEX MODEL WITH RW- **FIGURE 5-16**

30° BUG ✓ TURN

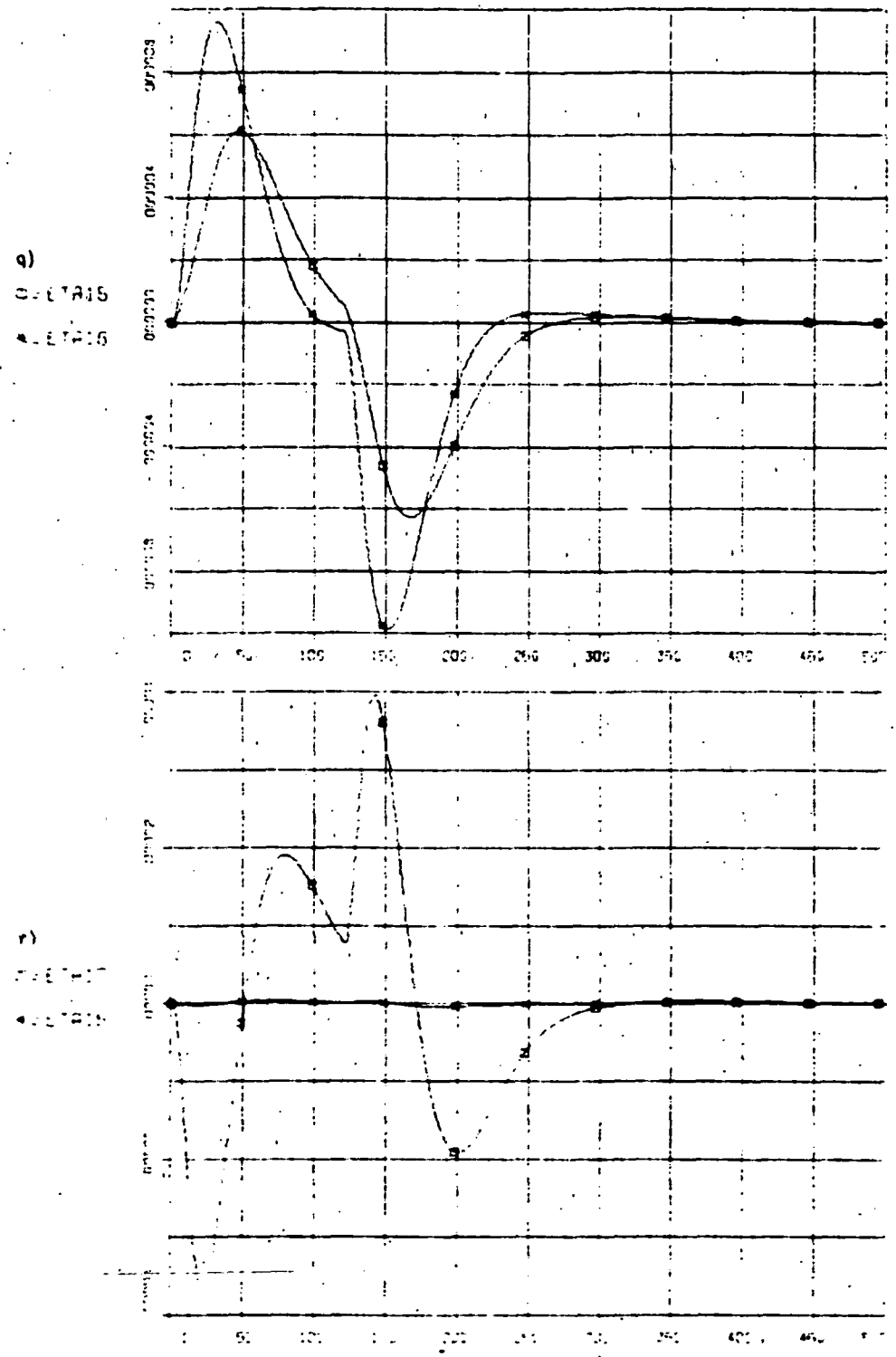

FIGURE 5-17

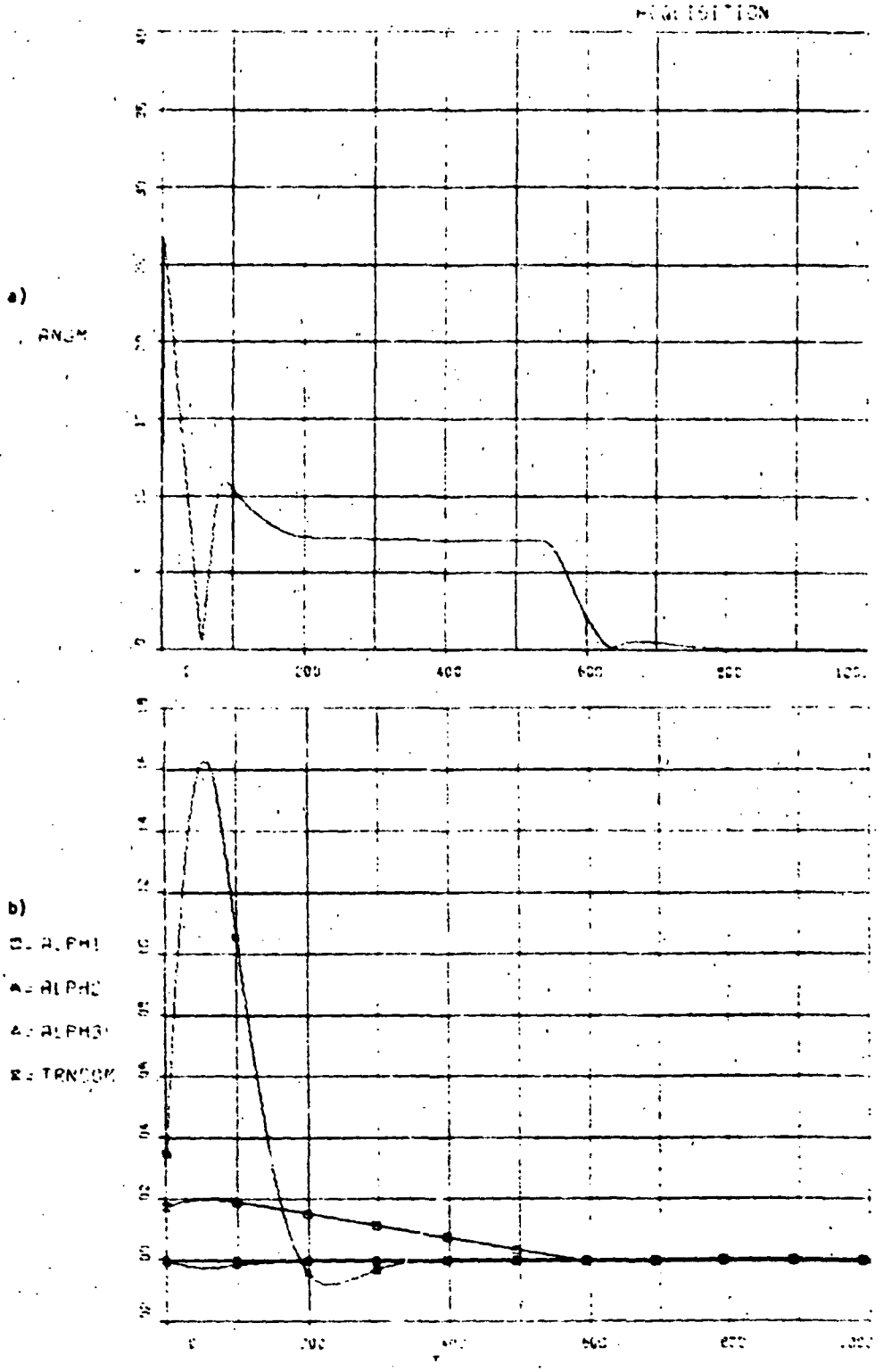

-600 seconds required for this particular set of acquisition initial conditions.

FIGURE 5-17

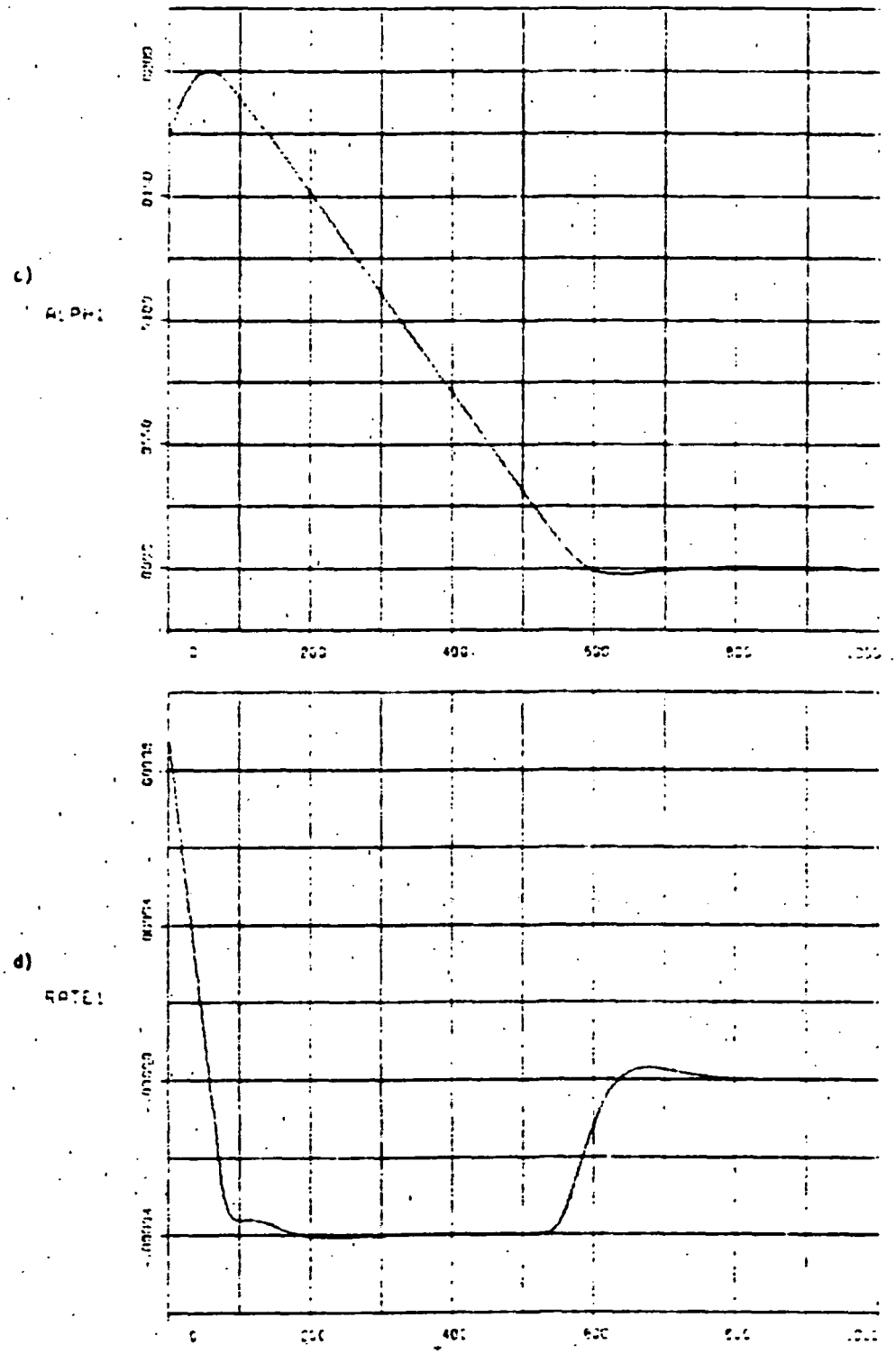

X RW stops vehicle and starts to bring it back but RW saturates at T=100, loosing its torquing capability. Vehicle coasts towards null with wheel saturated until T=530 seconds at which time control error changes sign and commands RW to decelerate, causing it to come out of saturation and regain control of vehicle. See also i), j), o) and r).

FULL FLEX MODE, with RWR

FIGURE 5-17
ACQUISITION

e)

ALPH2

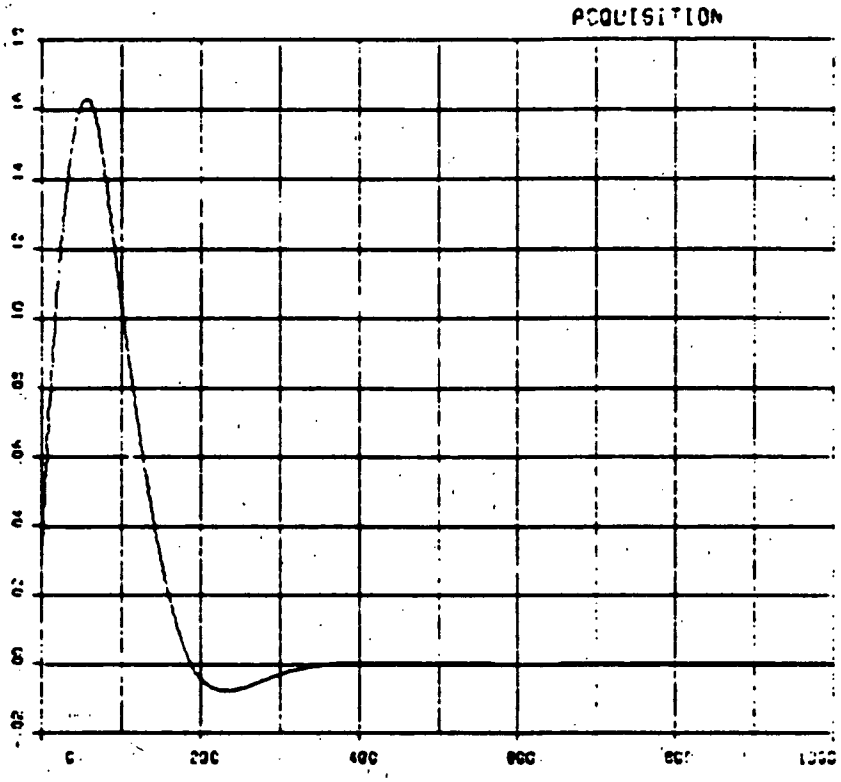

f)

RATE2

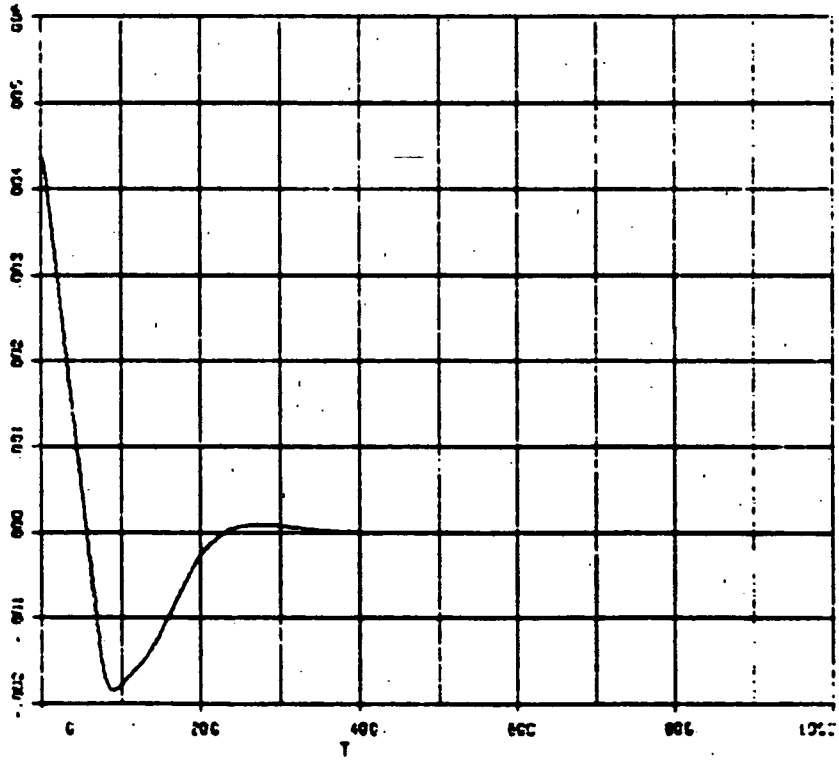

Yaw overshoots -7.4° before turning around due to low available torque. Acquisition in yaw is achieved in 350 seconds. See also h), i), p) and r).

FULL FLEX MODEL with Sh=

FIGURE 5-17
ACQUISITION

g)
ALPH3

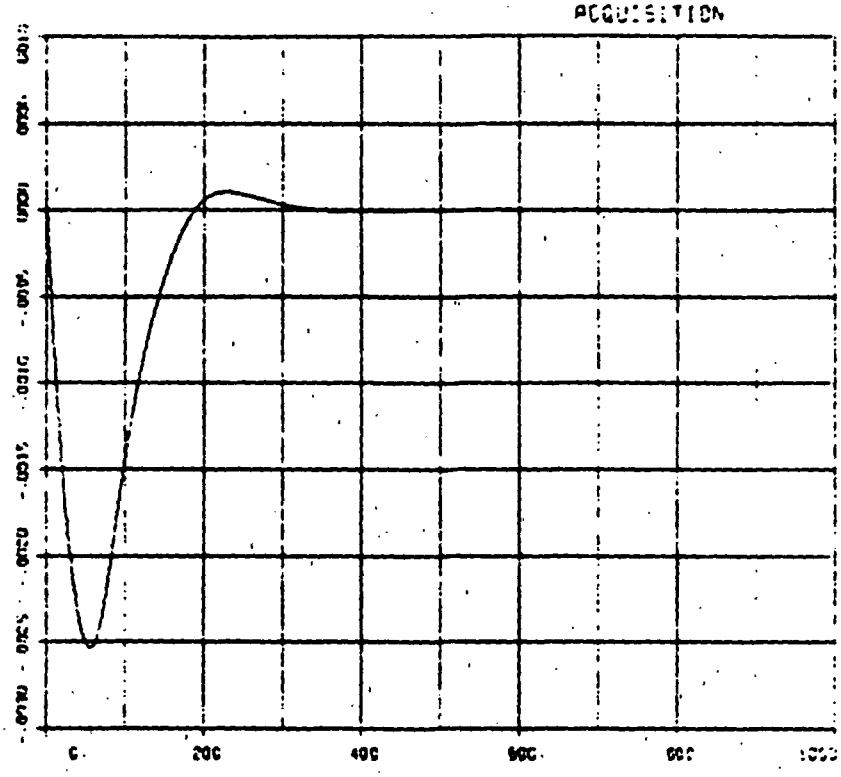

h)
RATE3

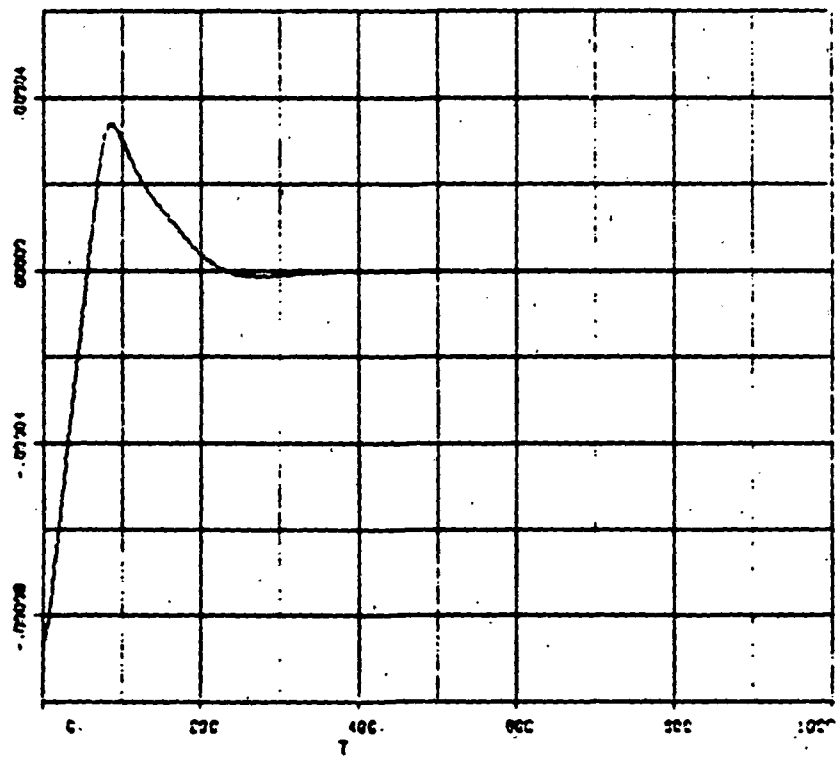

Roll reaches -0.15° before being turned around. Acquisition achieved in ~250 seconds. See also m), n), g), and r).

FULL FLEX MODEL WITH RAM

FIGURE 5-17 (cont)
ACQUISITION

i)

COERR1

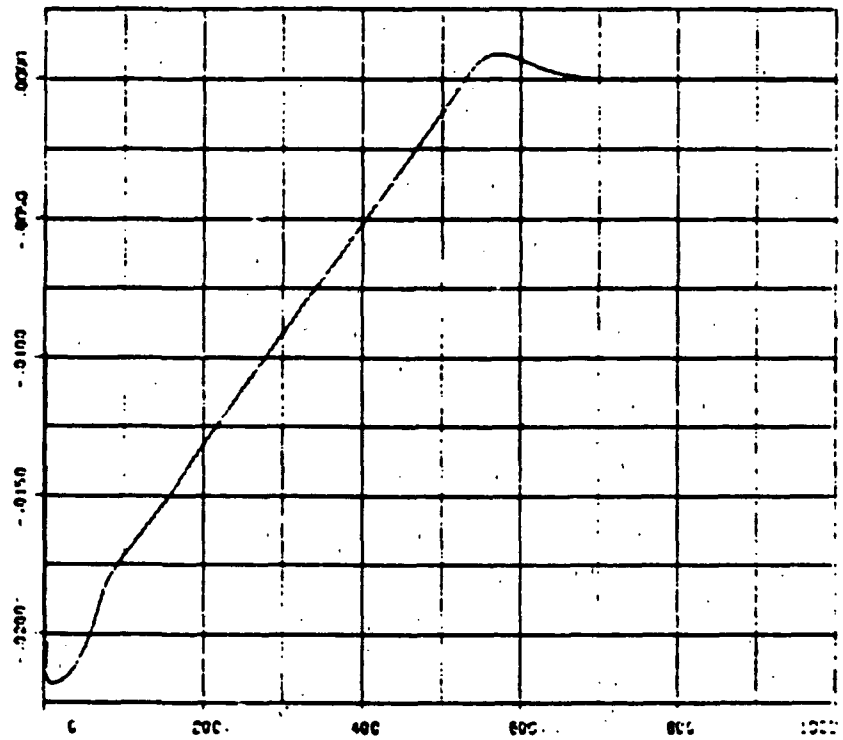

j)

□= TBL

×= TDESRK

△= TRWX

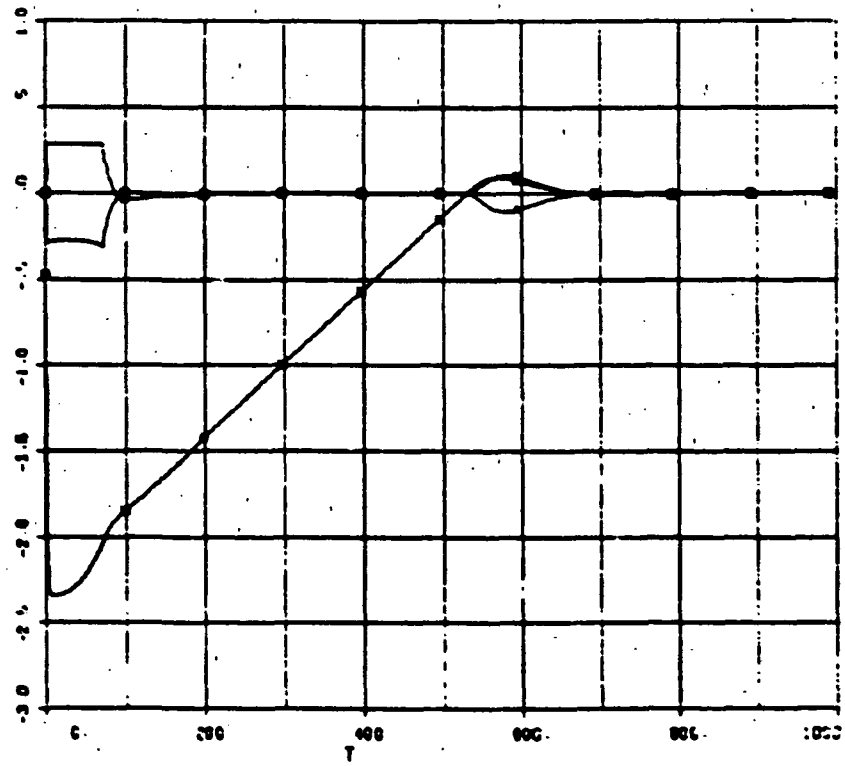

j) Shows saturated pitch wheel effect.

FULL FLEX MODEL WITH PWM

FIGURE 5-17
ACQUISITION

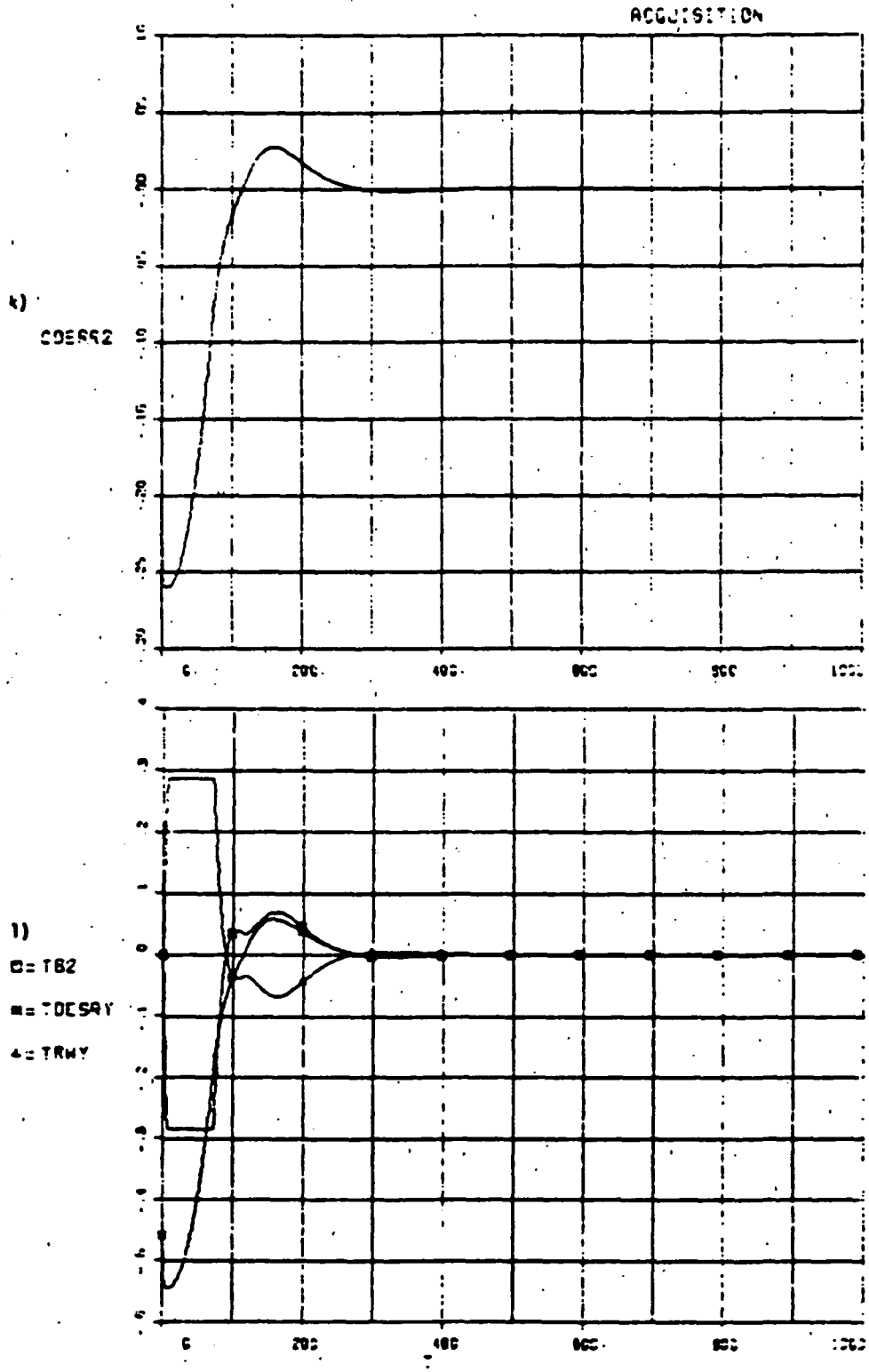

FULL FLEX MODEL WITH RWA

FIGURE 5-17
ACQUISITION

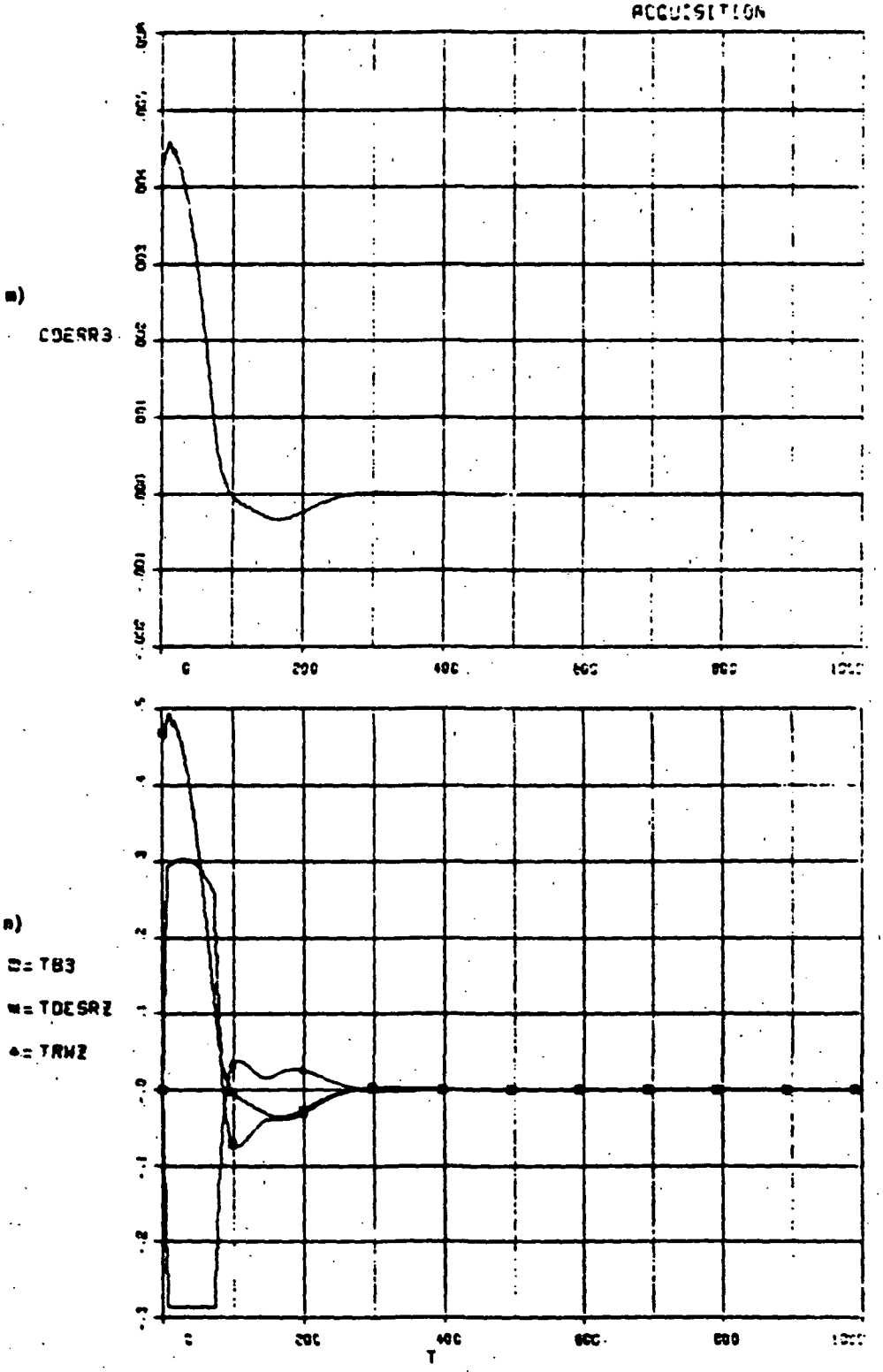

FULL FLEX MODEL WITH RWA

FIGURE 5-17
ACQUISITION

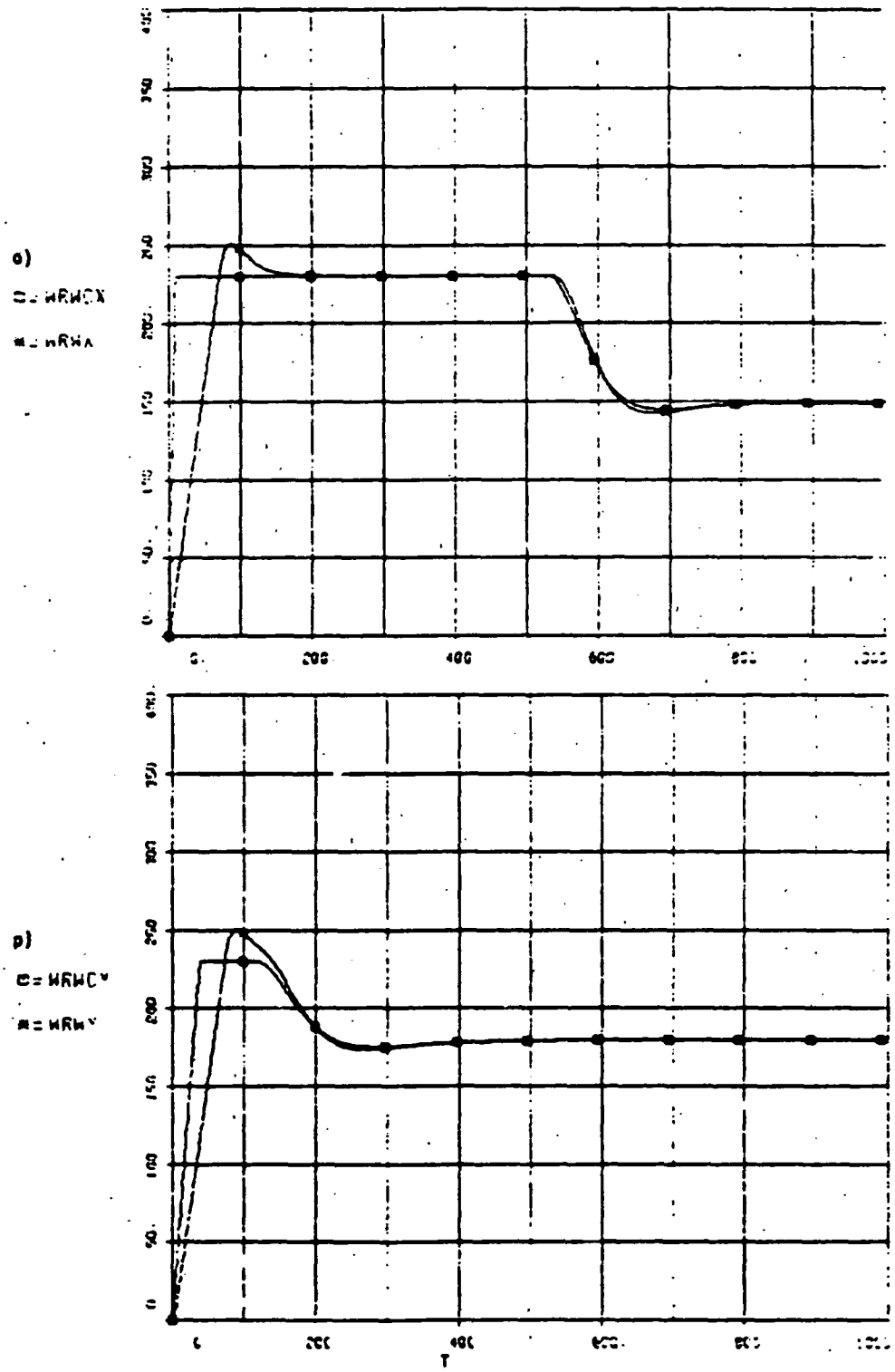

a) Saturated pitch wheel. p) Yaw nearly saturates.

FULL FLEX MODEL WITH RWA

FIGURE 5-17
ACQUISITION

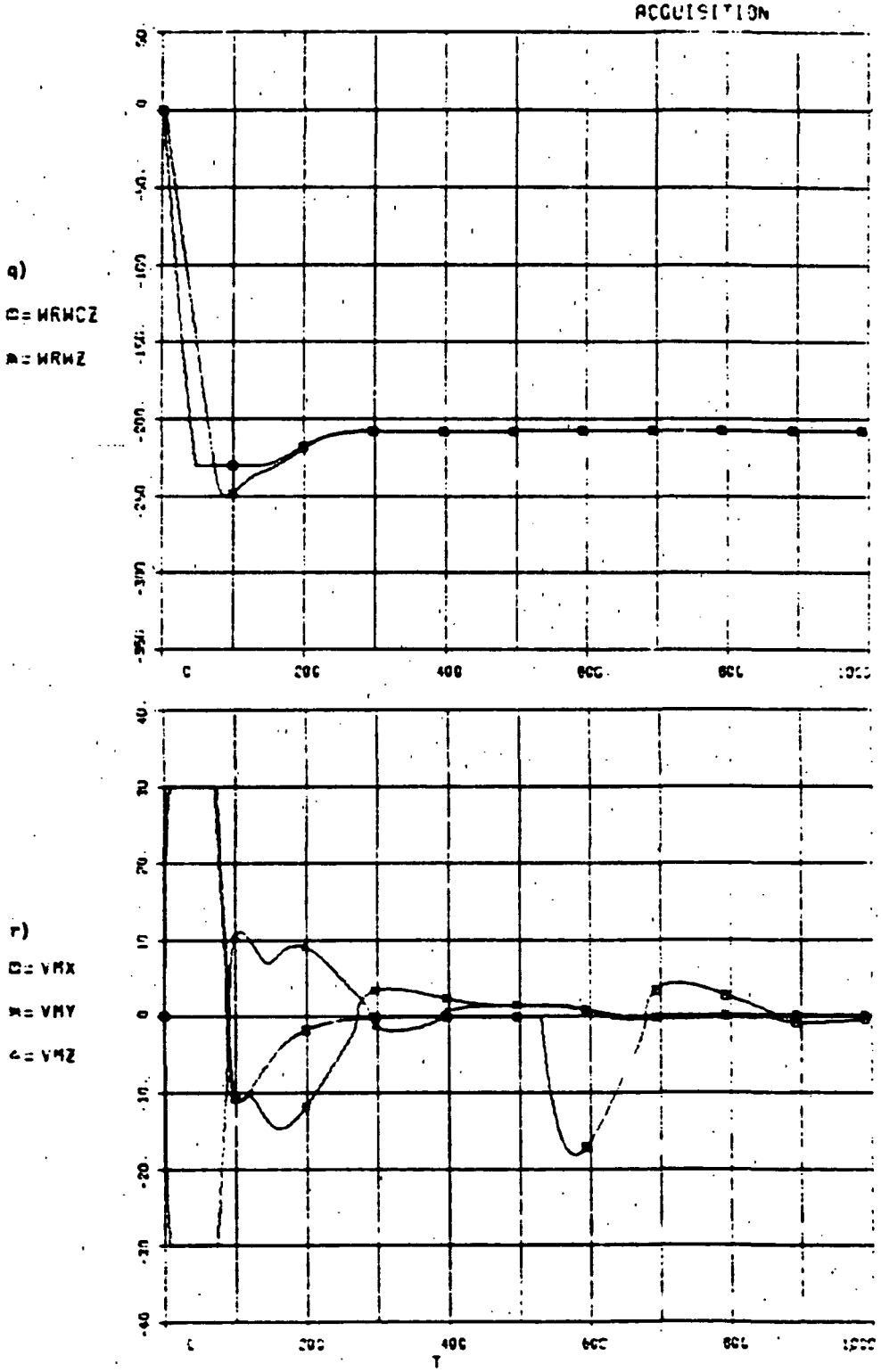

q) Roll RW nearly saturates. r) Shows max 30V being commanded to each of the three wheels at start of acquisition.

FULL FLEX MODEL WITH BAR **FIGURE 5-17**
REQUISITION

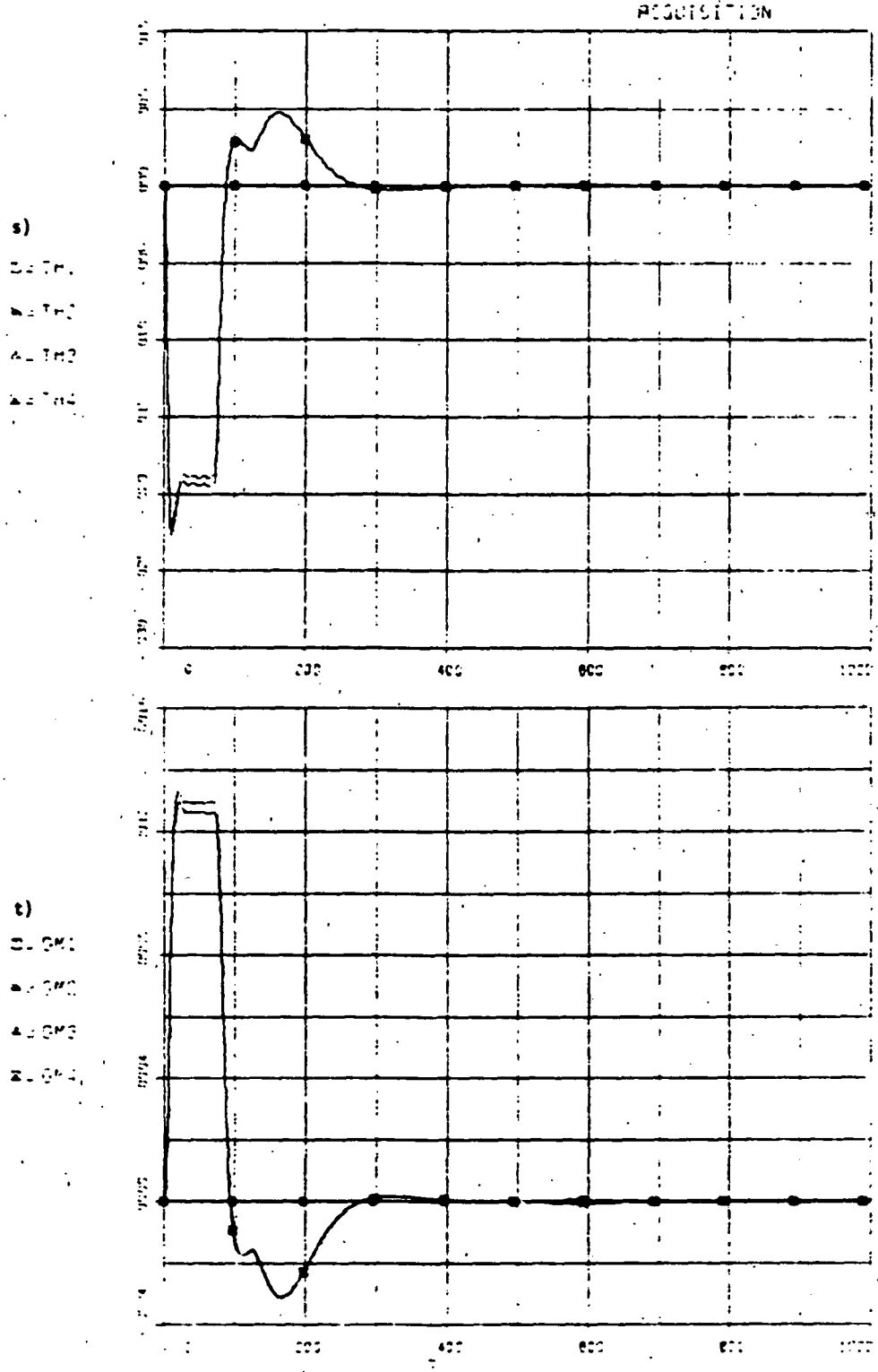

Small hinge torques and deflections.

FULL FLEX MODEL WITH RWA

FIGURE 5-17
ACQUISITION

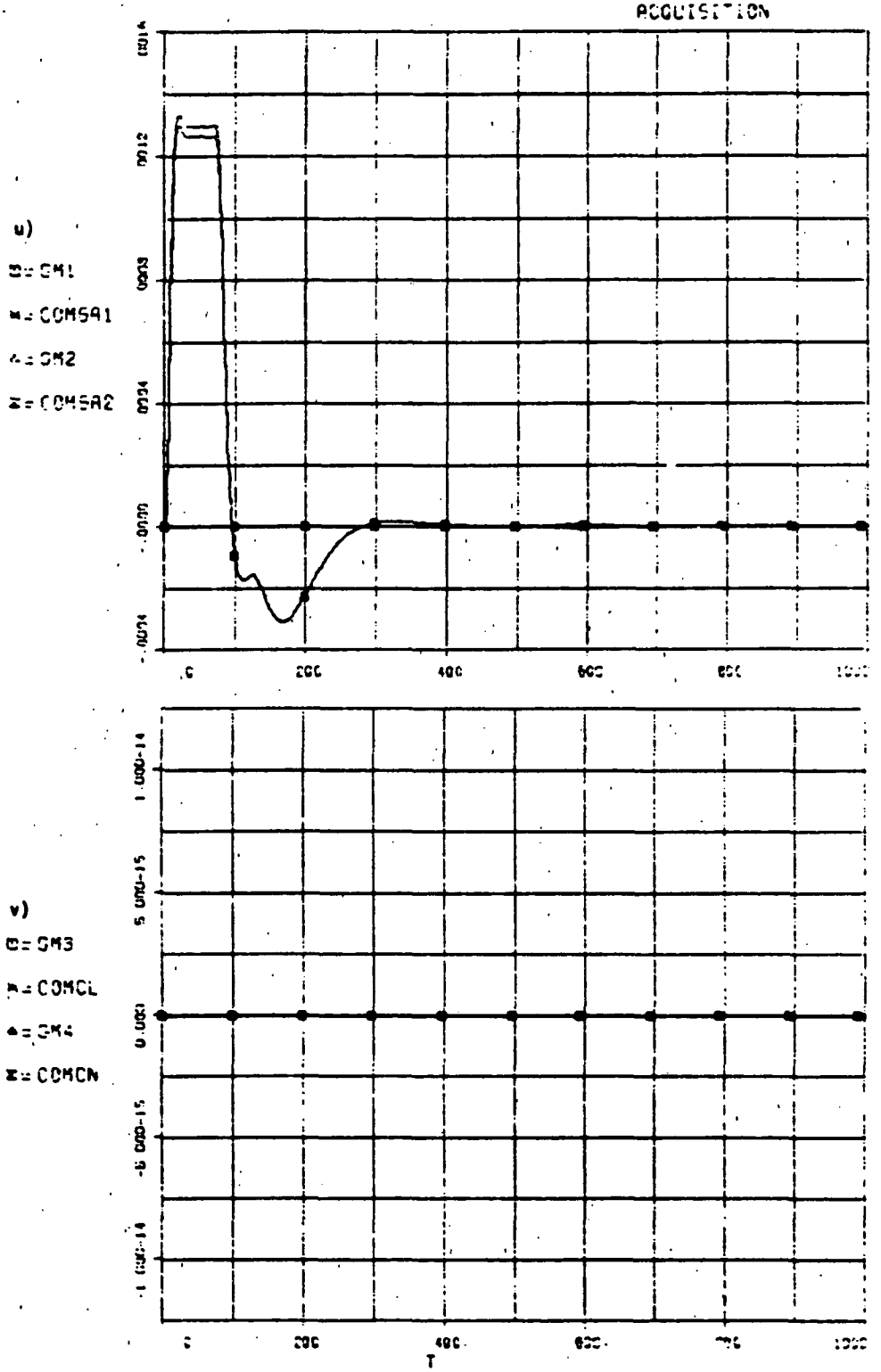

u) SA maximum hinge angle transient of -0.07°. v) Scan platform locked in place for this maneuver.

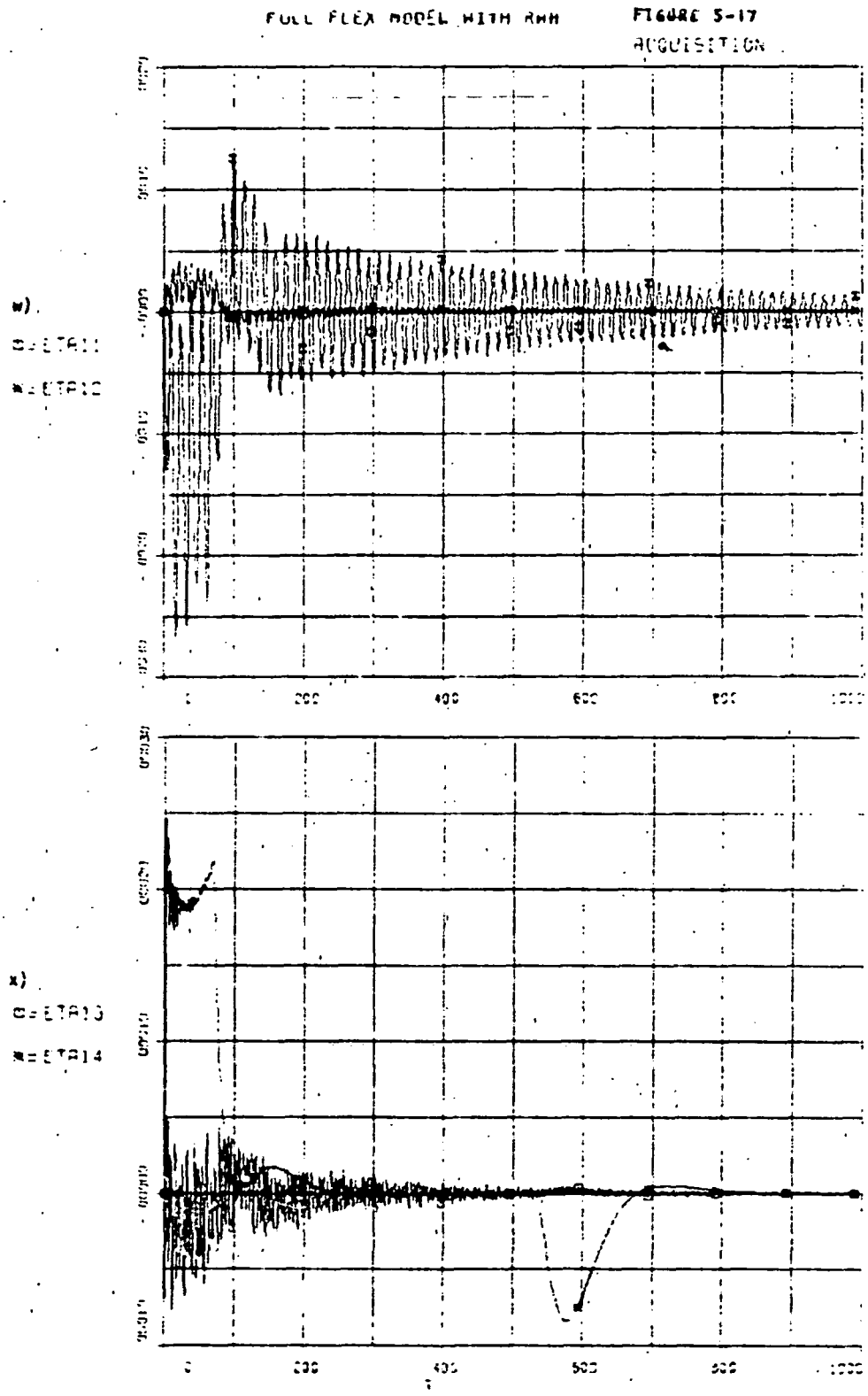

FIGURE 5-17

w) through z)
SA deformation generalized coordinates showing predominant mode 1 out-of-plane deformation of SA. Note that residual vibration levels are higher than for the two preceding maneuvers (because of the drastic square pulse-like torques applied by RW's in this maneuver - See j), l), and n).

FULL FLEX MODEL WITH RHC

FIGURE 5-17
ACQUISITION

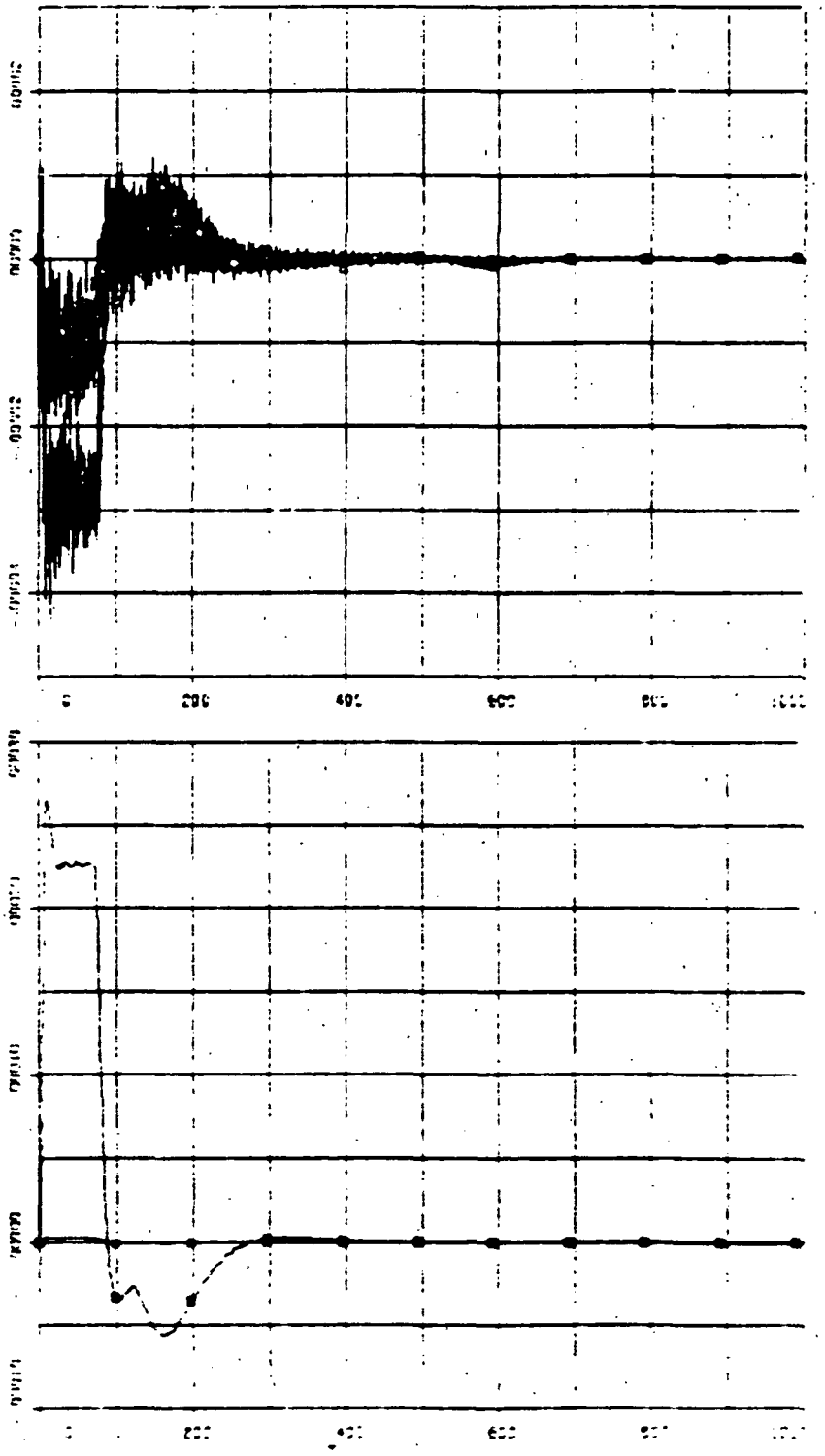

FIGURE 5-18

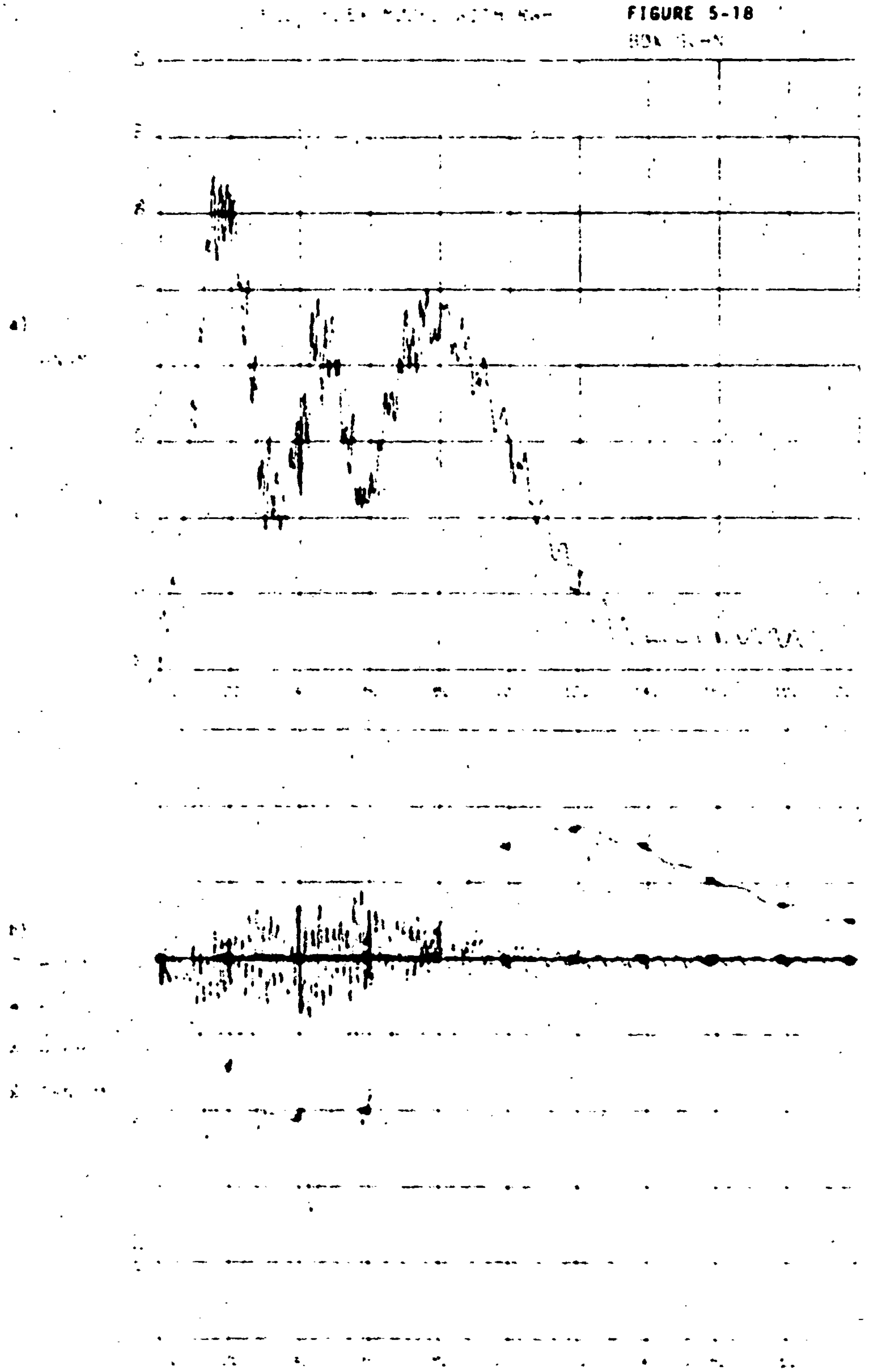

RW's keep vehicle attitude within 165 µrad of initial position under the disturbance created by the box slew sequence used.

FULL FLEX MODEL WITH RHH

FIGURE 5-18

50X SCAN

c)

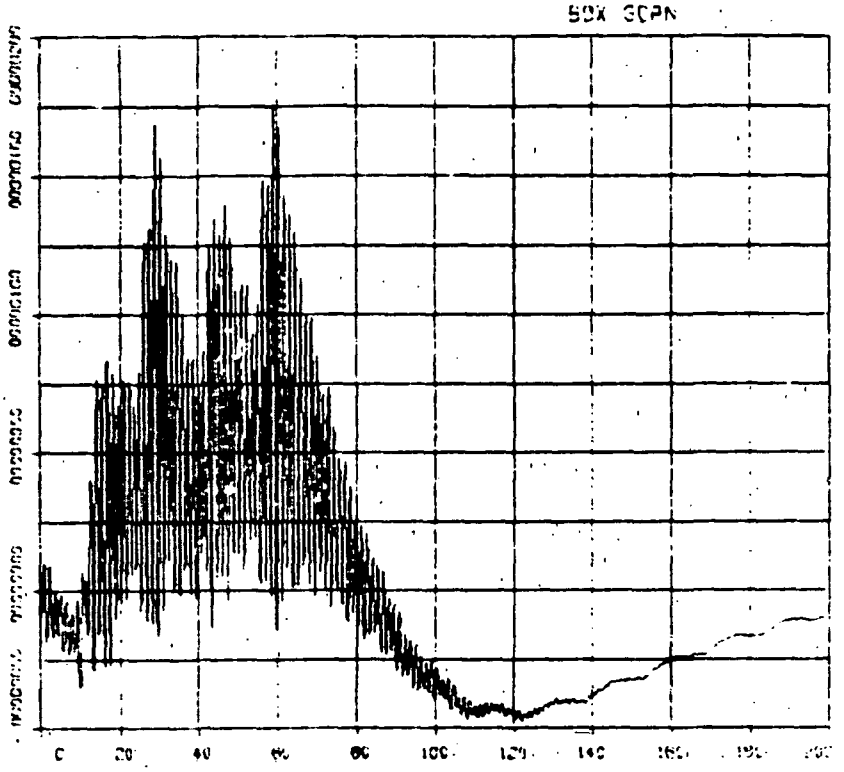

ALPHI

d)

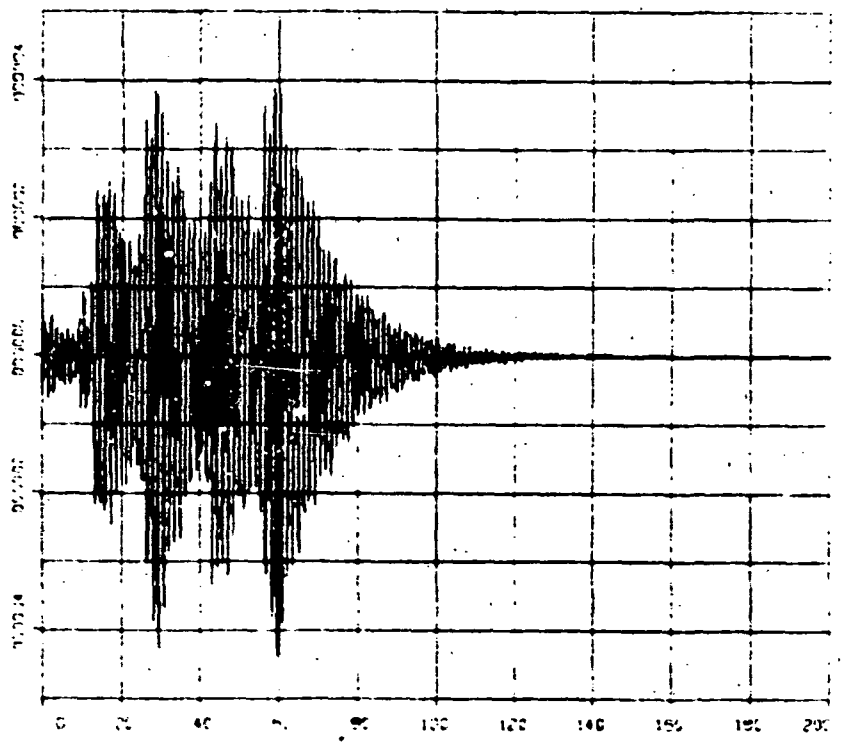

RATE

Induced pitch position and rate errors are very small (<2 urad and <4 urad/s, respectively).

FIGURE 5-18

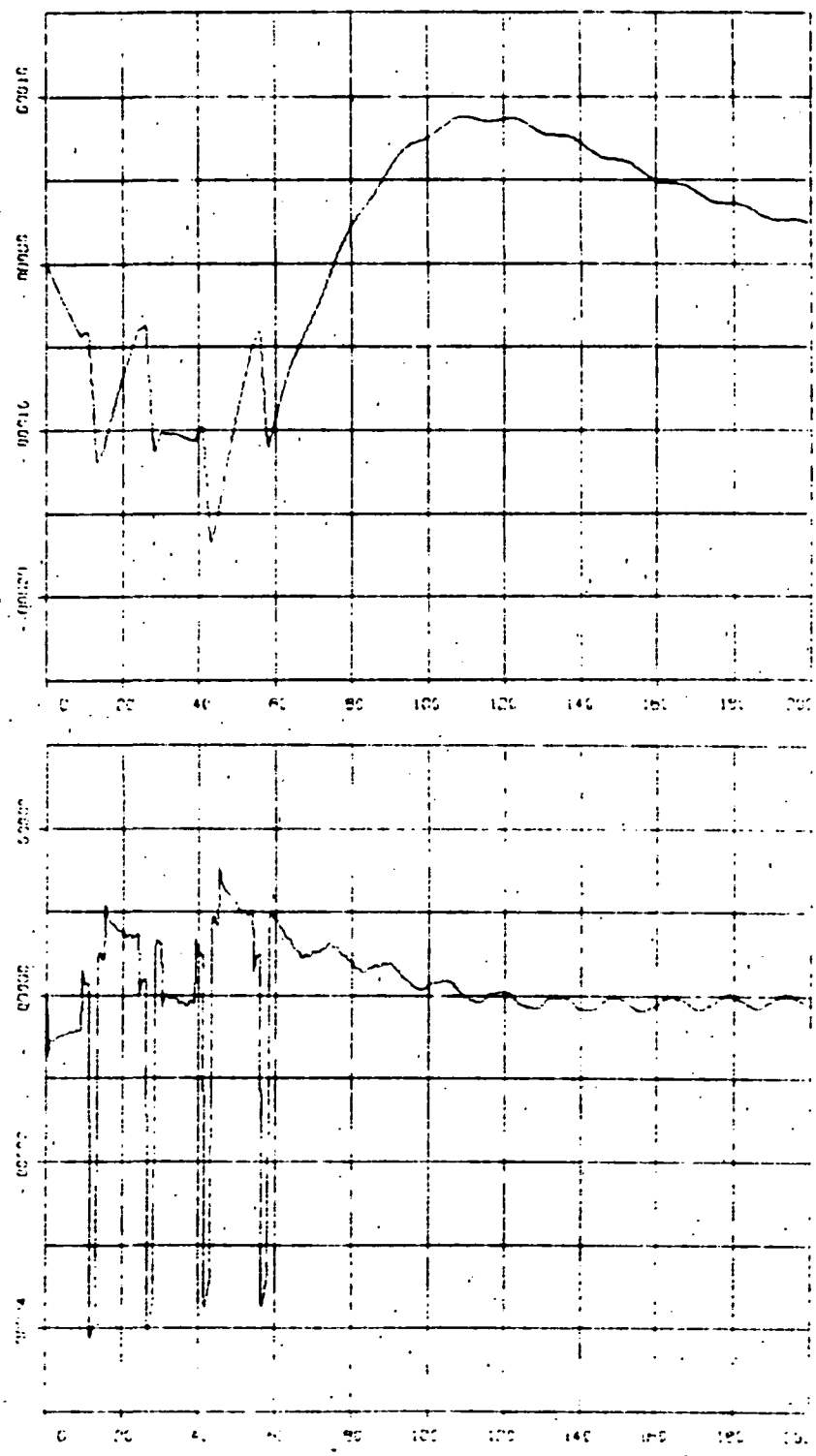

Predictably, the largest disturbance is in yaw (the axis of least inertia). Max position error 165 urad. Max rate 40 urad/s (due predominantly to scan start-stops, not to A/C).

FULL FLEX MODEL WITH RWA

FIGURE 5-18
50K SCAN

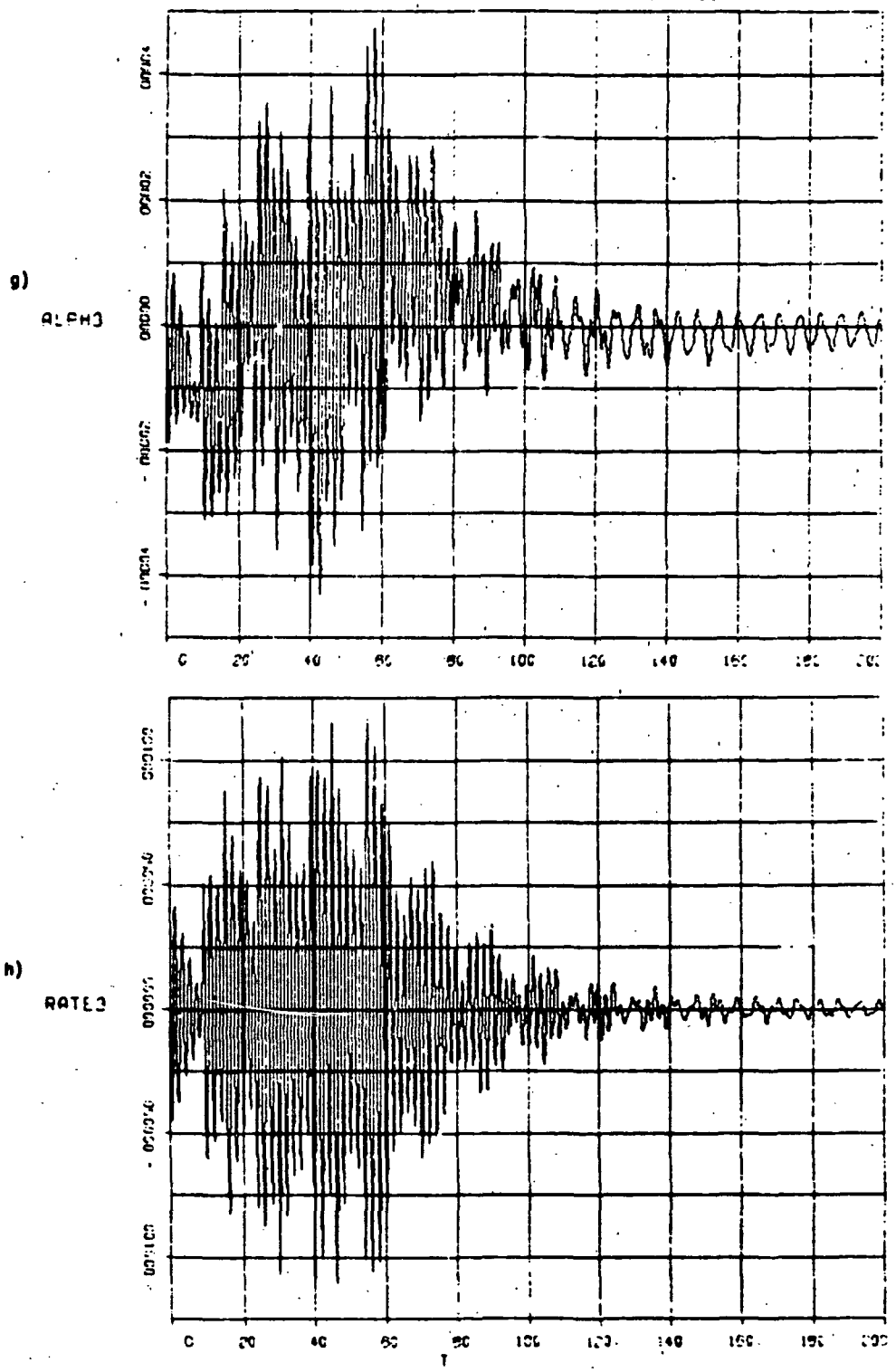

Induced roll position and rate errors of 45 μrad and 120 μrad/s, respectively. Noticeable interaction of scan with structure and RW control See 1), o), p), and u).

FULL FLEX MODEL WITH RWH

FIGURE 5-18
50X SCAN

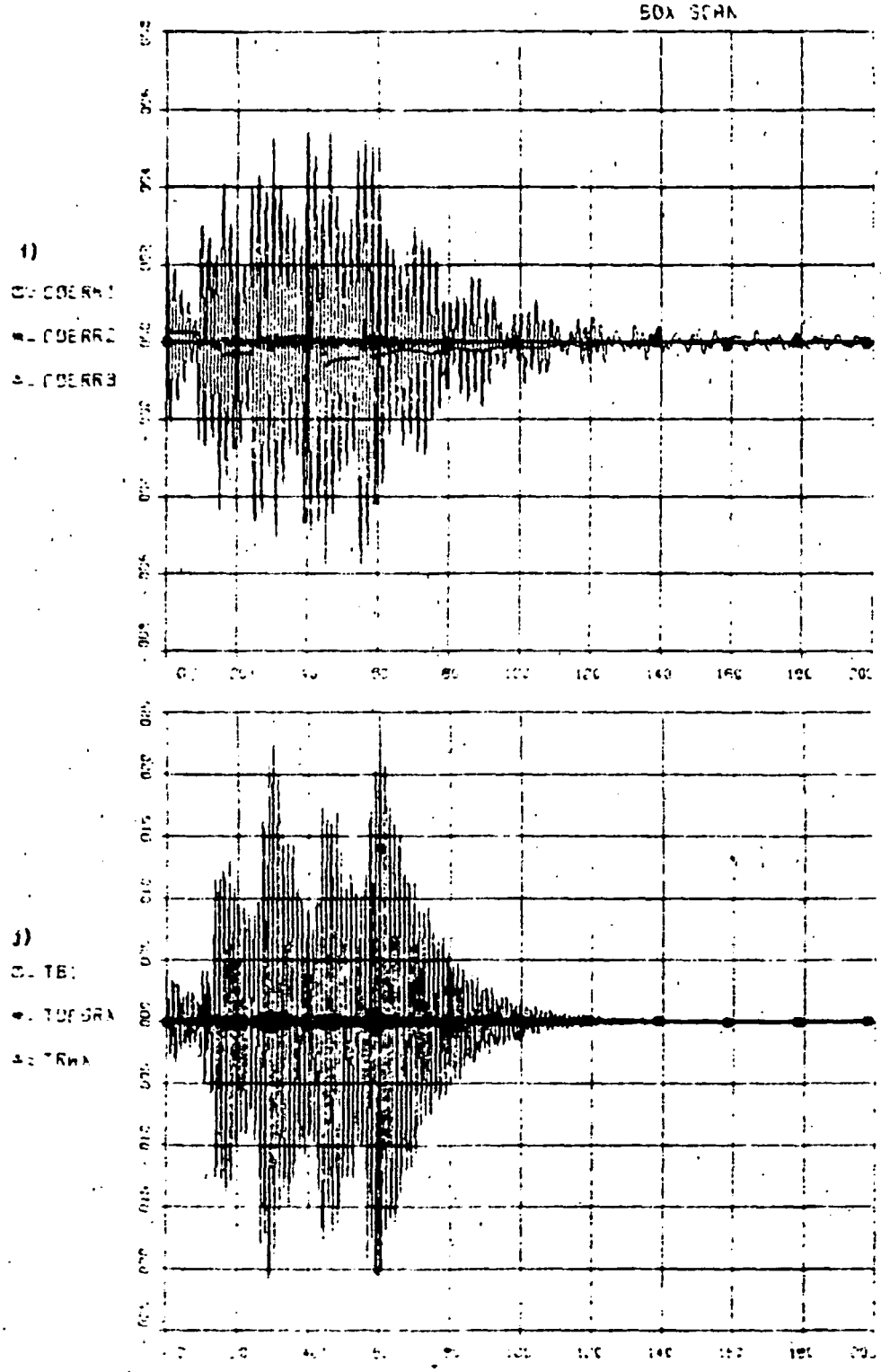

FULL FLEX MODEL WITH RWH

FIGURE 5-18
90X SCAN

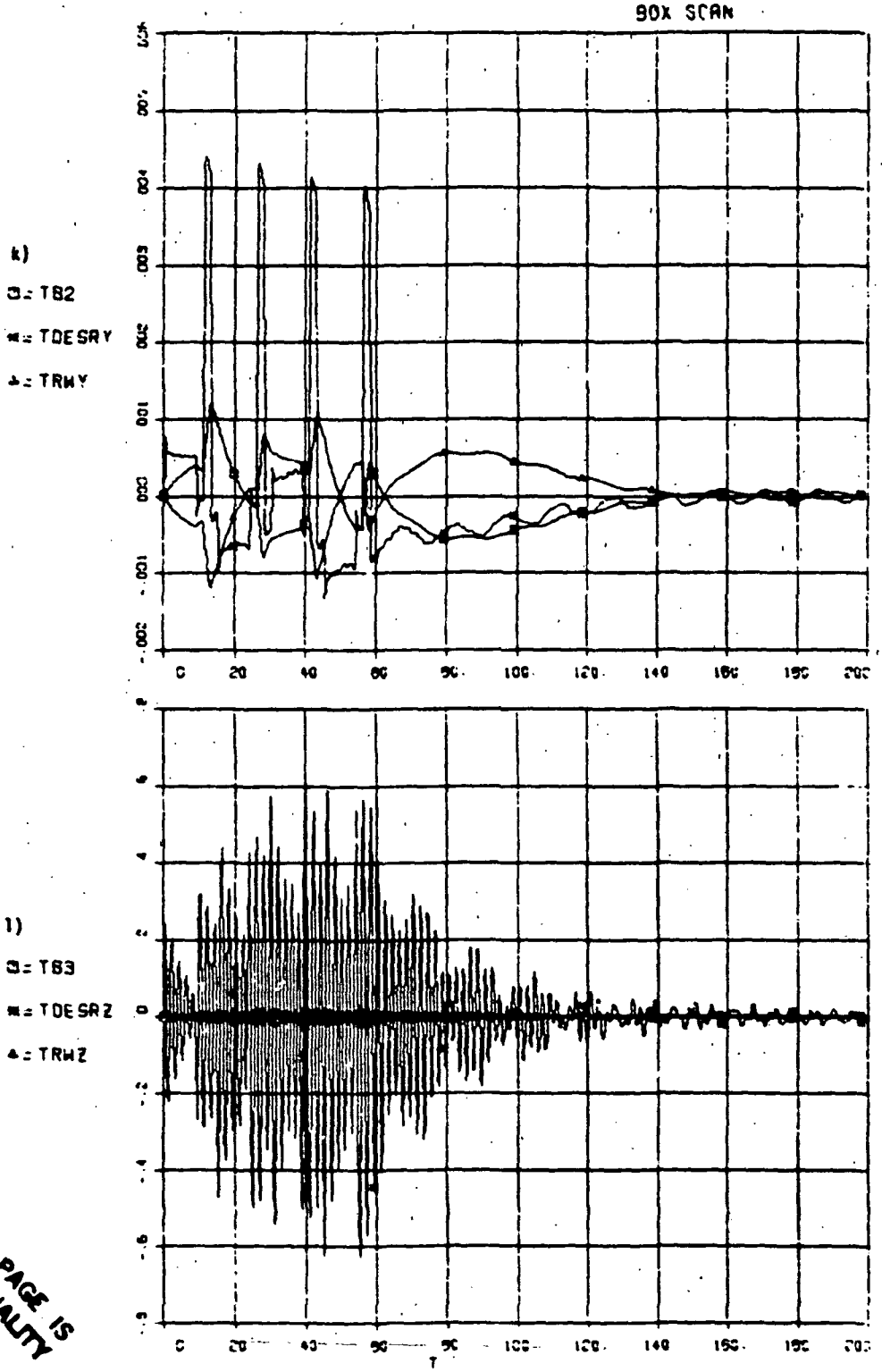

FULL FLEX MODEL WITH Rwc

FIGURE 5-18
90X SCAN

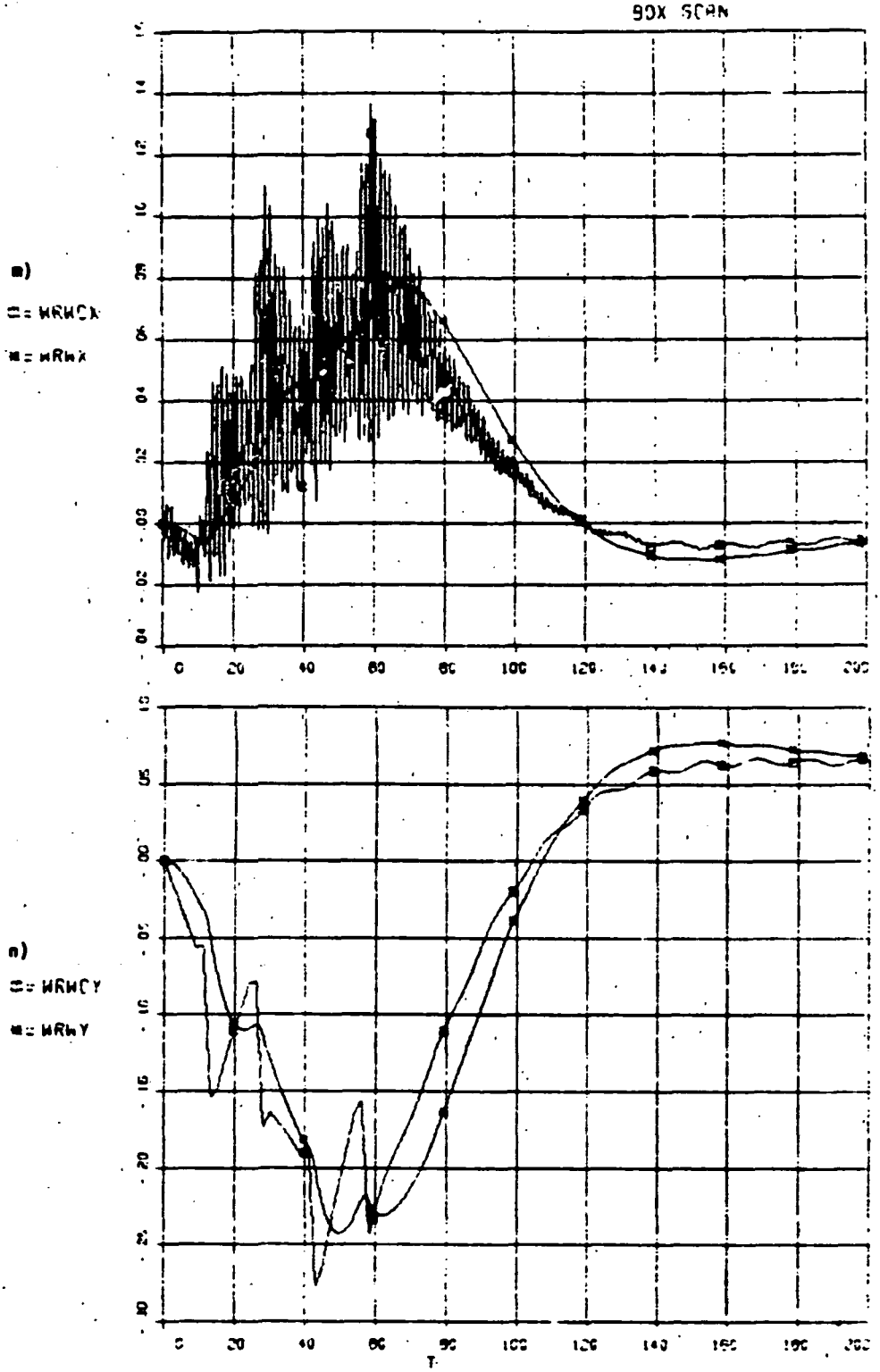

m), n), o). Commands and wheel speeds. Note fairly high ripple content on roll (due to high loop gain, which magnifies flexible interaction).

FULL FLEX MODEL WITH RWA

FIGURE 5-18
BOX SCAN

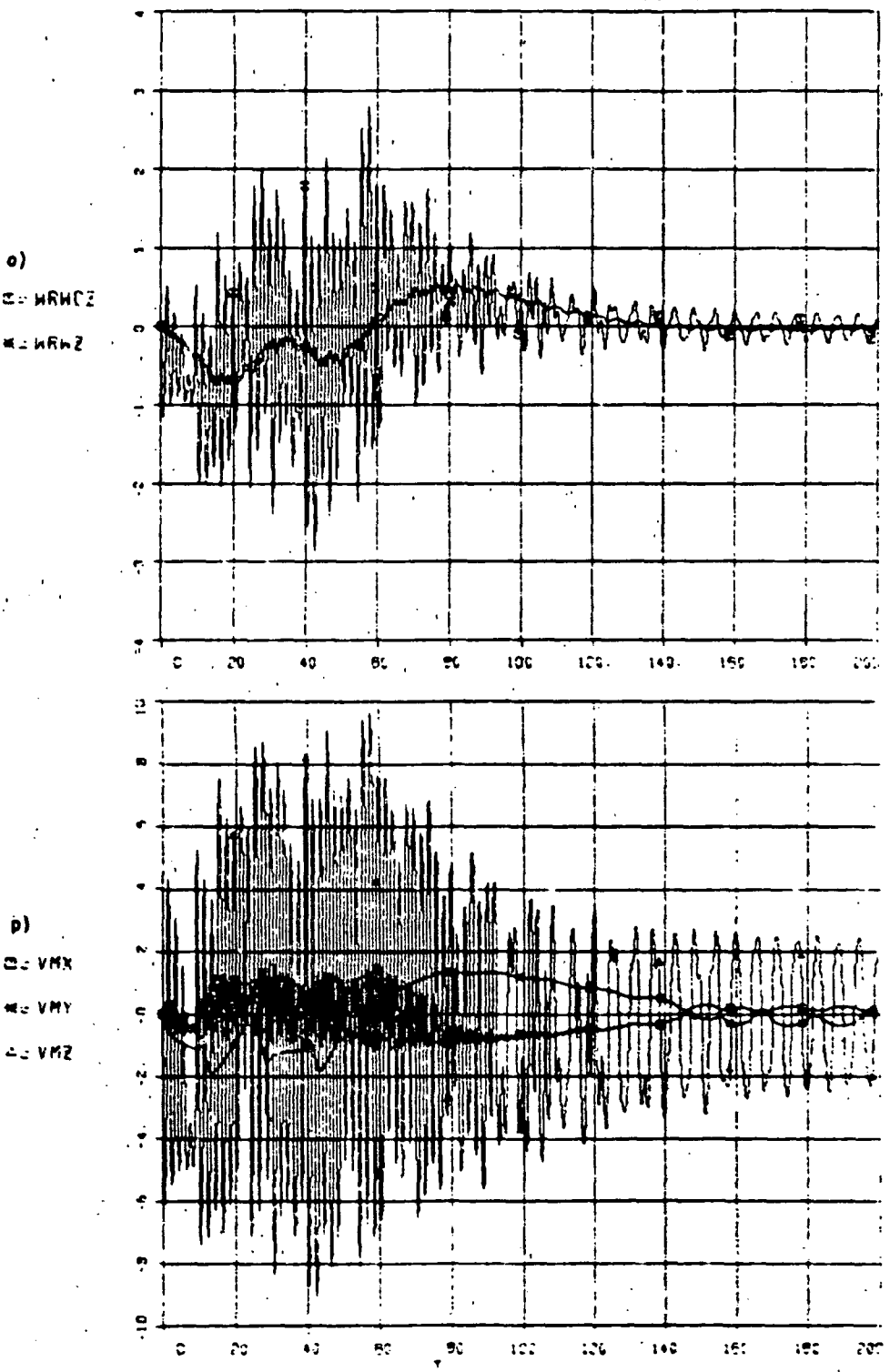

FULL FLEX MODEL WITH EMF

FIGURE 5-18
BOX SCAN

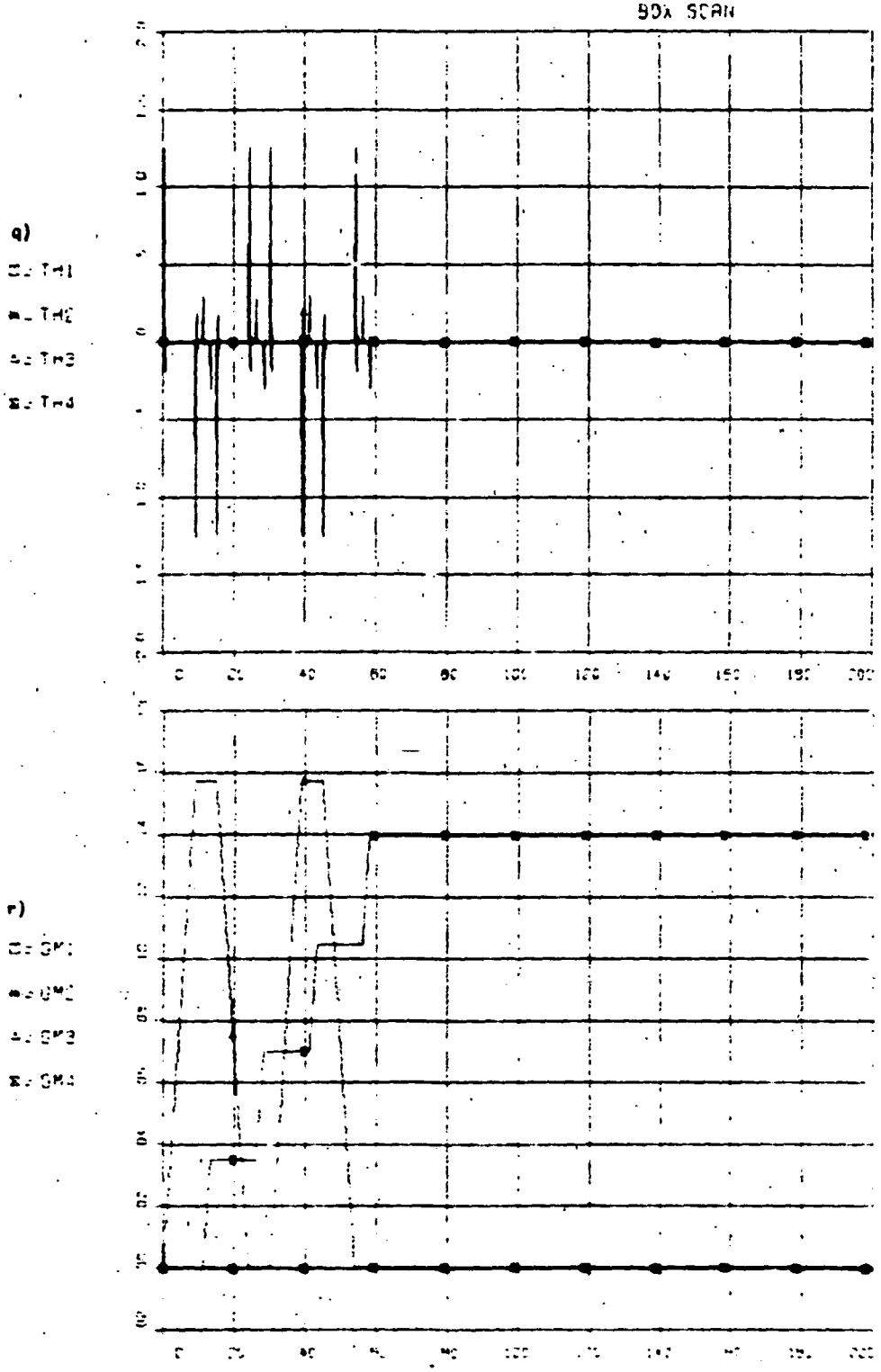

q) Note predominant scan torque spikes at scan start-stops r)

FULL FLEX MODEL WITH RAM

FIGURE 5-18
SOX SCAN

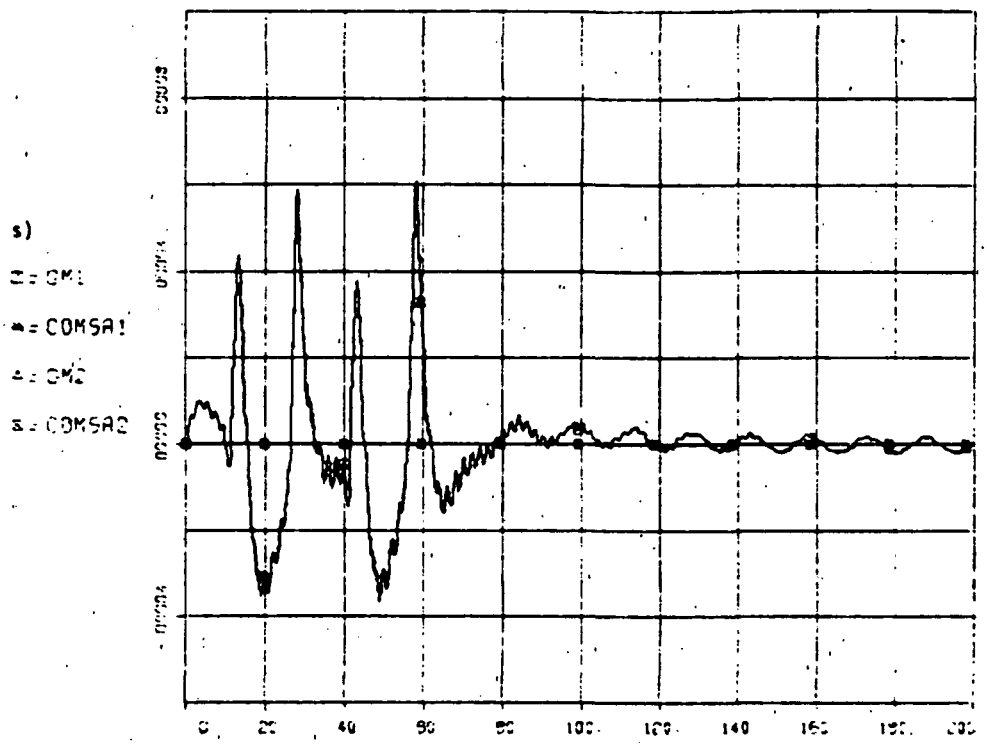

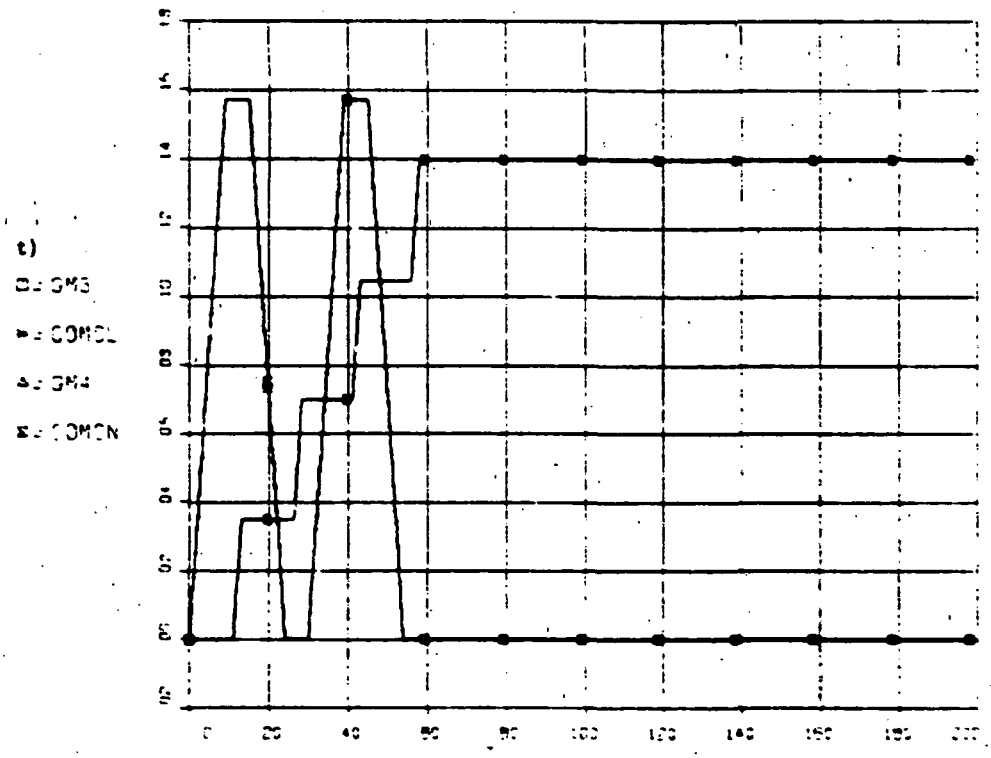

FIGURE 5-18
BOX SCAN

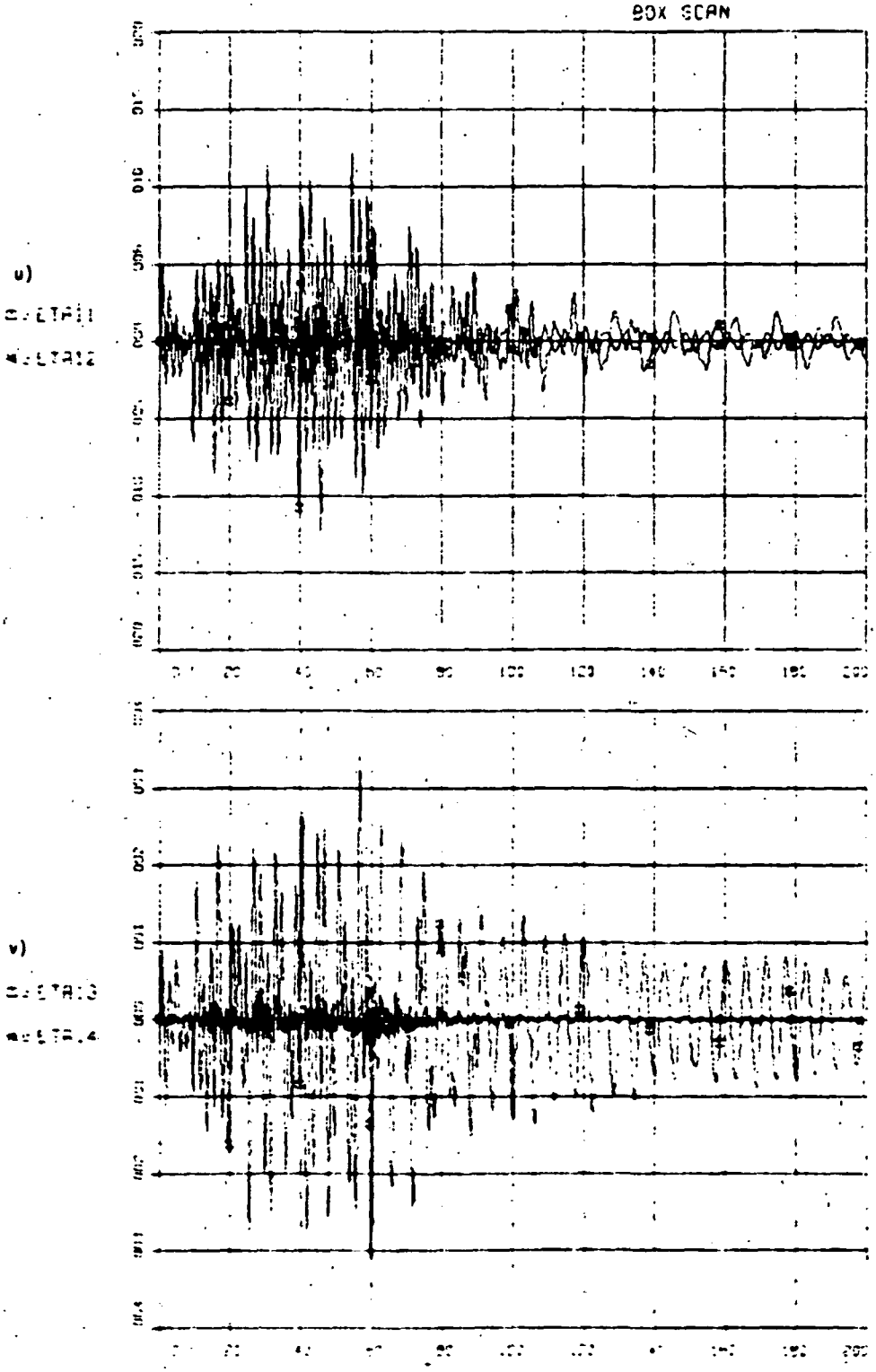

u) through z)
Higher vibration levels in the structure. Predominant mode is #1 (out-of-plane).

FULL FLEX MODEL WITH RAM

FIGURE 5-18

90X 3 N

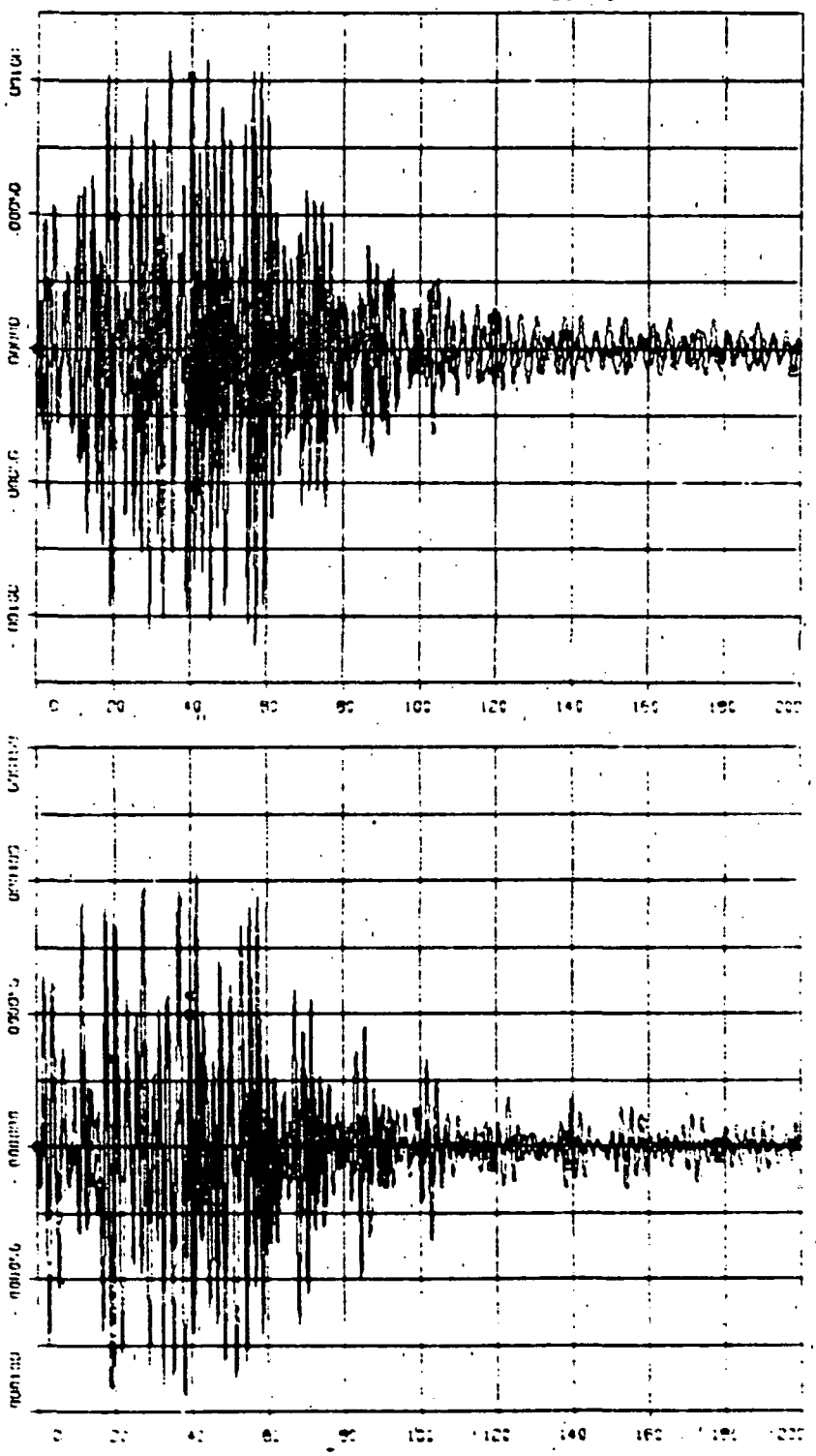

w)

x)

```
CR4DFL/TVC-MASTER
PROGRAM THREE AXES TVC CID FLEX 2 SOLAR PANELS UNDEPLOYED MAG BOOM    ...
      TWO DEGREE OF FREEDOM SCAN PLATFORM (BODY B3)                   ...
      STOWED HIGH GAIN ANTENNA                                        ...
      CONDITIONS AT TEMPLE 2 RENDEZVOUS
 COMMENT                                                              ...
      REVISED 10 OCT 79                                               ...
      METRIC UNITS THROUGHOUT                                         ...
      BUS DATA FROM H. PRICE'S MOM PROGRAM                            ...
      PANEL DATA FROM K. GUPTA'S FINITE EL MODEL (SPAR OCT 79)        ...
      THRUST VECTOR CONTROL LOOP WITH LEDLAG OR KRP  (NOV 79)         ...
      FOR SPECIFIC MANEUVER PARAMETERS SEE LINE 143
 COMMENT
  INTEGER NC,NF,M(3,2),F(2,3),PI(5),J,K,PLTNBR,L,M,N,NN,MANNBR
  ARRAY CMSLV(3)      , CMSLV(3,3)    ,HINGLV(3,3)    ,   TEMPST(8)   ....
        MB(7)         ,    MS(3,7)    ,    PB(3,3)    ,    PS(3,3,3)  ....
        C(4,3)        ,    TH(4)      ,    TB(3)      ,    TS(3,3)    ....
        FB(3)         ,    FS(3,3)    ,    GM(4)      ,   GMD(4)      ....
        GMDD(4)       ,  DIG(2,6,15),   REC(2,6,15),    RF(2,1,3)  ....
        WF(2,15)      ,    ZF(2,15)   ,    TF(2,1,3)  ,    FF(2,1,3)  ....
        FT(2,15)      ,  FTD(2,15)    ,    WO(3)      ,  WFHZ(2,15)  ....
        CK(2,3)       ,  CMSCLV(3)    ,    SENG1(3)   ,    SENG2(3)   ....
        ENG1LV(3)     ,  ENG2LV(3)    ,    RENG1(3)   ,    RENG2(3)
  DOUBLE PRECISION WDOT(7),ETDD(2,15) $ LOGICAL NOPLOT $ DROP
  DATA ((H(I,J),J=1,2)/0,1/
  DATA ((H(2,J),J=1,2)/0,1/
  DATA ((H(3,J),J=1,2)/0,2/
  DATA ((F(1,J),J=1,3)/1,1,15/ $ DATA ((F(2,J),J=1,3)/2,1,15/
  DATA PI/0,0,1,1,1/
 COMMENT
 COMMENT  DEFINE THE MASS PROPERTIES OF THE 4 BODIES
  DATA MB...
  /1824.304, 2635.642, 1769.269, -50.133, -114.634, -46.249, 1756.479/
  DATA ((MS(I,J),J=1,7)...
    /22084.00, 234.61, 21876.00, +158.02, 0.00, 0.00, 176.818/
  DATA ((MS(2,J),J=1,7)...
    /22084.00, 234.61, 21876.00, -158.02, 0.00, 0.00, 176.818/
  DATA ((MS(3,J),J=1,7)...
    /13.3  ,  7.5  , 16.5  , +2.1  , -0.2  , -1.0  , 90.19 /
 COMMENT
 COMMENT POS VEC SPECIF LOCATION OF CM'S & HINGES-IN S/C COORDINATES
  DATA CMSLV /.0703, .0190, .6266 /
  DATA ((CMSLV(1,J),J=1,3)/ 0.00, +19.37645 ,+0.2/
  DATA ((CMSLV(2,J),J=1,3)/ 0.00, -19.37645 ,+0.2/
  DATA ((CMSLV(3,J),J=1,3)/-1.3691,  -0.370, -0.7893/
  DATA ((HINGLV(1,J),J=1,3)/ 0.00 ,0.00 ,+0.2/
  DATA ((HINGLV(2,J),J=1,3)/ 0.00 ,0.00 ,+0.2/
  DATA ((HINGLV(3,J),J=1,3)/-1.3691,  -0.370, -0.7893/
 COMMENT
 COMMENT  ION ENGINES LOCATIONS - IN S/C COORDINATES
  DATA ENG1LV /0.0,+0.5,3.21/ $ DATA ENG2LV /0.0,-0.5,3.21/
 COMMENT
 COMMENT HINGE ORIENTATIONS
  DATA ((G(I,J),J=1,3)/ 0.000000,+1.000000, 0.000000/
  DATA ((G(2,J),J=1,3)/ 0.000000,+1.000000, 0.000000/
  DATA ((G(3,J),J=1,3)/ 0.000000, 0.000000,+1.000000/
  DATA ((G(4,J),J=1,3)/ 0.000000,+1.000000, 0.000000/
```

```
COMMENT
COMMENT RIGID ELASTIC COUPLING COEFFICIENTS FOR THE 2 PANELS ...
        SPAR MODEL BY K. GUPTA OF OCT 79                      ...
        CONDITIONS AT TEMPLE 2 RENDEZVOUS
 DATA ((RFC(1,J,K),J=1,6),K=1,12)/...
-11.18700,    .06995,   -.04629,   -.55239,    .03969,  68.52600,...
  -.51909,   -.09919,    .08782,   1.02460,   -.04128, -88.99000,...
 -3.13460,    .08922,   -.19750,  -2.21670,    .03269,  -4.53950,...
  -.13292,   -.01158,   9.57620, 104.93000,   -.65980,    .76180,...
   .80208,    .06203,    .11783,   1.25900,    .04004,  25.28500,...
  1.46540,   -.04164,   -.02503,   -.29815,  -1.37720,  10.39600,...
   .15877,   -.00148,    .00865,    .05069, 12.17000,    1.12110,...
   .04663,    .00457,    .01924,    .11299,    .13019,    .54573,...
   .07472,    .00979,    .02564,    .13027,   4.03855,    1.15200,...
   .04915,    .02260,    .00615,    .06512,   -.47812,  11.24900,...
  -.07393,    .00837,    .02850,    .10434,    .26855,   -1.51880,...
  -.23045,    .01450,    .03038,    .08424,   2.25460,   -2.39780/
 DATA ((RFC(1,J,K),J=1,6),K=13,15)/...
   .81469,   -.00625,    .00957,    .00618,    .87656,   7.36440,...
  -.11917,   -.01331,   -.03352,   -.05150,   -.33515,  -1.13710,...
   .09823,    .00182,    .00037,    .00137,    .23342,   5.35990/
 DATA ((RFC(2,J,K),J=1,6),K=1,12)/...
-11.18700,   -.06995,    .04629,   -.55239,   -.03969, -68.52600,...
  -.51909,    .09919,   -.08782,   1.02460,    .04128,  88.99000,...
 -3.13460,   -.08922,    .19750,  -2.21670,   -.03269,   4.53950,...
  -.13292,    .01158,  -9.57620, 104.93000,    .65980,   -.76180,...
   .80208,   -.06203,   -.11783,   1.25900,   -.04004, -25.28500,...
  1.46540,    .04164,    .02503,   -.29815,   1.37720, -10.39600,...
   .15877,    .00148,   -.00865,    .05069, -12.17000,  -1.12110,...
   .04663,   -.00457,   -.01924,    .11299,   -.13019,   -.54573,...
   .07472,   -.00979,   -.02564,    .13027,  -4.03855,  -1.15200,...
   .04915,   -.02260,   -.00615,    .06512,    .47812, -11.24900,...
  -.07393,   -.00837,   -.02850,    .10434,   -.26855,   1.51880,...
  -.23045,   -.01450,   -.03038,    .08424,  -2.25460,   2.39780/
 DATA ((RFC(2,J,K),J=1,6),K=13,15)/...
   .81469,    .00625,   -.00957,    .00618,   -.87656,  -7.36440,...
  -.11917,    .01331,    .03352,   -.05150,    .33515,   1.13710,...
   .09823,   -.00182,   -.00037,    .00137,   -.23342,  -5.35990/
COMMENT
COMMENT PANELS FREQUENCIES (IN HERTZ) AND DAMPING
 DATA (WFHZ(1,J),J=1,15)/...
  0.065226 , 0.126145 , 0.192507 , 0.226612 ,...
  0.261074 , 0.329296 , 0.353713 , 0.351529 ,...
  0.376027 , 0.393748 , 0.410395 , 0.443883 ,...
  0.453118 , 0.478315 , 0.501820 /
 DATA (WFHZ(2,J),J=1,15)/...
  0.065226 , 0.126145 , 0.192507 , 0.226612 ,...
  0.261074 , 0.329296 , 0.353713 , 0.351529 ,...
  0.376027 , 0.393748 , 0.410395 , 0.443883 ,...
  0.453118 , 0.478315 , 0.501820 /
 DATA (ZF(1,J),J=1,15)/15*0.004/
 DATA (ZF(2,J),J=1,15)/15*0.004/
       DO L2 K=1,15
        WF(1,K)=WFHZ(1,K)*2.*PIF
        WF(2,K)=WFHZ(2,K)*2.*PIF
 L2..  CONTINUE
COMMENT
```

```
      COMMENT  CALCULATE THE S/C CENTER OF MASS
               DO CM1 K=1,3
               CMSCLV(K)=MB(7)*CMBLV(K)+MS(1,7)*CMSLV(1,K)+MS(2,7)*CMSLV...
               (2,K)+MS(3,7)*CMSLV(3,K)
               CMSCLV(K)=CMSCLV(K)/(MB(7)+MS(1,7)+MS(2,7)+MS(3,7))
               CM1..  CONTINUE
               WRITE (6,F3) CMSCLV
      COMMENT COMPUTATION OF PH AND PS VECTORS AND CMB TO ENG VECTORS
               DO L1 K=1,3
               RENG1(K)=ENG1LV(K)-CMBLV(K) $ RENG2(K)=ENG2LV(K)-CMBLV(K)
               SENG1(K)=ENG1LV(K)-CMSCLV(K) $ SENG2(K)=ENG2LV(K)-CMSCLV(K)
               PH(1,K)=HINGLV(1,K)-CMBLV(K)
               PH(2,K)=HINGLV(2,K)-CMBLV(K)
               PH(3,K)=HINGLV(3,K)-CMBLV(K)
               PS(1,1,K)=HINGLV(1,K)- CMSLV(1,K)
               PS(2,2,K)=HINGLV(2,K)-CMSLV(2,K)
               PS(3,3,K)=HINGLV(3,K)-CMSLV(3,K)
        L1..   CONTINUE
     PICKUP
    INITIAL
     COMMENT  ************************************************************
              *                                                          *
              *      DEFINE THE BUS FIXED AXES AS FOLLOWS:               *
              *      -------------------------------------               *
              *                                                          *
              *      AXIS3 = Z ( ION ENGINE PLUME EXHAUST AXIS )         *
              *                                                          *
              *      AXIS2 = Y ( SOLAR ARRAY AXIS )                      *
              *                                                          *
              *      AXIS1 = X                                           *
              *                                                          *
              ************************************************************
              *                                                          *
              *      SELECT THE MANEUVER BY ITS NUMBER                   *
              *      ---------------------------------                   *
              *                                                          *
              *      1 - TURN ENTIRE SPACECRAFT ABOUT AXIS1              *
              *                                                          *
              *      2 - TURN ENTIRE SPACECRAFT ABOUT AXIS2              *
              *                                                          *
              *      3 - TURN ENTIRE SPACECRAFT ABOUT AXIS3              *
              *                                                          *
              *      4 - TURN  BUS ONLY ABOUT AXIS2                      *
              *          WHILE KEEPING ARRAYS ON THE SUN                 *
              *                                                          *
              *      5 - ACQUISITION OF CEL REFERENCES                   *
              *                                                          *
              *      6 - SCAN PLATFORM SLEW OR BOXSCAN                   *
              *                                                          *
              ************************************************************
              *                                                          *
              *                                                          *
    CONSTANT                      MANEUV = 1.0
     COMMENT  *                                                          *
              *                                                          *
              ************************************************************
```

```
                    ***********************************************
                    *                                             *
                    *      SET SIMULATION TIME                    *
                    *      -------------------                    *
                    *                                             *
CONSTANT            *                  FINTIM =  9.9              *
 COMMENT            *                                             *
                    ***********************************************
                    *                                             *
                    *      SET INITIAL CONDITIONS                 *
                    *      ----------------------                 *
                    *                                             *
                    *      AXIS1          AXIS2          AXIS3    *
                    *      -----          -----          -----    *
                    *                                             *
                    *   DISTURBANCE TORQUES                       *
                    *                                             *
CONSTANT            *    TDIST1=0.0    *   TDIST2=.2094E-4*  TDIST3=0.0
 COMMENT            *                                             *
                    *   INITIAL RATES                             *
                    *                                             *
CONSTANT            *    RATE1I=0.0    *   RATE2I=0.0    *   RATE3I=0.0
 COMMENT            *                                             *
                    *   INITIAL ANGULAR POSITION ERRORS           *
                    *                                             *
CONSTANT            *    ALPH1I=0.0    *   ALPH2I=0.0    *   ALPH3I=0.0
 COMMENT            *                                             *
                    *   TURN COMMANDS                             *
                    *                                             *
CONSTANT            *    TRNTIM= 200.00
CONSTANT            *  TRN1RT=8.72664E-5*TRN2RT=8.56332E-3*TRN3RT=8.72664E-5
 COMMENT            *                                             *
                    *                                             *
                    *      SOLAR ARRAY                            *
                    *      -----------                            *
                    *                                             *
                    *   SOLAR ARRAY COMMANDS                      *
                    *                                             *
CONSTANT            *    SAPSON=0.0    *   SALOCK=1.0    *   SASLEW=0.0
 COMMENT            *                                             *
                    *                                             *
                    *      SCAN PLATFORM                          *
                    *      -------------                          *
                    *                                             *
                    *   SCAN PLATFORM COMMANDS                    *
                    *                                             *
CONSTANT            *    SCANON=0.0    *   SLEWON=0.0    *   BOXON =0.0
 COMMENT            *                                             *
                    *                                             *
                    ***********************************************
 COMMENT
 COMMENT
 COMMENT
```

```
                TRN1ON=0.0 $ TRN2ON=0.0 $ TRN3ON=0.0
                SAPSUN=0.0 $ SCANON=0.0
                MANNBR = MANEUV + .5
                GO TO (M1,M2,M3,M4,M5,M6), MANNBR
   M1..         TRN1ON=1.0
                GO TO MEND
   M2..         TRN2ON=1.0
                GO TO MEND
   M3..         TRN3ON=1.0 $ SALOCK=1.0
                GO TO MEND
   M4..         TRN2ON=1.0 $ SAPSUN=1.0
                GO TO MEND
   M5..         GO TO MEND
   M6..         SCANON=1.0 $ SLEWON=0.0 $ BOXON=1.0
   MEND..       CONTINUE
COMMENT
COMMENT
COMMENT  ****************************************
COMMENT  ******  TVC CONTROLLER PARAMETERS  ******
COMMENT SPECIFY FILTER,S&E LEAD-LAGS, AND KRP PARAMETERS
   CONSTANT     SLOWLL = 1.0   ,  FASTLL= 0.0,  KPPON = 0.0      ****
                SKX=3.52       ,  FKX=39.66   ,  KKX=39.66       ****
                SKY=0.11       ,  FKY= 0.77   ,  KKY=0.77        ****
                SKZ=15.7       ,  FKZ=214.96  ,  KKZ=214.96      ****
                TAUF=15.                      ,  KKRPK=49.96     ****
                STAU1L=200.    ,  FTAU1L=60.  ,  KKRPY=49.96     ****
                STAU2L=10.     ,  FTAU2L=10.  ,  KKRPZ=49.96
          LLAGON=SLOWLL+FASTLL
          KX     =   SKX*SLOWLL+   FKX*FASTLL
          KY     =   SKY*SLOWLL+   FKY*FASTLL
          KZ     =   SKZ*SLOWLL+   FKZ*FASTLL
          TAU1LL=STAU1L*SLOWLL+FTAU1L*FASTLL
          TAU2LL=STAU2L*SLOWLL+FTAU2L*FASTLL+KPPON*99.
COMMENT GIMBALLED ENGINE INERTIAS (EACH "GIMBALLED ENGINE" IS A  ...
        BANK OF 4 ACTUAL ENGINES)
          IGENG1=4*0.475      $     IGENG2=4*0.475
          MGENG1=4*8.9        $     MGENG2=4*8.9
COMMENT  FORCE OF 4 ENGINES = 1 NEWTON
   CONSTANT     FC=1.0
COMMENT  ******  TVC CONTROLLER PARAMETERS END  ******
COMMENT  ****************************************
COMMENT  ******  CELESTIAL SENSOR PARAMETERS  ********
   CONSTANT     TAUS=1.0
COMMENT  ******  SA AND SP  CHARACTERISTICS  *********
COMMENT SPECIFY SA FILTER , S&F LEAD-LAGS , AND KRP PARAMETERS
   CONSTANT     SKSA=3.41      , FKSA=2000.    ,  KKSA=.32397     ****
                KA=0.01
   CONSTANT     STAU1A=200.    , FTAU1A=60.    ,  KKRPSA=57.6     ****
                STAU2A=20.     , FTAU2A=20.                       ****
                TAUFSA=15.
          KSA    =  SKSA*SLOWLL+  FKSA*FASTLL
          TAU1SA=STAU1A*SLOWLL+FTAU1A*FASTLL
          TAU2SA=STAU2A*SLOWLL+FTAU2A*FASTLL+KPPON*99.
          KSAKA=KSA*KA/2.
COMMENT     SOLAR ARRAY SELECTION
   IF(SALOCK.GT.0.9)SASLEW=0.0
   IF(SAPSUN.LT.0.9)GO TO SA1
```

```
    SALOCK=0.
    SASLEW=0.0
   SA1..CONTINUE
    CONSTANT A1SLBG=    0.00  .  A1SLEN=    50.00  .  A1SLRT=0.00438
    CONSTANT A2SLBG=    0.00  .  A2SLEN=    50.00  .  A2SLRT=0.00438
COMMENT
  COMMENT SP CONTROL LOOP PARAMETERS AND IC'S
   CONSTANT KCL    =1500.     .  KCN    =1500.
   CONSTANT BCL    = 148.50   .  BCN    = 220.25
  COMMENT SCAN SELECTION
   IF(SLEWON.GT.0.9)BOXON=0.0
   IF(SCANON.GT.0.9)GO TO SC1
   SLEWON=0.0
   BOXON =0.0
  SC1..CONTINUE
   CONSTANT CLRATE=0.017453  .  CNRATE=0.017453
   CONSTANT CLSLBG=20.00     .  CLSLEN=   50.00
   CONSTANT CNSLBG=120.0     .  CNSLEN=  150.00
   CONSTANT CLBXB1=20.00     .  CLBXFQ=   30.00  .  CLBXWD=9.0
   CONSTANT CLBXB2=35.00
   CONSTANT CNBXBG=31.00     .  CNBXFQ=   15.00  .  CNBXWD=2.00
   CONSTANT BOXEND=80.00
   CONSTANT TINITL=0..00000
   CONSTANT PIE=3.14159265
  COMMENT
  COMMENT    SET INITIAL  SS. FILTER. AND LL VALUES
   FLSA1I=-ALPH2I*SAPSUN
   FLSA2I=-ALPH2I*SAPSUN
   LLSA1I=FLSA1I
   LLSA2I=FLSA2I
   THTA1I=ALPH1I
   THTA2I=ALPH2I
   THTA3I=ALPH3I
   FILXI=-THTA1I
   FILYI=-THTA2I
   FILZI=-THTA3I
   LLXI=FILXI
   LLYI=FILYI
   LLZI=FILZI
  COMMENT
  COMMENT   SET UP PLOTTING INFORMATION
            NOPLOT = .FALSE.
   CONSTANT PLTNBR=0                 ....
            INTRV1=10.0              ....
            NEWINT=100.0             ....
            INTRV2=50.0
            SWITCH=NEWINT
  COMMENT
   NC=3   $  NF=2
   NXQDYN=0.
   NXODER=0.
   NXOTER=0.
   NXQINT=NXQINT+1.
  COMMENT
   CALL NODYFL(NC,H,MB,MS,PB,PS,G,PI,NF,F,EIG,REC,RF,WF,ZF)
   DEBUG
END
```

```
      COMMENT
*  DYNAMIC
      VARIABLE T=TINITL
      DERPDY=NXQDER-NXDERL
      NXDERL=NXQDER
      NXQDYN=NXQDYN+1.
      IF (NCPLOT) GO TO NOSAVE
      IF (T.GT.SWITCH) GO TO INT2
      YESPLT=PLTNBR*INTRV1
      GO TO SL1
      INT2..  CONTINUE
      CHECKP=PLTNBR*INTRV1
      IF (CHECKP.GE.NEWINT) NEWINT=NEWINT+INTRV2
      YESPLT = NEWINT
      SL1..  CONTINUE
      TIMEP=T+.0001
      IF (TIMEP.LT.YESPLT) GO TO NOSAVE
      WRITE (6,F1) PLTNBR,T
      WRITE (6,F2) PZ,P1,P2,P3
      WRITE (6,F2) GM(1),GM(2),GM(3),GM(4)
            DO SL2 J=1,2
            L=
            DO SL2 K=1,3
            WRITE (6,F2) (ET(J,L+M),M=1,5)
            F2..  FORMAT (1X,5G14.8)
            L=L+5
            SL2..  CONTINUE
         WRITE (6,F3) ((CK(N,NN),NN=1,5),N=1,2)
         F3..  FORMAT (1X,3G14.8)
      PLTNBR=PLTNBR+1
      IF (T.GT.SWITCH) NEWINT=NEWINT+INTRV2
      NOSAVE..  CONTINUE
      IF(T.GT.FINTIM)GO TO FIN
      OUTPUT  200                                          ....
                  TRNCO1,    TRNCO2,    TRNCO3,    ...
                  ERROR1,    ERROR2,    ERROR3,    ...
                  ALPH1 ,    ALPH2 ,    ALPH3 ,    ...
                  RATE1 ,    RATE2 ,    RATE3 ,    ...
                  TSC1  ,    TSC2  ,    TSC3  ,    ...
                  TB1   ,    TB2   ,    TB3   ,    ...
                  GM1   ,    ETA11 ,    ETA21 ,    ...
                  GM2   ,    ETA12 ,    ETA22 ,    ...
                  GM3   ,    ETA13 ,    ETA23 ,    ...
                  GM4   ,    ETA14 ,    ETA24 ,    ...
                  TH1   ,    ETA15 ,    ETA25 ,    ...
                  TH2   ,    ETA16 ,    ETA26 ,    ...
                  TH3   ,    ETA17 ,    ETA27 ,    ...
                  TH4   ,    ETA18 ,    ETA28 ,    ...
                  ANGM  ,    DERPDY,    NXGINT,    ...
                  COMSA1,    COMCL ,    NXQDYN,    ...
                  COMSA2,    COMCN ,    NXGDER,    ...
                  GIMA1 ,    GIMP1 ,    NXQTER,    ...
                  GIMA2 ,    GIMP2 ,    GM4D  ,    ...
                  GMA1D ,    GMB1D ,    GM3D  ,    ...
                  GMA2D ,    GMB2D ,    GM2D  ,    ...
                  COERR1,    COERR2,    GM1D  ,    ...
                  COERR3
```

```
    PREPAR  20                                          ....
                  TDESR1.    TDESR2.    TDESR3.    ...
                  TSC1  .    TSC2  .    TSC3  .    ...
                  ERROR1.    ERROR2.    ERROR3.    ...
                  ALPH1 .    ALPH2 .    ALPH3 .    ...
                  RATE1 .    RATE2 .    RATE3 .    ...
                  GM1   .    ETA11 .    COMSA1.    ...
                  GM2   .    ETA12 .    COMSA2.    ...
                  GM3   .    ETA13 .    COMCL .    ...
                  GM4   .    ETA14 .    COMCN .    ...
                  TH1   .    ETA15 .    GIMA1 .    ...
                  TH2   .    ETA16 .    GIMA2 .    ...
                  TH3   .    ETA17 .    GIMB1 .    ...
                  TH4   .    ETA18 .    GIMB2 .    ...
                  GMA1D .    GMA2D .    GMB1D .    ...
                  ANGM  .    TRNCOM.    GMB2D .    ...
                  COERR1.    COERR2.    COERR3
     RANGE ...
                  TRNCO1.    TRNCO2.    TRNCO3.    ...
                  ERROR1.    ERROR2.    ERROR3.    ...
                  ALPH1 .    ALPH2 .    ALPH3 .    ...
                  RATE1 .    RATE2 .    RATE3 .    ...
                  TH1   .    TH2   .    TH3   .    ...
                  TSC1  .    TSC2  .    TSC3  .    ...
                  GM1   .    ETA11 .    ETA21 .    ...
                  GM2   .    ETA12 .    ETA22 .    ...
                  GM3   .    ETA13 .    ETA23 .    ...
                  GM4   .    ETA14 .    ETA24 .    ...
                  TH1   .    ETA15 .    ETA25 .    ...
                  TH2   .    ETA16 .    ETA26 .    ...
                  TH3   .    ETA17 .    ETA27 .    ...
                  TH4   .    ETA18 .    ETA28 .    ...
                  ANGM  .    DERMDY.    NXGINT.    ...
                  COMSA1.    COMSA2.    NXGDYN.    ...
                  COMCL .    COMCN .    NXGDER.    ...
                  GIMA1 .    GIMB1 .    NXGTER.    ...
                  GIMA2 .    GIMB2 .    GM4D  .    ...
                  GMA1D .    GMB1D .    GM3D  .    ...
                  GMA2D .    GMB2D .    GM2D  .    ...
                  COERR1.    COERR2.    GM1D  .    ...
                  COERR3
DERIVATIVE.CID
    CINTERVAL CI=0.05
    XERROR ...
    GM1D  =1.E-8 .GM2D  =1.E-8 .GM1   =1.E-8 .GM2   =1.E-8 ....
    GM3D  =1.E-8 .GM4D  =1.E-8 .GM3   =1.E-8 .GM4   =1.E-8 ....
    RATE1 =1.E-6 .RATE2 =1.E-6 .RATE3 =1.E-6
    MERROR ...
    GM1D  =1.E-8 .GM2D  =1.E-8 .GM1   =1.E-8 .GM2   =1.E-8 ....
    GM3D  =1.E-8 .GM4D  =1.E-8 .GM3   =1.E-8 .GM4   =1.E-8 ....
    RATE1 =1.E-6 .RATE2 =1.E-6 .RATE3 =1.E-6
    NOSORT
    NXGDER=NXGDER+1.
    GMD(1)=GM1D   $  GM(1)=GM1
    GMD(2)=GM2D   $  GM(2)=GM2
    GMD(3)=GM3D   $  GM(3)=GM3
    GMD(4)=GM4D   $  GM(4)=GM4
```

```
  ETD(1,1) =ETD11    $  ET(1,1) =ETA11
  ETD(1,2) =ETD12    $  ET(1,2) =ETA12
  ETD(1,3) =ETD13    $  ET(1,3) =ETA13
  ETD(1,4) =ETD14    $  ET(1,4) =ETA14
  ETD(1,5) =ETD15    $  ET(1,5) =ETA15
  ETD(1,6) =ETD16    $  ET(1,6) =ETA16
  ETD(1,7) =ETD17    $  ET(1,7) =ETA17
  ETD(1,8) =ETD18    $  ET(1,8) =ETA18
  ETD(1,9) =ETD19    $  ET(1,9) =ETA19
  ETD(1,10)=ETD110   $  ET(1,10)=ETA110
  ETD(1,11)=ETD111   $  ET(1,11)=ETA111
  ETD(1,12)=ETD112   $  ET(1,12)=ETA112
  ETD(1,13)=ETD113   $  ET(1,13)=ETA113
  ETD(1,14)=ETD114   $  ET(1,14)=ETA114
  ETD(1,15)=ETD115   $  ET(1,15)=ETA115
  ETD(2,1) =ETD21    $  ET(2,1) =ETA21
  ETD(2,2) =ETD22    $  ET(2,2) =ETA22
  ETD(2,3) =ETD23    $  ET(2,3) =ETA23
  ETD(2,4) =ETD24    $  ET(2,4) =ETA24
  ETD(2,5) =ETD25    $  ET(2,5) =ETA25
  ETD(2,6) =ETD26    $  ET(2,6) =ETA26
  ETD(2,7) =ETD27    $  ET(2,7) =ETA27
  ETD(2,8) =ETD28    $  ET(2,8) =ETA28
  ETD(2,9) =ETD29    $  ET(2,9) =ETA29
  ETD(2,10)=ETD210   $  ET(2,10)=ETA210
  ETD(2,11)=ETD211   $  ET(2,11)=ETA211
  ETD(2,12)=ETD212   $  ET(2,12)=ETA212
  ETD(2,13)=ETD213   $  ET(2,13)=ETA213
  ETD(2,14)=ETD214   $  ET(2,14)=ETA214
  ETD(2,15)=ETD215   $  ET(2,15)=ETA215
  WO(1)=RATE1  $  WO(2)=RATE2  &  WO(3)=RATE3  $  ANGM=HM
COMMENT
  MACRO MACRO SSLEAD Q
  MACRO REDEFINE W,WD
     WD=(G(2)-W)/Q(5)
     W=INTEG(WD,Q(3))
     W(1)=W+Q(4)*WD
  MACRO END
 COMMENT SCAN PLATFORM CONTROLLER
  CLSLON=PULSE(CLSLBG,50000.,(CLSLEN-CLSLBG),T)*SLEWON
  CNSLON=PULSE(CNSLBG,50000.,(CNSLEN-CNSLBG),T)*SLEWON
  IF(T.GT.BOXEND)BOXON=0.0
  CLBXON=(PULSE(CLBXB1,CLBXFQ,CLBXWD,T)...
         -PULSE(CLBXB2,CLBXFQ,CLBXWD,T))*BOXON
  CNBXON= PULSE(CNBXBG,CNBXFQ,CNBXWD,T)*BOXON
  COMCL=INTEG((CLSLON+CLBXON)*CLRATE,0.)
  COMCN=INTEG((CNSLON+CNBXON)*CNRATE,0.)
 COMMENT SOLAR ARRAYS CONTROLLER
  A1SLON=PULSE(A1SLBG,50000.,(A1SLEN-A1SLBG),T)*SASLEW
  COMSA1=(-ALPH2*SAPSUN+INTEG(A1SLON+A1SLRT,0.))*(1.-SALOCK)
  A2SLON=PULSE(A2SLBG,50000.,(A2SLEN-A2SLBG),T)*SASLEW
  COMSA2=(-ALPH2*SAPSUN+INTEG(A2SLON+A2SLRT,0.))*(1.-SALOCK)
 COMMENT SOLAR ARRAY HINGE TORQUES
  ERRSA1=(COMSA1-GM1)
  ERRSA2=(COMSA2-GM2)
  FILSA1=REALPL(TAUFSA,ERRSA1,FLSA1I)
  FILSA2=REALPL(TAUFSA,ERRSA2,FLSA2I)
```

```
      SSLEAD  LLSA1,FILSA1,LLSA1I,TAU1SA,TAU2SA
      SSLEAD  LLSA2,FILSA2,LLSA2I,TAU1SA,TAU2SA
      ERPPA1=ERRSA1-KKRPSA*GM1D
      ERPPA2=ERRSA2-KKRPSA*GM2D
      TM1=KSAKA*LLSA1*LLAGON + KKSA*ERPPA1*RPPON
      TM2=KSAKA*LLSA2*LLAGON + KKSA*ERPPA2*RPPON
    COMMENT SCAN PLATFORM HINGE TORQUES
      TM3=-KCL*(GM3-COMCL)-BCL*GM3D
      TM4=-KCN*(GM4-COMCN)-BCN*GM4D
   COMMENT
  COMMENT   GENERATE TURN RAPP INPUT SIGNALS
      TRNTRU=PULSE(20.0,3000.0,TRNTIM,T)
      TRNCO1 =INTEG(TRN1ON*TRN1RT*TRNTRU,0.)
      TRNCO2 =INTEG(TRN2ON*TRN2RT*TRNTRU,0.)
      TRNCO3 =INTEG(TRN3ON*TRN3RT*TRNTRU,0.)
      TRNCOM = TRNCO1 + TRNCO2 + TRNCO3
  COMMENT  CELESTIAL SENSORS
      THETA1=REALPL(TAUS,ALPH1,THTA1I)
      THETA2=REALPL(TAUS,ALPH2,THTA2I)
      THETA3=REALPL(TAUS,ALPH3,THTA3I)
      ERROR1=TRNCO1 -THETA1
      ERROR2=TRNCO2 -THETA2
      ERROR3=TRNCO3 -THETA3
  COMMENT  **********************************************
  COMMENT  ****** TVC CONTROLLER DYNAMICS SECTION ******
  COMMENT  COMPUTE GAMMA COMMANDS
      FILX=REALPL(TAUF,ERROR1,FILXI)
      FILY=REALPL(TAUF,ERROR2,FILYI)
      FILZ=REALPL(TAUF,ERROR3,FILZI)
      SSLEAD  LLX,ERROR1,LLXI,TAU1LL,TAU2LL
      SSLEAD  LLY,ERROR2,LLYI,TAU1LL,TAU2LL
      SSLEAD  LLZ,ERROR3,LLZI,TAU1LL,TAU2LL
      ERPPX=ERROR1-KKRPX*RATE1
      ERPPY=ERROR2-KKRPY*RATE2
      ERPPZ=ERROR3-KKRPZ*RATE3
      COERR1=LLX*LLAGON + ERPPX*RPPON
      COERR2=LLY*LLAGON + ERPPY*RPPON
      COERR3=LLZ*LLAGON + ERPPZ*RPPON
      GAMXC=LLX*KY*LLAGON + ERPPX*KKY*RPPON
      GAMYC=LLY*KY*LLAGON + ERPPY*KKY*RPPON
      GAMZC=LLZ*KZ*LLAGON + ERPPZ*KKZ*RPPON
  COMMENT   COMPUTE THE DESIRED TORQUES
      TDESR1 = GAMXC*FC*SENG1(3)
      TDESR2 = GAMYC*FC*SENG1(3)
      TDESR3 = GAMZC*FC*SENG1(2)
  COMMENT  COMPUTE GIMBAL ANGLE COMMANDS FROM GAMMA COMMANDS
      GIMA1C=-GAMYC*GAMZC
      GIMA2C= GAMYC*GAMZC
      GIMB1C=-GAMXC
      GIMB2C= GAMXC
  COMMENT  COMPUTE GIMBAL DYNAMICS
      GMA1DD=GIMA1C*.04-0.283*GMA1D-.04*GIMA1
      GMA2DD=GIMA2C*.04-0.283*GMA2D-.04*GIMA2
      GMB1DD=GIMB1C*.04-0.283*GMB1D-.04*GIMB1
      GMB2DD=GIMB2C*.04-0.283*GMB2D-.04*GIMB2
      GMA1D=LIMINT(GMA1DD,0.,-0.1745,0.1745)
      GMA2D=LIMINT(GMA2DD,0.,-0.1745,0.1745)
```

```
    GMB1D=LIMINT(GMB1DD,0.,-0.1745,0.1745)
    GMB2D=LIMINT(GMB2DD,0.,-0.1745,0.1745)
    GIMA1=LIMINT(GMA1D,0.,-0.5235,0.5235)
    GIMA2=LIMINT(GMA2D,0.,-0.5235,0.5235)
    GIMB1=LIMINT(GMB1D,0.,-0.5235,0.5235)
    GIMB2=LIMINT(GMB2D,0.,-0.5235,0.5235)
COMMENT  COMPUTE GIMBALLED ENGINES REACTION TORQUES ...
         TAIL-WAGS-DOG (TWD) EFFECT OF GIMBALLING ENGINES
    TWD1X = -IGENG1*GMB1DD
    TWD1Y = -IGENG1*(GMA1DD*COS(GIMB1)-GMB1D*GMA1D*SIN(GIMB1))
    TWD1Z = -IGENG1*(GMA1DD*SIN(GIMB1)+GMB1D*GMA1D*COS(GIMB1))
    TWD2X = +IGENG2*GMB2DD
    TWD2Y = +IGENG2*(GMA2DD*COS(GIMB2)-GMB2D*GMA2D*SIN(GIMB2))
    TWD2Z = -IGENG2*(GMA2DD*SIN(GIMB2)+GMB2D*GMA2D*COS(GIMB2))
    TWDX = TWD1X + TWD2X
    TWDY = TWD1Y + TWD2Y
    TWDZ = TWD1Z + TWD2Z
COMMENT  RAISING THRUST UP IN 20 SEC
    FCHALF=FC*(1-COS(PIF*T/20.0))/4.0
    IF (T.GT.19.999995) FCHALF=FC/2.0
COMMENT  COMPUTE FORCE AND TORQUE ON BUS
    FB1X=-FCHALF*SIN(GIMA1)
    FB1Y=+FCHALF*SIN(GIMB1)*COS(GIMA1)
    FB1Z=-FCHALF*COS(GIMB1)*COS(GIMA1)
    FB2X=+FCHALF*SIN(GIMA2)
    FB2Y=-FCHALF*SIN(GIMB2)*COS(GIMA2)
    FB2Z=-FCHALF*COS(GIMB2)*COS(GIMA2)
    FBX=FB1X+FB2X
    FBY=FB1Y+FB2Y
    FBZ=FB1Z+FB2Z
    TENG1X=+FB1Z*RENG1(2)-FB1Y*RENG1(3)
    TENG1Y=-FB1Z*RENG1(1)+FB1X*RENG1(3)
    TENG1Z=+FB1Y*RENG1(1)-FB1X*RENG1(2)
    TENG2X=+FB2Z*RENG2(2)-FB2Y*RENG2(3)
    TENG2Y=-FB2Z*RENG2(1)+FB2X*RENG2(3)
    TENG2Z=+FB2Y*RENG2(1)-FB2Y*RENG2(2)
    TBX=TENG1X+TENG2X+TWDX
    TBY=TENG1Y+TENG2Y+TWDY
    TBZ=TENG1Z+TENG2Z+TWDZ
COMMENT  COMPUTE TORQUE ON S/C CENTER OF MASS
    TENG1X=+FB1Z*SENG1(2)-FB1Y*SENG1(3)
    TENG1Y=-FB1Z*SENG1(1)+FB1X*SENG1(3)
    TENG1Z=+FB1Y*SENG1(1)-FB1X*SENG1(2)
    TENG2X=+FB2Z*SENG2(2)-FB2Y*SENG2(3)
    TENG2Y=-FB2Z*SENG2(1)+FB2X*SENG2(3)
    TENG2Z=+FB2Y*SENG2(1)-FB2X*SENG2(2)
    TSCX=TENG1X+TENG2X+TWDX
    TSCY=TENG1Y+TENG2Y+TWDY
    TSCZ=TENG1Z+TENG2Z+TWDZ
COMMENT  ****** TVC CONTROLLER SECTION END ******
COMMENT  ****************************************
  COMMENT
COMMENT  ****************************
COMMENT  ******  FLEX DYNAMICS ******
  COMMENT FORCES AND TORQUES ACTING ON BUS AND HINGES
    TB1=TBX+TDIST1              $  TB(1)=TB1
    TB2=TBY+TDIST2              $  TB(2)=TB2
```

```
      TH3=TH2+TDIST3              $  TB(3)=TB3
      FM(1)=FBX
      FM(2)=FBY
      FM(3)=FBZ
      TM(1)=TH1
      TM(2)=TH2
      TM(3)=TH3
      TM(4)=TH4
   COMMENT  TORQUES ON S/C
      TSC1 = TSCX + TDIST1
      TSC2 = TSCY + TDIST2
      TSC3 = TSCZ + TDIST3
      COMMENT
   COMMENT   SOLVE FOR SYSTEM ACCELERATIONS
      CALL MRATE(NC,TH,TP,TS,FB,FS,TF,FF,GM,GMD,GMDD,ET,ETD,...
                 WO,WDOT,ETDD,HW,CK)
      COMMENT
      COMMENT SYSTEM RATES AND POSITIONS
      COMMENT
      RATE1 =INTEG(WDOT(1),RATE11)
      RATE2 =INTEG(WDOT(2),RATE21)
      RATE3 =INTEG(WDOT(3),RATE31)
      ALPH1 =INTEG(RATE1,ALPH11)
      ALPH2 =INTEG(RATE2,ALPH21)
      ALPH3 =INTEG(RATE3,ALPH31)
      P20,P10,P2D,P3D=HC*(HCK,P2,P1,P2,P3,RATE1,RATE2,RATE3)
      P2    =INTEG(P2D,1.000)
      P1    =INTEG(P1D,0.000)
      P2    =INTEG(P2D,0.000)
      P3    =INTEG(P3D,0.000)
      GM1D  =INTEG(WDOT(4),0.)
      GM2D  =INTEG(WDOT(5),0.)
      GM3D  =INTEG(WDOT(6),0.)
      GM4D  =INTEG(WDOT(7),0.)
      GM1   =INTEG(GM1D,0.)
      GM2   =INTEG(GM2D,0.)
      GM3   =INTEG(GM3D,0.)
      GM4   =INTEG(GM4D,0.)
      ETD11 =INTEG(ETDD(1,1) ,0.)   $  ETA11 =INTEG(ETD11 ,0.)
      ETD12 =INTEG(ETDD(1,2) ,0.)   $  ETA12 =INTEG(ETD12 ,0.)
      ETD13 =INTEG(ETDD(1,3) ,0.)   $  ETA13 =INTEG(ETD13 ,0.)
      ETD14 =INTEG(ETDD(1,4) ,0.)   $  ETA14 =INTEG(ETD14 ,0.)
      ETD15 =INTEG(ETDD(1,5) ,0.)   $  ETA15 =INTEG(ETD15 ,0.)
      ETD16 =INTEG(ETDD(1,6) ,0.)   $  ETA16 =INTEG(ETD16 ,0.)
      ETD17 =INTEG(ETDD(1,7) ,0.)   $  ETA17 =INTEG(ETD17 ,0.)
      ETD18 =INTEG(ETDD(1,8) ,0.)   $  ETA18 =INTEG(ETD18 ,0.)
      ETD19 =INTEG(ETDD(1,9) ,0.)   $  ETA19 =INTEG(ETD19 ,0.)
      ETD110=INTEG(ETDD(1,10),0.)   $  ETA110=INTEG(ETD110,0.)
      ETD111=INTEG(ETDD(1,11),0.)   $  ETA111=INTEG(ETD111,0.)
      ETD112=INTEG(ETDD(1,12),0.)   $  ETA112=INTEG(ETD112,0.)
      ETD113=INTEG(ETDD(1,13),0.)   $  ETA113=INTEG(ETD113,0.)
      ETD114=INTEG(ETDD(1,14),0.)   $  ETA114=INTEG(ETD114,0.)
      ETD115=INTEG(ETDD(1,15),0.)   $  ETA115=INTEG(ETD115,0.)
      ETD21 =INTEG(ETDD(2,1) ,0.)   $  ETA21 =INTEG(ETD21 ,0.)
      ETD22 =INTEG(ETDD(2,2) ,0.)   $  ETA22 =INTEG(ETD22 ,0.)
      ETD23 =INTEG(ETDD(2,3) ,0.)   $  ETA23 =INTEG(ETD23 ,0.)
      ETD24 =INTEG(ETDD(2,4) ,0.)   $  ETA24 =INTEG(ETD24 ,0.)
```

```
      ETD25 =INTEG(ETDD(2,5) ,0.)   $  ETA25 =INTEG(ETD25 ,0.)
      ETD26 =INTEG(ETDD(2,6) ,0.)   $  ETA26 =INTEG(ETD26 ,0.)
      ETD27 =INTEG(ETDD(2,7) ,0.)   $  ETA27 =INTEG(ETD27 ,0.)
      ETD28 =INTEG(ETDD(2,8) ,0.)   $  ETA28 =INTEG(ETD28 ,0.)
      ETD29 =INTEG(ETDD(2,9) ,0.)   $  ETA29 =INTEG(ETD29 ,0.)
      ETD210=INTEG(ETDD(2,10),0.)   $  ETA210=INTEG(ETD210,0.)
      ETD211=INTEG(ETDD(2,11),0.)   $  ETA211=INTEG(ETD211,0.)
      ETD212=INTEG(ETDD(2,12),0.)   $  ETA212=INTEG(ETD212,0.)
      ETD213=INTEG(ETDD(2,13),0.)   $  ETA213=INTEG(ETD213,0.)
      ETD214=INTEG(ETDD(2,14),0.)   $  ETA214=INTEG(ETD214,0.)
      ETD215=INTEG(ETDD(2,15),0.)   $  ETA215=INTEG(ETD215,0.)
COMMENT  ******  FLEX DYNAMICS END  ******
COMMENT  ********************************
END
END
END
TERMINAL
      FIN.. CONTINUE
      DEBUG
      NXQTER=NXQTER+1.
      WRITE(6,F23)T,NXQINT,NXQDYN,NXQDER,NXQTER
END
END
```

```
CRABFL/GAS-MASTER
PROGRAM THREE AXES GAS CID FLEX 2 SOLAR PANELS UNDEPLOYED MAG BOOM    ...
      TWO DEGREE OF FREEDOM SCAN PLATFORM (BODY B5)                   ...
      STOWED HIGH GAIN ANTENNA                                        ...
      CONDITIONS AT TEMPLE 2 RENDEZVOUS
 COMMENT                                                              ...
      REVISED 04 NOV 79                                               ...
      METRIC UNITS THROUGHOUT                                         ...
      BUS DATA FROM H. PRICE'S MOM PROGRAM                            ...
      PANEL DATA FROM K. GUPTA'S FINITE EL MODEL (SPAR OCT 79)        ...
      NEON GAS JETS CONTROL LOOP WITH LEDLAG OR KRP  (NOV 79)         ...
      FOR SPECIFIC MANEUVER PARAMETERS SEE LINE 143
 COMMENT
  INTEGER NC,NF,H(3,2),F(2,3),PI(5),J,K,PLTNBR,L,M,N,NN,MANNBR
  ARRAY CMBLV(3)      , CMSLV(3,3)    ,HINGLV(3,3)    ,   TEMPST(8)   ....
        MM(7)         ,    MS(3,7)    ,    PB(3,3)    ,    PS(3,3,3)  ....
        C(4,3)        ,    TM(4)      ,    TB(3)      ,    TS(3,3)    ....
        FB(3)         ,    FS(3,3)    ,    GM(4)      ,   GMD(4)      ....
        GMDD(4)       ,   EIG(2,6,15),   REC(2,6,15),    RF(2,1,3)  ....
        WF(2,15)      ,    ZF(2,15)   ,    TF(2,1,3)  ,    FF(2,1,3)  ....
        ET(2,15)      ,   ETD(2,15)   ,    WO(3)      ,   WFMZ(2,15)  ....
        CK(2,3)       ,   CMSCLV(3)   ,    SJTC1(3)   ,    SJTC2(3)   ....
        JTC1LV(3)     ,   JTC2LV(3)   ,    RJTC1(3)   ,    RJTC2(3)
  DOUBLE PRECISION WDOT(7),ETDD(2,15) $ LOGICAL NOPLOT $ DROP
  DATA ((H(I,J),J=1,2)/0,1/
  DATA ((H(2,J),J=1,2)/0,1/
  DATA ((H(3,J),J=1,2)/0,2/
  DATA ((F(1,J),J=1,3)/1,1,15/ $ DATA ((F(2,J),J=1,3)/2,1,15/
  DATA PI/3,0,1,1,1/
 COMMENT
  DATA MM...
  /1824.304, 2635.642, 1769.269, -50.133, -114.634, -46.249, 1756.474/
  DATA ((MS(1,J),J=1,7)...
    /22084.00, 234.61, 21876.00, +158.02, 0.00, 0.00, 176.818/
  DATA ((MS(2,J),J=1,7)...
    /22084.00, 234.61, 21876.00, -158.02, 0.00, 0.00, 176.818/
  DATA ((MS(3,J),J=1,7)...
    /13.3  ,  7.5  , 16.5  , +2.1  , -0.2  , -1.0  , 90.19 /
 COMMENT
 COMMENT POS VEC SPECIF LOCATION OF CM'S & HINGES-IN S/C COORDINATES
  DATA CMPLV /.0703, .0190, .6266 /
  DATA ((CMSLV(1,J),J=1,3)/ 0.00, +19.37645 ,+0.2/
  DATA ((CMSLV(2,J),J=1,3)/ 0.00, -19.37645 ,+0.2/
  DATA ((CMSLV(3,J),J=1,3)/-1.3691,  -0.370, -0.7893/
  DATA ((HINGLV(1,J),J=1,3)/ 0.00 ,0.00 ,+0.2/
  DATA ((HINGLV(2,J),J=1,3)/ 0.00 ,0.00 ,+0.2/
  DATA ((HINGLV(3,J),J=1,3)/-1.3691,  -0.370, -0.7893/
 COMMENT
 COMMENT  JET CLUSTERS LOCATIONS - IN S/C COORDINATES
  DATA JTC1LV /0.0,+1.27,3.21/ $ DATA JTC2LV /0.0,-1.27,3.21/
 COMMENT
 COMMENT HINGE ORIENTATIONS
  DATA ((G(1,J),J=1,3)/ 0.000000,+1.000000, 0.000000/
  DATA ((G(2,J),J=1,3)/ 0.000000,+1.000000, 0.000000/
  DATA ((G(3,J),J=1,3)/ 0.000000, 0.000000,+1.000000/
  DATA ((G(4,J),J=1,3)/ 0.000000,+1.000000, 0.000000/
 COMMENT
```

```
COMMENT RIGID ELASTIC COUPLING COEFFICIENTS FOR THE 2 PANELS ...
        SPAR MODEL BY K. GUPTA OF OCT 79                    ...
        CONDITIONS AT TEMPLE 2 RENDEZVOUS
 DATA (((REC(I,J,K),J=1,6),K=1,12)/...
-11.18730,    .06995,   -.04629,   -.05239,    .03969,  68.52600,...
  -.51909,   -.09919,    .08782,   1.02460,   -.04128, -88.99000,...
 -3.13480,    .08922,   -.19750,  -2.21670,    .03269,  -4.53950,...
  -.13282,   -.01158,   9.57620, 104.93000,   -.65980,    .76180,...
   .80228,    .06203,    .11783,   1.25900,    .04004,  25.28500,...
  1.46382,   -.04164,   -.02803,   -.24815,  -1.37720,  10.39600,...
   .15877,   -.00148,    .00585,    .05069,  12.17000,   1.12110,...
   .06603,    .00457,    .01828,    .11299,   -.13019,    .54573,...
   .07572,    .00979,    .02564,    .13027,   4.03850,   1.15200,...
   .54315,    .02260,    .00615,    .06512,   -.47812,  11.24900,...
  -.07393,    .00837,    .02850,    .10434,    .26855,  -1.51880,...
  -.23045,    .01450,    .03038,    .08424,   2.25460,  -2.39780/
 DATA (((REC(I,J,K),J=1,6),K=13,15)/...
   .81469,   -.00525,    .00957,    .00618,    .87656,   7.36440,...
  -.11917,   -.01331,   -.03352,   -.05150,   -.33515,  -1.13710,...
   .29823,    .00182,    .00337,    .00137,    .23342,   5.35990/
 DATA (((REC(2,J,K),J=1,6),K=1,12)/...
-11.18730,   -.06995,    .04629,   -.05239,   -.03969, -68.52600,...
  -.51909,    .09919,   -.08782,   1.02460,    .04128,  88.99000,...
 -3.13480,   -.08922,    .19750,  -2.21670,   -.03269,   4.53950,...
  -.13282,    .01158,  -9.57620, 104.93000,    .65980,   -.76180,...
   .80228,   -.06203,   -.11783,   1.25900,   -.04004, -25.28500,...
  1.46382,    .04164,    .02803,   -.24815,   1.37720, -10.39600,...
   .15877,    .00148,   -.00585,    .05069, -12.17000,  -1.12110,...
   .06603,   -.00457,   -.01828,    .11299,   -.13019,   -.54573,...
   .07572,   -.00979,   -.02564,    .13027,  -4.03850,  -1.15200,...
   .54315,   -.02260,   -.00615,    .06512,   -.47812, -11.24900,...
  -.07393,   -.00837,   -.02850,    .10434,   -.26855,   1.51880,...
  -.23045,   -.01450,   -.03038,    .08424,  -2.25460,   2.39780/
 DATA (((REC(2,J,K),J=1,6),K=13,15)/...
   .81469,    .00525,   -.00957,    .00618,   -.87656,  -7.36440,...
  -.11917,    .01331,    .03352,   -.05150,    .33515,   1.13710,...
   .29823,   -.00182,   -.00337,    .00137,   -.23342,  -5.35990/
COMMENT
COMMENT PANELS FREQUENCIES (IN HERTZ) AND DAMPING
 DATA (WFHZ(1,J),J=1,15)/...
  0.065226 , 0.126145 , 0.192507 , 0.226612 ,...
  0.261074 , 0.329296 , 0.333713 , 0.351529 ,...
  0.378027 , 0.397748 , 0.410395 , 0.443883 ,...
  0.453118 , 0.478315 , 0.501820 /
 DATA (WFHZ(2,J),J=1,15)/...
  0.065226 , 0.126145 , 0.192507 , 0.226612 ,...
  0.261074 , 0.329296 , 0.333713 , 0.351529 ,...
  0.378027 , 0.397748 , 0.410395 , 0.443883 ,...
  0.453118 , 0.478315 , 0.501820 /
 DATA (ZF(1,J),J=1,15)/15*0.004/
 DATA (ZF(2,J),J=1,15)/15*0.004/
       DO L2 K=1,15
        WF(1,K)=WFHZ(1,K)*2.*PIF
        WF(2,K)=WFHZ(2,K)*2.*PIF
 L2..  CONTINUE
COMMENT
COMMENT
```

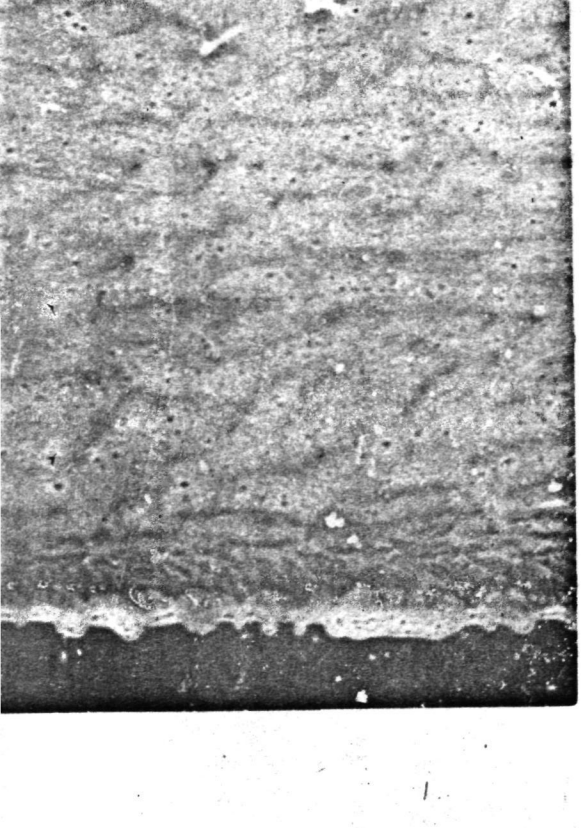

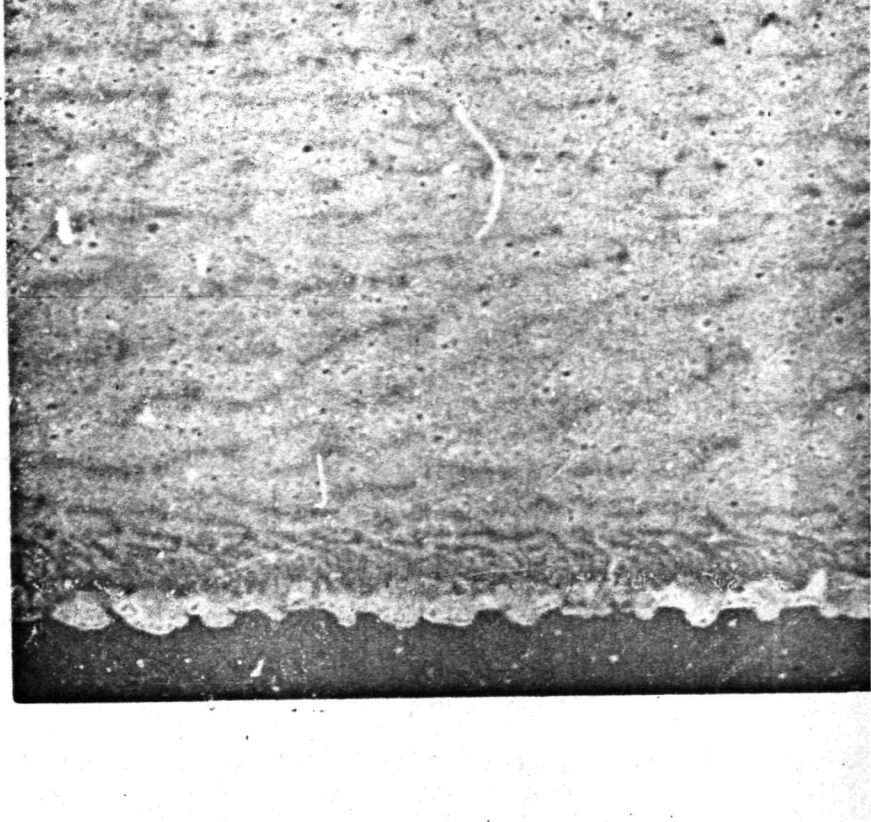


```
SLV(1,K)+MS(2,7)*CMSLV...

MS(2,7)+MS(3,7))

ND CMB TO ENG VECTORS

(K)=JTC2LV(K)-CMBLV(K)
2(K)=JTC2LV(K)-CMSCLV(K)
```

```
**********************    ...
                      *    ...
 FOLLOWS:             *    ...
---------             *    ...
                      *    ...
 EXHAUST AXIS )       *    ...
                      *    ...
 )                    *    ...
                      *    ...
                      *    ...
                      *    ...
**********************    ...
                      *    ...
UMBER                 *    ...
-----                 *    ...
```

```
      **********************************
      *
      *     SET SIMULATION TIME
      *     -------------------
      *
CONSTANT                 FINTIM =  9.9
 COMMENT *
      **********************************
      *
      *     SET INITIAL CONDITIONS
      *     ----------------------
      *
      *     AXIS1            AXIS2
      *     -----            -----
      *
      *  DISTURBANCE TORQUES
      *
CONSTANT     TDIST1=0.0   ,   TDIST2=.209E-
 COMMENT *
      *  INITIAL RATES
      *
CONSTANT     RATE1I=0.0   ,   RATE2I=0.0
 COMMENT *
      *  INITIAL ANGULAR POSITION ERRORS
      *
CONSTANT     ALPH1I=0.0   ,   ALPH2I=0.0
 COMMENT *
      *  TURN COMMANDS
      *
CONSTANT     TRNTIM= 200.00
CONSTANT   TRN1RT=8.72664E-5,TRN2RT=4.36332E-
 COMMENT *
      *  ------------------------------
      *     SOLAR ARRAY
```

```
                                                                    ...
                                                                    ...
        ************************************************************...
        *                                                          *...
        *      SET SIMULATION TIME                                 *...
        *      -------------------                                 *...
        *                                                          *
CONSTANT                    FINTIM =  9.9
 COMMENT *                                                         *...
        ************************************************************...
        *                                                          *...
        *      SET INITIAL CONDITIONS                              *...
        *      ----------------------                              *...
        *                                                          *...
        *      AXIS1            AXIS2            AXIS3             *...
        *      -----            -----            -----             *...
        *                                                          *...
        *   DISTURBANCE TORQUES                                    *...
        *                                                          *
CONSTANT      TDIST1=0.0    ,   TDIST2=.209E-4,  TDIST3=0.0
 COMMENT *                                                         *...
        *   INITIAL RATES                                          *...
        *                                                          *
CONSTANT      RATE1I=0.0    ,   RATE2I=0.0    ,   RATE3I=0.0
 COMMENT *                                                         *...
        *   INITIAL ANGULAR POSITION ERRORS                        *...
        *                                                          *
CONSTANT      ALPH1I=0.0    ,   ALPH2I=0.0    ,   ALPH3I=0.0
 COMMENT *                                                         *...
        *   TURN COMMANDS                                          *...
        *                                                          *
CONSTANT      TRNTIM= 200.00
CONSTANT   TRN1RT=8.72664E-5,TRN2RT=4.36332E-3,TRN3RT=8.72664E-5
 COMMENT *                                                         *...
        *                                                          *...
        *      SOLAR ARRAY                                         *...
        *      -----------                                         *...
        *                                                          *...
        *   SOLAR ARRAY COMMANDS                                   *...
        *                                                          *
CONSTANT      SAPSUN=0.0    ,   SALOCK=1.0    ,   SASLEW=0.0
 COMMENT *                                                         *...
        *                                                          *...
        *                                                          *...
        *      SCAN PLATFORM                                       *...
        *      -------------                                       *...
        *                                                          *...
        *   SCAN PLATFORM COMMANDS                                 *...
        *                                                          *
CONSTANT      SCANON=0.0    ,   SLEWON=0.0    ,   BOXON =0.0
 COMMENT *                                                         *...
        *                                                          *...
        *                                                          *...
        ************************************************************
 COMMENT
 COMMENT
 COMMENT
```

```
  COMMENT   CALCULATE THE S/C CENTER OF MASS
            DO CM1 K=1,3
            CMSCLV(K)=MB(7)*CMBLV(K)+MS(1,7)*CMSLV(1,K)+MS(2,7)*CMSLV...
            (2,K)+MS(3,7)*CMSLV(3,K)
            CMSCLV(K)=CMSCLV(K)/(MB(7)+MS(1,7)+MS(2,7)+MS(3,7))
            CM1..  CONTINUE
            WRITE (6,F3) CMSCLV
  COMMENT COMPUTATION OF PB AND PS VECTORS AND CMB TO ENG VECTORS
            DO L1 K=1,3
            RJTC1(K)=JTC1LV(K)-CMBLV(K) $ RJTC2(K)=JTC2LV(K)-CMBLV(K)
            SJTC1(K)=JTC1LV(K)-CMSCLV(K) $ SJTC2(K)=JTC2LV(K)-CMSCLV(K)
            PB(1,K)=HINGLV(1,K)-CMBLV(K)
            PB(2,K)=HINGLV(2,K)-CMBLV(K)
            PB(3,K)=HINGLV(3,K)-CMBLV(K)
            PS(1,1,K)=HINGLV(1,K)- CMSLV(1,K)
            PS(2,2,K)=HINGLV(2,K)-CMSLV(2,K)
            PS(3,3,K)=HINGLV(3,K)-CMSLV(3,K)
   L1..     CONTINUE
 PICKUP
INITIAL
 COMMENT ********************************************************    ...
         *                                                      *    ...
         *      DEFINE THE BUS FIXED AXES AS FOLLOWS:           *    ...
         *      -------------------------------------           *    ...
         *                                                      *    ...
         *      AXIS3 = Z ( ION ENGINE PLUME EXHAUST AXIS )     *    ...
         *                                                      *    ...
         *      AXIS2 = Y ( SOLAR ARRAY AXIS )                  *    ...
         *                                                      *    ...
         *      AXIS1 = X                                       *    ...
         *                                                      *    ...
         ********************************************************    ...
         *                                                      *    ...
         *      SELECT THE MANEUVER BY ITS NUMBER               *    ...
         *      ---------------------------------               *    ...
         *                                                      *    ...
         *      1 - TURN ENTIRE SPACECRAFT ABOUT AXIS1          *    ...
         *                                                      *    ...
         *      2 - TURN ENTIRE SPACECRAFT ABOUT AXIS2          *    ...
         *                                                      *    ...
         *      3 - TURN ENTIRE SPACECRAFT ABOUT AXIS3          *    ...
         *                                                      *    ...
         *      4 - TURN   BUS ONLY ABOUT AXIS2                 *    ...
         *          WHILE KEEPING ARRAYS ON THE SUN             *    ...
         *                                                      *    ...
         *      5 - ACQUISITION OF CEL REFERENCES               *    ...
         *                                                      *    ...
         *      6 - SCAN PLATFORM SLEW OR BOXSCAN               *    ...
         *                                                      *    ...
         ********************************************************    ...
         *                                                      *    ...
         *                                                      *
CONSTANT                      MANEUV = 1.0
 COMMENT *                                                      *    ...
         *                                                      *    ...
         ********************************************************    ...
                                                                     ...
```

```
    IF(SALOCK.GT.0.9)SASLEW=0.0
    IF(SAPSUN.LT.0.9)GO TO SA1
    SALOCK=0.
    SASLEW=0.0
   SA1..CONTINUE
    CONSTANT A1SLBG=    0.00  ,  A1SLEN=    50.00  ,  A1SLRT=0.00438
    CONSTANT A2SLBG=    0.00  ,  A2SLEN=    50.00  ,  A2SLRT=0.00438
COMMENT
   COMMENT SP CONTROL LOOP PARAMETERS AND IC'S
    CONSTANT KCL    =1500.     ,  KCN    =1500.
    CONSTANT BCL    = 148.50   ,  BCN    = 220.25
   COMMENT SCAN SELECTION
    IF(SLEWON.GT.0.9)BOXON=0.0
    IF(SCANON.GT.0.9)GO TO SC1
    SLEWON=0.0
    BOXON =0.0
   SC1..CONTINUE
    CONSTANT CLRATE=0.017453 ,  CNRATE=0.017453
    CONSTANT CLSLBG=    0.00  ,  CLSLEN=    30.00
    CONSTANT CNSLBG=  100.00  ,  CNSLEN=   130.00
    CONSTANT CLBXB1=    0.0   ,  CLBXFQ=    30.00  ,  CLBXWD=9.0
    CONSTANT CLBXB2=15.00
    CONSTANT CNBXBG=11.00     ,  CNBXFQ=    15.00  ,  CNBXWD=2.00
    CONSTANT BCYEND=60.00
    CONSTANT TINITL=0.000000
    CONSTANT PIE=3.14159265
   COMMENT
COMMENT    SET INITIAL  SS, FILTER, AND LL VALUES
    FLSA1I=-ALPH2I*SAPSUN
    FLSA2I=-ALPH2I*SAPSUN
    LLSA1I=FLSA1I
    LLSA2I=FLSA2I
    THTA1I=ALPH1I
    THTA2I=ALPH2I
    THTA3I=ALPH3I
    FILXI=-THTA1I
    FILYI=-THTA2I
    FILZI=-THTA3I
    LLXI=FILXI
    LLYI=FILYI
    LLZI=FILZI
COMMENT
COMMENT     SET UP PLOTTING INFORMATION
             NOPLOT = .FALSE.
    CONSTANT PLTNBR=0                 ,...
             INTRV1=10.0              ,...
             NEWINT=100.0             ,...
             INTRV2=50.0
             SWITCH=NEWINT
COMMENT
    NC=3  $  NF=2
    NXQDYN=0.
    NXQDER=0.
    NXQTER=0.
    NXQINT=NXQINT+1.
    CALL XRDYFL(NC,H,MB,MS,PH,PS,G,PI,NF,F,EIG,REC,RF,WF,ZF)
    DEBUG
```

```
              TRN1ON=0.0 $ TRN2ON=0.0 $ TRN3ON=0.0
              SAPSUN=0.0 $ SCANON=0.0
              MANNBR = MANFUV + .5
              GO TO (M1,M2,M3,M4,M5,M6), MANNBR
*   M1..      TRN1ON=1.0
              GO TO MEND
    M2..      TRN2ON=1.0
              GO TO MEND
    M3..      TRN3ON=1.0 $ SALOCK=1.0
              GO TO MEND
    M4..      TRN2ON=1.0 $ SAPSUN=1.0
              GO TO MEND
    M5..      GO TO MEND
    M6..      SCANON=1.0 $ SLEWON=0.0 $ BOXON=1.0
    MEND..    CONTINUE
COMMENT
COMMENT
COMMENT  ***************************************
COMMENT  ******  GAS CONTROLLER PARAMETERS  ******
COMMENT SPECIFY FILTER,S&F LEAD-LAGS, AND KRP PARAMETERS
    CONSTANT  SLOWLL = 1.0  ,  FASTLL= 0.0,  RPPON = 0.0      ****
              SKX=0.5       ,  FKX=0.5     ,  KKX=0.5         ****
              SKY=0.5       ,  FKY=0.5     ,  KKY=0.5         ****
              SKZ=0.5       ,  FKZ=0.5     ,  KKZ=0.5         ****
              TAUF=15.                     ,  KKRPX=20.0      ****
              STAU1L=200.   ,  FTAU1L=60.  ,  KKRPY=20.0      ****
              STAU2L=10.    ,  FTAU2L=10.  ,  KKRPZ=20.0
          LLAGON=SLOWLL+FASTLL
          KX     =   SKX*SLOWLL+   FKX*FASTLL
          KY     =   SKY*SLOWLL+   FKY*FASTLL
          KZ     =   SKZ*SLOWLL+   FKZ*FASTLL
          TAU1LL=STAU1L*SLOWLL+FTAU1L*FASTLL
          TAU2LL=STAU2L*SLOWLL+FTAU2L*FASTLL+RPPON*99.
COMMENT SPECIFY DEADBANDS DB20 AND DB100 WHICH ARE          ***
        THE MIN ON TIME (20 MS) DB AND THE FULL-ON (100 MS) DB
    CONSTANT DB20=4.36332E-3  ,  DB100=8.72665E-3
COMMENT GAS JET ADJUSTMENT FOR 20 MS MOT
    FONEJT=0.0445*3./2.
    CONSTANT ISP=75.
    GASFAC=2.*1000./(9.81*ISP)
    TTONX1=0.  $  TTONY1=0.  $  TTONZ=0.
COMMENT  ******  GAS CONTROLLER PARAMETERS END  ******
COMMENT  ***************************************
COMMENT  ******  CELESTIAL SENSOR PARAMETERS  ********
    CONSTANT  TAUS=1.0
COMMENT  ******  SA AND SP  CHARACTERISTICS  *********
COMMENT SPECIFY SA FILTER , S&F LEAD-LAGS , AND KRP PARAMETERS
    CONSTANT  SKSA=3.41     , FKSA=43.16    ,  KKSA=15.000     ****
              KA=0.015
    CONSTANT  STAU1A=200.   , FTAU1A=60.    ,  KKRPSA=5.53     ****
              STAU2A=20.    , FTAU2A=20.                       ****
              TAUFSA=15.
          KSA    =  SKSA*SLOWLL+  FKSA*FASTLL
          TAU1SA=STAU1A*SLOWLL+FTAU1A*FASTLL
          TAU2SA=STAU2A*SLOWLL+FTAU2A*FASTLL+RPPON*99.
          KSAKA=KSA*KA/2.
COMMENT    SOLAR ARRAY SELECTION
```

```
          ERROR1,   ERROR2,   ERROR3,   ...
          COERR1,   COERR2,   COERR3,   ...
          ALPH1 ,   ALPH2 ,   ALPH3 ,   ...
          RATE1 ,   RATE2 ,   RATE3 ,   ...
          TSC1  ,   TSC2  ,   TSC3  ,   ...
          FBX   ,   FBY   ,   FBZ   ,   ...
          TB1   ,   TB2   ,   TB3   ,   ...
          GM1   ,   ETA11 ,   ETA21 ,   ...
          GM2   ,   ETA12 ,   ETA22 ,   ...
          GM3   ,   ETA13 ,   ETA23 ,   ...
          GM4   ,   ETA14 ,   ETA24 ,   ...
          TH1   ,   ETA15 ,   ETA25 ,   ...
          TH2   ,   ETA16 ,   ETA26 ,   ...
          TH3   ,   ETA17 ,   ETA27 ,   ...
          TH4   ,   ETA18 ,   ETA28 ,   ...
          TRNCOM,   DERPDY,   NXQINT,   ...
          COMSA1,   COMCL ,   NXQDYN,   ...
          COMSA2,   COMCN ,   NXQDER,   ...
          TGASGR,   ANGM  ,   NXQTER,   ...
          XGASGR,   YGASGR,   ZGASGR,   ...
          TPONX ,   TPONY ,   TPONZ ,   ...
          TTONX ,   TTONY ,   TTONZ
PREPAR  1(                                ....
          TSC1  ,   TSC2  ,   TSC3  ,   ...
          ERROR1,   ERROR2,   ERROR3,   ...
          ALPH1 ,   ALPH2 ,   ALPH3 ,   ...
          RATE1 ,   RATE2 ,   RATE3 ,   ...
          GM1   ,   ETA11 ,   COMSA1,   ...
          GM2   ,   ETA12 ,   COMSA2,   ...
          GM3   ,   ETA13 ,   COMCL ,   ...
          GM4   ,   ETA14 ,   COMCN ,   ...
          TH1   ,   ETA15 ,   TGASGR,   ...
          TH2   ,   ETA16 ,   XGASGR,   ...
          TH3   ,   ETA17 ,   YGASGR,   ...
          TH4   ,   ETA18 ,   ZGASGR,   ...
          TPONX ,   TPONY ,   TPONZ ,   ...
          TTONX ,   TTONY ,   TTONZ ,   ...
          ANGM  ,   TRNCOM,           ...
          COERR1,   COERR2,   COERR3
RANGE   ...
          TRNCO1,   TRNCO2,   TRNCO3,   ...
          ERROR1,   ERROR2,   ERROR3,   ...
          COERR1,   COERR2,   COERR3,   ...
          ALPH1 ,   ALPH2 ,   ALPH3 ,   ...
          RATE1 ,   RATE2 ,   RATE3 ,   ...
          TSC1  ,   TSC2  ,   TSC3  ,   ...
          FBX   ,   FBY   ,   FBZ   ,   ...
          TB1   ,   TB2   ,   TB3   ,   ...
          GM1   ,   ETA11 ,   ETA21 ,   ...
          GM2   ,   ETA12 ,   ETA22 ,   ...
          GM3   ,   ETA13 ,   ETA23 ,   ...
          GM4   ,   ETA14 ,   ETA24 ,   ...
          TH1   ,   ETA15 ,   ETA25 ,   ...
          TH2   ,   ETA16 ,   ETA26 ,   ...
          TH3   ,   ETA17 ,   ETA27 ,   ...
          TH4   ,   ETA18 ,   ETA28 ,   ...
          TRNCOM,   DERPDY,   NXQINT,   ...
```

```
END
   COMMENT
DYNAMIC
   VARIABLE T=TINITL
   DERPDY=NXDDER-NXDERL
   NXDERL=NXDDER
   NXDDYN=NXDDYN+1.
   IF (NOPLOT) GO TO NOSAVE
   IF (T.GT.SWITCH) GO TO INT2
   YESPLT=PLTNBR*INTRV1
   GO TO SL1
   INT2..  CONTINUE
   CHECKP=PLTNBR*INTRV1
   IF (CHECKP.GL.NEWINT) NEWINT=NEWINT+INTRV2
   YESPLT = NEWINT
   SL1..  CONTINUE
   TIMEP=T+.0001
   IF (TIMEP.LT.YESPLT) GO TO NOSAVE
   WRITE (6,F2) PLTNBR,T
   WRITE (6,F2) PZ,P1,P2,P3
   WRITE (6,F2) GM(1),GM(2),GM(3),GM(4)
         DO SL2 J=1,2
         L=0
         DO SL2 K=1,3
         WRITE (6,F2) (FT(J,L+M),M=1,5)
         F2..  FORMAT (1X,5G14.8)
         L=L+5
         SL2..  CONTINUE
      WRITE (6,F3) ((CK(N,NN),NN=1,3),N=1,2)
      F3..  FORMAT (1X,3G14.8)
   PLTNBR=PLTNBR+1
   IF (T.GT.SWITCH) NEWINT=NEWINT+INTRV2
   NOSAVE..  CONTINUE
   IF(T.GT.FINTIM)GO TO FIN
COMMENT CALCULATION OF JET EQUIVALENT ON TIME
   PWCALC  GAMXC,DB2C,PWX,CI,TPONX,DB1CC
   PWCALC  GAMYC,DB2C,PWY,CI,TPONY,DB1CC
   PWCALC  GAMZC,DB2C,PWZ,CI,TPONZ,DB1CC
COMMENT
COMMENT
COMMENT  MACRO TO CALCULATE PULSE WIDTH
  MACRO  MACRO  PWCALC  P
      MACRO  RELABEL  GL1,GL2,GL3
      P(5)=0.
      IF(ABS(P(1))-P(2))  GL1,GL2,GL2
      GL1 ..  P(3)=0.
      GOTO GL3
      GL2 ..  CONTINUE
      P(3)=P.02*(ABS(P(1))-P(2))+0.08/(P(6)-P(2))
      IF(P(3).GT.P(4))  P(3)=P(4)
      IF(P(1).GT.0.)  P(5)=1.
      IF(P(1).LT.0.)  P(5)=-1.
      P(5)=P(5)*P(3)/P(4)
      GL3 ..  CONTINUE
  MACRO  END
   OUTPUT  200                                          ....
                TRNC01,   TRNC02,   TRNC03,    ...
```

```
    MACRO REDEFINE W,WD
       WD=(Q(2)-W)/Q(5)
       W=INTEG(WD,Q(3))
       Q(1)=W+Q(4)*WD
    MACRO END
   COMMENT SCAN PLATFORM CONTROLLER
    CLSLON=PULSE(CLSLBG,50000.,(CLSLEN-CLSLBG),T)*SLEWON
    CNSLON=PULSE(CNSLBG,50000.,(CNSLEN-CNSLBG),T)*SLEWON
    IF(T.GT.BOXEND)BOXON=0.0
    CLBXON=(PULSE(CLBXB1,CLBXFQ,CLBXWD,T)...
           -PULSE(CLBXB2,CLBXFQ,CLBXWD,T))*BOXON
    CNBXON= PULSE(CNBXBG,CNBXFQ,CNBXWD,T)*BOXON
    COMCL=INTEG((CLSLON+CLBXON)*CLRATE,0.)
    COMCN=INTEG((CNSLON+CNBXON)*CNRATE,0.)
   COMMENT SOLAR ARRAYS CONTROLLER
    A1SLON=PULSE(A1SLBG,50000.,(A1SLEN-A1SLBG),T)*SASLEW
    COMSA1=(-ALPH2*SAPSUN+INTEG(A1SLON+A1SLRT,0.))*(1.-SALOCK)
    A2SLON=PULSE(A2SLBG,50000.,(A2SLEN-A2SLBG),T)*SASLEW
    COMSA2=(-ALPH2*SAPSUN+INTEG(A2SLON+A2SLRT,0.))*(1.-SALOCK)
   COMMENT SOLAR ARRAY HINGE TORQUES
    ERRSA1=(COMSA1-GM1)
    ERRSA2=(COMSA2-GM2)
    FILSA1=REALPL(TAUFSA,ERRSA1,FLSA1I)
    FILSA2=REALPL(TAUFSA,ERRSA2,FLSA2I)
    SSLEAD  LLSA1,ERRSA1,LLSA1I,TAU1SA,TAU2SA
    SSLEAD  LLSA2,ERRSA2,LLSA2I,TAU1SA,TAU2SA
    ERPPA1=ERRSA1-KKRPSA*GM1D
    ERPPA2=ERRSA2-KKRPSA*GM2D
    TH1=KSAKA*LLSA1*LLAGON + KKSA*ERPPA1*RPPON
    TH2=KSAKA*LLSA2*LLAGON + KKSA*ERPPA2*RPPON
   COMMENT SCAN PLATFORM HINGE TORQUES
    TH3=-KCL*(GM3-COMCL)-BCL*GM3D
    TH4=-KCN*(GM4-COMCN)-BCN*GM4D
  COMMENT
 COMMENT   GENERATE TURN RAMP INPUT SIGNALS
    TRNTRU=PULSE(0.0,50000.0,TRNTIM,T)
    TRNCO1 =INTEG(TRN1ON*TRN1RT*TRNTRU,0.)
    TRNCO2 =INTEG(TRN2ON*TRN2RT*TRNTRU,0.)
    TRNCO3 =INTEG(TRN3ON*TRN3RT*TRNTRU,0.)
    TRNCOM = TRNCO1 + TRNCO2 + TRNCO3
 COMMENT  CELESTIAL SENSORS
    THETA1=REALPL(TAUS,ALPH1,THTA1I)
    THETA2=REALPL(TAUS,ALPH2,THTA2I)
    THETA3=REALPL(TAUS,ALPH3,THTA3I)
    ERROR1=TRNCO1 -THETA1
    ERROR2=TRNCO2 -THETA2
    ERROR3=TRNCO3 -THETA3
 COMMENT  **********************************************
 COMMENT  ****** GAS CONTROLLER DYNAMICS SECTION ******
 COMMENT  COMPUTE GAMMA COMMANDS
    FILX=REALPL(TAUF,ERROR1,FILXI)
    FILY=REALPL(TAUF,ERROR2,FILYI)
    FILZ=REALPL(TAUF,ERROR3,FILZI)
    SSLEAD  LLX,ERROR1,LLXI,TAU1LL,TAU2LL
    SSLEAD  LLY,ERROR2,LLYI,TAU1LL,TAU2LL
    SSLEAD  LLZ,ERROR3,LLZI,TAU1LL,TAU2LL
    ERPPX=ERROR1-KKRPX*RATE1
```

```
              COMSA1,   COMCL ,   NXQDYN,   ...
              COMSA2,   COMCN ,   NXQDER,   ...
              TGASGR,   ANGM  ,   NXQTER,   ...
              XGASGR,   YGASGR,   ZGASGR,   ...
              TPONX ,   TPONY ,   TPONZ ,   ...
              TTONX ,   TTONY ,   TTONZ
DERIVATIVE CIDGAS
  CINTERVAL CI=0.05
  XERROR ...
  GM1D  =1.E-7 ,GM2D  =1.E-7 ,GM1   =1.E-7 ,GM2   =1.E-7 ,...
  GM3D  =1.E-7 ,GM4D  =1.E-7 ,GM3   =1.E-7 ,GM4   =1.E-7 ,...
  TTONX =1.E-3 ,TTONY =1.E-3 ,TTONZ =1.E-3 ,...
  RATE1 =1.E-6 ,RATE2 =1.E-6 ,RATE3 =1.E-6
  MERROR ...
  GM1D  =1.E-7 ,GM2D  =1.E-7 ,GM1   =1.E-7 ,GM2   =1.E-7 ,...
  GM3D  =1.E-7 ,GM4D  =1.E-7 ,GM3   =1.E-7 ,GM4   =1.E-7 ,...
  TTONX =1.E-3 ,TTONY =1.E-3 ,TTONZ =1.E-3 ,...
  RATE1 =1.E-6 ,RATE2 =1.E-6 ,RATE3 =1.E-6
  NOSORT
  NXQDER=NXQDER+1.
  GMD(1)=GM1D  $  GM(1)=GM1
  GMD(2)=GM2D  $  GM(2)=GM2
  GMD(3)=GM3D  $  GM(3)=GM3
  GMD(4)=GM4D  $  GM(4)=GM4
  ETD(1,1) =ETD11   $  ET(1,1) =ETA11
  ETD(1,2) =ETD12   $  ET(1,2) =ETA12
  ETD(1,3) =ETD13   $  ET(1,3) =ETA13
  ETD(1,4) =ETD14   $  ET(1,4) =ETA14
  ETD(1,5) =ETD15   $  ET(1,5) =ETA15
  ETD(1,6) =ETD16   $  ET(1,6) =ETA16
  ETD(1,7) =ETD17   $  ET(1,7) =ETA17
  ETD(1,8) =ETD18   $  ET(1,8) =ETA18
  ETD(1,9) =ETD19   $  ET(1,9) =ETA19
  ETD(1,10)=ETD110  $  ET(1,10)=ETA110
  ETD(1,11)=ETD111  $  ET(1,11)=ETA111
  ETD(1,12)=ETD112  $  ET(1,12)=ETA112
  ETD(1,13)=ETD113  $  ET(1,13)=ETA113
  ETD(1,14)=ETD114  $  ET(1,14)=ETA114
  ETD(1,15)=ETD115  $  ET(1,15)=ETA115
  ETD(2,1) =ETD21   $  ET(2,1) =ETA21
  ETD(2,2) =ETD22   $  ET(2,2) =ETA22
  ETD(2,3) =ETD23   $  ET(2,3) =ETA23
  ETD(2,4) =ETD24   $  ET(2,4) =ETA24
  ETD(2,5) =ETD25   $  ET(2,5) =ETA25
  ETD(2,6) =ETD26   $  ET(2,6) =ETA26
  ETD(2,7) =ETD27   $  ET(2,7) =ETA27
  ETD(2,8) =ETD28   $  ET(2,8) =ETA28
  ETD(2,9) =ETD29   $  ET(2,9) =ETA29
  ETD(2,10)=ETD210  $  ET(2,10)=ETA210
  ETD(2,11)=ETD211  $  ET(2,11)=ETA211
  ETD(2,12)=ETD212  $  ET(2,12)=ETA212
  ETD(2,13)=ETD213  $  ET(2,13)=ETA213
  ETD(2,14)=ETD214  $  ET(2,14)=ETA214
  ETD(2,15)=ETD215  $  ET(2,15)=ETA215
  WO(1)=RATE1  $  WO(2)=RATE2  $  WO(3)=RATE3  $  ANGM=MM
COMMENT
  MACRO MACRO SSLEAD Q
```

```
      TH(1)=TH1
      TH(2)=TH2
      TH(3)=TH3
      TH(4)=TH4
COMMENT  TORQUES ON S/C
      TSC1 = TSCX + TDIST1
      TSC2 = TSCY + TDIST2
      TSC3 = TSCZ + TDIST3
      COMMENT
COMMENT   SOLVE FOR SYSTEM ACCELERATIONS
      CALL MRATE(NC,TH,TB,TS,FB,FS,TF,FF,GM,GMD,GMDD,ET,ETD,...
                 WO,WDOT,ETDD,HM,CK)
      COMMENT
      COMMENT SYSTEM RATES AND POSITIONS
      COMMENT
      RATE1 =INTEG(WDOT(1),RATE1I)
      RATE2 =INTEG(WDOT(2),RATE2I)
      RATE3 =INTEG(WDOT(3),RATE3I)
      ALPH1 =INTEG(RATE1,ALPH1I)
      ALPH2 =INTEG(RATE2,ALPH2I)
      ALPH3 =INTEG(RATE3,ALPH3I)
      PZD,P1D,P2D,P3D=HCK(HCK,PZ,P1,P2,P3,RATE1,RATE2,RATE3)
      PZ    =INTEG(PZD,1.000)
      P1    =INTEG(P1D,0.000)
      P2    =INTEG(P2D,0.000)
      P3    =INTEG(P3D,0.000)
      GM1D  =INTEG(WDOT(4),0.)
      GM2D  =INTEG(WDOT(5),0.)
      GM3D  =INTEG(WDOT(6),0.)
      GM4D  =INTEG(WDOT(7),0.)
      GM1   =INTEG(GM1D,0.)
      GM2   =INTEG(GM2D,0.)
      GM3   =INTEG(GM3D,0.)
      GM4   =INTEG(GM4D,0.)
      ETD11 =INTEG(ETDD(1,1) ,0.)  $  ETA11 =INTEG(ETD11 ,0.)
      ETD12 =INTEG(ETDD(1,2) ,0.)  $  ETA12 =INTEG(ETD12 ,0.)
      ETD13 =INTEG(ETDD(1,3) ,0.)  $  ETA13 =INTEG(ETD13 ,0.)
      ETD14 =INTEG(ETDD(1,4) ,0.)  $  ETA14 =INTEG(ETD14 ,0.)
      ETD15 =INTEG(ETDD(1,5) ,0.)  $  ETA15 =INTEG(ETD15 ,0.)
      ETD16 =INTEG(ETDD(1,6) ,0.)  $  ETA16 =INTEG(ETD16 ,0.)
      ETD17 =INTEG(ETDD(1,7) ,0.)  $  ETA17 =INTEG(ETD17 ,0.)
      ETD18 =INTEG(ETDD(1,8) ,0.)  $  ETA18 =INTEG(ETD18 ,0.)
      ETD19 =INTEG(ETDD(1,9) ,0.)  $  ETA19 =INTEG(ETD19 ,0.)
      ETD110=INTEG(ETDD(1,10),0.)  $  ETA110=INTEG(ETD110,0.)
      ETD111=INTEG(ETDD(1,11),0.)  $  ETA111=INTEG(ETD111,0.)
      ETD112=INTEG(ETDD(1,12),0.)  $  ETA112=INTEG(ETD112,0.)
      ETD113=INTEG(ETDD(1,13),0.)  $  ETA113=INTEG(ETD113,0.)
      ETD114=INTEG(ETDD(1,14),0.)  $  ETA114=INTEG(ETD114,0.)
      ETD115=INTEG(ETDD(1,15),0.)  $  ETA115=INTEG(ETD115,0.)
      ETD21 =INTEG(ETDD(2,1) ,0.)  $  ETA21 =INTEG(ETD21 ,0.)
      ETD22 =INTEG(ETDD(2,2) ,0.)  $  ETA22 =INTEG(ETD22 ,0.)
      ETD23 =INTEG(ETDD(2,3) ,0.)  $  ETA23 =INTEG(ETD23 ,0.)
      ETD24 =INTEG(ETDD(2,4) ,0.)  $  ETA24 =INTEG(ETD24 ,0.)
      ETD25 =INTEG(ETDD(2,5) ,0.)  $  ETA25 =INTEG(ETD25 ,0.)
      ETD26 =INTEG(ETDD(2,6) ,0.)  $  ETA26 =INTEG(ETD26 ,0.)
      ETD27 =INTEG(ETDD(2,7) ,0.)  $  ETA27 =INTEG(ETD27 ,0.)
      ETD28 =INTEG(ETDD(2,8) ,0.)  $  ETA28 =INTEG(ETD28 ,0.)
```

```
      ERPPY=ERROR2-KKRPY*RATE2
      ERPPZ=ERROR3-KKRPZ*RATE3
      COERR1=LLX*LLAGON + ERPPX*RPPON
      COERR2=LLY*LLAGON + ERPPY*RPPON
      COERR3=LLZ*LLAGON + ERPPZ*RPPON
      GAMXC=LLX*KX*LLAGON + ERPPX*KKX*RPPON
      GAMYC=LLY*KY*LLAGON + ERPPY*KKY*RPPON
      GAMZC=LLZ*KZ*LLAGON + ERPPZ*KKZ*RPPON
COMMENT   COMPUTE FORCES AND TORQUES
      FB1X=(+TPONY-TPONZ)*FONEJT
      FB1Y=0.
      FB1Z=+TPONX*FONEJT
      FB2X=(+TPONY+TPONZ)*FONEJT
      FB2Y=0.
      FB2Z=-TPONY*FONEJT
      FBX=FB1X+FB2X
      FBY=FB1Y+FB2Y
      FBZ=FB1Z+FB2Z
      TJTC1X=+FB1Z*RJTC1(2)-FB1Y*RJTC1(3)
      TJTC1Y=-FB1Z*RJTC1(1)+FB1X*RJTC1(3)
      TJTC1Z=+FB1Y*RJTC1(1)-FB1X*RJTC1(2)
      TJTC2X=+FB2Z*RJTC2(2)-FB2Y*RJTC2(3)
      TJTC2Y=-FB2Z*RJTC2(1)+FB2X*RJTC2(3)
      TJTC2Z=+FB2Y*RJTC2(1)-FB2X*RJTC2(2)
      TBX=TJTC1X+TJTC2X
      TBY=TJTC1Y+TJTC2Y
      TBZ=TJTC1Z+TJTC2Z
COMMENT  COMPUTE TORQUE ABOUT S/C CENTER OF MASS
      TJTC1X=+FB1Z*SJTC1(2)-FB1Y*SJTC1(3)
      TJTC1Y=-FB1Z*SJTC1(1)+FB1X*SJTC1(3)
      TJTC1Z=+FB1Y*SJTC1(1)-FB1X*SJTC1(2)
      TJTC2X=+FB2Z*SJTC2(2)-FB2Y*SJTC2(3)
      TJTC2Y=-FB2Z*SJTC2(1)+FB2X*SJTC2(3)
      TJTC2Z=+FB2Y*SJTC2(1)-FB2X*SJTC2(2)
      TSCX=TJTC1X+TJTC2X
      TSCY=TJTC1Y+TJTC2Y
      TSCZ=TJTC1Z+TJTC2Z
COMMENT GAS EXPENDITURES
      TTONX=INTEG(ABS(TPONX),TTONXI)
      TTONY=INTEG(ABS(TPONY),TTONYI)
      TTONZ=INTEG(ABS(TPONZ),TTONZI)
      XGASGR=GASFAC*FONEJT*TTONX
      YGASGR=GASFAC*FONEJT*TTONY
      ZGASGR=GASFAC*FONEJT*TTONZ
      TGASGR=XGASGR+YGASGR+ZGASGR
COMMENT  ****** GAS CONTROLLER SECTION END  ******
COMMENT  ********************************************
  COMMENT
COMMENT  ****************************
COMMENT  ******  FLEX DYNAMICS ******
 COMMENT FORCES AND TORQUES ACTING ON BUS AND HINGES
      TB1=TBX+TDIST1            $  TB(1)=TB1
      TB2=TBY+TDIST2            $  TB(2)=TB2
      TB3=TBZ+TDIST3            $  TB(3)=TB3
      FB(1)=FBX
      FB(2)=FBY
      FB(3)=FBZ
```

```
    CR4BFL/RWHGYROSC
PROGRAM THREE AXES RWH CID FLEX 2 SOLAR PANELS UNDEPLOYED MAG BOOM    ...
      TWO DEGREE OF FREEDOM SCAN PLATFORM (BODY 83)                   ...
      STOWED HIGH GAIN ANTENNA                                        ...
      CONDITIONS AT TEMPLE 2 RENDEZVOUS
  COMMENT                                                             ...
      REVISED 10 OCT 79                                               ...
      METRIC UNITS THROUGHOUT                                         ...
      BUS DATA FROM H. PRICE'S MOM PROGRAM                            ...
      PANEL DATA FROM K. GUPTA'S FINITE EL MODEL (SPAR OCT 79)        ...
      REACTION WHEEL CONTROL LOOP (SEP 79)                            ...
      FOR SPECIFIC MANEUVER PARAMETERS SEE LINE 127
  COMMENT
   INTEGER NC,NF,H(3,2),F(2,3),PI(5),J,K,PLTNBR,L,M,N,NN,MANNBR
   ARRAY CMBLV(3)      , CMSLV(3,3)    ,HINGLV(3,3)    ,   TEMPST(8)    ....
         MB(7)         ,    MS(3,7)    ,    PB(3,3)    ,    PS(3,3,3)   ....
         G(4,3)        ,    TH(4)      ,    TB(3)      ,    TS(3,3)     ....
         FB(3)         ,    FS(3,3)    ,    GM(4)      ,   GMD(4)       ....
         GMDD(4)       ,  EIG(2,6,15),   REC(2,6,15),    RF(2,1,3)   ....
         WF(2,15)      ,    ZF(2,15)   ,    TF(2,1,3)  ,    FF(2,1,3)   ....
         ET(2,15)      ,   ETD(2,15)   ,    WO(3)      ,   WFHZ(2,15)   ....
         CK(2,3)
   DOUBLE PRECISION WDOT(7),ETDD(2,15)
   LOGICAL NOPLOT
  COMMENT
 DROP
   DATA (H(1,J),J=1,2)/0,1/
   DATA (H(2,J),J=1,2)/0,1/
   DATA (H(3,J),J=1,2)/0,2/
   DATA (F(1,J),J=1,3)/1,1,15/
   DATA (F(2,J),J=1,3)/2,1,15/
   DATA PI/0,3,1,1,1/
  COMMENT
   DATA MB...
   /1824.304, 2635.642, 1769.269, -50.133, -114.634, -46.249, 1756.474/
   DATA (MS(1,J),J=1,7)...
     /22084.00, 234.61, 21876.00, +158.02, 0.00, 0.00, 176.818/
   DATA (MS(2,J),J=1,7)...
     /22084.00, 234.61, 21876.00, -158.02, 0.00, 0.00, 176.818/
   DATA (MS(3,J),J=1,7)...
     /13.3  ,  7.5  , 16.5  , +2.1  , -0.2  , -1.0  , 90.19 /
  COMMENT
  COMMENT POS VEC SPECIF LOCATION OF CM'S & HINGES-IN S/C COORDINATES
   DATA CMBLV /.0703, .0190, .6266 /
   DATA (CMSLV(1,J),J=1,3)/ 0.00, +19.37645 ,+0.2/
   DATA (CMSLV(2,J),J=1,3)/ 0.00, -19.37645 ,+0.2/
   DATA (CMSLV(3,J),J=1,3)/-1.3691,  -0.370, -0.7893/
   DATA (HINGLV(1,J),J=1,3)/ 0.00 ,0.00 ,+0.2/
   DATA (HINGLV(2,J),J=1,3)/ 0.00 ,0.00 ,+0.2/
   DATA (HINGLV(3,J),J=1,3)/-1.3691,  -0.370, -0.7893/
  COMMENT
  COMMENT HINGE ORIENTATIONS
   DATA (G(1,J),J=1,3)/ 0.000000,+1.000000, 0.000000/
   DATA (G(2,J),J=1,3)/ 0.000000,+1.000000, 0.000000/
   DATA (G(3,J),J=1,3)/ 0.000000, 0.000000,+1.000000/
   DATA (G(4,J),J=1,3)/ 0.000000,+1.000000, 0.000000/
  COMMENT
```

```
    ETD29 =INTEG(ETDD(2,9) ,0.)   $  ETA29 =INTEG(ETD29 ,0.)
    ETD210=INTEG(ETDD(2,10),0.)   $  ETA210=INTEG(ETD210,0.)
    ETD211=INTEG(ETDD(2,11),0.)   $  ETA211=INTEG(ETD211,0.)
    ETD212=INTEG(ETDD(2,12),0.)   $  ETA212=INTEG(ETD212,0.)
    ETD213=INTEG(ETDD(2,13),0.)   $  ETA213=INTEG(ETD213,0.)
    ETD214=INTEG(ETDD(2,14),0.)   $  ETA214=INTEG(ETD214,0.)
    ETD215=INTEG(ETDD(2,15),0.)   $  ETA215=INTEG(ETD215,0.)
COMMENT  ******  FLEX DYNAMICS END  ******
COMMENT  **********************************
END
END
END
TERMINAL
    FIN.. CONTINUE
    DEBUG
    NXQTER=NXQTER+1.
    WRITE(6,F2)T,NXQINT,NXQDYN,NXQDER,GO
END
END
```

```
          DO L1 K=1,3
          PB(1,K)=HINGLV(1,K)-CMBLV(K)
          PB(2,K)=HINGLV(2,K)-CMBLV(K)
          PB(3,K)=HINGLV(3,K)-CMBLV(K)
          PS(1,1,K)=HINGLV(1,K)- CMSLV(1,K)
          PS(2,2,K)=HINGLV(2,K)-CMSLV(2,K)
          PS(3,3,K)=HINGLV(3,K)-CMSLV(3,K)
    L1..  CONTINUE
  PICKUP
   COMMENT
   COMMENT
 INITIAL
    CONSTANT TINITL=0.000000
    CONSTANT PIF=3.14159265
  COMMENT ***************************************************** ...
          *                                                   * ...
          *      DEFINE THE BUS FIXED AXES AS FOLLOWS:        * ...
          *      -------------------------------------        * ...
          *                                                   * ...
          *      AXIS3 = Z ( ION ENGINE PLUME EXHAUST AXIS )  * ...
          *                                                   * ...
          *      AXIS2 = Y ( SOLAR ARRAY AXIS )               * ...
          *                                                   * ...
          *      AXIS1 = X                                    * ...
          *                                                   * ...
          ***************************************************** ...
          *                                                   * ...
          *      SELECT THE MANEUVER BY ITS NUMBER            * ...
          *      ---------------------------------            * ...
          *                                                   * ...
          *      1 - TURN ENTIRE SPACECRAFT ABOUT AXIS1       * ...
          *                                                   * ...
          *      2 - TURN ENTIRE SPACECRAFT ABOUT AXIS2       * ...
          *                                                   * ...
          *      3 - TURN ENTIRE SPACECRAFT ABOUT AXIS3       * ...
          *                                                   * ...
          *      4 - TURN   BUS ONLY ABOUT AXIS2              * ...
          *          WHILE KEEPING ARRAYS ON THE SUN          * ...
          *                                                   * ...
          *      5 -ACQUISITION OF CEL REFERENCES             * ...
          *                                                   * ...
          *      6 - SCAN PLATFORM SLEW OR BOXSCAN            * ...
          *                                                   * ...
          ***************************************************** ...
          *                                                   * ...
          *                                                   *
CONSTANT                       MANEUV = 2.0
  COMMENT *                                                   * ...
          *                                                   * ...
          ***************************************************** ...
                                                                ...
                                                                ...
                                                                ...
                                                                ...
                                                                ...
                                                                ...
                                                                ...
                                                                ...
                                                                ...
```

```
COMMENT RIGID ELASTIC COUPLING COEFFICIENTS FOR THE 2 PANELS ...
        SPAR MODEL BY K. GUPTA OF OCT 79                      ...
        CONDITIONS AT TEMPLE 2 RENDEZVOUS
 DATA ((REC(1,J,K),J=1,6),K=1,12)/...
-11.18700,    .06995,   -.04629,   -.55239,    .03969,  68.52600,...
  -.51909,   -.09919,    .08782,   1.02460,   -.04128, -88.99000,...
 -3.13480,    .08922,   -.19750,  -2.21670,    .03269,  -4.53950,...
  -.13282,   -.01158,   9.57620, 104.93000,   -.65980,    .76180,...
   .80208,    .06203,    .11783,   1.25900,    .04004,  25.28500,...
  1.46380,   -.04164,   -.02503,   -.24815,  -1.37720,  10.39600,...
   .15877,   -.00148,    .00685,    .05069,  12.17000,   1.12110,...
   .06603,    .00457,    .01928,    .11299,    .13019,    .54573,...
   .07672,    .00979,    .02564,    .13027,   4.03850,   1.15200,...
   .54915,    .02260,    .00615,    .06512,   -.47812,  11.24900,...
  -.07393,    .00837,    .02850,    .10434,    .26855,  -1.51880,...
  -.23045,    .01450,    .03038,    .08424,   2.25460,  -2.39780/
 DATA ((REC(1,J,K),J=1,6),K=13,15)/...
   .81469,   -.00625,    .00957,    .00618,    .87656,   7.36440,...
  -.11917,   -.01331,   -.03352,   -.05150,   -.33515,  -1.13710,...
   .29823,    .00182,    .00037,    .00137,    .23342,   5.35990/
 DATA ((REC(2,J,K),J=1,6),K=1,12)/...
-11.18700,   -.06995,    .04629,   -.55239,   -.03969, -68.52600,...
  -.51909,    .09919,   -.08782,   1.02460,    .04128,  88.99000,...
 -3.13480,   -.08922,    .19750,  -2.21670,   -.03269,   4.53950,...
  -.13282,    .01158,  -9.57620, 104.93000,    .65980,   -.76180,...
   .80208,   -.06203,   -.11783,   1.25900,   -.04004, -25.28500,...
  1.46380,    .04164,    .02503,   -.24815,   1.37720, -10.39600,...
   .15877,    .00148,   -.00685,    .05069, -12.17000,  -1.12110,...
   .06603,   -.00457,   -.01928,    .11299,   -.13019,   -.54573,...
   .07672,   -.00979,   -.02564,    .13027,  -4.03850,  -1.15200,...
   .54915,   -.02260,   -.00615,    .06512,    .47812, -11.24900,...
  -.07393,   -.00837,   -.02850,    .10434,   -.26855,   1.51880,...
  -.23045,   -.01450,   -.03038,    .08424,  -2.25460,   2.39780/
 DATA ((REC(2,J,K),J=1,6),K=13,15)/...
   .81469,    .00625,   -.00957,    .00618,   -.87656,  -7.36440,...
  -.11917,    .01331,    .03352,   -.05150,    .33515,   1.13710,...
   .29823,   -.00182,   -.00037,    .00137,   -.23342,  -5.35990/
COMMENT
COMMENT PANELS FREQUENCIES (IN HERTZ) AND DAMPING
 DATA (WFHZ(1,J),J=1,15)/...
  0.065226 , 0.126145 , 0.192507 , 0.226612 ,...
  0.261074 , 0.329296 , 0.333713 , 0.351529 ,...
  0.378027 , 0.393748 , 0.410395 , 0.443883 ,...
  0.453118 , 0.478315 , 0.501820 /
 DATA (WFHZ(2,J),J=1,15)/...
  0.065226 , 0.126145 , 0.192507 , 0.226612 ,...
  0.261074 , 0.329296 , 0.333713 , 0.351529 ,...
  0.378027 , 0.393748 , 0.410395 , 0.443883 ,...
  0.453118 , 0.478315 , 0.501820 /
 DATA (ZF(1,J),J=1,15)/15*0.004/
 DATA (ZF(2,J),J=1,15)/15*0.004/
       DO L2 K=1,15
        WF(1,K)=WFHZ(1,K)*2.*PIE
        WF(2,K)=WFHZ(2,K)*2.*PIE
 L2..  CONTINUE
COMMENT
COMMENT COMPUTATION OF PR AND PS VECTORS
```

```
            GO TO MEND
   M2..     TRN2ON=1.0
            GO TO MEND
   M3..     TRN3ON=1.0
            GO TO MEND
   M4..     TRN2ON=1.0 $ SAPSUN=1.0
            GO TO MEND
   M5..     GO TO MEND
   M6..     SCANON=1.0 $ SLEWON=0.0 $ BOXON=1.0
   MEND..   CONTINUE
   COMMENT
    COMMENT
COMMENT  ****************************************
COMMENT  ****** RWH CONTROLLER PARAMETERS  ******
  COMMENT RATE+POSITION CONTROLLER PARAMETERS
   CONSTANT KX  =107.48287 , KY  =  2.1016216  ,  KZ  =107.48287
   CONSTANT KRPX=49.961418 , KRPY=  49.961418  ,  KRPZ=49.961418
  COMMENT RW SPEED CONTROL LOOP PARAMETERS AND IC'S
   CONSTANT JRW=0.0868117
   CONSTANT KW=0.0003177
   CONSTANT KRW=32.790066 , KIRW=0.03
   CONSTANT VLIM=900.
   CONSTANT WRWXI=0.
   CONSTANT WRWYI=0.
   CONSTANT WRWZI=0.
COMMENT  ******  RWH CONTROLLER PARAMETER END  ******
COMMENT  ****************************************
  COMMENT  CELESTIAL SENSOR PARAMETERS
   CONSTANT  TAUS=1.0
COMMENT SA AND SP  CHARACTERISTICS
  COMMENT SOLAR ARRAY SELECTION
   IF(SALOCK.GT.0.9)SASLEW=0.0
   IF(SAPSUN.LT.0.9)GO TO SA1
   SALOCK=0.
   SASLEW=0.0
  SA1..CONTINUE
   CONSTANT A1SLBG=   0.00 , A1SLEN=   50.00  , A1SLRT=0.00438
   CONSTANT A2SLBG=   0.00 , A2SLEN=   50.00  , A2SLRT=0.00438
  COMMENT
  COMMENT SP CONTROL LOOP PARAMETERS AND IC'S
   CONSTANT KCL   =1500.    , KCN   =1500.
   CONSTANT BCL   = 148.50  , BCN   = 220.25
   CONSTANT KSA1  =15.00    , KSA2  =15.00
   CONSTANT BSA1  =  83.05  ,  BSA2  =  83.05
  COMMENT SCAN SELECTION
   IF(SLEWON.GT.0.9)BOXON=0.0
   IF(SCANON.GT.0.9)GO TO SC1
   SLEWON=0.0
   BOXON =0.0
  SC1..CONTINUE
   CONSTANT CLRATE=0..17453 , CNRATE=0.017453
   CONSTANT CLSLBG=   0.00  , CLSLEN=   30.00
   CONSTANT CNSLBG= 100.00  , CNSLEN=  130.00
   CONSTANT CLBXB1= 0.00    , CLBXFQ=   30.00  , CLBXWD=9.0
   CONSTANT CLBXB2=15.00
   CONSTANT CNBXBG=11.00    , CNBXFQ=   15.00  , CNBXWD=2.00
   CONSTANT BOXEND=60.00
```

```
          ****************************************************************
          *                                                              *
          *      SET SIMULATION TIME                                     *
          *      -------------------                                     *
          *                                                              *
CONSTANT                    FINTIM =  199.999
 COMMENT  *                                                              *
          ****************************************************************
          *                                                              *
          *      SET INITIAL CONDITIONS                                  *
          *      ----------------------                                  *
          *                                                              *
          *      AXIS1            AXIS2            AXIS3                 *
          *      -----            -----            -----                 *
          *                                                              *
          *   DISTURBANCE TORQUES                                        *
          *                                                              *
CONSTANT       TDIST1=0.0    ,   TDIST2=.209E-4,  TDIST3=0.0
 COMMENT  *                                                              *
          *   INITIAL RATES                                              *
          *                                                              *
CONSTANT       RATE11=0.0    ,   RATE21=0.0    ,   RATE31=0.0
 COMMENT  *                                                              *
          *   INITIAL ANGULAR POSITION ERRORS                            *
          *                                                              *
CONSTANT       ALPH11=0.0    ,   ALPH21=0.0    ,   ALPH31=0.0
 COMMENT  *                                                              *
          *   TURN COMMANDS                                              *
CONSTANT       TRNTIM= 200.00
CONSTANT    TRN1RT=8.72664E-5,TRN2RT=4.36332E-5,TRN3RT=8.72664E-5
 COMMENT  *                                                              *
          *                                                              *
          *      SOLAR ARRAY                                             *
          *      -----------                                             *
          *                                                              *
          *   SOLAR ARRAY COMMANDS                                       *
          *                                                              *
CONSTANT       SAPSUN=1.0    ,   SALOCK=1.0    ,   SASLEW=1.0
 COMMENT  *                                                              *
          *                                                              *
          *                                                              *
          *      SCAN PLATFORM                                           *
          *      -------------                                           *
          *                                                              *
          *   SCAN PLATFORM COMMANDS                                     *
          *                                                              *
CONSTANT       SCANON=1.0    ,   SLEWON=1.0    ,   BOXON =1.0
 COMMENT  *                                                              *
          *                                                              *
          ****************************************************************

 COMMENT
               TRN1ON=0.0 $ TRN2ON=0.0 $ TRN3ON=0.0
               SAPSUN=0.0 $ SCANON=0.0
               MANEUR = MANEUV + .5
               GO TO (M1,M2,M3,M4,M5,M6), MANEUR
   M1..        TRN1ON=1.0
```

```
          RATE1 ,   RATE2 ,   RATE3 ,  ...
          TB1   ,   TB2   ,   TB3   ,  ...
          TDESRX,   TDESRY,   TDESRZ,  ...
          TRWX  ,   TRWY  ,   TRWZ  ,  ...
          VMX   ,   VMY   ,   VMZ   ,  ...
          WRWEX ,   WRWEY ,   WRWEZ ,  ...
          IWRWEX,   IWRWEY,   IWRWEZ,  ...
          WRWCX ,   WRWCY ,   WRWCZ ,  ...
          WRWX  ,   WRWY  ,   WRWZ  ,  ...
          GM1   ,   ETA11 ,   ETA21 ,  ...
          GM2   ,   ETA12 ,   ETA22 ,  ...
          GM3   ,   ETA13 ,   ETA23 ,  ...
          GM4   ,   ETA14 ,   ETA24 ,  ...
          TH1   ,   ETA15 ,   ETA25 ,  ...
          TH2   ,   ETA16 ,   ETA26 ,  ...
          TH3   ,   ETA17 ,   ETA27 ,  ...
          TH4   ,   ETA18 ,   ETA28 ,  ...
          ANGM  ,   DERPDY,   NXQINT,  ...
          COMSA1,   COMSA2,   NXQDYN,  ...
          COMCL ,   COMCN ,   NXQDER,  ...
          NXQTER
PREPAR  10                                ....
          COERR1,   COERR2,   COERR3,  ...
          ALPH1 ,   ALPH2 ,   ALPH3 ,  ...
          RATE1 ,   RATE2 ,   RATE3 ,  ...
          TB1   ,   TB2   ,   TB3   ,  ...
          TDESRX,   TDESRY,   TDESRZ,  ...
          TRWX  ,   TRWY  ,   TRWZ  ,  ...
          VMX   ,   VMY   ,   VMZ   ,  ...
          WRWCX ,   WRWCY ,   WRWCZ ,  ...
          WRWX  ,   WRWY,     WRWZ  ,  ...
          GM1   ,   TH1   ,   COMSA1,  ...
          GM2   ,   TH2   ,   COMSA2,  ...
          GM3   ,   TH3   ,   COMCL ,  ...
          GM4   ,   TH4   ,   COMCN ,  ...
          TRNCOM,   ETA11 ,   ETA12 ,  ...
          ANGM  ,   ETA13 ,   ETA14 ,  ...
                    ETA15 ,   ETA16 ,  ...
                    ETA17 ,   ETA18
RANGE   ...
          TRNC01,   TRNC02,   TRNC03,  ...
          ALPH1 ,   ALPH2 ,   ALPH3 ,  ...
          ERROR1,   ERROR2,   ERROR3,  ...
          COERR1,   COERR2,   COERR3,  ...
          RATE1 ,   RATE2 ,   RATE3 ,  ...
          TB1   ,   TB2   ,   TB3   ,  ...
          TDESRX,   TDESRY,   TDESRZ,  ...
          TRWX  ,   TRWY  ,   TRWZ  ,  ...
          VMX   ,   VMY   ,   VMZ   ,  ...
          WRWEX ,   WRWEY ,   WRWEZ ,  ...
          IWRWEX,   IWRWEY,   IWRWEZ,  ...
          WRWCX ,   WRWCY ,   WRWCZ ,  ...
          WRWX  ,   WRWY,     WRWZ  ,  ...
          GM1   ,   ETA11 ,   ETA21 ,  ...
          GM2   ,   ETA12 ,   ETA22 ,  ...
          GM3   ,   ETA13 ,   ETA23 ,  ...
          GM4   ,   ETA14 ,   ETA24 ,  ...
```

```
   COMMENT
   COMMENT  SET UP PLOTTING INFORMATION
            NOPLOT = .FALSE.
    CONSTANT PLTNBR=0                 ****
             INTRV1=10.0              ****
             NEWINT=100.0             ****
             INTRV2=30.0
             SWITCH=NEWINT
   COMMENT
    NC=3  $  NF=2
    NXQDYN=0.
    NXQDER=0.
    NXQTER=0.
    NXQINT=NXQINT+1.
   COMMENT
    CALL VARDYFL(NC,H,MP,MS,PB,PS,G,PI,NF,F,EIG,REC,RF,WF,ZF)
    DEBUG
END
   COMMENT
DYNAMIC
   VARIABLE T=TINITL
   CALL ZZMON('AFTRWG',T,1.0,60)
   DERPDY=NXQDER-NXDERL
   NXDERL=NXQDER
   NXQDYN=NXQDYN+1.
   IF (NOPLOT) GO TO NOSAVE
   IF (Y.GT.SWITCH) GO TO INT2
   YESPLT=PLTNBR*INTRV1
   GO TO SL1
   INT2..  CONTINUE
   CHECKP=PLTNBR*INTRV1
   IF (CHECKP.GE.NEWINT) NEWINT=NEWINT+INTRV2
   YESPLT = NEWINT
   SL1..  CONTINUE
   TIMEP=T+.0001
   IF (TIMEP.LT.YESPLT) GO TO NOSAVE
   WRITE (6,F2) PLTNBR,T
   WRITE (6,F2) PZ,P1,P2,P3
   WRITE (6,F2) GM(1),GM(2),GM(3),GM(4)
         DO SL2 J=1,2
         L=0
         DO SL2 K=1,3
         WRITE (6,F2) (ET(J,L+M),M=1,5)
         F2..  FORMAT (1X,5G14.8)
         L=L+5
         SL2..  CONTINUE
      WRITE (6,F3) ((CK(N,NN),NN=1,3),N=1,2)
      F3..  FORMAT (1X,3G14.8)
   PLTNBR=PLTNBR+1
   IF (T.GT.SWITCH) NEWINT=NEWINT+INTRV2
   NOSAVE..  CONTINUE
   IF(T.GT.FINTIM)GO TO FIN
   OUTPUT  200                                  ****
                TRNC01,   TRNC02,   TRNC03,    ...
                ALPH1 ,   ALPH2 ,   ALPH3 ,    ...
                ERROR1,   ERROR2,   ERROR3,    ...
                COERR1,   COERR2,   COERR3,    ...
```

```
    CLSLON=PULSE(CLSLBG,50000.,(CLSLEN-CLSLBG),T)*SLEWON
    CNSLON=PULSE(CNSLBG,50000.,(CNSLEN-CNSLBG),T)*SLEWON
    IF(T.GT.BOXEND)BOXON=0.0
    CLBXON=(PULSE(CLBXB1,CLBXFQ,CLBXWD,T)...
           -PULSE(CLBXB2,CLBXFQ,CLBXWD,T))*BOXON
    CNBXON= PULSE(CNBXBG,CNBXFQ,CNBXWD,T)*BOXON
    COMCL=INTEG((CLSLON+CLBXON)*CLRATE,0.)
    COMCN=INTEG((CNSLON+CNBXON)*CNRATE,0.)
  COMMENT SOLAR ARRAYS CONTROLLER
    A1SLON=PULSE(A1SLBG,50000.,(A1SLEN-A1SLBG),T)*SASLEW
    COMSA1=(-ALPH2*SAPSUN+INTEG(A1SLON*A1SLRT,0.))*(1.-SALOCK)
    A2SLON=PULSE(A2SLBG,50000.,(A2SLEN-A2SLBG),T)*SASLEW
    COMSA2=(-ALPH2*SAPSUN+INTEG(A2SLON*A2SLRT,0.))*(1.-SALOCK)
  COMMENT SOLAR ARRAY HINGE TORQUES
    TH1=-KSA1*(GM1-COMSA1)-BSA1*GM1D
    TH2=-KSA2*(GM2-COMSA2)-BSA2*GM2D
  COMMENT SCAN PLATFORM HINGE TORQUES
    TH3=-KCL*(GM3-COMCL)-BCL*GM3D
    TH4=-KCN*(GM4-COMCN)-BCN*GM4D
 COMMENT
COMMENT   GENERATE TURN RAMP INPUT SIGNALS
    TRNTRU=PULSE(0.0,50000.0,TRNTIM,T)
    TRNCO1=INTEG(TRN1ON*TRN1RT+TRNTRU,0.)
    TRNCO2=INTEG(TRN2ON*TRN2RT+TRNTRU,0.)
    TRNCO3=INTEG(TRN3ON*TRN3RT+TRNTRU,0.)
    TRNCOM=TRNCO1+TRNCO2+TRNCO3
COMMENT  CELESTIAL SENSORS
    THETA1=REALPL(TAUS,ALPH1,0.)
    THETA2=REALPL(TAUS,ALPH2,0.)
    THETA3=REALPL(TAUS,ALPH3,0.)
    ERROR1=TRNCO1-THETA1
    ERROR2=TRNCO2-THETA2
    ERROR3=TRNCO3-THETA3
COMMENT  **************************************************
COMMENT  ******  RWH CONTROLLER DYNAMICS SECTION  ******
  COMMENT RATE+POSITION CONTROLLER
    COERR1=ERROR1-KRPX*RATE1
    COERR2=ERROR2-KRPY*RATE2
    COERR3=ERROR3-KRPZ*RATE3
    TDESRX=KX*COERR1+JRW*(-RATE3*TACHWY+RATE2*TACHWZ)
    TDESRY=KY*COERR2+JRW*(+RATE3*TACHWX-RATE1*TACHWZ)
    TDESRZ=KZ*COERR3+JRW*(-RATE2*TACHWX+RATE1*TACHWY)
    WRWCX=LIMINT(-TDESRX/JRW,0.,-230.38345,+230.38345)
    WRWCY=LIMINT(-TDESRY/JRW,0.,-230.38345,+230.38345)
    WRWCZ=LIMINT(-TDESRZ/JRW,0.,-230.38345,+230.38345)
  COMMENT RW SPEED CONTROL LOOP MODEL
    WRWEX=WRWCX-WRWX
    WRWEY=WRWCY-WRWY
    WRWEZ=WRWCZ-WRWZ
    IWRWEX=LIMINT(KIRW*WRWEX,0.,-27.447,+27.447)
    IWRWEY=LIMINT(KIRW*WRWEY,0.,-27.447,+27.447)
    IWRWEZ=LIMINT(KIRW*WRWEZ,0.,-27.447,+27.447)
    VCX=KRW*(WRWEX+IWRWEX)
    VCY=KRW*(WRWEY+IWRWEY)
    VCZ=KRW*(WRWEZ+IWRWEZ)
    VLX=BOUND(-VLIM,+VLIM,VCX)
    VLY=BOUND(-VLIM,+VLIM,VCY)
```

```
                TH1    ,   ETA15 ,   ETA25 ,   ...
                TH2    ,   ETA16 ,   ETA26 ,   ...
                TH3    ,   ETA17 ,   ETA27 ,   ...
                TH4    ,   ETA18 ,   ETA28 ,   ...
                ANGM   ,   DERPDY,   NXQINT,   ...
                COMSA1,    COMSA2,   NXQDYN,   ...
                COMCL  ,   COMCN  ,   NXQDER,   ...
                NXQTER
DERIVATIVE CID
  CINTERVAL CI=0.05
  XERROR ...
  GM1D  =1.E-8 ,GM2D  =1.E-8 ,GM1   =1.E-8 ,GM2   =1.E-8 ,...
  GM3D  =1.E-8 ,GM4D  =1.E-8 ,GM3   =1.E-8 ,GM4   =1.E-8 ,...
  RATE1 =1.E-6 ,RATE2 =1.E-6 ,RATE3 =1.E-6
  MERROR ...
  GM1D  =1.E-8 ,GM2D  =1.E-8 ,GM1   =1.E-8 ,GM2   =1.E-8 ,...
  GM3D  =1.E-8 ,GM4D  =1.E-8 ,GM3   =1.E-8 ,GM4   =1.E-8 ,...
  RATE1 =1.E-6 ,RATE2 =1.E-6 ,RATE3 =1.E-6
  NOSORT
  NXQDER=NXQDER+1.
  GMD(1)=GM1D  $  GM(1)=GM1
  GMD(2)=GM2D  $  GM(2)=GM2
  GMD(3)=GM3D  $  GM(3)=GM3
  GMD(4)=GM4D  $  GM(4)=GM4
  ETD(1,1) =ETD11   $  ET(1,1) =ETA11
  ETD(1,2) =ETD12   $  ET(1,2) =ETA12
  ETD(1,3) =ETD13   $  ET(1,3) =ETA13
  ETD(1,4) =ETD14   $  ET(1,4) =ETA14
  ETD(1,5) =ETD15   $  ET(1,5) =ETA15
  ETD(1,6) =ETD16   $  ET(1,6) =ETA16
  ETD(1,7) =ETD17   $  ET(1,7) =ETA17
  ETD(1,8) =ETD18   $  ET(1,8) =ETA18
  ETD(1,9) =ETD19   $  ET(1,9) =ETA19
  ETD(1,10)=ETD110  $  ET(1,10)=ETA110
  ETD(1,11)=ETD111  $  ET(1,11)=ETA111
  ETD(1,12)=ETD112  $  ET(1,12)=ETA112
  ETD(1,13)=ETD113  $  ET(1,13)=ETA113
  ETD(1,14)=ETD114  $  ET(1,14)=ETA114
  ETD(1,15)=ETD115  $  ET(1,15)=ETA115
  ETD(2,1) =ETD21   $  ET(2,1) =ETA21
  ETD(2,2) =ETD22   $  ET(2,2) =ETA22
  ETD(2,3) =ETD23   $  ET(2,3) =ETA23
  ETD(2,4) =ETD24   $  ET(2,4) =ETA24
  ETD(2,5) =ETD25   $  ET(2,5) =ETA25
  ETD(2,6) =ETD26   $  ET(2,6) =ETA26
  ETD(2,7) =ETD27   $  ET(2,7) =ETA27
  ETD(2,8) =ETD28   $  ET(2,8) =ETA28
  ETD(2,9) =ETD29   $  ET(2,9) =ETA29
  ETD(2,10)=ETD210  $  ET(2,10)=ETA210
  ETD(2,11)=ETD211  $  ET(2,11)=ETA211
  ETD(2,12)=ETD212  $  ET(2,12)=ETA212
  ETD(2,13)=ETD213  $  ET(2,13)=ETA213
  ETD(2,14)=ETD214  $  ET(2,14)=ETA214
  ETD(2,15)=ETD215  $  ET(2,15)=ETA215
  WD(1)=RATE1  $  WD(2)=RATE2  $  WD(3)=RATE3  $  ANGM=HM
COMMENT
 COMMENT SCAN PLATFORM CONTROLLER
```

```
   ETD11 =INTEG(ETDD(1,1) ,0.)  $  ETA11 =INTEG(ETD11 ,0.)
   ETD12 =INTEG(ETDD(1,2) ,0.)  $  ETA12 =INTEG(ETD12 ,0.)
   ETD13 =INTEG(ETDD(1,3) ,0.)  $  ETA13 =INTEG(ETD13 ,0.)
   ETD14 =INTEG(ETDD(1,4) ,0.)  $  ETA14 =INTEG(ETD14 ,0.)
   ETD15 =INTEG(ETDD(1,5) ,0.)  $  ETA15 =INTEG(ETD15 ,0.)
   ETD16 =INTEG(ETDD(1,6) ,0.)  $  ETA16 =INTEG(ETD16 ,0.)
   ETD17 =INTEG(ETDD(1,7) ,0.)  $  ETA17 =INTEG(ETD17 ,0.)
   ETD18 =INTEG(ETDD(1,8) ,0.)  $  ETA18 =INTEG(ETD18 ,0.)
   ETD19 =INTEG(ETDD(1,9) ,0.)  $  ETA19 =INTEG(ETD19 ,0.)
   ETD110=INTEG(ETDD(1,10),0.)  $  ETA110=INTEG(ETD110,0.)
   ETD111=INTEG(ETDD(1,11),0.)  $  ETA111=INTEG(ETD111,0.)
   ETD112=INTEG(ETDD(1,12),0.)  $  ETA112=INTEG(ETD112,0.)
   ETD113=INTEG(ETDD(1,13),0.)  $  ETA113=INTEG(ETD113,0.)
   ETD114=INTEG(ETDD(1,14),0.)  $  ETA114=INTEG(ETD114,0.)
   ETD115=INTEG(ETDD(1,15),0.)  $  ETA115=INTEG(ETD115,0.)
   ETD21 =INTEG(ETDD(2,1) ,0.)  $  ETA21 =INTEG(ETD21 ,0.)
   ETD22 =INTEG(ETDD(2,2) ,0.)  $  ETA22 =INTEG(ETD22 ,0.)
   ETD23 =INTEG(ETDD(2,3) ,0.)  $  ETA23 =INTEG(ETD23 ,0.)
   ETD24 =INTEG(ETDD(2,4) ,0.)  $  ETA24 =INTEG(ETD24 ,0.)
   ETD25 =INTEG(ETDD(2,5) ,0.)  $  ETA25 =INTEG(ETD25 ,0.)
   ETD26 =INTEG(ETDD(2,6) ,0.)  $  ETA26 =INTEG(ETD26 ,0.)
   ETD27 =INTEG(ETDD(2,7) ,0.)  $  ETA27 =INTEG(ETD27 ,0.)
   ETD28 =INTEG(ETDD(2,8) ,0.)  $  ETA28 =INTEG(ETD28 ,0.)
   ETD29 =INTEG(ETDD(2,9) ,0.)  $  ETA29 =INTEG(ETD29 ,0.)
   ETD210=INTEG(ETDD(2,10),0.)  $  ETA210=INTEG(ETD210,0.)
   ETD211=INTEG(ETDD(2,11),0.)  $  ETA211=INTEG(ETD211,0.)
   ETD212=INTEG(ETDD(2,12),0.)  $  ETA212=INTEG(ETD212,0.)
   ETD213=INTEG(ETDD(2,13),0.)  $  ETA213=INTEG(ETD213,0.)
   ETD214=INTEG(ETDD(2,14),0.)  $  ETA214=INTEG(ETD214,0.)
   ETD215=INTEG(ETDD(2,15),0.)  $  ETA215=INTEG(ETD215,0.)
COMMENT  ******  FLEX DYNAMICS END  ******
COMMENT  ************************************
END
END
END
TERMINAL
   FIN.. CONTINUE
   DEBUG
   NXQTER=NXQTER+1.
   WRITE(6,F2)T,NXQINT,NXQDYN,NXQDER,NXQTER
END
END
```

```
   VLZ=BOUND(-VLIM,+VLIM,VCZ)
   VMX=SQRT(ABS(VLX))*SIGN(1.,VCX)
   VMY=SQRT(ABS(VLY))*SIGN(1.,VCY)
   VMZ=SQRT(ABS(VLZ))*SIGN(1.,VCZ)
   TRWX=KM*VMX*ABS(VMX)
   TRWY=KM*VMY*ABS(VMY)
   TRWZ=KM*VMZ*ABS(VMZ)
   WRWX=INTEG(TRWX/JRW,WRWXI)
   WRWY=INTEG(TRWY/JRW,WRWYI)
   WRWZ=INTEG(TRWZ/JRW,WRWZI)
   TACHWX=WRWX-RATE1
   TACHWY=WRWY-RATE2
   TACHWZ=WRWZ-RATE3
   TBX=-TRWX-JRW*(-RATE3*TACHWY+RATE2*TACHWZ)   $  FBX=0.0
   TBY=-TRWY-JRW*(+RATE3*TACHWX-RATE1*TACHWZ)   $  FBY=0.0
   TBZ=-TRWZ-JRW*(-RATE2*TACHWX+RATE1*TACHWY)   $  FBZ=0.0
COMMENT  ******  RWH CONTROLLER DYNAMICS END  ******
  COMMENT
COMMENT  ****************************
COMMENT  ******  FLEX DYNAMICS ******
 COMMENT FORCES AND TORQUES ACTING ON BUS AND HINGES
   TB1=TBX+TDIST1              $  TB(1)=TB1
   TB2=TBY+TDIST2              $  TB(2)=TB2
   TB3=TBZ+TDIST3              $  TB(3)=TB3
   FB(1)=FBX
   FB(2)=FBY
   FB(3)=FBZ
   TH(1)=TH1
   TH(2)=TH2
   TH(3)=TH3
   TH(4)=TH4
   COMMENT
 COMMENT SOLVE FOR SYSTEM ACCELERATIONS
   CALL MRATE(NC,TH,TB,TS,FB,FS,TF,FF,GM,GMD,GMDD,ET,ETD,...
              WO,WDOT,ETDD,HM,CK)
   COMMENT
   COMMENT SYSTEM RATES AND POSITIONS
   COMMENT
   RATE1 =INTEG(WDOT(1),RATE1I)
   RATE2 =INTEG(WDOT(2),RATE2I)
   RATE3 =INTEG(WDOT(3),RATE3I)
   ALPH1 =INTEG(RATE1,ALPH1I)
   ALPH2 =INTEG(RATE2,ALPH2I)
   ALPH3 =INTEG(RATE3,ALPH3I)
   P2D,P1D,P2D,P3D=HCK(HCK,PZ,P1,P2,P3,RATE1,RATE2,RATE3)
   PZ    =INTEG(PZD,1.000)
   P1    =INTEG(P1D,0.000)
   P2    =INTEG(P2D,0.000)
   P3    =INTEG(P3D,0.000)
   GM1D  =INTEG(WDOT(4),0.)
   GM2D  =INTEG(WDOT(5),0.)
   GM3D  =INTEG(WDOT(6),0.)
   GM4D  =INTEG(WDOT(7),0.)
   GM1   =INTEG(GM1D,0.)
   GM2   =INTEG(GM2D,0.)
   GM3   =INTEG(GM3D,0.)
   GM4   =INTEG(GM4D,0.)
```

```
 COMMENT   CALCULATE THE S/C CENTER OF MASS
           DO CM1 K=1,3
           CMSCLV(K)=MB(7)*CMBLV(K)+MS(1,7)*CMSLV(1,K)+MS(2,7)*CMSLV...
           (2,K)+MS(3,7)*CMSLV(3,K)
           CMSCLV(K)=CMSCLV(K)/(MB(7)+MS(1,7)+MS(2,7)+MS(3,7))
           CM1..  CONTINUE
           WRITE (6,F3) CMSCLV
 COMMENT COMPUTATION OF PB AND PS VECTORS AND CMB TO ENG VECTORS
           DO L1 K=1,3
           RJTC1(K)=JTC1LV(K)-CMBLV(K) $ RJTC2(K)=JTC2LV(K)-CMBLV(K)
           SJTC1(K)=JTC1LV(K)-CMSCLV(K) $ SJTC2(K)=JTC2LV(K)-CMSCLV(K)
           PB(1,K)=HINGLV(1,K)-CMBLV(K)
           PB(2,K)=HINGLV(2,K)-CMBLV(K)
           PB(3,K)=HINGLV(3,K)-CMBLV(K)
           PS(1,1,K)=HINGLV(1,K)- CMSLV(1,K)
           PS(2,2,K)=HINGLV(2,K)-CMSLV(2,K)
           PS(3,3,K)=HINGLV(3,K)-CMSLV(3,K)
   L1..    CONTINUE
  PICKUP
INITIAL
 COMMENT ********************************************************
         *                                                      *
         *      DEFINE THE BUS FIXED AXES AS FOLLOWS:           *
         *      -------------------------------------           *
         *                                                      *
         *      AXIS3 = Z ( ION ENGINE PLUME EXHAUST AXIS )     *
         *                                                      *
         *      AXIS2 = Y ( SOLAR ARRAY AXIS )                  *
         *                                                      *
         *      AXIS1 = X                                       *
         *                                                      *
         ********************************************************
         *                                                      *
         *      SELECT THE MANEUVER BY ITS NUMBER               *
         *      ---------------------------------               *
         *                                                      *
         *      1 - TURN ENTIRE SPACECRAFT ABOUT AXIS1          *
         *                                                      *
         *      2 - TURN ENTIRE SPACECRAFT ABOUT AXIS2          *
         *                                                      *
         *      3 - TURN ENTIRE SPACECRAFT ABOUT AXIS3          *
         *                                                      *
         *      4 - TURN   BUS ONLY ABOUT AXIS2                 *
         *          WHILE KEEPING ARRAYS ON THE SUN             *
         *                                                      *
         *      5 - ACQUISITION OF CEL REFERENCES               *
         *                                                      *
         *      6 - SCAN PLATFORM SLEW OR BOXSCAN               *
         *                                                      *
         ********************************************************
         *                                                      *
         *                                                      *
CONSTANT                    MANEUV = 1.0
 COMMENT *                                                      *
         *                                                      *
         ********************************************************
```

END

DATE

FILMED

MAY 7 1980